A network analysis based proteomic and transcriptomic investigation into HIV-Tat induced neuronal dysfunction and the neuroprotective effect of lithium

By

Tariq Ahmad Ganief

GNFTAR001

Dissertation submitted for the degree of Doctor of Philosophy

In the Department of Integrative Biomedical Sciences

University of Cape Town

October 2015

Supervisor: Professor Jonathan M. Blackburn

Declaration

I, Tariq Ahmad Ganief, declare that this thesis is my own work (except where acknowledgements indicate otherwise). Neither the whole work nor part thereof has been, is being, or is to be submitted for any degree or examination at any other university.

I empower the University of Cape Town to reproduce for the purposes of research either the whole or any part of the contents of this thesis, in any manner whatsoever.

Signature of candidate: Tariq Ganief

Signed on the 28 day of October, 2015

Acknowledgements

During the years of my PhD, I have received a tremendous amount of support both personally and professionally; without which, this road would have proved significantly more arduous. While words are an abysmal return for all your friendship and counsel, please do accept them, even if only as an acknowledgement in gratitude.

Shaun, through all the debates and discussions in the years we have worked together I have come to appreciate your single-minded determination to achieve. Through your determination and help, I myself have learned and achieved. Your help and friendship has been invaluable.

Nelson, despite being a 'recent' addition to our lab, you quickly proved your value and became indispensable to the success of our group. Your knowledge and advice has and will always be appreciated.

To my supervisor and mentor, Professor Jonathan Blackburn; your brilliant mind, positive attitude, simple solutions countering seemingly incalculable complexity, unwavering support, patience and guidance have been a source of inspiration and motivation throughout this PhD. You have undoubtedly shaped me as a scientist and I truly and sincerely appreciate all the opportunities you have given me. I am proud to have been your student.

Lastly and most importantly; to my dear my parents, Sofwaan and Mariam Ganief; I thank you for the years of quiet sacrifice, continued support and pride in spite of difficulties. I thank you for raising me with a sense of wonder, perseverance and determination; traits which have been paramount to the completion of this PhD.

Table of Contents

Abbreviations

2DE	Two-dimensional gel electrophoresis
AAN	American Academy of neurology
ABC	Ammonium bicarbonate
AD	Alzheimer's disease
AGC	Automatic gain control
AKT	Protein kinase B
ANI	Asymptomatic neurocognitive impairment
APP	Amyloid precursor protein
AQUA	Absolute Quantification peptides
ARP	Actin related protein
ARV	Antiretroviral
ATP	Adenosine triphosphate
Aβ	Ameloid-β
BBB	Blood-Brain Barrier
BCA	Bicinchoninic acid assay
Bcl-2	B-cell lymphoma 2
BD	Bipolar disorder
BDNF	Brain-derived neurotropic factor
BH4	Tetrahydrobiopterin
BSA	Bovine serum albumin
BMVEC	Brain microvascular endothelial cell
c18	Octadecyl bonded silica
CCR5	Chemokine receptor type 5
CD8	Cluster of differentiation 8
cdc42	Cell division control 42
CDK5	Cyclin dependant kinase 5
CDK9	Cyclin Dependant kinase-9
CHGA	Chromogranin A
CHK	Serine/threonine-protein kinase Chk1
CNS	Central nervous system
con	Contaminant
CPE	CNS penetrating effectiveness
CREB	cAMP response element-binding protein
CRMP1	Collapsin Response Mediator Protein 1
CSTA	Cystatin A
CXCR4	C-X-C chemokine receptor 4
CYP 3A4	Cytochrome p450 3A4
D1	Dopamine receptor 1
DBH	Dopamine B-hydroxylase
DMEM	Dulbecco's Modified Eagle's medium
DMSO	Dimethyl sulphoxide
DNA	Deoxyribonucleic acid
DTT	Dithiothreitol
ECM	Extracellular matrix

EEF	Eukaryotic elongation factor
EIF	Eukaryotic initiation factor
EIF2α	Eukaryotic initiation factor 2α
eNOS	Nitric oxide synthase 3
ER	Endoplasmic reticulum
ERK	Extracellular signal-regulated kinases
ESI	Electrospray ionisation
FA	Formic acid
FASP	Filter aided sample preparation
FCS	Foetal calf serum
FDR	False discovery rate
FTICR	Fourier-transform ion cyclotron resonance
FXS	Fragile X syndrome
GCN2	General control nonderepressible 2
GNAI	Guanine Nucleotide Binding Protein/G protein subunit
GO	Gene ontology
GP120	Glycoprotein 120
GP160	Glycoprotein 160
GRB2	Growth factor receptor-bound protein 2
GSK-3β	Glycogen synthase kinase - 3β
GTP	Guanosine triphosphate
HAART	Highly active antiretroviral therapy
HAD	HIV-associated dementia
HAND	HIV-associated neurocognitive disorder
HCD	High-energy collision dissociation
HCV	Hepatitis C virus
HIV	Human immunodeficiency disease
HIV-Tat	HIV transactivator of transcription
HRI	Heme-regulated inhibitor kinase
HSF-1	Heat shock factor protein 1
IAA	Iodoacetamide
IFN	Interferon
IGF-1	Insulin growth factor-1
IGHA1	Immunoglobulin Heavy Constant Alpha 1
IGLL5	Immunoglobulin Lambda-Like Polypeptide 5
IIDMM	Institute of infectious disease and molecular medicine
IKK	Inhibitor of NF-κB kinase
IKβ	Inhibitor of NF-κB
IL	Interleukin
iNOS	Inducible nitric oxide synthase
IPA	Ingenuity pathway analysis
IRF	IFN regulatory factor
ISGs	Interferon-stimulated genes
iTRAQ	Isobaric tag for relative and absolute quantitation
IVA	Influenza A
KCTD15	Potassium Channel Tetramerization Domain Containing 15

LC	Liquid chromatography
LFQ	Label-free quantification
LIT	Linear ion trap
LTD	Long-term depression
LTP	Long-term potentiation
LTR	Long Terminal Repeat
m/z	Mass-to-charge ratio
MALDI	Matrix assisted laser desorption ionisation
MAPK	Mitogen-activated protein kinases
MCP-1	Macrophage chemotactic protein-1
MMHP	Mitochondrial membrane hyperpolarisation
MMP	Matrix-metalloproteases
MND	Mild cognitive disorder
mRNA	Messenger Ribonucleic acid
MS	mass spectrometry
mTOR	Mammalian target of rapamycin
MTT	3-(4,5-dimethylthiazol-2-yl)-2,5-diphenyltetrazolium bromide
MUCL1	Mucin-like protein 1
NaCl	Sodium chloride
NADPH	Nicotinamide adenine dinucleotide phosphate
NBP	4-(4-Nitrobenzyl)pyridine
NCE	Normalized collision energy
NE	Norepinephrine
Nef	Negative Regulatory Factor)
NFκB	Nuclear factor kappa B
NGF	Nerve growth factor
NHS	*N*-hydroxy-succinimide
NO	Nitric oxide
p53	Tumour protein p53
PAF	Platelet Activating Factor
PAMP	Pathogen-associated molecular patterns
PAR2	Proteinase activated receptor 2
PBS	Phosphate-buffered saline
PCBD	Pterin-4alpha-carbinolamine dehydratase
PD	Parkinson's disease
PERK	PKR-like endoplasmic reticulum-resident kinase
Pi3K	Phosphoinositol-3-kinase
PIC	Pre-integration complex
PITPa	Phosphatidylinositol transfer protein a
PITPB	Phosphatidylinositol transfer protein b
PKA	Protein kinase A
PKC	Protein kinase C
PP1	Protein phosphatase 1
PP2A	Protein phosphatase 2A
PP2ABα/PPP2R2A	Protein Phosphatase 2, Regulatory Subunit B
PPP2CA	Protein Phosphatase 2, Catalytic Subunit

PPP2R	Protein Phosphatase 2, regulatory subunit
PRK	Double-stranded RNA-activated protein kinase
PRR	Pattern recognition receptors
PRRC2C	Proline-Rich Coiled-Coil 2C
PSAQ	Protein Standard Absolute Quantification
PSME2	Activator Of Multicatalytic Protease Subunit 2
p-TEFb	Positive transcription elongation factor b
p-TEFb	Positive transcription elongation factor b
PTM	Post-translational modifications
PTPN11/SHP-2	Protein Tyrosine Phosphatase, Non-Receptor Type 11
Rac	RAS-Related C3 Botulinum Toxin Substrate
RAS	Renin-angiotensis system
rev	Reverse
Rho	RAS Homolog Family Member
RhoA	RAS Homolog Family Member A
RhoGDI	Rho GDP dissociation inhibitor
RNA	Ribonucleic acid
ROS	Reactive Oxygen species
RP	Reverse phase
sd	Standard deviation
SDS	Sodium dodecyl sulfate
Sept	Septin
SHROOM3	Shroom Family Member 3
SILAC	Stable isotope labelling by amino acids in cell culture
SNP	Single nucleotide polymorphism
TAR	HIV transactivation response
TFAP-2α	Transcription factor AP-2
TH	Tyrosine hydrolase
TLR	Toll-like receptor
TMT	Tandem mass tags
TNFR	Tumour necrosis factor - α receptor
TNFα	Tumour necrosis factor – α
TOF	Time-of-flight
Tris-HCl	Tris(hydroxymethyl)aminomethane - hydrochloric acid
TrKA	Tropomyosin receptor kinase A
tRNA	Transfer ribonucleic acid
TWEAK	Tumour necrosis factor-like weak inducer of apoptosis
UHPLC	Ultra-high pressure HPLC
UTR	Untranslated region
Vpr	Viral protein R
WASP	Wiskott–Aldrich syndrome protein

Abstract

HIV-associated neurocognitive disorders (HAND) affect up to 70% of HIV positive individuals and are the leading cause of dementia in patients under 40 years. Despite this, the molecular mechanisms involved in the onset of HAND are not well understood. Among a number of plausible etiological agents of HAND, HIV-Tat has been shown to be neurotoxic *in vitro* and *in vivo*, but the basis of its induced neuronal dysregulation remains relatively poorly characterised, giving rise to various competing theories. This thesis describes differential, quantitative proteomic analyses of HIV-Tat-treated neuronal cells *in vitro*, the goal being to gain deeper insight into the underlying molecular basis of this HIV-Tat-mediated dysregulation, as well as to potentially inform better patient treatments in the future. To achieve this goal, deep, quantitative proteomic analysis of HIV-Tat treated SILAC-labelled SH-SY5Y neuroblastoma cells was carried out, alongside transcriptomic analysis of the same system in which 3077 proteins were identified and quantified with 407 proteins and 1074 genes being differentially expressed. Subsequently, label-free proteomics analysis was used to study the ability of lithium – a proposed new treatment for HAND – to suppress the HIV-Tat induced dysregulated molecular phenotype in SH-SY5Y cells in which 3757 were identified and quantified with 360 and 531 being significantly differentially expressed in HIV-Tat and HIV-Tat + lithium treated cells, respectively.

Detailed analysis of all three datasets enabled delineation of a sequence of signalling events which not only lead to HIV-Tat-induced apoptosis but which also account for degeneration of neuronal cell function. Interestingly, this analysis identified dysregulation of neurodegenerative processes thought to be involved in other dementias such as Alzheimer's disease and Parkinson's disease and, usefully, also confirmed the dysregulated of numerous pathways known to be important to HIV replication. In particular, HIV-Tat induced activation of several proinflammatory pathways including Toll-like Receptor, Interferon Regulatory Factor, RIG-1 and MDA-5 signalling was observed. This implies involvement of a proinflammatory response in the dysregulation of cytoskeletal reorganisation pathways, attenuation of protein synthesis pathways and the induction of apoptosis. In cytoskeletal regulatory pathways, Rho, Rac and cdc42 signalling were found to be dysregulated; in protein synthesis pathways, EIF2 signalling was attenuated, as seen by the inhibition of several critical eukaryotic initiation factors,

and mTOR and P70S6K were also dysregulated; & initiation of apoptosis could be attributed to the accumulation, and resultant signalling, of ceramide due to the proinflammatory response.

Pathway analysis revealed that lithium activated AKT and reversed the activation of several pro-apoptotic pathways such as ceramide and TNFR1 signalling, but also showed that lithium did not ameliorate, but instead increased HIV-Tat induced protein synthesis attenuation. Furthermore, several key cytoskeletal regulatory factors, including RhoA and ARP proteins, remained dysregulated after lithium treatment. Importantly, while lithium was found to decrease the apparent overall dysregulation of most HIV-Tat dysregulated pathways, numerous proteins and pathways implicated in neurodegenerative processes remained dysregulated or were specifically newly dysregulated by lithium.

While it is unlikely that HIV-Tat is the sole contributor toward HAND development, the data presented in this thesis provides considerable new understanding of the extent to which HIV-Tat is able to induce significant dysregulation of the neural proteome, ultimately contributing to the neurodegeneration and synaptodendritic injury associated with disease onset and progression. Furthermore, the work described in this thesis also suggests that lithium is not able to prevent the dysregulation which underlies the HIV-Tat-induced neurodegeneration, an observation which may have direct clinical relevance.

Chapter 1

General introduction

HIV-Associated Dementia

Infection with human immuno-deficiency virus type 1 (HIV) is a significant global health concern and is known to have adverse neurological effects. A significant portion of HIV-infected patients develop some form of HIV-Associated Neurocognitive Disorder (HAND). HAND describes three formal disease classifications; asymptomatic impairment (ANI), mild cognitive disorder (MND) and HIV-associated dementia (HAD). Up to 70% of HIV+ patients develop HAND[1] and 90% of patients display autopsy evidence of neuropathology. Although the incidence of HAD have decreased since the implementation of Highly Active Antiretroviral Treatment (HAART), the incidence of minor cases of HAND have increased.[2,3] The high incidence of HAND poses significant socio-economic challenges to South Africa as it has negative implications for behavioural and health outcomes, adherence to medication, rates of employment, and functional impairment.[4] There are no current treatment possibilities for HAND other than HAART. Several studies have shown that patients treated with HAART improve in their neurocognition scores, but never fully remit. This implies that patients have had either significant neurological damage before the commencement of HAART, or that the neurotoxic environment was not removed. Whether or not the former is true it can be difficult to assess while the latter is a definite possibility.

There is, currently, no rapid test for HAND. Diagnosis relies on neuropsychological, psychiatric and medical evaluation. Several diagnostic approaches have been proposed, however, due to variability in disease presentation and possible limitation in busy or recourse poor medical centres, there is a need for standardisation. In 2007, the American Academy of neurology (AAN) updated their proposed diagnostic procedure and established criteria for the diagnosis of three HAND syndromes: ANI, MND and HAD. A notable improvement over the previous procedure is that neurocognitive impairment is now required for HAND diagnosis. Previously, HIV neurocognitive disorders could be diagnosed on the basis of neuromotor and non-cognitive psychiatric changes such as changes in personality or mood.[5] HAND diagnosis also requires that all other possible sources of neurocognitive impairment.

HIV Life cycle

As an obligate intracellular parasite, HIV requires a permissive human cell for most of the machinery involved in its life cycle. The factors required are recruited and manipulated in order to facilitate maximal viral replication. In response to the threat of viral infection, host cells have developed several physical and functional mechanisms in order to limit infection and replication.

HIV's initial requirement is a host cell; the infection of which is governed by the cells' expression of CD4 and CXCR4 or CCR5 of their surfaces. $CD4^+$ T-lymphocytes and cells of the monocytic lineage along with several smaller populations of cells such as dendritic cells are the predominant host cells. $CD4^+$ cell state also plays a significant role in the HIV life cycle where both active and resting cells are permissive to infection, but only active cells are permissive to viral replication. Since the majority of $CD4^+$ cells are resting, there is typically a large population of latently infected cells which can be activated. Once bound to the surface of permissive cells through GP120 interaction with the CD4, GP120 undergoes conformational changes. In this process, GP120 engages with either CXCR4 or CCR5 which, in turn activate GP41 mediated fusion of the viral and cellular membrane. Fusion leads to the ejection of the viral capsid containing its nuclear material into the cytoplasm. At this point, the virus faces a physical barrier to infection in the form of a dense cortical actin mass below the cell membrane. It is believed that interaction of the viral Env protein with the chemokine receptors initiates a cascade leading to the activation of actin depolymerising protein, cofilin, which degrades the cortical actin barrier. Once beyond the cortical actin barrier the capsid is transported along the cytoskeleton toward the nucleus. During this time, the viral genome is reverse transcribed and the preintegration complex is formed. Premature uncoating may be facilitated by the host cellular restriction factor, TRIM5α, and results in aborted infection.[6] Once at the nuclear surface, the viral pre-integration complex (PIC) must traverse the nuclear membrane; a significant challenge as the PIC is 56 nm in diameter while the nuclear pore has a 28 nm central channel.[7] Although it is not well defined, several factors including importin 7, histone H1, HIV-Vpr, matrix and integrase are required for importing the PIC into the nucleus.[8,9] Following entry into the nucleoplasm, the PIC releases the viral DNA and integrase to allow 3' processing and covalent strand transfer into the host genome. While integrase co-ordinates the process, several host proteins such as DNA repair enzymes are

required.[10,11] Although several genes have been expressed from the incoming cytoplasmic genome copies, transcription of the full genome only takes place after integration. Transcription of the HIV genome is primarily driven by HIV-Tat and several recruited host proteins such as RNA polymerase II. Once viral mRNA has been processed and exported to the cytoplasm by Rev, another major challenge is encountered. Viral protein synthesis relies entirely on the host translation machinery and, theoretically, has to compete with host transcripts for translation. Translation is also primarily co-ordinated by HIV-Tat through its binding to the 5' HIV transactivating response element (TAR) mRNA sequence.[12,13] There are several established examples of HIV actively dysregulating host protein synthesis machinery.

One of the most studied and well recognised of these is the interaction between PKR, HIV-Tat and TAR. Briefly, PKR surveys the cytoplasm for viral replication and is activated by the resultant dsRNA. Through the phosphorylation of Eukaryotic initiation factor 2α (EIF2α), PKR is able to induce a global attenuation of protein synthesis. This process limits of completely inhibits the translation of most host mRNA's but also serves to prevent active viral replication. To prevent this, it is reported that HIV-Tat binds and prevents the phosphorylation of EIF2α. There is, however, significant uncertainty about the mechanisms of this process in HIV-infected cells. The HIV mRNA translation process will be discussed in detail later. The final stage of the HIV life cycle is assembly, budding and maturation; each of which is co-ordinated by the polyprotein, gag, and its proteolytic products. The N-terminus of the Gag polyprotein, MA, targets and binds the plasma membrane and completely co-ordinates viral assembly by recruiting essential components such as Env, viral enzymes and the RNA genome. Although there is sufficient evidence that Gag and genomic RNA associates with actin structures, an intact actin cytoskeleton does not seem to be essential for assembly.[14,15]

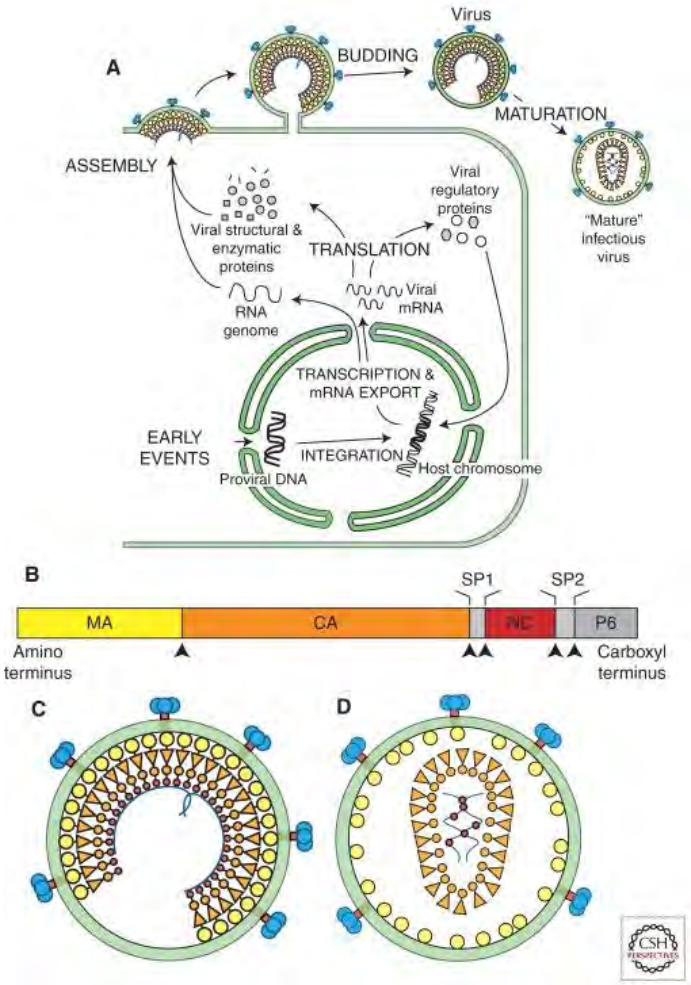

Figure 1:A The figure represents brief depiction of the viral life cycle adapted from Sundquist and Kräusslich.[16] A) During assembly, Gag polyproteins targets and binds the host plasma membrane via interaction with its N-terminal Matrix (MA). Gag continues to recruit essential components such as the viral RNA genome, Env products, gp120 and gp41 and the viral enzymes, IN, PR and RT. Gp120 and gp41 are impregnated into the plasma membrane and the RNA genome is packaged and bound the Gag C-terminal nucleoprotein, NC. As the budding process progresses, host ESCRT complex proteins are recruited to facilitate the membrane fission between the nascent virion particle and the plasma membrane. B) The Gag polyprotein and arrangement of the protein products within it. C) After fission, the immature virion then activates the viral protease which cleaves the Gag polyprotein into individual proteins which rearrange to form the mature, infectious virus (D). After Gag cleavage by the protease, MA proteins are structured below the membrane, the capsid protein arranges to form the core structure and the nucleocapsid (NC) associate with the RNA genome within the core.

As the spherical immature virion is formed by co-ordinated Gag protein-protein interactions at the cell membrane, host ESCRT proteins are recruited to the budding particle and facilitates the fission between the nascent particle and the plasma membrane.[17] Once budding is complete, unknown signals activate the viral protease which cleaves the Gag polyprotein into the individual proteins which rearrange to form the mature virus.[16] The major steps in the HIV life cycle are illustrated in **Figure 1**.

As neurons are not $CD4^+$ and are, therefore, not typically infected by HIV, direct viral infection cannot be causative of neuronal degradation in HAND. The central nervous system (CNS) is, however, not immune to HIV.

HIV in the brain

The blood-brain barrier (BBB) is a continuous layer of tightly linked brain microvascular endothelial cells tasked with separating the CNS from the periphery. The BBB is a selectively permeable membrane which regulates the tracking of molecules into and out of the brain parenchyma and the bloodstream. HIV has been shown to infect the brain very early after initial infection.[18] While the mechanism is not entirely clear, HIV must have a means through which to cross the BBB in order to enter the brain. The Trojan horse theory suggests that HIV enters the CNS in infected monocytes migrating across the BBB into the brain parenchyma (**Figure 2**).

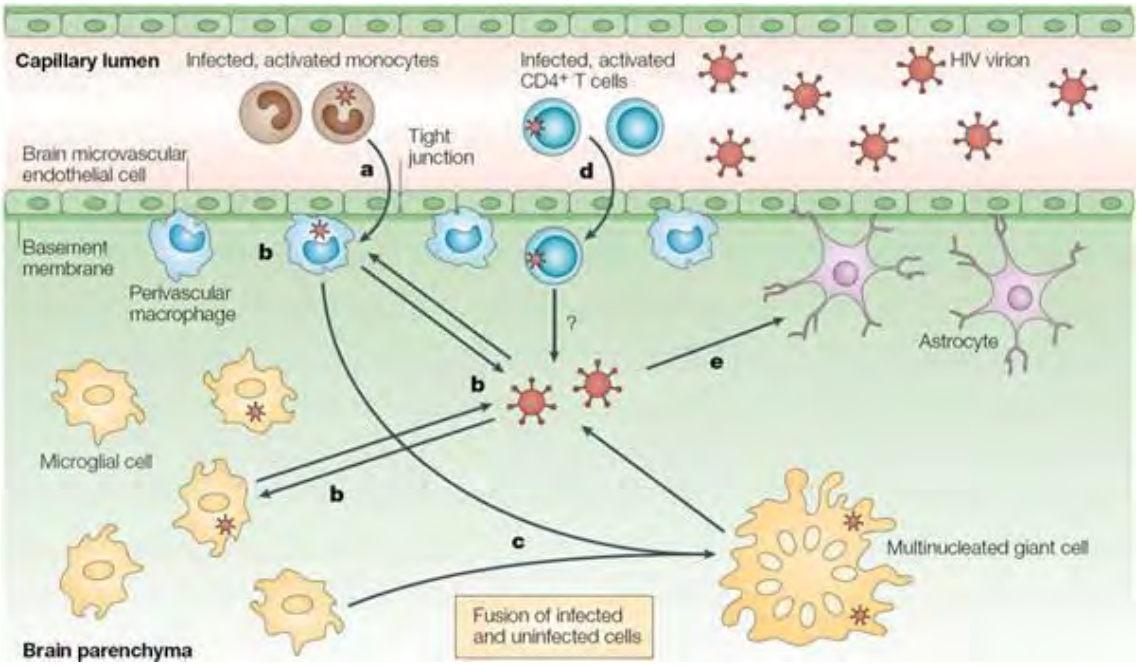

Figure 2: Trojan horse theory: While there is evidence that HIV can migrate through BMVEC's, it typically accepted that HIV initially enters the brain through invading, infected perivascular monocytes migrating across the BBB. These cells then shed replicative viral particles which go on to infect brain resident HIV permissive cells such as microglia. Once infected, microglia can be activated and induce and maintain an inflammatory environment in the brain.[19]

Other work has shown that brain microvascular endothelial cells (BMVEC) in infected individuals contain HIV DNA which suggests that HIV may be couriered across the BBB through BMVEC's. Invading virus or those shed from invading monocytes then infect resident brain cells, the majority of which are astrocytes and microglia, which then serve as both latent and active CNS reservoirs for HIV. Active or productive infection implies that HIV is constantly being shed from the cell surface whereas latent infection implies that the HIV genomic material is present, but is not being actively transcribed. It is believed that perivascular macrophages are the most common peripheral cell type to enter the CNS during infection. Together with microglia, these cells are capable of

forming multinucleated giant cells, or syncytia, which are a hallmark of HIV-encephalitis. While astrocytes are typically not productively infected, latent infection leads to the secretion of monocyte chemoattractant protein, MCP-1, which contributes to the recruitment of activated macrophages into the CNS.[20,21] Furthermore, the BBB is actively degraded during HIV infection which exposes the CNS to insults that it would not ordinarily encounter as well as increase the potential for continuous HIV entry.[22] Blood plasma molecules have access to the CNS via a disrupted BBB and have been shown to accumulate in neural tissues.[23] This accumulation has a plethora of its own toxic effects. HIV has been shown to activate matrix-metalloproteases (MMP's) which break down the BBB.[24] Several mechanisms proposed to be involved in HIV induced BBB degradation are illustrated in (**Figure 3)**.

Due to unique selective pressure, the immune privileged environment in the CNS results in the accumulation of unique HIV genomic sequences in the CNS.[25] HIV genomic sequences isolated post mortem from HIV Dementia patients' brains have showed that CNS derived genomic sequences cluster separately from peripheral HIV genomic sequences relative to HIV-Tat.[26] Furthermore, sequences also cluster relative to the brain area from which the sequences were isolated. This may be resultant of decreased immune surveillance in the CNS which alters the selective pressure and affects HIV genomic sequence evolution.

As neurons are not productively infected by HIV, interaction with the infected cells or neurotoxic factors released by them must be causative of HAND pathologies. Infected microglia and brain resident macrophages can be activated by HIV infection itself, interaction with viral proteins or cytokine secretion by infected cells. Once infected and activated, these cells can secrete an array of neurotoxic factors including inflammatory cytokines IL-1β, IL-6, TNF-α, VCAM-1, ICAM-1, MCP-1 and PAF as well as excitotoxic amino acids.[20,27,28,29,30]

Evidently, HIV induces significant alterations to cellular signalling during the infection and replication processes. To facilitate cell entry and movement through the cell, HIV modifies cytoskeletal regulation and structures. During replication HIV needs to hijack host protein translation machinery to ensure efficient synthesis of its proteins. Furthermore, these critical cellular functions need to be regulated by HIV despite the activation of innate antiviral response characteristic of HIV infection.[31,32]

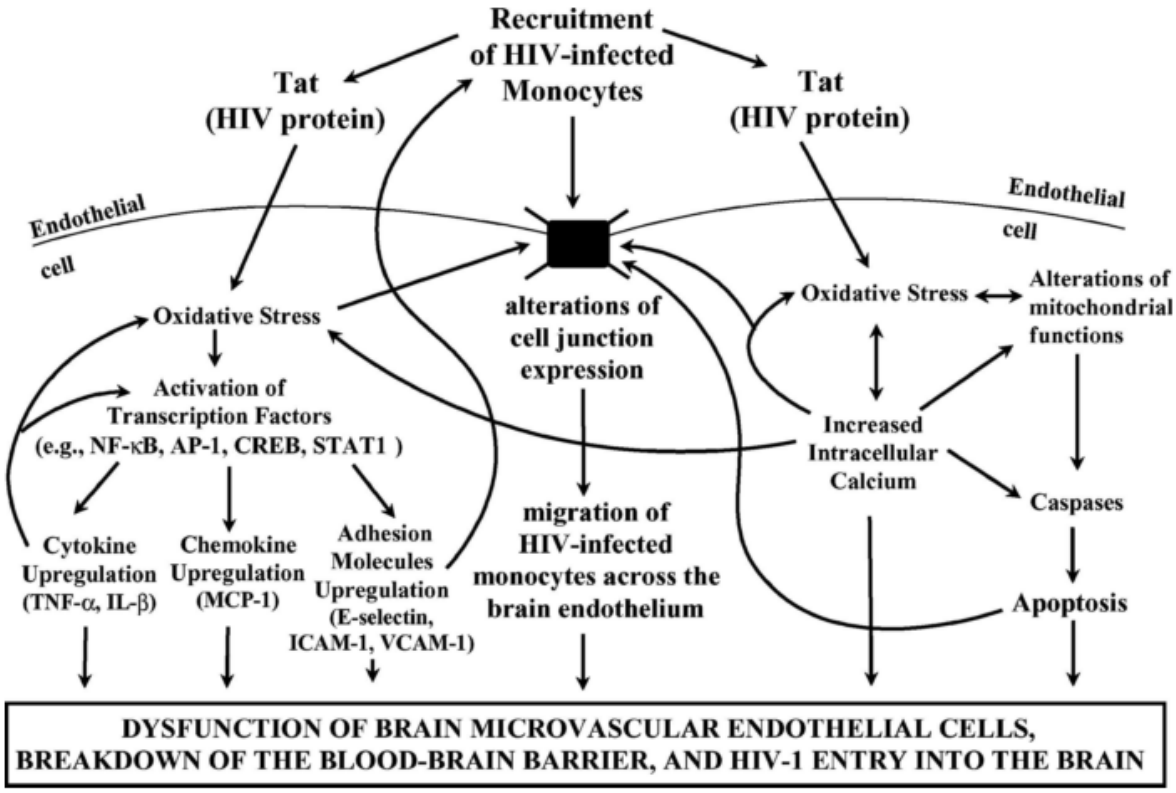

Figure 3: The mechanisms by which HIV exerts it toxic effects on the brain are numerous and complex. The image described several mechanisms through which HIV-Tat can alter the microvascular system and, ultimately, result in the degeneration of the BBB. Image adapted from Toborek *et al*.[23]

Innate antiviral response and inflammation

To successfully replicate in a human host, many viruses have developed means through which to modulate the host's ability to activate the IFN mediated innate antiviral response. To achieve this, the activation of IFN regulatory factors by toll-like receptors, MDA-5 and RIG-1 are inhibited.[33,34] No such ability has been reported for HIV. Ironically, sustained IFN production is characteristic of *in vivo* HIV infection. Although there are several different interferons, type-1 interferons of the alpha (IFNα) and beta (IFNβ) classes are the most studied and well characterised interferons released by host cells in response to viral infection. IFNα/β signals through a ubiquitously expressed receptor to activate a signal transduction cascade in response to viral infection. The specific antiviral response is mediated thereafter by any number of several hundred interferon response genes (ISG).[35]

Given the diversity of potential human infective viruses present, it is no surprise that there is an array of distinct cell surveillance mechanisms by which the cell can detect viruses and mount a response. Interferon production through the recognition of

pathogen-associated molecular patterns (PAMPs) by pattern recognition receptors (PRRs) is the first step in this process. While the specific mechanisms of activation vary between PRRs, they converge on downstream components. For example, the PRR's RIG-I and MDA-5 are closely related in function but are non-redundant and induce interferon production by distinct means. Activated PRR's induce the phosphorylation of the C-terminus of IFN regulatory factors (IRF) which then translocate to the nucleus where they induce the expression of IFNα/β. Activated PRR's also result in the activation of the inhibitor of NF-κB kinase (IKK) and the subsequent phosphorylation, ubiquitination and destruction of inhibitor of NF-κB (IKβ) which results in the activation and nuclear translocation of nuclear factor kappa B (NF-κB) (**Figure 4**). Together with c-Jun, each of these pathways can induce the transcription and subsequent production of IFNα/β. Through the subsequent IFNα/β activation, the antiviral pathways are engaged by specific compliments of ISGs being expressed. These ISGs number in the hundreds and are largely responsible for the innate antiviral effect of IFN.[36,32] Since their discovery, much has been learned about the molecular cascades resulting in the activation of IFN and the subsequent antiviral pathways. However, much less is known about the specific genes being activated and their functions in the antiviral response.[37] The diverse array of functions of ISGs include cytoskeleton reorganisation, [38,35,39] protein translation blockade [39,40,41] and apoptosis.[42,43,44]

However, that some viruses are able to replicate despite the induction of a powerful antiviral response evidences the fact that they are able to overcome the intended inhibition caused. The mechanisms employed by viruses to overcome the antiviral response are diverse. Furthermore, there are several elegant descriptions of a viral requirement of the host antiviral response in order to replicate successfully. That the antiviral response primarily attenuates cellular protein translation evidences the importance of this system to viral replication. This also implies that viruses need to develop efficient means through which to overcome translational blockades. Indeed, several viruses are reported to not only antagonize the host's efforts to inhibit viral protein synthesis but to require global protein translation suppression to replicate most efficiently. These include but are not limited to influenza, Hepatitis C virus (HCV) and dengue fever.[45,46,47,48,49]

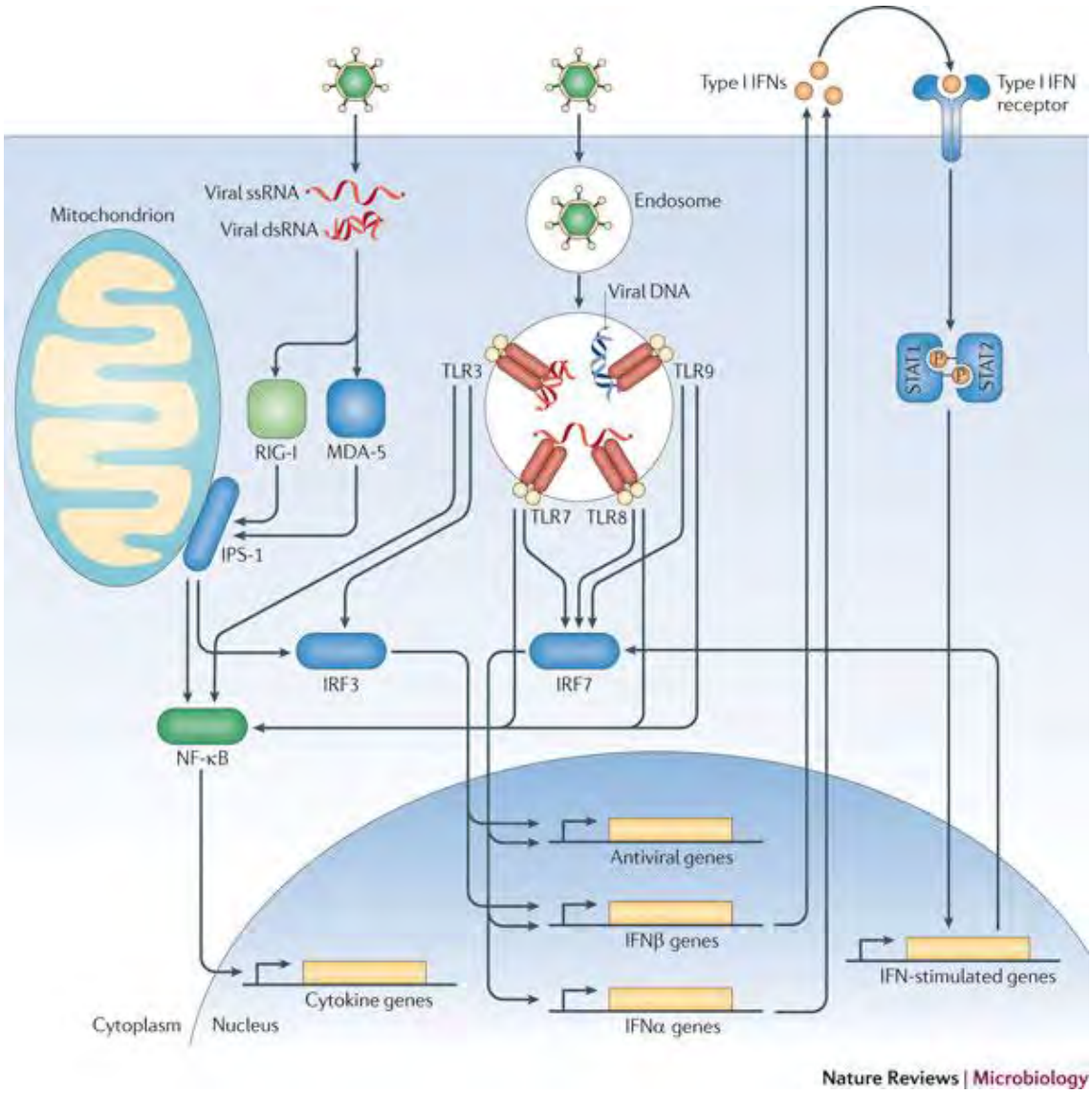

Figure 4: Viral RNA binding induces the activation and subsequent signalling of RIG-1 and MDA-5. This activation cascade leads to NF-κB and IRF activation and nuclear translocation where they induce the expression of IFN-stimulated, antiviral and various proinflammatory genes.[50]

Primarily, the cytoskeletal effects of IFN play a role in barrier disruption and immune cell migration. It is well-documented that IFNα/β increase the permeability of epithelial barriers to facilitate immune cell migration into areas of inflammation. Similarly, IFN directly affects cytoskeletal reorganisation[51] and its inflammatory effects are mediated by the cytoskeleton.[52] The effects of IFN and inflammation on cytoskeletal reorganisation are discussed in detail by Ivanov *et al*.[52]

Maintained activation of PRR's, which results from the cells' inability to effectively overcome the infection, the antiviral system induces apoptosis. Inflammation can induce apoptosis in many ways, through any of the stress responses it induces. The

involvement of viruses with the induction of apoptosis is not as much to do with replication directly but with prolonging access to replicative machinery.

Neuroinflammation and neurodegeneration

Inflammation creates a stress response in cells. If the inflammation is not resolved, this stress response persists and is associated with tissue damage and is involved in diseases such as asthma, Crohn's disease, rheumatoid arthritis, gastritis, otitis, celiac disease, and inflammatory bowel disease. Furthermore, many neurodegenerative diseases such as HAND, Alzheimer's disease (AD) and Parkinson's disease (PD) have an established inflammatory component.[53] Since the acceptance that AD and PD patient brains contained an extensive milieu of proinflammatory molecules, extensive knowledge has been generated outlining the sources and some effects of this inflammation. In both AD and PD, the causative agents of this inflammation was fairly easy to discern; Aβ and α-synuclein deposits respectively.[54] Furthermore, the resultant cell death in these diseases elicits an additional inflammatory response. However, teasing apart the effects of these deposits and the ensuing inflammatory response is more challenging.

Aβ is neurotoxic and induces apoptosis when added to neuronal cultures alone, however, this effect is significantly increased when neurons are pre-treated with IFNγ.[55] The inflammation resulting from Aβ and tangles further increases the expression of amyloid precursor protein (APP) which subsequently increases the formation of Aβ. A key marker of AD is tau hyperphosphorylation which is facilitated by CNS inflammation. Interestingly, acute and lasting increased cognitive impairment in AD patients have been correlated with peripheral infection events. The inflammatory events uncovered in AD brains are well-documented to be cytotoxic in the periphery; it is therefore improbable that they would be neurotoxic as well. Furthermore, upregulated inflammatory markers localize within areas of the brain with high AD pathology. Several clinical trials have provided evidence that classic anti-inflammatory treatment delay the onset or progression of AD.[56]

There is significant evidence for the involvement of inflammatory markers in PD. Studies have shown that both TNFα and IFNγ levels are altered in PD brains post mortem. Proinflammatory cytokines also correlate with disease severity in PD patients. Patients receiving therapeutic IFNα have been reported to exhibit a PD-like syndrome

including tremors, muscle rigidity and a generalized paucity of movement. Similarly, PD patients exhibit fewer infections and malignancies which may stem from increased systemic inflammation.[57] The effects of IFN on neurons is predominantly thought to be exacted through microglia, however, IFN also has direct effects on neurons. IFN treatment increased calcium influx and nitric oxide production which subsequently depleted cellular ATP which lead to dendritic beading.[58] While there may be significantly more biochemical events which are not outlined in this study, it provides evidence for the neurotoxicity of proinflammatory cytokines.

Given the evidence that inflammation can cause neurodegeneration in well studied diseases, the inflammatory environment present in HAND patient brains likely plays a role in disease as well. Thus, it is reasonable to assume that the same effects elicited by inflammation in AD and PD are taking place in HAND. Although both PD and AD are, evidently, very complex diseases, HAND might be even more so. While there are certainly genetic predispositions involved in PD and AD, HAND has the additional complexity of a replicating virus within the CNS. A virus which is known to alter host biochemistry in order to favour its replication and which produces and secretes many non-host proteins, many of which are known to have deleterious effects on cells.

To assess the inflammatory involvement in neurodegenerative disease, one must also consider the involvement of the brain resident macrophage: microglia. In common with other viral infections in other tissues, HIV infection induces an inflammatory response in the CNS. This response is typically beneficial and helps in the removal of the offending antigens. However, in the case of HIV infection, the virus persists and results in chronic inflammation in the CNS and periphery. Then, considering the cytotoxic environment induced by inflammation, it is not surprising that chronic CNS inflammation would have deleterious effects on CNS cells and, importantly, neuronal function. In healthy, non-inflamed brains, resting microglia are dominant with small cell bodies and many branched processes. Upon activation by various PAMPs or damage-associated molecular pattern molecules (DAMPs), microglia begin actively producing proteins such as iNOS and COX-II together with proinflammatory cytokines such as IFN and TNFα. These not only affect local neurons but also activate other microglia and astrocytes. This active state is maintained as long as antigen is present. Activated microglia can kill pathogens but are also capable of killing neurons directly.[59]

Possible origins of disease

HIV, even when well managed, is a chronic disease which elicits an inflammatory response. In addition, viral proteins are present and circulating throughout the entire infection. Compounding this, HIV antiretroviral (ARV) treatments are inherently cytotoxic. ARV's are certainly not required for HAND onset and progression, although, they do not inhibit the progression. Therefore, it is reasonable to suggest that HAND is caused by either the secretion of viral products interacting with neurons, the secretion of neurotoxic inflammatory molecules from infected or non-infected immune cells or a combination of these.

ARV therapy and HIV Dementia

The increase in minor HAND cases in the post HAART era raised questions pertaining to the involvement of ARVs in the development of HAND. HAND has been shown to persist while patients are on treatment despite supressed CNS viral loads.[60] These observations have raised the simple question as to why HAND is persisting and increasing in incidence. Here, several possibilities may be causative: 1. HIV may be protected from the ARVs by the BBB. This would result in the unchallenged replication of HIV in the CNS facilitating continued CNS exposure to neurotoxins resultant of HIV infection. 2. ARVs themselves may be neurotoxic, thus eliciting similar symptoms to HIV-mediated toxicity. 3. Patients have suffered irreversible neuron loss before the commencement of HAART.

Patients with advanced HIV being treated with drug cocktails with higher CNS penetrating effectiveness (CPE) values have lower CNS viral loads. However, patients in this cohort with higher CPE scores performed lower on neurocognitive tests.[61] This trend was also found in patients treated with a greater number of drugs within their regiments.[61] Higher CPE scores were also correlated with decreased or undetectable CNS viral counts which suggests that uncontrolled CNS replication of HIV is unlikely the cause of the persistence of HAND. Studies in developed countries have shown that patients on treatment do improve in their neurocognitive scores, although the symptoms sometimes do not fully remit. This suggests that either significant neuronal loss was present before the commencement of treatment or that the treatment is facilitating HAND development.[60] Since the BBB is often severely compromised in HIV^+ patients,[62] it is not inconceivable that the levels of ARVs in the CNS rise considerably. It has been shown that several proteins achieve plasma levels in the CNS when the BBB is

compromised.[63,64] Since the hypothesis that ARVs may be neurotoxic is relatively new, very little information is available on the topic. Consequently, we have not found possible mechanisms through which ARVs might be neurotoxic, although, it is widely accepted that ARVs are toxic to peripheral tissues.

HAND is clearly a highly multifactorial disease. HIV is the most common form of encephalitis and neuroinflammation. Since viral burden does not correlate well with disease severity, it is most likely that secondary products of infection are key disease agents. This alone introduces a vast array and possible combinations of neurotoxic proinflammatory cytokines and viral proteins. The most prominent of the latter group would be GP120 and HIV-Tat as both are neurotoxic and secreted into the CNS despite undetectable viral replication,[65,27,66,67] although, other viral proteins certainly have effects as well. As is evident in other well studied neurodegenerative diseases; there is scope for a large number of cellular functions to be dysregulated in HAND and contribute to the phenotype of neurodegeneration.

Neuroinflammation in HIV infection

Microglia can become activated in response to viral infection, viral proteins such as GP120 and HIV-Tat or factors released by other activated cells. It is known that HIV enters the brain early after infection and infected microglia have been detected 15 days after infection; suggesting that the brain is exposed to early inflammation. A prominent feature of microglial infection by HIV is the development of microglial nodules. HIV patients who developed HAND showed increased microglial density, decreased synaptic and dendritic density and neuronal loss between successive follow-ups. Cases with severe HAD suffered a 40% loss of dendritic area in frontal cortex and a 40–60% loss of dendritic spine density in comparison with non-demented controls.[68] Several studies, however, showed that neuronal loss was not correlative with viral burden and apoptotic neurons did not localize with infected microglia but were topographically associated with markers of microglial activation. Furthermore, the cytotoxic cytokine, TNFα and its receptor, TNFR, are elevated in microglia in HAD patients. TNFα affects neurons in many ways including cytoskeletal reorganisation, protein translation modulation and inhibition of neurite outgrowth.[69] HAD patient microglia also contain increased levels of IL-1B which is can induce the expression of TNFα and iNOS. NO regulates the release of many neurotransmitters such as

acetylcholine, catecholamines, excitatory and inhibitory amino acids, serotonin, histamine, and adenosine.[70] Therefore, the release of NO may further contribute to neuronal dysfunction and injury.

Inflammation in the brain is associated with impaired neural plasticity.[71] The term "neural plasticity" encompasses an array of mechanisms, from the birth, survival, migration, and integration of new neurons to neurite outgrowth, synaptogenesis, and the modulation of mature synapses. Impairment in neuronal plasticity is an early hallmark of neurodegeneration and is intimately linked to the symptoms of neurodegeneration. High degrees of neuronal plasticity are particularly important in brain areas involved in regulation of memory, learning, perception, self-awareness, consciousness, and higher brain functions as these require a life-long re-fitting of connectivity. By extension, these are the first functions affected by impaired neural plasticity.[72]

In general, inflammation brings about many cellular changes in order to respond to viral infection. The effects influence regulation of protein synthesis replication and cytoskeletal regulation. Attenuation of protein synthesis is the primary means through which cells counter viral replication before the initiation of apoptosis. Cytoskeletal reorganisation is essential for immune cells to travel toward site of inflammation. Similarly, epithelial cells need to increase membrane permeability which is primarily induced through cytoskeletal regulation.

Neurotoxic viral proteins

GP120

Glycoprotein 120 is the envelope protein of HIV and functions in the attachment and penetration of HIV into host cells. HIV-1 cell entry is initiated by the interaction between gp120 and CD4, and chemokine coreceptors C-X-C chemokine receptor 4 (CXCR4) and C-C chemokine receptor type 5 (CCR5). Although they typically referred to as immune receptors on CD4 cells, neurons also express both coreceptors; where they have been reported to be involved in neuronal migration [73] and proliferation.[74] Exogenous GP120 binding to these receptors induces apoptosis in neurons which can be blocked by inhibitors to the receptors. Interestingly, pre-treatment with brain-

derived neurotropic factor (BDNF) protects against GP120 induced apoptosis, mediated by BDNF-induced internalization of CXCR4.[75]

HIV Transactivator of transcription

HIV-Tat function

HIV-Tat is the most important regulator of HIV gene regulation and expression.[76] HIV-Tat has been shown to activate Long Terminal Repeat (LTR) directed transcription. It performs this function by binding a Transactivating Response Region (TAR) RNA stem loop immediately downstream of the initiation sequence. This is followed by the assembly of the positive transcription elongation factor b (p-TEFb) containing Cyclin Dependant kinase-9 (CDK9) and Cyclin T1.[77,76] The HIV-Tat/p-TEFb complex then phosphorylates the C-terminus of RNA polymerase II (**Figure 5**).[78] In phosphorylating RNA polymerase II, both its initiation and elongation functions are enhanced resulting in the rapid transcription and translation of its RNA genome. Although HIV-Tat forms complex interactions with host cellular machinery to achieve HIV replication, it does not interact only with them. Many of HIV-Tat deleterious effects are resultant of its ability to bind many host proteins, transcription factors and promoters.[79,76,80,81,77,78]

HIV-Tat Protein structure

HIV-Tat consists of two exons, the first of which composes of the functional domains while the functions of exon two are possibly situation specific and complimentary to the functions of exon 1.[82] Exon 1 codes for 72 amino acids while exon 2 has a highly variable length.[83] The crystal structure of HIV-1 Tat complexed to human p-TEFb has recently been determined.[84] Although these domains, illustrated in **Figure 6,** have been studied before, the crystal structure aided in understanding the roles of these domains regarding both structure and function. The determination of the structure emphasised the role of the cysteine-rich region in the structure of HIV-Tat as well as the recruitment and binding of P-TEFb, which is essential to HIV-Tat's transactivation function.[84]

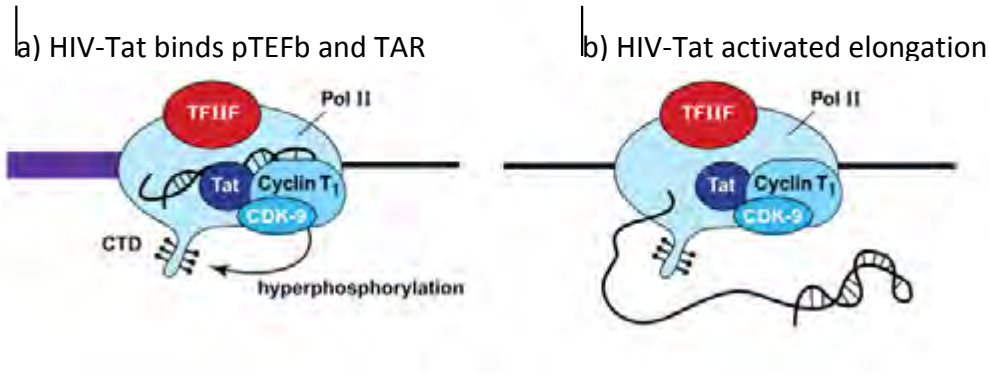

Figure 5: Showing the p-TEFb complex formation initiated by HIV-Tat. Once the p-TEFb complex is assembled, the C-terminus of RNA polymerase II is phosphorylated (b) which increases the rate of initiation and elongation. Image adapted from Karn, 2000.[85]

The seven cysteines in the cysteine-rich region help coordinate the formation of a novel zinc finger like structure with two Zn2+ molecules.[84] Previous work has shown that oxidising conditions destroy HIV-Tat function and result in aggregation.[86]

HIV-1 Tat protein is extremely variable in its peptide sequence which results from viral replication by the error prone Polymerase II.[87] HIV-Tat is reported to tolerate ~40 % mutations overall without losing biological activity.[84] This high tolerance for mutation supported by the high mutation rate of HIV replication results in an enormous diversity in HIV-Tat genomic sequences found *in vivo*. It also promotes the selection of viruses able to exploit any tissue it may infect. This mutation rate also affects the length of exon two which results in variant proteins with 72aa, 86aa and 101aa being the commonly referred to lengths, though HIV-Tat proteins larger than 101aa have also been reported.[82,86]

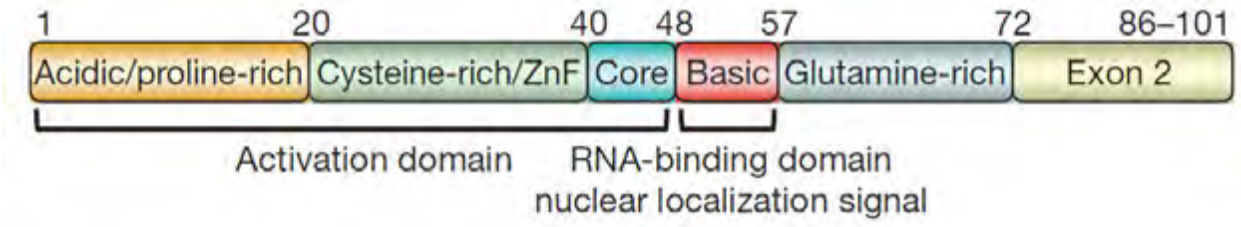

Figure 6: A linear representation of the functional domains of HIV-Tat protein. Exon 1 is thought to contain all the functional domains while exon two functions are unclear. Image adapted from Tahirov *et al.*[84]

While they retain their transactivation function, the different lengths of HIV-Tat protein have significantly different properties such as cellular localization, transactivation and membrane transduction.[88,89] Based on current knowledge of protein function, it is conceivable that different sequences of HIV-Tat have diverse *in*

vivo characteristics. Since HIV can infect a variety of cells in different tissues,[90,91,92,93,94] it is also conceivable that various protein sequences arise to exploit different tissues. It is possible that the diversity in protein sequences add to HIV-Tat's ability to bind a variety of host molecules [95,96] and therefore its toxicity.

HIV-Tat toxicity

While HIV-Tat acts as a pro-survival factor in many tissues,[97,98] it induces apoptosis in neurons.[99,98] Despite extensive research efforts and suggested mechanisms by which HIV-Tat causes apoptosis in neurons, there is no consensus. One commonality in the suggestions is that it acts through the activation of Glycogen Synthase Kinase-3β (GSK-3β) to induce apoptosis.[100,101,99] In addition to being directly neurotoxic, HIV-Tat has various other effects such as promoting the production of cytokines[65] and cytokine receptors,[102] proliferation and migration of different cell types and exerting angiogenic activity *in vitro* and *in vivo*.

The specific mechanisms of these phenotypes are unclear but may result from either HIV-Tat's protein binding characteristics through which it may directly alter protein function or transactivating activity by altering expression patterns. HIV-Tat protein has been shown to activate many host genes as well as bind to many host proteins. Each of these genes and proteins may have an effect on the cell state. Additionally, HIV-Tat is able to bind to many cytokine receptors, which may result in signal cascades having significant effects.[21,103]

A likely *in vivo* candidate pathway is the platelet activating factor (PAF) pathway.[101] In an HIV-infected brain, infected and activated microglia, macrophages and neurons all release TNF-α.[104] TNF-α in turn initiates the proinflamatory release of PAF from microglia and macrophages.[105,101] Through the activation of PAF receptors on neurons, AKT and PI3K are inactivated.[106] This results in active GSK-3β which is able to activate caspase mediated apoptosis pathways.[107,108] This proposed pathway requires PAF production by microglia and macrophages. It has, however, been shown that HIV-Tat is able to stimulate apoptosis *in vitro* without the involvement of PAF.[65] These studies have also shown an increase in GSK-3β activity when treated with HIV-Tat,[27] suggesting that there are other pathways activated by HIV-Tat that can lead to apoptosis. Two popular mechanisms proposed are the production of reactive oxygen species (ROS) and an increase in cellular calcium levels.

The generation of ROS and the increase in cellular calcium are interlinked and are resultant of one another. HIV-Tat induces the release of ROS in neurons and microglia, which in turn induces oxidative stress in neurons.[105,65] HIV-Tat has been shown to induce mitochondrial membrane hyperpolarisation (MMHP) and calcium influx.[109] MMPH possibly results in increase proton-motive activity and therefore, increased ATP production.[105] This process in turn results in increased oxidative stress and neuronal toxicity.[110] Increased Ca^{2+} has an additional effect on astrocytes' cytokine production. It has been shown that increased astrocyte intracellular Ca^{2+} can activate NF-κB.[110] This in turn increases the production of neurotoxic cytokines such as TNF-α by Astrocytes.[105] TNF-α increases ROS production in microglia,[111] thus, perpetuating the neurotoxic effects due to chronic exposure to HIV-Tat.

While HIV-Tat may have direct effects influencing neuronal survival, it also indirectly affects neurons through NF-κB. Astrocytes induce the activation NF-κB as a neuroprotector in response to stress in the CNS.[99,112] During HIV infection, HIV-Tat decreases the neuroprotective activity of NF-κB through the activation of GSK-3β via the PI3K/AKT pathway. GSK-3β phosphorylates serine 468 on NF-κB subunit rel-A which decreases its transactivation activity and limits its ability to initiate pro-survival expression within neurons. [99,113] This is surprising as NF-κB is a transcription factor controlling TNF- α expression. TNF- α increases the production of HIV virions in cells of monocytic lineages[114] as well as activate GSK-3β. There is certainly a very delicate equilibrium between GSK-3β and NF-κB activity resulting in the expression of various proinflammatory cytokines.

HIV and protein translation

Due to the activity of the antiviral inflammatory response in attenuating protein synthesis so as to combat viral replication, HIV's obvious ability to thrive under or circumvent the intended effects are being investigated. There are four mammalian kinases capable of phosphorylating and inactivation eukaryotic initiation factor 2α (EIF2α): general control nonderepressible 2 (GCN2), double-stranded RNA-activated protein kinase (PRK), PKR-like endoplasmic reticulum-resident kinase (PERK) and heme-regulated inhibitor kinase (HRI).[115] Of these, PKR is activated through inflammation and the presence of dsRNA, thus, it is the primary means through which cells attempt to attenuate viral replication in virally infected cells. PKR would,

therefore, be an obvious target of investigation in HIV related protein synthesis research. However, there seems to be contention over the role of PKR during HIV infection.

A common opinion is that PKR autophosphorylation and, thus, activation, is inhibited by binding to HIV-Tat, thus, it is unable to phosphorylate its target, EIF2α. However, it is evident that HIV-Tat requires phosphorylation by PKR for maximal activity. This, therefore, suggest that PKR is not inhibited, but that it may be modulated by competitive binding with HIV-Tat. This is further supported by the evidence that HIV replication is strongly inhibited in PKR knockout cells. It is, therefore, clear that HIV replication requires some level of PKR activity. Contradictory to this, however, is research suggesting that any PKR activity is inhibitory to HIV replication.[116] In their review, Clerzius *et al*, also claim that PKR is strongly inhibiting of HIV replication and that PKR is inactivated during late stage infection, due to high levels of TAR RNA which inhibit PKR and then allow for HIV replication.[117] This model assumes that HIV transcription can proceed while PKR is actively inhibiting protein synthesis until sufficient TAR RNA can be accumulated. This work, however, was performed *in vitro* and without directly measuring the resultant HIV replication rates. Furthermore, the authors propose that, due to dsRNA binding and PKR dimerization requirements, high concentrations of TAR would inhibit PKR activation.[118,119] Similar work, but including HIV-Tat, shows that the concentration of dsRNA required to activate PKR *in vitro* increases with HIV-Tat concentration present.[120] Furthermore, if HIV required inhibition of PKR, its replication would not be strongly inhibited in PKR knockout models. It is clear that there is significant confusion over the role of the most studied antiviral protein, PKR, and its regulation and requirement during HIV infection.

Mammalian protein translation is a sequential, multi-step process which begins with the formation of the preinitiation complex. The initiator Met-tRNA$_i^{Met}$ is bound by EIF2 to initiate the formation of an eIF2/GTP/Met-tRNAi complex which is delivered to the P site of the 40S ribosomal subunit to form the 43S preinitiation complex. The 43S preinitiation complex must then be recruited to the mRNA. EIF4E binds the m^{7}GpppX 5’ cap sequence and forms the EIF4F complex with EIF4G and EIF4A. EIF4EBP bind and inactivates EIF4E which inhibits protein synthesis by preventing cap recognition.EIF4A helicase activity is increased 10 fold when increasing its affinity for ATP when bound to EIF4B. Additionally, EIF4B promotes the formation of the 48S complex. EIF3 plays a role

in the formation of the preinitiation complex as well as the 43S complex. Following the recruitment of the 43S complex to the mRNA, the AUG codon needs to be located by 5' untranslated region (UTR) scanning. Beginning at the 5' cap, the 43S complex scans the UTR for the AUG and translation is initiated when a favourable pairing between Met-$tRNA_i^{Met}$ and AUG forms which completes the formation of the 48S complex. EIF1 and EIF1A also function to promote the formation of the 48S complex at the AUG codon.[121,122,123]

While PKR and its phosphorylation of EIF2α are likely the most studied relationships between HIV and host protein translation, HIV is known to affect other Eukaryotic initiation factors and ribosomal proteins. Since many proteins and protein complexes are required to initiate and maintain protein synthesis, dysregulation of any required protein would dysregulate the entire process. HIV protease has been shown to cleave EIF4G and, thereby, inhibit cap-dependant mRNA translation; upon which host mRNA translation is dependant.

HIV and the cytoskeleton

Cytoskeletal components play a major role in the execution of a diverse array of cellular functions including cell shape maintenance, cell polarity and movements as well as cytoplasmic trafficking of molecules determining cell fate and including apoptosis. As a result, the cytoskeleton plays a role in the entire life cycle of HIV.

Cytoskeletal dynamics are controlled by the Rho small GTPases composed of the Rho, Rac and cdc42 protein superfamilies. Since HIV modulates cytoskeleton dynamics, these cytoskeletal regulating proteins are a potential source of the HIV induced cytoskeletal dysregulation, through either direct or indirect activity. It has been suggested that actin microfilament redistribution and cytoskeletal contraction facilitate receptor clustering in the cell membrane.[124,125] HIV entry is dependent on the process or co-receptor clustering by Rho-dependant cytoskeletal reorganisation which is responsible for the process of receptor clustering. Statins, which inhibit Rho activity block HIV envelope fusion with the target cell and, thereby, reduces cell infection.

Cells have a physical barrier against viral and endocytic vesical entry below the cell membrane known as the cortical actin network. For viruses to infect the cell, they must overcome this barrier.[126] It is believed that HIV Nef protein binding and activating

Rho GTPases dysregulates the cytoskeleton and allows HIV to circumvent this barrier during infection. Furthermore, Nef induces actin reorganisation such as to facilitate the movement of the viral core [127] which makes use of dynein to move toward the nuclear pore complex.[128] A Nef binding domain was identified in SH3-domain containing proteins and is believed to be required for its Nef mediated inhibition.[129]

Viral assembly and budding also require specific cytoskeletal reorganisation. Although the mechanism is not clear, virion self-assembly occurring at the plasma membrane is thought to induce the formation of a cellular protrusion.[130] The formation of a cellular protrusion requires the formation of a focal adhesion and actin polymerisation behind the focal adhesion. This process would, presumably, be controlled by the cytoskeletal regulators, Rho, Rac and cdc42. The protrusion formed continues to grow until the virion is released from the membrane. The final release is mediated by proteins traditionally involved in the generation of endosomal compartments called multivesicular bodies.[131]

Glycogen Synthase Kinase in HAND

Glycogen Synthase Kinase (GSK) is expressed in many tissues with particularly high levels in the brain and phosphorylates over 40 target substrates.[132] It functions as a key component to several pathways including cell fate regulation. GSK homologs are found in all eukaryotes with high degrees of homology. Protein function is also conserved across all eukaryotes. Two isoforms with over 98% conservation in their kinase domains have been isolated: GSK-3α and GSK-3β. Despite the high levels of similarity, their functions are non-redundant *in vivo*. [133] It is believed that GSK-3α and GSK-3β are inhibited by S21/S9 phosphorylation respectively by Phosphoinositol-3-Kinase (PI3K).[134] Mutation studies substituting S21/S9 for alanine have since revealed that these are less important than previously thought. This was supported when Y216 was identified as being phosphorylated *in vivo* which was later shown to increase GSK kcat fivefold.[135] The mechanism responsible for GSK tyrosine phosphorylation is currently controversial.[136]

HIV-Tat was shown to increase GSK-3β activity but not protein levels *in vivo*. Although HIV-Tat does co-precipitate with GSK-3β, it does not directly dysregulate its activity which suggests that its dysregulation is resultant of dysregulation induced in upstream pathways.[27] While no data is available pertaining to *in vivo* GSK-3β activity in HAND

patients, data regarding AD patients has been reported. These studies have shown a correlation between GSK-3β activity and AD development.[137] In AD, GSK-3β is of particular importance as it directly phosphorylates tau protein and its inhibition inhibits Aβ induced neuronal apoptosis. Similarly, its inhibition by lithium inhibits HIV-Tat induced neuronal apoptosis.[27]

Lithium

Lithium has been prescribed for the treatment of Bipolar Disorder (BD) for nearly 60 years.[138] Despite having received approval for treatment of BD, the molecular targets and mode of action responsible for the behavioural alterations remains poorly understood.

Very little is known about lithium molecular targets other than its activation of AKT. Several phosphorylation events such as tau phosphorylation, have been shown to be inhibited by lithium. The effect on tau protein is predicted to be via the inhibition of GSK-3β as it is a tau kinase. A mechanism for the lithium-induced inactivation of GSK-3β is outlined in the review by Freland and Beaulieu.[139] In addition to direct GSK-3β inhibition, lithium also activates AKT by promoting the dissociation of its inhibitory complex composed of AKT:βArr2 and PP2A.[139] Lithium is also reported to favour the dissociation of the PP2A regulatory subunit which abolishes its activity.[140] The work by Chen *et al*, does not address lithium's effect on other PP2A regulatory subunits but it may be that they are similarly affected. In addition to its effects on GSK-3β, AKT and PP2A, lithium has also been shown to inhibit inositol monophosphatases, bisphosphate 3'-nucleotidase and cyclooxygenase. Whether or not these effects are linked is not known.

Since its initial use as a mood stabiliser, lithium has found therapeutic value in many neurodegenerative and neurotoxic settings. While lithium is certainly able to inhibit apoptosis induced by a variety of neuronal insults, it has not produced particularly promising results *in vivo*.[141,142,143]

Due to lithium's apparently safety as chronic treatment and its inhibition of HIV-Tat induced neuronal apoptosis *in vitro*, it has been proposed as a treatment for HAND. While it is widely accepted that lithium has several cellular targets beyond GSK-3β, an exhaustive list of targets has not been generated. Whether or not lithium's mood

stabilising ability is due to GSK-3β inhibition or not is still unclear. In spite of this, several small trials have been performed to test lithium's efficacy as a HAND therapeutic agent. While one prominent and often cited publication by Letendre *et al*, show neurocognitive improvement by HAND patients treated with lithium over 10 weeks, they do not rule out the possibility of practiced effects, spontaneous remission and test error due to the uncontrolled study design.[141] Others suggest that lithium is safe to use and propose further studies, but they do not report significant improvements in HAND patients.[142] However, an early study reported that lithium was not well tolerated by HIV positive men and that most patients did not complete the study due to toxicity.[143]

Lithium was essentially proposed as a treatment possibility due to the involvement of a single molecule, GSK-3β and its role in HIV-Tat induced neuronal apoptosis. Considering the results of previously performed clinical trials, it is clear that the involvement of GSK-3β and the subsequent use of lithium should be carefully evaluated. In addition, it is clear that the molecular aetiology responsible for HAND onset and progression is poorly understood. HAND mechanisms have been studied for many years, yet there are still a great many contradictions and even greater uncertainty in the molecular events facilitating HAND onset and progression as well as the possible cellular effects they induce or contribute to. While understanding the basic molecular dysregulation that occurs in and contributes to HAND is interesting and important, we also need to link these molecular events to cellular functions and resultant phenotypic alterations which ultimately lead to the symptoms. Given the probable complexity present in HAND onset and progression, it is becoming imperative that we study these multifactorial diseases in a manner that allows us to view the interactions of multiple cellular systems together. This would allow us to gauge the contributions and interplay between many systems in disease development and, thereby, generate new models which take the complexity into account and allow us to better identify drug targets which may be more specific for dysregulations contributing to disease. In addition, it is important to understand the effect of lithium on HAND beyond its effect on GSK-3β. Such a study might allow us to gauge the involvement GSK-3β in the dysregulation of cellular functions responsible for disease onset and progression.

Unfortunately, typical biochemistry approaches to identifying dysregulation induced by potential causative agents require a hypothesis. This limits the scope of the work to identifying disease contributors which were previously implicated. This approach is unable to identify novel outcomes nor is it able to consider any proteins and pathways not specifically targeted in the experiment. To understand a disease as complex as HAND is proving to be, viewing a snapshot of the dysregulated cell state in comparison to a healthy cell may allow us to provide a comprehensive overview of the dysregulation underlying disease as well as to better describe those molecular features in the context of disease onset and development. Such an analysis would require the analysis as large a proportion of the cells' machinery as possible and identify differences between a 'disease' and 'healthy' state.

Teasing apart the Differences

The determination of specific pathways integral to the development of HAND is hindered by the intricate interactions and, often, conflicting pathways implicated to date. An all-encompassing explanation of these interactions has not yet been presented. It is likely that a global "snap shot" of these pathways interacting with one another will identify specific pathways central to the development of HAND. Such a snapshot would compose all the cellular proteins presents in forms and levels relevant to the physiological stress being studied. Generating such data is possible through mass spectrometry (MS) based techniques. Using MS, researchers are theoretically able to identify all forms and levels of all proteins representing the exact state of the cell. Computational differential analysis between stressed and unstressed sample groups allows the identification of differentially expressed or activated proteins between the two states. Using gene ontology, it is possible to use this information to identify pathways activated during the particular stress.

Assaying complex biology using proteomics

To begin assessing the complexity present in a biological system, we need to be able to measure as many contributory components as possible, simultaneously. Genome sequencing has revealed that the human genome is composed of approximately 20, 000 genes, a subset of which is actively transcribed in individual cells. Current technology already allows us to determine the transcription rates of the entire human genome in single experiments. The proteome, however, is significantly more complex

and is incongruent with transcription levels. While the true values are not known, there are an excess of 1 million individual functional protein species that can theoretically be formed from the ~20 000 human genes.[144,145] This is due to alternate splicing, post-translational modifications and cleavage products. This is to say that singly, doubly or triply phosphorylated versions of the same primary amino acid sequence with the same fold are in fact different proteins as they potentially have different functions. Complimentary to genomics, proteomics enables the high throughput analyses of the protein complexity representing a snapshot of the cell state at any point in time.

Two-dimensional gel electrophoresis

Classically, proteomics has entailed the analysis of complex protein samples by two-dimensional gel electrophoretic (2D-PAGE) methods which relies on two dimensions of protein separation. The first is separation performed by loading proteins on isoelectric focusing (IEF) strip which contains regions of varying pH. As proteins migrate along the strip under the influence of an electric current, they reach their isoelectric pH at which they carry no charge, and stop migrating. The strip is then placed lengthwise atop an SDS-PAGE gels and resolved in the second dimension as per standard SDS-PAGE methods. The resultant protein 'spots' can then be quantitated by densitometry. Based on this quantitation, spots of interest are excised and the proteins identified by MS. A drawback of this technique is that it is time-consuming and poorly reproducible. The most modest shifts in mobility in either dimension can result in spot mismatching during quantitative analysis and identification.[146] Furthermore, it is unable to efficiently resolve the complexity of whole proteomes due to multiple proteins migrating together. This meant that the densitometric quantitation was of undefined protein mixtures rather than a single protein. This made differential analysis between samples troublesome and relatively few proteins could feasibly be identified in an experiment.[147,148,149] As a result, 2DE is an inefficient means with which to analyse proteome complexity.[150]

A major advancement in 2D-PAGE technology was the development of 2D-DIGE. One of the major advantages of 2D-DIGE over 2D-PAGE is that samples can be analysed together on the same gel; this mitigates the possibility of spots in one sample shifting

its relative position compared to the other.[151] In addition, spots can be quantitated and directly compared between samples.

The spot position variability between 2D-PAGE gels is eliminated by the addition of a differential labelling step followed by sample mixing prior to IEF focusing. Up to three samples can be compared by labelling proteins with different, spectrally resolvable cyanine dyes (CyDyes). Once labelled, equal protein quantities of each sample are mixed and loaded onto a suitable IPG strip for IEF focusing as in 2DE. After separation in the first and second dimensions is complete, the gels are analysed by CyDye specific scanners which are able to differentiate between fluorescence from each CyDye. This allows for direct relative quantitative comparison between samples for each spot.[152]

Both 2D-gel methodologies rely on MS to identify proteins within each spot. Spots of interest are excised from the gel and subjected to in-gel digestion which is a common process employed to extract proteins from PAGE gels for MS identification. Despite addressing the reproducibility of 2DE, 2D-DIGE was inherently low throughput. The requirement for every spot of interest to be excised from the gel and processed for MS identification could not be avoided and was labour intensive. In addition, there was still a high possibility that each spot of interest contained many proteins and that neither of them are significantly differentially regulated. Over time, advances in MS and protein/peptide ionisation techniques, MS-based proteomics emerged as an answer to the limitations of gel based proteomics.

A new 'proteomics'

As proteomics was being ported from gel-based methods to MS-based methods, another important reform occurred. Gel based methods typically analysed intact proteins whereas MS methods typically analysed the peptides resultant from chemical or enzymatic cleavage of those intact proteins. Intact protein analysis became known as top-down proteomics, which contrasted bottom-up proteomics, which refers to the analysis of protein derived peptides in order to extrapolate the data generated to identify and quantify proteins in a given sample. Both techniques rely on direct intensity measurements and protein/peptide sequencing for quantification and identification, respectively. Modern MS based bottom-up proteomics proved capable of significantly higher throughput and reproducibility than top-down methods and quickly dominated proteome analysis workflows. Despite its advantages, top-down MS

is typically limited to the analysis of single proteins or simple mixtures. One caveat of bottom-up vs top-down approaches is that bottom-up analysis, unlike top-down experiments, very rarely yields 100% protein sequence coverage of individual proteins. Coupled to inherent variability in peptide ionisation efficiencies, this creates a problem for quantification and identification. Data analysis for bottom-up proteomics will be discussed in more detail later.

Mass spectrometry

Modern advancements in proteomics, specifically the capabilities of MS, have allowed for the side-by-side quantitative comparison of a large proportion of proteins within a biological sample. MS has fast become an invaluable tool in the proteomic analysis of complex protein samples ordinarily used for biomarker discovery. Shotgun proteomics is a method of identifying proteins in complex mixtures using a combination of high performance liquid chromatography combined with MS.[153] By definition a mass spectrometer consist of an ion source, mass analyser and a detector which records data allowing the mass and abundance of each ion species present to be determined. MS has a lower detection limit than any other high-throughput discovery technique.[154,150] MS provides an unrivalled platform from which to perform an in depth proteomic analysis of a complex biological sample.

There are several mass analysers used in an array of mass spectrometers, but the most popular are time-of-flight (TOF), Fourier-transform ion cyclotron resonance (FTICR), linear ion trap (LIT) and Orbitrap mass analyser. Each operates by different physical principles to achieve the same basic function; to separate ions according to their mass/charge ratio. The TOF instrument is essentially a long tube into which ions uniformly accelerating toward a detector. Due to the uniform acceleration, larger ions travel slower than smaller ions with the same charge and are, therefore, separated in time. A modification of this is TOF/TOF which increases resolution by increasing the flight path with a second TOF tube.

FTICR-mass analysers differ from TOF instruments in that the ions are not separated in time; instead, ions are maintained within a strong radial magnetic field and an axial electric field applied by trapping plates (**Figure 7**). Ions are briefly excited upon entering the magnetic field; when the excitation is removed, the ions are rotating in phase at their cyclotron frequency. The ions are, thereby, maintained in an orbital

motion within the magnetic and retained axially by the electric field. As all ions entering are excited together, ions with higher m/z values adopt different rotation patterns to those with lower m/z.[155,156]

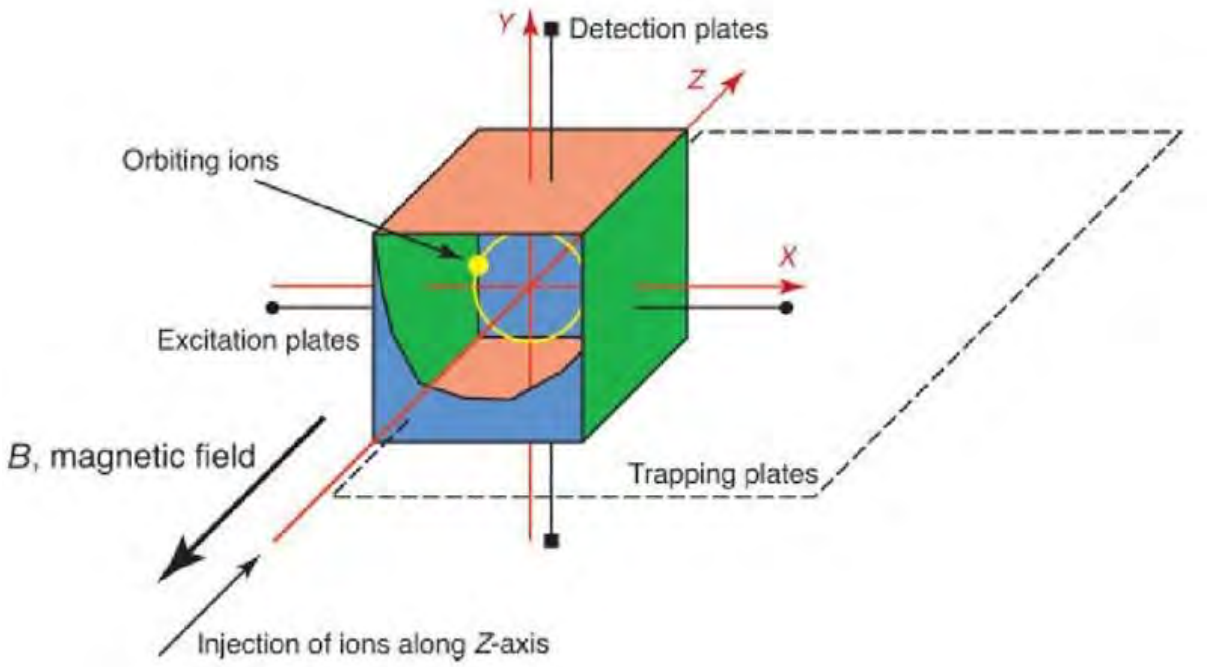

Figure 7: Schematic FTICR-cell. Ions are injected coaxial to the magnetic field. Excitation and detection plates can be seen with the trapping plates at each end of the cell. (Image adapted from: http://what-when-how.com/proteomics/ft-icr-proteomics/)

The linear quadrupole ion trap consists of four rods with hyperbolic inner surfaces arranged to create a hollow central channel. In addition, each rod consists of three regions; front, centre and back (**Figure 8**). This design allows ions to be contained and controlled radially in the central channel by applying a radio frequency (RF) voltage across the four rods and axially by applying DC potentials in the front and back of each rod. In order to facilitate mass selection and MS/MS, additional AC voltage is applied across x-rods.[157]

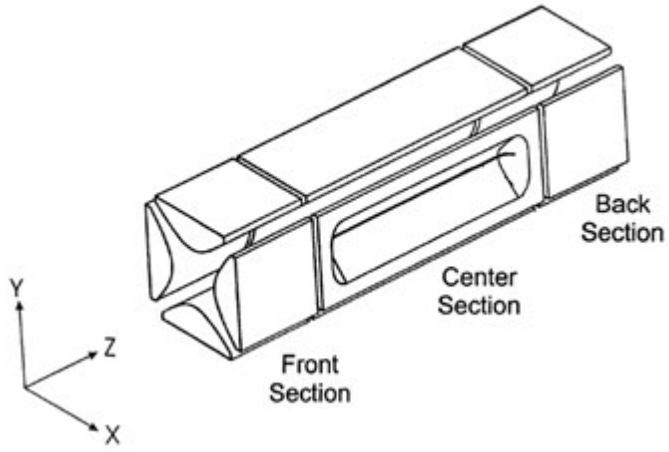

Figure 8: A schematic diagram of the linear quadrupole ion trap.[157]

The orbitrap mass analyser is relatively comparable to the FTICR in principle. Orbitraps also maintain ions in orbital motion, but this motion is maintained by an electrostatic field generated between an outer barrel and an inner spindle-like electrode. Unlike FTICR, ions don't require excitation to assume a harmonic oscillation pattern in the electric field after being squeezed into the orbitrap perpendicular to the inner spindle.

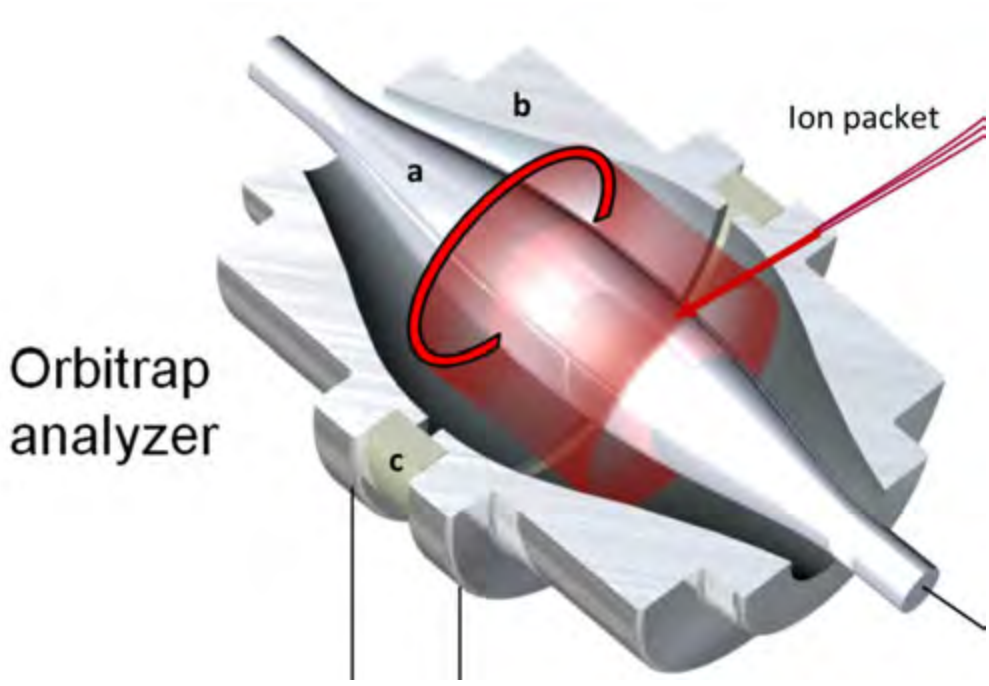

Figure 9: A cutoff representation of the Orbitrap analyser. The inner (a) and outer (b) electrodes can be seen with the amplifying detector (c) situated in the outer electrode. (Image adapted from: https://en.wikipedia.org/wiki/Orbitrap)

The oscillating ions induce an image current which is detected via a differential amplifier positioned between the two halves of the outer electrode (**Figure 9**). Each

ion rotation induces an image current which is recorded into a frequency spectrum and, using fast fourier transformation, is converted into a mass spectrum. [158,159,160,] FTICR detectors work on the same principle where ions create an image current on the amplifying detector plate. In contrast to the differential amplifying, non-destructive detectors present in the FTICR and orbitrap mass analysers, destructive electron multipliers, are another common detector used in MS. In electron multipliers, the ions impacting the first dynode generate secondary electrons which are accelerated to a secondary dynode where each electron generates several more electrons. As this process is repeated, the original sample is multiplied, thereby, increasing sensitivity.[161]

Mass spectrometry-based proteomics

Since its entry into the proteomics arena, MS has become an indispensable technology in the analysis of complex protein samples. A mass spectrometer is typically composed of three parts, an ion source to produce the gas phase ions, a mass analyser to separate the ionised analytes according to their mass-to-charge ratio (m/z), and a detector that records the number of ions at each m/z value. Two main achievements have facilitated MS based proteomics: the availability of genome sequence databases to provide the means by which to identify and peptides and proteins; and the development of soft protein ionisation methods for which the 2002 Nobel Prize in Chemistry was awarded. Since then, two primary means of ionisation were developed and are widely used today; matrix assisted laser desorption ionisation (MALDI) and electrospray ionisation (ESI). In MALDI-MS, the samples to be analysed are co-spotted onto a target plate with a suitable matrix. While there are an extensive variety of MALDI matrices, each with specific uses, they serve a common purpose; to ionise and facilitate vaporization of the analyte. Once dried on the target plate, matrix-analyte mixtures are ionised softly by laser radiation which is absorbed by the matrix leading to desorption and ionisation of the analytes. Ions are then accelerated by an electrostatic field generated around the target (**Figure 10**).[162] MALDI has historically been used in conjunction with 2DE to identify excised spots by peptide mass fingerprinting.[163,164] However, a powerful use has arisen from MALDI's ability maintain the spatial distribution of the sample. Thus, MALDI is increasingly being used for imagining experiments where, for example, a tissue section is laid onto a target plate and overlaid with a suitable matrix. Protein spatial distribution across the section can then be determined by selectively ionising specific areas of the section.[165]

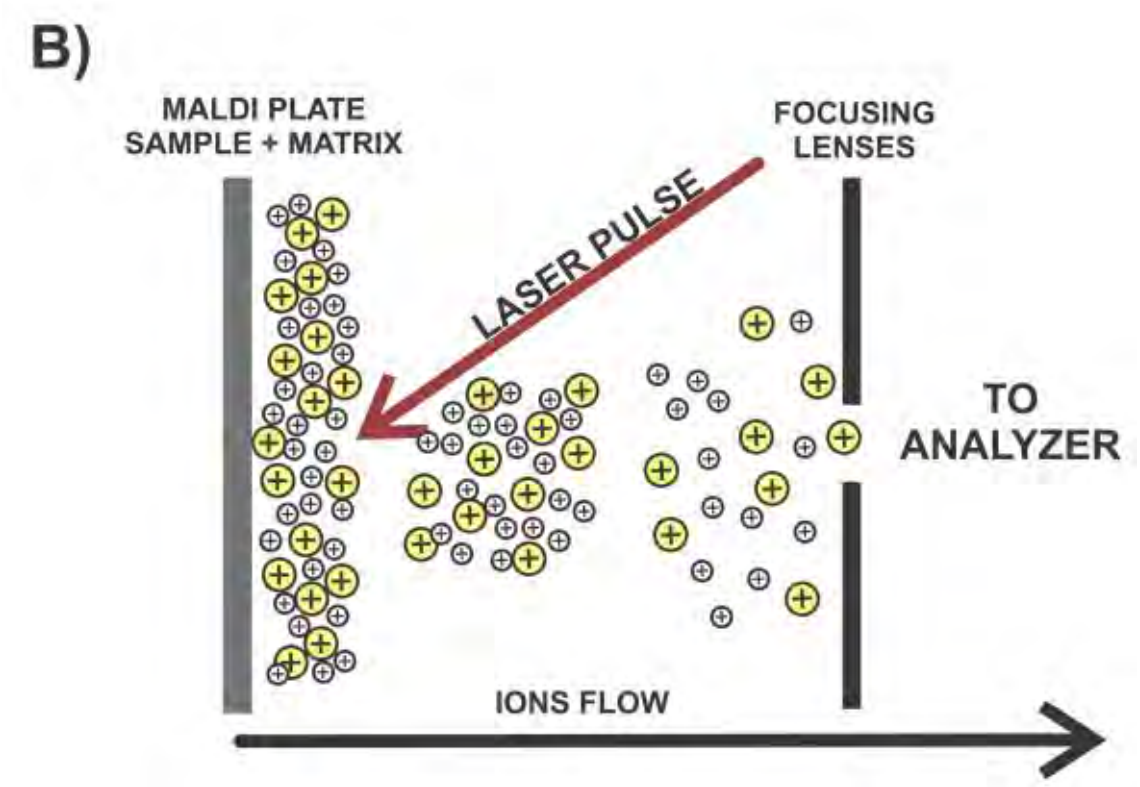

Figure 10: A simplified representation of MALDI ionisation. Once the mixture of analyte and matrix have dried on the MALDI target, laser pulses are used to excite the matrix which impart a charge onto the analyte. The charged analytes are then accelerated into the mass spectrometer by an electrostatic field generated around the target plate. Image adapted from Demartini.[166]

ESI is characterised by the ionisation of a sample in liquid phase and its subsequent transfer into the gas phase. Due to the pressurised flow through the LC emitter and acidified mobile phase, tiny positively charged, analyte containing droplets are propelled toward the MS by a charge imparted onto the emitter. The positively charged droplet shrinks due to solvent evaporation once exposed to the atmosphere. As the droplet shrinks, it becomes increasingly unstable due to increasing density of positive charges on the droplet. These droplets break up due to coulombic explosions to form smaller droplets which continue to evaporate and break up into exponentially smaller droplets. This process continues until the charged analyte is released from the droplet and available for analysis in the gas phase (Figure 11). However, the process by which the charged analyte is released is poorly understood and discussed in detail by Konermann *et al.*[167]

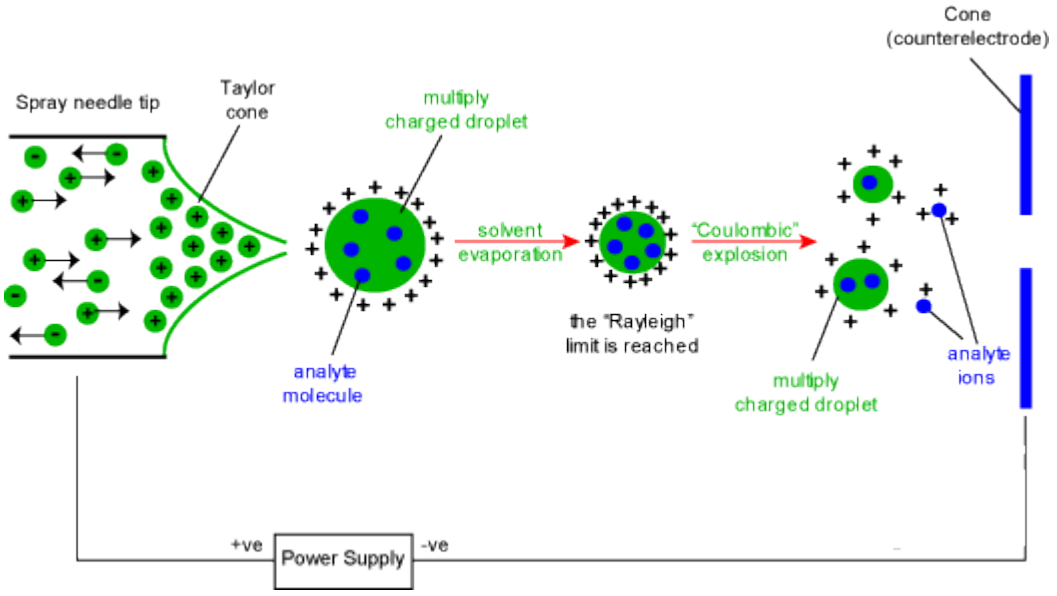

Figure 11: In source dynamics of analyte entry into the gas phase: As charged droplets are released from the LC emitter, they begin to reduce in size due to solvent evaporation. As the droplet shrinks, the density of charges increases which results in coulombic explosions. This process occurs until charged analytes are released and become available for MS analysis. The image is adapted from the university of Bristol (http://www.bris.ac.uk/).

As ESI requires the analyte to be in a liquid phase, it is particularly amenable to coupling with liquid chromatography (LC) systems; however, MALDI MS can also be coupled to offline LC systems. The practical limitation of MS with regard to sample complexity is that there is a dynamic range of two-three orders of magnitude detectable per spectrum. This is insufficient to analyse any complex, raw biological sample in its entirety. The dynamic range of proteins in serum spans twelve orders of magnitude [168] with cell culture and tissue samples spanning 5 – 6 orders or magnitude. Together with the dynamic range, typical mammalian cell lysates contain 500 000+ protein species after alternative splicing and post-translational modifications (PTM). Typically, proteomic analysis of these complex samples is performed at the peptide level which compounds the challenge. As a result, protein/peptide separation methodologies are essential for the analysis of most complex protein mixtures.

Peptide fragmentation and, subsequently, using peptide fragmentation patterns to generate a peptide primary sequence through which it can be identified is not a trivial matter. Two common MS/MS fragmentation methods are used in proteomics; collision induced dissociation (CID) and electron transfer dissociation (ETD). As the name suggests, ETD relies on the transfer of electrons from radical anions such as anthracene or azobenzene to the peptide. ETD typically results in peptide breakage on the N-terminal side of the primary carbon which produces c and z ions (**Figure 12**). A

powerful advantage of ETD is that it has a greater capability of maintaining labile PTM's such as phosphorylation and is, therefore, favoured for PTM analysis.[169] Under ideal CID conditions, charged peptides break along the backbone at amide bonds and produce b and y series ions as illustrated in **Figure 12**. The fragmentation pattern generated from a peptide depends on many factors such as the peptide size, charge state, collision energy, collision gas and collision gas pressure.[170] The resultant fragments masses and intensities are measured by the detector and, together with MS1 mass and intensity data, account for the majority of the data in MS raw files.

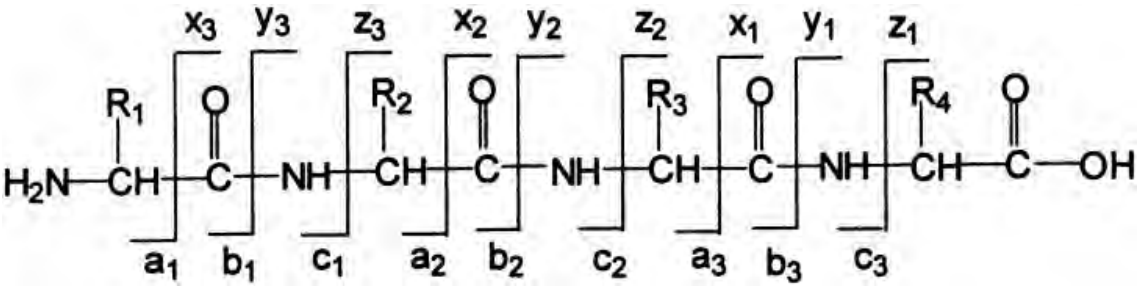

Figure 12: Nomenclature of peptide fragment ions. Image adapted from Harrison.[170]

Limitations of MS

Although researchers are able to detect low fmol quantities of protein with high confidence using shotgun MS technology and methodology, MS has several limitations. One of the greatest limitations facing current methodologies is the limited dynamic range of detection per spectrum.[171] This means that abundant analytes will overshadow the less abundant analytes. This poses a significant problem as most proteomes are dominated by a small subset of proteins [171] which effectively renders the remainder of the proteome "invisible" to MS. Two methods for overcoming this are depletion and fractionation. The depletion route aims to remove the most abundant analytes before analysis, thereby enriching the less abundant analytes for MS analysis.[172] The use of depletion in shotgun proteomics is currently limited by insufficient selectivity and specificity.[173] This means that many non-targeted molecules are removed from the sample either by non-specificity or by being bound to target molecules. Fractionation on the other hand is based on producing many less complex fractions of the original sample, ideally with a lower dynamic range per sample.[174] After being analysed individually, all fractions can be compiled to represent the original complex sample. However, fractionation on its own may still be plagued by the "dynamic range" problem as the abundant molecules will still be present in select

fractions. Fractionation can be performed both online and offline. Offline fractionation strategies produce multiple individual samples, which need to be combined bioinformatically to represent the whole, original sample. Online fractionation may be coupled to offline fractionation and will be discussed later.

Current bottom-up shotgun proteomics requires that protein samples are digested, fractionated and then analysed by MS. This is the preferred route as sequencing intact high molecular weight proteins using high-throughput shotgun proteomics methodologies is extremely challenging.[175] bottom-up methodologies, however, pose an inherent bioinformatic challenge where peptides from a single protein are spread across any fractions due to fractionation. This complicates analysis as splice variants or activity states of proteins cannot be elucidated unless specific spliced or post translationally modified peptides are identified.[176]

Decreasing biological complexity for MS analysis

Protein separation ahead of MS has is a critical and indispensable component of high-throughput MS-based proteomics. To address this, various gel and liquid based methods have been developed to fractionate complex protein samples into several less complex samples which, together, represent the full complexity of the original sample in more manageable portions.

In light of this challenge, LC techniques have earned an unrivalled position in MS based proteomics. Typically, reverse phase (RP) chromatography is used for peptide chromatography with octadecyl bonded silica (c18) used as the solid phase packing material. RP separation is based on the partitioning of peptides between the non-polar solid phase and the polar liquid phase. RP chromatography is not only favoured as a peptide separation method in proteomics due to its high resolving power, but also for its compatibility. The mobile phase typically contains water and a water soluble organic solvent such as acetonitrile. This solution is typically acidified with low concentrations of formic, acetic or triflouroacetic acid to ensure all peptides are positively charged. Despite the high resolving power of RP-HPLC, the complexity of biological samples has demanded even more. It has been shown that ultra-high pressure HPLC (uHPLC) outperforms HPLC by increasing separation speed and, thereby, decreasing analysis time. A further benefit of uHPLC is reduced sample requirement due to lower column volumes and flow rates. The increased pressure tolerance of

uHPLC's has allowed for longer columns and has typically resulted in increased resolution and identification rates. Column lengths cannot be increased indefinitely, however. Several phenomena affecting chromatographic resolution occur inside a column. The most important of these is the effect of mobile phase diffusion into the chromatographic particles. As chromatographic particles are typically hollow, the mobile phase can enter the particle as well as travel passed it unrestricted. Mobile phase entering the particle is slowed and takes a longer time to exit the end of the column. If the column length is increased, the time delay is increased proportionally to the column length and this decreases resolution as peak width increases. This inherent limitation of chromatographic separation and means to mitigate it will be discussed in greater detail later.

To achieve additional fractionation ahead of LC-MS analysis, samples can be fractionated at the protein level before digestion. This simplifies the samples even further by decreasing the number of proteins from which peptides can be generated in each fraction. Jafari *et al*, performed a comparison between various whole protein fractionation techniques and found 1D-PAGE gels to yield the highest protein identifications.[177] Although 1D SDS-PAGE gels have relatively low resolution, they are capable of efficiently gross separation of a protein sample and have successfully been used as a fractionation technique upstream of LC-MS analysis. The major limitation of this, however, is that it decreases the reproducibility of the workflow. While LC-MS is capable of very high reproducibility, PAGE coupled with in-gel digestion is significantly less reproducible. Reports of protein and peptide loss during PAGE and in-gel digestion vary between 15% and 50%.[178] This inconsistency makes limits the quantitative capacity of such experiments. However, labelling and combining samples before PAGE separation mitigates the possibility of differential sample loss between control and experimental samples.

Chromatographic particle/bead size

Typically, increasing the length of the analytical column on nLC systems results in increased sample separation and a resultant increased identification rate. The column lengths are, however, limited by the resultant system pressure increases. Theoretically, resolving power increases with an increased chromatographic surface area until a critical limit is reached whereby peaks widths begin to broaden, thus, beginning to

increase the chromatographic area occupied by highly abundant peaks masking low abundant peaks. In part, this phenomenon is caused by the diffusion required for peptides bound inside beads to transfer from the solid phase to the mobile phase. Larger beads also create larger spaces between beads which creates turbulence in the column and decreases the chromatographic surface area to column volume ratio. Together, these serve to increase eddy diffusion inside the column and, thereby, decrease performance (**Figure 13**). To counter this effect, solid core beads with increasingly small diameters were developed. This decreases the effect of diffusion in the analytical column and increases the theoretical plate count. Low diameter, solid core beads have a relatively thin surface coating into which peptides can diffuse and be bound to. Coupled to optimal pore sizes of ~100Å, peptides are transferred from solid phase to mobile phase much faster which results in smaller peak widths and higher theoretical plate counts.[179,180]

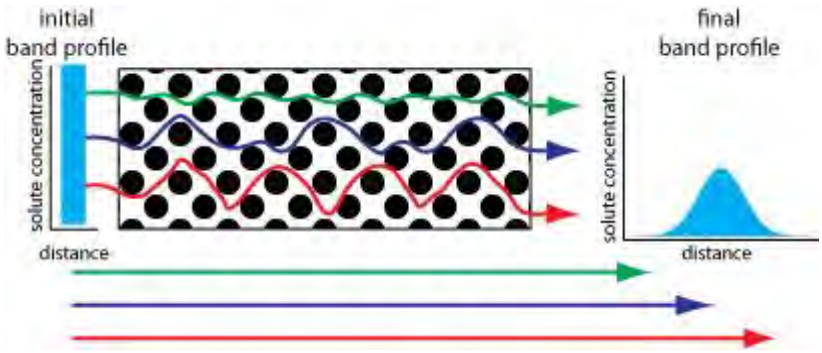

Figure 13: Depiction of eddy flow and its effects on peak width. Adapted from http://community.asdlib.org/imageandvideoexchangeforum/ (access date: 27.09.2015)

However, using smaller beads results in dramatic increases in the system pressure, which prohibits the use of small beads in long columns. The advent of nUHPLC systems which tolerate pressures up to and exceeding 800 bar has removed this limitation. Thus far, these systems have out-performed lower pressure nHPLC systems in literature. The increased performance is not a function of increased pressure but of the capabilities the increased pressure bestows: decreased bead size and increased column length.

Bottom-up proteomics data processing

Protein identification

The aim of proteomics is to generate meaningful data about a biological system with the aim of increasing our understanding of that system. To acquire this information,

however, the raw MS data needs to be transformed into a validated list of quantified proteins which can then be used in further analyses. Possibility-based database searches remain the most efficient means through which to identify MS/MS spectra. This, however, depends on the presence of a suitable database containing the proteins being analysed. Thus, large scale, high-throughput proteomics absolutely depends on the availability of fully sequenced genomes. From these, theoretical proteins and proteolytic peptides can be generated *in silico*. These *in silico* peptides are then used to create *in silico* fragmentation spectra based on the fragmentation patterns discussed earlier. Experimental MS/MS spectra are compared and scored based on their similarity to the theoretical spectrum. Several free and commercial software packages available make use of algorithms employing this approach, such as Andromeda and Mascot.[181,182] SEQUEST makes use of the same principle of matching experimental spectra to theoretical spectra, but it first reduces the size of the database against which it searches each spectrum. Based on the precursor mass, SEQUEST creates a list of possible peptide matches with similar masses. Theoretical spectra are generated from this reduced list and compared to the experimentally derived spectra to produce a list of 500 best fit sequences. These 500 possible matches are subjected to a correlation-based analysis to generate a final probability score where the best score is selected.[183] Andromeda is based on the mascot algorithm and assesses two basic criteria; precursor mass and the number and masses of MS/MS fragment masses. Based on the overlap between the experimental and theoretical spectra, the algorithms score the spectra with a possibility score indicating the likelihood of a positive match which also considers the likelihood of the match occurring by random chance. Furthermore, higher scores are assigned if the matched peaks are higher intensity.[182] Probability-based searches, however, are only applicable when the peptide is present in a database. However, if peptides are not in an available database, *de novo* sequencing of MS/MS spectra is possible, as it does not require prior knowledge of the proteins being identified. *De novo* sequencing makes use of the same MS/MS spectra generated and used in probability-based searches, but instead of matching to theoretical spectra, peaks are assigned amino acids based on the mass differences between peaks. However, the sheer quantity of data and possible MS/MS spectra which may arise creates significant challenges for *de novo* sequencing entire shotgun experiments. A major challenge in this approach is the ability of algorithms to

correctly distinguish peaks from noise. Added to this, missing peaks and PTM's merely compound the problem.[184,185,186] Due to the high possibility of false positives, stringent criteria are required to obtain sufficiently high confidence peptide and protein identifications. Criteria stringency aiming to decrease false positives needs to be balanced by the likelihood of excluding false negatives. A minimum list of protein identifications are then inferred from the peptides identified. Since many proteins share non-proteotypic peptides, if proteotypic peptides are not identified in the experiment, it is impossible to assign a single protein identification with certainty. As a result, protein groups which contain all proteins which may have contributed the peptides identified are reported.

Protein quantitation

Rather than just produce a list of protein identified in a sample, proteomics also aims to quantify those proteins in the sample. An unfortunate drawback of shotgun proteomics is that it only allows for confidence in proteins identified, but cannot assign confidence in the absence of a protein which is not detected. Due to this limitation, shotgun proteomic analyses typically entail comparing proteins identified and quantified in all conditions being tested. To facilitate the comparison of two or more physiological states in a biological setting, the proteins present must be accurately quantitated. The quantitation method may either be absolute or relative. Absolute quantitation allows for the exact molar amount of each peptide to be determined. Far more commonly, however, peptides and proteins are quantified such as to facilitate relative quantitation. Absolute quantitation requires that known amounts of MS discernible isotopes of the target peptide be quantitated simultaneously with the target peptide. Two common methods for absolute quantification are AQUA^{tm} and PSAQ.[187,188]

Several labelling techniques have been developed to increase the accuracy of relative quantitation. Of those, labelling techniques such as Stable isotope labelling by amino acids in cell culture (SILAC), Isobaric tags for relative and absolute quantitation (iTRAQ) and Tandem Mass Tags (TMT) are the most popular. iTRAQ and TMT are similar in that they are both isobaric mass tags with which peptides can be labelled after digestion. In both techniques, the tags make use of *N*-hydroxy-succinimide (NHS) chemistry which permits near complete tagging of peptide amine groups. As the tags are isobaric, the

same peptide labelled with the different tag masses would have the same precursor mass. This allows peptides from different samples to be selected together during the MS1 precursor scan and during MS/MS. Peptides from different samples are discernible only upon peptide fragmentation in MS/MS, during which the relative ratios of each samples' contribution is identified. iTRAQ and TMT allow for the analysis of up to eight and ten samples simultaneously, respectively.[189,190] The rationale behind using labelling techniques is that samples being compared can be mixed together and analysed together. This serves to eliminate any sample specific variability introduced after labelling and subsequent sample mixing. Following this, the sooner samples can be mixed together, the further one can reduce the technical variability introduced by sample processing. To date, SILAC is the gold standard for labelling techniques as samples can, theoretically, be combined immediately after harvesting cells from culture. These benefits can be realized in the detection of smaller biological differences present between two cell states. These differences might otherwise be missed by techniques with greater inherent variability. SILAC labelling makes use of isotopically labelled amino acids in which certain nuclei are replaced with their heavy isotopes (deuterium, 13C and 15N). To SILAC label cells in culture, cells are grown in chemically identical media, except that each contains heavy or light isotopes of specific amino acids. Typically, heavy lysine and arginine are used as they ensure that efficient tryptic digestion results in a single heavy amino acid per peptide, although, many others are available. Cells typically require ~5 passages to achieve near complete label incorporation, although, incorporation efficiency should be tested before using the cells experimentally. Although the technique is typically restricted to cell culture, larger organisms can be labelled and are available; albeit at very high cost.[191,192] While the technique is very powerful when applicable, it can be difficult or impossible to label certain samples due to the size of the animal or metabolic inactivity of the target cells and tissues.[193] In order to address this limitation, CDIT and, more recently, super-SILAC have been developed.[194,195] Both techniques employ metabolically labelled proteins from a related cell culture mixed with the unlabelled tissue as an internal standard. As opposed to CDIT, super-SILAC makes use of multiple cell lines in the SILAC labelled internal standard which results in greater coverage of the proteome being analysed.

Due to methodological and instrumentation developments in proteomics, many of the benefits endowed by labelling methodologies have been offset relative to label-free

approaches. As the name suggests, label-free quantification does not involve any labelling of peptides/proteins before analysis and each sample is analysed individually. Label-free approaches are, therefore, not necessarily quantified as a ratio between experimental conditions. Two approaches exist for label-free quantification; spectral counting and ion intensity. Spectral counting functions on the assumption that the number of peptide spectrum matches, total number of peptides identified and the sequence coverage correlates with protein abundance. Since this method relies on simple counting of spectra rather than measuring physical data, it has remained controversial.[196] The second method calculates the cumulative area under the curve for the monoisotopic mass for each precursor ion. The area under the peak has been shown to correlate linearly with peptide abundance which makes the method highly amenable to quantitative proteomics.[197] Despite relatively higher systematic error being introduced to label-free approaches, there are several advantages as well.[198] Since samples are analysed individually, label-free samples are significantly simpler which equates to a greater analysis depth in single MS runs. Increased analysis depth is also facilitated by a higher dynamic range of quantification. Additionally, there is no limit of the number of biological comparisons that can be made in an experiment. While always important, a stable LC-MS system is integral to label-free experiments. Changes to the system during the course of an experiment could render the resultant data incomparable.

Understanding the biology

Currently, the challenge to understanding biological systems is no longer our ability to generate data representative of the system. The challenge lies in our ability to understand those massive datasets and draw biologically meaningful information from them. Proteomics is inherently a systems science that studies not only proteins and their expression levels but the interplay between proteins, complexes and the pathways they function in. However, after the database search, we have a list of proteins rather than information about the protein and pathway interactions. These lists then contain extensive potential information which may not be immediately apparent as a mere protein list with quantitation. Pathway and gene ontology analyses are typically used to view the data within the biological context. Before the widespread usage of MS and genome-wide gene expression methodologies to assay biological systems, significantly fewer proteins were identified in experiments. In those

instances, it was feasible to search each differentially regulated protein individually and determine a biologically relevant explanation for its dysregulation as well as postulate about its effect. In some cases, a few proteins/genes signifying the most differentially regulated elements of the data are individually analysed. This, however, has a major limitation in that it can miss important regulatory information and intermediates in signalling. Furthermore, modest changes in multiple proteins in a pathway can have a large effect on the overall activity of the pathway. Thus, making use of as much of the dataset as possible infers obvious advantages. Analysing single proteins/genes individually is, however, impossible when thousands of proteins are identified and quantified and hundreds are significantly dysregulated. Furthermore, most pathways function with incredible complexity and significant cross talk with other pathways that it is simply not feasible to attempt to understand the interactions one protein at a time. In addition, this approach can be very subjective.

One means through which to analyse large datasets for biological significance is through gene ontology (GO) analysis. GO analysis attempts to identify biologically meaningful functions taking place in the biological system. It does this by assigning one or more functional term to each queried gene or protein, then identifies statistically significant enrichment of terms within the dataset against a background dataset. This approach, however, considers each query as a separate event and, thereby, decouples pathways and networks. This means that individual proteins are not validated by the presence of interacting partners. In addition, many proteins have multiple functions and, analysing each individually does not necessarily identify the specific functional role in which that protein is being dysregulated. Perhaps the biggest drawback of GO annotation and enrichment analyses is that they do not make use of quantitative data.

Pathway and network analysis helps simplify unwieldly amounts of data by grouping proteins into smaller functional compartments. These compartments may be defined by interaction in a function or canonical pathway. Many pathways may work together in complex networks to bring about certain biological functions. Data can, therefore, be analysed in increasing complexity in order to understand the activity of pathways and their relationship to the biological system. An advantage of pathway and network analysis over GO analysis is that pathway and network analysis allows for direct visualisation of proteins with their interaction partners and regulatory elements.

Furthermore, many knowledge bases, such as Ingenuity Pathway Analysis (IPA) contains information upon which biological implications of protein, pathway and network information can be made with respect to a functional outcome.

An inherent problem with all automated analyses, however, is that they rely on incomplete knowledge.[199] Firstly, our knowledge of protein/gene functions and their *in vivo* interactions, regulation, functions and localization is incomplete. Secondly, as the knowledge bases are manually curated, the curators may miss some already published information. More commonly, however, there is a lag in incorporating newly published data into the knowledge bases. Thus, it will always be the responsibility of the user to evaluate the data, and understand the basis of predictions made by automated software. The user will also be required to understand and address the functional implication of all possible interactions within pathways as well as across different pathways. It is a common assumption that pathways function linearly and each pathway produces and 'output' which then goes on to interact with other pathways. In reality, individual proteins within canonical pathways are constantly being regulated by external and internal proteins. Therefore, despite the use of extensive and very well constructed and curated knowledge bases, there will always be a need to manually assess the data output of pathway analyses. Furthermore, many proteins are ubiquitously expressed in many different cell types. They may not have identical functions due to PTM's and cellular localization. Where they do have the same function, their functional outcomes may vary. A simple example can be made with the cytoskeleton. Neurons and macrophages have highly overlapping cytoskeletal regulatory mechanisms and proteins. However, in macrophages, cytoskeletal projections are the basis for pseudopodia. In neurons, however, they are the initial structure in a developing neurite, axon, dendrite and, ultimately, a neuronal synapse. Thus, downstream bioinformatic analysis of the primary quantitative data is a critical part of the overall results obtained from proteomic experiments today.

Despite the overwhelming research efforts into understanding HIV-Tat mediated neuronal dysregulation, the mechanisms involved remain poorly understood. This is, in part, due to the nature of classical mechanistic experiments, which require a hypothesis to be tested. The limitation of this approach is that the proteins or pathways of interest must be specifically targeted while concurrently ignoring the vast

majority of processes taking place. This limitation is compounded by the apparent complexity of the mechanisms involved in HIV-tat treated neurons. High throughput, hypothesis generating MS analyses coupled to detailed pathway analysis may be capable of providing a global view of the mechanisms underlying HIV-Tat induced neuronal dysregulation. Furthermore, by using these techniques, the potential therapeutic value of drugs could be assessed by characterising the effects they have on the dysregulated pathways and their ability to restore normal signalling.

Aims of This Thesis

In this work, the goal was to use shotgun proteomics to understand and describe the molecular mechanism of HIV-Tat induced neuronal apoptosis. The achieve these, the aims of this thesis were:

1. To develop an in vitro model system for HAND.
2. To perform quantitative differential genomic and proteomic analysis to characterise the perturbation of the model system by HIV-Tat.
3. To perform quantitative differential proteomic analysis to characterise the effect of lithium on HIV-Tat dysregulated neuronal proteome.
4. To perform detailed pathway analysis of the data generated in (2) and (3) to identify the underlying mechanisms of HIV-Tat induced neurotoxicity and the effect of lithium on those perturbations induced by HIV-Tat.

Chapter 2

Establishing a model for HIV-Tat induced neuronal cell death

Introduction

There are approximately 36.9 million people living with HIV (WHO, 2014, http://www.who.int/hiv/en/), up to 70% of whom develop HIV-associated neurocognitive disorders (HAND). HAND describe three formal disease classifications; asymptomatic impairment (ANI), mild cognitive disorder (MND) and HIV-associated dementia (HAD).[5] Before the widespread implementation of HAART, disease onset and progression was associated with neuronal apoptosis which resulted in neurological and cognitive impairment. However, in the post HAART era, HAD incidence has decreased while the incidence of milder forms has increased. This phenomenon is associated with patients living longer with varying degrees of viral replicative suppression. As a result, patients are exposed to decreased levels of the causative agents over an extended period. HAND progression is, therefore, no longer associated with apoptosis but with synaptodendritic loss. Despite significant research efforts, molecular mechanism underlying the neurodegeneration evident in HAND brains remains poorly understood. To identify molecular cascades in an array of diseases, *in vitro* cell culture models have been invaluable.

Currently, the biomedical research field relies on appropriate models to study disease states and develop therapies for many human diseases. Furthermore, the CNS is composed of a heterogeneous cell population predominantly composed of neurons and glia (astrocytes, dendritic and microglia). The difficulties of molecular analysis in heterogeneous organs are compounded when dealing with complex, multigenic diseases such as neurodegenerative diseases. When analysing molecular responses, it is nearly impossible to delineate the responses within individual cell population. In comparison to this, in vivo cell culture allows the analysis of a homogeneous cell population. As HIV is not known to directly infect neurons, it is feasible to assume that

the neurodegeneration is due to the host response, secreted viral factors or a combination of the two acting on neurons.

Several HIV proteins, including gp120 and HIV-Tat have been shown to be neurotoxic. One critical feature unique to HIV-Tat is that it is continually secreted from infected cells despite replicative suppression. HIV-Tat primary sequence is highly variable and reported to tolerate ~40% mutations while maintaining function and occurs in many active length variants *in vivo*. Typically, cysteine comprises ~2.26% of amino acids in mammalian proteins.[200] Although the HIV-Tat primary sequence is highly variable, seven cysteines are maintained within a 16 amino acid cysteine-rich motif[201] which equates to at least 7% cysteine occupancy across the entire protein (ignoring any cysteines outside the cysteine-rich region). This region is believed to be integral to HIV-Tat structure, function and toxicity through the formation of specific disulphide bonds.[202,203]

The SH-SY5Y neuroblastoma cell line has long been used as a model human neuronal cell line and is widely used in HAND mechanistic studies involving HIV-Tat.[204,205] An ever present and legitimate concern about using cell lines is their ability to adequately represent and replicate in vivo tissue responses. Unfortunately, cell lines will never replicate complex human tissues; however, work by Krishna *et al* assessed the validity of SH-SY5Y as an appropriate cell line for studying neurodegenerative diseases. After analysis of genomic, transcriptomic and proteomic data derived from the cell line and performed disease specific network analysis. The concluded that most genes involved in PD, AD, Huntington's disease and Amyotrophic Lateral Sclerosis were intact.[206]

Herein, we provide a brief description of the establishment of an SH-SY5Y model for HIV-Tat induced neuronal dysregulation. In particular, the maintenance of monomeric, active HIV-Tat required particular attention. We show that multimeric HIV-Tat is unable to induce cell death and that the buffer used to resuspend lyophilized HIV-Tat is critical to its long-term *in vitro* activity. As many publications fail to identify the resuspension buffer used, this may be the source of the conflicting information present in literature. Furthermore, we show that the inclusion of a wash step, not present in many MTT protocols, is required for accurate MTT data.

Materials and Methods

Cell culture

The SH-SY5Y neuroblastoma cell line was kindly provided by Dr. K. Wilkinson (IIDMM, University of Cape Town Faculty of Health Sciences). Cells were expanded in Dulbecco's modified Eagle's medium (DMEM) - high glucose (Sigma-Aldrich D6429), supplemented with Penicillin-Streptomycin (100 units/ml penicillin and 0.1 mg/mL streptomycin (Sigma-Aldrich D4333)) and 10% (v/v) heat-inactivated foetal calf serum (FCS) (Sigma-Aldrich F7524). Cells were seeded on 10 cm Greiner adherent cell culture plates (Lasec SA, South Africa) at 1.5 X 10^6 cells/plate and maintained at 37 °C in a humidified atmosphere containing 5% CO_2.

Subculture

Cell culture media was removed and cells are gently washed with warmed PBS. After removal of the wash buffer, 1.25 ml of trysin solution was added to the 10 cmØ culture dish and spread evenly across the surface. The plate was then incubated for approximately 1 minute or until cells have visibly lifted from the dish. Once cells are loosened from the plate, the trypsin was immediately quenched with trypsin inhibitor. 20 µl of well mixed cell suspension was mixed with 20 µl of trypan blue and loaded into a cell counting slide and viable cells are manually counted using a microscope. Depending on the application, specific amounts of cells are then diluted in 10% FBS, DMEM and aliquoted into appropriate dishes and incubated the 5% CO^2, humidified 37^{o}C incubator.

MTT assay

Following treatment, cell culture media was removed and the cells are gently washed with warmed 0% FBS, DMEM. After the wash buffer was removed, 0% FBS containing 0.5 mg MTT/ml was added and cells are incubated in the 5% CO_2, humidified 37^{o}C incubator for approximately 30 minutes or until formazan crystals are visible. All treatments were performed when cells were at ~80% confluence in three biological replicates while MTT assays were measured in two technical replicates.

To evaluate our ability to detect changes in cell viability using the MTT assay, we performed dose response tests with staurosporine. While maintaining a constant 0.2% DMSO in all wells, we treated the cells with a range on staurosporine concentrations (100 nM, 50 nM and 25 nM) suspended in 100% DMSO as well as a 0.2% DMSO

control. We then also tested the effect of washing the cells in warmed DMEM media prior to treatment with 0.5 mg/ml MTT reagent. Briefly, after treatment, the culture media was removed and warmed media was added very gently over the cells. After a gentle swirl, this media was again removed and media containing 0.5 mg/ml MTT reagent was added to the cells gently.

After sufficient formazan crystals formed, the media was removed. We then added 200 µl 100% DMSO and incubated the dishes at room temperature with gentle agitation for 10 minutes. Thereafter, 80 µl of the suspended formazan was added to clear, flat bottomed 96 well plates and analysed by iMARK (BIORAD) plate reader at 595 nm. If the highest $A_{595} \geq 1$, mixtures were diluted equally until the highest $A_{595} < 1$.

Results and Discussion

HIV-Tat was suspended in sterile PBS and diluted to a range of concentrations such that the volume added to each well remained constant. Cells were treated with HIV-Tat for 24 hours then assayed for cell death using the MTT assay **Figure 14**. A wide range of HIV-Tat toxic concentrations have been reported in literature and our CD_{50} fell within the reported range.

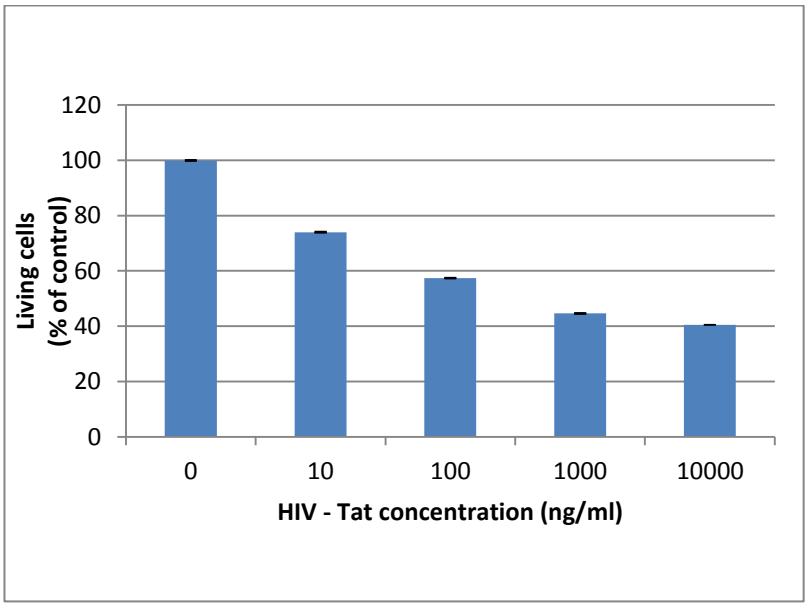

Figure 14: A dose response assay perfomed using indicated concentrations of HIV-Tat. The data was expressed as the number of live cells as a percentage of PBS treated control cells. Based on the trend line fitted to the data, the CD_{50} was calculated to 575 ng/ml.

Following this result, we performed ELISA assays to determine cellular expression levels of GSK-3β after HIV-Tat treatment (data not shown). The data we received from

the ELISAs were in accordance with expected results as it was previously reported that the activity and not expression levels of GSK-3β is altered by HIV-Tat.[27] Before continuing with ELISAs to determine the levels of phosphorylated, activeGSK-3β and MS analysis of perturbed cells, I attempted to confirm the results in **Figure 14** were reproducible.

Remnants of apoptotic cells produce formazan

Using HIV-Tat from the same source suspended in the same manner, we were unable to reproduce these results. To confirm that the cell culture and assay technique applied was capable of accurately and reproducibly detect and measure cell death, we tested the protocol using a known apoptotic agent, staurosporine. [207,208] To do this, we performed a dose response experiment using staurosporine (**Figure 15**). Staurosporine was suspended in 100% DMSO which served as the control. Following treatment, we determined that the MTT assay was capable of identifying dose dependant cell death induced by staurosporine.

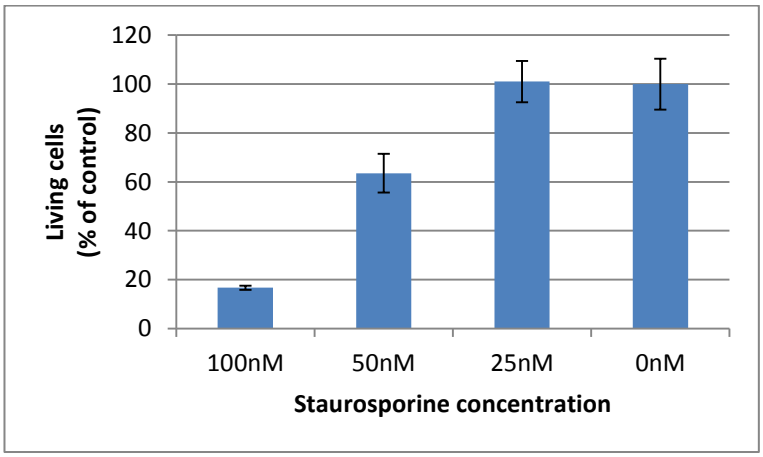

Figure 15: Staurosporine dose response showing that the MTT assay was able to detect cell death in SH-SY5Y. The data is expressed as a percentage of the carrier (DMSO) treated control.

Satisfied that our MTT assay was able to detect and quantify cell death in SH-SY5Y reproducibly, we determined whether our technique was producing accurate data. Given that cells are undergoing cell death, it is to be expected that cell debris will be present during the MTT assay. To determine whether dead cells influenced the result, we tested the effect of washing the cells prior to performing the MTT assay. **Figure 16** shows that the dead cells do contribute significantly and cause the assay to overestimate live cells present when using 50 mM staurosporine.

We are unable to find any literature reference to this drastic effect of dead cells present in the MTT assay but we hypothesize that this effect is due to lactate dehydrogenase (LDH) which is not degraded during cell death and is present and active in the cell bodies and culture media after cell death.[209] LDH is able to convert the soluble MTT to the same insoluble formazan salt formed by live, intact mitochondria.[210] The presence of active LDH therefore skews the result by increasing the amount of insoluble formazan formed. We therefore concluded that it is important to remove dead cells and replace the media prior to performing the MTT assay.

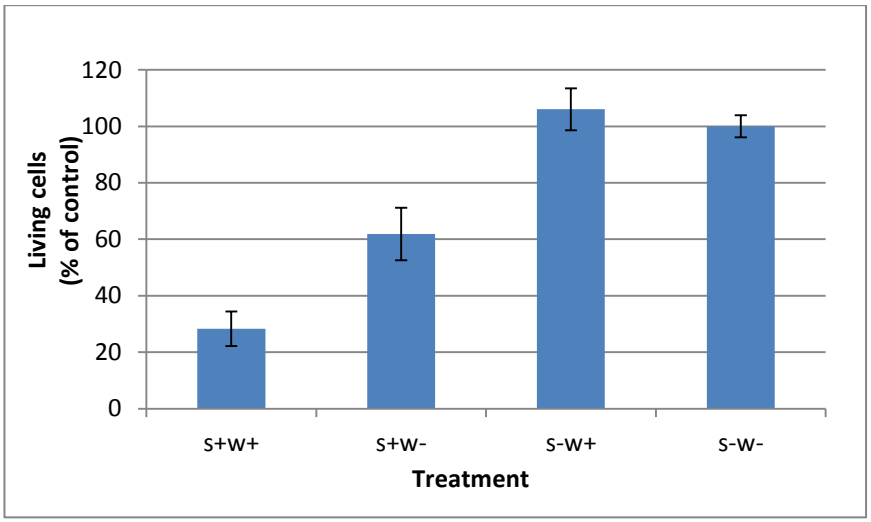

Figure 16: Determining the effect of removing dead cells prior to the MTT assay. Cells were treated with either 50 nM staurosporine (s+) or DMSO (control) (s-). Cells were then either washed (w+) or not washed (w-) prior to performing the MTT assay.

After refining the assay using staurosporine, we attempted to induce cell death with HIV-Tat again. Using up to 10, 000 ng/ml HIV-Tat, we were unable to show any cell death in SH-SY5Y cells (data not shown). Despite acquiring several new vials (all from the same batch) we were not able to reproduce the data in **Figure 14**. Following this, we shifted our focus to determining why the HIV-Tat we received was inactive.

Reduced, monomeric HIV-Tat is essential for the induction of cell death

We separated the HIV-Tat suspended in PBS by 12% SDS-PAGE. This revealed that the sample consisted of proteins larger than the expected monomeric mass of 9.7 kDa seen in **Figure 17**.

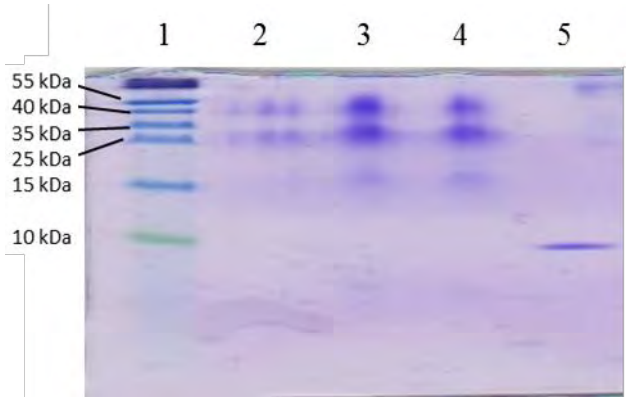

Figure 17: A 12% SDS-PAGE of NIH supplied HIV-Tat (1 µg, 4 µg and 2 µg)(lanes 2-4) and ubiquitin at 8.5 kDa (1 µg) (lane 5). It is clear that there are no bands in lanes 2, 3 and 4 close to the expected molecular mass of 9.7 kDa. Only high molecular mass proteins are present in the sample.

We then analysed that same sample by MALDI-MS, which revealed the presence of only high molecular mass proteins (**Figure 18**). The mass spectrum consisted of a series of peaks ranging from 39.657 – 78.457, each separated by ~9.7 kDa. This suggested that these peaks represent high order structures of HIV-Tat protein. While this spectrum does not confirm multimeric HIV-Tat, it does support the gel data showing high molecular weight proteins which are likely HIV-Tat multimers.

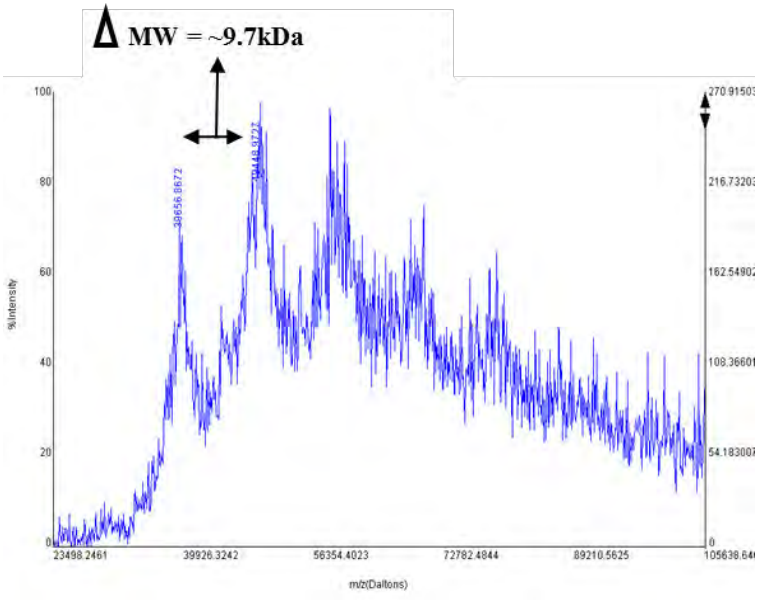

Figure 18: A mass spectrum of NIH HIV-Tat showing the high order HIV-Tat structures with peaks 9.7 kDa apart.

We then wanted to determine why the protein was predominantly represented by multimeric forms. Additionally, we acquired another HIV-Tat variant (HIV-Tat from Clade-B) from a different source (Diatheva, Italy). Notably, DTT was used in their isolation protocol, which raised a concern because the cysteines are highly important to HIV-Tat confirmation and activity [211,84]. DTT is well known to oxidise rapidly and

spontaneously in solution, so it seemed plausible that by the time the HIV-Tat was resuspended for use, no effective reducing agent was present which enabled the formation of inter-molecular disulphides. To test this hypothesis, we treated an aliquot of the same HIV-Tat used in Error! Reference source not found. and **Figure 18** with 200 M β-mercaptoethanol (βMe), 10% SDS; after thorough mixing, this mixture was heated to 95^{o}C for 15 minutes. As can be seen in **Figure 19**, this reversed most of the high order structures present in the sample. Lanes 2 and 4 are clade-B HIV-Tat and it can clearly be seen that nearly all the multimers have been reduced to monomers. We also tested lower concentrations of βME but these had no effect on reversing multimers, even after boiling. Since 200mM βME alone (i.e. without 10% SDS and heating) was not sufficient to restore the monomeric form (data not shown), we generated a βME dose response curve for SH-SY5Y to determine the highest possible concentration of βME tolerated by the cells (data not shown).

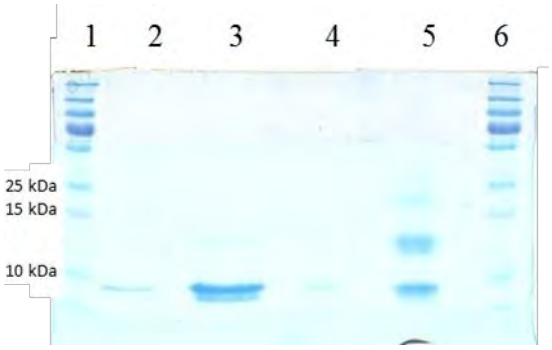

Figure 19: HIV-Tat superstructures reversed by 200 mM βME treatment. Lanes 2 and 3 are treated with 200 mM βME, 10% SDS and heating. Lanes 4 and 5 are suspended in plain strerile water. Lane 2 shows significantly reduced compared to lane 4. Lane has no visible multimers, though there are fewer multimers in lane 3 without βME.

From this, we determined that we could treat the HIV-Tat stocks with up to 350 mM βME which would result in 3.5 mM final βME concentration when diluted to working HIV-Tat concentrations in cell culture. Unfortunately, 350 mM βME was not enough to reverse multimers that have already formed (Data not shown).

Since the formation of disulphide bonds requires alkaline pH and oxygen,[212] we suspended new vial of clade-B HIV-Tat in a nitrogen bubbled, degassed solution of 0.05% TFA in water. However, this HIV-Tat was still unable to induce cell death and was multimeric (data not shown). However, when we resuspended clade-B and C HIV-Tat in degassed, 0.05% TFA containing 350 mM βME the resultant solution was able to induce cell death (Figure 20). The presence of monomeric HIV-Tat upon resuspension was confirmed by MALDI-MS as can be seen in **Figure 21** along with an SDS-PAGE (not

shown). A single clear, defined peak is present at ~9.7 kDa, while a doubly charged ion can be seen at ~4.8 kDa along with an SDS-PAGE (not shown).

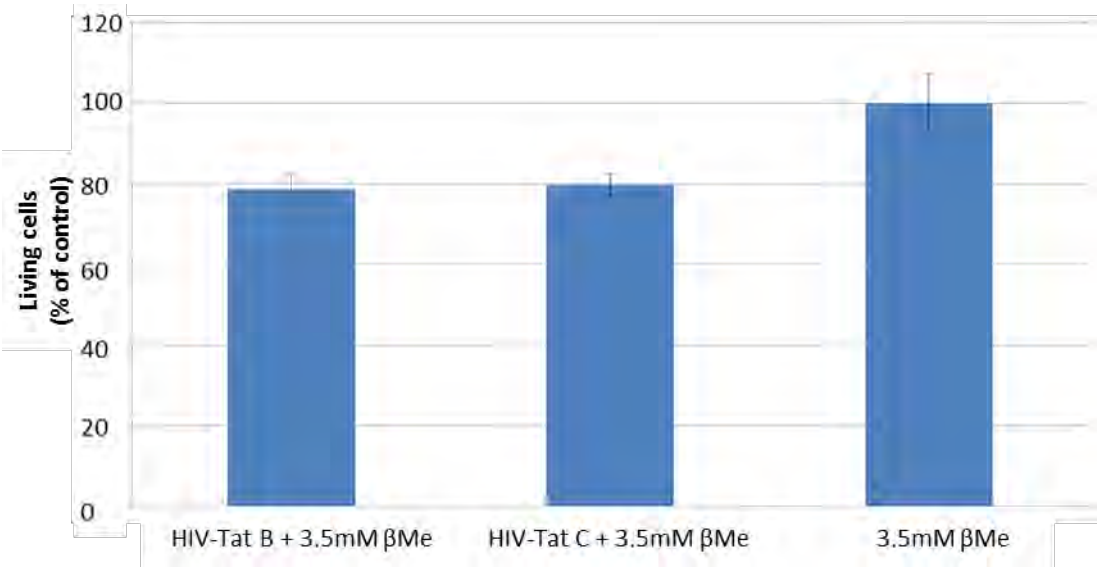

Figure 20: SH-SY5Y cells treated with two variants of HIV-Tat (clade-B and C) resuspended in degassed water containing 350 mM βME, 0.05% TFA. The final concentration of βME in cell culture was 3.5 mM which was also used as the control. All data is expressed as percentage of control live cells.

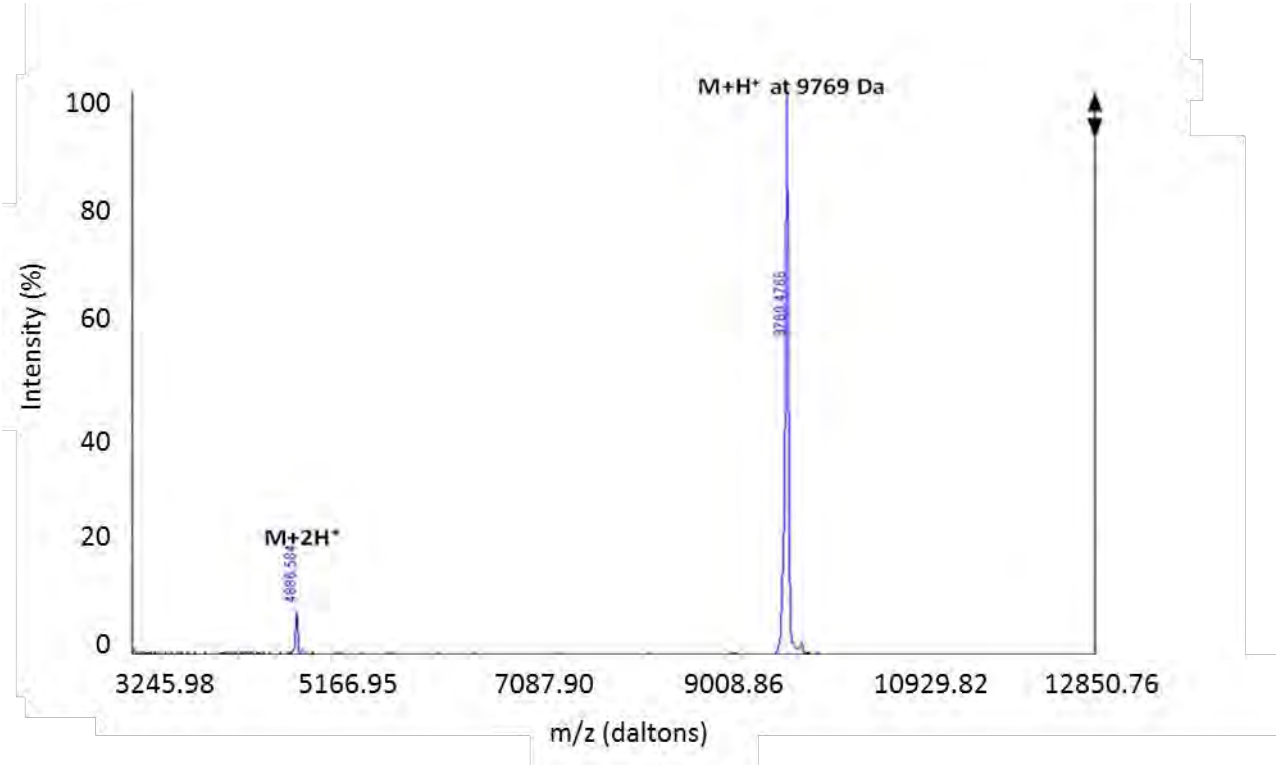

Figure 21: MALDI mass spectrum of singly and doubly charged monomeric HIV-Tat.

We also showed that clade-B HIV-Tat resuspended in this manner was able to induce cell death both when used immediately upon resuspension, as well as after three months of storage at -80^{0}C, with the same level of activity at both time points (**Figure 22**).

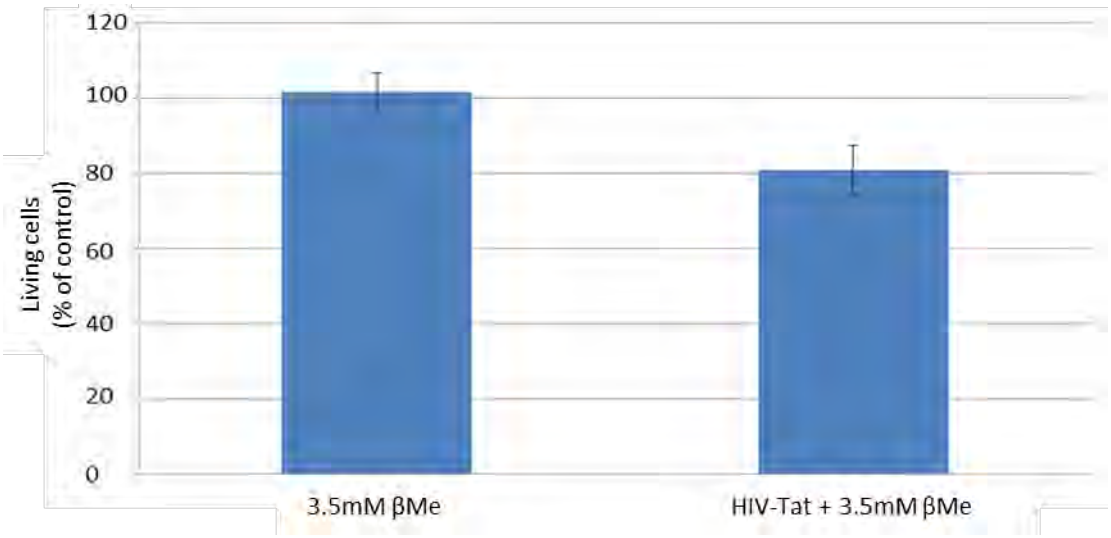

Figure 22: Clade-B HIV-Tat resuspended in 0.05% TFA, 350 mM βMe degassed water after 3 months of storage at -80^{0}C.

Our model was, therefore, one in which 1 ug/ml HIV-Tat reproducibly induced ~20% neuronal cell death as measured by MTT. Using this model, we were then able to pursue more advanced proteomic analyses. Despite 3.5 mM βMe not inducing any measurable cell death, we wanted to reduce its concentration so as to have as little effect as possible in cell culture. Toward this, we tested using 50 mM βMe in the resuspension buffer as opposed to 350 mM and found the resultant HIV-Tat suspension to be monomeric (**Figure 23A)** and able to induce 20% cell death at 1 µg/ml (**Figure 23B**).

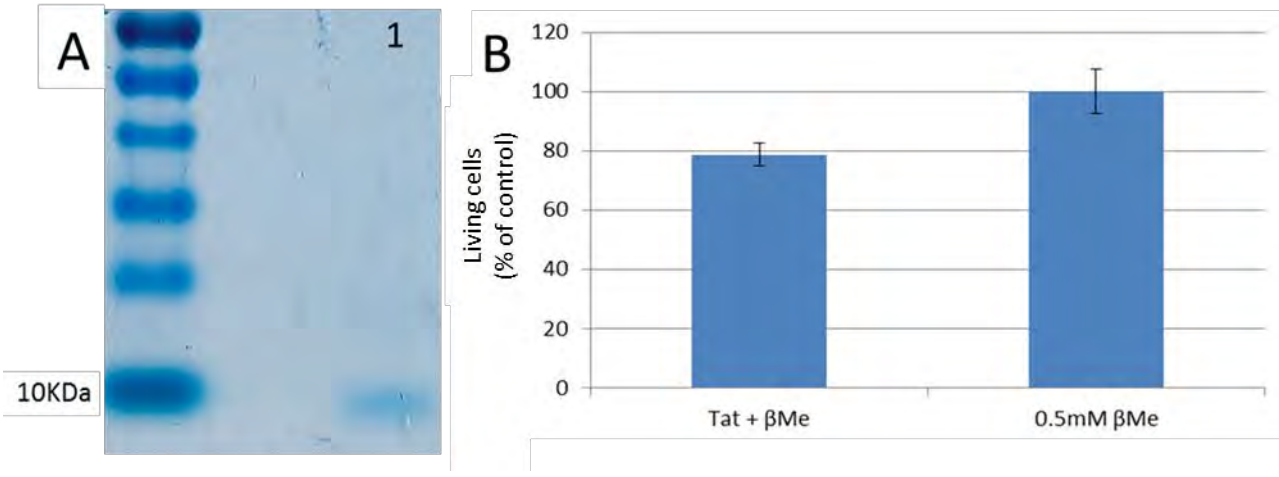

Figure 23: HIV-Tat resuspended in 0.05% TFA, 50 mM βMe degassed water induced cell death as effectively as earlier experiments using higher βMe concentrations.

This work confirms that HIV-Tat must be in its monomeric form to induce cell death. Since establishing the cell culture model and reproducibly inducing ~20% cell death, we progressed on to MS analysis of this model.

Chapter 3

Quantitative proteomic analysis of HIV-1 Tat-induced damage in SH-SY5Y neuroblastoma cells

Abstract

Despite affecting up to 70% of HIV^+ patients and being the leading cause of dementia in patients under 40 years, the molecular mechanisms involved in the onset of HAND is not well understood. To this end, we performed SILAC-based quantitative proteomic analysis on HIV-Tat treated neuroblastoma (SH-SY5Y) cells. Isolated protein was fractionated by SDS-PAGE and analysed by nLC-MS/MS on a Orbitrap Velos. Using MaxQuant, we identified and quantitation 3077 unique protein groups. Using the student's t-test, we identified 407 differentially regulated proteins of which 29 were identified as highly significantly and stably dysregulated using an additional 2sd cutoff. GO-term analysis shows dysregulation in both protein translation machinery as well as cytoskeletal regulation which have both been implicated in other dementias. In addition, several key cytoskeletal regulatory proteins such as ARHGEF17, the Rho GTPase, SHROOM3 and CMRP1 are down-regulated. Together, we that HIV-Tat can dysregulate neuronal cytoskeletal regulatory proteins which leads to the major HAND clinical manifestation; synapse loss.

Keywords: Proteomics , SILAC, HIV dementia, pathway analysis, neurodegeneration

Introduction

A major complication of human immunodeficiency virus type-1 infection, affecting 70% of HIV positive individuals in South Africa in its more severe form, is HIV-associated neurocognitive disorders (HAND).[213] HAND encompasses a set of neuropathological disorders characterised by varying degrees of cognitive, motor and behavioural dysfunction as a result of HIV infection in the central nervous system (CNS).[5] HAND comprises an array of conditions that range from asymptomatic neurocognitive disorder (ANI) and mild neurocognitive disorder (MND) to the most severe form, HIV-associated dementia (HAD).[5] Since the implementation of highly active antiretroviral therapy (HAART), the life expectancy of HIV+ patients has increased. As a result, more patients have presented with HAND. The incidence of HAD has decreased since the implementation of HAART, however HAND cases have increased.

HIV has been shown to enter the brain during early infection[214] which results in significant alterations in the volumes of various brain regions.[215] HAND patients generally present with minor cognitive and motor disorders as well as depressive disorders.[216] Studies have shown that neurocognitive and psychiatric scores of HAND/HAD patients correlate most strongly with loss of synapses rather than neuronal loss or encephalitis.[217]

The causative agent for the development of HAND must be considered as either an HIV protein or a host response to HIV infection. In reality, it is most likely that the exact pathology involves a combination of HIV and the host inflammatory response to HIV. However, a great wealth of information has been published which shows that HIV transactivator of transcription (HIV-Tat) alone is capable of causing neuronal damage and eliciting an inflammatory response *in vivo* and *in vitro*. However, the deregulatory effect of HIV-Tat protein in the CNS has been studied extensively, the underlying molecular mechanism involved remain to be elucidated. There is, therefore, no complete mechanism describing the proteomic changes in neurons when treated with HIV-Tat. In addition, despite the large amount of work dedicated to this area, no diagnostic nor prognostic markers have been used clinically.[218]

Lately, there has been increased evidence suggesting that the HIV-1 Tat has a major impact at the gene and protein levels of infected host cells. For example, a recent study has demonstrated that Jurkat cells treated with HIV-Tat resulted in the

dysregulation of 49 host proteins involved in diverse functions such as protein metabolism, energy and amino acid metabolism. [219] In another similar study it has been suggested that HIV-Tat is responsible for changes in expression pattern of proteins relevant for the integrity of endothelial tight junctions, interestingly those changes result in increased permeability of blood-brain barrier.[220–222] In neuronal cells, such as SH-SY5Y cells it has been reported that HIV-Tat is responsible for the differential expression of multiple MicroRNAs. [223] HIV-Tat is a highly variable protein derived from a two-exon *HIV-Tat* gene. The first, 72bp, exon is stable in its length while exon 2 may be completely absent to 39+bp in length. It is reported that HIV-Tat can remain functional with ~40% variability in its primary sequence.[84] While its primary function relative to HIV is simple; transactivation of the viral genome,[76] its highly variant sequence lends itself to performing a vast array of secondary biological functions [95,224,102]. These functions may or may not be targeted functions of the HIV life cycle. Added to its protein binding capacity, HIV-Tat has been shown to bind the genome of a human cell line at 2074 discreet sites.[225] Taken together, this suggests a startlingly high capacity for HIV-Tat to influence host signalling pathways and cellular functions.

In lieu of the disparity in our understanding of HAND molecular mechanisms of onset and HIV-Tat's apparent ability to affect host biological functions, we have performed a global quantitative proteomic analysis of SILAC labelled SH-SY5Y neuroblastoma cells treated with HIV-Tat. We present a rigorous bioinformatics approach capable of identifying gross proteomic changes in the cell. Using this approach, we were able to quantitate 3077 proteins and identify 407 proteins as stably and significantly differentially regulated with 29 passing an additional standard deviation (sd) test and being deemed highly dysregulated. We have, to our knowledge, for the first time, identified the molecular basis for HIV-Tat induced neuronal degradation. Several proteins identified can be linked to the major clinical manifestation of HAND, synaptic degeneration. Additionally, we have identified several secretory proteins which deserve further study as putative diagnostic or prognostic markers.

Materials and Methods

Cell culture and SILAC labelling

The SH-SY5Y neuroblastoma cell line was kindly provided by Dr. K. Wilkinson (IIDMM, University of Cape Town Faculty of Health Sciences). Cells were expanded in DMEM - high glucose (Sigma-Aldrich D6429), supplemented with Penicillin-Streptomycin (100 units/ml penicillin and 0.1 mg/mL streptomycin (Sigma-Aldrich D4333)) and 10% (v/v) heat-inactivated FCS (Sigma-Aldrich F7524). Cells were seeded on 10 cm Greiner adherent cell culture plates (Lasec SA, South Africa) at 1.5 X 10^6 cells/plate and maintained at 37 °C in a humidified atmosphere containing 5% CO_2.

Cells were expanded for a minimum of five passages (>15 doublings) in arginine and lysine deficient high glucose DMEM (Sigma-Aldrich) supplemented with Penicillin-Streptomycin and 10% dialysed heat-inactivated FCS (Thermo Fisher Scientific 88212) and containing the respective concentration of L-lysine and L-arginine isotopes (Thermo Fisher Sientific): light 0.8 mM $6C_{12}2N_{14}$ (K^0) and 0.2 mM $6C_{12}4N_{14}$ (R^0) or heavy 0.8 mM $6C_{13}2N_{15}$ (K^8) and 0.2 mM $6C_{13}4N_{15}$ (R^{10}). Incorporation efficiency and Arg – Pro conversion was tested through analysis of the heavy labelled sample as described in Soares *et al*. 2013.[226]

Treatment with recombinant HIV-1 Tat CLADE-B:

HIV-1 Tat (rec-HIV-1 Tat CLADE-B, Catalogue # REP0002B, Lot 013-0511, Diatheva, Fano, PU, Italy) was reconstituted at a concentration of 0.1ug/µl in 50 mM βMe, nitrogen bubbled water acidified with 0.01% TFA. βMe was essential to maintain HIV-1 Tat functionality by preventing disulphide bond formation which created inactive multimeric HIV-1 Tat. Cells at 80% confluence were incubated for 24 hours in DMEM (no FCS) with Tat (1ug/ml HIV-Tat and 0.5mM βMe final concentration) or only 0.5mM βMe (vehicle).

In parallel with experiments for protein extraction, cell viability was determined using the [4,5-Dimethylthiazol]-2,5-diphenyltetrazolium (MTT) (Sigma, M2128) cell proliferation assay in 24 well plates. After 24 hours of HIV-Tat treatment, wells were washed with DMEM and incubated in 0.5 mg/mL MTT in DMEM for 30 – 90 minutes. The resultant formazan crystals were solubilised in dimethyl sulphoxide (DMSO)

(Sigma-Aldrich), and measured at 560 nm using a BioRad iMARK™ Microplate Reader UV-Vis Spectrophotometer (BioRad Laboratories Pty Ltd, Parklands, Johannesburg).

Sample preparation

K^0/R^0 labelled cells were treated with vehicle, whereas K^8/R^{10} cells with HIV-Tat on 10 cm dishes in triplicate ($8x10^6$ cells per dish). After dead cells were washed away with heated phosphate buffer saline (PBS), the remaining attached cells were lifted with trypsin (Sigma-Aldrich, T4049**)** which was immediately quenched using trypsin inhibitor (T6522). Cells were pelleted at 600 g and washed in Tris-HCl Wash Buffer (50 mM Tris-HCl, 10 mM NaCl, pH 7.5) before lysis. After washing, cells were counted using the trypan blue assay and mixed in a 1:1 ratio. The pellet was then lysed at <4^{o}C according to the QIAGEN Phosphoprotein Kit (Catalogue #37101). Briefly, the washed pellet, containing 16 x 10^6 cells was resuspended by gentle pipetting, and incubated for 40 minutes with occasional vortexing in cold 5 mL PhosphoProtein Lysis Buffer containing protease phosphatase inhibitors (provided in the kit), 10 µL of 25 units/µL Benzonase® Nuclease Stock, and 0.25% (w/v) CHAPS). The suspension was then clarified by centrifugation at 14,000 *g*, and the clarified supernatant was transferred into a clean vial for further processing.

Following the lysis protocol, the clarified lysate was quantitated and passed through the PhosphoProtein Purification Columns (QIAGEN, Catalogue #37101) at room temperature as per the manufacturer's instruction. Briefly, total protein was quantitated using the Bradford Protein Quantiation Assay following manufacturer's instructions, the total lysate diluted to 0.1 mg/mL with PhosphoProtein lysis Buffer. The diluted lysate was then passed through the column and the flow through was retained as the phosphodepleted (PD) sample. The column was then washed with 6 mL PhosphoProtein Lysis Buffer and retained. Thereafter, bound phosphorprotein was eluted using four 500 µL volumes of phosphoprotein elution buffer (50 mM K_2PO_4, pH 7.5 , 50 mM NaCl, 0.25% CHAPS) pooled and labelled phospho-enriched (PE). PD and PE were then concentrated using 3 kDa molecular weight cutoff (MWCO) filtration columns (Nanosep®) to final volumes of ~1 mL and ~100 µL respectively. Bradford protein quantitation showed that PE contained ~180 µg each, whereas the PD contained ~1.8 mg each.

100 µg of protein from each of the three PE and PD replicates were fractionated by 1D-SDS-PAGE, ten gel slices were cut from each lane, and subjected to in-gel digestion. Proteins were reduced with 10 mM DTT, alkylated with 55 mM iodocetamide and digested with 200 ng Trypsin (Promega). Peptides were extracted twice with 70% Acetonitrile (ACN), 0.1% Formic Acid for 30 minutes, cleaned using stage tips then dried. Briefly, ziptips where equilibrated using 80% ACN acidified with 0.1% TFA then washed twice using 5% ACN, 0.1% TFA. Peptides were loaded onto the column and washed using 5% ACN, 0.1% TFA. Peptides were there eluted from the column using two volumes of 80% ACN, 0.1% TFA and dried down. Peptides were reconstituted in 5% ACN, 0.1% formic acid for LC injection.

Mass spectrometry

The LC-MS/MS was performed on a Proxeon EASY-nLC II system (Proxeon Biosystems, Odense, Denmark now Thermo, Bremen), which was coupled in-line via a nanoelectrospray (nESI) source to a LTQ-Orbitrap Velos™ instrument (Thermo Fisher Scientific) for MS analysis. 10 µL The peptide mixtures were applied onto a 10 cm ProxeonEASY column (ID 75 µm, 3 µm, C18-A2 medium) analytical column and peptide elution was achieved at a flow rate of 300 nL/minute with a linear gradient of 5-40% Solvent B (95%Acetonitrile, 0.1% formic acid) for 60 minutes (samples were injected in duplicate).

Data dependent mass spectral acquisition was programmed on Xcalibur as follows: precursor MS1 scans from *m/z* 380 – *m/z* 1600 acquired in the Orbitrap mass analyser with a resolution of 60,000 (at full-width half-maximum at *m/z* 400) with lock mass option enabled for the *m/z* 445.120025 ion. For full scans, 1 x 10^6 ions were accumulated within a maximum injection time of 150 ms. The ten most intense ions with a minimum charge state of +2 were then sequentially isolated with a 2 m/z isolation window and an AGC target of 30000 with a maximum injection time set to 100 ms. Higher energy collisional dissociation (HCD) fragmented was performed at a normalized collision energy (NCE) of 35. The corresponding MS/MS scans were acquired and detected in the Orbitrap mass analyser at a resolution of 7500. Precursor masses were placed on a dynamic exclusion list for 70s following MS/MS selection.

Data processing and bioinformatic analysis

The raw data files were searched using MaxQuant (1.3.0.5) against the Human Uniprot Global Proteome, (12 January 2013, taxonomy id 9606) and the MaxQuant built in common contaminant database, using a reverse decoy database with global FDR set at 5%. Trypsin was used as the protease, allowing two missed cleavages and a fixed modification of Carbamidomethyl (C) and variable modifications of Oxidation (M) and Acetyl (Protein N-term). Only unique, unmodified peptides were used for quantitation. MaxQuant assigns detected peptides to proteins, however, proteins that are not identified by proteotypic peptides are reported in protein groups. All files were run simultaneously to ensure all protein groups were the same across samples and normalized together. Replicates were separated through the MaxQuant experimental design facility.

The text outputs from MaxQuant (proteingroups.txt, peptides.txt, evidence.txt, paramters.txt, summary.txt) were imported into the statistical language R (http://www.r-project.org/). Decoy Hits (Rev) and Contaminants (Con) were removed. Data was further curated by removing any protein with an H/L variability greater than 300, indicating greater than 3 sd across all redundant quantifiable peptides for the protein within a sample, thereby removing inaccuracies in protein quantitation from the data. A two-tailed t-test was then performed on the entire dataset, using a subset of the entire dataset, those proteins within 1sd and with a variance below 0.25, against which to assess differential regulation of the dataset. Proteins with a t-test p-value below 0.05 were identified as significantly differentially expressed and those with a t-test p-value below 0.05 and average expression above the 2SD cutoff were deemed highly and significantly differentially expressed.

Functional enrichment analysis

To identify the biological processes altered by HIV-Tat treatment, we assessed the significantly differentially expressed proteins (by t-test only) for GO-term enrichment using the PANTHER online software suite.[227] For each core analysis investigated, GO-terms identified with less than Three proteins were ignored.

Results

Given the unavailability of diseased primary neuronal tissue, establishing models of disease are a necessity for studying causative pathway dysregulation in disease. To identify pathways responsible for HIV-Tat mediated neuronal dysregulation, we SILAC labelled and treated the commonly used neuroblastoma cell line, SH-SY5Y, with recombinant HIV-1 Tat protein. The resultant isolated proteins representing the proteomic state of the cell under both control and treated conditions were mixed and analysed by Orbitrap Velos mass spectrometer. The resultant data was analysed to identify and quantify proteins prior to differential bioinformatic analysis to identify dysregulated proteins. These dysregulated proteins were then further analysed in order to elucidate the pathways and cellular functions dysregulated by HIV-1 Tat.

Monomeric HIV-Tat is required to induced cell death in SH-SY5Y cells

Previous studies described the identification of several oligomerization forms of HIV-Tat protein spontaneously forming in solution and particularly stable to denaturing and reducing conditions.[228] Accordingly, our SDS-PAGE based assay revealed that HIV-Tat multimeric form was highly stable once formed and it remains stable after treatment with high concentrations of βMe (**Chapter 2**). However, HIV-Tat multimer formation was prevented when lyophilized HIV-Tat is suspended in milliQ water with 50 mM βMe, 0.05% TFA and deoxygenated by nitrogen bubbling. Earlier evidences indicate that the monomeric form of exogenous HIV-Tat is the only functional form capable of transactivating the HIV-1 LTR. This prompted us to investigate the effects of different forms of HIV-Tat (monomeric or multimeric) on SH-SY5Y cell viability *in vitro*. Our results confirmed that the multimeric form of HIV-Tat had no effect on cell viability, whereas monomeric HIV-Tat suspended in deoxygenated 50 mM βMe, 0.05% TFA resulted in 20% cell death. Therefore, in order to treat SH-SY5Y cells with exogenous active HIV-Tat protein, the latter conditions were used for further experiments involving HIV-Tat treatment. Here, SH-SY5Y cells were treated with 1µg/mL of monomeric HIV-Tat, which is within the range of in vivo HIV-Tat levels[229] and we chose to harvested HIV-Tat treated cells at 80% viability assuming that most of the cells would be highly stressed but alive and intact. We reason that this would allow us to

have a snap shot of late stage molecular events preceding, but ultimately resulting in apoptosis.

Proteome dynamics

We performed a typical SILAC experiment that compared two differentially labelled cell cultures: SH-SY5Y untreated cells (Arg^0; Lys^0) and treated with HIV-Tat (Arg^{10}; Lys^8) with three biological replicates. The incorporation efficiency of the SILAC amino acid was greater than 99.9 % (Identified peptides: Appendix 1) and the Arg –Pro conversion was calculated as 6.5%. For the subsequently analysis, we employed 1D SDS-PAGE protein separation, and subsequent in-gel protein digestion of 10 fractions from each biological replicate. After MS analysis and MaxQuant STY phosphorylation identification, we saw no evidence of phospho-enrichment (**Data not shown).** We, therefore, treated the phospho-enrichment as a further fractionation step in downstream analysis. Combined proteome of the SILAC experiments resulted in the identification of 1348896 MS/MS spectra corresponding to 19672 non-redundant peptides sequences and 3077 protein groups. The false discovery rate (FDR) was set at 1% at the peptide level and 5% at protein group level. In order to determine the extent of relative expression changes in proteome, a histogram was generated to determine the distribution of the data, due to there being outliers in the data, the histogram was trimmed including everything within 2SD and regenerated returning a normally distributed data set, shown in **Figure 24**.

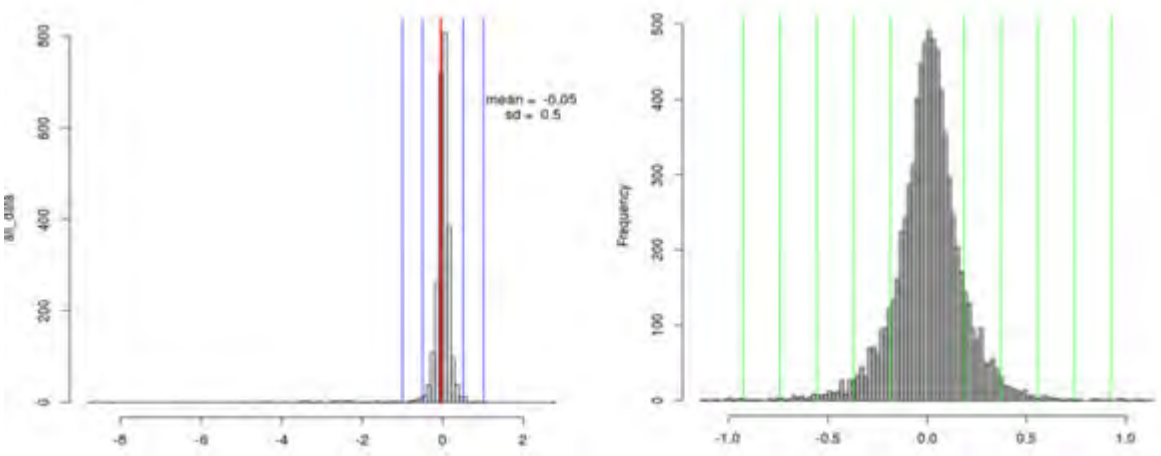

Figure 24: A histogram of protein H/L ratios showing a normal distribution of H/L ratios across the dataset after highly variant data was removed.

The reproducibility of quantitation between biological replicates was assessed by a Pearson Correlation analysis and was found to be between 0.75 and 0.96 as shown in **Figure 25**.

A two-tailed student's t-test was then used to test each protein against a stably expressed set of the data defined as those proteins within 1sd of the mean with a variance below 0.25 between replicates. A total of 407 protein groups scored a t-test p-value below 0.05 and were identified as significantly differentially expressed. Of these, 29 displayed a greater than 2SD variance from the data mean and were deemed highly and significantly differentially expressed (**Table 1)**.

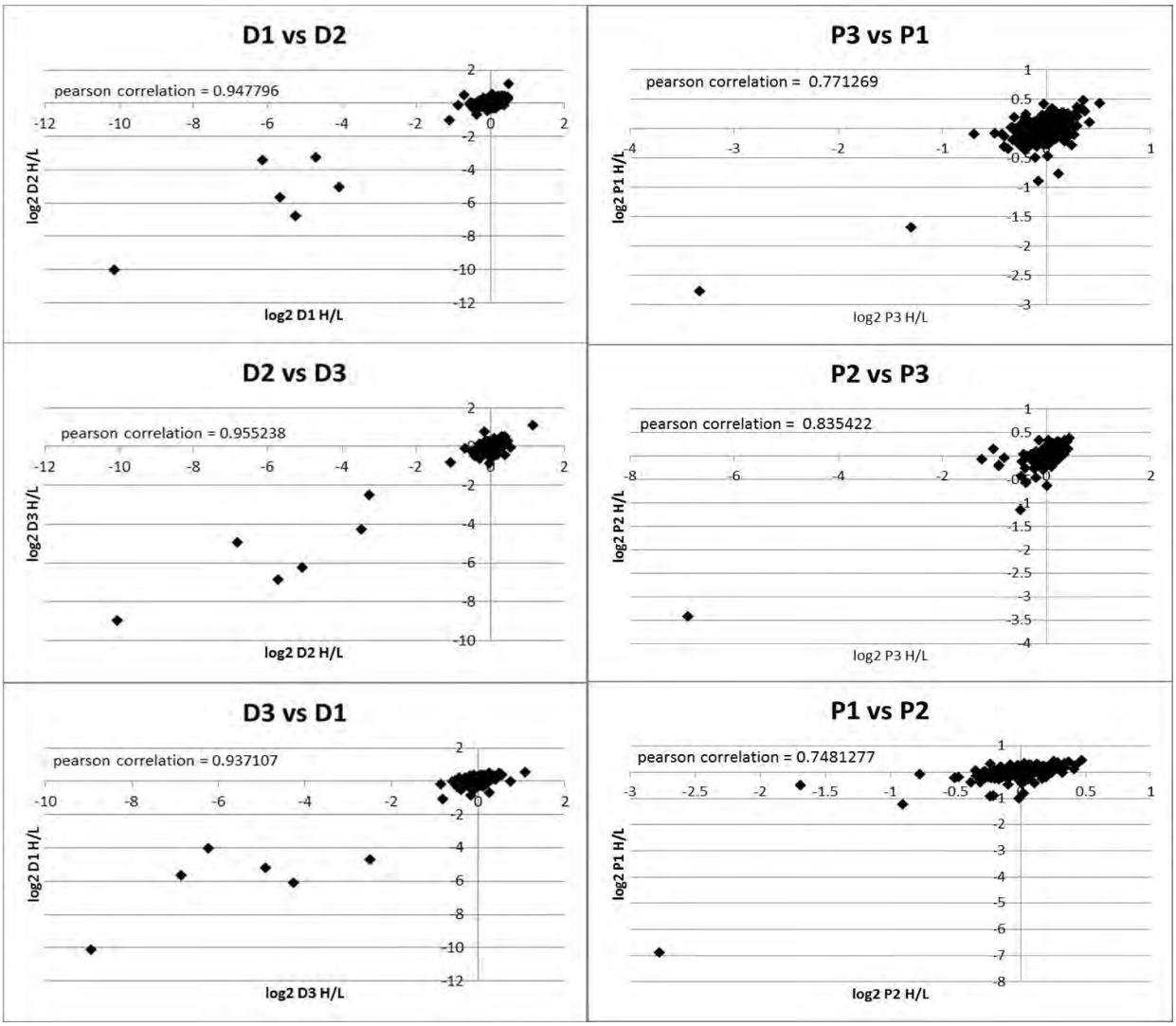

Figure 25: Reproducibility of quantitation between biological replicates. Despite the extensive fractionation performed, the biological replicates retain high correlations which will allow for more sensitive significance analysis downstream.

Of these, six proteins were upregulated and 23 were downregulated in response to HIV-Tat treatment. In order to have an overview of the potential biological processes affected by HIV-Tat infection, differential and highly differentially expressed proteins

were analysed by GO-term enrichment or individually classified by their putative function respectively.

Table 1: The set of 29 stably and highly significantly differentially regulated proteins as well as number of identified peptides, fold change and p-value.

Gene Name	Unique Peptides	PEP	Fold Change	p-value	Protein Names
ARHGEF17	1	0.011871	-8.56	0.035	Rho guanine nucleotide exchange factor 17
BPIFA1	5	7.9E-109	-26.41	0.009	BPI fold-containing family A member 1
CASP14	3	2.16E-25	-2.45	0.028	Caspase-14
CDO1	1	0.012644	1.45	0.005	Cysteine dioxygenase type 1
CHGA	6	2E-173	2.10	0.009	Chromogranin-A
CRMP1	7	1.1E-152	-1.75	0.026	Dihydropyrimidinase-related protein 1
CSTA	3	9.71E-23	-4.74	0.037	Cystatin-A
DBH	15	6E-193	1.67	0.028	Dopamine beta-hydroxylase
DCD	4	4.77E-43	-10.77	0.002	Dermcidin
DSP	28	1.1E-106	-5.51	0	Desmoplakin
IGHA1	8	1.17E-72	-9.97	0.022	Ig alpha-1 chain C region
IGLL5	1	5.21E-26	-5.04	0.001	Immunoglobulin lambda-like polypeptide 5
KCTD15	7	2.98E-17	-1.33	0.026	BTB/POZ domain-containing protein KCTD15
KIAA1429	2	0.000126	-1.45	0	Protein virilizer homolog
KRT2	1	0	-6.46	0.031	Keratin, type II cytoskeletal 2 epidermal
LRMP	2	0.001908	-418.48	0	Lymphoid-restricted membrane protein
MUCL1	2	0.000325	-6.65	0.001	Mucin-like protein 1
PITPNB	10	3.74E-35	1.39	0.02	Phosphatidylinositol transfer protein beta isoform
PRRC2C	3	9.04E-05	-31.89	0.019	Protein PRRC2C
PRSS3	1	2.46E-46	-10.90	0.043	Trypsin-3
PSME2	12	1.2E-174	1.40	0	Proteasome activator complex subunit 2
S100A8	5	6.84E-18	-5.53	0.021	Protein S100-A8
SHROOM3	1	0.000739	-103.75	0.002	Protein Shroom3
SLC2A1	2	0.000103	-1.34	0.02	Solute carrier family 2
SMYD5	3	7.99E-14	-1.37	0.013	SET and MYND domain-containing protein 5
TFPI2	1	0.034087	6.52	0.028	tissue factor protease inhibitor 2
TOMM34	3	1.71E-09	-1.30	0.014	Mitochondrial import receptor subunit TOM34
UBXN7	3	1.48E-08	-3.56	0.004	UBX domain-containing protein 7
ZG16B	4	1.37E-34	-11.81	0.023	Zymogen granule protein 16 homolog B

Using the full complement of 407 differentially regulated proteins, we performed GO-term enrichment analysis using PANTHER.[227] **Figure 26** shows that the most highly enriched functions are catalytic activity and binding. In our data, catalytic activity describes a vast array of enzyme mediated cellular functions which are dominated by

hydrolase activity. More interestingly, however, is that the second most enriched function is the GO-term, binding (GO:0005488). In our data, this function is dominated by nucleic acid as well as protein binding, the components of which can be seen in **Figure 27A** and **Figure 27B**, respectively.

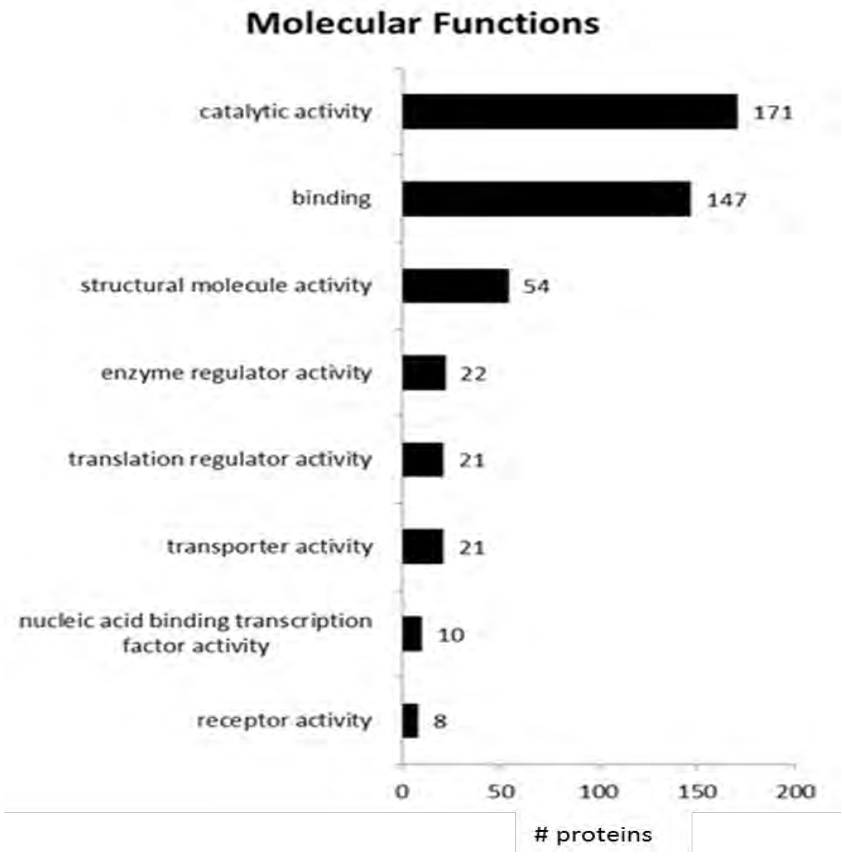

Figure 26: PANTHER GO-term, molecular functions components.

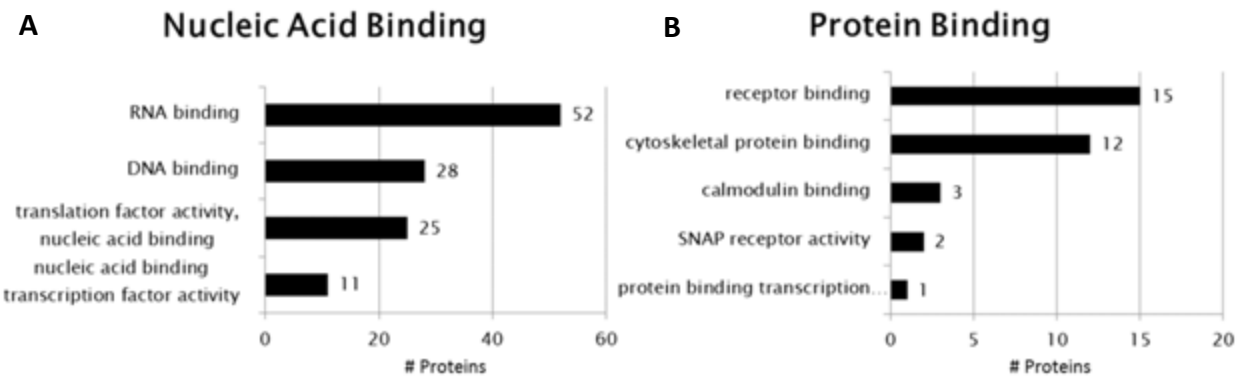

Figure 27: PANTHER GO analysis of the respective component functions of nucleic acid and protein binding.

Discussion

HIV-Tat has been known to cause varying degrees of neuronal damage *in vivo* and *in vitro*. Due to the subjective nature of many of these past experiments, clear, conclusive mechanisms by which this damage takes place has remained elusive. To this end, we have performed a quantitative global proteomic analysis of HIV-Tat treated SILAC labelled SH-SY5Y human neuroblastoma cells. With this data, we were able to attribute HIV1-Tat specific proteomic dysregulation to the most prominent clinical feature correlating with disease severity; synapse degradation and loss.

HIV clade-B Tat as an HIV dementia causative agent

Despite HIV clade-B being most associated with HIV dementia worldwide, South Africa's burden is most associated with clade-C.[230] This was recently attributed to the HIV-Tat S31C mutation, most associated with clade-B HIV-Tat, being present in South African isolates.[231] Furthermore, CNS derived sequences from HIV dementia patients typically contained the S31C mutation. However, clade-C HIV-Tat with the S31C mutation was, to our knowledge, not commercially available at the time of this study. For these reasons, we chose to use clade-B HIV-Tat in our studies. Current studies using HIV-Tat to induce neuronal apoptosis use varying concentrations of HIV-Tat and culture conditions and rarely confirm the HIV-Tat to be monomeric.

Bioinformatic identification of dysregulated proteins upon HIV-Tat treatment

In the current study we have identified a total of 3077 protein groups; a significant proportion of the SH-SY5Y proteome and overall this study resulted in one of the largest proteomic data reported in SH-SY5Y published to date. We selected the unconventional use of an FDR of 5% as our peptide and protein identification because we reasoned that any false positives would become evident in downstream analysis by our use of pathway analysis. Our reasoning is that all protein entries in the UniProt database used in our MaxQuant searches have an equal opportunity of being identified as a false positive in our final protein lists. Furthermore, pathway analysis relies on associated proteins being present in the given dataset. The basis of the non-real protein assignments dictate that there is a very low possibility that a non-real protein identified will fall into a pathway with many other members selected by our bioinformatic analysis. Therefore, most, if not all, false positive proteins selected by

our differential analysis should not fall into pathways and can thus be excluded from further analyses on that basis. Highly dysregulated proteins which do not fall into known pathways selected for further analysis will be analysed using targeted MS methods

Conventionally, any proteins with greater than 2SD variance from the dataset mean are considered differentially expressed. 2SD is, however, a completely arbitrary value as it has no biological relevance when used on its own. We also deemed that the commonly used 2X fold change was also not a reliable nor acceptable criterion as the cellular relevance of any change in protein abundance would surely be dependent on the cell state and would be highly variable between proteins. Furthermore, the 2SD average variance from the mean criterion does not take variance among samples into account.

As can be seen in **Figure 28,** we present two examples of proteins with a greater than 2SD variance from the mean, but they have large variability between samples. These two proteins are, therefore, excluded from further analysis due to their high inter-sample variance Alternatively, differentially expressed proteins which have a greater than 2SD variance and small inter-sample variance as determined as a function of a significant p-value in the two-tailed students t-test are deemed significantly differentially regulated. While we have not presented the data, 2X fold change would suffer similar short falls since it too will not take inter-sample variance into account. To this end, we argue that any protein with a significant difference as determined by a two-tailed students t-test is stably and significantly different and should not be ignored. We included the 2SD cutoff as described in order to generate a high confidence list of differentially expressed proteins with both a significant and large difference between treated and untreated samples which could highlight the most significant cellular changes brought about by HIV-Tat treatment (**Figure 29**).

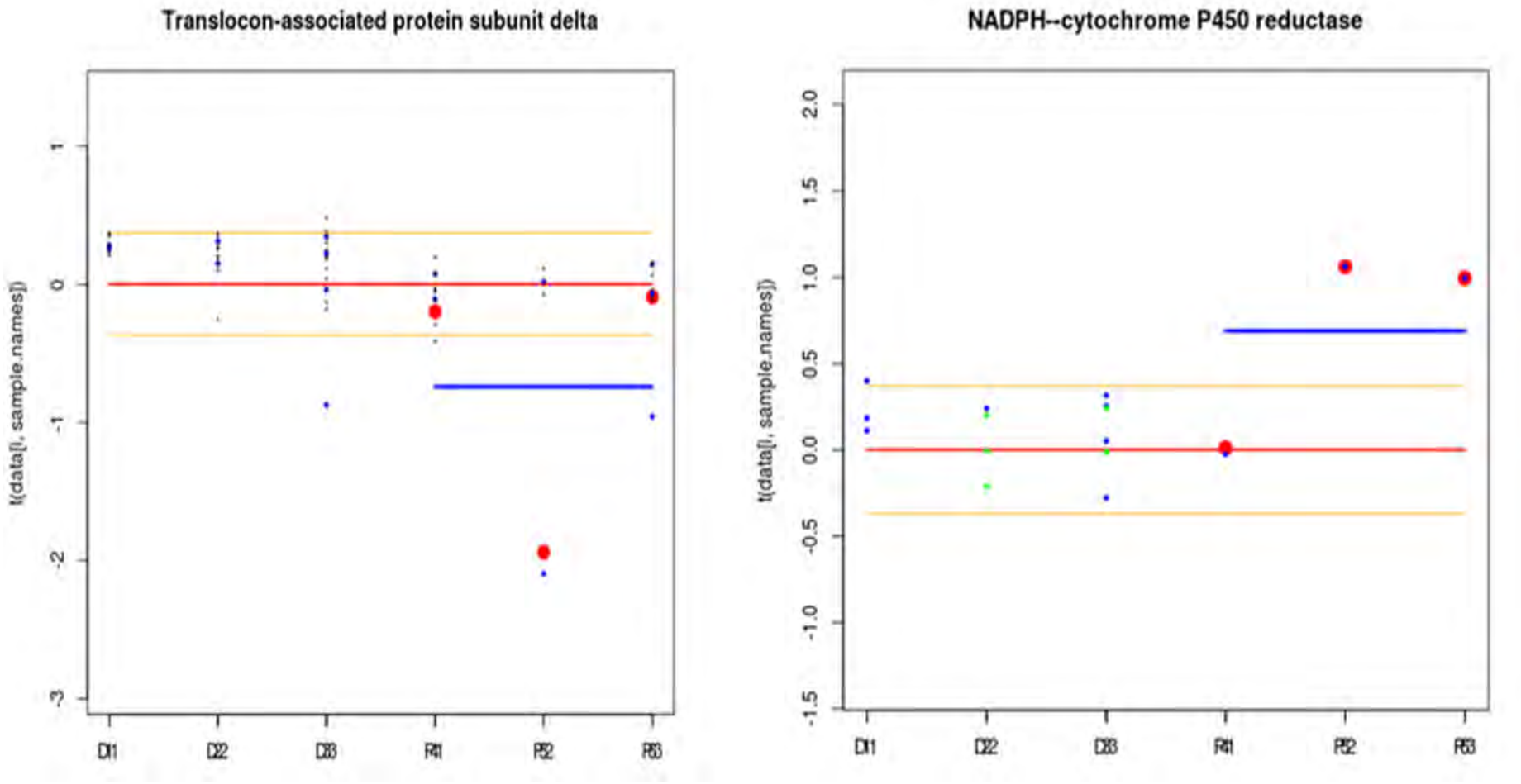

Figure 28: Two examples of proteins which have an average expression greater than 2SD but have a large variability and are therefore not regarded as significantly differentially regulated.

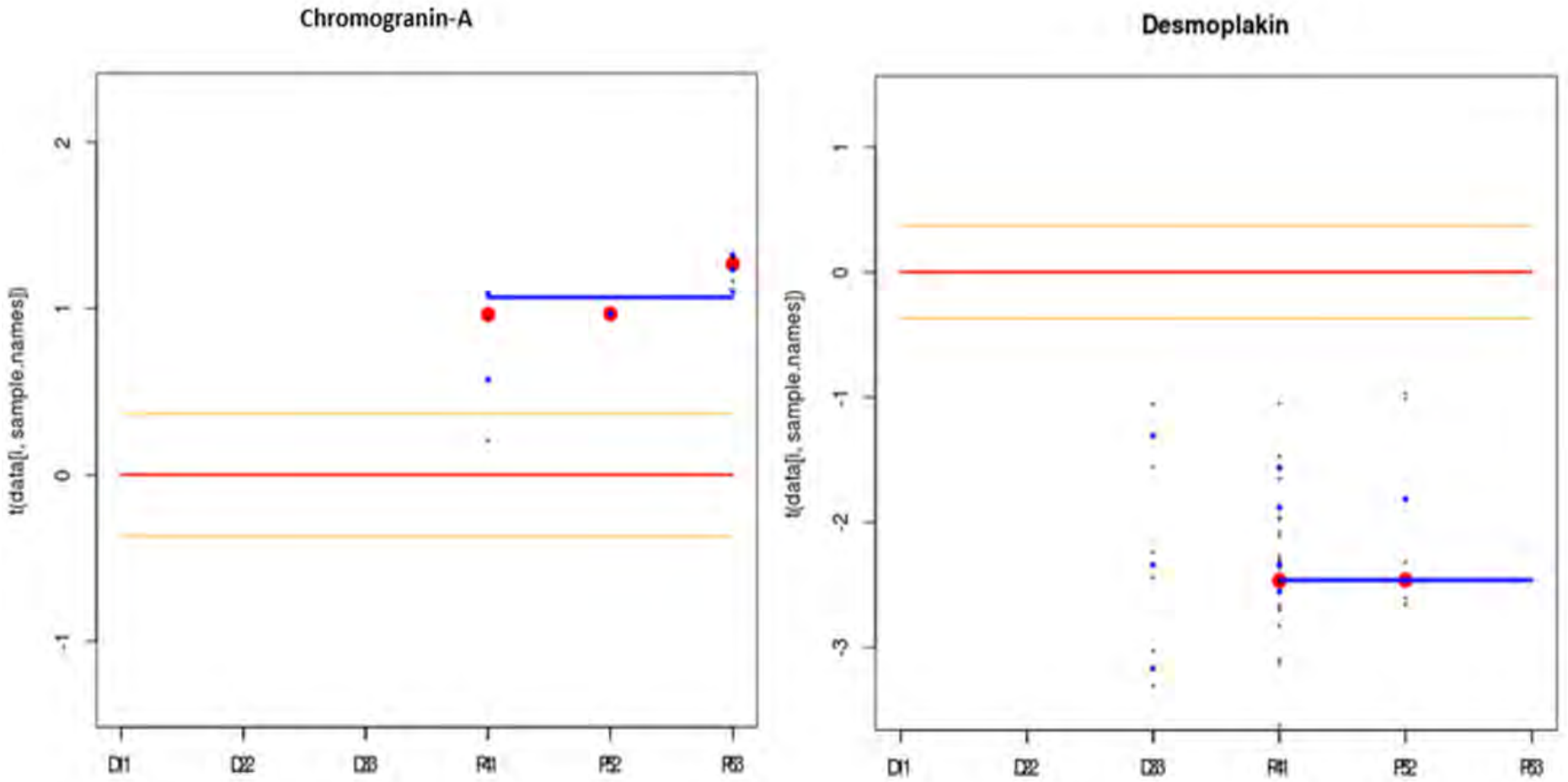

Figure 29: Two examples of proteins which have an average expression greater than 2SD with sufficiently small variation, therefore, selected as significantly differentially regulated

HIV-Tat alters protein translation and cytoskeletal regulation

Using the full complement of 407 differentially regulated protein groups, we performed GO-term enrichment analysis using PANTHER.[227] Other publications performing large scale discovery work to identify HIV-Tat induced dysregulation have identified similar dysregulated pathways to those identified in this study. Liao *et al* [232] performed qRT-PCR on selected few amino acid metabolism enzymes and, while we did not identify differential regulation specific enzymes analysed, we did identify differential regulation of 13 amino acid metabolism proteins. Alteration of amino acid metabolism is possibly due to altered energy metabolism as a result of HIV-Tat treatment. Additionally, among the array of observations outlined in Jarboui *et al*, [219] ribosomal biogenesis and the ubiquitin proteasome pathway were noted. Our data also shows a dysregulation in the ubiquitin proteasome pathway and we see increased expression of a wide array of ribosomal proteins. Following from this, the PANTHER molecular functions enriched in the differential data highlight HIV-Tat's ability to dysregulate several key cellular functions is apparent. In our data, the GO-term, binding, predominantly describes nucleic acid and protein binding functions. HIV-Tat's ability to alter nucleic acid metabolism is not at all surprising given that its primary function relative to HIV is to increase the HIV genome transcription through established mechanisms.[233] Complementary to this, HIV-Tat is, evidently, capable of altering the expression of a vast array of eukaryotic initiation factors (EIF) and ribosomal proteins; these form the bulk of the GO-term, *RNA binding* within the nucleic acid binding description. HIV-Tat has been shown to bind 2074 discrete DNA loci within the human genome.[225] It is, therefore, not surprising to see an increase in DNA binding in our data and it serves to validate our findings. In addition to the dysregulation seen by the downregulation of EIF's, we also see the opposite, upregulation of ribosomal proteins. From the findings, it is clear that HIV-Tat is able to effectively alter neurons' ability to regulated protein translation.

The protein binding term is dominated by cytoskeletal protein and receptor binding (**Figure 27B**). The purpose, relative to HIV, of dysregulating receptor proteins is not immediately clear and requires further investigation. However, it may be that HIV-Tat is capable of modulating the cellular antiviral response as these cellular cascades are

primarily initiated by ligand-receptor binding (INF, TNFα, TLR3 etc.).[234,235,29] Furthermore, HIV is known to bind and signal through integrin receptors. Thus, HIV1-Tat may be capable of increasing these proteins' abundance such as to provide HIV with greater effective binding on cell surfaces. Given that the dominant clinical manifestation of HAND is the loss of synapses, it is very interesting to see that the actin cytoskeleton, its inner and outer membrane binding partners and regulators are dysregulated within the protein binding term. Establishing and maintaining synapses relies heavily on the cytoskeleton, not only for structural support, but also for guidance queues.[236] As the cytoskeleton is a dynamic structure, dysregulation of its subunits and regulatory proteins will undoubtable impede the neurons' ability to maintain and establish properly functioning synapses or may lose them entirely. [237] Furthermore, analysis of the protein classes in PANTHER provides further support of HIV-Tat's ability to impede proper synapse function.

Cytoskeletal dysregulation features prominently in highly differentially regulated dataset

After applying the 2SD cutoff to the 407 significantly dysregulated proteins, we identified 29 as highly and stably differentially regulated as a result of HIV-Tat treatment. While classical pathway analysis was not feasible for such a small dataset, following from the GO-term analysis of the entire dysregulated set, we were able to postulate as to the biological impact of these highly differentially regulated proteins.

We have identified eight proteins, which we believe are indicative of synaptic damage. The process of building and maintaining synapses involves several cellular functions such as cell – cell adhesion, cytoskeletal reorganisation and axonal and synaptic guidance.[236] The maintenance of these is essential to the maintenance of synapses. Interestingly, each of these functions are represented in our list of highly significantly dysregulated proteins and were all down-regulated.

PRSS3 is a form of trypsin expressed in neural tissue and released into the extracellular space as a stress response. PRSS3 then specifically cleaves proteinase activated receptor 2 (PAR^2) which is a G protein coupled receptor. Among others, PAR^2 functions to alter cell adhesion by activating Rho. Interestingly, we also identified the Rho

guanine nucleotide exchange factor 17 as being down-regulated in our data. As the name suggests, this protein controls the activity of Rho by regulating its access to GTP. Together, this suggests a decrease in Rho activity. Decreased Rho activity is further supported by the decrease in SHROOM3 which is a potent Rho recruiting protein.[238] Rho is the primary co-ordinator of the actin cytoskeleton which forms the structural basis of neural extension and, thus, synapses.[239,240] If Rho activity is decreased, it is feasible to assume that the cells' ability to maintain synapses is decreased as well since Rho is a major cytoskeletal regulator in synapses.[237] In addition to providing structural support for cell extensions, the cytoskeleton also plays a role in cell adhesion, which is important for synapse stability as well. S100-A8 is involved in a multitude of cellular functions including but not limited to oncogenesis, signal transduction and energy metabolism.[241] While some of these activities may be relevant in HAD, its role in the modulation of the actin dependant cytoskeleton [241,242] is particularly interesting and relevant. There is limited information regarding its involvement in the cytoskeleton, however, its decrease seems relevant in lieu of the decreases of other observed cytoskeletal proteins. Its calcium binding properties are important to the polymerisation of actin [243,244] and they may be structurally important to desmosomes. [245] There are a multitude of cell adhesion molecules present in synapses and axons including the integral desmosome protein, desmoplakin. Desmoplakin is most well-known for its role in epidermal and cardiac cell adhesion but has also been identified in hippocampal granular cell synapses [246,247] where it functions in cell adhesion. Interestingly, the hippocampus is one of the most notably damaged areas in HAD patients with respect to synapse loss.[248] The desmoplakin binder, CSTA [249,250], and regulator, SHROOM3 [238,251], were also found to be down-regulated in our data. A decrease in the Rho-dependant CRMP1 has been shown to result in a loss of hippocampal synapses.[252] CRMP1 is known to function in axonal outgrowth and guidance via its interaction with Rho-dependant Semaphorins.[253] PSME2 belongs to a family of proteasomal proteins shown to be involved in synaptic regulation and neuronal plasticity.[254]

A surprising find was that two Immunoglobulin-like proteins, IGHA1 and IGLL5 were identified as being severely decreased. While we cannot draw any firm conclusions

about their involvement, it is interesting to note that Ig-like proteins have now been shown to be involved in synapse adhesion.[255] It is plausible that IGHA1 and IGLL5 are yet to be discovered neuronal adhesion molecules.

HIV-Tat affects key systems seemingly unrelated to protein translation or cytoskeletal regulation

Several other interesting and relevant dysregulated proteins were identified; however, further analysis will be required to speculate about their function in HIV-Tat induced neuronal toxicity as they seem to appear to function independently of the other dysregulated proteins identified in this study. Both PITPB and its isoform, PITPa with which it shares 77% sequence and 94% structural homology are expressed in the hippocampus. [256] However, only PITPa is known to contribute to axonal guidance and synaptic establishment.[257] Increased PITPb has been known to inhibit cells growth and a complete loss results in nonviable cells [258] and plays a role in neuronal vesicular trafficking.[259] An increase in Dopamine B-hydroxylase (DBH) results in increased norepinephrine (NE) production which has been shown to increase infectivity and replication of HIV in immune cells. [260,261] Consequently, increased DBH and production of NE may be depleting CNS dopamine levels. [262,263] Our data suggests that KCTD15, a TFAP-2α suppressor, expression is decreased by HIV-Tat treatment. TFAP-2α is a transcription factor capable of transcribing several known viral enhancer elements in the human genome. [264,265] This, therefore, suggests that HIV-Tat is promoting the transcription of host viral enhancer elements. Along with the above mentioned functional alterations induced by HIV-Tat, several proteins identified to be dysregulated are secreted (TFPI2, CHGA, MUCL1) and certainly warrant further investigation as putative diagnostic or prognostic markers for HAD. Furthermore, CHGA [266] and PRRC2C are thought to be diagnostic in AD; these too, certainly require further investigation using targeted methods.

In Summary, the data presented here provide clear evidence for HIV-Tat's ability to, at least in part, contribute to the major clinical HAND phenotype; synapse loss. Go-Term enrichment analysis in PANTHER reveals that several well established neurodegeneration and axonal guidance pathways are dysregulated. Furthermore, we have identified several other dysregulated cellular functions which undoubtedly

contribute to the overall phenotype of HAND. Protein translation dysregulation has not previously been implicated in HAND, but is known to contribute to other neurodegenerative diseases such as AD, Huntington's, Schizophrenia, PD.[267,268,269] While we report direct evidence for synapse dysregulation via cytoskeletal dysregulation, dysregulation of protein translation may also play a significant role in synapse loss as was shown to be the case in AD.[270]

Chapter 4

Extensive pathway analysis of SILAC labelled proteomic and transcriptomic data from HIV-Tat treated SY-SY5Y neuroblastoma cells

Abstract

Despite affecting up to 70% of HIV^+ patients and being the leading cause of dementia in patients under 40 years, the molecular mechanisms involved in the onset of HAND is not well understood. To this end, we performed SILAC-based quantitative proteomic and transcriptomic analysis of HIV-Tat treated neuroblastoma (SH-SY5Y) cells. We identified 407 proteins and 1074 transcripts as significantly differentially regulated. In depth analysis of the dysregulated pathways identified by pathway analysis tools revealed overwhelming evidence that HIV-Tat activates numerous antiviral and inflammatory response pathways. In other cell types, these may aid in the specific dysregulation of the protein synthesis and cytoskeletal functions to aid efficient HIV replication. In neural cells, dysregulation of these pathways likely have a profound effect on the neurons' ability to maintain synapses, which can lead to neuronal loss of function and, ultimately, dementia.

Introduction

HIV-1 infection can induce an array of neurocognitive impairments termed HIV-associated neurocognitive disorders (HAND). The HAND complex describes three standardised measures of dysfunction; asymptomatic impairment (ANI), mild cognitive disorder (MND) and HIV-associated dementia (HAD).[271] Currently, there are no biomarkers to predict or diagnose the disease and there are no specific treatments for HAND. Initially, the disease was classified as being the result of neuronal loss in various brain regions. Recently, however, it has been shown that cognitive scores correlate most closely with synapse loss rather than neuronal loss.[217] This switch in the disease profile may be directly linked to the advent and availability of highly active antiretroviral treatment (HAART). Indeed, since the implementation of HAART, there has been a decrease in the incidence of HAD but an increase in MND.[1,272] This can be attributed to increased life expectancy of HIV patients. In this model, however, a source of neurotoxic agents must still exist which leads to a slower but notable neurocognitive decline in patients. HAND has been shown to persist and progress despite undetectable CNS viral loads.[273,60] It was showed that HIV-Tat protein is still secreted and detectable in blood despite HIV-treatment and undetectable CSF and serum viremia in the majority of patients.[274] Depending on the specific Antiviral regiment being administered, this may be even more pronounced within the brain which may serve as a viral reservoir of actively replicating virus.[275] None the less, it is highly likely that the CNS and other tissues are exposed to HIV-Tat in most HIV patients despite controlled HIV replication.

HIV-Tat has been studied as a possible HAND causative agent for many years and has been shown to dysregulate neurons in several ways. The most prominent of these has been the induction of apoptosis.[276] As HIV-Tat has been shown to induce apoptosis in neuronal cells, significant efforts have gone into elucidating a molecular mechanism of this apoptosis induction. However, given the multifunctional nature of HIV-Tat and the myriad of cellular pathways that can result in apoptosis, it is not surprising that several different pathways have been implicated. One undeniable, central feature is that GSK-3β activity is increased.[27] A popular proposed mechanism demonstrates that, upon HIV-Tat treatment, TNFα and PAF function to inhibit the PI3K/AKT pathway, thereby,

resulting in active GSK-3β which is then capable of facilitating apoptosis induction.[106,101] However, the upstream source of TNFα upregulation is not elucidated.

A popular alternative to this involves increased cellular calcium and ROS production. It has been shown that HIV-Tat treatment results in increased cellular calcium in neurons as well as mitochondrial dysfunction. When cellular calcium increases as a result of Endoplasmic reticulum (ER) calcium efflux, mitochondrial calcium influx in increased. This calcium influx results in mitochondrial membrane hyperpolarisation (MMHP).[109] This, in turn, results in increased ATP and ROS production. ER stress and subsequent calcium induced MMHP are known to induce apoptosis in neurons.[277] Normal *et al* present excellent work demonstrating that this is possible by HIV-Tat binding to the Ryanodine receptor and inducing ER stress.[229]

While, in their isolation, all these pathways are seemingly able to induce apoptosis, we do not yet know how all of these pathways contribute, if they do at all, to the HIV dementia phenotype. Added to that, HIV dementia has been show to correlate most closely with synapse loss rather than neuronal apoptosis. Based on this, together with the observation that HIV-Tat is able to bind 2074 sites in the human genome,[225] there are other possible molecular events taking place in response to HIV-Tat. Together with this wealth of literary information about the cellular dysregulations induced by HIV-Tat, unfortunately, there exists contradictory data; much of which can be attributed to work being done in different cell types. These contradictions exist on so grand a scale that HIV-Tat is reported to be both pro and anti-apoptotic.[278] Understanding these dysregulated pathways may allow us to inform better treatments for HAD patients. To identify as many of these events as possible, we need to circumvent a downfall inherent to classical molecular biology techniques used to identify pathway involvement in a particular setting which is that it ignores all non-target molecules and pathways. As a result, for one to present a unified set of molecular events to consolidate the great wealth of information published in this area, one has to rely on conjecture of possible outcomes of interactions.

Such a proposal can only be realized by a few high-throughput cell state analysis techniques such as MS and gene expression analysis. These two incredibly powerful

platforms allow us to take a snapshot of the cell state at a chosen time and identify non-targeted, global dysregulation in the cell. Along with identifying currently unknown functions, these platforms could allow us to determine the pathways ultimately responsible for apoptosis and whether those are also responsible for other clinical symptoms observed. Such a global analysis would also provide insight into additional, unknown, pathways HIV-Tat might be dysregulating.

A key requirement for any global MS experiment seeking to perform a differential analysis is sound statistical methodology. Typically, a fold change approach is used to identify differentially regulated proteins. However, given the recent advancements in peptide mass spectrometry and nanoLC allowing highly reproducible data generation, new statistical approaches are being explored. Recently, several publications have employed a t-test based statistical differential analysis. [279] In comparison to a fold change based approach, the t-test allows for much smaller changes in protein abundance to be deemed significant which equates to greater sensitivity and specificity in identifying differential expression.

In this Chapter, we describe the analysis of both the SILAC-labelled proteome and complimentary transcriptome of HIV-Tat treated SH-SY5Y neuroblastoma cells. We identify and quantitate 3077 SILAC protein group pairs, of which 407 were identified as statistically significantly dysregulated. Additionally, we identified 1074 differentially regulated transcripts. Pathway analysis on both these datasets reveal rather interesting cascade of pathways. It is apparent from the gene expression analysis that HIV-Tat activates pattern recognition receptors (PRR) such as RIG-1 and TLR's which are cellular dsRNA sensors. These can be seen to activate an antiviral response via the activation of INFα/γ. A primary means by which the antiviral system resists viral infection is to modulate the protein synthesis pathways but it also signals through and alters cytoskeletal regulation. Both of these are evidenced in the proteomic data. Together, these data provide a cascade map of the dysregulation induced by HIV-Tat and can be seen to adversely affect neuronal synapse maintenance and apoptosis.

Materials and Methods

Proteomic data used for pathway analysis

The highly significantly dysregulated proteomic data presented in Chapter 3 was generated by applying an additional 2 SD cutoff to the significantly dysregulated data identified by t-tests (as described in Chapter 3, section: Data processing and bioinformatic analysis). In this chapter, the t-test derived significantly dysregulated data was further analysed using IPA (QIAGEN Redwood City, www.qiagen.com/ingenuity).

RNA extractions

Since SILAC has no impact on cellular functions, RNA was extracted from unlabelled, HIV-tat treated cells. The cells were treated identical to those used to generate the data represented in Chapter 2, **Figure 23B**.

RNA extractions were performed using the QIAzol^{tm} (QIAGEN) reagent and a modified manufacturer's protocol. The entire protocol was completed as per the manufacturer's instructions except that all incubation steps were performed on ice and all centrifugations were performed at 4^{o}C. We found that this yielded higher quality RNA. Briefly, cells were removed from the plate by removing media and washing the cells in warmed PBS. Trypsin was then used to detach cells from the culture dish and was then immediately quenched with trypsin inhibitor once cells are visibly lifted. The cell suspension was then transferred to a 2ml vial and centrifuged and 600g for 10minutes. The cells are then washed with warmed PBS and centrifuged at 600 g for 10 minutes. The cell pellet was the suspended in 500 µl of QIAzol^{tm} reagent and was incubated on ice for 25 minutes with occasional gentle end over end mixing. I then added 100 µl of cold chloroform and shaken vigorously for 15 seconds. The tube was then incubated on ice for 3 minutes followed by centrifugation at 12000 g for 15 minutes at 4^{o}C. The upper aqueous phase was transferred to a clean vial and 250 µl ice-cold isopropanol was added to the aqueous phase and mixed by vortexing. The mixture was then incubated on ice for 10 minutes followed by centrifugation at 12000g at 4^{o}C for 10 minutes. The RNA pellet was then recovered by removing the supernatant, washed with 1 ml of ice-cold 75% absolute ethanol and centrifuged at 7500 g at 4^{o}C for 5

minutes. The RNA pellet was the air-dried completely and suspended in RNA free water for quantitation and quality assessment by UV spectroscopy using a nanodrop instrument.

Affymetrix Gene array analysis

Samples were analysed on two separate occasions where four samples (2 treated and two untreated) were run initially and two samples (one treated and one untreated) were analysed at a later date. The gene expression analysis was performed using the Affymetrix platform and HuGene-1_0-st-v1. The quality and concentration of the samples were assessed using the Nanodrop (spectrophotometer) and the RNA integrity determined using the Agilent Bioanalyser. Using the Ambion WT Expression assay the samples were labelled in accordance with the protocol. A control RNA sample was included to monitor the assay performance. For the purpose of ensuring sufficient labelled target for hybridisation to the Human Gene ST array, 200ng of RNA was used for cDNA synthesis. Following cDNA synthesis, *in vitro* transcription was carried out to generate antisense RNA (cRNA). The cRNA was cleaned up in accordance with the protocol and the concentration and assessment of size distribution determined using the Nanodrop spectrophotometer and Agilent Bioanalyser respectively. Using 15µg of cRNA, 1st strand cDNA synthesis was carried out followed by cRNA hydrolysis. The sense strand cDNA was cleaned up in accordance with the protocol and the concentration and the size distribution determined using the Nanodrop spectrophotometer and Agilent Bioanalyser respectively. In order to proceed with labelling, 5.5µg of sense strand cDNA was fragmented, assessed on the Agilent Bioanalyser for complete fragmentation and subsequently end-labelled. The prepared targets were hybridised to the arrays for 17 hours. After the hybridisation period, the arrays were washed and stained using the GeneChip® Fluidics Station 450 and scanned using the GeneChip® Scanner 3000 7G.

Gene expression data analysis

The data analysis including the differential analysis of the transcriptomic data was performed by Katie Viljoen, a fellow PhD student at the time. Although, I will include a brief description of the raw data analysis performed. I performed the pathway analysis of the differentially expressed data.

The data was preprocessed in R using the Bioconductor packages,[280] frma[281] and ComBat[282] for normalization and batch correction respectively. The data was generated in two separate experiments in which the cell culture, RNA extractions and Affymetrix array hybridisation were duplicated. However, batch effects were identified and corrected for using ComBat. Differential expression analysis was performed using the Bioconductor package, Limma. Limma uses a moderated t-test to compute p-values in which both the standard error and the degrees of freedom are modified. A p-value cutoff of 0.01 was applied in the selection of significantly differentially regulated transcripts.

Pathway analysis

Pathway analysis for both gene expression and proteomic data were performed in the IPA software package. Significantly dysregulated gene names and log-fold or ratios for each gene/protein, respectively, were submitted into the IPA core analysis function. The IPA core analysis function generates an activity profile for the pathways and functions dysregulated in HIV-Tat treated cells. Dysregulated genes/proteins were used as overlays on pathways to easily identify and display significantly dysregulated pathway members. Biological significance of the data was determined by comparing the differences in dysregulation induced by both experimental conditions. Briefly, the pathways were grouped into common functions and matched to dysregulated functions identified by IPA. Based on literature and the IPA analyses, the dysregulation induced was interpreted relative to HIV replication as well as neurodegenerative functions. Where possible, mechanisms underlying the dysregulation as well as their implications are proposed.

Pathway maps displaying dysregulated genes are generated from transcriptomic data while all pathway maps displaying dysregulated proteins are generated from proteomic data.

Results

HIV-Tat induces cell death and widespread functional dysregulation

We elected to harvest protein when approximately 20% cell death was reached as determined by MTT assay on parallel experiments (data shown in Chapter 2). The

proteomic (Dysregulated SILAC proteins; Appendix 2) and transcriptomic (Genes dysregulated in transcriptomic analysis: Appendix 3) analysis identified 1074 and 407 proteins as differentially regulated respectively. Although some overlap in gene/protein identifications was observed, the large majority were restricted to one dataset or the other. A similar observation was reported by Woodhouse, *et al*.[283] Despite several cellular functions and pathways being specifically or better represented in one dataset over the other, there was a large overlap between dysregulated pathways and functions. Obvious trends in the pathway can be discerned from the most highly dysregulated aspects of the data. The proteomic pathway analysis displayed a wider variety of cellular effects with the most highly dysregulated canonical pathways indicative of protein translation dysregulation (EIF2 signalling, mTOR signalling and the regulation of EIF4 and p70S6K signalling), protein degradation (protein ubiquitination pathway) and cytoskeletal regulation (remodelling of epithelial adherens junctions) (**Table 2A**). The transcriptomic pathway analysis also provided evidence for functions highlighted in the proteomic data, but was dominated by pathways indicative of an immune activation (**Table 2B**).

However, all the dysregulated pathways, their interactions with each other and their contributions to the dysregulated functions should be analysed for a deeper and more meaningful analysis. Given HIV-Tat's function as a transactivator of transcription, it is unsurprising that fewer pathways are inhibited (**Figure 30**) than activated (**Figure 31**). As the primary regulator of protein synthesis, the inhibition of EIF2 signalling at the gene level is interesting. Similarly, the inhibition of several cell-surface receptors including but not limited to G protein subunits, Gαs (Gai3) and GNRH signalling is noteworthy.

Table 2: An IPA generated summary of the pathways, disease and cellular functions dysregulated in the proteomic (A) and transcriptomic (B) data respectively. While the most highly dysregulated pathways do not overlap, the functional implications do. Both datasets are indicative of neurological disease and cell survival deficits.

A

Proteomic pathway analysis summary	
Pathway	**p-value**
EIF2 Signaling	2.95E-18
Regulation of eIF4 and p70S6K Signaling	6.19E-11
Protein Ubiquitination Pathway	1.37E-07
mTOR Signaling	1.59E-07
Remodeling of Epithelial Adherens Junctions	7.05E-07

Disease and Disorder	p-value
Dermatological Diseases and Conditions	2.01E-09
Neurological Disease	1.73E-08
Psychological Disorders	4.27E-08
Skeletal and Muscular Disorders	4.27E-08
Infectious Disease	2.03E-07

Molecular and Cellular Function	p-value
Cellular Growth and Proliferation	5.13E-17
Protein Synthesis	4.90E-15
Cell Death and Survival	1.33E-12
Gene Expression	5.19E-12
Cellular Development	2.05E-11

B

Transcriptome pathway analysis summary	
Pathway	**p-value**
Activation of IRF by Cytosolic Pattern Recognition Receptors	5.93E-05
Role of RIG1-like Receptors in Antiviral Innate Immunity	3.38E-04
TWEAK Signaling	7.84E-04
Role of PKR in Interferon Induction and Antiviral Response	2.20E-03
Hypoxia Signaling in the Cardiovascular System	2.85E-03

Disease and Disorder	p-value
Cardiovascular Disease	2.27E-03
Organismal Injury and Abnormalities	2.27E-03
Neurological Disease	3.25E-03
Cancer	6.60E-03
Inflammatory Response	1.12E-02

Molecular and Cellular Function	p-value
Cell Morphology	3.73E-04
Cellular Assembly and Organization	3.73E-04
Cellular Development	4.17E-04
Cell Death and Survival	4.89E-04
Cellular Function and Maintenance	4.89E-04

The regulation of DARPP-32 is very complex and relies on many kinases and phosphatases,[284] however, the inhibition of *Dopamine-DARPP32 Feedback in cAMP Signalling* is significant as it is associated with traumatic brain injury and executive function, learning, and memory deficits.[285] The inhibition of death receptor signalling is counter intuitive given that HIV-Tat is known to induce apoptosis. A strong activation of immune functions can be seen in the activation of *Role of RIG1-like Receptors in Antiviral Innate Immunity, Role of Pattern Recognition Receptors in Recognition of Bacteria and Viruses, Activation of IRF by Cytosolic Pattern Recognition Receptors, TNFR1* and *TNFR2 Signalling* and many others. The activation of inflammatory pathways is complimented by the predicted activation and recruitment of many immune cell types (**Figure 32**) In the discussion of the apparent activation of an inflammatory response, it is not being suggested that these neuroblastoma cells have the ability to induce a classical inflammatory response as would be produced by cells of the immune system. Instead, the inflammatory and antiviral responses described herein are those typical of non-immune cells, which are capable of producing and responding to inflammatory cytokines in order to recruit immune cells and mount an initial response to a cellular stress such as viral infection. The induction of apoptosis

can be seen in the activation of *apoptosis* and *ceramide* signalling as well as *induction of apoptosis by HIV1*. In conjunction with the inhibition of one G protein subunit (Gai3), Gα12/13 and Gαi signalling is activated.

Transcriptomic data identified a comprehensive inflammatory response

Pathway analysis of the transcriptomic data revealed strong activation of several inflammatory antiviral pathways and molecules. We see a strong upregulation of Interferon regulatory factor (IRF) 7 as well as type-1 interferon-α and type-2 interferon-γ (**Figure 33A**). These are likely functions of the activated PRR pathways such as TLR or RIG-1 activation as displayed in **(Figure 33B).** The activation of the cytoplasmic dsRNA receptors, RIG-1 and MDA5 lead to the activation of IRF and a subsequent activation of an interferon mediated inflammatory response.[286] This is accompanied by activation of several other antiviral, proinflammatory pathways such as *TWEAK signalling* which activates and signals through FADD and TRAF which are both pro-apoptotic **(Figure 34A)**. Complimentary to an inflammatory activation, several TNFα family members are upregulated along with their receptor signalling; TNFR1, TNFR2 and TREM1. Central to immune activation and many other cellular processes, NF-κB is strongly activated. NF-κB plays a role in a diverse array of cellular pathways and functions as it regulates the transcription of many genes. Since NF-κB is such a multifunctional transcription factor, we wanted to determine which aspects of the data are being influenced by its activation. **Figure 34B** shows that dysregulated proteins involved in NF-κB also signals in a host of antiviral inflammatory pathways. As may be expected given the inflammatory environment predicted in the HIV-Tat treated cells, NF-κB is also signalling in a pro-apoptotic capacity. The antiviral response brings about several alterations in cellular dynamics; most importantly, its effects on protein translation and cytoskeletal regulation play an important role in the process.

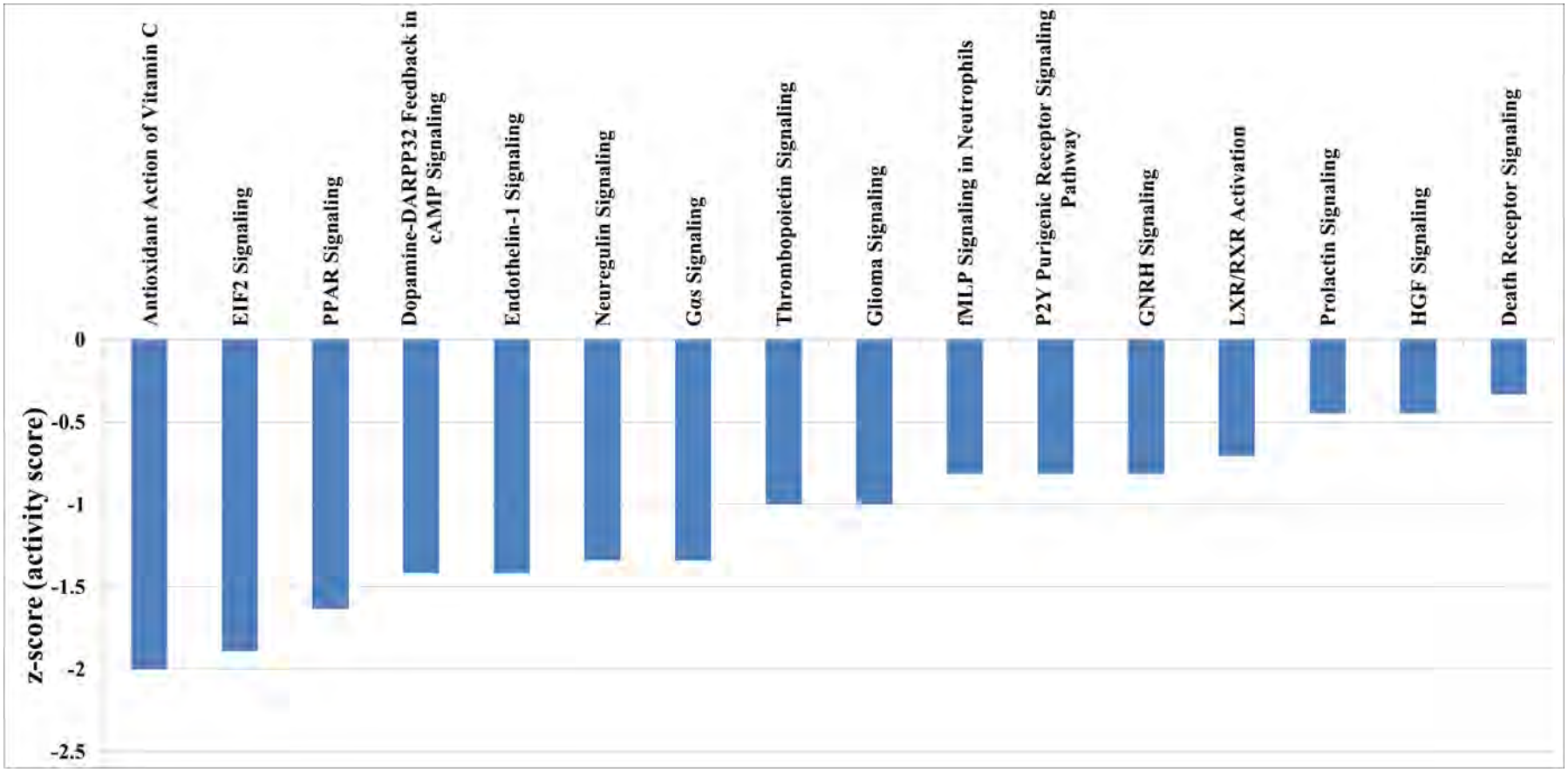

Figure 30: HIV-Tat inhibited pathways identified in transcriptomic data.

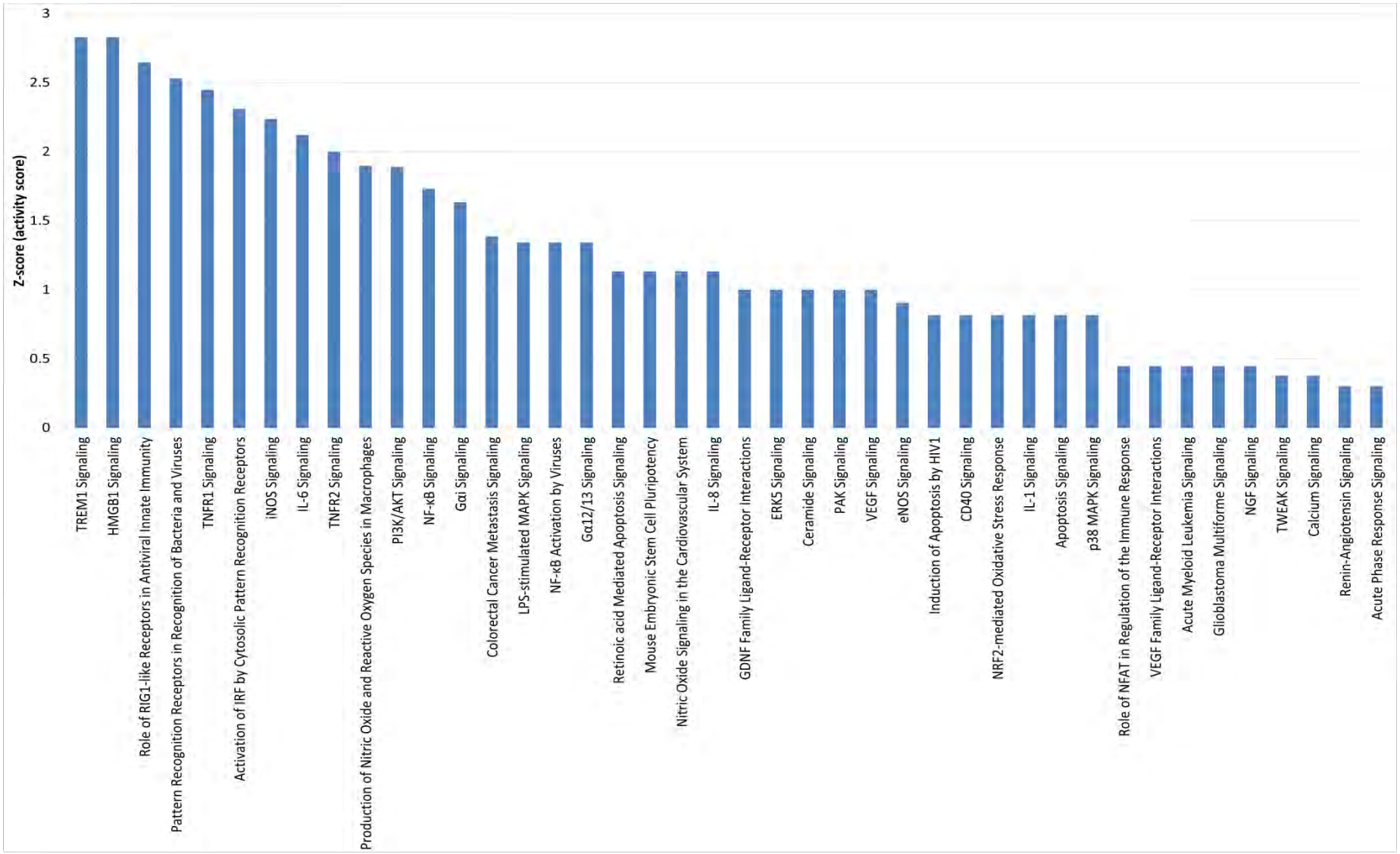

Figure 31: HIV-Tat activated canonical pathways identified in the transcriptomic data evidences a comprehensive inflammatory activation

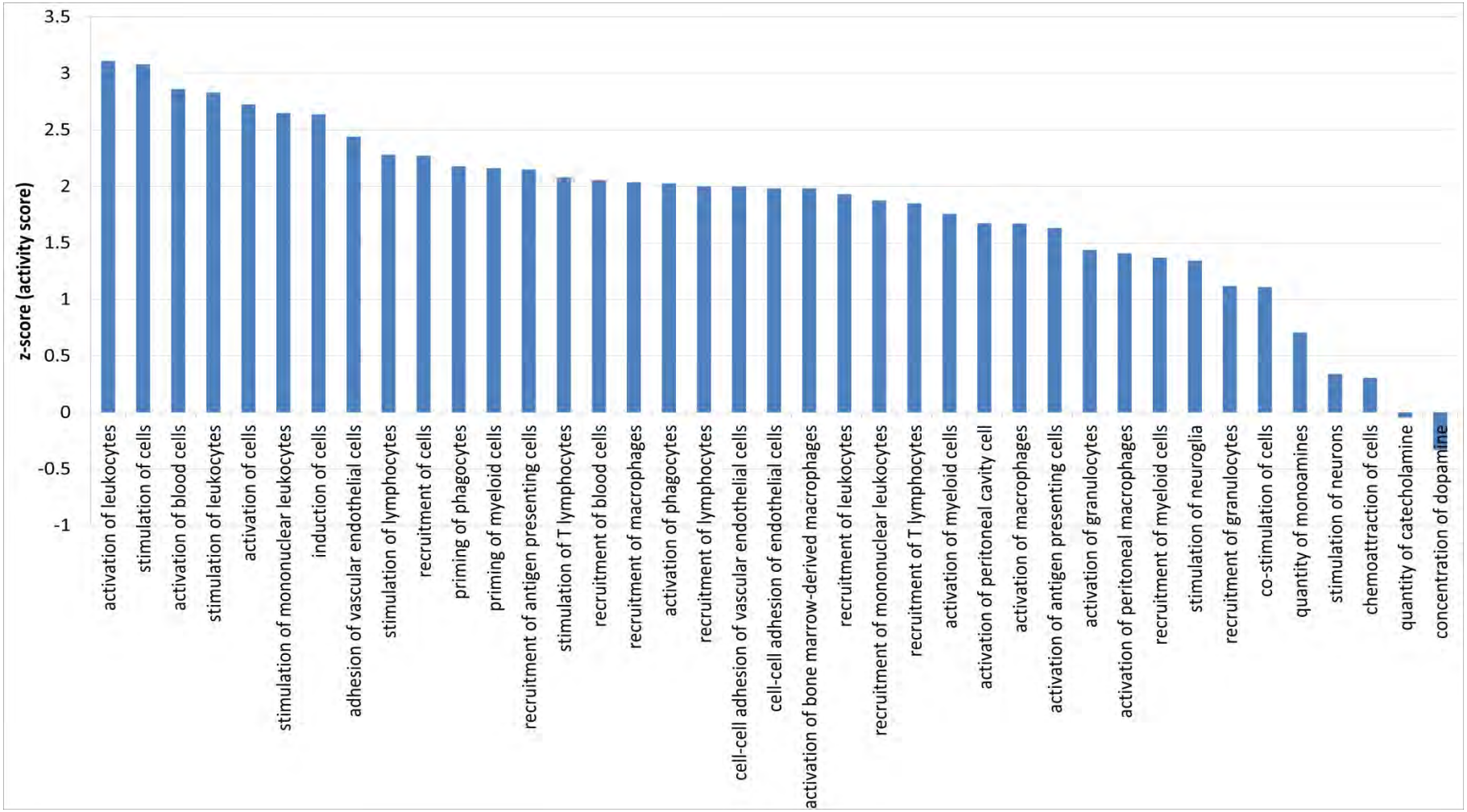

Figure 32: Cell - Cell signalling functions predicted by IPA analysis of the transcriptomic data. Some of the most dramatic function activation occurs in functions related to immune activation in the recruitment of immune cells.

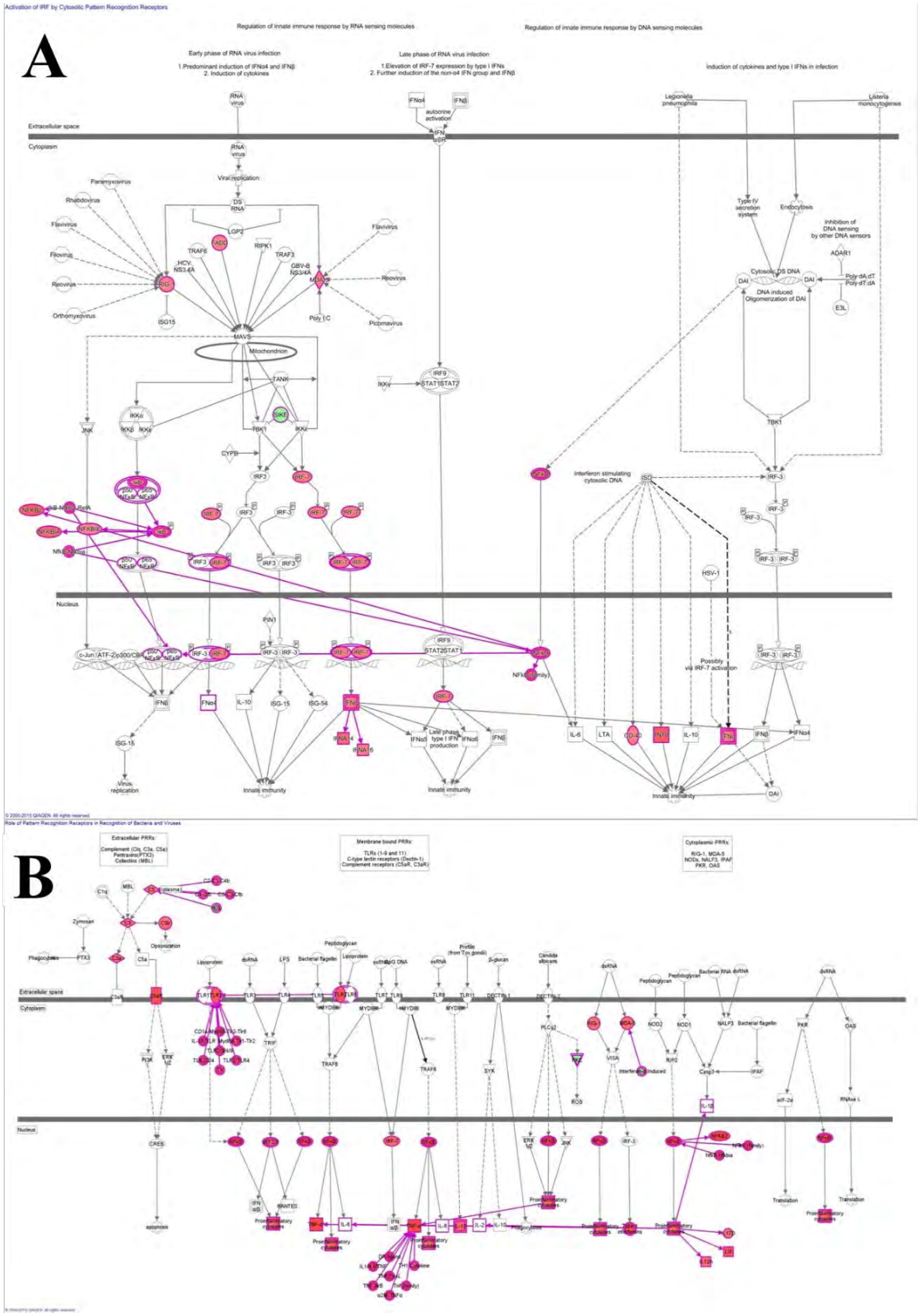

Figure 33: Pathway maps of differentially regulated genes in the (A) Interferon regulatory factor (IRF) and (B) Pattern recognition receptor pathways. These pathways show the activation of a vast array of proinflammatory cytokines as well as the activated receptors which mediate and regulate the inflammatory response. Green shaded proteins are identified and are decreased compared to the control while red shaded proteins have increased abundance.

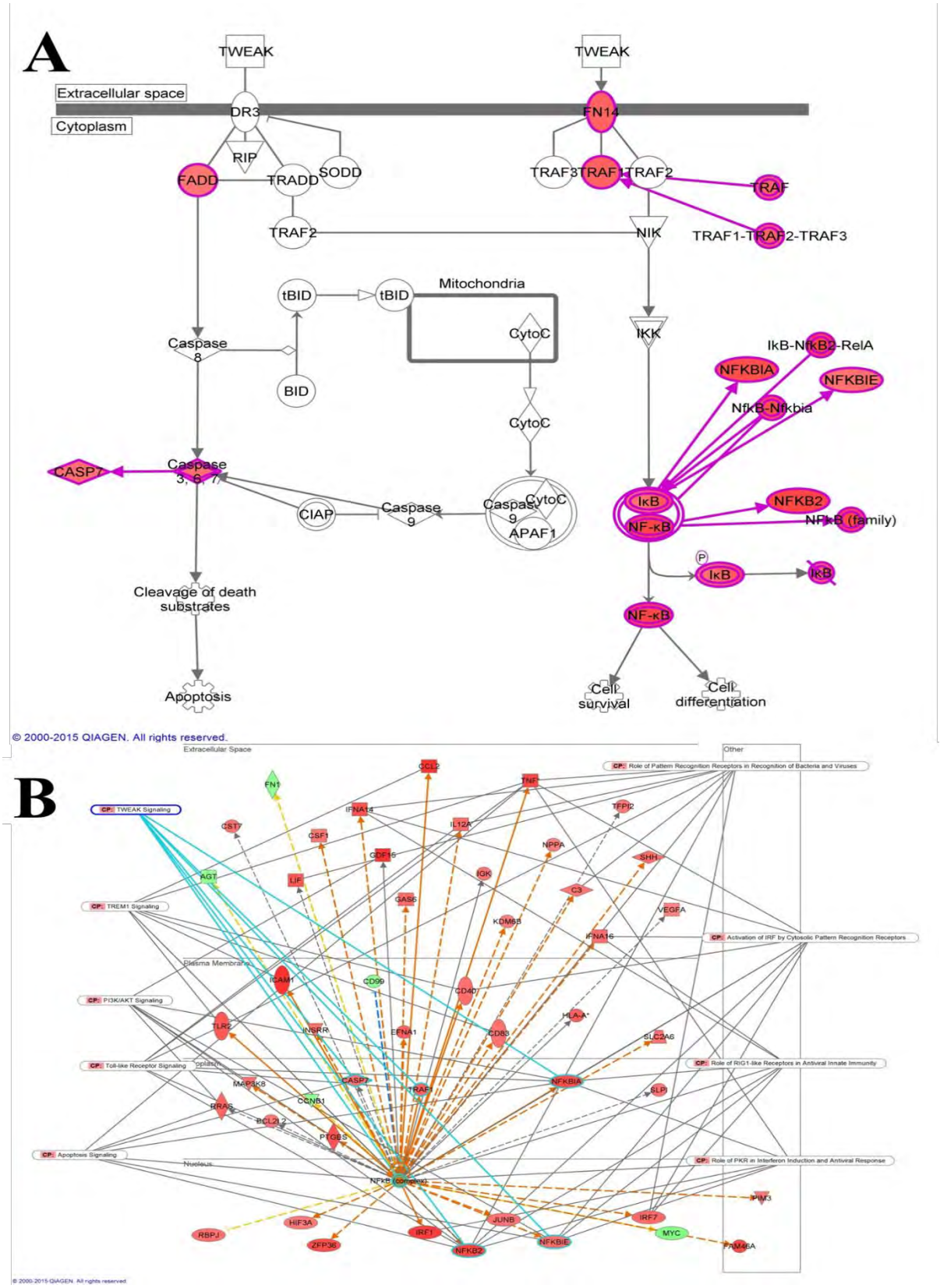

Figure 34: A) Dysregulated genes identified in the transcriptomic data overlaid onto the TWEAK pathway. TWEAK regulated the induction of several inflammatory cytokines and can induce apoptosis. B) Dysregulated NF-κB associated genes identified in the transcriptomic data overlaid. NF-κB activation is central to the inflammatory response activation as seen in the transcriptomic data. Several pathways, in which NF-κB plays a central signalling role have been overlaid onto the NF-κB associated proteins identified. Green shaded proteins are identified and are decreased compared to the control while red shaded proteins have increased abundance.

Inhibition of several EIF's indicate attenuation of protein synthesis

EiF2 signalling was the pathway most highly dysregulated by HIV-Tat treatment. From the pathway map in **Figure 35A** it is evident that all but two eukaryotic initiation factor (EIF3H and EIF4B) were upregulated in the differentially expressed dataset. Ribosomal protein expression is less uniformly affected with ~60% being decreased with the remainder increased in the differentially regulated set of proteins. Although EIF2 signalling pathway receives regulatory input from a host of pathways, it remains the master regulator of protein synthesis.[287] It is therefore the primary pathway by which to assess the regulation of protein within the cell. Protein synthesis is, however, influenced by a number of other pathways which cascade onto the EIF2 signalling pathway. Together with this, it must be noted that loss of individual proteins in the protein translation pathways can offset increases of other proteins. Along with the loss of EIF3H and EIF4B, the increase in EIF4E inhibitor, 4EBP would serve to inhibit 40s ribosome binding and scanning.

Since the EIF2 signalling pathway describes only protein synthesis, the physiological implications are not easily discernible from this data alone. The functional implications of the dysregulation of protein synthesis can be seen in **Figure 35B** which shows that functions related to protein synthesis are seemingly activated by HIV-Tat treatment despite the observed decrease of several EIF and ribosomal proteins.

Endoplasmic reticulum stress could account for the attenuation of protein synthesis

As can be seen in **Figure 35A** the ER, via PERK, is one of four major protein synthesis regulators capable of inhibiting global protein synthesis. Coupled to the activation of the unfolded protein response (UPR) (**Figure 36A**), IPA diseases and functions analysis predicts general ER stress. This serves as another means through which HIV-Tat can attenuate global protein synthesis. As part of UPR, protein degradation is also increased by proteasomal activation which is evidenced in the data by the upregulation of several proteasomal proteins and protein ubiquitination in (**Figure 36B**).

Attenuated protein synthesis is associated with other neurodegenerative diseases

Defects in the regulation of protein translation has been linked to an array of neurodegenerative diseases including AD, Huntington's, PD, Schizophrenia. [267,268,269]

The importance of the dysregulation of protein synthesis in neurological and psychological diseases as well as neuronal cell death which share 17, 13 and 5 dysregulated proteins with protein synthesis pathways respectively can be seen in **Figure 38**. This serves to highlight the relationship between individual dysregulated pathways and functions and phenotypic manifestation of disease.

Endoplasmic reticulum stress could account for the mitochondrial dysfunction

An additional consequence of ER stress and the reported interaction between HIV-Tat and the Ryanodine receptor, is that cytoplasmic calcium levels increase.[229] This is further evidenced by the increase in calcium signalling (**Figure 31**)**.** The mitochondria are particularly sensitive to cellular calcium where increases result in mitochondrial membrane hyperpolarisation (MMHP) and altered energy production. As with protein synthesis, energy production is tightly controlled by many pathways and proteins. Our data not only shows dysregulation of proteins related to mitochondrial dysregulation, but we also see dysregulation of the function, energy production. All cellular functions rely on energy, thus, dysregulation in energy production may have significant effects on cellular homeostasis. Once more, the complex cellular interplay and regulatory systems involved in energy production share many proteins which play a role in known neurological and psychological diseases. An additional consequence of MMPH is the increased generation of ROS.[288] **Figure 37** shows that the production of ROS is not only altered, but also shares proteins with, and is therefore associated with infectious diseases, neurological disease, gene expression and apoptosis.

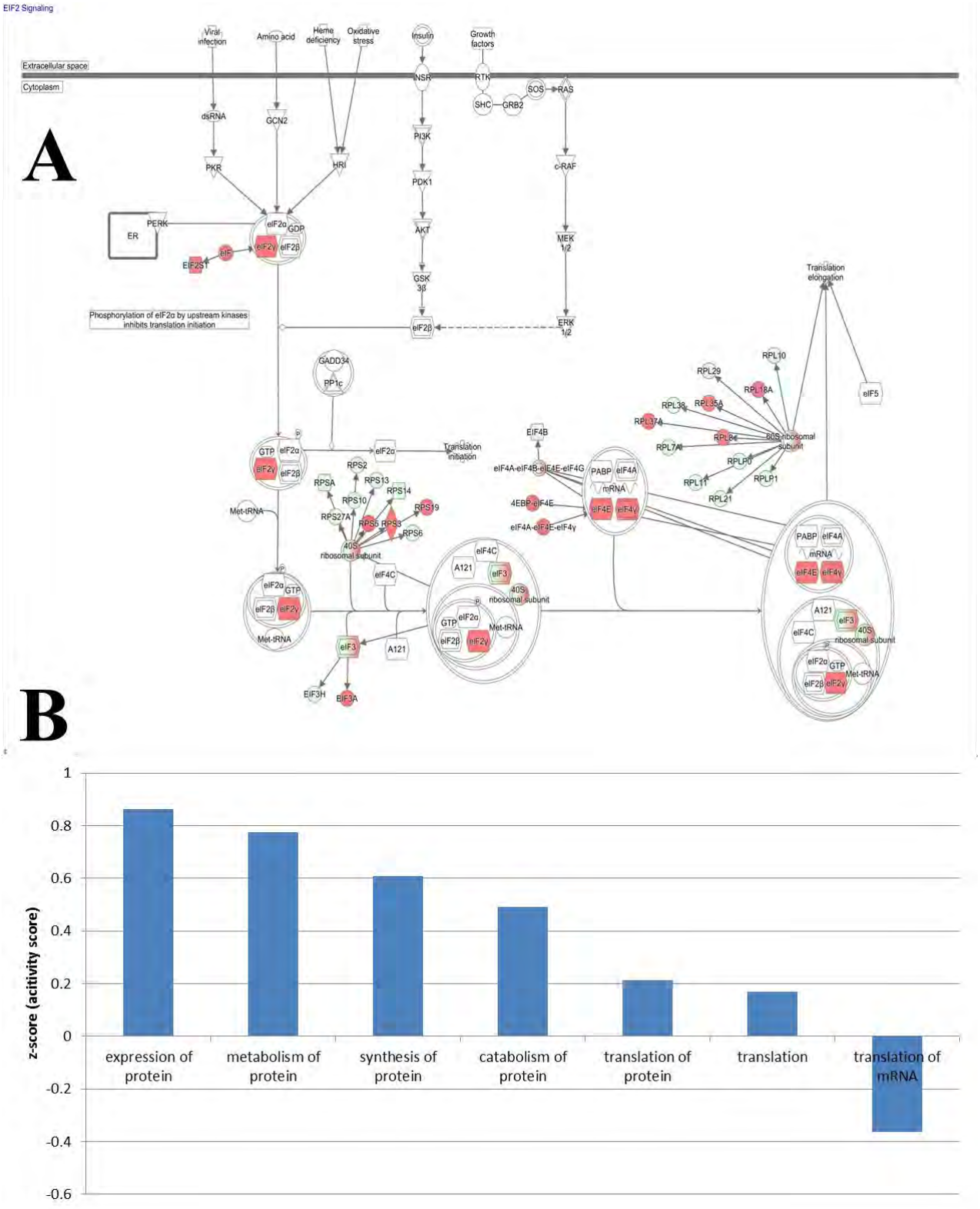

Figure 35: A) Proteins dysregulated in the proteomic data overlaid onto the EIF2 signalling pathway. Green shaded proteins are identified and are decreased compared to the control while red shaded proteins have increased abundance. B) Functions relating to protein synthesis. All functions relating to protein synthesis are activated except for translation of mRNA.

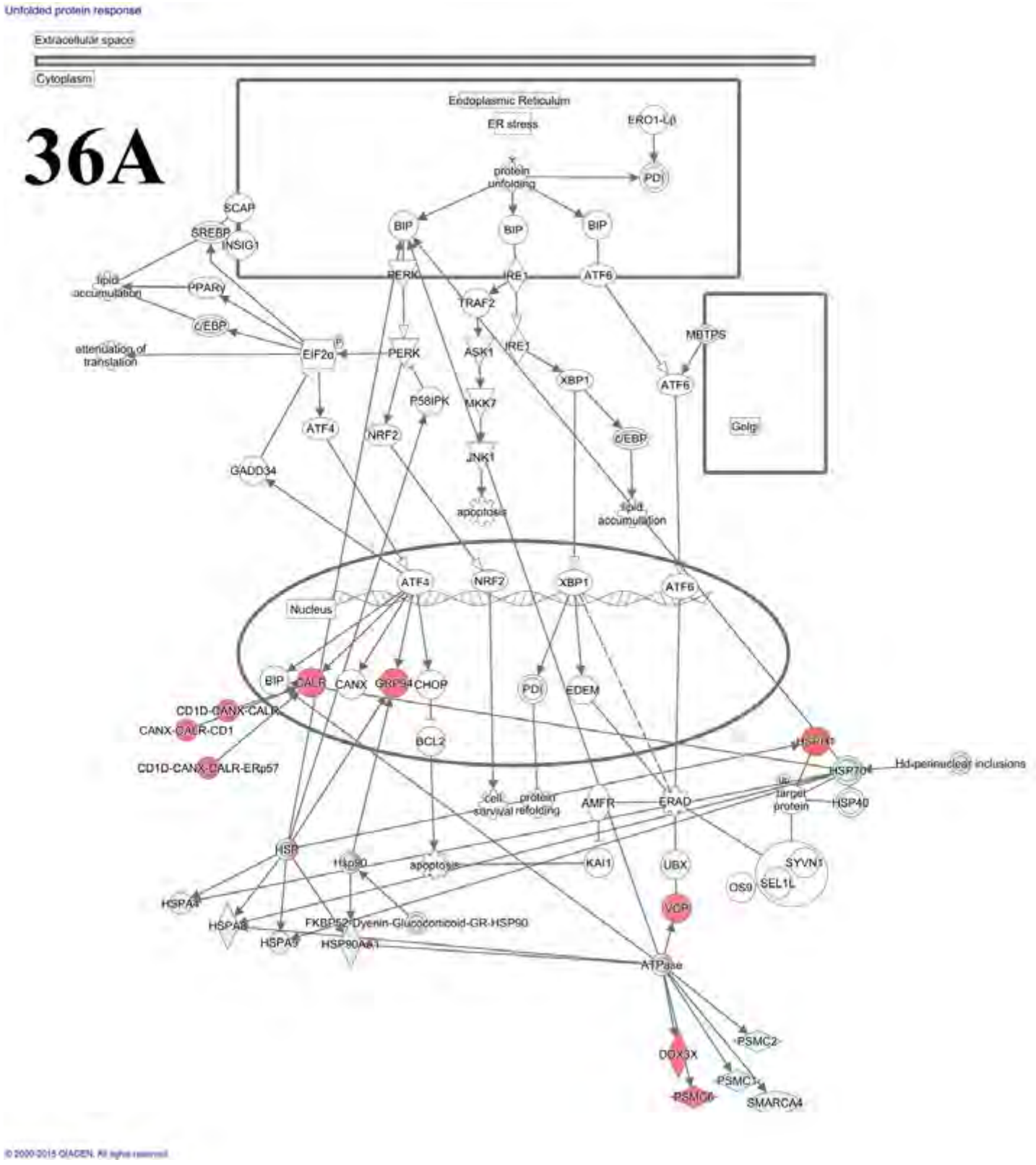

36B

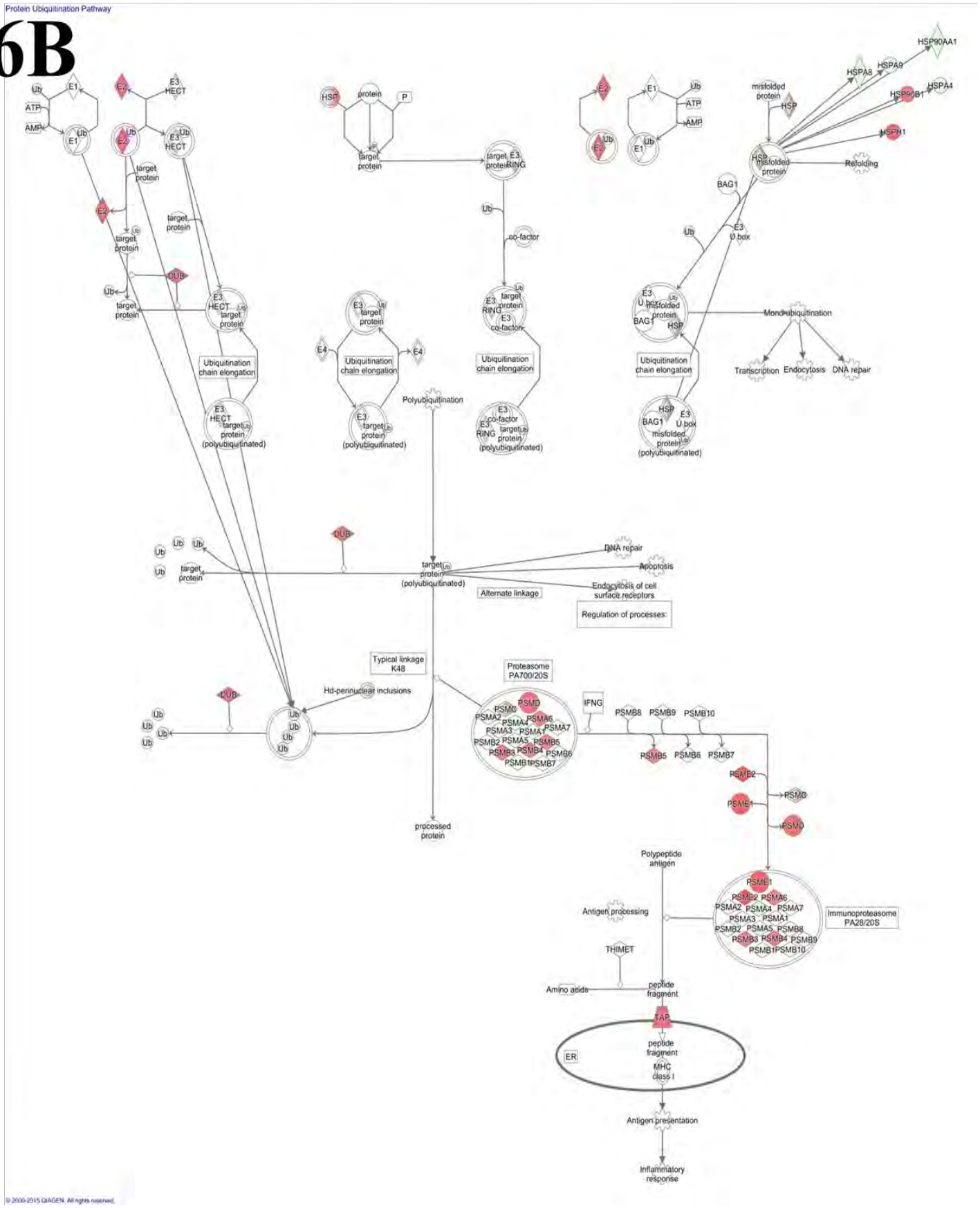

Figure 36: Proteins dysregulated in the proteomic data overlaid onto the (A) unfolded protein response pathway and (B) protein ubiquitination pathway. Most of the dysregulation occurs in protein chaperones and ATPases. UPR initiation typically occurs together with increased protein ubiquitination which functions to target proteins for degradation. Green shaded proteins are identified and are decreased compared to the control while red shaded proteins have increased abundance.

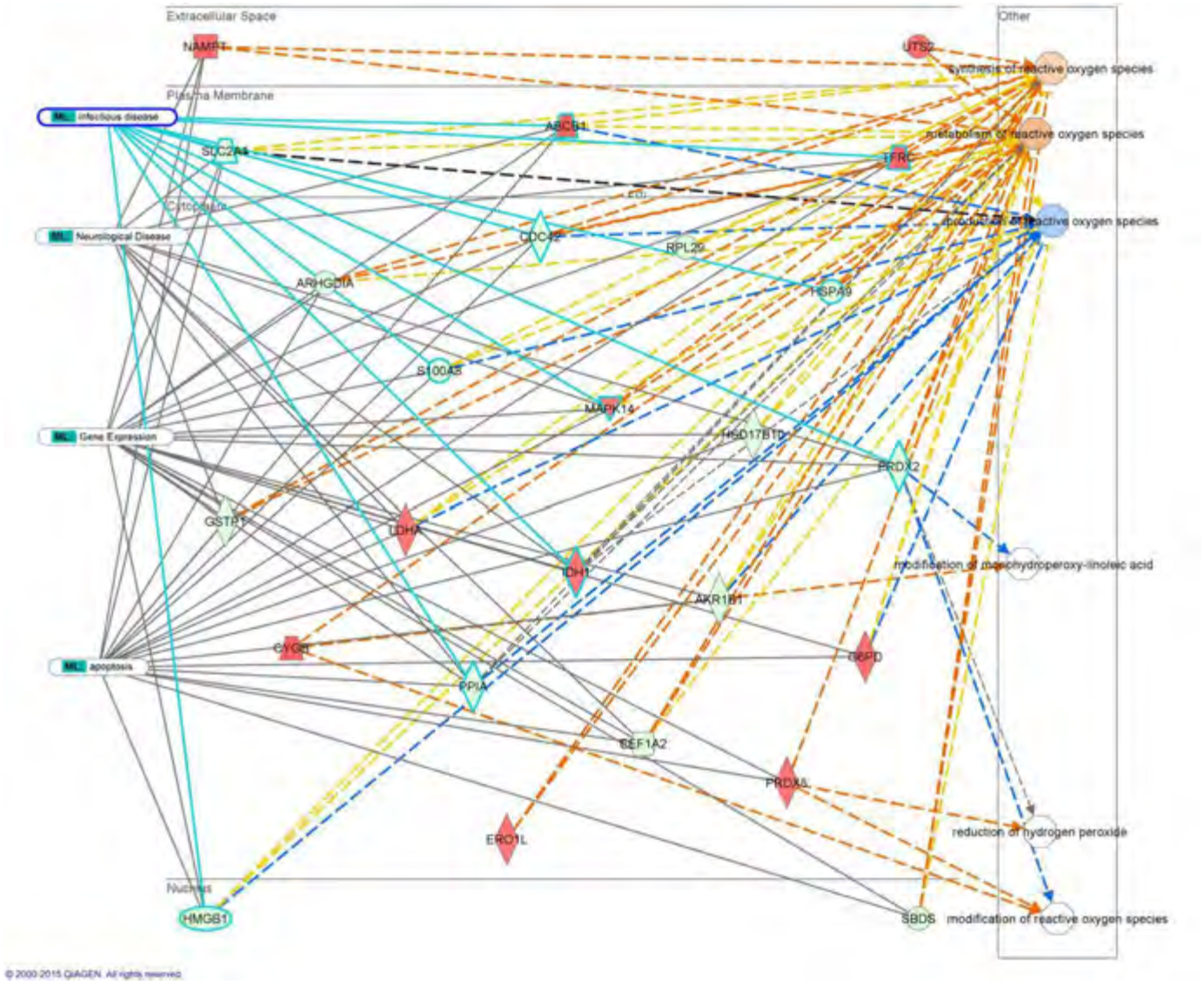

Figure 37: Functions and dysregulated proteins identified in the proteomic data relating to the production and metabolism of ROS. ROS plays a role in several cellular functions and diseases, some of which are overlaid to identify shared proteins. Those shared proteins will undoubtedly play a role in the respective functions.

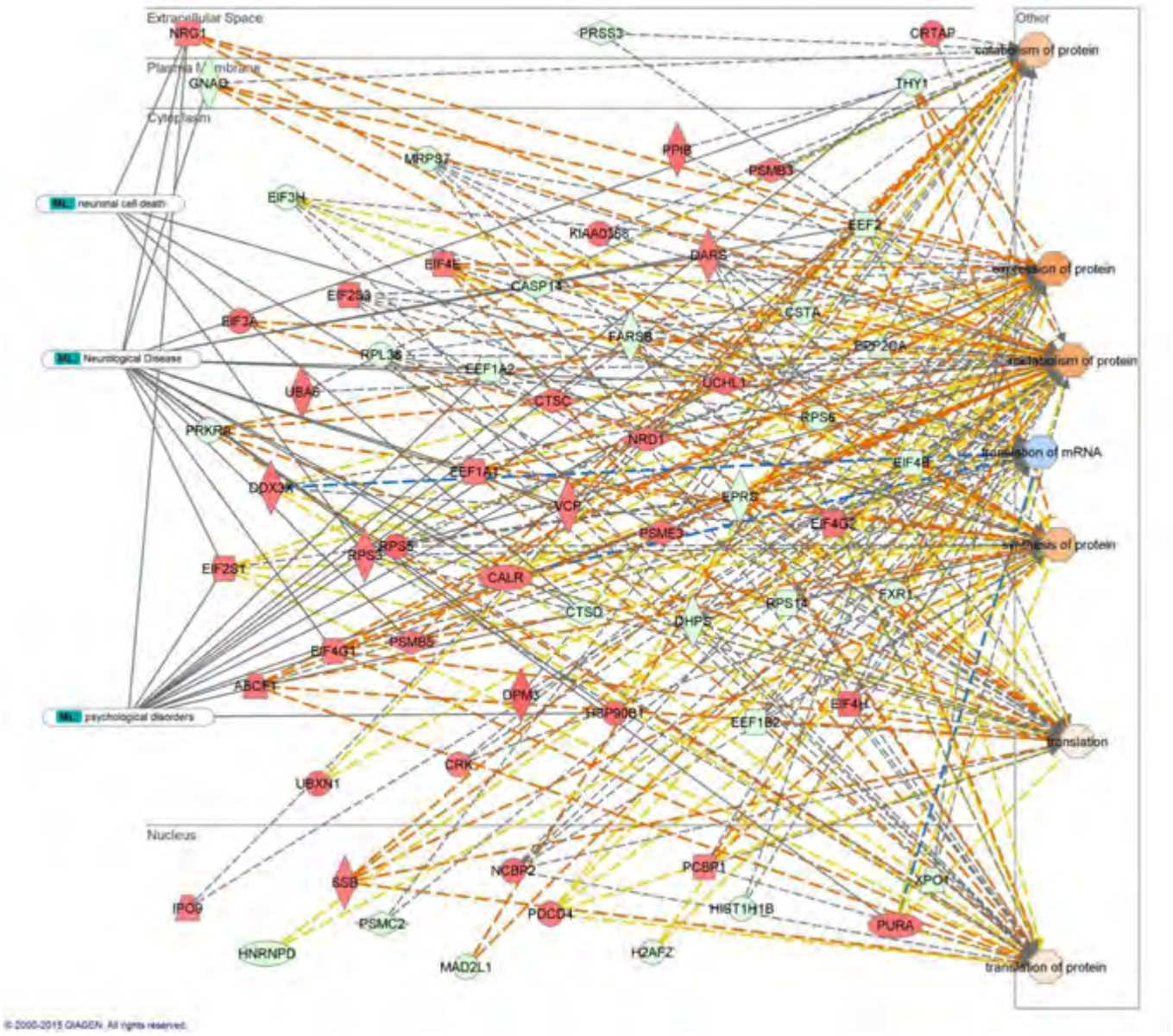

Figure 38: Protein synthesis functions identified in the proteomic data overlaid with proteins associated with psychological disorders, neurological disease and neuronal cell death. This serves to illustrate the involvement of dysregulation in protein synthesis and the development of neurodegenerative diseases. Green shaded proteins are identified and are decreased compared to the control while red shaded proteins have increased abundance. Orange and blue shaded functions are predicted to activated and inhibited, respectively.

Major cytoskeletal regulatory pathways and proteins are dysregulated

The differentially regulated data presented here enriched for canonical pathways involved in cytoskeletal regulation. Most proteins relating to cytoskeletal regulation are upregulated with notable exceptions being the RhoGDI nucleotide exchanger and the cdc42 family of proteins. Cdc42 proteins are strong positive regulators of actin reorganisation. Thus, their loss may be related to a cells inability to regulate its actin

cytoskeleton. It is similarly interesting to note that all the actin related proteins (ARP) as well as cofilin are upregulated. These directly facilitate the polymerisation and depolymerisation of F-actin respectively (**Figure 39**).[289] Given that integrins function as mediators between the external and internal cellular environment, the activated integrin signalling may play a role in regulating the cytoskeleton. Among others, ezrin, cdc42, Rho, Rac and ARP family proteins function downstream of integrins[239,290,291] (**Figure 40**).Given that cytoskeletal dysregulation has been implicated in many diseases including neurodegenerative disease, it is interesting to note that dysregulated proteins involved in the cytoskeleton and its dysregulation signal in other important pathways as well (**Figure 41)**. Several pathways relating to the cytoskeleton, but more intimately known to affect synapse formation were seen to be dysregulated.

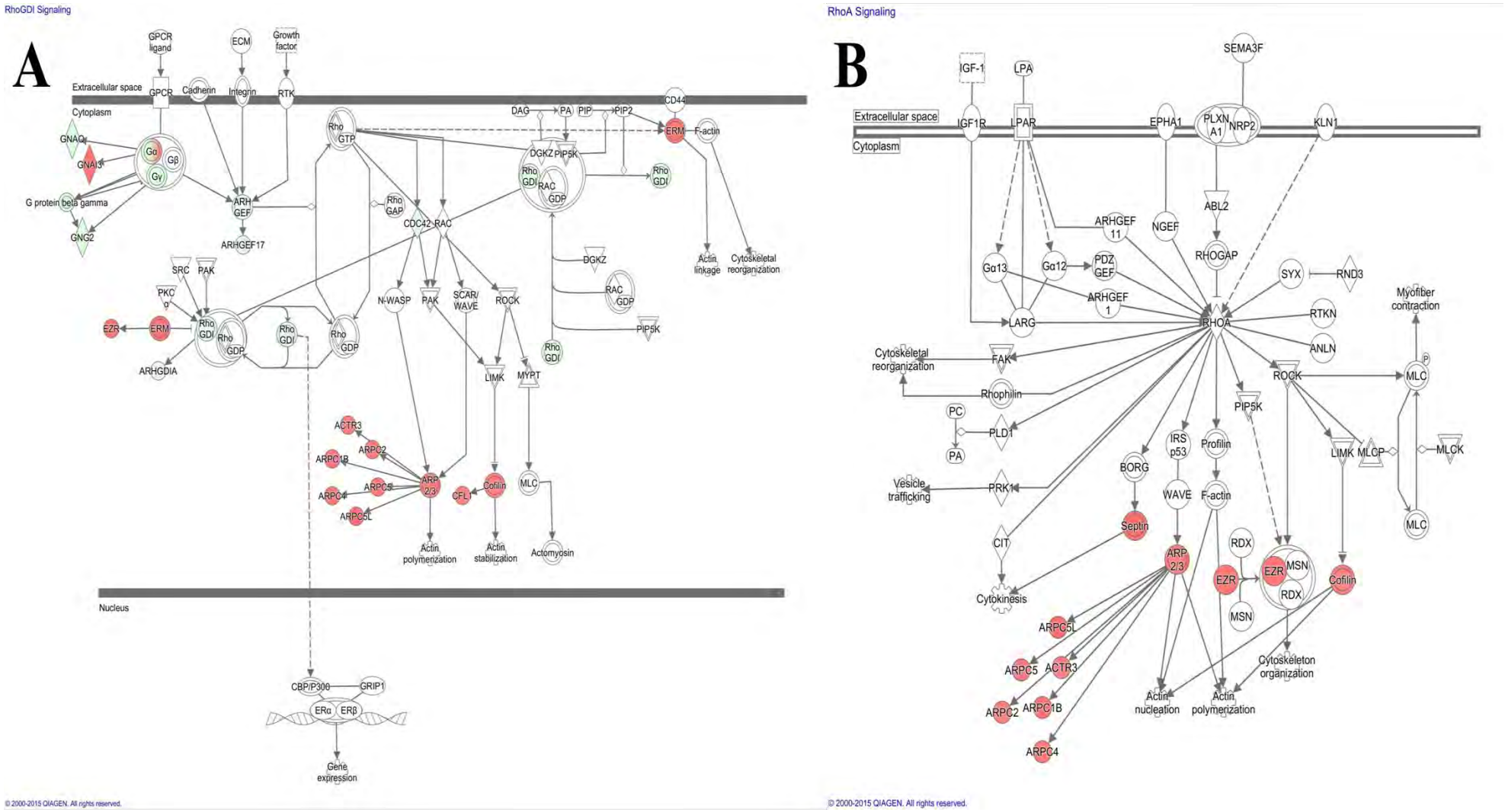

Figure 39: Dysregulated proteins identified in the proteomic data overlaid onto the (A) RhoGDI and (B) RhoA signalling pathways. These pathways play a role in signal transduction between the external and the internal cellular environment. Primarily, they regulate the cytoskeletal response in accordance with those signals plays integral roles in many pathways and cellular functions. Green shaded proteins are identified and are decreased compared to the control while red shaded proteins have increased abundance.

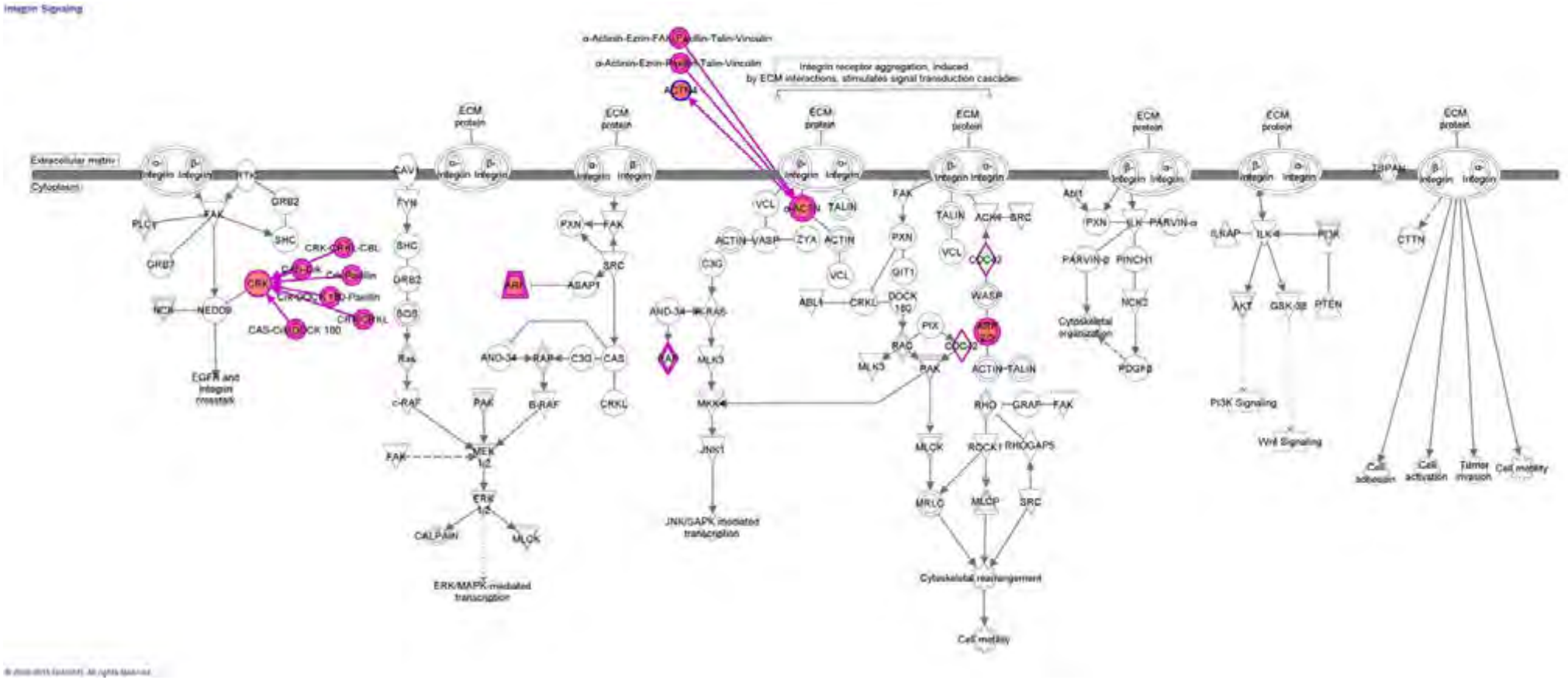

Figure 40: Proteins identified in the proteomic data overlaid onto the Integrin signalling. Integrins serve as connections between the exterior and interior of the cell and the subsequent signalling dictates the cellular response to the exterior environment. Additionally, integrins are partially responsible for cell adherence to the extracellular matrix which is of importance to the development and maintenance of cellular projections such as dendrites. Green shaded proteins are identified and are decreased compared to the control while red shaded proteins have increased abundance.

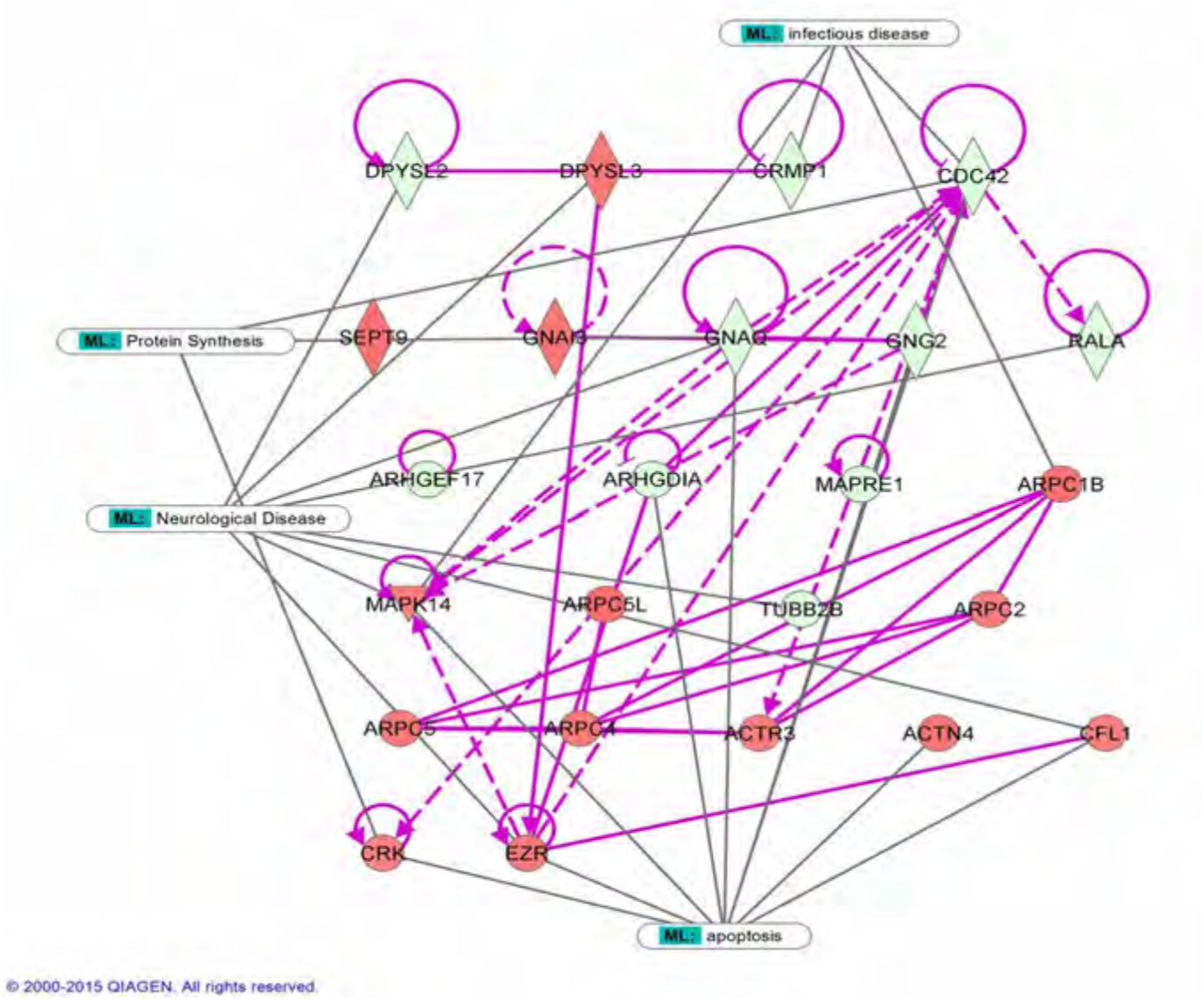

Figure 41: Dysregulated proteins involved in cytoskeletal regulation identified in the proteomic data have been plotted in an interaction map with several functions overlaid to highlight the relationship between cellular functions. The cytoskeleton plays a role in many cellular functions, thus its dysregulation influences those functions as well. Notably, many cytoskeletal proteins are associated with neurological disease. Green shaded proteins are identified and are decreased compared to the control while red shaded proteins have increased abundance.

HIV-Tat induced dysregulation is strongly associated with increased cell death and decreased cell survival

While there are classical apoptotic pathways and markers, they are the end-points of other cascades which regulate the initiation of apoptosis. In this study, we believe that tracking and understanding the upstream regulators of apoptosis which ultimately result in that final end-point decision are more important. The wealth of literature as well as our own data showing that HIV-Tat induces apoptosis in neurons is sufficient evidence of the event. Since the regulation of apoptosis cannot be described using a specific canonical pathway, it can be described only as a cellular function resultant of

several pathways and other functions; thus, we will present it as such. IPA analysis has revealed connections with cell death and apoptosis in a variety of cell types; however, we have chosen to only present those related to neuronal cell loss and apoptosis in general (Figure 42). Due to the cell wide regulation of apoptosis, we sought to identify the pathways and functions which, in our data, contribute to the apoptotic phenotype. Dysregulation in these functions are, therefore, the strongest contributors to apoptosis induced by HIV-Tat. The large dysregulation of gene expression proteins is not surprising given the HIV-Tat function in the HIV life cycle.

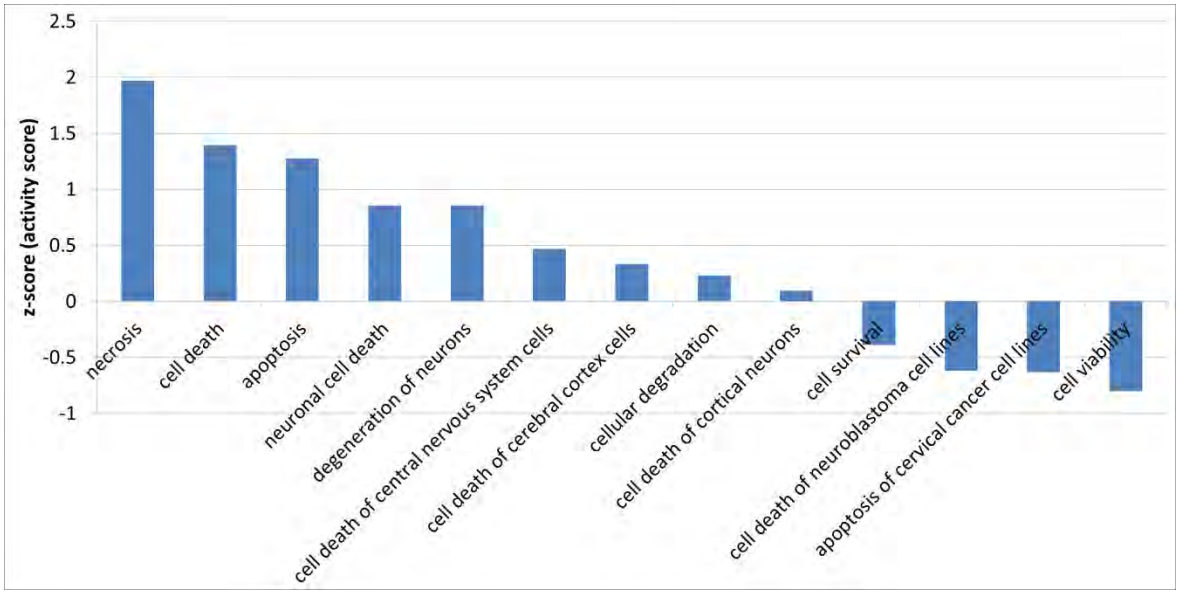

Figure 42: Cell death and survival functions. Several relevant functions depicting evidence for cell death and survival based on the proteomic data. Cell death and apoptosis are predicted as activated while cell survival and cell viability are predicted to be inhibited as a result of HIV-Tat treatment

To assess the interplay between apoptosis and other functions we have described which are known to play a role in neurodegenerative diseases, we overlaid those functions onto a network map of proteins and functions involved in apoptosis (**Figure 43**). It is, therefore, clear that dysregulation of any single function affects many others. Such complex interactions also highlights the value of a global approach such as this as it is not possible to predict the extent of these interactions based on the expression of just a few proteins.

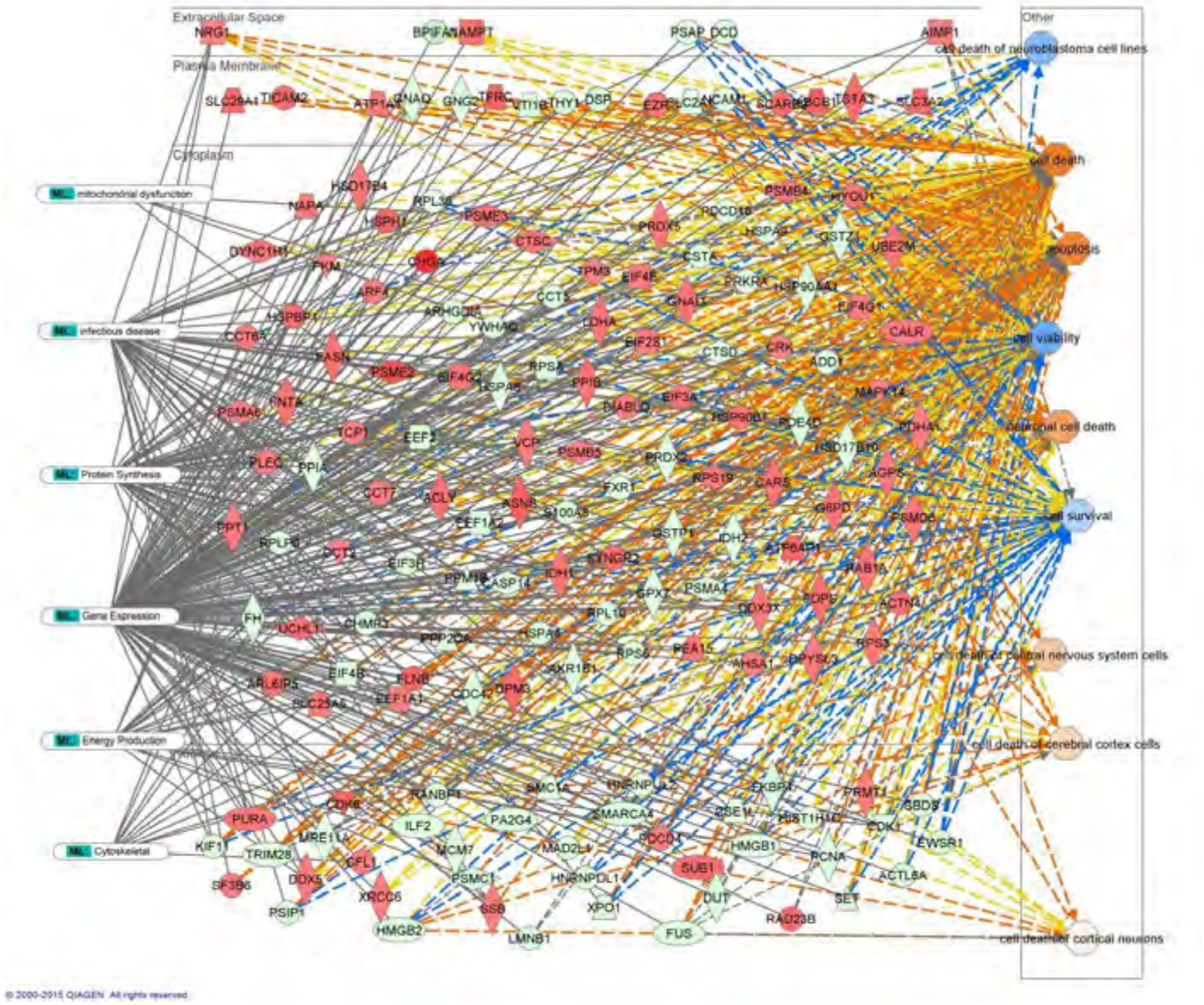

Figure 43: Functional network map generated from proteins identified in the proteomic data showing the involvement of various cellular functions in the dysregulation and apoptosis of neurons via proteins shared by the different cellular functions depicted. The network contains 166 proteins related to cell death or apoptosis; of these, 157 are shared by Gene Expression functions, 49 to infectious disease, 45 to protein synthesis, 22 to energy production, 11 are cytoskeletal and 4 to mitochondrial dysfunction. Green shaded proteins are identified and are decreased compared to the control while red shaded proteins have increased abundance. Orange and blue shaded functions are predicted to be activated and inhibited, respectively. Yellow, orange and blue dotted lines show connections between dysregulated proteins and the neuronal apoptotic functions they are known to contribute to. Grey lines denote involvement of these proteins to other important cellular functions.

Discussion

The most widely studied neurodegenerative disease is AD. From this wealth of knowledge, it is clear that neurodegenerative diseases are multifactorial. The list of molecules, pathways and risk factors implicated in the onset of disease is extensive.

Thus, it is becoming increasingly important to address these multifactorial diseases in a manner that allows us to view as many of these factors as possible. Within the HAD research sphere, neuronal cell culture experiments treated with HIV-Tat allow for the presumption that gross cellular changes resulting in neurite retraction and apoptosis are taking place.[105] This approach, however, cannot divulge any information about the specific pathway dysregulation resulting in these changes. While there is a great wealth of information published in this area, the data is often derived in a wide array of cell types with inconsistent experimental methodologies. This created difficulty in linking these studies and postulating about the involvement of different proteins and pathways. To unravel the molecular basis of HAD, an all-encompassing experiment was performed in which the involvement of each protein, pathway and function could be determine simultaneously. While proteomic and transcriptomic approaches do not allow us to identify external triggers of the disease, they do allow us to discern the means by which these external triggers dysregulate a cell and, thereby, bring about the disease phenotype. This approach is particularly useful when attempting to uncover underlying molecular phenotypes which later manifest as a disease phenotype. This is especially important given that the disease of interest is multifactorial and that the molecular events being analysed are multifunctional. This is to say that neither of the factors implicated in these diseases functions independently. Thus, it is of critical importance to view them synchronously so as to elucidate the means by which they interact and co-regulate specific cellular functions which foster disease progression and onset. In order to delve deeper into the molecular milieu responsible for the pathway dysregulation and ultimately, the gross phenotypic changes observed, we performed rigorous proteomic and gene expression analyses on HIV-Tat treated neuroblastoma cells. From this data, we identified genes and proteins that are differentially regulated by HIV-Tat treatment. Using IPA, we performed pathway analysis on these and, thus, identified cellular functions linked to and possibly responsible for HIV dementia development.

An important realization to maintain throughout this pathway analysis is that pathways act to bring about one specific action. Typically, many pathways are involved in executing a particular cellular function. For this reason, one cannot engage in

pathway analysis with the view that pathways are static such as to assume that pathways function independently to bring about cellular functions. Pathway analysis requires understanding of each pathway's contribution to bringing about a function and the hierarchy of those contributions. Similarly, it is important to note that pathways share members; some more than others. This seems to be particularly true for pathways linked to multiple cellular functions. Furthermore, multiple cellular functions can act synchronously to bring about a single or few phenotypic changes in the cell.

Cytoplasmic dsRNA sensors contribute to the Inflammatory response

The antiviral response is, imaginably, the cells' first line of defence against viral infections. This response is primarily instigated and maintained by the upregulation of type-1 interferon (IFN) and its response genes, ISG's. IFN expression is rapidly induced by IRF's after the activation of PRR. PRR's are predominantly composed of RIG-1, MDA5 and toll-like receptors (TLR).[292] Upregulation of all of these proteins and pathways provides significant support that inflammation and the antiviral response are initiated. As RIG-1, MDA5 and TLR-2 are activated by dsRNA or viral components,[293,294,295] this observation would be expected in a virus infected cell, but not so where no exogenous nucleic acids are present. This then presents the interesting question as to whether HIV is specifically activating the host's inflammatory and antiviral response via HIV-Tat. It seems apparent that, in HIV permissive cells, HIV replication requires the cellular alterations we have presented here for efficient replication. It is also interesting that the attenuation of protein synthesis[296] and cytoskeletal regulation[297,52] are both functions of inflammation and the antiviral response. The activation of several proinflammatory TNFα family cytokines as well as their receptor, TNFR1, is congruent with an antiviral response.[298,299] Several downstream effects of this activation can be seen in the data, among which is a strong NF-κB activation, upon which an inflammatory response is dependant.[300] The dysregulation of PKR is indicative of the activation of NF-κB and may be the result of the upregulation of TNFα.[301] None the less, PKR associated pathways have been dysregulated in the transcriptomic data. PKR is a particularly interesting kinase as it is the source of much controversy within literature regarding HIV-Tat function. Some

reports show PKR being inactivated by HIV-Tat binding while others report its activation and function to be highly important to HIV-Tat function.[302,303,304,305] It may be that both are true and that the means by which the results are obtained are responsible for the contradiction. It seems clear that HIV-Tat binding to TAR RNA as well as LTR activation is improved by PKR phosphorylation of HIV-Tat.[303] Also, it is reported that HIV-Tat inhibits the activation of PKR by dsRNA[304] and that this inhibition is competitive with dsRNA binding.[120] This implies that PKR is not inhibited such that it cannot phosphorylate EIF2α but that this function may be decreased. Furthermore, interferon-α directly activates PKR.[306] This interplay likely results in our reported dysregulation without a specific directionality. It is also likely that there is some PKR phosphorylation activity toward its targets. It is interesting to note that complete loss of PKR results in a potent inhibition of HIV replication.[307] Primarily, PKR antiviral activity functions to inhibit global protein translation once activated by dsRNA so as to limit viral protein synthesis. Although many inflammatory regulating pathways can alter the regulation of protein synthesis, PKR is likely the most widely studied. TNFα induced inflammation is known to result in the global attenuation of protein synthesis via PKR activation and phosphorylation of EIF2-α.[301] This effect would be compounded by the activation of several IFN genes which are also known to attenuate protein synthesis via modulation of EIF activity.[306]

The HIV-Tat induced inflammatory response favours HIV replication

There are several antiviral responses initiated by host cells upon viral infection or pre-emptively when neighbouring cells are infected. These systems illicit a variety of cellular responses including the initiation of cytokine release, blockade of protein translation and preparation for apoptosis. Intuitively, these measures should decrease or abolish the rate of viral replication in cells. Counter intuitively, however, we and others show that HIV-1 activates NF-κB which is a potent antiviral transcription factor, [307,308,309] although it has a wide variety of transcription targets. Interestingly, the HIV-LTR contains flanking NF-κB binding domains[310,311] and an inhibition of NF-κB activation by various means leads to a decrease in HIV-1 transcription.[312] It is also feasible that HIV-Tat can alter the function of active NF-κB since it has been shown to bind NF-κB directly.[76] Thus, it is reasonable to assume that HIV has the means to overcome the blockade intended by the host antiviral response.

There is significant evidence in the literature that other viral as well HIV infections still trigger the antiviral inflammatory response. However, despite this, HIV and other viruses are still able to replicate very efficiently inside host cells. This, therefore, implies that efficient strategies have been developed by the various viruses in order to overcome any intended replicative impedance by the antiviral and inflammatory systems. This does not exclude the possibility that these viruses succeed in spite of the antiviral response. However, HIV may be specifically evolved to replicate maximally in the cellular environment created by inflammation. It is not impossible to envisage a situation whereby HIV-Tat can prime cells to this state in preparation for HIV Infection; especially in lieu of the data presented here. HIV may be initiating the inflammatory response as a simple means to bring about cell wide environment conducive to its replication which is typically initiated by this system. It may then specifically alter the expression of a few genes to bring about a favourable replicative environment. Or, it may have altered its life cycle such that it thrives in an otherwise classical antiviral environment.

The inflammatory response attenuates protein translation

Our data does not allow us to conclusively determine the purpose of HIV-Tat stimulating the antiviral response, but we can speculate based on knowledge of other viral mechanisms of overcoming the host antiviral response. It is well established that the induction of the antiviral response induces a cell wide blockade on protein synthesis. This blockage includes most, but not all, host transcripts.[313] Many publications state that HIV prevents this blockade via inhibition of eukaryotic initiation factor 2α kinase, PKR. This work proposes that HIV-Tat binds and is phosphorylated by PKR and, in this process, blocks EIF2α phosphorylation and inactivation. While our data does not allow us to see PKR activity specifically, its signalling is dysregulated by HIV-Tat treatment. Despite little literature evidence for a cellular shutoff induced by HIV, there is significant evidence for the process in other viral infections.[46,314,315] Influenza is known to decrease both host transcription and translation and, thereby, favour synthesis of its own proteins.[45,316] Evidence for exactly this is seen in our data whereby mRNA transcription and translation is predicted to be decreased. If, in our model, protein translation is not inhibited by PKR activity, as is the case in influenza shutoff, the entire PRR antiviral system can induce a protein translation blockade. Interestingly,

like HIV-Tat, influenza induces the degradation of EIF4B in order to attenuate host protein synthesis.[45] Specifically, activation of RIG-1, MDA-5 and TLR's induce the rapid production of interferon. The resultant interferon mediated antiviral inflammatory response induces a global protein translation blockade.

The inflammatory response is a potent cytoskeletal regulator

Similarly, inflammation is known to affect the regulation of the cytoskeleton from the altered membrane permeability due to alterations in cellular adhesion[52] to altered neuronal migration.[317,318] This can easily be rationalised due to the fact that the immune system cells are typically recruited to sites of inflammation; This recruitment relies on a cytoskeletal response to chemotactic signals in order to direct cellular movement. Furthermore, inflammatory agents such as TNFα and IFN increase Rho-dependant signalling and disassembly of cellular junctions which increases membrane permeability. Inflammation is also attributed to increased F-actin disassembly due to increases cofilin activity.[52] Classically, the renin-angiotensin (RAS) system is involved in the regulation of blood pressure. More recently, however, basic research and animal studies have implicated the RAS as an important proinflammatory mediator in response to TNFα stimulation.[319,320] Furthermore, the RAS system is known to be activated in HIV-infected podocytes and is associated with a compromised actin cytoskeleton.[321] The RAS has been shown to be capable of mediating cytoskeletal reorganisation by signalling through RhoA and Rac via Ezrin.[322] Thus, the dysregulated cytoskeletal reorganisation in our study is possibly directly due to the proinflammatory environment. Furthermore, the dysregulation identified in this work is capable of altering neuronal cytoskeletal reorganisation pathways such that cellular extensions such neurites and dendrites cannot be initiated nor maintained.[323]

Protein translation blockade favours replication in many viruses

The dysregulation in the EIF2 signalling pathway and general dysregulation of the protein synthesis functions seen are very interesting not only because it is the most highly dysregulated system, but because of its importance to viral infection. Since viruses rely entirely on the host cell for its translation machinery, cells have, therefore, appropriately developed an array of mechanisms through which to inhibit viral replication once infected. Similarly, successful viruses have developed mechanisms

with which to overcome the efforts by their hosts to stifle their replication. It is, therefore, well established that viruses specifically target and dysregulate host protein translation in an effort to subvert the effects of the host antiviral system in order to specifically translate their RNA's while inhibiting the translation of host RNA.[49]

Protein translation is attenuated in AD

Interestingly, dysregulation of protein synthesis is known to play a role other neurodegenerative diseases such as AD and PD.[324,325] In AD patients' brains, inhibition of global protein synthesis was elevated compared to non-AD age matched patients.[326] This inhibition was associated with activated PKR.[327] In another study, knockout of ER resident EIF2α kinase, PERK, ameliorated the inhibitory effects of Aβ on LTP in hippocampal slices.[270] This is likely because LTP requires *de novo* protein synthesis, thus, inhibition of protein synthesis inhibits long lasting LTP is blocked.[328,329]

Activated UPR attenuates protein synthesis

PERK is one of four master regulators of EIF2α activity and responds to various ER stresses; specifically, the UPR which requires modulation of protein synthesis.[330] The primary function of UPR is to reduce the influx of protein due to the presence of unfolded protein in the ER/cell. While attenuating protein synthesis, protein degradation is also increased by proteasomal activation.[331] Norman, *et al*, 2008, reports that HIV-Tat can indeed activate UPR in neurons through binding to and activation of ryanodine receptors in the ER.[229] However, why HIV would evolve a function which places additional stress on cellular protein synthesis is not apparent from this work. Work in other RNA viruses including, but not limited to, West Nile Virus, Coronavirus and Influenza A virus shows that they too activate UPR upon infection and require UPR activation for optimal replication.[332,333,334,335] In addition, global protein translation is also attenuated in those cells. Another UPR function is to increase levels of protein folding chaperones. HIV makes extensive use of the ER for protein folding, glycosylation and disulphide formation, possibly due to its ideal folding environment.[336] Despite this, a large proportion of synthesized GP160 is retained in the ER in insoluble aggregates.[337] Given this, it seems plausible that HIV-Tat activates the UPR in cells such that the ER becomes better equipped for large scale, rapid viral protein production. However, the UPR is a stress response and, therefore, induces

several negative effects inside the cell, not least of which is the suppression of protein synthesis. Additionally, chronic UPR activation leads to apoptosis via the activation of CHOP. Following from the work by Norman, *et al*, ryanodine receptor activation leads to ER calcium depletion [229] and, consequently, cytoplasmic calcium enrichment. Given that mitochondria are highly sensitive to cytoplasmic calcium, this may explain the mitochondrial dysfunction we report.

Our data shows a decrease in PPP2CA which is a catalytic subunit of the multifunctional phosphatase, PP2A, forming part of the core enzyme and Holoenzyme. It has been shown that the ratio between core enzyme and holoenzyme are important for the HIV-Tat mediated HIV-LTR transcription. Ruediger *et al*, showed that by increasing levels of core enzyme, HIV-LTR transcription was inhibited 5-fold.[338] Conversely, it is feasible to assume that by decreasing the levels of the core enzyme, HIV-LTR transcription would be increased. Our data shows that HIV-Tat is capable of decreasing the levels of PPP2CA which, following from Ruediger *et al*, 1997, would decrease the levels of core enzyme.[338] PP2A is one of four major cellular phosphatases and is a negative regulator of cell cycle and survival. It responds to many pathways; of interest to us are protein synthesis regulators such as PKR and mTOR where it regulates the activities of AKT/PI3K and EIF4B. In addition, HIV protein Vpr has been shown to bind with PP2A subunits which affirm PP2A as a target for dysregulation by HIV. Our data, thus, shows that HIV-Tat is capable of decreasing its level in the cell as well. Furthermore, as is outlined in the review by Ruediger *et al,* many viruses target and dysregulate PP2A in their life cycles.[339] Targeted PP2A dysregulation may be a means by which HIV-Tat can alter the protein synthesis machinery to suit HIV replication. Interestingly, PP2A is also responsible for the synaptodendritic regulation of EIF4B mediated mRNA translation and is essential for neuronal plasticity.[340]

Our data shows an bidirectional expression effect on dysregulated ribosomal proteins. It is known that several ribosomal proteins are members of a diverse range of signalling pathways, although, little is known about this. It may be that HIV requires a specific ribosomal expression pattern for protein synthesis modulation as well as other functions. It may be that those ribosomal proteins activated are specifically required to translate HIV mRNA while maintaining suppression of host mRNA translation. Jarboui

et al, also reported dysregulation of several ribosomal proteins as well as HIV-Tat trafficking to the nucleolus; the site of ribosomal protein synthesis.[219]

EIF4B is responsible for the recruitment of the 40s ribosome to the translation initiation complex. Thus, loss of EIF4B will result in impaired 40s ribosomal recruitment, mRNA scanning and subsequent translation initiation.[121] Interestingly, Influenza A also decreases levels of EIF4B in order to inhibit host mRNA translation which dramatically increases IAV replication.[45] Similarly, the decrease in EIF3H would attenuate translation initiation due to its core role in recruiting and stabilising the 40s ribosome preinitiation complex. Thus, its loss would either compound or further facilitate the protein translation attenuation caused by EIF4B. It is important to note that this is most important for the vast majority of mammalian mRNA transcripts as they contain 5' structured untranslated region (UTR) which would result in the global attenuation of translation.[341] Cimermancic *et al* identified 497 HIV protein-host interactions involving 435 host proteins including many EIF3 subunits.[342]

Given the integral involvement of EIF4B in the recruitment of the 40s ribosome to mRNA, its loss would certainly attenuate the translation of all transcripts requiring it. While the exact mechanism by which IAV overcomes the loss of EIF4B is not known, HIV may employ a similar mechanism or, at least, the effect may be for a similar reason. Most human mRNA initiation begins by the 40s scanning which is already attenuated by the loss of EIF4B. It is likely that the highly structured 5' UTR prevents 40s access to the UTR and thus scanning may not be possible. Indeed, the TAR secondary hairpin structure decreases EIF4B access and mutation studies removing the hairpin structure increased EIF4B access[343] and, presumably, 40s pre-scanning. The TAR hairpin sequence and structure in HIV mRNA is absolutely required for efficient transcription and translation in infected cells. This implies that the TAR specifically prevents EIF4B dependent translation of HIV RNA.

When the TAR sequence is removed, basal HIV protein translation increases 190 fold in healthy cells. However, logic dictates that under cellular conditions present during HIV infection and replication, the TAR sequence results in greater or more efficient viral protein translation. Following this logic, it may be that there is a translational blockade

within infected cells and that HIV has developed a means through which to efficiently translate its own proteome. Furthermore, the HIV-Tat bound TAR sequence was shown to sequester EIF2s1 with greater affinity that mammalian mRNA sequences.[344] This would allow HIV mRNA transcripts to outcompete host mRNA for translation even further under compromised cellular conditions.

It is feasible to assume that HIV-Tat might use the antiviral and inflammatory systems to bring about a favourable environment in which it can replicate. By our analysis, this would involve the removal of host mRNA's ability to compete with HIV transcripts for translation machinery. It has been shown that HIV protease cleaves EIF3D[342] and that interferon induced the suppression of EIF3's ability to bind the 40s ribosome for translation initiation. Thus, interferon functions to suppress global protein upon viral infection.[345] Similarly, HIV-Tat has decreased the levels of EIF4B which is essential for cap-dependent mRNA translation. Furthermore, higher EIF4B levels promote cap-dependent translation over internal ribosome entry site (IRES) translation.[346] Thus, a reduction of EIF4B would favour IRES translation. Taken together, a reduction in EIF3H and EIF4B would severely decrease the efficacy of cap-dependent mRNA scanning and translation and would favour IRES translation. Indeed, HIV translation has been shown to make use of the cap-independent translation, IRES.[347] Ventoso*, et al*, show that HIV protease cleaves EIF4G and, in doing so, attenuates host cap-dependent protein synthesis and favours and IRES mechanism. To our knowledge, HIV-Tat has not previously been shown to attenuate EIF functions or protein synthesis. Via this mechanism, HIV can effectively decrease competition from host capped mRNA's and thus promote its own translation.

HIV's biological purpose is to replicate itself. The requirements for replication are energy in the form of ATP and GTP, monomers for its protein and genetic material and replication machinery. By limiting the cells' ability to use these recourses, viral replication has access to them with decreased competition. Toward this, a human cell likely has several thousand mRNA transcripts present and competing for translation at any point in time. If these were to be translated along with the HIV transcript species with the same efficiency, HIV replication would be sorely hampered.

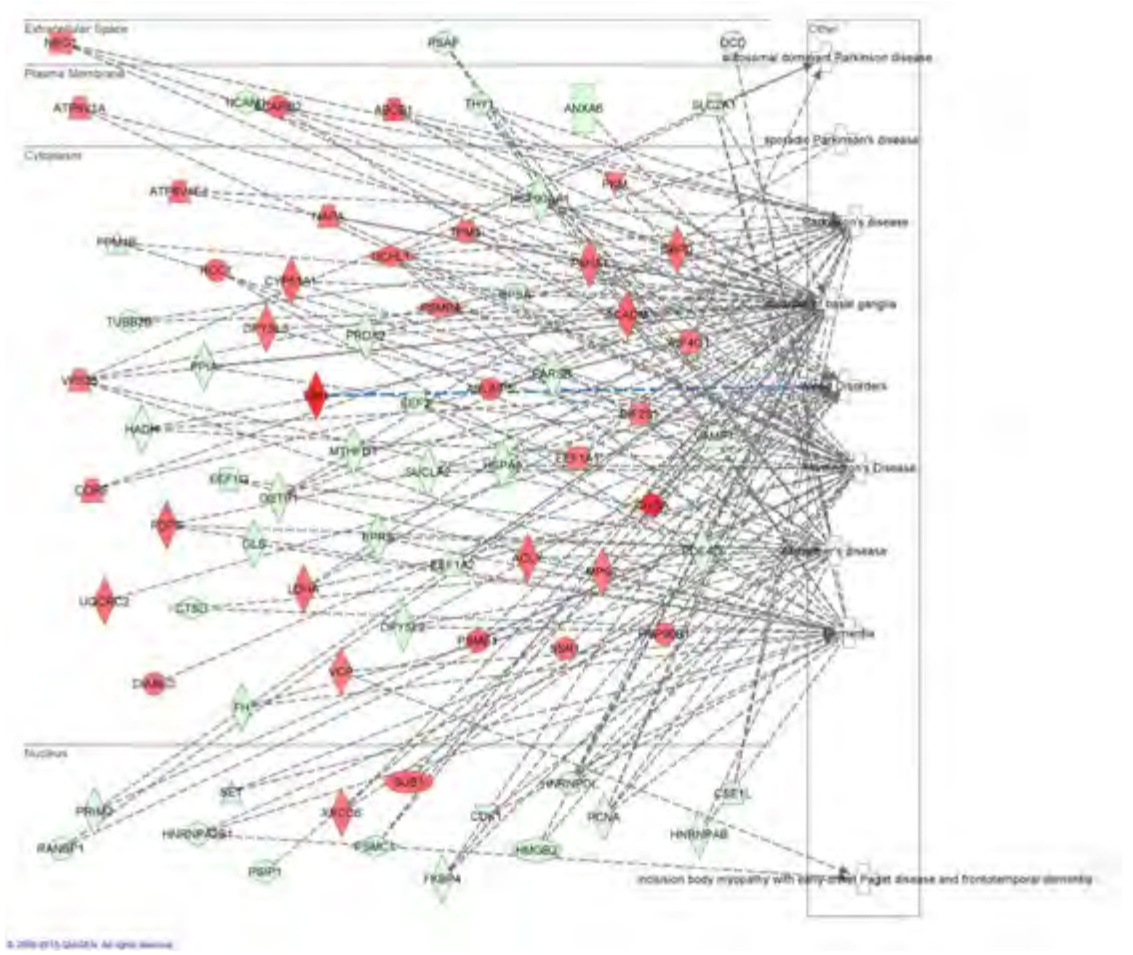

Figure 44: Psychological disorders. Associated proteins don't match known disease patterns. This, however, also serves to show that HIV-Tat dysregulates proteins implicated in other similar diseases but is molecularly distict from them. Green shaded proteins are identified and are decreased compared to the control while red shaded proteins have increased abundance.

Cytoskeletal dysregulation underpins synaptic degradation

We tend to believe that a pathway has a loss of function when its members' expression is decreased and a converse increase in function when its members' expression is increased. However, any dysregulation should be seen as a loss of function especially when the function is regulation. This is due to the fact that cells can no longer regulate these key functions to the same degree as in healthy cells. This problem likely becomes exacerbated when dealing with such an important, tightly controlled and multifunctional cellular systems as the cytoskeleton.

Cytoskeletal components play a major role in the human immunodeficiency virus-1 (HIV-1) infection.[348] A wide variety of molecules belonging to the microfilament system, including actin filaments and actin binding proteins, as well as microtubules

have a key role in regulating both cell life and death.[349,350] Cell shape maintenance, cell polarity and cell movements as well as cytoplasmic trafficking of molecules determining cell fate, including apoptosis, are regulated by the cytoskeleton.[351] Additionally, cytoskeletal dysregulation plays a role in the development of many diseases including many neurodegenerative diseases like AD, PD and Huntington's Disease.[352] While the cytoskeleton plays a role in many cellular functions such as cell-cell communication, attachment, cellular transport, etc., in neurons, it is also plays a central role in the establishment and maintenance of synapses.[237,353]

Neuronal synapse maintenance and function relies heavily on the neurons ability to accurately regulate its actin remodelling pathways.[354,240] Synaptic actin spans a wide array of functions including pre and post synaptic shape, restraining and directing synaptic vesicles toward the synapse and maintaining the entire synapse in its specific space. The roles of specific actin structures within synapses are largely unknown, however, despite this, it is known that dysregulation of actin remodelling pathways can disrupt synapse function and integrity. Several actin reliant pathways are dysregulated in our proteomic data and they are united in their ability to regulate actin remodelling. Our proteomic data show that ARP proteins are being upregulated. Interestingly, *Korobova and Svitkina,* 2009, report that ARP2/3 is integral to both stable and dynamic actin fibres in post synaptic boutons.[240] While we can see that actin remodelling is dysregulated by HIV-Tat, our proteomic data does not allow us to speculate about the source of the dysregulation. The gene expression data, however, does provide insight into the upstream regulators of the dysregulated actin remodelling pathways.

Cofilin activity promotes the depolymerisation of actin and an increased production of free barbed ends from F-actin chains. Conversely, these free barbed ends provide binding sites for ARP2/3 and subsequent actin polymerisation.[289] This process inhibits the formation of stable long F-actin filaments. Furthermore, induction of long-term potentiation requires stabilisation of F-actin chains; A process is facilitated by the inhibition of cofilin.[355,356] Overexpression of cofilin results in the formation of actin/cofilin rods and is thought to be an early event in the neurodegeneration

associated with AD and PD. The actin/cofilin rods are also reported to impede distal neurite function without killing the neuron.[352]

Along with the maintenance of LTP, stabilisation of the F-actin in synapses plays several other roles such as dendritic spine and post synaptic bouton density and morphology which are important to their function.[357] While we cannot be sure about the effect of increased ARP proteins along with increased cofilin, it is certain that the cytoskeletal role in synapse function and maintenance is impaired. In addition to this, the observed decreased cdc42 correlated with increased cofilin and ARP activity. Cdc42 is a known cytoskeletal regulator and its loss in neurons was shown to result in gross brain abnormalities as well as, but not limited to, impaired abilities to form axons. [358] Wegner, *et al*, 2008, showed that ARP2/3 function was critical to the formation of dendritic spines and synapses. Similarly, decreased cdc42 levels reduced the number of synapses and dendritic spines on neurons via impedance of ARP2/3 function.[359]

Relative to HIV replication, the observed dysregulation of the actin cytoskeleton can be explained. HIV requires the cytoskeleton to be reorganised such as to allow efficient transportation of its components through the cell throughout the infection, replication and release process. In addition, cortical actin structures present an initial, physical barrier to HIV infection. Active cofilin and ARP2/3 loosen this barrier and allow release of the viral core into the cytoplasm.[15] Furthermore, the transport of viral cores from the membrane to the nucleus is facilitated by free barded ends and actin polymerisation.[15] This may explain HIV's need for the production of free barded ends by cofilin and the polymerisation functions of ARP's. This same process of removing actin structures likely aids in the disruption of neuronal cytoskeletal structures as well as function.[360] Protein kinase C (PKC) is known to regulate cofilin and is an important cytoskeletal mediator.[361] Active cofilin is also associated with increases membrane permeability which would allow HIV greater and faster infiltration into tissues. Additionally, activation of the multifunctional NF-KB is critical to HIV replication where its loss decreases replication. Furthermore, NF-KB activation in HIV was shown to be reliant on the activation of the RAS system. Chandel *et al*, showed that the activation of RAS signalling was central to the loss of cytoskeletal regulation during HIV infection [362]

As has been mentioned, the regulation of protein synthesis plays a role in cytoskeletal regulation and synapse maintenance and function. In addition to its effects on protein synthesis, a further consequence of decreased EIF3H may be due to it having several regulatory functions beyond protein translation. It is reported to be important for brain development in zebrafish.[363] *Sertie et al*, showed a further neuron-specific interaction whereby EIF3H interacts with the neuron-specific GDP/GTP exchange factor, Collybistin, which plays a role in cytoskeletal regulation via Rho, Rac and cdc42. This interaction was shown to include the receptor-anchoring protein, gephyrin, which plays a role in the maintenance of synapses. They further propose that this interaction may regulate synapse specific protein translation.[364] It is known that long-term potentiation in neurons requires *de novo* protein synthesis and that this process needs to be very tightly regulated. Interestingly, HIV has been reported to alter the expression of BDNF which is known to be a powerful regulator of synapse specific protein translation and well as many other neuronal and synaptic functions.[365,366] HIV decreases the levels of BDNF in synapses and consequently increase the levels of its antagonist, pro-BDNF. Additionally, the predicted decrease of BDNF activity further supports impaired LTP where sustained BDNF activity is shown to be critical to LTP induction and maintenance.[367] Furthermore, MEK and protein kinase A (PKA) are critical to BDNF-induced LTP, [368,369] thus, their inhibition seen in our gene expression data would function to further hinder LTP induction. PKA is well known as a cytoskeletal regulator and its decrease in the data correlates with the loss of cdc42 proteins and increase in Rho, both of which are central cytoskeletal regulators.[370]

BDNF is thought to regulate synaptic protein synthesis through regulation of eukaryotic elongation factor 2 (EEF2) which is decreased in our data. Interestingly, EEF1A is the only upregulated EEF in our data and is known to be important for the reverse transcription complex. Reduction of EEF1A levels resulted in a significant decrease in HIV reverse transcription.[371] BDNF promotes expression of certain mRNA's and is said to increase levels of active EEF2 through EEF2 kinase inhibition and EEF2 phosphatase activation.[372]

Apoptosis

Apoptosis is a well-documented end result of HIV-Tat treated neurons with a wealth of literature on the topic. Due to a wealth of literature on the subject, it is indisputable that GSK-3β activity is responsible for or at least greatly involved in apoptosis in HIV-Tat treated neurons and that apoptosis can be inhibited by activating the PI3K/AKT pathway by lithium. What is not known, however, is what molecular events lead to the sustained inactivation of the PI3K/AKT pathway, and therefore, the activation of GSK-3β. While the downstream effectors in this model are known and described, the upstream effectors are not clear and their elucidation is certainly more pertinent.

As mentioned previously, apoptosis is regulated by a fine balance between anti and pro-apoptotic stimuli contributed by external or internal stimuli which signal through a vast array of pathways. By extension, these pathways regulate an array of cellular functions including protein synthesis and cytoskeletal reorganisation. Similarly, due to the wide scope of apoptosis regulating proteins, it is not surprising that proteins and pathways implicated in diseases such as neurodegeneration also contribute to apoptosis regulation. Following this, we were interested to see how the pathways and cellular functions dysregulated in our datasets contribute to or may initiate apoptosis. What was of interest was the relationship between the dysregulation of other pathways and cellular functions and apoptosis. As mentioned above, there is no single pathway that leads to apoptosis; instead, it is mediated by several pathways.

Literature has shown that TNF-α exacerbates the apoptotic effect of HIV-Tat treatment.[65] The cause of this, however, remains unknown. The IPA analysis of the data we present shows that TNFR, TNFR2 and strong TREM1 signalling is activated by HIV-Tat treatment in addition to upregulation of several TNF family genes. Since TNFa signals through both pro and anti-apoptotic TNFR1 and TNFR2 respectively, further cellular input is required to favor cell survival or death.[298,373,374,375] TNFα treatment typically increases the activity of GSK-3β via PI3K/AKT inhibition. HIV-Tat is reported to increase phosphatase, PTEN, expression which, therefore, increases PI3K/AKT dephosphorylation and results in dephosphorylated and, therefore, active GSK-3β. Several publications have shown that HIV-Tat treated neurons exhibit increased PTEN levels, which, when inhibited, inhibits apoptosis. Increased hippocampal PTEN activity

has been shown to be responsible for AKT mediated apoptosis.[376,377] PTEN activity may also be a direct effect of HIV-Tat's ability to bind its promoter.[378] Along with PTEN, fellow phosphatase, PP2A, are central inflammatory mediators in the cell whereby PTEN favours inflammation and PP2A is inhibitory.[379,380,381] There is, however, some contradiction within literature as to the activity of PP2A. PP2A inhibition can function as a pro-survival mediator due to its phosphatase activity toward PI3K/AKT.[339] This mechanism should function to decrease GSK-3β activity. Conversely, decreased PP2A activity in an AD brain model correlated with neurodegeneration and increased GSK-3β activity.[382] Despite the obvious complexity of PP2A activity, we believe PP2A to function in a pro-apoptotic and neurodegenerative capacity in our model due to possible regulatory mechanisms outlined below. Furthermore, a decrease in PP2A activity is paramount to the induction and maintenance of an inflammatory response.[383,384] Thus, despite the complexity of PP2A activity, the use of additional proxy pathways makes it feasible to conclude that PP2A is functioning in a pro-apoptotic and cellular degenerative capacity.

There is a very significant interplay reported between PP2A, BDNF, GSK-3β and NF-κB. NF-κB is a highly complex transcription factor with multiple levels of regulation, some of which is controlled by GSK-3β and PTEN.[385,386,387] While the regulatory functions of each of these phosphorylation events remains unclear, they must be tightly regulated as NF-κB can be both pro and anti-apoptotic.[388] The exact activity likely depends on the cellular localization together with the specific phosphorylation status and subunit composition; all of which would influence binding partners. GSK-3β has been shown to activate NF-κB via Rel-A subunit phosphorylation.[389] Activation of TNF-like weak inducer of apoptosis (TWEAK) signalling correlates with the phonotypic apoptosis. Although the TWEAK signalling cascade is poorly understood, it is known to activate and signal through the NF-κB pathway and inhibit the AKT/PI3K pathway, thereby activating GSK-3β.[390] Given that HIV-Tat induced GSK-3β is pro-apoptotic, it may be fair to assume that its activation of NF-κB in this state is also pro-apoptotic. Following from this, PP2A may be a potent regulator of apoptosis in HIV-Tat induced neuronal apoptosis and several other functions. Despite massive complexity in NF-κB signalling, many pro-apoptotic NF-κB activators are known; among them is TNFα signalling

through TNFR1. This pro-apoptotic event is known to be inhibited by PP2A activity. It is important to note here that the specific compliment of cellular stimuli will define the activation status of each of these factors and thereby, ultimately, decide the cells apoptotic status. Interestingly, PKC and PKA show decreased expression and are PP2A regulators. Both PKA and PKC are reported to activate PP2A [391, 392] thus, their loss could explain the loss in PP2A.

While NF-κB can be either pro or anti-apoptotic, it seems clear from both the data presented here and literature, that HIV-Tat mediated apoptosis is NF-κB dependent. It is also likely that, given the multifunctional nature of NF-κB, chronic pro-apoptotic signalling from multiple pathways is required for an apoptotic phenotype. In our description of HIV-mediated neuronal apoptosis, TNFR1/2, UPR, PKR/pEIF2α and TWEAK together with other proinflammatory signalling seem to contribute to apoptosis. It is certainly feasible that chronic activation of the inflammatory, antiviral pathways by HIV-Tat would result in apoptosis.

Since the implementation of HAART, the disease has changed significantly such that HAND correlates less with neuronal cell loss and more so with synapse loss. Our data clearly shows how pathways and cellular functions we have shown to be involved in neuronal degeneration are also involved in apoptosis. Thus, given that this study made use of stressed but live, intact cells, the apoptotic signals from these proteins must still be offset by anti-apoptotic signals in the cell. The *in vivo*, pro-apoptotic signals may be further offset by local support cells such as the astrocytes and microglia. Using stressed cells, however, does allow us to isolate candidate systems and pathways that may ultimately lead to apoptosis as those systems are likely active and dysregulated in the stressed cells.

Conclusion

It is undeniable that HIV is an incredibly efficient replicator within its target cells. Furthermore, the HIV genome is highly error prone; errors that the virus relies on for its ability to overcome the immune system and ARV treatments through rapid evolution. Thus, any cellular environment present during HIV infection is likely as a result of HIV influence or HIV has managed to overcome any intended inhibitory

effects; the latter of which is evidenced by the global HIV pandemic. Therefore, it is no mere coincidence that the transcriptomic and proteomic data presented here evidence favourable dysregulation of so many pathways integral to HIV replication within permissive cells. That a large portion of this data can be explained within the context of HIV replication lends additional support for the validity of those pathways described as playing a role in the most studied synaptopathy, AD. As such, this work has highlighted the similarity in molecular mechanisms responsible for neurodegeneration in HAND and AD. Indeed, Perry *et al* also suggest that HAND and AD neurodegeneration may be via similar mechanisms.[105] The causative agents certainly are different, but the pathways dysregulated share many similarities. However, we show that the pattern of dysregulation induced by HIV-Tat does not match that of any other neurodegenerative disease. This means that, although proteins and pathways implicated in other neurodegenerative diseases are dysregulated by HIV-Tat, the patterns of dysregulation differ in those diseases.

Despite HIV not typically infecting neurons, many ubiquitous cellular functions share very similar cellular machinery. Thus, although HIV-Tat has likely evolved to specifically target systems to enable maximal replication within host cells, if the machinery is the same, it will have the same effects in neurons. In the model we propose, HIV-Tat inhibits the translation of host cellular mRNA in order to favour the translation of its own transcripts via cap-independent mechanisms despite global translation attenuation. HIV is known to disrupt cytoskeletal signalling in order to facilitate infection and transport of its components throughout the cell during replication. Not only does this work show that HIV-Tat is capable of inducing the cytoskeletal dysregulation, but that it is likely responsible or, at least, contributory to synaptic degradation in HAND. This work serves to highlight the strength of global protein and transcription analyses and subsequent pathway analysis to unravel and visualise complex cellular interactions in various cell states.

Chapter 5

The effect of lithium on HIV-Tat dysregulated SH-SY5Y Neuroblastoma cells

Abstract

One of the few molecular hallmarks of HAND is the activation of GSK and its inhibition rescues neurons from HIV-Tat induced apoptosis. Additionally, activation of GSK is strongly associated with other neurodegenerative diseases such as AD. Not unexpectedly, the widely described neuroprotector and potent GSK inhibitor, lithium, was proposed as a treatment for HAND. However, several clinical trials have shown limited success. To this end, we sought to characterise the effect of lithium on HIV-Tat dysregulation of neuronal proteins, pathways and cellular functions. In addition to identifying known effects of lithium such as the activation of the PI3K/AKT pathway, many previously undescribed effects on protein translation and cytoskeletal regulation, which are known to play a role in neurodegenerative diseases, are described in detail. Additionally, prominent features of the cytoskeletal dysregulation, such as RhoA and Rac, involved directly in the development of dendrites and synapses correlate strongly with the observed inhibition of NGF signalling which is maintained after lithium treatment. Interestingly, NGF modulates inflammatory signalling and inhibits HIV replication. It is, therefore, feasible that NGF inhibition facilitates the inflammatory signalling required for HIV replication and, consequently, results in the loss of synaptodendritic density in HAND. While lithium reverses the dysregulation of several HIV-Tat dysregulated proteins, many are specifically or further dysregulated by lithium which results in its inability to prevent the neuronal functional deficits induced by HIV-Tat.

Introduction

HIV-1 infection can induce an array of neurocognitive impairments termed HIV-associated neurocognitive disorders (HAND). The HAND complex describes three standardised measures of dysfunction; asymptomatic impairment (ANI), mild cognitive disorder (MND) and HIV-associated dementia (HAD).[271] Although HAD was fairly common, its incidence has decreased since the widespread implementation of highly active antiretroviral therapy (HAART). However, the incidence of milder forms of the disease has increased.[1,272] Furthermore, the disease has persisted in such cases where the peripheral and CNS viral loads were undetectable.[273] It is, therefore, clear that frontline anti-retrovirals (ARV) are not a sufficient treatment for HAND complex diseases. Given that disease progression may continue despite undetectable virus in the CNS and that neurons are very rarely infected with HIV, the whole virus is not likely to be the primary cause of disease.[393] An effective treatment would, therefore, have to nullify or reverse the cellular dysregulation induced during HIV infection. Furthermore, HIV transactivator of transcription (Tat) protein remains detectable despite undetectable viral load.[274] This, therefore, implies that viral proteins and the host response to them are capable of inducing disease onset and maintain its progression.

While the molecular dysregulation underpinning the functional dysregulation leading to HAND progression is not well understood, a key molecular event in HIV-Tat induced neurotoxicity is the activation of GSK-3β which, when inhibited by lithium, protects against apoptosis.[276,394] Lithium is a commonly prescribed bipolar treatment which has well-documented GSK-3β inhibitory activity.[395] However, it has a variety of other protein targets and likely many unknown as well.[396] The inhibition of GSK-3 along with that of other pro-apoptotic genes and the activation of bcl-2 is proposed as its primary means of cytoprotection in neurodegenerative diseases.[397] It is not known whether lithium's inhibition of apoptosis is solely responsible for its therapeutic effects in BD patients, nor whether the other targets have beneficial or adverse effects in patients. Lithium has been reported to induce a wide variety of dysregulations in cellular functions such as dendritic density, protein synthesis, immunity and inflammation[398] and neuronal signalling.[399,400] It has been shown to both increase and decrease

dendritic densities *in vitro* and *in vivo*. These contradictions may be related to the cell type and underlying disease state being tested. Despite the therapeutic mechanisms being poorly understood,[139] lithium is being studied for efficacy in a variety of neurodegenerative diseases including HAND.[401,402] Several short term studies have previously investigated lithium as a treatment for HAND and have, to some degree, found the drug to have had little effect.[402] This has led some of them to suggest further trials as lithium produced no negative effects in their trials. Such studies have also been performed in other disease states such as AD and produced similar conclusions. However, what has not yet been determined is the extent to which lithium dysregulates cells in these disease states.

GSK-3β plays a role in a diverse array of cellular functions such as cell survival and proliferation, development and an array of neuronal functions including aspects of neuronal function, such as gene expression, neurogenesis, synaptic plasticity, neuronal structure, and neuronal death and survival[403] and phosphorylates a range of targets including CREB, NF-κB, AP-1, HSF-1, β-catenin and p53.[404] Its inhibition, therefore, may affect these processes as well. Despite much research toward identifying the molecular aetiology of HAND, little is known about the cellular dysregulations that lead to disease onset.[405,406] While apoptosis is a central feature in many neurodegenerative diseases, HAND prognosis and symptom progression correlates most closely with synapse loss.[217] While GSK-3β does play a role in the synaptic plasticity, its inhibition has not been shown to restore normal plasticity. In BD, GSK-3β inhibition reduces dendritic density. In contrast, fragile X syndrome (FXS) is associated with increased dendritic spine density.

The functional implications of impaired synaptic plasticity are however, not simply equivalent to the number of dendrites and functional synapses present. Synapses need to be both formed and destroyed adequately for normal neuronal/brain function. If either function is sufficiently dysregulated, impairment will ensue. With up to 70% of patients showing partial or no response to lithium,[407] it is feasible to assume that the underlying aetiology is different, if only modestly. Additionally, 37 single nucleotide polymorphisms (SNPs) were weakly associated with increased risk of BD.[408] Added to the variability contained within the BD pathology, BD is vastly different to dementia's.

It is, therefore, not possible to predict whether lithium would have a positive effect on HAND patients. To evaluate the effects lithium might have on HIV-Tat induced neuronal dysregulation, we designed a MS-based cell culture experiment to ascertain the effects of lithium on HIV-Tat dysregulated neuroblastoma cells.

Herein, we describe the analysis cell cultures treated with HIV-Tat and HIV-Tat + lithium as well as their controls using label-free MS techniques. We identified and quantitated 3757 proteins with 360 and 531 being significantly dysregulated in HIV-Tat and HIV-Tat + lithium respectively. With this data, we aimed to determine whether the cellular dysregulation we previously identified and described (Chapter 4) could be reversed by lithium. To do this, we preformed pathway analysis using IPA and evaluated the effects on individual key proteins, pathways identified as well as activity predictions of the cellular functions. While the dysregulation of several pathways such as PTEN and IL-1 signalling were decreased or removed, most remained dysregulated after lithium treatment. To our knowledge, this is the first global proteomic analysis of lithium's effects on HIV-Tat induced neuronal dysregulation and may be the first global proteomic analysis of any lithium-induced dysregulation.

Materials and Methods

Label-free method development

Given the challenges regarding quantitation in label-free proteomics, we performed extensive tests to determine whether a label-free approach was sufficient for our work. We prepared samples with the FASP protocol.[409] Both, technical and biological replicates were analysed on 180 minute gradients. The most important factors to test were the reproducibility of technical as well as biological replicates with regards to the stability of protein quantitation as well as ID's. With this approach, we were able to test our entire label-free workflow, from cell culture to MS data acquisition. Of importance one sample was run in triplicate, which allowed us to assess the stability of our LC-MS workflow, and the remaining samples analysed once.

LC and Q-Exactive method optimisation

This work was done in conjunction with Shaun Garnett and Dr. Nelson Soares. After using standard protocols provided by Thermo Scientific^{tm} during the Q-Exactive

installation as well as another in-house method, we began a series of experiments to test effect of each parameter in the MS method setup on the rate of MS and MS/MS acquisition and protein an peptide identifications per time. To this end, our starting point was a set of settings published by, Pirmoradien *et al*.[410] To get an accurate understanding of the effect of all the settings, we both increased and decreased the respective settings and then tried combinations that yielded the best results.

After identifying optimal MS methods to use, we also developed new LC methods. To do this, we maximised sample elution time by determining the lag time as well as identifying the sample elution range such that we can focus on this area with an appropriate gradient. Following the development of optimal linear gradients, we developed new non-linear gradients. Briefly, the entire sample elution range is not occupied by the same number of peptides/time. Thus, all areas of the chromatogram are not used to the same efficiency. To this end, we increased the gradient in the beginning and end of the chromatogram and decreased it in the centre.

Lithium treatment

In order to determine the toxicity of lithium on SH-SY5Y cells, we performed a dose response assay. We then used to 10mM lithium chloride in subsequent experiments with HIV-Tat. When cells have grown to approximately 70% confluency, cells are washed twice with heated DMEM and cultured in 0% FBS, DMEM for 24hours prior to treatment. After 24 hours, cells are treated with 10mM LiCl and/or HIV-Tat suspended in 0.01% TFA, 50mM βMe and N_2 bubbled water to 100ng/µl was added to 1µg/ml and mixed gently. HIV-Tat treated cells are then incubated 5% CO_2, humidified 37^oC incubator for 24 hours.

Label-free sample processing

After cells are washed with warmed DMEM, they are immediately treated with 1ml of ice-cold RIPA lysis buffer (150mM NaCl, 50mM Tris-HCl pH 8**,** 0.1% SDS, 0.5% sodium deoxycholate with protease and phosphatase inhibitors). The lysate was then removed and the culture dish was washed with an additional 500 µl and added to the lysate to which 250 units of benzonase was added and mixed. This lysate was incubated, mixing end over end, at 4^oC for 24hours. After 24 hours, the SDS concentration was increased

to 1% and mixed thoroughly. Protein was then quantitated in duplicate using the micro-BCA method with a 7-point BSA standard curve. After quantitation, 100 µg was prepared and digested using the Filter Aided Sample Preparation (FASP) protocol.[409] Briefly, approximately 100 µg of protein was added to a 30 kDa microcon filter and diluted to 450 µl with 8M urea and centrifuged at 14000g for 15minutes. 200 µl 100mM DTT was added to the filter, mixed and incubated at room temperature for 30minutes in the dark. Following the incubation, samples are centrifuged at 14000g for 15minutes. 100 µl of 8M urea was added and the filters are centrifuged at 14000g for 15minutes. Thereafter, 200 µl of 50mM IAA was added, mixed and incubated in the dark at room temperature for 30 minutes. The filters were centrifuged at 14000g for 15 minutes. This was followed by the addition of 200 µl of 8M urea and centrifuged at 14000g for 15minutes; this step was repeated twice. Following this, 200 µl of 50mM ammonium bicarbonate (ABC) was added and centrifuged at 14000g for 15minutes; this step was repeated twice. Filters were then transferred to fresh, clean tubes and 20 µl of 0.06µg/µl Trypsin (Promega gold) suspended in ice-cold 50mM ABC was then added to the filters at a 1:75 trypsin to protein ratio. The digests were then mixed and incubated in a humidified 37^{o}C chamber for ~16hours. Following the incubation, the filters are centrifuged at 14000g for 10minutes. 50 µl of 50mM ABC was added to the filter followed by centrifuging at 14000g for 10minutes; this step was repeated twice. Peptides were then acidified with 5 µl 1% formic acid.

Reverse phase peptide clean-up

In-house packed stage tips are used for peptide clean-up. Briefly, ~1mmØ disks are cut and packed into 200 µl plastic pipette tips. Columns are activated by adding 100 µl 80% acetonitrile (ACN), 0.1% formic acid (FA) and centrifuging at 5000g for 1 minute; this was repeated thrice. The column was then washed by adding 100 µl 2%, 0.1% FA and centrifuged at 5000g for 1 minute; this was repeated twice. 10 µg of peptide (assuming no loss through digestion) was loaded onto the column, diluted to 100 µl in wash buffer (2% ACN, 0.1% FA) and centrifuged at 500g for 5 minutes. The column was then washed by adding 50 µl wash buffer and centrifuging at 5000g for 1 minute; this was repeated thrice. After washing, a tapered glass vial was added such that the stage tip was inside the vial. Peptides are eluted into the glass vial by adding 50 µl of 60% ACN,

0.1% FA and centrifuging at 5000g for 1 minute; this was repeated thrice. Samples were then dried completely in a speedyVac.

Q-Exactive settings

Standard settings were used for all Q-Exactive analyses unless otherwise mentioned. Spectra were captured in a data dependant manner with automatic switching between MS and MS/MS scans using a top 10 method. MS spectra were acquired at a resolution of 70000 with and AGC of $3X10^6$ with a maximum fill time of 250ms with an underfill ratio of 1%. The MS scan range was 400m/z to 1750m/z with a fixed first mass of 100m/z. MS/MS spectra were acquired at a resolution of 17500 with a AGC target of $2X10^5$ with an underfill ratio of 1% and a maximum fill time of 120ms. Peptide fragmentations were performed by high-energy collision dissociation with the NCE set to 25. MS/MS ion selection was performed using a 4m/z window including only $6 \leq z \geq 2$.

Label-Free data analysis

Raw files are analysed in MaxQuant^{tm} [279], version 1.5.1.2 applying a 1% peptide and protein FDR, a maximum of two missed cleavages, LFQ based quantitation and the MaxLFQ algorithm for normalization. To assess LC and MS reproducibility, shared proteins' LFQ values in the technical replicate data where compared to each other using regression curves. Regression curves were plotted and Pearson's correlation calculations were used to assess reproducibility between biological and technical replicates. Although these samples were not SILAC labelled, we wanted to compare the data to the SILAC labelled data presented in Chapters 3 and 4 respectively. To do this, we generated ratios between randomly selected pairs of HIV-Tat : βMe and HIV-Tat + lithium : βMe treated cells, respectively. These ratios were then tested for significance using the t-test method as described in Chapter 3 (section: Data processing and bioinformatic analysis). However, only t-tests and not a 2sd cutoff were applied to identify significant dysregulation.

Ingenuity Pathways Analysis

Total proteins identified and significantly dysregulated lists were submitted for IPA (QIAGEN Redwood City, www.qiagen.com/ingenuity) analysis. Gene names and ratios

for each protein were submitted into the IPA software package and analysed by the core analysis function. The IPA core analysis function generates an activity profile for the pathways and functions dysregulated by HIV-Tat and HIV-Tat + lithium treatment relative to the control. Significantly dysregulated proteins and their log- mean ratios were also analysed by the core analysis function. These were used as overlays on pathways annotated with all proteins identified for that pathway to easily identify significantly dysregulated pathway members. Biological significance of the data was determined by comparing the differences in dysregulations induced by both experimental conditions. Briefly, the pathways were grouped into common functions and matched to dysregulated functions identified by IPA. Based on literature and the IPA analyses, the dysregulations induced were interpreted relative to HIV replication as well as neurodegenerative functions. Where possible, mechanisms underlying the dysregulations as well as their implications are proposed.

Results

Non-linear LC gradients produce higher identifications

When starting this work, our group was routinely using linear LC gradients across the entire peptide elution range. However, linear gradients tend to produce TIC profiles such as is depicted in **Figure 45** which have a steep slope up to a peak which then slopes back down to baseline. The downfall of this approach is that fewer peptides are eluted at the base of the peak, which underutilises the mass spectrometer. Conversely, too many peptides are co-eluted around the peak of the chromatogram, which can result in a greater proportion of peptides not being selected for MS/MS analysis. This was confirmed by determining the identifications per time window across the chromatogram. To address this, the gradient was decreased over the centre of the chromatogram and increased at the start and end (**Figure 46**). An additional benefit of running non-linear gradients is that the sample load could be increased significantly. Adopting non-linear gradients increased our peptide identifications from ~9000 to ~16000 and protein identification rates from ~2700 to ~3400 per 120 minute gradient. These results were obtained using an earlier version 1.3; if reanalysed, these identification rates will likely decrease as identification rates tend to decrease when using the latest version.

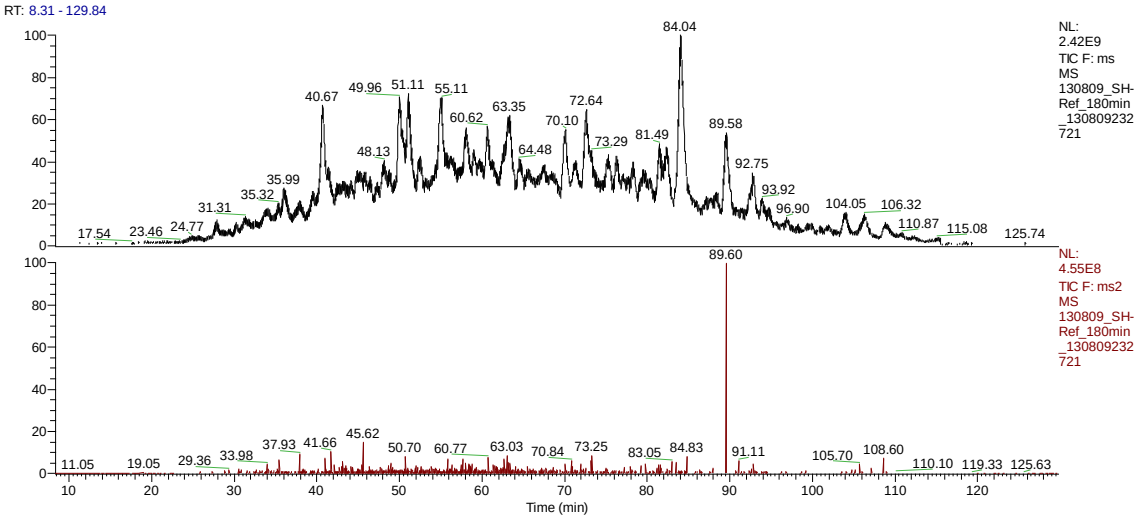

Figure 45: A representative TIC generated from a 120 minute linear LC gradient

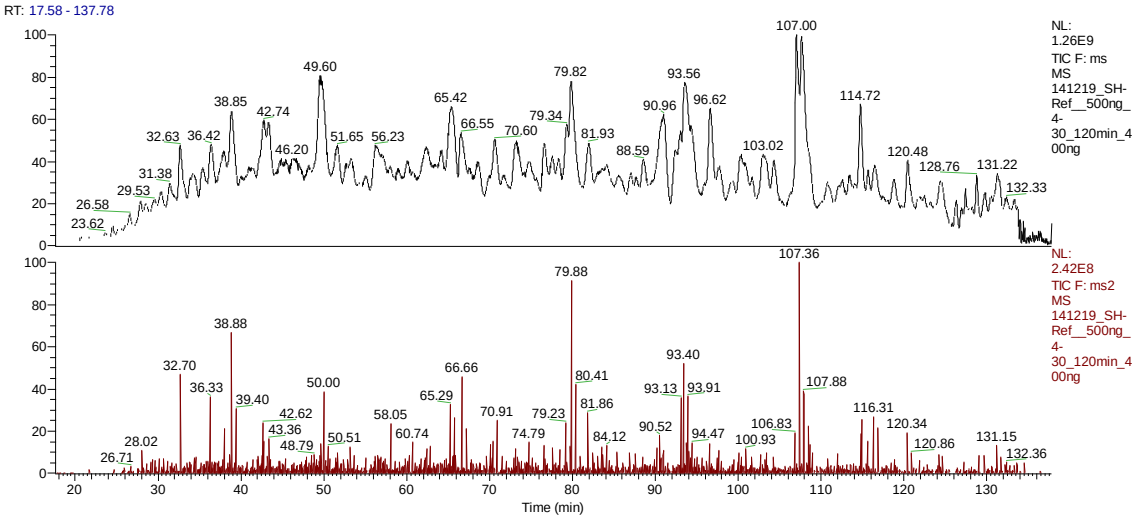

Figure 46: A representative TIC generated from a 120 minute non-linear LC gradient

Similar 180minute, non-linear gradients were used to analyse the label-free HIV-Tat and HIV-Tat + lithium treated samples; a representative of which is displayed in **Figure 47.**

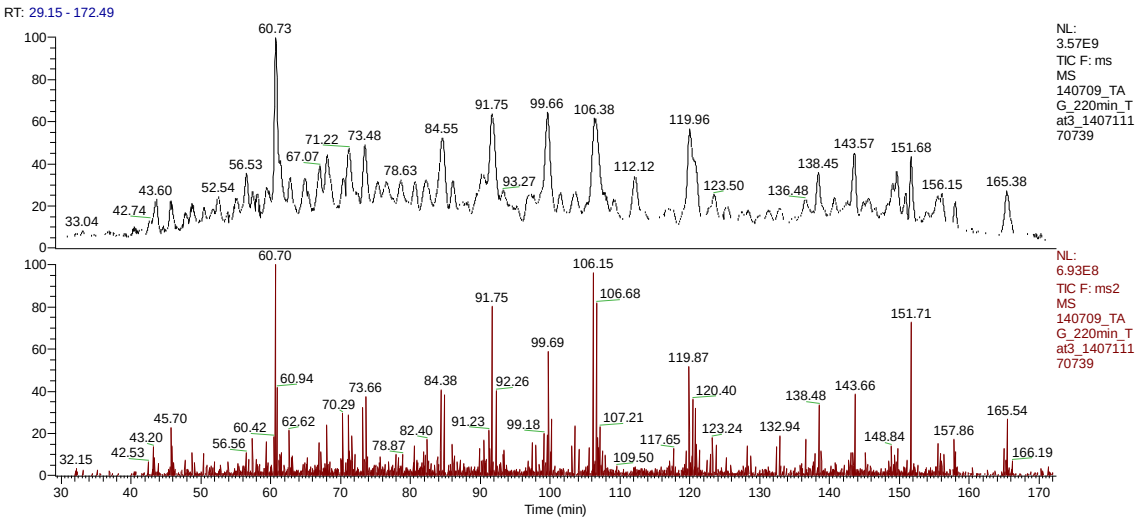

Figure 47: A representative TIC generated from a 180 minute linear LC gradient used to analyse the label-free HIV-Tat and HIV-Tat + lithium samples.

Label-free peptides generated from HIV-Tat and HIV-Tat + lithium treated cells were analysed on 180 minute gradients on a Q-Exactive Orbitrap. The resultant raw files were analysed using the MaxQuant software package; the results of which are summarised in **Table 3.**

Table 3: A summary of the Label-free metadata obtained from the MaxQuant analysis.

MS spectra	134643
MS/MS Spectra submitted	755896
MS/MS Spectra Identified	304637
Total unique peptides identified	29817
Total protein groups	3757
0 missed cleavages	86%
1 missed cleavage	13%
2 missed cleavage	1%

Differential analysis performed on the quantitated 3757 proteins identified in the label-free experiments identified 360 (Dysregulated-LF_TatvsBme proteins; Appendix 4) and 531 (Dysregulated LF_TatLivsBme proteins; Appendix 5) being significantly dysregulated in HIV-Tat and HIV-Tat + lithium, respectively, when compared to the βMe treated control.

Label-free experiments were highly reproducible

One of the primary concerns in applying label-free proteomics techniques is that they are inherently less reproducible than labelling techniques such as SILAC, it was

important for us to assess the quantitative reproducibility of the methodology. To assess reproducibility, we performed Pearson's correlation tests on the three biological replicates as well as three technical replicates. Technical replicates achieved Pearson's correlation scores above 0.98 (**Figure 48**). Pearson's correlation scores for biological replicates were above 0.98 for twelve comparisons and 0.94 and 0.95 for the remaining two (**Figure 49**). As MaxQuant^{tm} normalizes the data,[279] LFQ intensities were used for the Pearson's correlation scores and significance analysis with no further normalization applied.

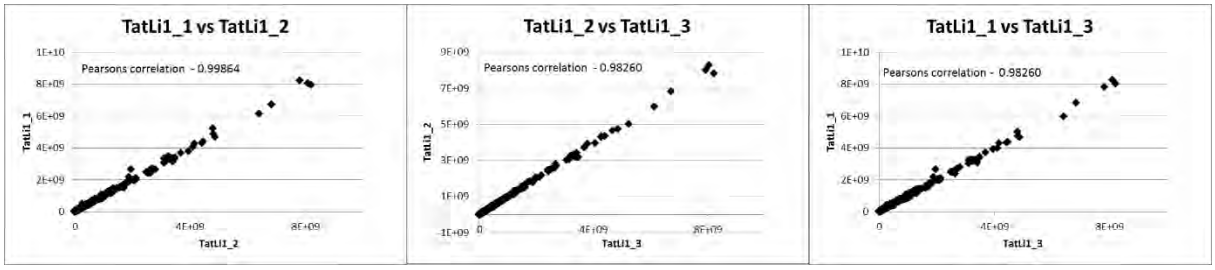

Figure 48: Regression curves and Pearson's correlations of three technical replicates of TatLi1; Pearson's correlations above 0.98 suggest that the LC-MS were operating stably.

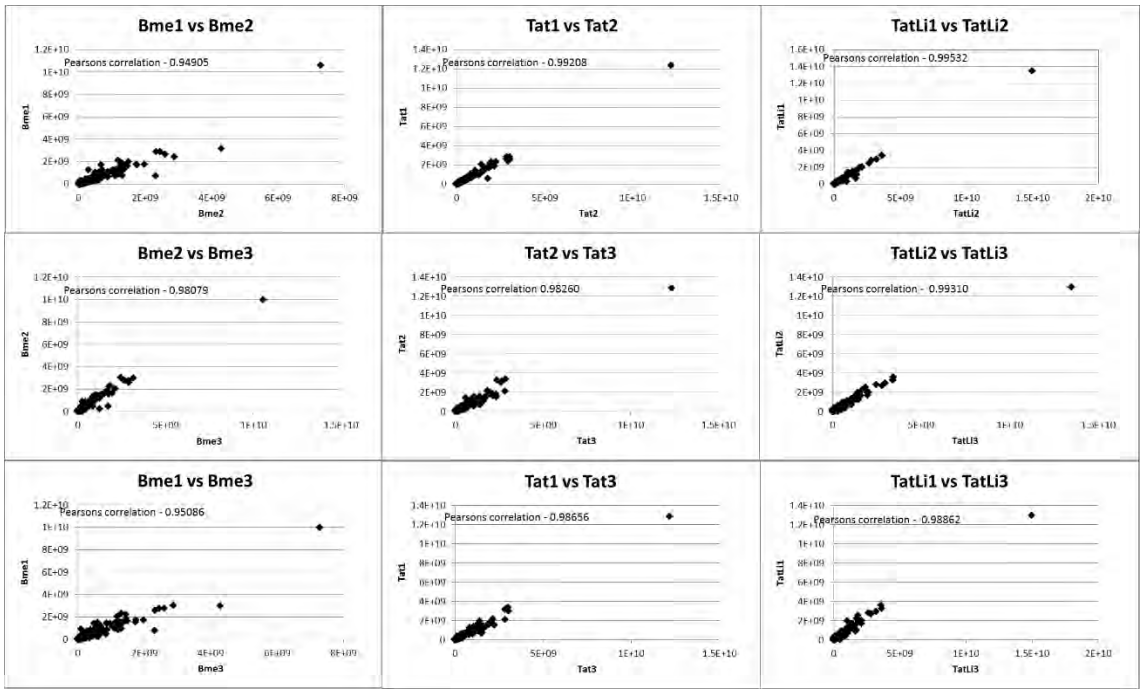

Figure 49: Regression curves and Pearson's correlation scores for biological replicates show that the sample preparation was highly reproducible within each set of biological replicates.

Lithium inhibits HIV-Tat induced neuronal apoptosis

To determine the effect of lithium on HIV-Tat treated neuroblastoma cells, we performed a dose response experiment using a range of lithium concentrations and 1 µg/ml of HIV-Tat (**Figure 50**). HIV-Tat induced cell death was completely inhibited by 5 mM – 20 mM lithium whereas 2.5mM had minimal effect.

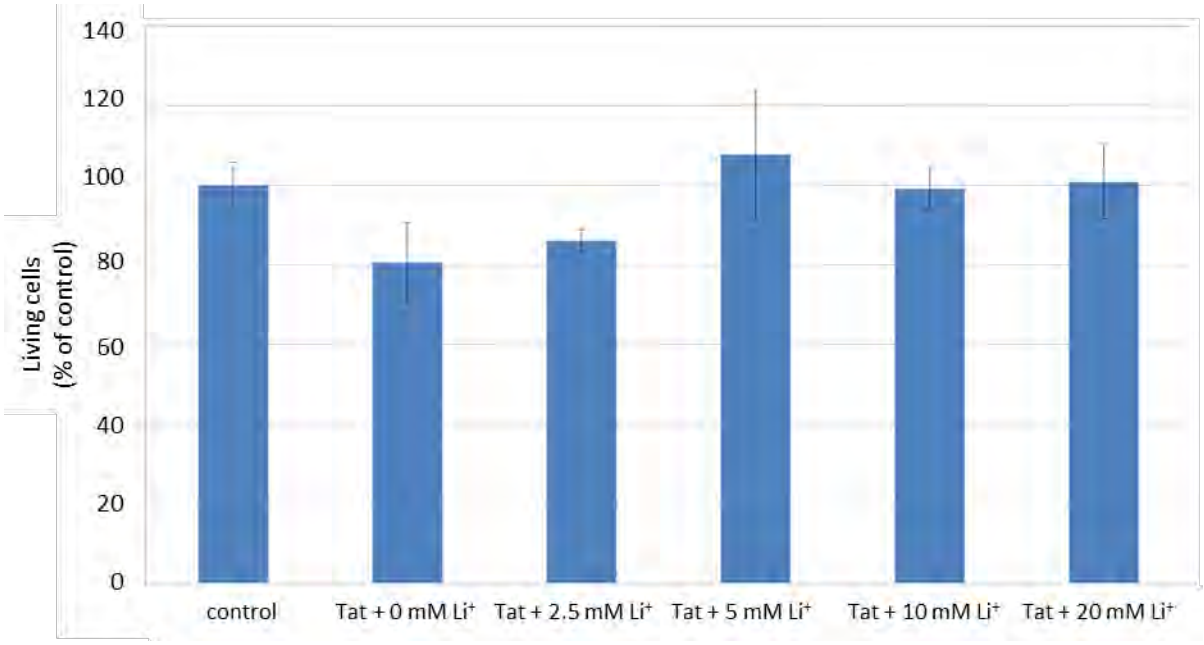

Figure 50: Cell viability of HIV-Tat treated cells with a range of lithium concentrations. HIV-Tat induced apoptosis can be inhibited by lithium at various concentrations with no lithium-induced cell death evident.

Lithium alters the gross dysregulation induced by HIV-Tat

To determine gross effects lithium had on HIV-Tat induced dysregulation, we determined the directionality of dysregulation across all the pathways significantly dysregulated in the HIV-Tat and HIV-Tat + lithium experiments (**Figure 51**). HIV-Tat + lithium had 81 while HIV-Tat treated had 93 dysregulated pathways and 79 were shared between both experimental groups. There were 65 and 49 (55 and 48 shared) inhibited pathways and 24 and 20 (20 and 19 shared) activated pathways in HIV-Tat and HIV-Tat + lithium treated experiments respectively. HIV-Tat has fourteen unique dysregulated pathways while HIV-Tat + lithium has two.

To more directly compare the effects on shared dysregulated pathways, we assessed the directional and magnitude effects of those pathways which are dysregulated in both experiments (**Figure 52**). Of the 79 shared pathways that were dysregulated, 47 maintained the directionality of the dysregulation induced by HIV-Tat after lithium

treatment and 30 changed. Of those inhibited, the magnitudes of 11 were increased and 22 were decreased. Of those activated, the magnitudes of two were increased and six were decreased and five were unchanged between HIV-Tat and HIV-Tat + lithium treated.

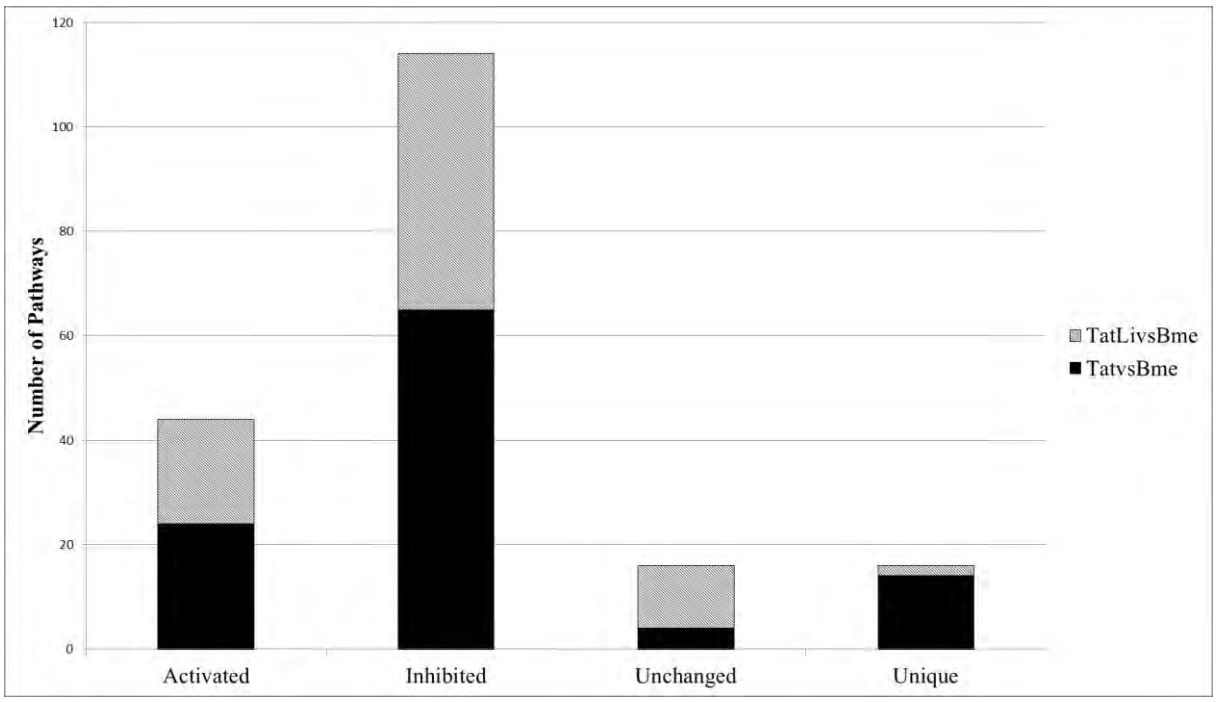

Figure 51: Gross pathway dynamics within each experiment. All pathways with activation scores in IPA were used irrespective of whether information was available for the pathway in the reciprocal experiment.

Lithium altered HIV-Tat induced dysregulated in a pathway dependant manner

The dysregulatory effect of lithium varies between pathways from a very modest effect seen in *relaxin* and *IL-8 signalling* to for more drastic effects seen in *cdc42 Signalling* and *eNOS signalling* (**Figure 53).** The inhibition of ERK/MAPK signalling in both treatments is significant as ERK activity is needed for BDNF control of dendritic density and in the establishment and maintenance of LTP/LDP which is essential to learning and memory functions.[411]

HIV-Tat dysregulation of cdc42 signalling is one of the most strongly affected by lithium. Not only is cdc42 known to be specifically decreased during latent HIV infection, [412] as a Rho regulator, it plays a central role in the regulation of F-actin and the cytoskeleton.[237] In addition, the cytoskeleton regulating pathways, *RhoGDI*

Signalling, *Signalling by Rho Family GTPases* and *Regulation of Actin-based Motility by Rho* and dysregulated by HIV-Tat; the latter two of which are mildly exacerbated by lithium.

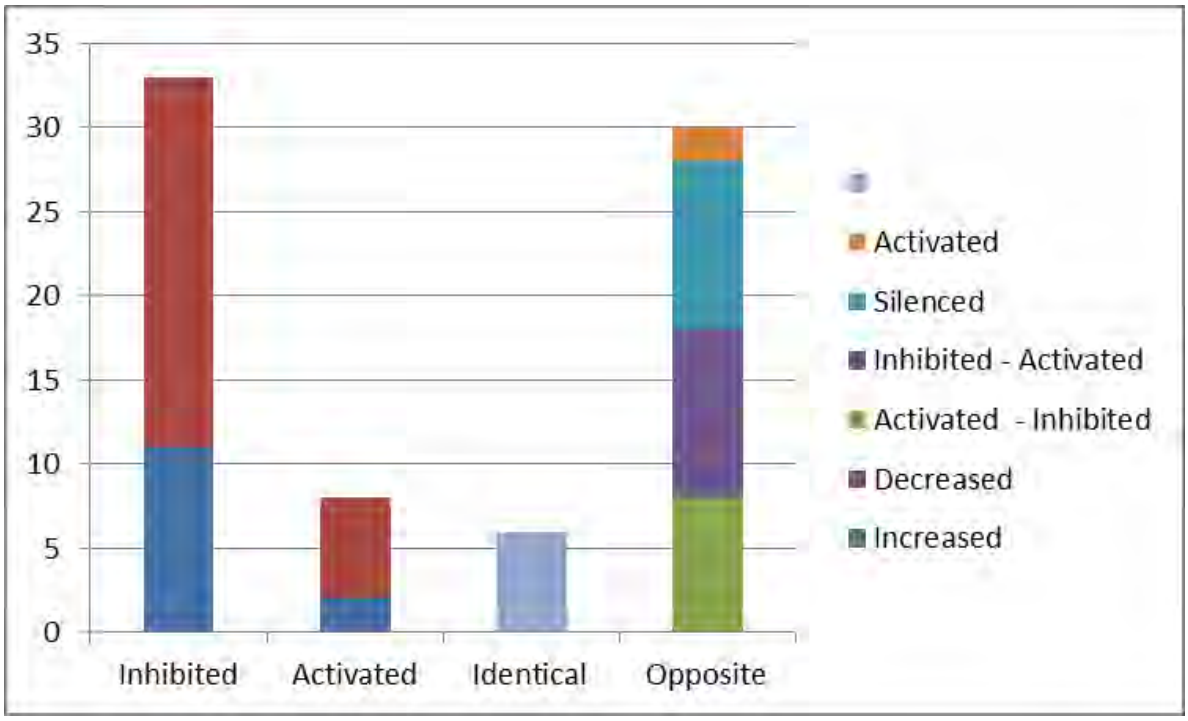

Figure 52: overview of lithium's effect on HIV-Tat induced dysregulation. Of those pathways where lithium treatment maintained the directionality of dysregulation, lithium tended to decrease the dysregulation. Lithium had no effect of the activation of six pathways. The dysregulation directionality of 30 pathways was reversed by lithium. 8 pathways activated by HIV-Tat were inhibited by lithium while 10 inhibited by HIV-Tat were activated by lithium. 10 pathways dysregulated by HIV-Tat are normal in lithium treated cells while 2 are uniquely dysregulated by lithium.

There are ten instances where lithium has completely abrogated the dysregulation induced by HIV-Tat; of these PTEN is likely directly related to its effect on apoptosis. A general observation is that lithium decreases the dysregulation in most HIV-Tat dysregulated pathways. Interestingly, although lithium inhibition of apoptosis is well established to act via the activation of AKT, there is little effect seen on the AKT signalling pathway. This may suggest that HIV-Tat dysregulation of the pathway is not via direct inhibition of the AKT, but rather that AKT is inhibited through a molecular cascade initiated by HIV-Tat. Furthermore, together with **Figure 57**, this data supports the direct activation of AKT by lithium. Although the immune activation previously

reported in Chapter 4 is less abundantly represented in **Figure 53,** *Activation of IRF by Cytosolic Pattern Recognition Receptors* is activated by HIV-Tat and, interestingly, this activation is decreased, but not abrogated by lithium. IRF7 activation has been shown to increase HIV replication.[413] Similarly, *the Induction of Apoptosis by HIV1* is activated by HIV-Tat and is appropriately inhibited by lithium. Dysregulation of *Dopamine receptor signalling* is important as it is one of the major neurotransmitters. Lithium decreases the magnitude of HIV-Tat induced activation. PCBD, a regulator of the Tyrosine hydrolase (TH) cofactor, BH4, which is critical to the production of dopamine[414,415] is significantly decreased in HIV-Tat treated cells but not in HIV-Tat + lithium treated cells.

The inhibition of ceramide and TNFR1 signalling correlates with apoptosis inhibition

Further involvement if HIV-Tat and lithium's effects on apoptosis are evident in **Figure 54.** *Ceramide* and *TNFR1 signalling* activation by HIV-Tat are both strongly inhibited by lithium and may, therefore, play prominent roles in HIV-Tat induced neuronal apoptosis. It is interesting to note that *Apoptosis signalling* is inhibited by HIV-Tat and that that inhibition is decreased by lithium. The protein synthesis regulators, *EIF2, mTOR* and *p70S6K signalling* as well as *Regulation of eIF4 and p70S6K Signalling* are all inhibited by HIV-Tat and activated by lithium. The cell cycle is also affected by HIV-Tat and can be seen in the dysregulation of *Cell Cycle: G2/M DNA Damage Checkpoint Regulation, Cell Cycle: G1/S Checkpoint Regulation, Role of CHK Proteins in Cell Cycle Checkpoint Control* and *CDK5 Signalling* in **Figure 53** and **Figure 54.** HIV-Vpr but not, HIV-Tat, has previously been described as stalling the cell cycle in the G2/M phase.[416] The strong inhibition of nerve growth factor (NGF) signalling in HIV-Tat treated cells is highly significant in relation to neurodevelopment and synaptic loss associated with HAND. By regulating the activity of cytoskeletal reorganisation machinery, NGF signalling regulates microtubule dependant axonal extension and maintenance in many neuronal types.[417] While the majority of pathways were identified in both experiments, several were unique to an experiment (**Figure 55**). Several significant pathways such as *long-term depression* were not identified in HIV-Tat + lithium treated cells.

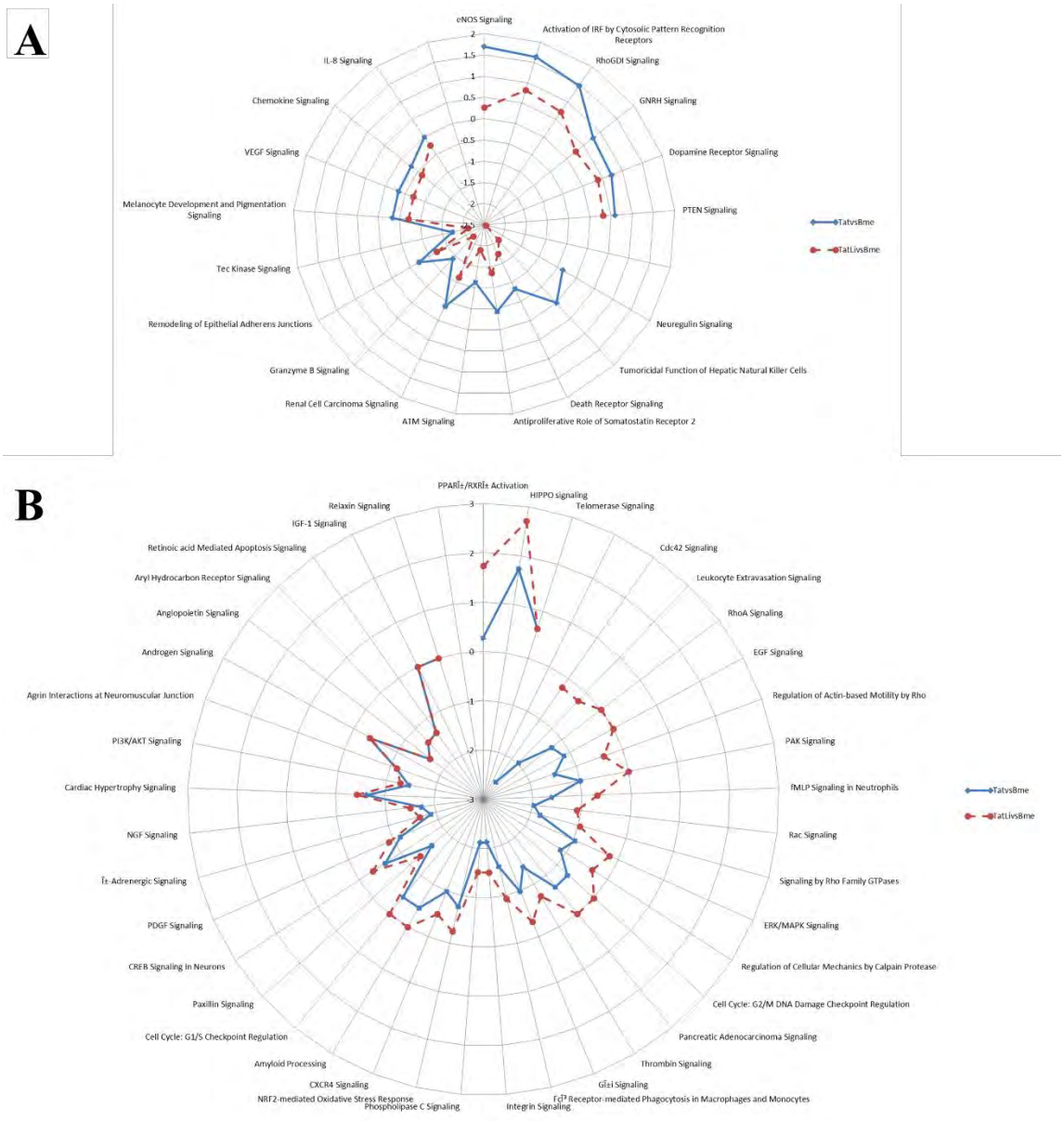

Figure 53: Radial plot showing the z-scores of both, HIV-Tat and HIV-Tat + lithium on pathways where the directionality of dysregulation was maintained. All pathways presented are, therefore, either inhibited further by lithium (red line outside) or the magnitude of the inhibition is decreased by lithium (blue line outside) but they remain inhibited. Each cluster of pathways is arranged from the most to least affected by HIV-Tat + lithium treatment relative to HIV-Tat treatment in a clockwise fashion.

Figure 54: Shared pathways where lithium reversed the directionality of the dysregulation induced by HIV-Tat. Both pathway clusters are arranged from the largest to smallest difference between HIV-Tat and HIV-Tat + lithium z-scores for each pathway in a clockwise fashion. Thus, the largest effects of lithium can be seen in ceramide and EIF2 signalling respectively.

Lithium increases the extent to which most pathways are dysregulated

As the magnitude of dysregulation varied between pathways and treatments so did the extent to which members of each pathway were dysregulated. Based on IPA canonical pathway outputs, the percentage of significantly dysregulated proteins in each pathway verses the total proteins identified for that pathway was calculated. Of the pathways the rate of dysregulation could calculated, 65 were common between both HIV-Tat and HIV-Tat + lithium treated analyses (**Figure 56**). The percentage of identified proteins of each pathway in each experimental condition that was dysregulated varied between 12.9% and 53.6%. As a general observation, lithium increased the rate of dysregulation in pathways when compared to HIV-Tat treated cells. A notable exceptions to this, however, are *insulin growth factor-1* (IGF-1) and *PI3K/AKT Signalling* which are, unsurprisingly, decreased by lithium. Their decreased rate of dysregulation may be a result of lithium's known effects on GSK-3β and AKT, respectively, which are regulators in those pathways.

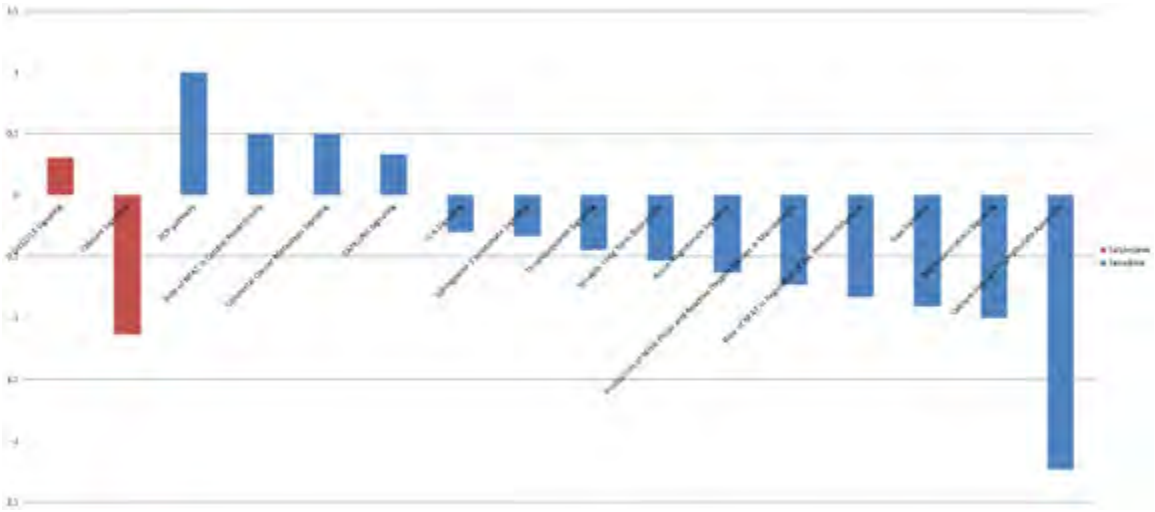

Figure 55: Several pathways with z-scores in each experiment were not found in the reciprocal experiment. These were not necessarily found in the reciprocal experiment, but did not have a uniform directionality to their dysregulation. HIV-Tat treated cells have many more dysregulated pathways than HIV-Tat + lithium treated cells.

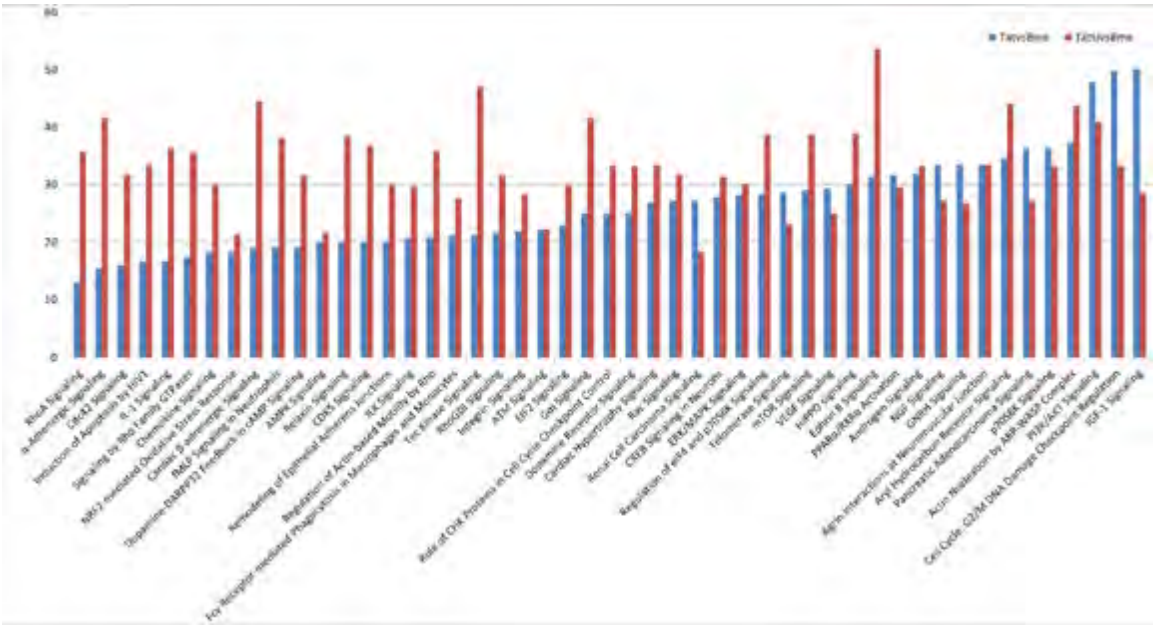

Figure 56: Rate of dysregulation. The percentage of proteins significantly dysregulated in each of the common pathways varies between 12.9% and 53.6%.

Lithium reverses the molecular signature of apoptosis

The effects of lithium on HIV-Tat induced apoptosis is the most important feature to characterise as it is the most documented feature in literature. While the molecular regulation of this effect is unknown, the phenotypic effect is well characterised. We see a predicted HIV-Tat induced decrease in AKT activity which correlates with the increased GSK3β activity (**Figure 57A**). Following lithium treatment, AKT activity is

predicted to increase which would signify a decrease in GSKβ activity due to increased ser9 phosphorylation (**Figure 57B**).[418]

The cell culture evidence showing that lithium is able to inhibit HIV-Tat induced cell death is clearly evident in the functional network analysis as well (**Figure 58**). The protein expression pattern induced by HIV-Tat is indicative of activated cell death and inhibited cell survival. Not unexpectedly, lithium treatment reversed almost all these effects such that cell death is predicted to be almost completely inhibited. Interestingly, however, cell survival and viability functions are inhibited further by lithium. Proteins involved in cell death and survival functions remain dysregulated despite lithium treatment and the inhibition of apoptosis; both, phenotypically and molecularly. **Figure 59** contains 106 dysregulated proteins involved in various cell death and survival functions as well as an array of other relevant pathways that they contribute to. This highlights the interconnectivity of pathways and cellular functions which further supports the need for detailed pathway analyses as dysregulation in individual pathways likely has widespread functional implications beyond those expected for a particular pathway.

Lithium specifically dysregulated several EIF proteins

Once more, EIF2 signalling was one of the most dysregulated pathways in both HIV-Tat and HIV-Tat + lithium treated cells. However, the effect of lithium on the pathway is qualitatively evident in that a greater proportion was significantly dysregulated in the HIV-Tat + lithium treated cells verses HIV-Tat treated only. While the directionality is reversed for some proteins, it is not for many others. HIV-Tat induced dysregulation of many EIF's was eliminated by lithium; however, most ribosomal proteins were dysregulated by lithium only. Interestingly, two specific EIF's discussed in Chapter 4, EIF4B and EIF3H which play a significant role in the regulation of protein synthesis 118 were inhibited in HIV-Tat and returned to normal levels in HIV-Tat + lithium treated cells. However, several EIF3 proteins, EIF4E and EIF4C remain significantly inhibited after lithium treatment. Nine phosphatases in EIF2 signalling were dysregulated; five in HIV-Tat and four in Tat + lithium treated cells respectively. Additionally, lithium inhibits the GTP-binding EIF2 subunit, EIF2β. The Full effects of lithium treatment on the EIF2 signalling pathway can be seen in (**Figure 60**).

HIV-Tat treated cells exhibit a marginal increase in initiation of translation of protein with 32 proteins identified as contributing to the function. Similarly, 29 proteins related to initiation of translation of protein were identified in HIV-Tat + lithium treated cells; 28 of which are shared with HIV-Tat treated cells. However, IPA reports no activation score in the HIV-Tat + lithium experiment.

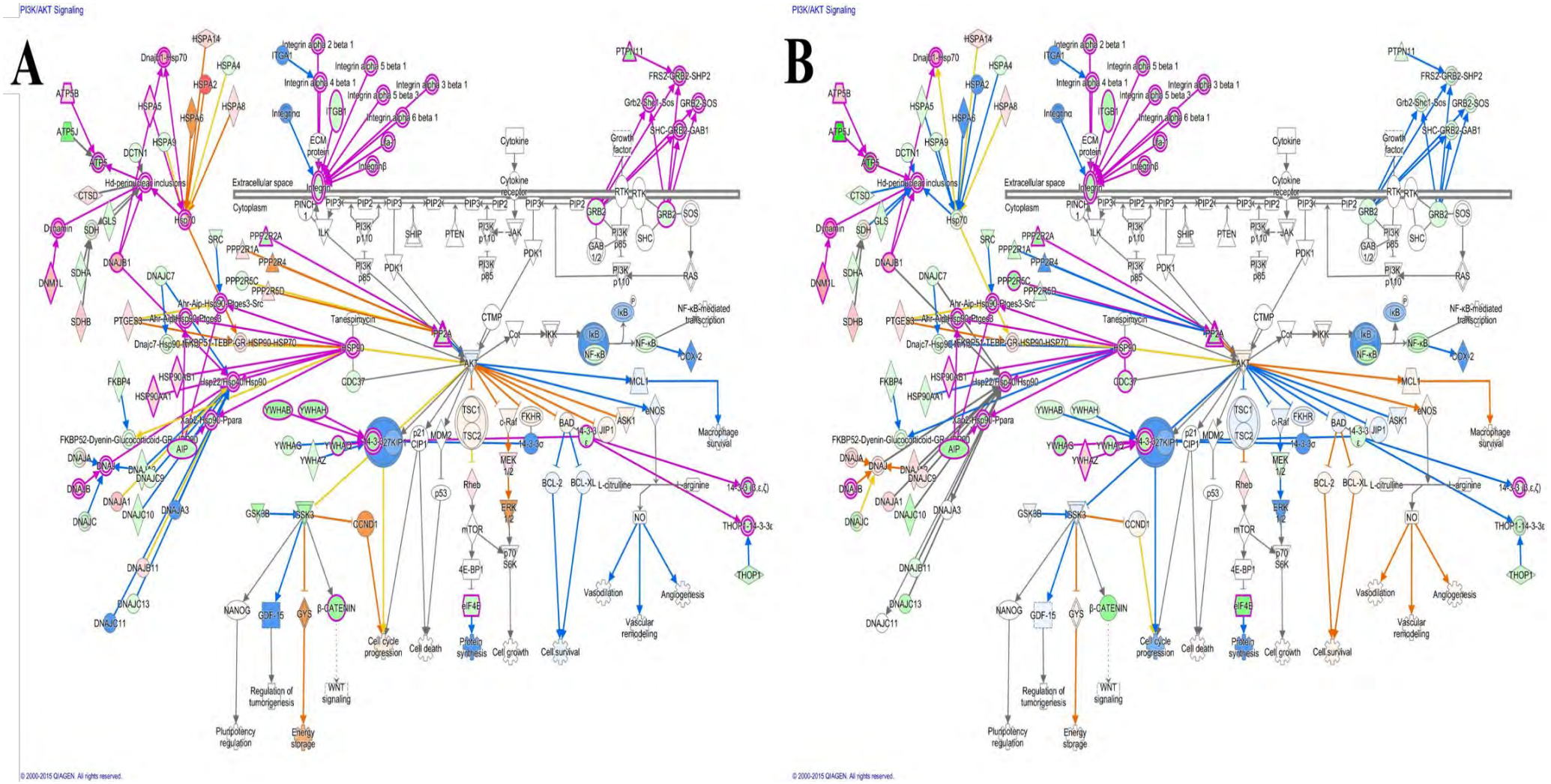

Figure 57: AKT signalling. AKT phosphorylates a diverse array of protein substrates; typically in a pro-survival, proliferative manner. Most importantly in this setting, AKT phosphorylates and inhibits GSK-3β. All proteins identified in the pathway are displayed with significantly dysregulated proteins and complexes highlighted in magenta. Green shaded proteins are identified and are decreased compared to the control while red shaded proteins have increased abundance. Additionally, blue shaded proteins and complexes are predicted to be inhibited while those predicted as activated are shaded in orange. A) HIV-Tat treated cells, B) HIV-Tat + lithium treated cells.

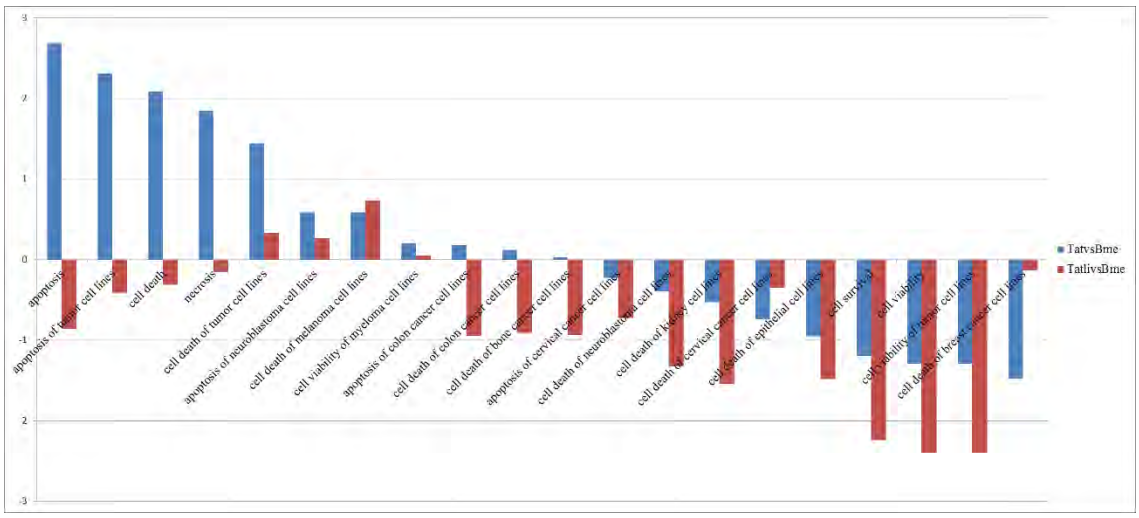

Figure 58: Cellular functions related to Cell death and survival depicting significant functions. IPA analysis predicts that Li^+ ameliorates most of the cell death functions and shows a clear relative decrease in cell death and an increase in cell survival. While lithium has a clear inhibitory effect on cell death and apoptosis, it also further inhibits cell survival and viability functions.

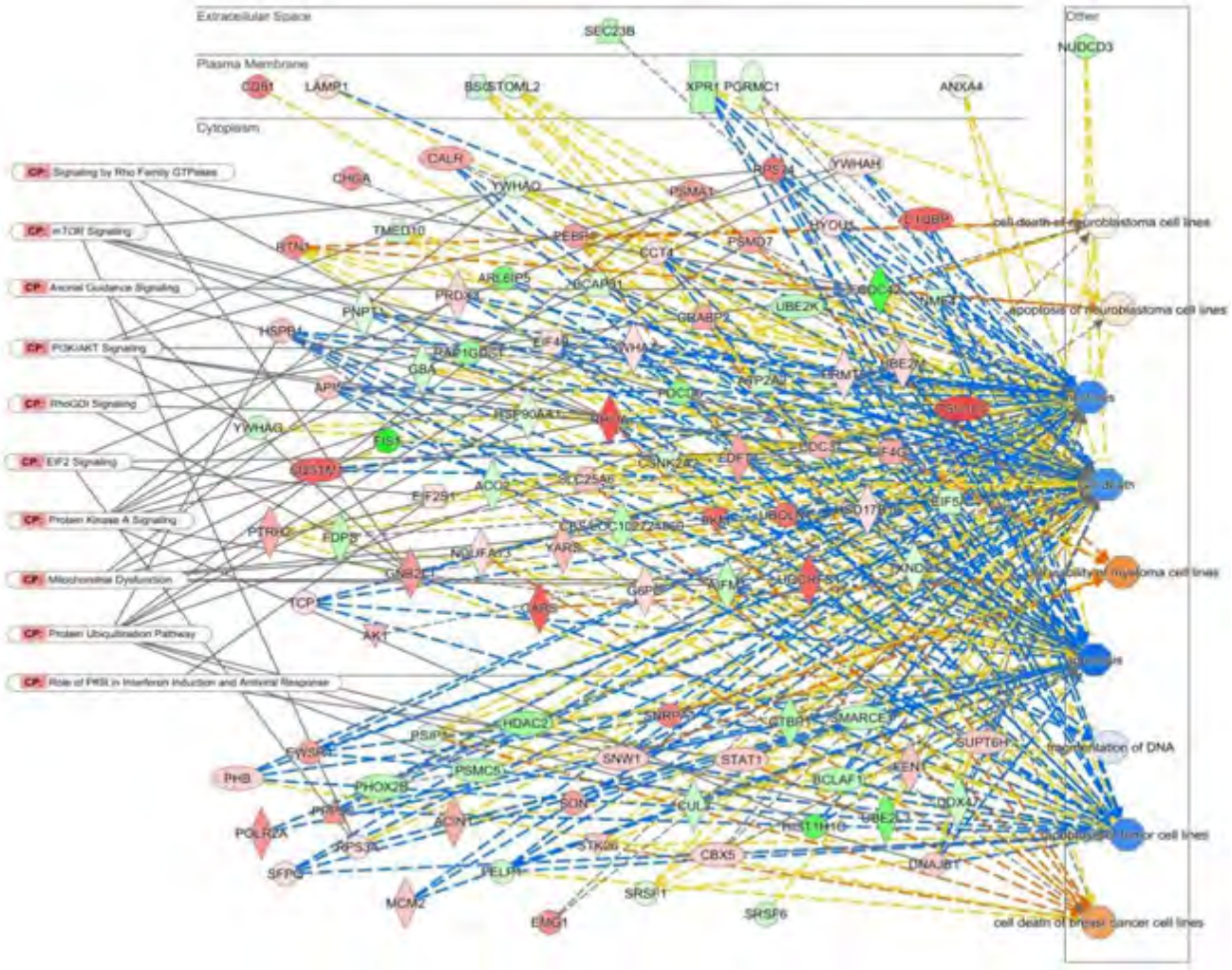

Figure 59: Cell death and survival functions: 106 significantly dysregulated proteins involved in cell death and survival functions in neuronal cells as well as an array of other important pathways. This indicates that many proteins and pathways contributing to the execution of apoptosis remain significantly dysregulated after lithium treatment.

Although the EIF2 signalling pathway is the most influential in the regulation of protein synthesis,[118] there are other pathways involved as well. The multifunctional mTOR pathway is involved in the regulation of many other pathways and functions including protein synthesis and cytoskeletal regulation.[419]

Given that protein synthesis occurs ubiquitously in all cells using conserved mechanisms, a great wealth of regulatory information exists with which to interpret the pathway data in (**Figure 60**)**.** Protein synthesis occurs in three defined steps with temporally and spatially defined requirements for each step. Thus, disruption of any step disrupts progression to subsequent steps and attenuates protein synthesis. Despite this, however, it was useful for us to analyse the IPA predictions of protein synthesis related functions based on expression patterns of proteins related to those functions. This analysis shows that functions related to protein synthesis are largely unchanged or decreased in HIV-Tat + lithium treated cells relative to HIV-Tat treated cells (**Figure 61**).

Along with the activation of several ER stress functions, Calpain (Capn1) signalling is inhibited by HIV-Tat treatment and is reversed by lithium. Calpain1 is known to associate with Pi3K [420] and its decrease led to decreased AKT activity and increased neuronal apoptosis. Capn1 loss is reported to decrease dendritic density and impair hippocampal LTP.[421,422]

60A

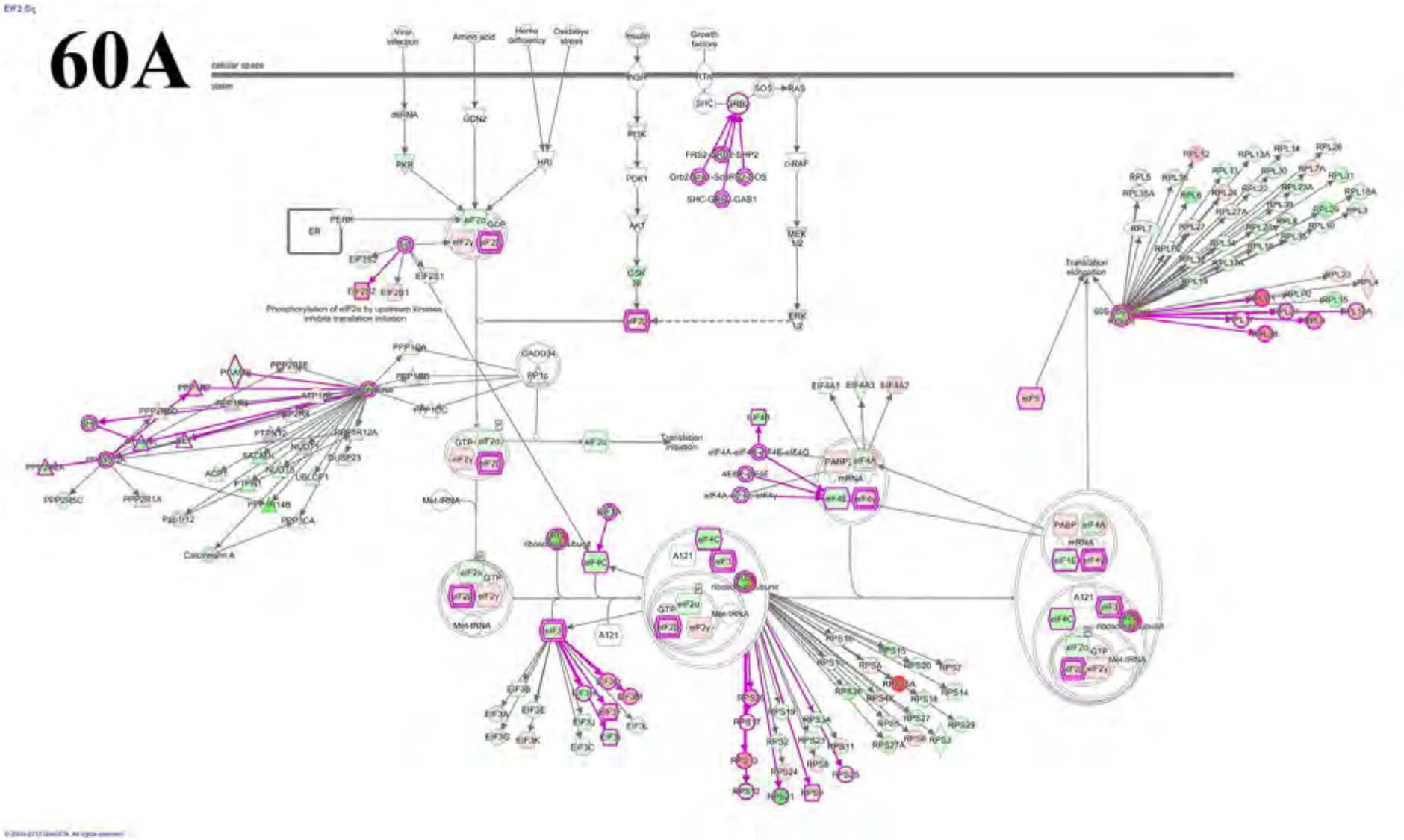
cellular space
cytosol
Viral infection
Amino acid
Heme deficiency
Oxidative stress
Insulin
Growth factors
dsRNA
GCN2
PKR
HRI
INSR
PI3K
PDK1
AKT
GSK 3β
SHC
GRB2
SOS
RAS
c-RAF
MEK 1/2
ERK 1/2
PERK
ER
eIF2α
eIF2γ
eIF2β
eIF2
EIF2S2
EIF2S1
EIF2B2
EIF2B1
Phosphorylation of eIF2α by upstream kinases inhibits translation initiation
PPP1CA
PPP1CB
PPP1CC
GADD34
RP1c
PPP2CB
PPP2R5E
PPP2R5D
PPP2R1A
PPP2R5C
PPP1R12A
PTPN12
NUDT1
NUDT5
SUSP23
UBLCP1
PPP1R14B
PPP1CA
Calcineurin A
GTP-eIF2α
Translation initiation
Met-tRNA
eIF4A1
eIF4A3
eIF4A2
eIF4B
eIF4A-eIF4E-eIF4G
PABP
mRNA
eIF4E
eIF4G
eIF5
Translation elongation
GDP
RPL12
RPL13A
RPL14
RPL26
RPL5
RPL36
RPL11
RPL30
RPL7A
RPL31
RPL35A
RPL6
RPL24
RPL22
RPL23A
RPL18A
RPL7
RPL27A
RPL29
RPL3
RPL27
RPL10
RPL34
RPL18
RPL35
RPL13
RPL19
RPL23
RPL4
RPL32
RPL15
RPL37A
RPL8
RPL38
eIF4C
A121
eIF3
ribosomal subunit
GTP
eIF2α
Met-tRNA
eIF2γ
eIF2
EIF3B
EIF3E
EIF3A
EIF3G
EIF3K
EIF3C
EIF3J
EIF3L
RPS10
RPS13
RPS12
RPS4A
RPS20
RPS7
RPS3A
RPS14
RPS18
RPS27
RPS29
RPS19
RPS3A
RPS23
RPS11
RPS27A
RPS8
RPS25
RPS24
RPS21
RPS15

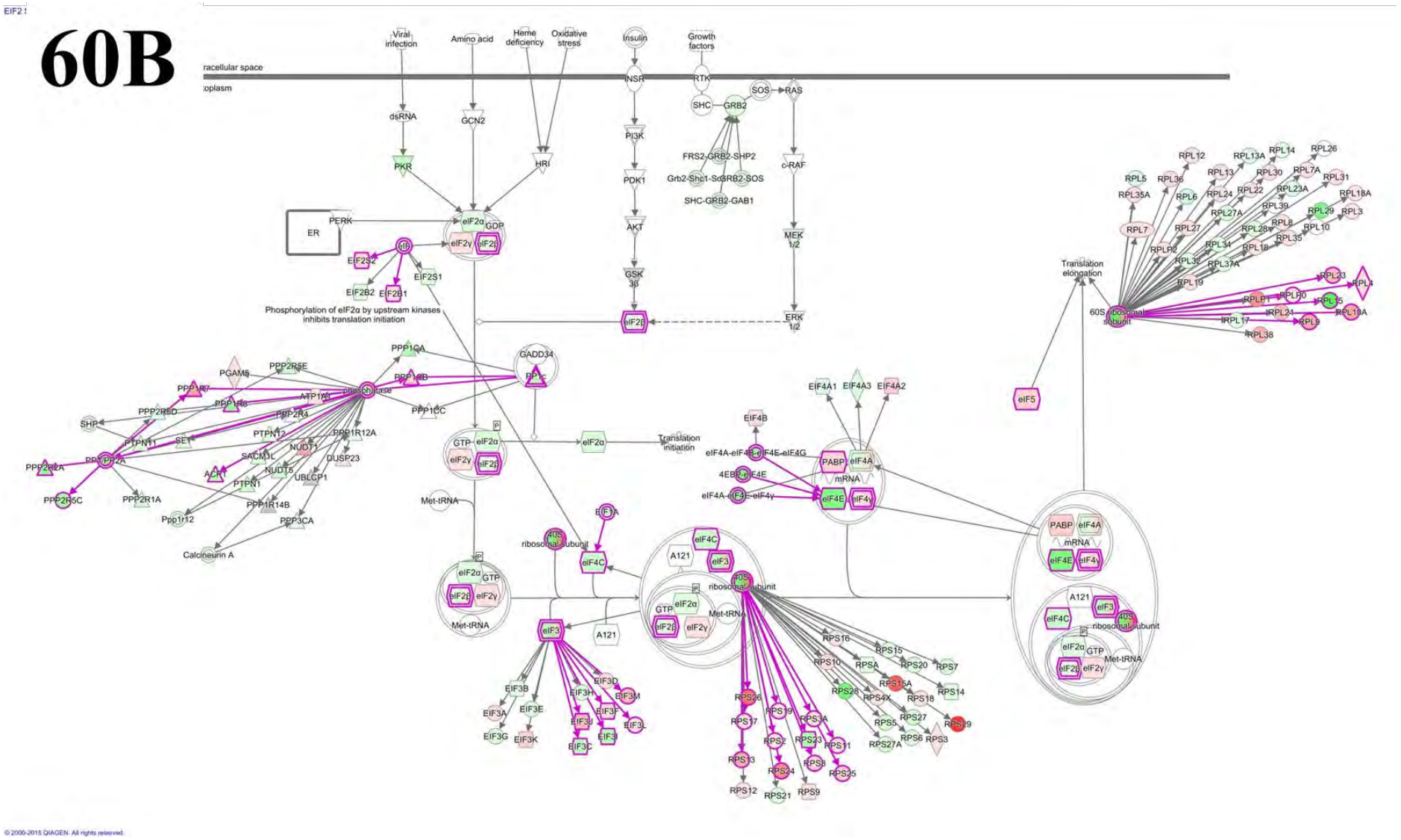

Figure 60: EIF2 signalling pathway; the primary protein synthesis regulator which integrates a diverse array of stress and proliferative signals to regulate the global and specific rates of protein synthesis. All protein identified in the pathway are displayed with significantly dysregulated proteins and complexes highlighted in magenta. Green shaded proteins are identified and are decreased compared to the control while red shaded proteins have increased abundance. A) HIV-Tat treated cells, B) HIV-Tat + lithium treated cells.

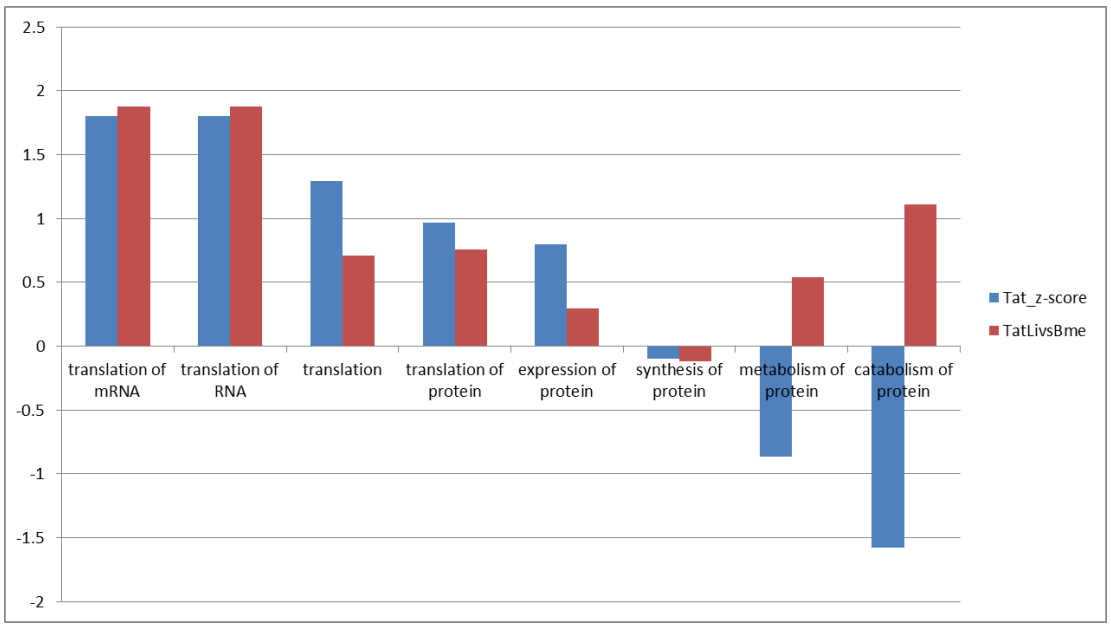

Figure 61: IPA predictions of shared protein synthesis functions. Functions related to protein synthesis shared HIV-Tat and HIV-Tat + lithium show the functional implication of the patterns of protein expression. Functions are plotted with IA calculated activation scores showing the extent of either activation or inhibition

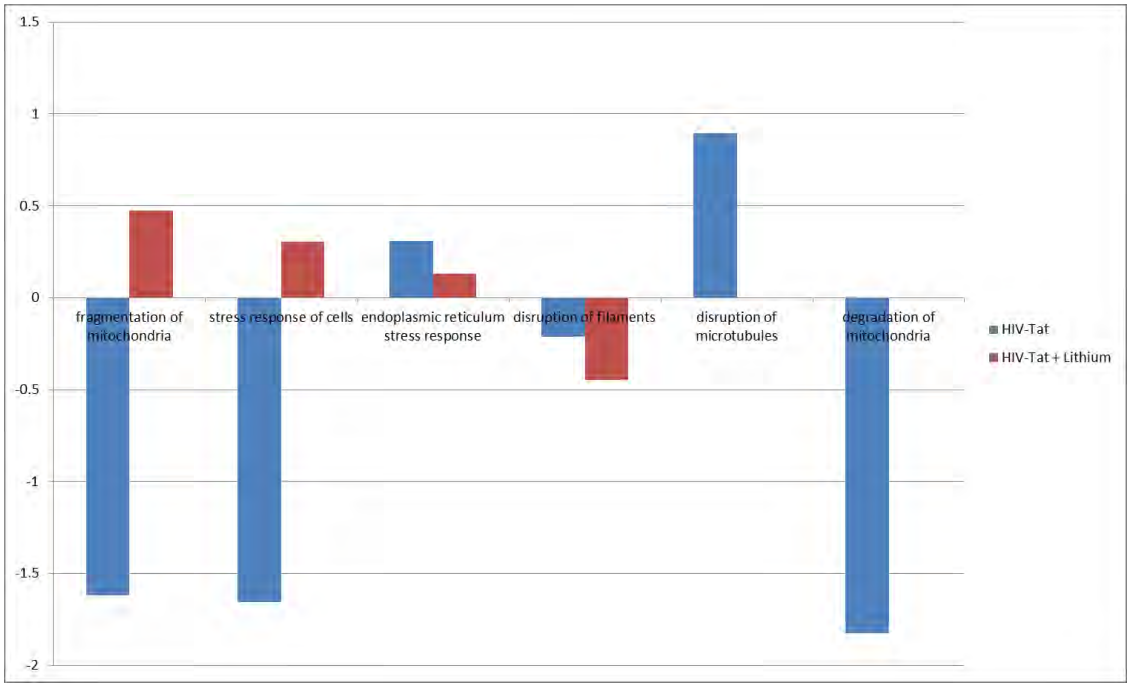

Figure 62: Cellular compromise functions: evidence for the activation of cellular stress functions. Functions related to the cellular stress response shared by HIV-Tat and HIV-Tat + lithium show the functional implication of the patterns of protein expression. Functions are plotted with IPA calculated activation scores showing the extent of either activation or inhibition

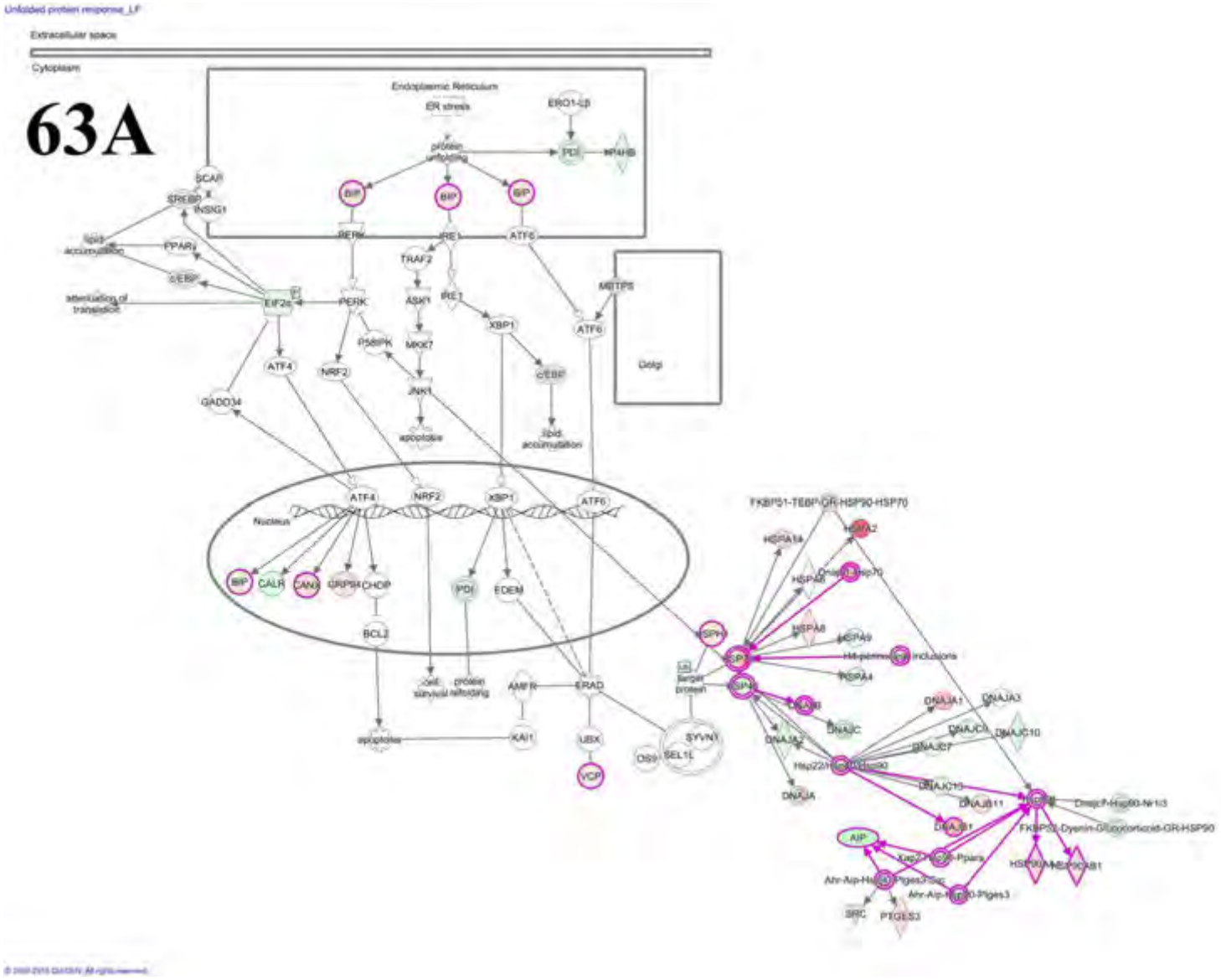
Unfolded protein response_LF
Extracellular space
Cytoplasm
63A
Endoplasmic Reticulum
ER stress
ERO1-Lβ
PDI
MTHFD
protein unfolding
SCAP
SREBP
INSIG1
BiP
PERK
IRE1
ATF6
TRAF2
PPARα
C/EBP
EIF2α
ASK1
MBTPS
XBP1
ATF4
NRF2
P58IPK
MKK7
JNK1
CHOP
GADD34
apoptosis
lipid accumulation
Golgi
Nucleus
CALR
CANX
GRP94
PDI
EDEM
BCL2
AMFR
ERAD
KAI1
UBX
VCP
SYVN1
SEL1L
HSPH1
HSPA2
HSPA1A
HSPA8
HSPA9
HSPA4
DNAJA1
DNAJA3
DNAJB1
DNAJC
DNAJC7
DNAJC10
DNAJA2
DNAJA
DNAJC10
DNAJB11
HSP90B1
AIP
SRC
PTGES3
FKBP51-TEBP-GR-HSP90-HSP70

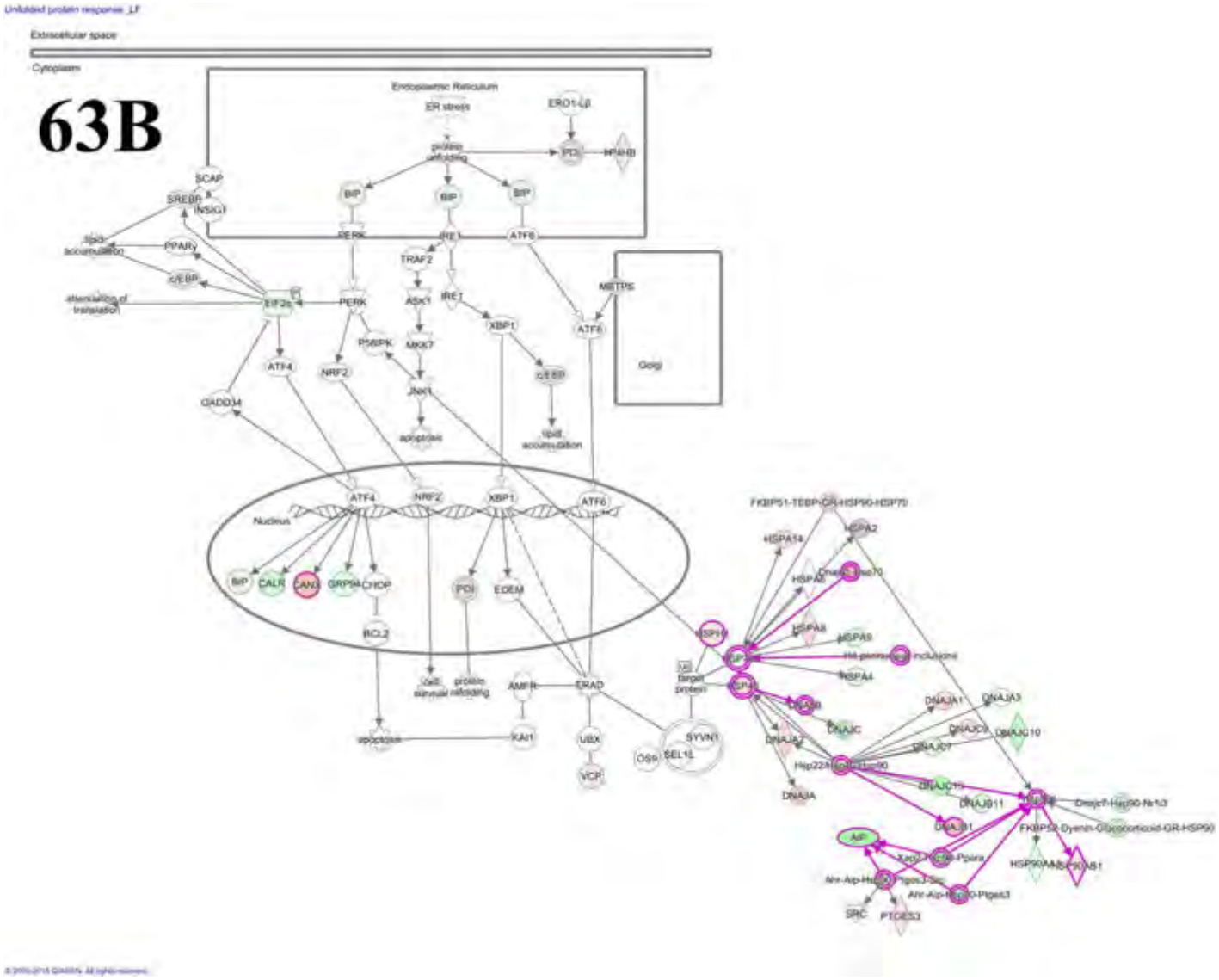

Figure 63: Unfolded protein response; A cellular stress response activated in response to ER stress and unfolded protein accumulation. All protein identified in the pathway are displayed with significantly dysregulated proteins and complexes highlighted in magenta. Green shaded proteins are identified and are decreased compared to the control while red shaded proteins have increased abundance. A) HIV-Tat treated cells, B) HIV-Tat + lithium treated cells.

64A

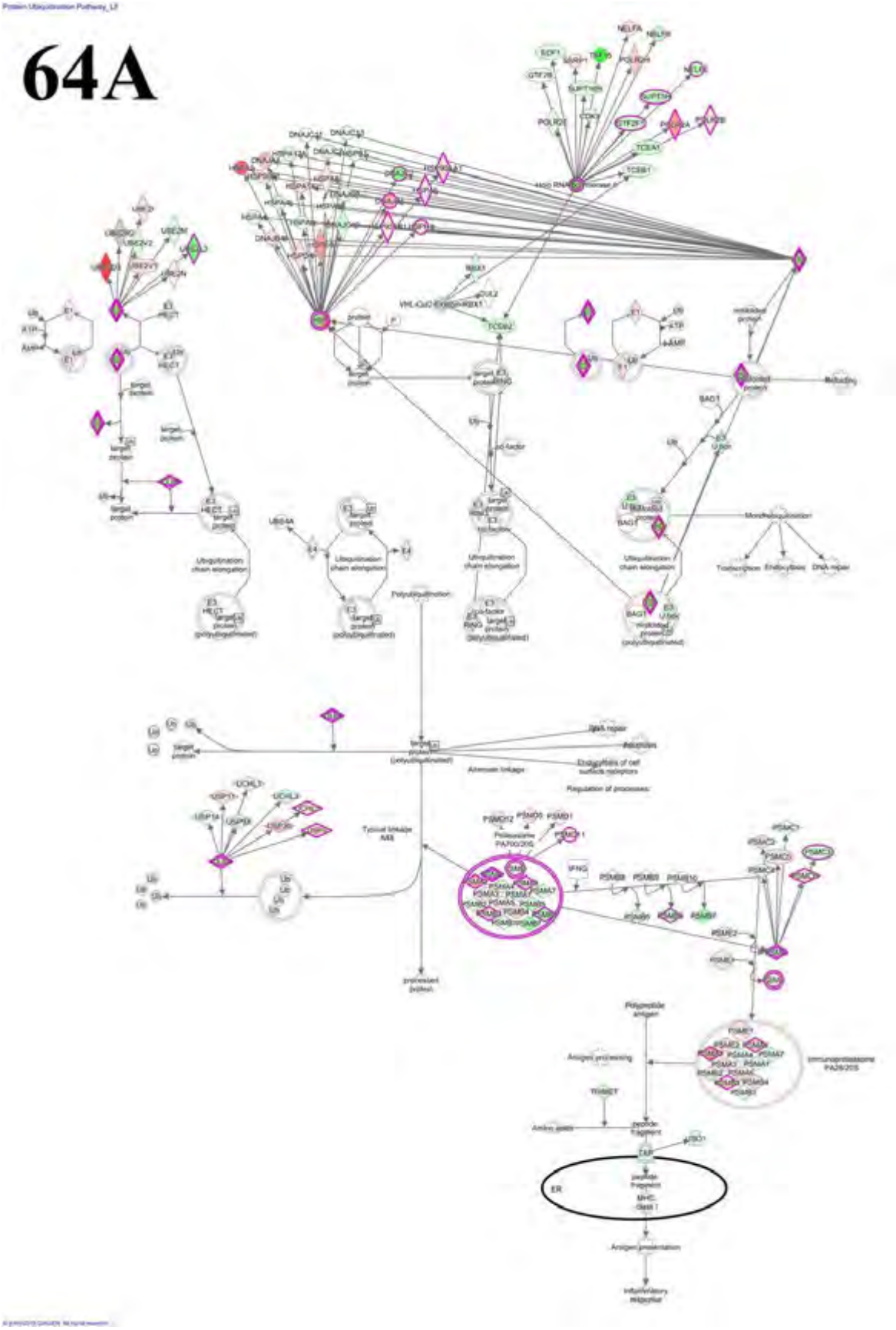

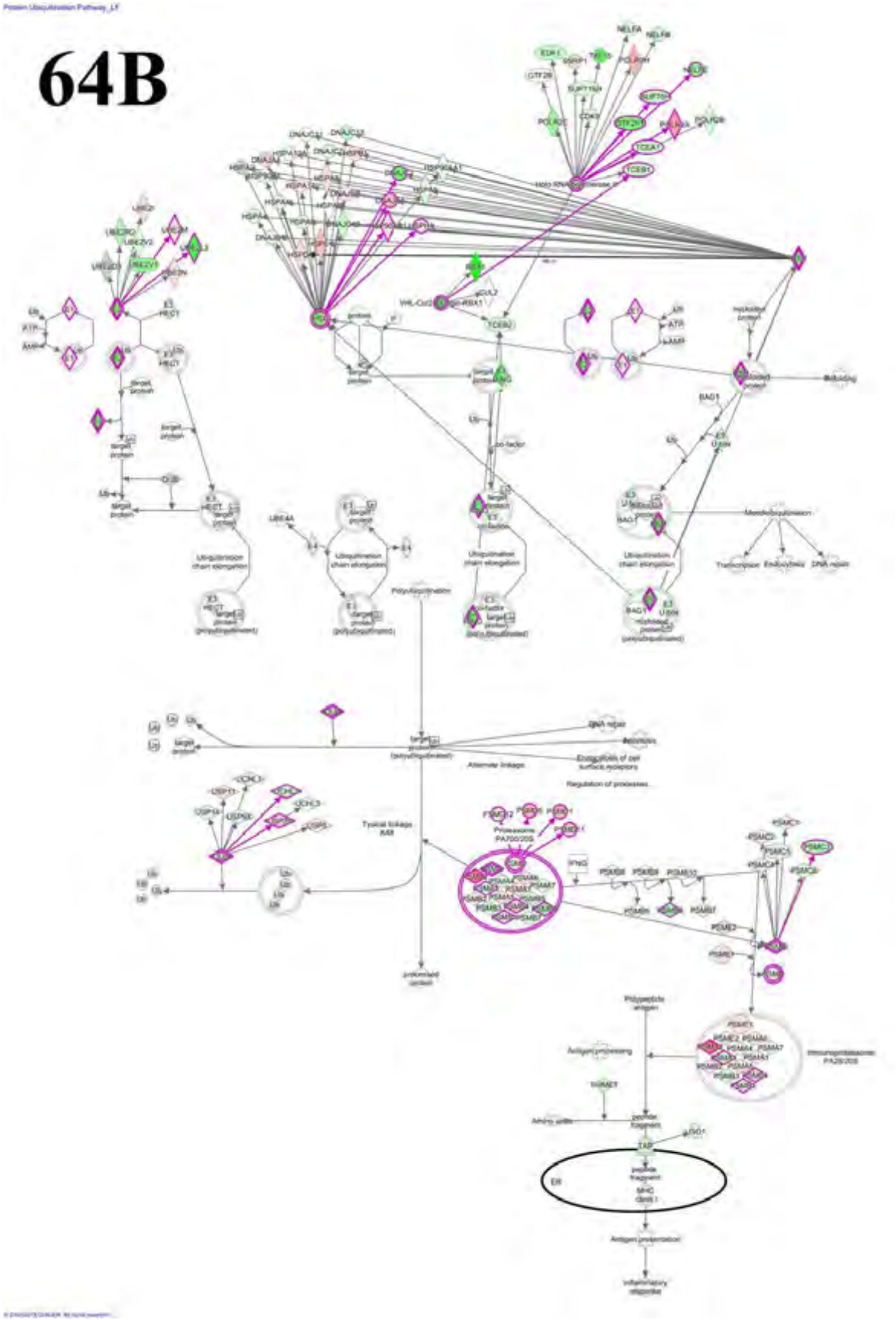

Figure 64: Protein Ubiquitination Pathway; protein ubiquitination functions as a post-translational modification which primarily targets proteins for proteasomal degradation. All protein identified in the pathway are displayed with significantly dysregulated proteins and complexes highlighted in magenta. Green shaded proteins are identified and are decreased compared to the control while red shaded proteins have increased abundance. A) HIV-Tat treated cells, B) HIV-Tat + lithium treated cells.

Lithium does not abrogate endoplasmic reticulum stress nor UPR activation

As was highlighted previously, global protein synthesis can be regulated by the endoplasmic reticulum resident kinase, PKR-like endoplasmic reticulum kinase, PERK.[115] PERK is phosphorylated and activated by endoplasmic reticulum stress resultant from, among others, unfolded protein accumulation.[423] The ensuing stress response then functions to decrease or completely inhibit global protein synthesis, increase protein ubiquitination and degradation and to increase levels of protein folding chaperones.[424] ER stress is activated by HIV-Tat treatment and is modestly attenuated by lithium (**Figure 62**). Interestingly, *fragmentation and degradation of mitochondria* are strongly inhibited by HIV-Tat with the former being activated by lithium. Functionally, ER stress induces protein ubiquitination and the UPR primarily to decrease the rate of protein synthesis and increase the clearance of unfolded protein by degradation and refolding. Interestingly, we see dysregulatory effects resultant from both HIV-Tat and HIV-Tat + lithium treatment in these cellular functions.

Two prominent unfolded protein response (UPR) induced ER chaperones, BiP and CANX and are significantly dysregulated by HIV-Tat. BiP is significantly upregulated in HIV-Tat treated cells but not Tat + lithium treated cells. HIV-Tat induced activation of CANX is maintained in HIV-Tat + lithium cells. Furthermore, while lithium does reverse the dysregulation of the chaperone, HSP90AA1, more remain dysregulated (**Figure 63**). Despite the large representation of chaperones in the UPR pathway, the majority were not differentially dysregulated by HIV-Tat (**Figure 63A**) nor by lithium (**Figure 63B**).

Protein ubiquitination and proteasomal activity function together and are represented in **Figure 64**, we see that many protein folding chaperones such as members of the DNAJ and HSP families are differentially regulated by HIV-Tat (**Figure 64A**). In some cases such as with HSPA5, lithium normalizes their abundance (**Figure 64B**). However, other chaperones are either specifically dysregulated by lithium or their dysregulation is maintained by lithium. Within the protein ubiquitination pathway, E2 ligases are responsible for actively ubiquitinating and targeting proteins for proteasomal degradation.[425] Our data shows that HIV-Tat dysregulates one E2 ligase and lithium maintains its dysregulation and additionally dysregulates another. In addition E1 and E3 are significantly dysregulated in lithium treated cells; both are important for protein

ubiquitination. As is the case in other elements of this pathway, several proteasome subunits are dysregulated by either or both treatments. As a general observation, most significantly dysregulated proteasomal proteins are activated.

Lithium effects on HIV-Tat induced Cytoskeletal dysregulation

The cytoskeleton is involved in many cellular functions beyond the structural integrity of the cell. Many cellular processes communicate with the exterior environment through the cytoskeleton as it extends throughout the cell, through the membrane and makes direct contact with the cell exterior and ECM. Its contacts with the ECM guide cellular movement and cell projections. Furthermore, synapse loss is an integral part of HAND pathology. Therefore, understanding the means through which HIV is able to dysregulate and destabilize synapses is paramount to understanding the disease and to guiding therapeutic intervention.[426]

The dysregulation of the cytoskeleton is likely the most important feature of HIV-Tat induced neuronal dysregulation as it is directly responsible for the degradation of neuronal dendrites and synapses. While the dysregulation of protein synthesis is certainly important as it is involved in many neurodegenerative diseases and is a prominent feature in our work, its dysregulation is likely not directly responsible for the loss of synapses although it may be contributory. To assess the impact of lithium on the regulation of the cytoskeleton, we investigated pathways involved in cytoskeletal functions as well as the functional implications of cytoskeleton regulating pathways.

Many cytoskeletal regulatory proteins are specifically dysregulated by lithium

Integrin signalling and the member proteins are major cell-surface proteins responsible for cell-ECM and cell-cell adhesion and interaction. They also function as binding sites for extracellular ligands and transduce signals to the cell interior. They can, however, transduce signals to the exterior as well. Many of these signalling events serve as regulators driving cytoskeletal reorganisation guided by extracellular cues.[427,428]

HIV-Tat induces significant dysregulation in many key proteins involved in integrin signalling such as ITGB1, PTPN11, ARF4, cdc42 and RhoA (**Figure 65A**). After lithium treatment, all but PTPN11 are maintained and others such as RhoG, CrkL, TSPAN6 and

ARP were significantly dysregulated in response to lithium (**Figure 65B**). As a central upstream regulator of many Rho-dependant cytoskeletal regulatory functions, RhoA and RhoG dysregulation may have a significant impact on cytoskeletal dynamics. TSPAN6 is associated with AD pathology[429] while loss of CrkL inhibits dendritogenesis.[430]

Key phosphatases are dysregulated by lithium

Actin nucleation by ARP-WASP complex (**Figure 66**) is primarily responsible for regulating actin polymerisation in several actin filaments and are critical in the development, establishment and maintenance of dendritic spines and synapses.[359] The process of actin polymerisation is primarily controlled by the ARP-WASP proteins. This is responsible for many functions including cell motility and plasma membrane protrusions in the formation of lamellipodia and filopodia. Lamellipodial and filopodial protrusions from neurons are integral to axon extension, guidance, the formation of axon branches, and synaptic structures.[323,354] ARP are responsible for polymerising and, therefore, lengthening F-actin filaments.[323] Loss of ARP2/3 proteins or its activators alters spine morphology and reduces their number.[431] Many cytoskeletal regulatory elements such as RhoA and an array of phosphatases such as PP2A and PP1 family members are dysregulated as well. A PP2A regulatory subunit (PPP2R) dysregulated by HIV-Tat is maintained by lithium while an additional subunit and several other phosphatases are dysregulated. The HIV-Tat induced dysregulation of growth factor receptor-bound protein 2 (GRB2) is inhibited by lithium. GRB2 is known to inhibit HIV induced activation of toll-like receptor (TLR) signalling.

Lithium dysregulates cytoskeletal regulatory G protein coupled receptor subunits

GTPases are small signalling molecules involved in the regulation of diverse cellular functions including reorganisation of the actin cytoskeleton,[432,251] morphogenesis,[251] transcriptional regulation,[432] cell-cell junctions,[251,433] vesicle trafficking,[237,432] neutrophil activation, phagocytosis, activation of the NADPH oxidase, mitogenesis, apoptosis and tumorigenesis.[434] Along with the already mentioned RhoA and RhoG dysregulation, we see differential GNAI dysregulation between HIV-Tat and HIV-Tat + lithium treated cells (**Figure 67**). GNAI3 is activated by HIV-Tat; this, along with the inhibition of GNAS, is maintained in lithium treated cells. Similarly, GNB1, GNB2,

GNB2L1 are specifically activated by lithium. These G-proteins are upstream regulators of the major cytoskeletal regulators, cdc42, Rac and Rho.[435,436] Although not significantly dysregulated, the increase in cofilin activity in **Figure 67B** results in the prediction of increased actin polymerisation, likely, by increasing barbed ends which are required for ARP2/3 mediated actin polymerisation. Cofilin is responsible for severing F-actin filaments and its increase leads to synaptic loss in AD.[437] Lithium maintains the HIV-Tat induced dysregulated Septins, Sept9 and Sept11 and additionally dysregulates Sept2 and Sept7. Septins not only regulate the cytoskeleton,[438] but have been found to play a role in AD.[439] ARP2/3 family proteins play major roles in synaptic plasticity[359] as they are the major actin polymerising proteins and are further dysregulated by lithium. Their dysregulation would result in the cell's inability to regulate the growth of actin filaments which are paramount to the structural integrity of synapses.

Neuronal cell protrusion functions remain dysregulated in lithium treated cells

Given the importance of the cytoskeleton and that it plays a role in many cellular functions and pathways, the specific functional implication of dysregulations in individual pathways may be difficult to assess. The IPA predicted effects of the cytoskeletal dysregulation induced in both HIV-Tat and HIV-Tat + lithium treated cells allows for comparison of the functional implication of the dysregulation (**Figure 68**)**.** Despite the continued dysregulation of cytoskeleton regulating pathways with lithium treatment, the functional effects of those dysregulations are typically less pronounced when compared to HIV-Tat treated cells. Important functions such as *neuritogenesis* and *morphogenesis of neurites* predicted only in HIV-Tat treated cells are not evident in HIV-Tat + lithium treated cells. Similarly, among others, lithium induces the inhibition of *extension of cellular protrusions*.

65A

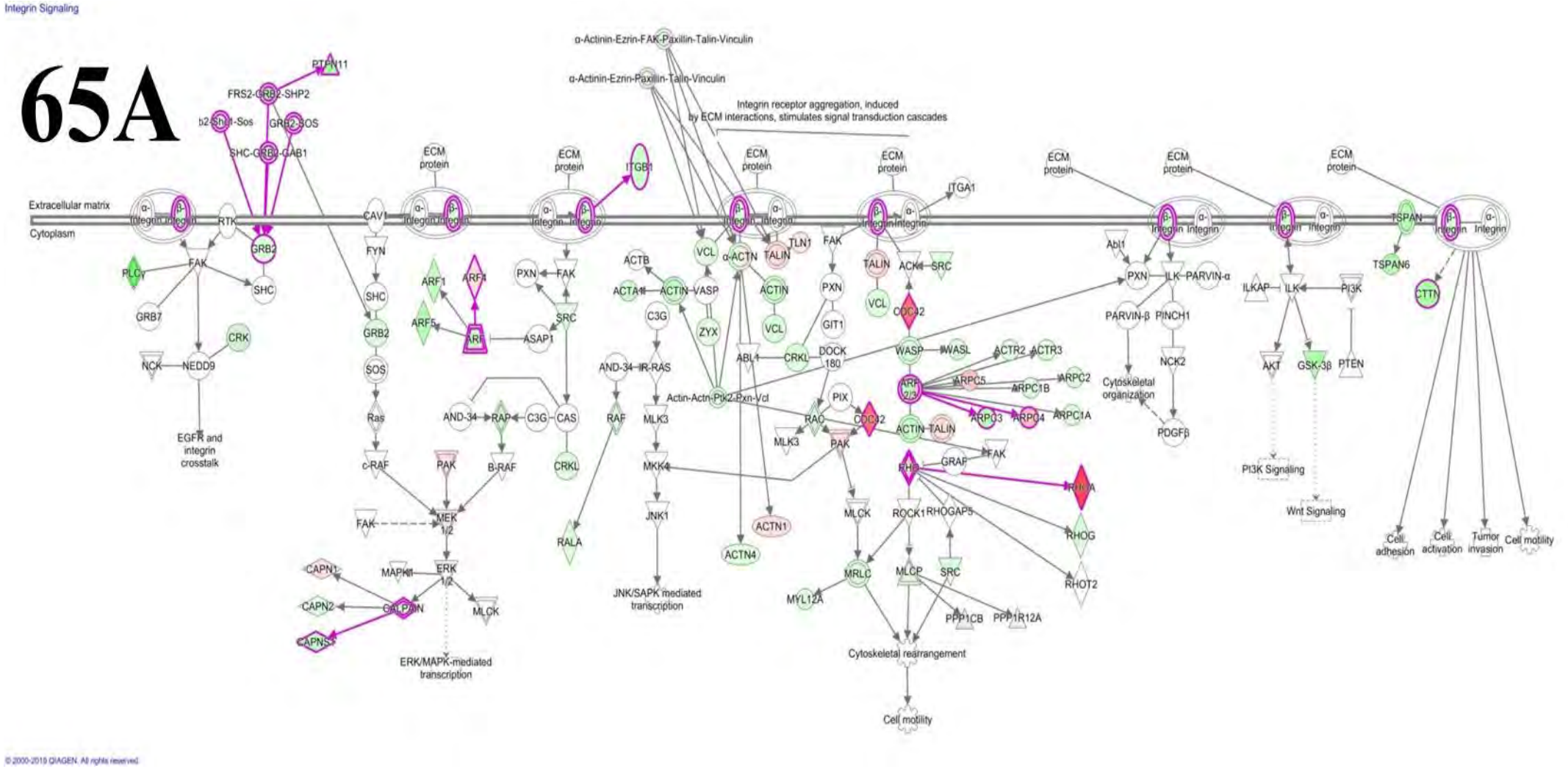
Integrin Signaling
α-Actinin-Ezrin-FAK-Paxillin-Talin-Vinculin
α-Actinin-Ezrin-Paxillin-Talin-Vinculin
Integrin receptor aggregation, induced by ECM interactions, stimulates signal transduction cascades
Extracellular matrix
Cytoplasm
PTPN11
FRS2-GRB2-SHP2
b2-Shc-Sos
GRB2-SOS
SHC-GRB2-GAB1
ECM protein
ITGB1
ITGA1
RTK
GRB2
CAV1
FYN
SHC
GRB2
SOS
Ras
c-RAF
MEK 1/2
ERK 1/2
MAPKII
CAPN1
CAPN2
CAPNS1
CALPAIN
MLCK
ERK/MAPK-mediated transcription
PLCγ
FAK
SHC
GRB7
CRK
NCK
NEDD9
EGFR and integrin crosstalk
PAK
B-RAF
ARF1
ARF4
ARF5
ARF
ASAP1
PXN
FAK
SRC
AND-34
RAP
C3G
CAS
CRKL
RALA
RAF
ACTB
ACTA1
ACTIN
VASP
C3G
ZYX
AND-34-IR-RAS
MLK3
MKK4
JNK1
JNK/SAPK mediated transcription
VCL
α-ACTN
TALIN
TLN1
ACTIN
VCL
ABL1
CRKL
DOCK 180
Actin-Actn-Ptk2-Pxn-Vcl
ACTN1
ACTN4
FAK
TALIN
ACK
SRC
PXN
GIT1
VCL
CDC42
WASP
WASL
ACTR2
ACTR3
ARP 2/3
ARPC5
ARPC2
ARPC1B
ARPC3
ARPC4
ARPC1A
PIX
RAC
CDC42
ACTIN-TALIN
MLK3
PAK
FAK
GRAF
RHO
RHOA
RHOG
RHOT2
MLCK
ROCK1
RHOGAP5
MRLC
MLCP
SRC
MYL12A
PPP1CB
PPP1R12A
Cytoskeletal rearrangement
Cell motility
Abl1
PXN
ILK
PARVIN-α
PARVIN-β
PINCH1
NCK2
Cytoskeletal organization
PDGFβ
ILKAP
ILK
PI3K
AKT
GSK-3β
PTEN
PI3K Signaling
Wnt Signaling
TSPAN
TSPAN6
CTTN
Cell adhesion
Cell activation
Tumor invasion
Cell motility
© 2000-2019 QIAGEN. All rights reserved.

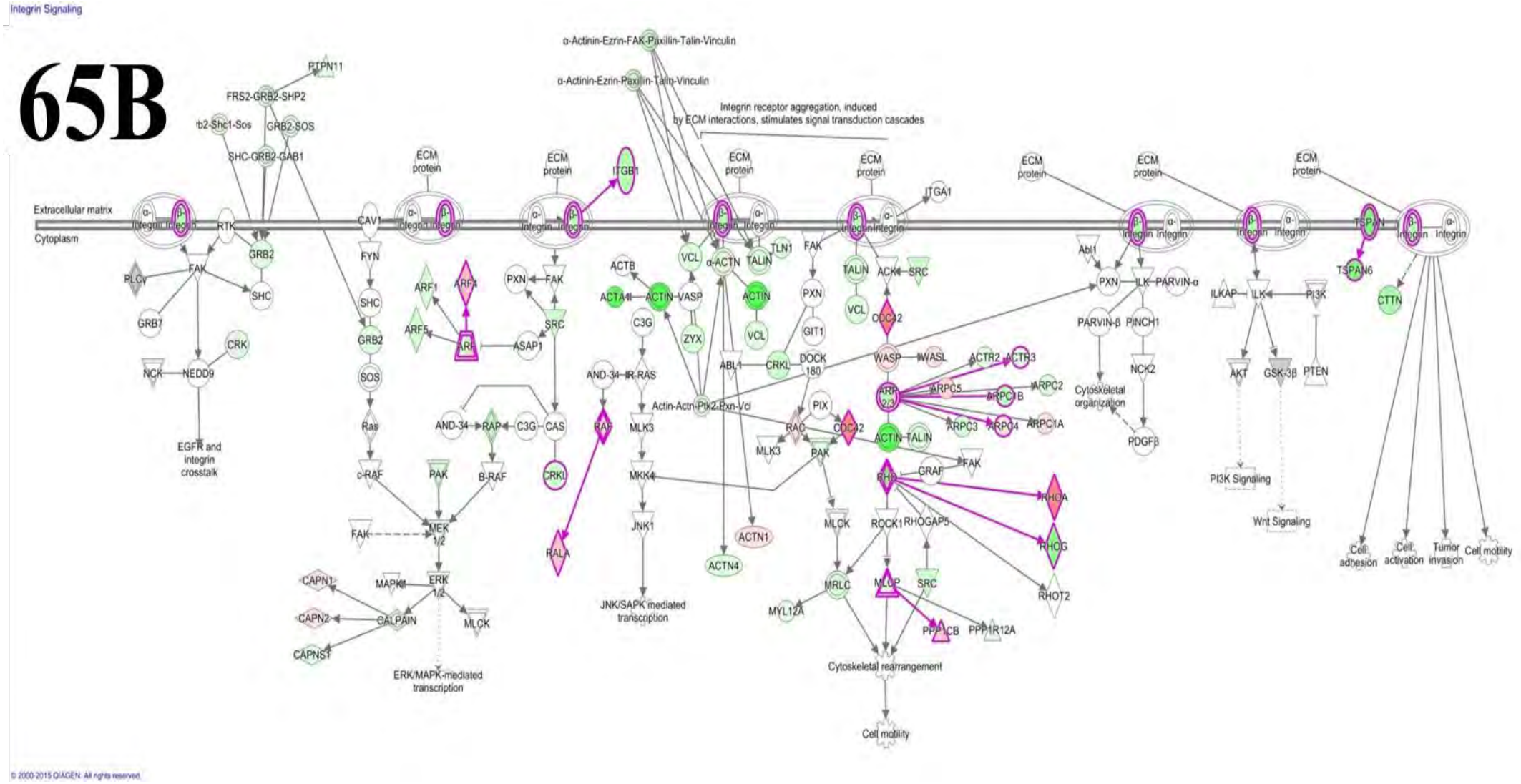

Figure 65: Integrin signalling pathway; A major family of cell-surface proteins responsible for cell-cell and cell-surface adhesion. Along with their downstream signalling proteins, they are responsible for signal transduction through the cell membrane. All protein identified in the pathway are displayed with significantly dysregulated proteins and complexes highlighted in magenta. Green shaded proteins are identified and are decreased compared to the control while red shaded proteins have increased abundance. A) HIV-Tat treated cells, B) HIV-Tat + lithium treated cells.

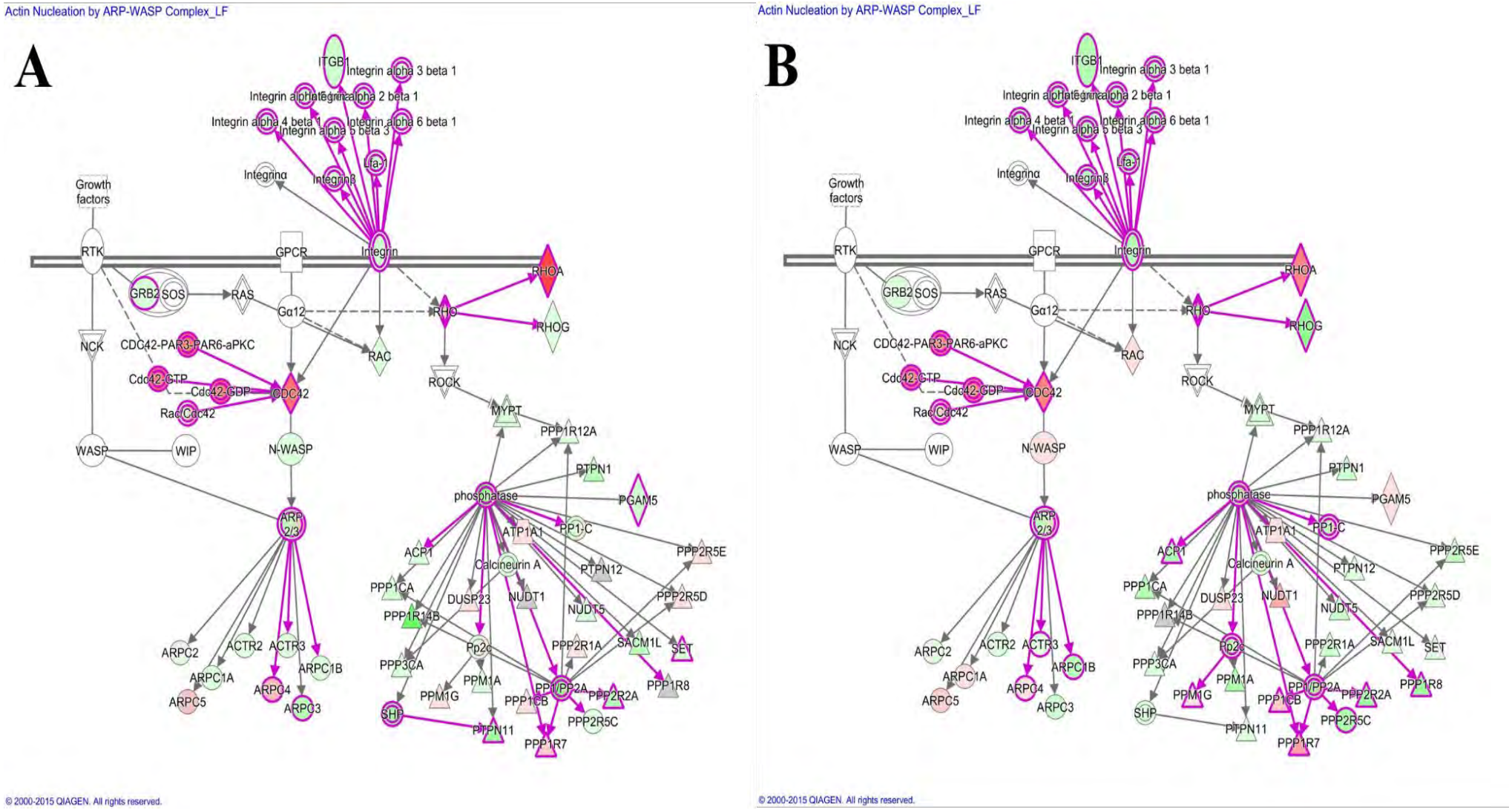

Figure 66: Actin nucleation by ARP-WASP complex. Along with their regulators, such as WASP, ARP proteins are responsible for actin polymerisation during cytoskeletal reorganisation. All protein identified in the pathway are displayed with significantly dysregulated proteins and complexes highlighted in magenta. Green shaded proteins are identified and are decreased compared to the control while red shaded proteins have increased abundance. A) HIV-Tat treated cells, B) HIV-Tat + lithium treated cells.

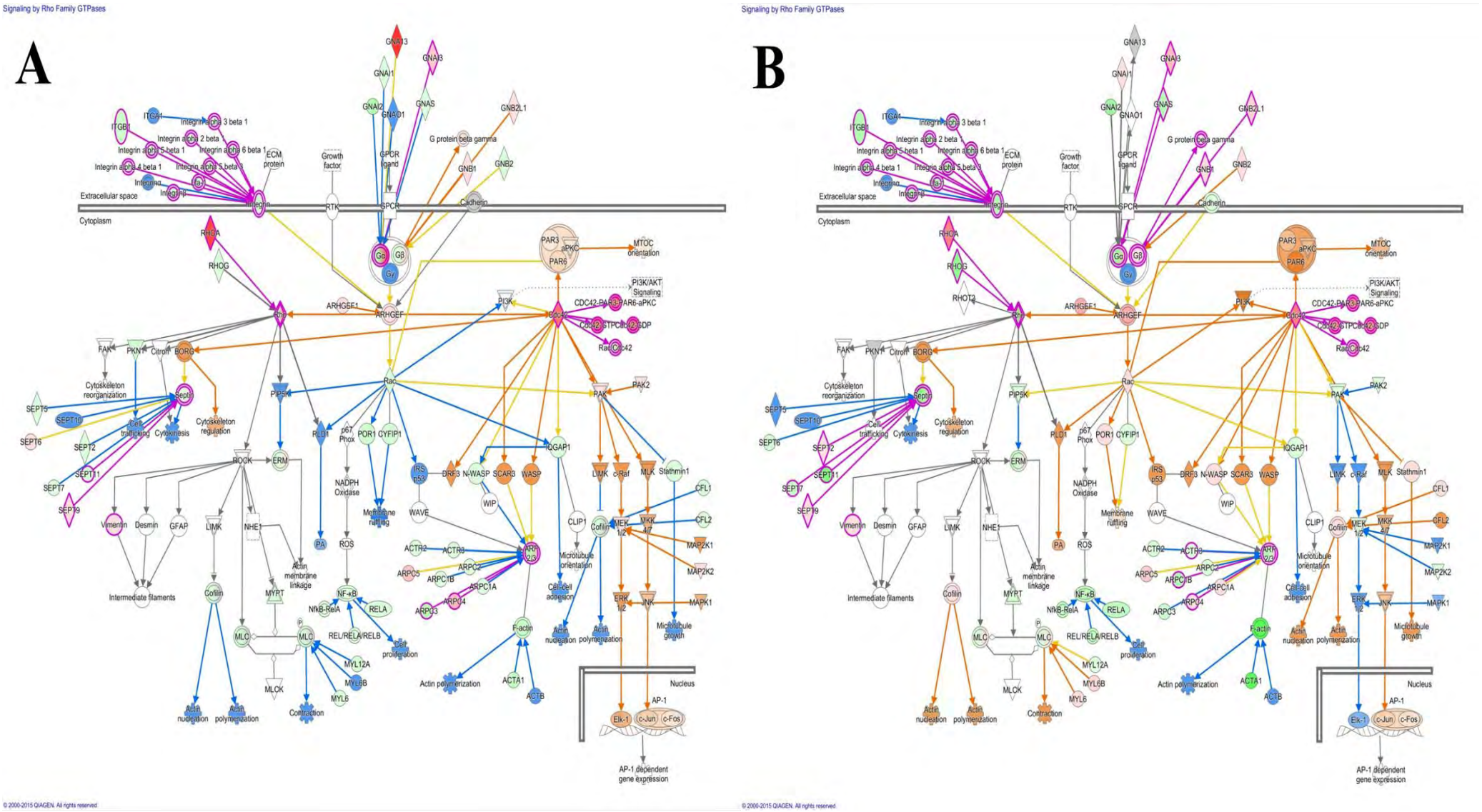

Figure 67: Signalling by Rho family GTPases. Molecule Activity Predictor (MAP) shows the predicted effect of the given protein abundance pattern on both relevant cellular functions and proteins. Blue and orange indicate predicted inhibition and activation respectively. Green and red shaded proteins are identified and decreased or increased respectively compared to the control. Proteins and complexes highlighted in magenta are significantly dysregulated in the respective experiment. A) HIV-Tat treated cells, B) HIV-Tat + lithium treated cells.

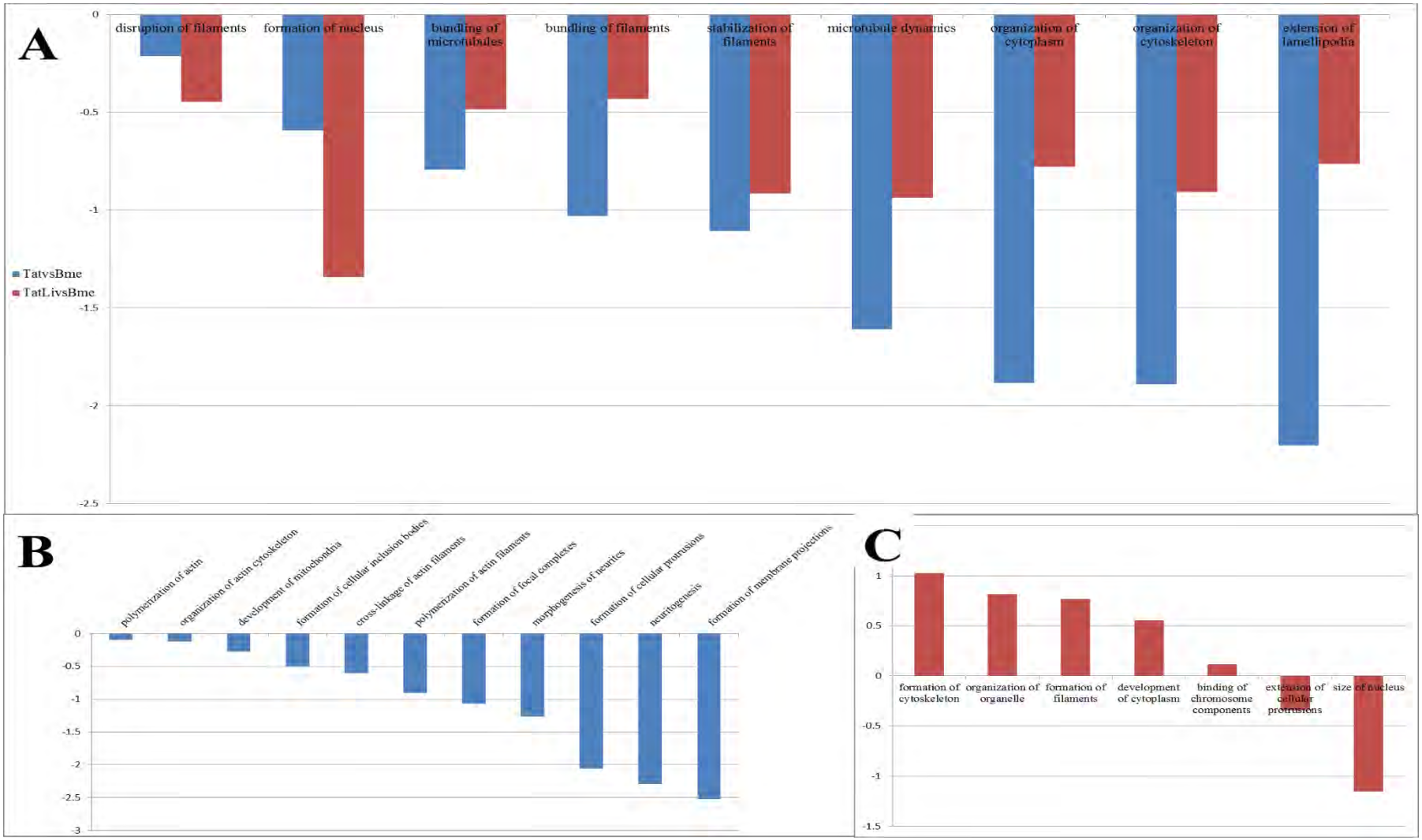

Figure 68: Several dysregulated cellular functions related to the cytoskeleton that are contained within the *Cellular Assembly and Organization* description in the *Disease and function* utility in IPA. The Degree of dysregulation induced by lithium on the pathways dysregulated by HIV-Tat varies between pathways. The majority of pathways dysregulated by HIV-Tat remain dysregulated after lithium treatment (A). Several Important functions such as *neuritogenesis* and *morphogenesis of neurites* are only identified in HIV-Tat treated cells (B). Similar functions such as *extension of cellular protrusions* are, however, are identified in HIV-Tat + lithium treated cells (C).

Discussion

Given the central and canonical role GSK-3β occupies in HIV-Tat mediated neurotoxicity, it is reasonable to investigate lithium for its therapeutic potential. However, despite the wide use of lithium, little is known about its molecular effects in a cell beyond that of inhibiting GSK-3β via AKT activation. We, therefore, aimed to elucidate the extent of the proteomic changes induced by lithium on HIV-Tat treated neuroblastoma cells as well as the functional implications of those changes. That lithium inhibited apoptosis in cell culture was clear, however, the mechanisms responsible are not well understood beyond the activation of AKT. With this data, we tried to further understand the cellular dysregulation induced by HIV-Tat as well as the mechanisms through which lithium alters that response. We also specifically aimed to determine the effect lithium has on the cytoskeletal dysregulation induced by HIV-Tat and whether that would affect neurite and, ultimately, synapse loss. Given that the current consensus is that HAND is the result of synaptic loss rather than neuronal loss, lithium's ability to effect neurite maintenance and function is significant. Ochs *et al*, showed that GSK-3β knockout resulted in a decrease in dendritic spine density in the hippocampus.[440] Takahashi *et al* investigated the effect of lithium on the development of primary rat hippocampal neurons. They found that the inhibition of GSK-3β and phosphorylated tau inhibited neurite growth and purpose that this would hinder axon and synapse formation.[441] Work by Shah *et al,* however, shows that neurite growth can be improved by low doses of lithium such that GSK3β is attenuated rather than completely inhibited in primary murine neuronal cultures.[442] The role of GSK-3β in neurodegenerative diseases is complex and often not well understood. FXS is associated with increased dendritic spine density and GSK-3β activation. Subsequently, GSK-3β inhibition in FXS alleviates behavioural deficits. [440] Thus, if the same trend is expected, GSK-3β inhibition in HAND may serve to further destabilize synapses.

From these, and many other works, it is clear that GSK-3β plays an important role in synapse formation and maintenance as well as being central to HIV-Tat induced apoptosis. Our previous work (Chapter 4) provides a detailed description of the proteomic alterations and the functional implications of HIV-Tat treatment in neurons.

We will, therefore, not detail the current data to the same extent, except for significant pathways and functions exclusive to this dataset.

Initially, the observation that HIV-Tat and HIV-Tat + lithium experiments shared so few differentially regulated proteins despite the overlap in identification was unexpected. However, both lithium and HIV-Tat have an array of target molecules and there is no reason, biological or other, for those targets to overlap. The wide range of targets for both molecules is reflected in the number of differentially regulated proteins in each experiment. That many HIV-Tat induced changes were ameliorated would hold promise for lithium's therapeutic benefit if not for the observation that lithium increased the dysregulation of many proteins and pathways as well as uniquely inducing an array of dysregulated proteins and pathways. Similarly, the vast majority of HIV-Tat dysregulated pathways remain dysregulated in lithium treated cells. Despite the observation that lithium generally increases the rate of dysregulation, a more detailed analysis of the proteins, pathways and functions dysregulated is required to gauge the effect of lithium on HIV-Tat treated cells.

Pathway analysis overview

It is well established that HIV-Tat is neurotoxic and induces gross neuronal morphological changes and apoptosis. It is also well established that Lithium treatment is able to protect neurons from HIV-Tat induced apoptosis. In the previous chapter (Chapter 4), several dysregulated pathways and cellular functions are described; these may or may not be consequent or causative of apoptosis and may, thus, be completely uncoupled from apoptotic signalling. Furthermore, it is accepted that *in vivo* neuronal apoptosis is not primarily responsible for the onset of HAND symptoms in patients. In this study, we aimed to ascertain whether lithium has any positive effects on the HIV-Tat-induced dysregulation of key pathways and cellular functions which contribute to and ultimately result in synapse loss.

It is well known that lithium treatment induces many unfavourable side effects along with the associated behavioural alterations.[443] There are, however, very few studies attempting to document the molecular dysregulations induced by lithium or the molecular source of the behavioural alterations it induces. Since lithium's effects are

non-specific, it is not unexpected that it induces cellular dysregulations of its own. It is, however, interesting that there are many HIV-Tat induced dysregulations which are ameliorated by lithium.

The extent to which GSK-3β inhibition by lithium would benefit HAND patients is difficult to assess by merely considering its effect on apoptosis or neurite growth and maintenance. The brain has a significant level of redundancy in its structure and function. The exact pathology in HAND patients is not known, but it is feasible that significant loss of neuronal functionality must develop before symptoms manifest. Indeed, this is supported by the observation that ~90% of HIV^+ patients display post mortem evidence of neuropathology whereas significantly fewer present with HAND during their lifetimes. It is undeniable that GSK-3β and its inhibition will affect the progression and development of HAND. As the dysregulated processes directly involved in the onset of apoptosis are likely not entirely responsible for the neurodegeneration seen in HAND patients, pathways intuitively related to other cellular functions may be more intimately involved. Given the previously discussed (Chapter 4) importance of cytoskeletal and protein synthesis regulation, their maintained dysregulation in HIV-Tat + lithium treated cells identifies them as targets for further investigation. The discussion will, henceforth, be focussed on proteins, pathways and functions which may directly influence neurodegenerative processes in HAND.

HIV-Tat induced dopamine receptor signalling

HIV replication is reported to increase when host cells are exposed to increasing dopamine levels[444] Congruent to this, HIV patients have higher CFS dopamine levels and develop hypersensitivity to dopamine antagonists. In addition to HIV-Tat's function as a HIV-LTR transactivator, it may increase dopamine signalling specifically to increase the rate of HIV replication. HAND affects patient brains asymmetrically with significantly more damage being caused in dopamine rich brain regions. Whether this results from increased sensitivity of these areas to HIV or whether HIV replicates more efficiently there and, therefore, the causative agents are in greater abundance is not known. Silver *et al,* show that inhibition of dopamine receptor, DR1, completely inhibited HIV-Tat induced apoptosis in rat midbrain primary neuronal cells but not in

hippocampal cells where DR1 expression is low.[445] Given that lithium reduced dopamine receptor signalling activation induced by HIV-Tat may suggest that lithium's activity on AKT/GSK-3β may be directed through the dopamine receptor.

Lithium inhibition of HIV-Tat induced neuronal apoptosis

HIV-Tat treatment induces dysregulation indicative of cell death and inhibits those of cell survival. Despite lithium's complete inhibition of apoptosis in cell culture, it is interesting that it further inhibits cell survival functions**.** It may be that lithium is merely capable of blocking the execution of apoptosis but not the signals which induce apoptosis during HIV-Tat treatment. Indeed, there remains significant dysregulation in AKT, particularly with chaperones and the phosphatases, PP2A and PP1, as well as other cell survival pathways. The dysregulation of chaperones and proteasomal proteins are likely indicative of cellar stress such as ER stress which can induce apoptosis.

Using global proteomic data as presented here to conclusively identify a molecular mechanism responsible for the induction of apoptosis is not trivial. This is especially so given the number of pathways and functions identified to be dysregulated. However, given that apoptosis is completely inhibited according to cell culture data as well as functional analysis of the resultant MS data, it is feasible to assume that the pathways and functions which are responsible for the execution of apoptosis should be activated in HIV-Tat treated cells and dramatically and notably inhibited by lithium. Following this reasoning, ceramide and TNFR1 signalling present themselves as obvious candidates. Both are strongly activated by HIV-Tat and inhibited by lithium treatment.

Ceramide signalling induces apoptosis by activating PP2A phosphatase which dephosphorylates and inactivates Bcl-2. Both TNFR1 signalling[446] and IL-1[447] have been shown to accumulate ceramide and induce ceramide dependant apoptosis. Furthermore, lithium has been shown to inhibit ceramide induced apoptosis by decreasing Bcl-2 dephosphorylation via PP2A inhibition.[140] While the proteomic data does not describe HIV-Tat effects on the inflammatory response as well as our gene expression data does, pathways such as *Activation of IRF by Cytosolic Pattern Recognition Receptor IL-1 signalling, IL-8 signalling and TNFR1 signalling* suggest that

lithium supresses the HIV-Tat induced activation of proinflammatory molecules, pathways and functions. Interestingly, PTPN11 (SHP-2) negatively regulates TLR mediated IRF-3 activation and proinflammatory cytokine (TNF-α, INF-β) production, and loss of the phosphatase exacerbates the proinflammatory response.[448,449] As may be expected of its involvement in cytoskeletal reorganisation, PTPN11 regulates the formation of Lamellipodia.[449] Furthermore, PTPN11 regulates cells adhesion and plays a role in hippocampal synapse formation.[450] Its loss impairs learning and memory in mice and induces neuronal and behavioural deficits in mice.[451] That lithium abrogates the significant decrease of PTPN11 induced by HIV-Tat supports proposition that the inflammatory response activated by HIV-Tat initiates pro-apoptotic signalling in HIV-Tat treated neurons. Interestingly, TNFR1 along with Fas contribute to death receptor signalling.

Inhibition of CREB blocks GSK-3β mediated inhibition of PP2A [452] which suggests that CREB is an intermediate between PP2A and GSK-3β activity. However, both seem capable of regulating each other; the outcomes of which are dependent on the stimulus. CREB activity is required for neuronal LTP and LTD in learning and memory functions.[368,367,453] Furthermore, AKT phosphorylates and activates CREB.[454] While CREB inhibition did decrease upon lithium treatment, it was not activated as would be expected from active AKT. Additionally, CREB activity is decreased in AD brains and Ameloid-β (Aβ) tangle treated neurons in cell culture.[455] Hippo signalling is also known to negatively regulate AKT signalling [456] and is known to be upregulated in HIV-infected CD8 T cells, but the exact role in HIV infection is not known.[457] Hippo activation, therefore, promotes apoptosis in its primary function to regulate organ development and size.[458] It is interesting that lithium further increases the HIV-Tat induced activation of Hippo signalling while concurrently activating AKT. This further supports our hypothesis that lithium merely disrupts the execution of apoptosis at the level of AKT while maintaining or exacerbating the original pro-apoptotic signals. While Hippo is activated during neuronal differentiation,[459] its role in differentiated neuronal cells is unknown. Although the specifics are unknown, it is clear that dysregulated hippo signalling contributes to neurodegeneration.

The relationships between and contributions of pathways to seemingly unrelated cellular functions is often overlooked in pathway analyses, although, they cannot be ignored. The attributed functions of canonical pathways are rarely their sole function in cells. The extent of inter-pathway relationships likely varies between pathways and may be dependent to some degree on the complexity of the pathway. As a practical example, *EIF2 signalling* is best known for its regulation of protein synthesis; indeed, that is its primary function in the cell. However, protein synthesis can be regulated by countless other cellular systems and pathways and, therefore, by extension, signals in those pathways as well. This then implies that dysregulation in EIF2 signalling would affect the regulation of those pathways as well as pathways reliant on protein synthesis for their regulation. Indeed, one such mechanism is the relationship between EIF2 signalling and apoptosis. Briefly, if EIF2 signalling is inhibited sufficiently, which invariably indicates chronic cell stress, apoptosis is initiated.[115,460] Therefore, pathway dysregulation, however small they may be, likely have far reaching effects on serveral other systems. Apoptosis is a cell function which must be tightly regulated and must be able to respond to a myriad of cellular stresses. Due to the obvious importance of tight regulation in apoptosis initiation and that it is a possible end-point function of chronic dysregulation of a vast array of pathways discussed; it is not surprising that it shares proteins with many important pathways. It is, therefore, feasible to postulate that any dysregulation in these pathways would ultimately contribute to and influence pro or anti-apoptotic signalling in cells. Thus, it is also feasible that all of the systems dysregulated by HIV-Tat or HIV-Tat + lithium contribute to the execution of apoptosis. Although apoptosis may have been inhibited by lithium, it is evident that many cell stresses induced by HIV-Tat are still present, even though the nature of the dysregulation may be altered after lithium treatment. There is, therefore, no doubt that lithium is merely altering the nature of the HIV-Tat induced dysregulation and not specifically alleviating all their effects. This may, however, have been expected as lithium does not have a specific, targeted function and is a broad spectrum inhibitor.

That lithium protects against HIV-Tat induced neuronal apoptosis does not necessarily imply that lithium would be a viable treatment option for HAND as HAND is not primarily resultant of neuronal loss. It is clear that lithium's effect on AKT and GSK-3β

are central to its inhibition of HIV-Tat induced apoptosis. However, what is not clear is whether the activation of AKT and GSK-3β inhibition play a role in the behavioural alterations induced by lithium in bipolar patients nor that they would alleviate HAND symptoms.

Protein synthesis

Although lithium evidently alters the dysregulation induced by HIV-Tat, the pathways and functions associated with protein synthesis and its regulation remain dysregulated. In this work and previously, we argued that protein synthesis is inhibited in HIV-Tat treated cells and that this would favour HIV replication. Briefly, protein synthesis takes place in several sequential stages; initiation, elongation and termination.[122] Regulation of these stages effects the rate of protein synthesis sequentially as well. Therefore, increases in elongation and termination machinery will not significantly increase the rate of protein synthesis if the initiation machinery is inhibited. Furthermore, there are sequential steps within the initiation process whereby EIF2 functionality initiates the process such that inhibition of EIF2 functions to globally suppress protein synthesis irrespective of other components of the pathway.[461,462] This observation is supported Bertsch *et al*, which showed that lithium reduced EIF2B activity and was ineffective at reducing the inhibition of protein synthesis.[463] This data, however, is from an unrelated disease in muscle cells. Rats fed with lithium chronically showed significant decrease in active, phosphorylated EIF2B in brain tissue.[464] Both FXS and BD are associated with increased protein synthesis rates. Lithium was shown to decrease the rate of neuronal protein synthesis in models of both these diseases.[465] This further supports our view that lithium will further attenuate the protein synthesis dysregulation induced by HIV-Tat.

Unlike BP and FXS, the rate of protein synthesis is decreased in AD and can be reversed by inhibition of the EIF2α kinases.[270] The inhibition of protein synthesis was directly linked to deficits in synaptic plasticity and special memory in an AD mouse model.[270] This may be due to the need for de novo protein synthesis in synapses to initiate and maintain LTP. Not only does this affirm the importance of tightly regulated protein synthesis, but also highlights the implication of potentially further decreasing the rate of protein synthesis in HAND by lithium. Several EIF's are dysregulated by HIV-Tat as

well as by the addition of lithium. Lithium would, therefore, likely serve to exacerbate the effects of a decreased rate of protein synthesis. Although **Figure 54** shows that lithium increases EIF2 signalling dramatically, **Figure 61** suggests that protein translation is decreased by lithium treatment. As we have previously argued (Chapter 4) loss of specific individual EIF proteins can attenuate the entire process of protein synthesis. As the vast majority of mammalian mRNA's requires binding and activity of multiple EIF's in sequence, the loss of any of them would decrease the efficiency of protein translation initiation and global protein translation. This remains true despite upregulation of individual EIF's and/or ribosomal components.

Cytoskeletal Dysregulation

Deficits in apoptosis signalling and protein synthesis are certainly involved in the dysregulation of synapse maintenance and their loss. In order to impair synapse structure, the structural components must be impaired. It is, therefore, reasonable to postulate that the elements regulating the synaptic structural components must be impaired. The structural component of the synapse is the cytoskeleton and its regulation forms the basis of synaptic plasticity. Functions that regulate synapse formation, maintenance and destruction must directly or indirectly influence the cytoskeleton. Therefore, discerning the effects on the cytoskeleton helps to gauge the state of the synapse's physical structure irrespective of the source of the effect. Whether or not the deregulation of synaptic functions is decreased, exacerbated or maintained by lithium is difficult to gauge without functional studies on the synapses under different treatments. However, that elements of their cytoskeletal structure remains dysregulated is clear.

One of the most prominent neuronal phosphatases, PP2A, along with PP1 show consistent dysregulation in many pathways, including those involved in cytoskeletal reorganisation, presented. In AD, PP2A and PP1 receive much attention due to their role as primary tau phosphatases as well as their ability to regulate microtubule structure and function. The involvement of tau hyperphosphorylation in HAND is debated, although, there are several publications showing increased tau phosphorylation in HAND patient brain tissue as well as CSF.[466] Certainly, the increased GSK-3β activity does support the notion of increased tau phosphorylation.[467] However,

while lithium does decrease the levels of phospho-tau in an AD mouse model, it did not improve their working memory.[468] This may be due to the involvement of GSK-3β in LTP/LTP. GSK-3β inhibition is integral to the induction of LTP, however, the inhibition must end for normal LTP function; [469] thus, highlighting the importance of regulation as opposed to directionality.

The specific functional implications of individual PP2A subunits is poorly understood, however, research by Martin *et al* shows the potential functional implication of the HIV-Tat induced loss PPP2R2A (PP2ABα). This work shows that loss of PP2Abα leads to hyperactivation of RhoA resulting in the cell's inability to regulate its cytoskeletal rearrangement. PP2ABα loss also lead to dysregulated cell–matrix adhesion regulation.[470] Synaptic plasticity relies on the cell's ability to rapidly and reliably rearrange its cytoskeletal structure such as to destroy and rebuild synapses. Similarly, accurate axonal guidance is important for proper synapse formation and this would be hindered by poor cell–matrix adhesion and communication. Interestingly, the PP2ABα subunit is also known to interact with PKR in its regulation of EIF4E. The interaction of HIV-Tat with PKR and its regulation of protein synthesis was discussed in Chapter 4. Chen, *et al*, show that lithium inhibited the methylation of the PP2A subunit C which is required for subunit B recruitment.[140] This would suggest that binding of all regulatory subunits would be inhibited by lithium. In either event, this may go toward explaining the array of side effects associated with lithium treatment.

Although there is little information regarding specific activities PP2A subunit, PPP2R5C, as well as other phosphatases specifically dysregulated by lithium treatment, it is feasible to assume that they will have major effects on homeostasis. Irrespective of the source of dysregulation, they will have major effects on the regulation of the cytoskeleton and, in turn, on all cellular functions reliant on the cytoskeleton such as synapse maintenance and function. Neurite outgrowth is controlled by tight regulation of cytoskeletal functions such as focal point contact formation and guidance and actin polymerisation to drive the formation of cellular protrusions.[471] RhoA inhibits neurite formation and is antagonized by Rac.[237] However, dysregulation of Rac in either direction retards proper neurite formation suggesting that tight regulation is absolutely necessary.[472] Additionally, Rac is required for the formation of point

contacts and the stabilisation of subsequent lamellar protrusions. Overexpression of Rac, however, does increase the frequency of protrusion formation but decreases the overall neurite outgrowth, thus, tight regulation is important. Furthermore, growth cone adhesion to the extracellular matrix (ECM) via point contacts which are enriched by molecules such as β1-integrin and paxillin.[473,474,475] Our data, therefore describes the loss proteins and dysregulation of pathways required for the initiation, formation, stabilisation and guidance of neurites which would ultimately relate to neurons' inability to form axons and synapses nor maintain them or their function. Furthermore, both Rho and Rac protein functions as well as their signalling pathways can be controlled through NGF signalling which promotes neurite outgrowth and, ultimately, synapse formation.[476,477] The down regulation of NGF signalling correlates with the observed activation and inactivation of RhoA and Rac respectively in our data. This dysregulation also accounts for the observed HIV-Tat induced loss of neurites in neuronal cell cultures as well as the synapse loss in HIV+ patients.[478]

Interestingly, NGF also functions in an inflammatory loop. TLR stimulation increases expression of NGF. In turn, NGF decreases the production of TLR induced proinflammatory cytokines, IL-1β, TNF-α, IL-6, and IL-8 and induces the release of anti-inflammatory cytokines, IL-10 and IL-1 receptor antagonist.[479] HIV-Tat may decrease NGF signalling in order to sustain the proinflammatory cellular environment. HIV infection is associated with chronic inflammation and maybe be due to inflammation resolution pathways being attenuated during HIV infection. While it is counter intuitive that HIV favours a proinflammatory cell state by activating antiviral mechanisms, HIV replication is dependent on this state. Equils *et al* show that LPS dependant activation of TLR-4 activates the HIV-LTR and that the inhibition of TLR-4 inhibits LPS induced HIV-LTR activation. Furthermore, this HIV-LTR transactivation occurs via IL-1 signalling.[480] TLR agonist and TLR induced proinflammatory cytokine, TNF-α, increased HIV replication [481]

Given all the arguments presented for HIV's dependence on a proinflammatory cell environment and the evidence presented showing that this proinflammatory environment may induce the cellular changes which ultimately result in synaptic loss, it is feasible that an anti-inflammatory drug co-treatment along with HIV-Tat could

protect neurons from the degeneration. However, a caveat to this is that it may prove dangerous to systemically treat HIV patients with anti-inflammatories. However, the NGF receptor, TrKA, agonists may prove sufficient to attenuate the HIV induced proinflammatory environment. Furthermore, it may serve to reverse the dysregulation seen in cytoskeletal regulatory pathways.

The mechanism proposed for the activation of the inflammatory response is central to HIV's ability to hijack the cell and replicate efficiently. TLR activation may be central to achieving the desired proinflammatory environment. That the inhibition of TLR activation inhibits HIV replication certainly supports this hypothesis.

To our knowledge, this is the first proteomic analysis of the effect of lithium on HIV-Tat treated cells. While this was not intended to serve as a complete description of lithium-induced cellular dysregulation, it is possibly the largest such description produced. Based on the data presented here and the modest clinical trials testing lithium for HAND therapeutic potential, it is unlikely that lithium is able to completely restore the HIV-Tat induced neuronal cell to a normal cell state. Schifitto *et al* found that lithium had no beneficial effect on cognitive performance of HAND patients.[402] It is, however, similarly clear that lithium is capable of abrogating or ameliorating several HIV-Tat induced dysregulations particularly regarding apoptosis and cytoskeletal reorganisation. Lithium may, therefore, have an effect over a significantly longer trial by slowing the rate of synaptic loss, thereby, slowing disease progression. However, in supporting the opinion that lithium is detrimental to neuronal regulation is a retrospective study performed on psychiatric patients in the Danish medical records. Although not intended to address lithium efficacy in HAND, they assessed the relationship between lithium usage and dementia onset. They identified all patients who had any exposure to lithium within the psychiatry registry and took a random sample of the rest of the population who had never taken lithium. Interestingly, the incidence of dementia was decreased to the same level as the rest of the population after a single lithium prescription. Unexpectedly, however, they report a slight increase in the incidence of dementia relative to subsequent prescriptions. This trend was not seen for other prescriptions such as anticonvulsants.[482] Thus, continued lithium exposure is, seemingly, detrimental to neuronal regulation. This data may suggest that

lithium would compound HIV-Tat induced dysregulation. However, considering the alterations to HIV-Tat induced dysregulation by lithium, it is more likely that lithium will attenuate some functions but maintain and exacerbate others. These data may also serve to begin addressing the molecular dysregulations induced by lithium which leads to the array of side effects associated with its administration. Lithium is often said to be neuroprotective as it inhibits apoptosis induced by many insults. However, inhibition of apoptosis does not equate to proper neuronal function. Irrespective the original source of dysregulation, lithium seemingly merely prevents the execution of apoptotic signals but does not silence the original signal. This may indeed be a benefit in such diseases where neuronal apoptosis is primarily responsible for the patient decline. However, it is less important in cases, such as HAND, where apoptosis is not the primary disease contributor. Additionally, merely blocking the final signalling in the cascade does not necessarily inhibit the other effects induced by the original signal. Unfortunately, literature is very unclear about the specific regulation and function of many PP2A and PP1 phosphatases. Based on our data and literature, lithium's functions may, at least in part, be due to the inhibition of phosphatases including the PP2A family. Given that PP2A accounts for 25% of cellular phosphatase activity, its general inhibition would have many side effects. In conclusion, we cannot rule out the possibility of therapeutic benefit to HAND patients, despite being certain that lithium would have side effects and that it does not completely abrogate HIV-Tat induced neuronal dysregulation.

Chapter 6

Closing summary

HAND affects up to 70% of HIV patients, which equates to ~26 million of the 36.9 million HIV-infected patients worldwide. Despite the prevalence of the disease and the continued global effort and research, we are as yet uncertain about the molecular mechanism of disease onset and progression. Humanised mouse studies have shown that HIV infection and HIV-Tat protein induces neurodegeneration. While HIV-GP120 is also neurotoxic, unlike GP120, HIV-Tat expression and secretion is not adversely affected by antiretroviral (ARV) therapy.

Using shotgun proteomics and genome-wide transcriptomics, we profiled the molecular dysregulation of neuroblastoma cells treated with HIV-Tat and found that it is capable of inducing a wide array of cellular dysregulations. Of these, the dysregulation of the inflammatory response, protein synthesis, cytoskeletal reorganisation and apoptosis are most prominent and relevant. Although neurons are not typically infected, these dysregulations are likely induced to prepare a cell for HIV infection. In many cases, literature has shown that inhibiting the induction of these dysregulations in HIV-infected cells inhibited HIV replication. One of the most prominent features of HIV-Tat treatment in neurons is the activation of GSK-3β and subsequent apoptosis. Recently, lithium has been suggested as probable therapeutic candidate for HAND. Indeed, lithium has well-documented neuroprotective effects against various neuronal insults and is commonly prescribed to BD (BP) patients. The symptomatic presentation and pathologies of HAND and BP are, however, significantly different. Furthermore, only a subset of BP patients responds to lithium which highlights the impact of disease pathology on lithium efficacy. Thus far, very little is known about molecular mechanism involved in lithium-induced behavioural alterations nor have broader effects of lithium treatment beyond AKT activation been classified.

In chapters 3 and 4, we described the proteomic alterations induced by HIV-Tat and linked these to HAND disease onset and progression. Following this, we wanted to determine whether lithium's neuroprotection extended to abrogating all dysregulation

induced by HIV-Tat. We found that lithium very effectively reversed the molecular signature of apoptosis via activation of AKT. As a great deal of cross talk occurs between pathways, any imposed dysregulation, no less to such broadly functioning kinases as AKT/Pi3K, would have dysregulatory effects on downstream targets. We also show that AKT inhibition by HIV-Tat is likely via activation of PP2A phosphatases which are the primary AKT phosphatases. In the functional analyses, HIV-Tat was shown to strongly activate cell death and strongly inhibit reciprocal cell survival functions. Lithium, however, inhibited cell death functions and increased the inhibition of cell survival. This suggests that lithium merely intercepts apoptotic signalling at AKT while leaving upstream signalling unaffected. This is important since the upstream inflammatory dysregulation we see and describe induces dramatic molecular alterations to support their function with chronic activation resulting in apoptosis. Before initiating apoptosis however, the antiviral inflammatory response attempts to control viral growth by attenuating protein synthesis. Similarly, cells' cytoskeletons respond to inflammation in a variety of ways such as epithelial cells decreasing adhesion in order to allow greater immune cell access to sites of inflammation. Similarly, immune cells respond by using their cytoskeletons to actively move toward sites of inflammation. Many publications highlight HIV's need of dysregulated host cytoskeletal regulation throughout its life cycle. Similarly, it is not surprising that HIV requires alterations to host protein synthesis machinery to support its own protein synthesis while decreasing competition for host protein synthesis machinery. Lithium's effects on protein synthesis and cytoskeletal reorganisation were, however, were not as promising as those seen in apoptotic pathways and functions. Prominent proteins and pathways contributing to both functions remained highly dysregulated. In addition, lithium induced the dysregulation of many novel proteins in these pathways.

We have shown that HIV intends to attenuate global protein synthesis through other proteins and add that HIV-Tat is capable of inducing previously undescribed alterations to host protein synthesis machinery. Indeed, host protein synthesis attenuation is essential in many other viruses. Although not formally described, HIV likely has the same requirement and HIV-Tat plays a role in its implementation. While there is dispute in literature, we provide evidence in support of HIV mRNA translation

occurring via cap-independent protein translation. Global protein synthesis inhibition in neurons is known to play a role in synapse loss in AD but has not been described in HAND. Lithium treatment did not remove the inhibition of protein synthesis.

While pro-apoptotic signalling and impaired protein synthesis certainly induce an unfavourable cellular environment within neurons, the loss of neuronal synapses is directly associated with dysregulated cytoskeletal reorganisation. We have explained the dysregulation of many of the associated functions with respect to their importance to HIV replication as well as their impact of synapse structure. Following from this, the roles of cdc42, Rho and Rac signalling and their dysregulation can be directly and unmistakably associated with impaired neurite outgrowth and stabilisation which ultimately corresponds with synapse dysregulation and loss. This, together with impaired lamellar protrusion, axonal guidance and cell adhesion functions, are entirely capable of inducing the synaptic loss observed in HAND patients.

HIV-Tat, on its own, is capable of inducing many cellular dysregulations identified in HIV-infected systems. Furthermore, although unquantifiable, it supports the validity of the data we have generated and it adds support to the myriad of dysregulations not previously attributed to HIV or HIV-Tat. In addition to identifying functions known to be associated with HIV infection, we have identified and described many functions known to play a role in neurodegenerative diseases including AD, which has proved similar to HAND.

Neuronal apoptosis, dysregulation of protein synthesis and cytoskeletal reorganisation can be explained as downstream effects of proinflammatory activity. Similarly, the described neurite and synaptic degradation can be attributed to RhoA and Rac dysregulation due to loss of NGF signalling. However, NGF loss cannot be explained by proinflammatory signalling. Interestingly, HIV replication decreases when host cells are treated with NGF. It is, therefore, feasible that HIV-Tat specifically and actively attenuates NGF signalling. As a consequence of this, not only are neurons unable to regulate their synapses properly, NGF attenuation of the proinflammatory response is also lost. NGF signalling remained strongly dysregulated after lithium treatment, as did RhoA and Rac signalling.

PP2A family phosphatases play diverse roles and regulate many proteins. The exact mechanisms through which the vast array of subunits are regulated is poorly understood. Thus, PP2A likely plays a very significant role in HIV-Tat induced dysregulation. However, we cannot, with certainty, identify the means through which specific subunits are dysregulated and it may be that HIV-Tat dysregulates them directly. Furthermore, lithium induced the significant dysregulation of additional PP2A and other phosphatases which certainly exacerbate HIV-Tat induced dysregulation.

Together, the data presented herein not only describes a vast diversity of cellular changes induced by HIV-Tat and lithium's effect on that dysregulation but also identifies a plausible and well supported mechanism of HAND onset and progression. In addition, the data provides insights into the wider functionality of HIV-Tat in its ability to transform healthy host cells into highly efficient HIV replicative machines. In using a virus free system, many dysregulated proteins and genes previously described only during HIV infection can be attributed to HIV-Tat function. It is important to note that although neurons are typically not infected by HIV, many of the systems we describe as dysregulated are ubiquitous to all cells and, therefore, HIV-Tat's mechanism to dysregulate them may be generally effective in all cells. Although, differences in the specific molecular mechanism may vary between different cell types; this may induce variable functional outcomes of the initial dysregulation induced. Our use of lithium has not only allowed us to speculate about the possible efficacy of lithium as a treatment for HAND, but has evidenced the power of MS-based proteomics to identify, describe and quantify drug effects in a cell system. Whether that system is in a disease or healthy state, we have shown our ability identify expected effects as well as to extend the analysis and enable the identification and description of novel effects. To this end, the proteomic data showed that lithium induced the well-described and expected inhibition of cell death. However, lithium failed to abrogate all the dysregulation induced by HIV-Tat and even further dysregulated several of them. Importantly, lithium did attenuate much of the pathway and functional dysregulation to cytoskeletal reorganisation. Theoretically, this seems to suggest that HIV-Tat induced synaptic degradation in HAND patients may be attenuated. However, maintained or exacerbated dysregulation to any cytoskeletal

component may and likely will offset decreases in others. This is especially relevant in this work as the dysregulated NGF signalling was only modestly affected by lithium. As has been mentioned, synapse regulation is highly complex and dysregulation in any of the contributory pathways and functions will impair their stability and function. For example, dysregulation of protein synthesis alone can impair synaptic function due to the requirement of *de novo* protein synthesis for LTP induction and maintenance. Furthermore, several publications describe lithium as having little or no beneficial, and sometimes detrimental, effects in HAND and AD patients. This supports our finding that lithium is capable of dysregulating pathways already dysregulated by HIV-Tat and that it may well exacerbate HIV-Tat induced neuronal degradation. Despite this, we cannot, based on our data, dismiss the possibility that lithium may have modest long-term benefits to HAND patients.

References

1. Maschke M, Kastrup O, Esser S, Ross B, Hengge U, Hufnagel a. Incidence and prevalence of neurological disorders associated with HIV since the introduction of highly active antiretroviral therapy (HAART). *J Neurol Neurosurg Psychiatry*. 2000;69(3):376-380. http://www.pubmedcentral.nih.gov/articlerender.fcgi?artid=1737101&tool=pmcentrez&rendertype=abstract.

2. Letendre S, Marquie-beck J, Capparelli E, et al. Validation of the CNS Penetration-Effectiveness Rank for Quantifying Antiretroviral Penetration Into the Central Nervous System. *October*. 2009;65(1):65-70. doi:10.1001/archneurol.2007.31.Validation.

3. Cysique LA, Brew BJ. Neuropsychological Functioning and Antiretroviral Treatment in HIV / AIDS : A Review. *Neuropsychol Rev*. 2009:169-185. doi:10.1007/s11065-009-9092-3.

4. Heaton RK, Cysique LA, Jin H, et al. Neurobehavioral effects of HIV infection among former plasma donors in rural China. 2010;14(6):536-549. doi:10.1080/13550280802378880.Neurobehavioral.

5. Antinori a, Arendt G, Becker JT, et al. Updated research nosology for HIV-associated neurocognitive disorders. *Neurology*. 2007;69(18):1789-1799. doi:10.1212/01.WNL.0000287431.88658.8b.

6. Arhel N. Revisiting HIV-1 uncoating. *Retrovirology*. 2010;7(1):96. doi:10.1186/1742-4690-7-96.

7. Miller MD, Farnet CM, Bushman FD. Human immunodeficiency virus type 1 preintegration complexes: studies of organization and composition. *J Virol*. 1997;71(7):5382-5390.

8. Fassati A, Görlich D, Harrison I, Zaytseva L, Mingot JM. Nuclear import of HIV-1 intracellular reverse transcription complexes is mediated by importin 7. *EMBO J*. 2003;22(14):3675-3685. doi:10.1093/emboj/cdg357.

9. Rivière L, Darlix J-L, Cimarelli A. Analysis of the viral elements required in the nuclear import of HIV-1 DNA. *J Virol*. 2010;84(2):729-739. doi:10.1128/JVI.01952-09.

10. Craigie R, Bushman FD. HIV DNA integration. *Cold Spring Harb Perspect Med*. 2012;2(7):1-18. doi:10.1101/cshperspect.a006890.

11. Delelis O, Carayon K, Saïb A, Deprez E, Mouscadet J-F. Integrase and integration: biochemical activities of HIV-1 integrase. *Retrovirology*. 2008;5:114. doi:10.1186/1742-4690-5-114.

12. Charnay N, Ivanyi-Nagy R, Soto-Rifo R, Ohlmann T, López-Lastra M, Darlix J-L. Mechanism of HIV-1 Tat RNA translation and its activation by the Tat protein. *Retrovirology*. 2009;6:74. doi:10.1186/1742-4690-6-74.

13. de Breyne S, Soto-Rifo R, López-Lastra M, Ohlmann T. Translation initiation is

driven by different mechanisms on the HIV-1 and HIV-2 genomic RNAs. *Virus Res*. 2012;171:366-381. doi:10.1016/j.virusres.2012.10.006.

14. Liu B, Dai R, Tian CJ, Dawson L, Gorelick R, Yu XF. Interaction of the human immunodeficiency virus type 1 nucleocapsid with actin. *J Virol*. 1999;73(4):2901-2908.

15. Stolp B, Fackler OT. How HIV takes advantage of the cytoskeleton in entry and replication. *Viruses*. 2011;3:293-311. doi:10.3390/v3040293.

16. Sundquist WI, Kräusslich H-G. HIV-1 assembly, budding, and maturation. *Cold Spring Harb Perspect Med*. 2012:1-24. doi:10.1101/cshperspect.a006924.

17. Bleck M, Itano MS, Johnson DS, et al. Temporal and spatial organization of ESCRT protein recruitment during HIV-1 budding. *Proc Natl Acad Sci U S A*. 2014;111(33). doi:10.1073/pnas.1321655111.

18. Davis LE, Hjelle BL, Miller VE, et al. Early viral brain invasion in iatrogenic human immunodeficiency virus infection. *Neurology*. 1992;42(9):1736-1739. doi:10.1212/WNL.42.9.1736.

19. Gonzalez-Scarano F, Martin-Garcia J. The neuropathogenesis of AIDS. *Nat Rev Immunol*. 2005;5(1):69-81. http://dx.doi.org/10.1038/nri1527.

20. El-Hage N, Bruce-Keller AJ, Yakovleva T, et al. Morphine exacerbates HIV-1 Tat-induced cytokine production in astrocytes through convergent effects on [Ca(2+)](i), NF-kappaB trafficking and transcription. *PLoS One*. 2008;3(12):e4093. doi:10.1371/journal.pone.0004093.

21. Ariani GIM, Abin ROLR, Arber JOMF, Oonan DOMN. HIV-1 Tat protein mimicry of chemokines. *Immunology*. 1998;95(October):13153-13158.

22. Otamis T, Ercal N, Nakaoke R, Banks WA. HIV-1 viral proteins gp120 and Tat induce oxidative stress in brain endothelial cells. *Brain Res*. 2005;1045:57-63. doi:10.1016/j.brainres.2005.03.031.

23. Toborek M, Lee YW, Flora G, et al. Mechanisms of the Blood – Brain Barrier Disruption in HIV-1 Infection. *Infection*. 2005;25(1):181-199. doi:10.1007/s10571-004-1383-x.

24. Ju SM, Song HY, Lee JA, Lee SJ. Extracellular HIV-1 Tat up-regulates expression of matrix metalloproteinase-9 via a MAPK-NF- κ B dependent pathway in human astrocytes. *Aids*. 2009;41(2):86-93. doi:10.3858/emm.2009.41.2.011.

25. Engelhardt B, Coisne C. Fluids and barriers of the CNS establish immune privilege by confining immune surveillance to a two-walled castle moat surrounding the CNS castle. *Fluids Barriers CNS*. 2011;8(1):4. doi:10.1186/2045-8118-8-4.

26. Bratanich AC, Liu C, Mcarthur JC, et al. Brain-derived HIV-1 tat sequences from AIDS patients with dementia show increased molecular heterogeneity. *J Neurovirol*. 1998;(April 1996):387-393.

27. Maggirwar SB, Tong N, Ramirez S, Gelbard HA, Dewhurst S. HIV-1 Tat-mediated activation of glycogen synthase kinase-3beta contributes to Tat-mediated

neurotoxicity. *J Neurochem*. 1999;73:578-586.

28. Lee YW, Eum SY, Nath A, Toborek M. Estrogen-mediated protection against HIV Tat protein-induced inflammatory pathways in human vascular endothelial cells. *Cardiovasc Res*. 2004;63(1):139-148. doi:10.1016/j.cardiores.2004.03.006.

29. Shi B, Raina J, Lorenzo a, Busciglio J, Gabuzda D. Neuronal apoptosis induced by HIV-1 Tat protein and TNF-alpha: potentiation of neurotoxicity mediated by oxidative stress and implications for HIV-1 dementia. *J Neurovirol*. 1998;4(3):281-290. http://www.ncbi.nlm.nih.gov/pubmed/9639071.

30. Kaul M, Lipton S a. Signaling pathways to neuronal damage and apoptosis in human immunodeficiency virus type 1-associated dementia: Chemokine receptors, excitotoxicity, and beyond. *J Neurovirol*. 2004;10 Suppl 1(April 2003):97-101. doi:10.1080/jnv.10.s1.97.101.

31. Chang JJ, Altfeld M. Innate Immune Activation in Primary HIV-1 Infection. *J Infect Dis*. 2010;202(Suppl 2):1-9. doi:10.1086/655657.Innate.

32. Mogensen TH, Melchjorsen J, Larsen CS, Paludan SR. Innate immune recognition and activation during HIV infection. *Retrovirology*. 2010;7:54. doi:10.1186/1742-4690-7-54.

33. Hengel H, Koszinowski UH, Conzelmann KK. Viruses know it all: New insights into IFN networks. *Trends Immunol*. 2005;26(7):396-401. doi:10.1016/j.it.2005.05.004.

34. García-Sastre A, Biron C a. Type 1 interferons and the virus-host relationship: a lesson in détente . *Science*. 2006;312(5775):879-882. doi:10.1126/science.1125676.

35. Wong M, Chen SS. Emerging roles of interferon-stimulated genes in the innate immune response to hepatitis C virus infection. *Cell Mol Immunol*. 2014;000(000):0. doi:10.1038/cmi.2014.127.

36. Boasso A. Type I Interferon at the Interface of Antiviral Immunity and Immune Regulation: The Curious Case of HIV-1. *Scientifica (Cairo)*. 2013;2013(2):580968. doi:10.1155/2013/580968.

37. Sen GC, Sarkar SN. The interferon-stimulated genes: Targets of direct signaling by interferons, double-stranded RNA, and viruses. *Curr Top Microbiol Immunol*. 2007;316:233-250. doi:10.1007/978-3-540-71329-6-12.

38. Zhang D, Zhang D-E. Interferon-stimulated gene 15 and the protein ISGylation system. *J Interferon Cytokine Res*. 2011;31(1):119-130. doi:10.1089/jir.2010.0110.

39. de Veer MJ, Holko M, Frevel M, et al. Functional classification of interferon-stimulated genes identified using microarrays. *J Leukoc Biol*. 2001;69:912-920.

40. Farrell PJ, Sen GC, Dubois MF, Ratner L, Slattery E, Lengyel P. Interferon action: two distinct pathways for inhibition of protein synthesis by double-stranded RNA. *Proc Natl Acad Sci U S A*. 1978;75(12):5893-5897. doi:10.1073/pnas.75.12.5893.

41. Lu J, O'Hara EB, Trieselmann B a., Romano PR, Dever TE. The interferon-induced double-stranded RNA-activated protein kinase PKR will phosphorylate serine, threonine, or tyrosine at residue 51 in eukaryotic initiation factor 2?? *J Biol Chem*. 1999;274:32198-32203. doi:10.1074/jbc.274.45.32198.

42. Thyrell L, Erickson S, Zhivotovsky B, et al. Mechanisms of Interferon-alpha induced apoptosis in malignant cells. *Oncogene*. 2002;21:1251-1262. doi:10.1038/sj.onc.1205179.

43. Balachandran S, Roberts PC, Kipperman T, et al. Alpha/beta interferons potentiate virus-induced apoptosis through activation of the FADD/Caspase-8 death signaling pathway. *J Virol*. 2000;74(3):1513-1523. doi:10.1128/JVI.74.3.1513-1523.2000.

44. Gil J, Esteban M. Induction of apoptosis by the dsRNA-dependent protein kinase (PKR): mechanism of action. *Apoptosis*. 2000;5(2):107-114. http://www.ncbi.nlm.nih.gov/pubmed/11232238.

45. Wang S, Chi X, Wei H, et al. Influenza A Virus-Induced Degradation of Eukaryotic Translation Initiation Factor 4B Contributes to Viral Replication by Suppressing IFITM3 Protein Expression. *J Virol*. 2014;88(15):8375-8385. doi:10.1128/JVI.00126-14.

46. Zürcher T, Marión RM, Ortín J. Protein synthesis shut-off induced by influenza virus infection is independent of PKR activity. *J Virol*. 2000;74(18):8781-8784. doi:10.1128/JVI.74.18.8781-8784.2000.

47. Villas-Bôas CS a, Conceição TM, Ramírez J, Santoro a. BM, Da Poian a. T, Montero-Lomelí M. Dengue virus-induced regulation of the host cell translational machinery. *Brazilian J Med Biol Res*. 2009;42(11):1020-1026. doi:10.1590/S0100-879X2009001100004.

48. Edgil D, Polacek C, Harris E. Dengue Virus Utilizes a Novel Strategy for Translation Initiation When Cap-Dependent Translation Is Inhibited Dengue Virus Utilizes a Novel Strategy for Translation Initiation When Cap-Dependent Translation Is Inhibited. *Society*. 2006;80(6):2976-2986. doi:10.1128/JVI.80.6.2976.

49. DerekWalsh, Michael B. Mathews IM. Tinkering with Translation : Protein Synthesis. *Cold Spring Harb Perspect Biol*. 2013;5(1).

50. Foxman EF, Iwasaki A. Genome–virome interactions: examining the role of common viral infections in complex disease. *Nat Rev Microbiol*. 2011;9(4):254-264. doi:10.1038/nrmicro2541.

51. Boccellino M, Giuberti G, Quagliuolo L, et al. Apoptosis induced by interferon-α and antagonized by EGF is regulated by caspase-3-mediated cleavage of gelsolin in human epidermoid cancer cells. *J Cell Physiol*. 2004;201(December 2003):71-83. doi:10.1002/jcp.20058.

52. Ivanov AI, Parkos C a, Nusrat A. Cytoskeletal regulation of epithelial barrier function during inflammation. *Am J Pathol*. 2010;177(2):512-524. doi:10.2353/ajpath.2010.100168.

53. Jayadev S, Yun B, Nguyen H, Yokoo H, Morrison RS, Garden G a. The glial response to CNS HIV infection includes p53 activation and increased expression of p53 target genes. *J Neuroimmune Pharmacol*. 2007;2(4):359-370. doi:10.1007/s11481-007-9095-x.

54. McGeer EG, McGeer PL. Inflammatory processes in Alzheimer's disease. *Prog Neuro-Psychopharmacology Biol Psychiatry*. 2003;27(5):741-749. doi:10.1016/S0278-5846(03)00124-6.

55. Bate C, Kempster S, Last V, Williams A. Interferon-gamma increases neuronal death in response to amyloid-beta1-42. *J Neuroinflammation*. 2006;3:7. doi:10.1186/1742-2094-3-7.

56. Etminan, M. Gill, S. , Samiim A. Effect of non-steroidal anti-inflammatory drugs on risk of Alzheimer's disease: systematic review and meta-analysis of observational studies. *Bmj*. 2003;327:128-131. doi:10.1136/bmj.327.7407.128.

57. Litteljohn D, Mangano E, Clarke M, Bobyn J, Moloney K, Hayley S. Inflammatory mechanisms of neurodegeneration in toxin-based models of Parkinson's disease. *Parkinsons Dis*. 2010;2011:713517. doi:10.4061/2011/713517.

58. Mizuno T, Zhang G, Takeuchi H, et al. Interferon-gamma directly induces neurotoxicity through a neuron specific, calcium-permeable complex of IFN-gamma receptor and AMPA GluR1 receptor. *FASEB J*. 2008;22(6):1797-1806. doi:10.1096/fj.07-099499.

59. Brown GC, Neher JJ. Inflammatory neurodegeneration and mechanisms of microglial killing of neurons. *Mol Neurobiol*. 2010;41(2-3):242-247. doi:10.1007/s12035-010-8105-9.

60. Sacktor N. The epidemiology of human immunodeficiency virus-associated neurological disease in the era of highly active antiretroviral therapy. *J Neurovirol*. 2002;8 Suppl 2:115-121. doi:10.1080/13550280290101094.

61. Marra CM, Zhao Y, Clifford DB, et al. Impact of Combination Antiretroviral Therapy on Cerebrospinal Fluid HIV RNA and Neurocognitive Performance. *Aids*. 2010;23(11):1359-1366. doi:10.1097/QAD.0b013e32832c4152.Impact.

62. Nath A, McArthur J. restoration in HAART-treated patients. *Aids*. 2003:1-35.

63. Stolp HB, Dziegielewska KM, Ek CJ, et al. Breakdown of the blood-brain barrier to proteins in white matter of the developing brain following systemic inflammation. *Cell Tissue Res*. 2005;320(3):369-378. doi:10.1007/s00441-005-1088-6.

64. Afonso PV, Ozden S, Schmitt C, et al. Human Blood-Brain Barrier Disruption by Retroviral-Infected Lymphocytes: Role of Myosin Light Chain Kinase in Endothelial Tight-Junction Disorganization. *J Immunol*. 2011;179:2576-2583.

65. Shi B, Raina J, Lorenzo A, Busciglio J, Gabuzda D. Neuronal apoptosis induced by HIV-1 Tat protein and TNF-alpha: potentiation of neurotoxicity mediated by oxidative stress and implications for HIV-1 dementia. *J Neurovirol*. 1998;4:281-290.

66. Hesselgesser J, Taub D, Baskar P, et al. Neuronal apoptosis induced by HIV-1 gp120 and the chemokine SDF-1 alpha is mediated by the chemokine receptor CXCR4. *Curr Biol*. 1998;8(10):595-598. http://www.ncbi.nlm.nih.gov/pubmed/9601645.

67. Snyder SH. Chemokines and activated macrophages in HIV gp120-induced neuronal apoptosis. *Neurobiology*. 1999;96(July):8212-8216.

68. Iskander S, Walsh K a, Hammond RR. Human CNS cultures exposed to HIV-1 gp120 reproduce dendritic injuries of HIV-1-associated dementia. *J Neuroinflammation*. 2004;1:7. doi:10.1186/1742-2094-1-7.

69. Neumann H, Schweigreiter R, Yamashita T, Rosenkranz K, Wekerle H, Barde Y-A. Tumor necrosis factor inhibits neurite outgrowth and branching of hippocampal neurons by a rho-dependent mechanism. *J Neurosci*. 2002;22(3):854-862. http://www.ncbi.nlm.nih.gov/pubmed/11826115.

70. Prast H, Philippu A. Nitric oxide as modulator of neuronal function. *Prog Neurobiol*. 2001;64(1):51-68. doi:10.1016/S0301-0082(00)00044-7.

71. Poluektova L, Meyer V, Walters L, Paez X, Gendelman HE. Macrophage-induced inflammation affects hippocampal plasticity and neuronal development in a murine model of HIV-1 encephalitis. *Glia*. 2005;52(4):344-353. doi:10.1002/glia.20253.

72. Arendt T. Neurodegeneration and plasticity. *Int J Dev Neurosci*. 2004;22(7):507-514. doi:10.1016/j.ijdevneu.2004.07.007.

73. Stumm RK, Zhou C, Ara T, et al. CXCR4 regulates interneuron migration in the developing neocortex. *J Neurosci*. 2003;23(12):5123-5130. doi:23/12/5123 [pii].

74. Stuart MJ, Corrigan F, Baune BT. Knockout of CXCR5 increases the population of immature neural cells and decreases proliferation in the hippocampal dentate gyrus. *J Neuroinflammation*. 2014;11(1):31. doi:10.1186/1742-2094-11-31.

75. Bachis A, Major EO, Mocchetti I. Brain-derived neurotrophic factor inhibits human immunodeficiency virus-1/gp120-mediated cerebellar granule cell death by preventing gp120 internalization. *J Neurosci*. 2003;23(13):5715-5722.

76. Dandekar DH, Ganesh KN, Mitra D. HIV-1 Tat directly binds to NFkB enhancer sequence : role in viral and cellular gene expression. *Aids*. 2004;32(4):1270-1278. doi:10.1093/nar/gkh289.

77. Hetzer C, Dormeyer W, Schnölzer M, Ott M. Decoding Tat : the biology of HIV Tat posttranslational modifications. 2005;7:1364-1369. doi:10.1016/j.micinf.2005.06.003.

78. Guendel I, Carpio L, Easley R, et al. 9-aminoacridine Inhibition of HIV-1 Tat Dependent Transcription. *Virol J*. 2009;14:1-14. doi:10.1186/1743-422X-6-114.

79. Turk G, Carobene M, Monczor A, Rubio AE, Gómez-carrillo M, Salomón H. Higher transactivation activity associated with LTR and Tat elements from HIV-1 BF intersubtype recombinant variants. *Access*. 2006;12:1-12. doi:10.1186/1742-4690-3-14.

80. Huang H, Wang K. Structural Characterization of the metal Binding Site in the Cysteine-Rich Region of HIV-1 Tat Protein. *Biochem Biophys Res Commun*. 1996;227:615-621.

81. Duyne R Van, Easley R, Wu W, et al. Lysine methylation of HIV-1 Tat regulates transcriptional activity of the viral LTR. *Access*. 2008;13:1-13. doi:10.1186/1742-4690-5-40.

82. Ma M, Nath a. Molecular determinants for cellular uptake of Tat protein of human immunodeficiency virus type 1 in brain cells. *J Virol*. 1997;71(3):2495-2499. http://www.pubmedcentral.nih.gov/articlerender.fcgi?artid=191362&tool=pmcentrez&rendertype=abstract.

83. Park J, Lee H, Lee Y, Kang YH, Rhim H, Choi SY. Expression of Human Immunodeficiency Virus Type 1 Tat Proteins in Escherichia coli and Application to Study Tat Functions. *J Biochem*. 2000;33(4):337-343.

84. Tahirov TH, Babayeva ND, Varzavand K, Cooper JJ, Sedore SC, Price DH. Crystal structure of HIV-1 Tat complexed with human P-TEFb. *Nature*. 2010;465(7299):747-751. doi:10.1038/nature09131.

85. Karn J. Tat , a novel regulator of HIV transcription and latency. 2000:2-18.

86. Pierleoni R, Menotta M, Antonelli A, et al. Effect of the redox state on HIV-1 tat protein multimerization and cell internalization and trafficking. *Mol Cell Biochem*. 2010;345(1-2):105-118. doi:10.1007/s11010-010-0564-9.

87. Marle G Van, Rourke SB, Zhang K, et al. HIV dementia patients exhibit reduced viral neutralization and increased envelope sequence diversity in blood and brain. *Aids*. 2002;(April).

88. Callejas S, Abia D, Mateos E, Dopazo A, Alcamı J. Modifications in host cell cytoskeleton structure and function mediated by intracellular HIV-1 Tat protein are greatly dependent on the second coding exon. *Nucleic Acids Res*. 2010;(3):1-21. doi:10.1093/nar/gkq037.

89. Mahlknecht U, Dichamp I, Varin A, Lint V, C, Herbein G. NF-kappaB-dependent control of HIV-1 transcription by the second coding exon of Tat in T cells. *J Leukoc Biol*. 2008;83:718-727.

90. Sugaya M, Loré K, Koup R a, Douek DC, Blauvelt A. HIV-infected Langerhans cells preferentially transmit virus to proliferating autologous CD4+ memory T cells located within Langerhans cell-T cell clusters. *J Immunol*. 2004;172(4):2219-2224. http://www.ncbi.nlm.nih.gov/pubmed/14764689.

91. Jayadev S, Yun B, Nguyen H, Yokoo H, Morrison RS, Garden G a. The glial response to CNS HIV infection includes p53 activation and increased expression of p53 target genes. *J Neuroimmune Pharmacol*. 2007;2(4):359-370. doi:10.1007/s11481-007-9095-x.

92. Tuyama AC, Hong F, Saiman Y, et al. Human Immunodeficiency Virus (HIV)-1 Infects Human Hepatic Stellate Cells and Promotes Collagen I and Monocyte Chemoattractant Protein-1 Expression: Implications for the Pathogenesis of

HIV/Hepatitis C Virus–Induced Liver Fibrosis. *Reporter*. 2010;52(2):612-622. doi:10.1002/hep.23679.Human.

93. Eugenin EA, Morgello S, Klotman ME, et al. Human Immunodeficiency Virus (HIV) Infects Human Arterial Smooth Muscle Cells in Vivo and in Vitro Implications for the Pathogenesis of HIV-Mediated Vascular Disease. *Pathology*. 2008;172(4):1100-1111. doi:10.2353/ajpath.2008.070457.

94. Avraham HK, Jiang S, Lee T, Prakash O, Avraham S. HIV-1 Tat-Mediated Effects on Focal Adhesion Assembly and Permeability in Brain Microvascular Endothelial Cells. 2010;173(10):6228-6233.

95. Caldwell RL, Gadipatti R, Lane KB, Shepherd VL. HIV-1 TAT represses transcription of the bone morphogenic protein receptor-2 in U937 monocytic cells. *J Leukoc Biol*. 2006;79:192-201. doi:10.1189/jlb.0405194.0741-5400/06/0079-192.

96. Caldwell RL, Egan BS, Shepherd VL. HIV-1 Tat represses transcription from the mannose receptor promoter. *J Immunol*. 2000;165(12):7035-7041. http://www.ncbi.nlm.nih.gov/pubmed/11120831.

97. Jope RS. The paradoxical pro- and anti-apoptotic actions of GSK3 in the intrinsic and extrinsic apoptosis signaling pathways. *Prog Neurobiol*. 2006;79:173-189. doi:10.1016/j.pneurobio.2006.07.006.

98. Chugh P, Fan S, Planelles V, Maggirwar SB, Dewhurst S, Kim B. Infection of human immunodeficiency virus and intracellular viral Tat protein exert a pro-survival effect in a human microglial cell line. *J Mol Biol*. 2007;366(1):67-81. doi:10.1016/j.jmb.2006.11.011.

99. Sui Z, Sniderhan LF, Fan S, et al. Human immunodeficiency virus-encoded Tat activates glycogen synthase kinase-3b to antagonize nuclear factor-jB survival pathway in neurons. *Neuroscience*. 2006;23(December 2005):2623-2634. doi:10.1111/j.1460-9568.2006.04813.x.

100. Maggirwar SB. Glycogen synthase kinase 3beta-mediated apoptosis of primary cortical astrocytes involves inhibition of nuclear factor kappaB signaling. *Mol Cell Biol*. 2003;23:4649-4662.

101. Tong N, Sanchez JF, Maggirwar SB, et al. Activation of glycogen synthase kinase 3 beta (GSK-3b) by platelet activating factor mediates migration and cell death in cerebellar granule neurons. *Neuroscience*. 2001;13:1913-1922.

102. Fanales-Belasio E, Moretti S, Nappi F, et al. Native HIV-1 Tat protein targets monocyte-derived dendritic cells and enhances their maturation, function, and antigen-specific T cell responses. *J Immunol*. 2002;168(1):197-206. http://www.ncbi.nlm.nih.gov/pubmed/11751963.

103. Siddappa NB, Venkatramanan M, Venkatesh P, et al. Transactivation and signaling functions of Tat are not correlated : biological and immunological characterization of HIV-1 subtype-C Tat protein. *Immunodeficiency*. 2006;20:1-20. doi:10.1186/1742-4690-3-53.

104. Ensoli F, Fiorelli V, Decristofaro M, et al. Inflammatory Cytokines and HIV-1-

Associated Neurodegeneration: Oncostatin-M Produced by Mononuclear Cells from HIV-1-Infected Individuals Induces Apoptosis of Primary Neurons 1. *Cytokines*. 1999;162:6268-6277.

105. Perry SW, Norman JP, Litzburg A, Zhang D, Dewhurst S, Gelbard H a. HIV-1 transactivator of transcription protein induces mitochondrial hyperpolarization and synaptic stress leading to apoptosis. *J Immunol*. 2005;174:4333-4344. doi:10.4049/jimmunol.174.7.4333.

106. Endo H, Nito C, Kamada H, Nishi T, Chan PH. Activation of the Akt / GSK3b signaling pathway mediates survival of vulnerable hippocampal neurons after transient global cerebral ischemia in rats. *Changes*. 2006;294002:1479-1489. doi:10.1038/sj.jcbfm.9600303.

107. Martinez A. Preclinical E ⁄ cacy on GSK-3 Inhibitors : T owards a Future Generation of Powerful Drugs. *Med Res Rev*. 2008;28(5):773-796. doi:10.1002/med.

108. Rowe MK, Wiest C, Ã DC. GSK-3 is a viable potential target for therapeutic intervention in bipolar disorder. *Apoptosis*. 2007;31:920-931. doi:10.1016/j.neubiorev.2007.03.002.

109. Haughey NJ, Holden CP, Nath A, Geiger JD. Involvement of Inositol 1 , 4 , 5-Trisphosphate-Regulated Stores of Intracellular Calcium in Calcium Dysregulation and Neuron Cell Death Caused by HIV-1 Protein Tat. 1999:1363-1374.

110. El-hage N, Bruce-keller AJ, Yakovleva T, et al. Morphine Exacerbates HIV-1 Tat-Induced Cytokine Production in Astrocytes through Convergent Effects on [Ca 2 +] i , NF-kB Trafficking and Transcription. *Inflammation*. 2008;3(12):1-14. doi:10.1371/journal.pone.0004093.

111. Wallace DR. HIV Neurotoxicity : Potential Therapeutic Interventions. *J Neurochem*. 2006;2006:1-10. doi:10.1155/JBB/2006/65741.

112. Peng L. Transactivation in astrocytes as a novel mechanism of neuroprotection. *Cell*. 2004;31(92):503-518.

113. Buss H, Dorrie A, Schmitz ML, et al. Phosphorylation of serine 468 by GSK3b negatively regulates basal p65 NF-kB activity. *J Biol Chem*. 2004;279:49571-49574.

114. Locardi C, Petrini C, Boccoli G, et al. Increased human immunodeficiency virus (HIV) expression in chronically infected U937 cells upon in vitro differentiation by hydroxyvitamin D3: roles of interferon and tumor necrosis factor in regulation of HIV production. *J Virol*. 1990;64(12):5874-5882. http://www.pubmedcentral.nih.gov/articlerender.fcgi?artid=248750&tool=pmcentrez&rendertype=abstract.

115. Baltzis D, Pluquet O, Papadakis AI, Kazemi S, Qu LK, Koromilas AE. The eIF2a kinases PERK and PKR activate glycogen synthase kinase 3 to promote the proteasomal degradation of p53. *J Biol Chem*. 2007;282(43):31675-31687. doi:10.1074/jbc.M704491200.

116. Clerzius G, Shaw E, Daher A, et al. HIV-1 replication changes the function of the PKR activator PACT. *Retrovirology*. 2013;10(Suppl 1):P35. doi:10.1186/1742-4690-10-S1-P35.

117. Guerline Clerzius, Jean-Francois Gatignol AG. Multiple levels of PKR inhibition during. *Rev Med Virol*. 2010;21(December 2010):42-53. doi:10.1002/rmv.

118. Lemaire P a, Anderson E, Lary J, Cole JL. Mechanism of PKR Activation by dsRNA. *J Mol Biol*. 2008;381(2):351-360. doi:10.1016/j.jmb.2008.05.056.Mechanism.

119. Heinicke L a, Wong CJ, Lary J, et al. RNA Dimerization Promotes PKR Dimerization and Activation. *J Mol Biol*. 2009;390(2):319-338. doi:10.1016/j.jmb.2009.05.005.RNA.

120. Cai R, Carpick B, Chun RF, Jeang KT, Williams BR. HIV-I TAT inhibits PKR activity by both RNA-dependent and RNA-independent mechanisms. *Arch Biochem Biophys*. 2000;373:361-367. doi:10.1006/abbi.1999.1583.

121. Pestova T V, Kolupaeva VG, Lomakin IB, et al. Molecular mechanisms of translation initiation in eukaryotes. *Proc Natl Acad Sci U S A*. 2001;98(13):7029-7036. doi:10.1073/pnas.111145798.

122. Richard J. Jackson, Christopher U.T. Hellen TVP. THE MECHANISM OF EUKARYOTIC TRANSLATION INITIATION AND PRINCIPLES OF ITS REGULATION. *Nat Rev Mol Cell Biol*. 2010;1(2):113-127. doi:10.1146/annurev-biochem-060713-035802.

123. Nahum Sonenberg AGH. Regulation of Translation Initiation in Eukaryotes: Mechanisms and Biological Targets. *Cell*. 2009;136(4):731-745. doi:10.1016/j.cell.2009.01.042.Regulation.

124. Jones JL, Walker R a. Integrins: a role as cell signalling molecules. *Mol Pathol*. 1999;52(4):208-213. doi:10.1136/mp.52.4.208.

125. Kirsch J, Wolters I, Triller A, Betz H. Gephyrin antisense oligonucleotides prevent glycine receptor clustering in spinal neurons. *Nature*. 1993;366(6457):745-748. doi:10.1038/366745a0.

126. Delorme-Axford E, Coyne CB. The actin cytoskeleton as a barrier to virus infection of polarized epithelial cells. *Viruses*. 2011;3:2462-2477. doi:10.3390/v3122462.

127. Schaeffer E, Geleziunas R, Warner C, Greene WC. Human Immunodeficiency Virus Type 1 Nef Functions at the Level of Virus Entry by Enhancing Cytoplasmic Delivery of Virions Human Immunodeficiency Virus Type 1 Nef Functions at the Level of Virus Entry by Enhancing Cytoplasmic Delivery of Virions. *Society*. 2001;75(6):2993-3000. doi:10.1128/JVI.75.6.2993.

128. McDonald D, Vodicka M a., Lucero G, et al. Visualization of the intracellular behavior of HIV in living cells. *J Cell Biol*. 2002;159(3):441-452. doi:10.1083/jcb.200203150.

129. Manninen a, Hiipakka M, Vihinen M, Lu W, Mayer BJ, Saksela K. SH3-Domain binding function of HIV-1 Nef is required for association with a PAK-related

kinase. *Virology*. 1998;250(2):273-282. doi:10.1006/viro.1998.9381.

130. Gladnikoff M, Shimoni E, Gov NS, Rousso I. Retroviral assembly and budding occur through an actin-driven mechanism. *Biophys J*. 2009;97(9):2419-2428. doi:10.1016/j.bpj.2009.08.016.

131. Morita E, Sundquist WI. Retrovirus Budding. *Annu Rev Cell Dev Biol*. 2004;20(1):395-425. doi:10.1146/annurev.cellbio.20.010403.102350.

132. Eom T, Jope RS. GSK3β N-terminus binding to p53 promotes its acetylation. *Mol Cancer*. 2009;7:1-7. doi:10.1186/1476-4598-8-14.

133. Doble BW, Woodgett JR. GSK-3 : tricks of the trade for a multi-tasking kinase. *J Cell Sci*. 2003;116:1175-1186. doi:10.1242/jcs.00384.

134. Sayas CL, Ariaens A, Ponsioen B, Moolenaar WH. GSK-3 is activated by the tyrosine kinase Pyk2 during LPA1-mediated neurite retraction. *Mol Biol Cell*. 2006;17:1834-1844.

135. Forde JE, Dale TC. Review Glycogen synthase kinase 3 : A key regulator of cellular fate. *Cell Mol Life Sci*. 2007;64:1930-1944. doi:10.1007/s00018-007-7045-7.

136. Sayas CL, Ariaens A, Ponsioen B, Moolenaar WH. GSK-3 Is Activated by the Tyrosine Kinase Pyk2 during LPA 1 -mediated Neurite Retraction. *Mol Biol Cell*. 2006;17(April):1834-1844. doi:10.1091/mbc.E05.

137. Hye A, Kerr F, Archer N, et al. Glycogen synthase kinase-3 is increased in white cells early in Alzheimer ' s disease. *Neurosci Lett*. 2005;373:1-4. doi:10.1016/j.neulet.2004.10.031.

138. Shorter E. The history of lithium therapy. *Bipolar Disord*. 2009;11(SUPPL. 2):4-9. doi:10.1111/j.1399-5618.2009.00706.x.

139. Freland L, Beaulieu J-M. Inhibition of GSK3 by lithium, from single molecules to signaling networks. *Front Mol Neurosci*. 2012;5(February):1-7. doi:10.3389/fnmol.2012.00014.

140. Chen C, Lin C, Chiang C, Jan M, Lin Y. Lithium Inhibits Ceramide- and Etoposide-Induced Protein Caspase-2 Activation , and Apoptosis. 2006;70(2):510-517. doi:10.1124/mol.106.024059.been.

141. Letendre SL, Woods SP, Ellis RJ, et al. Lithium improves HIV-associated neurocognitive impairment. *AIDS*. 2006;20(14):1885-1888. doi:10.1097/01.aids.0000244208.49123.1b.

142. Schifitto G, Zhong J, Gill D, et al. Lithium therapy for HIV-1 Associated Neurocognitive Impairment. *J Neurovirol*. 2009;15(2):176-186. doi:10.1080/13550280902758973.Lithium.

143. Parenti DM, Simon GL, Scheib RG, et al. Effect of lithium carbonate in HIV-infected patients with immune dysfunction. *J Acquir Immune Defic Syndr*. 1988;1(2):119-124.

144. Meri S, Meri S, Baumann M, Baumann M. Proteomics: posttranslational modi

cations, immune responses and current analytical tools. *Biomol Eng*. 2001;18:213-220.

145. Jensen ON. Modification-specific proteomics: Characterization of post-translational modifications by mass spectrometry. *Curr Opin Chem Biol*. 2004;8(1):33-41. doi:10.1016/j.cbpa.2003.12.009.

146. Morris JS, Clark BN, Wei W, Gutstein HB. Evaluating the performance of new approaches to spot quantification and differential expression in 2-dimensional gel electrophoresis studies. *J Proteome Res*. 2010;9(1):595-604. doi:10.1021/pr9005603.

147. Wang W, Sun J, Nimtz M, Deckwer W-D, Zeng A-P. Protein identification from two-dimensional gel electrophoresis analysis of Klebsiella pneumoniae by combined use of mass spectrometry data and raw genome sequences. *Proteome Sci*. 2003;1:6. doi:10.1186/1477-5956-1-6.

148. Lim H, Eng J, Yates JR, et al. Identification of 2D-gel proteins: A comparison of MALDI/TOF peptide mass mapping to ?? LC-ESI tandem mass spectrometry. *J Am Soc Mass Spectrom*. 2003;14(9):957-970. doi:10.1016/S1044-0305(03)00144-2.

149. Gygi SP, Corthals GL, Zhang Y, Rochon Y, Aebersold R. Evaluation of two-dimensional gel electrophoresis-based proteome analysis technology. *Proc Natl Acad Sci U S A*. 2000;97(17):9390-9395. doi:10.1073/pnas.160270797.

150. Gygi SP, Corthals GL, Zhang Y, Rochon Y, Aebersold R. Evaluation of two-dimensional gel electrophoresis- based proteome analysis technology. *Proteins*. 2010;97(17):3-8.

151. Unlu M, Morgan ME, Minden JS. Difference gel electrophoresis: A single gel method for detecting changes in protein extracts. *Electrophoresis*. 1997;18:2071-2077. doi:10.1002/elps.1150181133.

152. Issaq HJ, Veenstra TD. Two-dimensional polyacrylamide gel electrophoresis (2D-PAGE): Advances and perspectives. *Biotechniques*. 2008;44(5):697-700. doi:10.2144/000112823.

153. Alves P, Arnold RJ, Novotny M V, Reilly JP, Tang H. ADVANCEMENT IN PROTEIN INFERENCE FROM SHOTGUN PROTEOMICS USING PEPTIDE DETECTABILITY. *Pacific Symp Biocomput*. 2007;420:409-420.

154. Wei H, Dean SL, Parkin MC, Nolkrantz K, Callaghan JPO, Kennedy RT. Microscale sample deposition onto hydrophobic target plates for trace level detection of neuropeptides in brain tissue by MALDI-MS. *J Mass Spectrom*. 2005;(40):1338-1346. doi:10.1002/jms.916.

155. Schmid DG, Grosche P, Bandel H, Jung G. FTICR-mass spectrometry for high-resolution analysis in combinatorial chemistry. *Biotechnol Bioeng*. 2000;71(2):149-161. doi:10.1002/1097-0290(2000)71:2<149::AID-BIT1005>3.0.CO;2-C.

156. Scigelova M, Hornshaw M, Giannakopulos A, Makarov A. Fourier transform mass spectrometry. *Mol Cell Proteomics*. 2011;10(7):M111.009431.

doi:10.1074/mcp.M111.009431.

157. Schwartz JC, Senko MW, Syka JEP. A two-dimensional quadrupole ion trap mass spectrometer. *J Am Soc Mass Spectrom*. 2002;13(6):659-669. doi:10.1016/S1044-0305(02)00384-7.

158. Scigelova M, Makarov A. Orbitrap mass analyzer - Overview and applications in proteomics. *Proteomics*. 2006;1(1-2 SUPPL.):16-21. doi:10.1002/pmic.200600528.

159. Hu Q, Noll RJ, Li H, Makarov A, Hardman M, Cooks RG. The Orbitrap: A new mass spectrometer. *J Mass Spectrom*. 2005;40(4):430-443. doi:10.1002/jms.856.

160. Makarov A. Electrostatic axially harmonic orbital trapping: A high-performance technique of mass analysis. *Anal Chem*. 2000;72(6):1156-1162. doi:10.1021/ac991131p.

161. Micallef J, Dharsee M, Chen J, et al. Applying mass spectrometry based proteomic technology to advance the understanding of multiple myeloma. *J Hematol Oncol*. 2010;3:13. doi:10.1186/1756-8722-3-13.

162. De Carolis E, Vella A, Vaccaro L, et al. Application of MALDI-TOF mass spectrometry in clinical diagnostic microbiology. *J Infect Dev Ctries*. 2014;8(09). doi:10.3855/jidc.3623.

163. Henzel WJ, Watanabe C, Stults JT. Protein identification: The origins of peptide mass fingerprinting. *J Am Soc Mass Spectrom*. 2003;14(9):931-942. doi:10.1016/S1044-0305(03)00214-9.

164. Millares P, LaCourse EJ, Perally S, et al. Proteomic profiling and protein identification by MALDI-TOF mass spectrometry in unsequenced parasitic nematodes. *PLoS One*. 2012;7(3):1-11. doi:10.1371/journal.pone.0033590.

165. Schwamborn K, Caprioli RM. MALDI Imaging Mass Spectrometry - Painting Molecular Pictures. *Mol Oncol*. 2010;4(6):529-538. doi:10.1016/j.molonc.2010.09.002.

166. Demartini DR. A Short Overview of the Components in Mass Spectrometry Instrumentation for Proteomics Analyses. *Tandem Mass Spectrom - Mol Charact*. 2013;1. doi:10.5772/54484.

167. Konermann L, Ahadi E, Rodriguez AD, Vahidi S. Unraveling the Mechanism of Electrospray Ionization. 2013;85:2-9.

168. Mallick P, Kuster B. Proteomics: a pragmatic perspective. *Nat Biotechnol*. 2010;28(7):695-709. doi:10.1038/nbt.1658.

169. Elviri L. ETD and ECD Mass Spectrometry Fragmentation for the Characterization of Protein Post Translational Modifications. *Tandem Mass Spectrom - Appl Princ*. 2012:163-178. doi:DOI: 10.5772/35277.

170. Harrison AG. Cyclization of Peptide b9 Ions. *J Am Soc Mass Spectrom*. 2009;20(12):2248-2253. doi:10.1016/j.jasms.2009.08.013.

171. Liu X, Valentine SJ, Plasencia MD, Trimpin S, Naylor S, Clemmer DE. Mapping the

Human Plasma Proteome by SCX-LC-IMS-MS. *J Am mass Spectrom*. 2007;18:1249-1264. doi:10.1016/j.jasms.2007.04.012.

172. Callesen AK, Madsen JS, Vach W, Kruse TA, Mogensen O, Jensen ON. Serum protein profiling by solid phase extraction and mass spectrometry : A future diagnostics tool ? *Proteomics*. 2009;9. doi:10.1002/pmic.200800382.

173. Lei T, He QY, Wang YL, Si LS. , Heparin chromatography to deplete high-abundance proteins for serum proteomics. *Clin Chim Acta*. 2008;388:173-178.

174. Stoll DR, Li X, Wang X, Carr PW, Porter SEG, Rutan SC. Fast, comprehensive two-dimensional liquid chromatography. *J Chromatogr A*. 2007;1168(1-2):3-43; discussion 2. doi:10.1016/j.chroma.2007.08.054.

175. Tsai YS, Scherl A, Shaw JL, et al. Precursor ion independent algorithm for top-down shotgun proteomics. *J Am Soc Mass Spectrom*. 2009;20(11):2154-2166. doi:10.1016/j.jasms.2009.07.024.

176. Nesvizhskii AI, Aebersold R. Interpretation of Shotgun Proteomic Data. *Mol Cell Proteomics*. 2005:1419-1440. doi:10.1074/mcp.R500012-MCP200.

177. Mohieddin Jafari, Vincent Primo, Gary B. Smejkal, Eugene V. Moskovets WP, Kuo ARI. Comparison of in-gel protein separation techniques commonly used for fractionation in mass spectrometry-based proteomic profiling. *Electrophoresis*. 2012;33(16):2516-2526. doi:10.1002/elps.201200031.Comparison.

178. Granvogl B, Plöscher M, Eichacker LA. Sample preparation by in-gel digestion for mass spectrometry-based proteomics. *Anal Bioanal Chem*. 2007;389(4):991-1002. doi:10.1007/s00216-007-1451-4.

179. Tanaka N. Monolithic silica columns for high-efficiency chromatographic separations. 2002;965:35-49.

180. Hayes R, Ahmed A, Edge T, Zhang H. Core-shell particles: Preparation, fundamentals and applications in high performance liquid chromatography. *J Chromatogr A*. 2014;1357:36-52. doi:10.1016/j.chroma.2014.05.010.

181. Cold P, Harbor S, Creasy D. Probability-based protein identification by searching sequence databases using mass spectrometry data . Electrophoresis 20 : 3551-. 1999;(September 2015). doi:10.1002/(SICI)1522-2683(19991201)20.

182. Cox J, Neuhauser N, Michalski A, Scheltema R a, Olsen J V, Mann M. Andromeda: a peptide search engine integrated into the MaxQuant environment. *J Proteome Res*. 2011;10(4):1794-1805. doi:10.1021/pr101065j.

183. Eng JK, McCormack a L, Yates JR. An approach to correlate tandem mass spectral data of peptides with amino acid sequences in a protein database. *J Am Soc Mass Spectrom*. 1994;5(11):976-989. doi:10.1016/1044-0305(94)80016-2.

184. Allmer J. Sequencing of Peptides From Tandem Mass Spectra. *Expert Rev Proteomics*. 2011;8(5):645-657. doi:10.1586/epr.11.54.

185. Standing KG. Peptide and protein de novo sequencing by mass spectrometry. *Curr Opin Struct Biol*. 2003;13(5):595-601. doi:10.1016/j.sbi.2003.09.005.

186. Ari M. Frank, Mikhail M. Savitski, Michael N. Nielsen, Roman A. Zubarev and PAP. De Novo Peptide Sequencing and Identification with Precision Mass Spectrometry. *J Proteome Res*. 2007;6(1):114-123. doi:10.1055/s-0029-1237430.Imprinting.

187. Brun V, Dupuis A, Adrait A, et al. Isotope-labeled protein standards: toward absolute quantitative proteomics. *Mol Cell Proteomics*. 2007;6(12):2139-2149. doi:10.1074/mcp.M700163-MCP200.

188. Jaquinod M, Trauchessec M, Huillet C, et al. Mass spectrometry-based absolute protein quantification: PSAQ^{TM} strategy makes use of "noncanonical" proteotypic peptides. *Proteomics*. 2012;12(8):1217-1221. doi:10.1002/pmic.201100538.

189. Ross PL, Huang YN, Marchese JN, et al. Multiplexed protein quantitation in Saccharomyces cerevisiae using amine-reactive isobaric tagging reagents. *Mol Cell Proteomics*. 2004;3(12):1154-1169. doi:10.1074/mcp.M400129-MCP200.

190. Thompson A, Schäfer J, Kuhn K, et al. Tandem mass tags: A novel quantification strategy for comparative analysis of complex protein mixtures by MS/MS. *Anal Chem*. 2003;75(8):1895-1904. doi:10.1021/ac0262560.

191. Krüger M, Moser M, Ussar S, et al. SILAC Mouse for Quantitative Proteomics Uncovers Kindlin-3 as an Essential Factor for Red Blood Cell Function. *Cell*. 2008;134(2):353-364. doi:10.1016/j.cell.2008.05.033.

192. Zanivan S, Meves A, Behrendt K, et al. In Vivo SILAC-Based Proteomics Reveals Phosphoproteome Changes during Mouse Skin Carcinogenesis. *Cell Rep*. 2013;3(2):552-566. doi:10.1016/j.celrep.2013.01.003.

193. Kito K, Ito T. Mass spectrometry-based approaches toward absolute quantitative proteomics. *Curr Genomics*. 2008;9(4):263-274. doi:10.2174/138920208784533647.

194. Ishihama Y, Sato T, Tabata T, et al. Quantitative mouse brain proteomics using culture-derived isotope tags as internal standards. *Nat Biotechnol*. 2005;23(5):617-621. doi:10.1038/nbt1086.

195. Geiger T, Wehner A, Schaab C, Cox J, Mann M. Comparative proteomic analysis of eleven common cell lines reveals ubiquitous but varying expression of most proteins. *Mol Cell Proteomics*. 2012;11(3):M111.014050. doi:10.1074/mcp.M111.014050.

196. Bantscheff M, Lemeer S, Savitski MM, Kuster B. Quantitative mass spectrometry in proteomics: Critical review update from 2007 to the present. *Anal Bioanal Chem*. 2012;404(4):939-965. doi:10.1007/s00216-012-6203-4.

197. Bondarenko P V., Chelius D, Shaler T a. Identification and relative quantitation of protein mixtures by enzymatic digestion followed by capillary reversed-phase liquid chromatography - Tandem mass spectrometry. *Anal Chem*. 2002;74(18):4741-4749. doi:10.1021/ac0256991.

198. Liu NQ, Dekker LJM, Stingl C, et al. Quantitative proteomic analysis of microdissected breast cancer tissues: comparison of label-free and SILAC-based

quantification with shotgun, directed, and targeted MS approaches. *J Proteome Res*. 2013;12(10):4627-4641. doi:10.1021/pr4005794.

199. King OD, Lee JC, Dudley AM, Janse DM, Church GM, Roth FP. Predicting phenotype from patterns of annotation. *Bioinformatics*. 2003;19(SUPPL. 1):896-904. doi:10.1093/bioinformatics/btg1024.

200. Miseta a, Csutora P. Relationship between the occurrence of cysteine in proteins and the complexity of organisms. *Mol Biol Evol*. 2000;17(8):1232-1239. doi:10.1093/oxfordjournals.molbev.a026406.

201. Albini a, Benelli R, Giunciuglio D, et al. Identification of a novel domain of HIV tat involved in monocyte chemotaxis. *J Biol Chem*. 1998;273(26):15895-15900. doi:10.1074/jbc.273.26.15895.

202. Koken SEC, Greijer AE, Verhoef K, Van Wamel J, Bukrinskaya AG, Berkhout B. Intracellular analysis of in vitro modified HIV Tat protein. *J Biol Chem*. 1994;269(11):8366-8375.

203. Sarah J. Bertrand, Marina V. Aksenova, Charles F. Mactutus RMB. HIV-1 Tat protein variants: critical role for the cysteine region in synaptodendritic injury. *Exp Neurobiol*. 2013;248:228-235. doi:10.1016/j.expneurol.2013.06.020.HIV-1.

204. Recio J a, Martínez de la Mata J, Martín-Nieto J, Aranda a. Retinoic acid stimulates HIV-1 transcription in human neuroblastoma SH-SY5Y cells. *FEBS Lett*. 2000;469(1):118-122. http://www.ncbi.nlm.nih.gov/pubmed/10708768.

205. Soane L, Fiskum G. TAT-mediated endocytotic delivery of the loop deletion Bcl-2 protein protects neurons against cell death. *J Neurochem*. 2005:230-243. doi:10.1111/j.1471-4159.2005.03359.x.

206. Krishna A, Biryukov M, Trefois C, et al. Systems genomics evaluation of the SH-SY5Y neuroblastoma cell line as a model for Parkinson's disease. *BMC Genomics*. 2014;15(1):1154. doi:10.1186/1471-2164-15-1154.

207. Pregi N, Vittori D, Pérez G, Leirós CP, Nesse A. Effect of erythropoietin on staurosporine-induced apoptosis and differentiation of SH-SY5Y neuroblastoma cells. *Analysis*. 2006;1763:238-246. doi:10.1016/j.bbamcr.2005.12.011.

208. Giardina SF, Beart PM. Kainate receptor-mediated apoptosis in primary cultures of cerebellar granule cells is attenuated by mitogen-activated protein and cyclin-dependent kinase inhibitors. *Br J Pharmacol*. 2002:1733-1742.

209. Lobner D. Comparison of the LDH and MTT assays for quantifying cell death: Validity for neuronal apoptosis? *J Neurosci Methods*. 2000;96(2):147-152. doi:10.1016/S0165-0270(99)00193-4.

210. Abe K, Matsuki N. Measurement of cellular 3-(4,5-dimethylthiazol-2-yl)-2,5-diphenyltetrazolium bromide (MTT) reduction activity and lactate dehydrogenase release using MTT. *Neurosci Res*. 2000;38(4):325-329. doi:10.1016/S0168-0102(00)00188-7.

211. Slice LW, Codner E, Antelman D, et al. Characterization of Recombinant HIV-1 Tat and Its Interaction with TAR RNA. *Biochemistry*. 1992;(31):12062-12068.

212. Fülöp V, Szeltner Z, Polgár L. Catalysis of serine oligopeptidases is controlled by a gating filter mechanism. *EMBO Rep*. 2000;1(3):277-281. doi:10.1093/embo-reports/kvd048.

213. Joska J a, Hoare J, Stein DJ, Flisher a J. The neurobiology of HIV dementia: implications for practice in South Africa. *Afr J Psychiatry*. 2011;14(1):17-22. http://www.ncbi.nlm.nih.gov/pubmed/21509406.

214. Bissel SJ, Wiley CA. NIH Public Access. 2006;14(1):97-108.

215. Ragin AB, Du H, Ochs R, et al. Structural brain alterations can be detected early in HIV infection. *Neurology*. 2012;79(24):2328-2334. doi:10.1212/WNL.0b013e318278b5b4.

216. Dubé B, Benton T, Cruess DG, Evans DL. Neuropsychiatric manifestations of HIV infection and AIDS. 2005;30(4):237-246.

217. Ellis R, Langford D, Masliah E. HIV and antiretroviral therapy in the brain: neuronal injury and repair. *Nat Rev Neurosci*. 2007;8(1):33-44. doi:10.1038/nrn2040.

218. McGuire D. CSF biomarkers in HIV dementia: through a glass darkly. *Neurology*. 2009;73(23):1942-1944. doi:10.1212/WNL.0b013e3181c51a92.

219. Jarboui MA, Bidoia C, Woods E, et al. Nucleolar protein trafficking in response to HIV-1 Tat: rewiring the nucleolus. *PLoS One*. 2012;7(11):e48702. doi:10.1371/journal.pone.0048702.

220. Banerjee A, Zhang X, Manda KR, Banks W a, Ercal N. HIV proteins (gp120 and Tat) and methamphetamine in oxidative stress-induced damage in the brain: potential role of the thiol antioxidant N-acetylcysteine amide. *Free Radic Biol Med*. 2010;48(10):1388-1398. doi:10.1016/j.freeradbiomed.2010.02.023.

221. Gandhi N, Saiyed ZM, Napuri J, et al. Interactive role of human immunodeficiency virus type 1 (HIV-1) clade-specific Tat protein and cocaine in blood-brain barrier dysfunction: implications for HIV-1-associated neurocognitive disorder. *J Neurovirol*. 2010;16(4):294-305. doi:10.3109/13550284.2010.499891.

222. Banks W a, Robinson SM, Nath A. Permeability of the blood-brain barrier to HIV-1 Tat. *Exp Neurol*. 2005;193(1):218-227. doi:10.1016/j.expneurol.2004.11.019.

223. Chang JR, Mukerjee R, Bagashev A, et al. HIV-1 Tat protein promotes neuronal dysfunction through disruption of microRNAs. *J Biol Chem*. 2011;286(47):41125-41134. doi:10.1074/jbc.M111.268466.

224. Siddappa NB, Venkatramanan M, Venkatesh P, et al. Transactivation and signaling functions of Tat are not correlated: biological and immunological characterization of HIV-1 subtype-C Tat protein. *Immunodeficiency*. 2006;20:1-20. doi:10.1186/1742-4690-3-53.

225. Marban C, Su T, Ferrari R, et al. Genome-wide binding map of the HIV-1 Tat protein to the human genome. *PLoS One*. 2011;6(11):e26894. doi:10.1371/journal.pone.0026894.

226. Soares NC, Spät P, Krug K, Macek B. Global dynamics of the Escherichia coli proteome and phosphoproteome during growth in minimal medium. *J Proteome Res*. 2013;12(6):2611-2621. doi:10.1021/pr3011843.

227. Mi H, Muruganujan A, Thomas PD. PANTHER in 2013: modeling the evolution of gene function, and other gene attributes, in the context of phylogenetic trees. *Nucleic Acids Res*. 2013;41(Database issue):D377-D386. doi:10.1093/nar/gks1118.

228. Tosi G, Meazza R, Barbaro ADL, et al. Highly stable oligomerization forms of HIV-1 Tat detected by monoclonal antibodies and requirement of monomeric forms for the transactivating function on the HIV-1 LTR. 2000:1120-1126.

229. Norman JP, Perry SW, Reynolds HM, et al. HIV-1 Tat Activates Neuronal Ryanodine Receptors with Rapid Induction of the Unfolded Protein Response and Mitochondrial Hyperpolarization. *Stress Int J Biol Stress*. 2008;3(11). doi:10.1371/journal.pone.0003731.

230. Ranga U, Shankarappa R, Siddappa NB, et al. Tat Protein of Human Immunodeficiency Virus Type 1 Subtype C Strains Is a Defective Chemokine. *Society*. 2004;78(5):2586-2590. doi:10.1128/JVI.78.5.2586.

231. Rao VR, Neogi U, Talboom JS, et al. Clade C HIV-1 isolates circulating in Southern Africa exhibit a greater frequency of dicysteine motif-containing Tat variants than those in Southeast Asia and cause increased neurovirulence. 2013:1-16.

232. Liao W, Tan G, Zhu Z, et al. Combined Metabonomic and Quantitative Real-Time PCR Analyses Reveal Systems Metabolic Changes in Jurkat T‐Cells Treated with HIV‐1 Tat Protein. 2012.

233. Sakane N, Kwon H-S, Pagans S, et al. Activation of HIV transcription by the viral Tat protein requires a demethylation step mediated by lysine-specific demethylase 1 (LSD1/KDM1). *PLoS Pathog*. 2011;7(8):e1002184. doi:10.1371/journal.ppat.1002184.

234. Schroder K, Hertzog PJ, Ravasi T, Hume DA. Interferon-□: an overview of signals , mechanisms and functions. 2004;75(February). doi:10.1189/jlb.0603252.Journal.

235. Chan FK-M, Shisler J, Bixby JG, et al. A role for tumor necrosis factor receptor-2 and receptor-interacting protein in programmed necrosis and antiviral responses. *J Biol Chem*. 2003;278(51):51613-51621. doi:10.1074/jbc.M305633200.

236. Chia PH, Li P, Shen K. Cell biology in neuroscience: cellular and molecular mechanisms underlying presynapse formation. *J Cell Biol*. 2013;203(1):11-22. doi:10.1083/jcb.201307020.

237. Tolias KF, Duman JG, Um K. Control of synapse development and plasticity by Rho GTPase regulatory proteins. *Prog Neurobiol*. 2011;94(2):133-148. doi:10.1016/j.pneurobio.2011.04.011.

238. Nishimura T, Takeichi M. Shroom3-mediated recruitment of Rho kinases to the apical cell junctions regulates epithelial and neuroepithelial planar remodeling.

Development. 2008;135(8):1493-1502. doi:10.1242/dev.019646.

239. Sit S-T, Manser E. Rho GTPases and their role in organizing the actin cytoskeleton. *J Cell Sci*. 2011;124(Pt 5):679-683. doi:10.1242/jcs.064964.

240. Korobova F, Svitkina T. Molecular Architecture of Synaptic Actin Cytoskeleton in Hippocampal Neurons Reveals a Mechanism of Dendritic Spine Morphogenesis Farida Korobova and Tatyana Svitkina. 2010;21:165-176. doi:10.1091/mbc.E09.

241. Passey RJ, Xu K, Hume DA, Geczy CL. S100A8 : emerging functions and regulation Abstract : The functional importance of members. 1999;66(October).

242. Ehrchen JM, Sunderkötter C, Foell D, Vogl T, Roth J. The endogenous Toll-like receptor 4 agonist S100A8/S100A9 (calprotectin) as innate amplifier of infection, autoimmunity, and cancer. *J Leukoc Biol*. 2009;86(3):557-566. doi:10.1189/jlb.1008647.

243. Berthier S, Baillet A, Paclet M-H, Gaudin P, Morel F. How Important are S100A8/S100A9 Calcium Binding Proteins for the Activation of Phagocyte NADPH Oxidase, Nox2. *Antiinflamm Antiallergy Agents Med Chem*. 2009;8(4):282-289. doi:10.2174/187152309789839000.

244. Wolf M, Riethmüller C, Petersen B, Oberleithner H, Roth J, Vogl T. Crosslinking of microtubules and actin filaments by S100A8/S100A9. *Cell Commun Signal*. 2009;7(Suppl 1):A103. doi:10.1186/1478-811X-7-S1-A103.

245. Echelard S, Hoyaux D, Hermans M, et al. S100A8 and S100A9 calcium-binding proteins: localization within normal and cyclosporin A-induced overgrowth gingiva. *Connect Tissue Res*. 2002;43(2-3):419-424. http://www.ncbi.nlm.nih.gov/pubmed/12489193. Accessed June 25, 2013.

246. Lein ES, Zhao X, Gage FH. Defining a molecular atlas of the hippocampus using DNA microarrays and high-throughput in situ hybridization. *J Neurosci*. 2004;24(15):3879-3889. doi:10.1523/JNEUROSCI.4710-03.2004.

247. Benson DL, Tanaka H. N-cadherin redistribution during synaptogenesis in hippocampal neurons. *J Neurosci*. 1998;18(17):6892-6904. http://www.ncbi.nlm.nih.gov/pubmed/9712659.

248. Anderson E., Boyle J, Zink W., Persidsky Y, Gendelman H., Xiong H. Hippocampal synaptic dysfunction in a murine model of human immunodeficiency virus type 1 encephalitis. *Neuroscience*. 2003;118(2):359-369. doi:10.1016/S0306-4522(02)00925-9.

249. Blaydon DC, Nitoiu D, Eckl K-M, et al. Mutations in CSTA, encoding Cystatin A, underlie exfoliative ichthyosis and reveal a role for this protease inhibitor in cell-cell adhesion. *Am J Hum Genet*. 2011;89(4):564-571. doi:10.1016/j.ajhg.2011.09.001.

250. Marekov LN. Direct Evidence That Involucrin Is a Major Early Isopeptide Cross-linked Component of the Keratinocyte Cornified Cell Envelope. *J Biol Chem*. 1997;272(3):2021-2030. doi:10.1074/jbc.272.3.2021.

251. Terry S, Nie M, Matter K, Balda MS. Rho signaling and tight junction functions.

Physiology (Bethesda). 2010;25(1):16-26. doi:10.1152/physiol.00034.2009.

252. Su K-Y, Chien W-L, Fu W-M, et al. Mice deficient in collapsin response mediator protein-1 exhibit impaired long-term potentiation and impaired spatial learning and memory. *J Neurosci*. 2007;27(10):2513-2524. doi:10.1523/JNEUROSCI.4497-06.2007.

253. Yamashita N, Uchida Y, Ohshima T, et al. Collapsin response mediator protein 1 mediates reelin signaling in cortical neuronal migration. *J Neurosci*. 2006;26(51):13357-13362. doi:10.1523/JNEUROSCI.4276-06.2006.

254. James AB, Conway A, Morris BJ. Regulation of the Neuronal Proteasome by Zif268 (Egr1). 2006;26(5):1624-1634. doi:10.1523/JNEUROSCI.4199-05.2006.

255. Fogel AI, Stagi M, Perez de Arce K, Biederer T. Lateral assembly of the immunoglobulin protein SynCAM 1 controls its adhesive function and instructs synapse formation. *EMBO J*. 2011;30(23):4728-4738. doi:10.1038/emboj.2011.336.

256. Utsunomiya a, Owada Y, Yoshimoto T, Kondo H. Localization of gene expression for phosphatidylinositol transfer protein in the brain of developing and mature rats. *Brain Res Mol Brain Res*. 1997;45(2):349-352. http://www.ncbi.nlm.nih.gov/pubmed/9149113.

257. Cosker KE, Shadan S, van Diepen M, et al. Regulation of PI3K signalling by the phosphatidylinositol transfer protein PITPalpha during axonal extension in hippocampal neurons. *J Cell Sci*. 2008;121(Pt 6):796-803. doi:10.1242/jcs.019166.

258. Vordtriede PB, Doan CN, Tremblay JM, Helmkamp GM, Yoder MD. Structure of PITPbeta in complex with phosphatidylcholine: comparison of structure and lipid transfer to other PITP isoforms. *Biochemistry*. 2005;44(45):14760-14771. doi:10.1021/bi051191r.

259. Carvou N, Holic R, Li M, Futter C, Skippen A, Cockcroft S. Phosphatidylinositol-and phosphatidylcholine-transfer activity of PITPbeta is essential for COPI-mediated retrograde transport from the Golgi to the endoplasmic reticulum. *J Cell Sci*. 2010;123(Pt 8):1262-1273. doi:10.1242/jcs.061986.

260. Cole SW, Naliboff BD, Kemeny ME, Griswold MP, Fahey JL, Zack J a. Impaired response to HAART in HIV-infected individuals with high autonomic nervous system activity. *Proc Natl Acad Sci U S A*. 2001;98(22):12695-12700. doi:10.1073/pnas.221134198.

261. Cole SW, Korin YD, Fahey JL, Zack J a. Norepinephrine accelerates HIV replication via protein kinase A-dependent effects on cytokine production. *J Immunol*. 1998;161(2):610-616. http://www.ncbi.nlm.nih.gov/pubmed/9670934.

262. Koutsilieri E, Sopper S, Scheller C, ter Meulen V, Riederer P. Parkinsonism in HIV dementia. *J Neural Transm*. 2002;109(5-6):767-775. doi:10.1007/s007020200063.

263. Wang G-J, Chang L, Volkow ND, et al. Decreased brain dopaminergic transporters in HIV-associated dementia patients. *Brain*. 2004;127(Pt 11):2452-

2458. doi:10.1093/brain/awh269.

264. Eckert D, Buhl S, Weber S, Jäger R, Schorle H. The AP-2 family of transcription factors. *Genome Biol*. 2005;6(13):246. doi:10.1186/gb-2005-6-13-246.

265. Orso F, Corà D, Ubezio B, Provero P, Caselle M, Taverna D. Identification of functional TFAP2A and SP1 binding sites in new TFAP2A-modulated genes. *BMC Genomics*. 2010;11:355. doi:10.1186/1471-2164-11-355.

266. Jahn H, Wittke S, Zürbig P, et al. Peptide fingerprinting of Alzheimer's disease in cerebrospinal fluid: identification and prospective evaluation of new synaptic biomarkers. *PLoS One*. 2011;6(10):e26540. doi:10.1371/journal.pone.0026540.

267. Bando Y, Onuki R, Katayama T, et al. Double-strand RNA dependent protein kinase (PKR) is involved in the extrastriatal degeneration in Parkinson's disease and Huntington's disease. *Neurochem Int*. 2005;46(1):11-18. doi:10.1016/j.neuint.2004.07.005.

268. Mimi A. Trinh, Hanoch Kaphzan, Ronald C. Wek, Philippe Pierre, Douglas R. Cavener EK. Brain-specific Disruption of the eIF2α Kinase PERK Decreases ATF4 Expression and Impairs Behavioral Flexibility. *Cell Rep*. 2012;1(6):676-688. doi:10.1016/j.celrep.2012.04.010.Brain-specific.

269. Hetz C, Mollereau B. Disturbance of endoplasmic reticulum proteostasis in neurodegenerative diseases. *Nat Rev Neurosci*. 2014;15(4):233-249. doi:10.1038/nrn3689.

270. Ma T, Trinh M a, Wexler AJ, et al. Suppression of eIF2α kinases alleviates Alzheimer's disease-related plaasticity and memory deficits. *Nat Neurosci*. 2013;16(9):1299-1305. doi:10.1038/nn.3486.

271. Toro-nieves DM, Rodriguez Y, Plaud M, et al. Proteomic analyses of monocyte-derived macrophages infected with human immunodeficiency virus type 1 primary isolates from Hispanic women with and without cognitive impairment. 2009;15(1):36-50. doi:10.1080/13550280802385505.Proteomic.

272. McArthur JC. HIV dementia: An evolving disease. *J Neuroimmunol*. 2004;157(1-2 SPEC. ISS.):3-10. doi:10.1016/j.jneuroim.2004.08.042.

273. Bruce Shiramizu, Suzanne Gartner, Andrew Williams, Cecilia Shikuma, Silvia Ratto- Kim, Michael Watters, Joleen Aguon VV. Circulating proviral HIV DNA and HIV-associated dementia. *Aids*. 2005;19(1):45-52. doi:10.1016/j.biotechadv.2011.08.021.Secreted.

274. Mediouni, Sonia, Albert Darque, Gilbert Baillat, Isabelle Ravaux, Catherine Dhiver, Hervé Tissot-Dupont, Malika Mokhtari, Hervé Moreau, Catherine Tamalet CB, Pascale Paul, Françoise Dignat-George, Andreas Stein, Philippe Brouqui, Stephen A. Spector, 6Grant R. Campbell EPL. Antiretroviral Therapy Does Not Block the Secretion of the Human Immunodeficiency Virus Tat Protein. *Infect Disord - Drug Targets(Formerly Curr Drug Targets - Infect Disord*. 2012;12:81-86. doi:10.2174/187152612798994939.

275. Venturi G, Catucci M, Romano L, et al. Antiretroviral resistance mutations in human immunodeficiency virus type 1 reverse transcriptase and protease from

paired cerebrospinal fluid and plasma samples. *J Infect Dis*. 2000;181(2):740-745. doi:10.1086/315249.

276. New DR, Maggirwar SB, Epstein LG, Dewhurst S, Gelbard H a. HIV-1 Tat induces neuronal death via tumor necrosis factor-alpha and activation of non-N-methyl-D-aspartate receptors by a NFkappaB-independent mechanism. *J Biol Chem*. 1998;273(28):17852-17858. http://www.ncbi.nlm.nih.gov/pubmed/9651389.

277. Zhang Y, Soboloff J, Zhu Z, Berger SA. Inhibition of Ca 2 ƨ Influx Is Required for Mitochondrial Reactive Oxygen Species-Induced Endoplasmic Reticulum Ca 2 ƨ Depletion and Cell Death in Leukemia Cells. 2006;70(4):1424-1434. doi:10.1124/mol.106.024323.mulation.

278. Cummins NW, Badley AD. Anti-apoptotic mechanisms of HIV: Lessons and novel approaches to curing HIV. *Cell Mol Life Sci*. 2013;70(18):3355-3363. doi:10.1007/s00018-012-1239-3.

279. Cox J, Hein MY, Luber C a., Paron I, Nagaraj N, Mann M. MaxLFQ allows accurate proteome-wide label-free quantification by delayed normalization and maximal peptide ratio extraction. *Mol Cell Proteomics*. 2014:M113.031591 - . doi:10.1074/mcp.M113.031591.

280. Gentleman RC, Carey VJ, Bates DM, et al. Bioconductor: open software development for computational biology and bioinformatics. *Genome Biol*. 2004;5(10):R80. doi:10.1186/gb-2004-5-10-r80.

281. McCall MN, Jaffee H a., Irizarry R a. fRMA ST: frozen robust multiarray analysis for Affymetrix Exon and Gene ST arrays. *Bioinformatics*. 2012;28(23):3153-3154. doi:10.1093/bioinformatics/bts588.

282. Li C, Rabinovic A. Adjusting batch effects in microarray expression data using empirical Bayes methods. *Biostatistics*. 2007;8(1):118-127. doi:10.1093/biostatistics/kxj037.

283. Woodhouse SD, Narayan R, Latham S, et al. Transcriptome sequencing, microarray, and proteomic analyses reveal cellular and metabolic impact of hepatitis C virus infection in vitro. *Hepatology*. 2010;52:443-453. doi:10.1002/hep.23733.

284. Fernandez É, Schiappa R, Girault JA, Le Novère N. DARPP-32 is a robust integrator of dopamine and glutamate signals. *PLoS Comput Biol*. 2006;2(12):1619-1633. doi:10.1371/journal.pcbi.0020176.

285. James W. Balesa, Hong Q. Yana, Xiecheng Maa, Youming Lia R, Samarasingheb and CED. The dopamine and cAMP regulated phosphoprotein, 32 kDa (DARPP-32) signaling pathway: A novel therapeutic target in traumatic brain injury. *Exp Neurol*. 2011;229(2):300-307. doi:10.1016/j.biotechadv.2011.08.021.Secreted.

286. John W. Schoggins CMR. Interferon-stimulated genes and their antiviral effector functions. *Curr Opin Virol*. 2011;1(6):519-525. doi:10.1016/j.biotechadv.2011.08.021.Secreted.

287. de Haro C, Méndez R, Santoyo J. The eIF-2alpha kinases and the control of protein synthesis. *FASEB J*. 1996;10(12):1378-1387.

288. Yu T, Robotham JL, Yoon Y. Increased production of reactive oxygen species in hyperglycemic conditions requires dynamic change of mitochondrial morphology. *Proc Natl Acad Sci U S A*. 2006;103(8):2653-2658. doi:10.1073/pnas.0511154103.

289. Bamburg JR, Bernstein BW. Roles of ADF/cofilin in actin polymerization and beyond. *F1000 Biol Rep*. 2010;2(August):62. doi:10.3410/B2-62.

290. Hanna S, El-Sibai M. Signaling networks of Rho GTPases in cell motility. *Cell Signal*. 2013;25(10):1955-1961. doi:10.1016/j.cellsig.2013.04.009.

291. Ng T, Parsons M, Hughes WE, et al. Ezrin is a downstream effector of traf ® cking PKC ± integrin complexes involved in the control of cell motility. 2001;20(11).

292. Dabo S, Meurs EF. dsRNA-dependent protein kinase PKR and its role in stress, signaling and HCV infection. *Viruses*. 2012;4(11):2598-2635. doi:10.3390/v4112598.

293. Barbalat R, Barton G. Toll-like receptor 2 on inflammatory monocytes induces type I interferon in response to viral but not bacterial ligands. *Nat Immunol*. 2010;10(11):1200-1207. doi:10.1038/ni.1792.Toll-like.

294. Saito T, Gale M. Differential recognition of double-stranded RNA by RIG-I-like receptors in antiviral immunity. *J Exp Med*. 2008;205(7):1523-1527. doi:10.1084/jem.20081210.

295. Wu B, Peisley A, Richards C, et al. Structural basis for dsRNA recognition, filament formation, and antiviral signal activation by MDA5. *Cell*. 2013;152(1-2):276-289. doi:10.1016/j.cell.2012.11.048.

296. Connor JH, Lyles DS. Inhibition of host and viral translation during vesicular stomatitis virus infection: eIF2 is responsible for the inhibition of viral but not host translation. *J Biol Chem*. 2005;280(14):13512-13519. doi:10.1074/jbc.M501156200.

297. Rogers KR, Morris CJ, Blake DR, Street A. The cytoskeleton and its importance of inflammation. *Annu Rheum Dis*. 1992;51:565-571.

298. Ruby J, Bluethmann H, Peschon JJ. Antiviral activity of tumor necrosis factor (TNF) is mediated via p55 and p75 TNF receptors. *J Exp Med*. 1997;186(9):1591-1596. doi:10.1084/jem.186.9.1591.

299. Benedict C a. Viruses and the TNF-related cytokines, an evolving battle. *Cytokine Growth Factor Rev*. 2003;14(3-4):349-357. doi:10.1016/S1359-6101(03)00030-3.

300. Hiscott J, Kwon H, Génin P. Hostile takeovers: Viral appropriation of the NF-κB pathway. *J Clin Invest*. 2001;107(2):143-151. doi:10.1172/JCI11918.

301. Gilbert SJ, Duance VC, Mason DJ. Tumour necrosis factor alpha up-regulates protein kinase R (PKR)-activating protein (PACT) and increases phosphorylation of PKR and eukaryotic initiation factor 2-alpha in articular chondrocytes. *Biochem Soc Trans*. 2002;30(Pt 6):886-889. doi:10.1042/BST0300886.

302. Heinicke L a, Wong CJ, Lary J, et al. RNA Dimerization Promotes PKR Dimerization and Activation. 2009;390(2):319-338.

doi:10.1016/j.jmb.2009.05.005.RNA.

303. Endo-Munoz L, Warby T, Harrich D, McMillan N a J. Phosphorylation of HIV Tat by PKR increases interaction with TAR RNA and enhances transcription. *Virol J*. 2005;2:17. doi:10.1186/1743-422X-2-17.

304. Brand SR, Kobayashi R, Mathews MB. The Tat protein of human immunodeficiency virus type 1 is a substrate and inhibitor of the interferon-induced, virally activated protein kinase, PKR. *J Biol Chem*. 1997;272(13):8388-8395.

305. McMillan N a, Chun RF, Siderovski DP, et al. HIV-1 Tat directly interacts with the interferon-induced, double-stranded RNA-dependent kinase, PKR. *Virology*. 1995;213(2):413-424. doi:10.1006/viro.1995.0014.

306. Su Q, Wang S, Baltzis D, et al. Interferons induce tyrosine phosphorylation of the eIF2alpha kinase PKR through activation of Jak1 and Tyk2. *EMBO Rep*. 2007;8(3):265-270. doi:10.1038/sj.embor.7400891.

307. Demarchi F, Gutierrez MI, Giacca M. Human immunodeficiency virus type 1 tat protein activates transcription factor NF-kappaB through the cellular interferon-inducible, double-stranded RNA-dependent protein kinase, PKR. *J Virol*. 1999;73(8):7080-7086.

308. Lawrence T. The nuclear factor NF-kappaB pathway in inflammation. *Cold Spring Harb Perspect Biol*. 2009;1(6):1-10. doi:10.1101/cshperspect.a001651.

309. Fiume G, Vecchio E, De Laurentiis A, et al. Human immunodeficiency virus-1 Tat activates NF-κB via physical interaction with IκB-α and p65. *Nucleic Acids Res*. 2012;40(8):3548-3562. doi:10.1093/nar/gkr1224.

310. Montano M a, Kripke K, Norina CD, et al. NF-kappa B homodimer binding within the HIV-1 initiator region and interactions with TFII-I. *Proc Natl Acad Sci U S A*. 1996;93(22):12376-12381. doi:10.1073/pnas.93.22.12376.

311. Mulu A, Maier M, Liebert U. Triple NF-kB binding sites and LTR sequence similarities in HIV-1C isolates irrespective of helminth co-infection. *Parasit Vectors*. 2014;7(1):204. doi:10.1186/1756-3305-7-204.

312. Miyake A, Ishida T, Yamagishi M, et al. Inhibition of active HIV-1 replication by NF-κB inhibitor DHMEQ. *Microbes Infect*. 2010;12(5):400-408. doi:10.1016/j.micinf.2010.02.004.

313. Chen J-J. Translational Control by Heme-Regulated eIF2α Kinase during Erythropoiesis. *Curr Opin Hematol*. 2014;21(3):172-178. doi:10.1016/j.biotechadv.2011.08.021.Secreted.

314. Toribio R, Ventoso I. Inhibition of host translation by virus infection in vivo. *Proc Natl Acad Sci U S A*. 2010;107(21):9837-9842. doi:10.1073/pnas.1004110107.

315. Smiley JR. Herpes Simplex Virus Virion Host Shutoff Protein : Immune Evasion Mediated by a Viral RNase ? MINIREVIEW Herpes Simplex Virus Virion Host Shutoff Protein : Immune Evasion Mediated by a Viral RNase ? *J Virol*. 2004;78(3):1063-1068. doi:10.1128/JVI.78.3.1063.

316. Lyles DS. Cytopathogenesis and inhibition of host gene expression by RNA viruses. *Microbiol Mol Biol Rev*. 2000;64(4):709-724. doi:10.1128/MMBR.64.4.709-724.2000.Updated.

317. Belmadani A, Tran PB, Ren D, Miller RJ. Chemokines regulate the migration of neural progenitors to sites of neuroinflammation. *J Neurosci*. 2006;26(12):3182-3191. doi:10.1523/JNEUROSCI.0156-06.2006.

318. Bye N, Turnley AM, Morganti-Kossmann MC. Inflammatory regulators of redirected neural migration in the injured brain. *NeuroSignals*. 2012;20(3):132-146. doi:10.1159/000336542.

319. Jacoby DS, Rader DJ. Renin-angiotensin system and atherothrombotic disease: from genes to treatment. *Arch Intern Med*. 2003;163:1155-1164. doi:10.1001/archinte.163.10.1155.

320. Takeshita Y, Takamura T, Ando H, et al. Cross talk of tumor necrosis factor-alpha and the renin-angiotensin system in tumor necrosis factor-alpha-induced plasminogen activator inhibitor-1 production from hepatocytes. *Eur J Pharmacol*. 2008;579(1-3):426-432. doi:10.1016/j.ejphar.2007.11.016.

321. Chandel N, Sharma B, Husain M, et al. HIV compromises integrity of the podocyte actin cytoskeleton through downregulation of the vitamin D receptor. *Am J Physiol Renal Physiol*. 2013;304:F1347-F1357. doi:10.1152/ajprenal.00717.2012.

322. Hsu HH, Hoffmann S, Endlich N, et al. Mechanisms of angiotensin II signaling on cytoskeleton of podocytes. *J Mol Med*. 2008;86(12):1379-1394. doi:10.1007/s00109-008-0399-y.

323. Hotulainen P, Hoogenraad CC. Actin in dendritic spines: Connecting dynamics to function. *J Cell Biol*. 2010;189(4):619-629. doi:10.1083/jcb.201003008.

324. Segev Y, Michaelson DM, Rosenblum K. ApoE ε4 is associated with eIF2α phosphorylation and impaired learning in young mice. *Neurobiol Aging*. August 2012. doi:10.1016/j.neurobiolaging.2012.06.020.

325. Taymans J-M, Nkiliza A, Chartier-Harlin M-C. Deregulation of protein translation control, a potential game-changing hypothesis for Parkinson's disease pathogenesis. *Trends Mol Med*. 2015;21(8):466-472. doi:10.1016/j.molmed.2015.05.004.

326. Chang RCC, Wong AKY, Ng H-K, Hugon J. Phosphorylation of eukaryotic initiation factor-2alpha (eIF2alpha) is associated with neuronal degeneration in Alzheimer's disease. *Neuroreport*. 2002;13(18):2429-2432. doi:10.1097/01.wnr.0000048020.74602.bb.

327. Stern E, Chinnakkaruppan A, David O, Sonenberg N, Rosenblum K. Blocking the eIF2α kinase (PKR) enhances positive and negative forms of cortex-dependent taste memory. *J Neurosci*. 2013;33(6):2517-2525. doi:10.1523/JNEUROSCI.2322-12.2013.

328. Abraham WC, Mason SE, Demmer J, Williams JM, Richardson CL, Tate WP, Lawlor PA DM. Correlations between immediate early gene induction and the

persistence of long-term potentiation. 1993:717-727.

329. Hu N-W, Zhang H-M, Hu X-D, et al. Protein synthesis inhibition blocks the late-phase LTP of C-fiber evoked field potentials in rat spinal dorsal horn. *J Neurophysiol*. 2003;89(5):2354-2359. doi:10.1152/jn.01027.2002.

330. Dang Do AN, Kimball SR, Cavener DR, Jefferson LS. eIF2alpha kinases GCN2 and PERK modulate transcription and translation of distinct sets of mRNAs in mouse liver. *Physiol Genomics*. 2009;38(3):328-341. doi:10.1152/physiolgenomics.90396.2008.

331. Ferreiro E, Baldeiras I, Ferreira IL, et al. Mitochondrial- and endoplasmic reticulum-associated oxidative stress in alzheimers disease: From pathogenesis to biomarkers. *Int J Cell Biol*. 2012;2012. doi:10.1155/2012/735206.

332. Medigeshi GR, Lancaster AM, Hirsch AJ, et al. West Nile virus infection activates the unfolded protein response, leading to CHOP induction and apoptosis. *J Virol*. 2007;81(20):10849-10860. doi:10.1128/JVI.01151-07.

333. Ambrose RL, Mackenzie JM. West Nile virus differentially modulates the unfolded protein response to facilitate replication and immune evasion. *J Virol*. 2011;85(6):2723-2732. doi:10.1128/JVI.02050-10.

334. Bechill J, Chen Z, Brewer JW, Baker SC. Coronavirus infection modulates the unfolded protein response and mediates sustained translational repression. *J Virol*. 2008;82(9):4492-4501. doi:10.1128/JVI.00017-08.

335. Hassan IH, Zhang MS, Powers LS, et al. Influenza A viral replication is blocked by inhibition of the inositol-requiring enzyme 1 (IRE1) stress pathway. *J Biol Chem*. 2012;287(7):4679-4689. doi:10.1074/jbc.M111.284695.

336. Zhou T, Dang Y, Zheng Y-H. The Mitochondrial Translocator Protein, TSPO, Inhibits HIV-1 Envelope Glycoprotein Biosynthesis via the Endoplasmic Reticulum-Associated Protein Degradation Pathway. *J Virol*. 2014;88(6):3474-3484. doi:10.1128/JVI.03286-13.

337. Bültmann a, Muranyi W, Seed B, Haas J. Identification of two sequences in the cytoplasmic tail of the human immunodeficiency virus type 1 envelope glycoprotein that inhibit cell surface expression. *J Virol*. 2001;75:5263-5276. doi:10.1128/JVI.75.11.5263-5276.2001.

338. Ruediger R, Brewis N, Ohst K, Walter G. Increasing the ratio of PP2A core enzyme to holoenzyme inhibits Tat-stimulated HIV-1 transcription and virus production. *Virology*. 1997;238(2):432-443. doi:10.1006/viro.1997.8873.

339. Guergnon J, Godet AN, Galioot A, et al. PP2A targeting by viral proteins: A widespread biological strategy from DNA/RNA tumor viruses to HIV-1. *Biochim Biophys Acta - Mol Basis Dis*. 2011;1812(11):1498-1507. doi:10.1016/j.bbadis.2011.07.001.

340. Eom T, Muslimov I a., Tsokas P, et al. Neuronal BC RNAs cooperate with eIF4B to mediate activity-dependent translational control. *J Cell Biol*. 2014;207(2):237-252. doi:10.1083/jcb.201401005.

341. Mignone F, Gissi C, Liuni S, Pesole G. Untranslated regions of mRNAs. *Genome Biol*. 2002;3(3):REVIEWS0004. doi:10.1186/gb-2002-3-3-reviews0004.

342. Cimermancic P, Gulbahce N, Johnson JR, et al. Global landscape of HIV – human protein complexes. 2011;481(7381):1-6. doi:10.1038/nature10719.

343. Parkin NT, Cohen E a, Darveau a, Rosen C, Haseltine W, Sonenberg N. Mutational analysis of the 5' non-coding region of human immunodeficiency virus type 1: effects of secondary structure on translation. *EMBO J*. 1988;7(9):2831-2837.

344. Ben-Asouli Y, Banai Y, Hauser H, Kaempfer R. Recognition of 5'-terminal TAR structure in human immunodeficiency virus-1 mRNA by eukaryotic translation initiation factor 2. *Nucleic Acids Res*. 2000;28(4):1011-1018.

345. Terenzi F, Hui DJ, Merrick WC, Sen GC. Distinct induction patterns and functions of two closely related interferon-inducible human genes, ISG54 and ISG56. *J Biol Chem*. 2006;281(45):34064-34071. doi:10.1074/jbc.M605771200.

346. Hernández G, Vázques-Pianzola P, Zurbriggen A, Altmann M, Sierra JM, Rivera-Pomar R. Two functionally redundant isoforms of Drosophila melanogaster eukaryotic initiation factor 4B are involved in cap-dependent translation, cell survival, and proliferation. *Eur J Biochem*. 2004;271(14):2923-2936. doi:10.1111/j.1432-1033.2004.04217.x.

347. Ventoso I, Blanco R, Perales C, Carrasco L. HIV-1 protease cleaves eukaryotic initiation factor 4G and inhibits cap-dependent translation. *Proc Natl Acad Sci U S A*. 2001;98:12966-12971. doi:10.1073/pnas.231343498.

348. Lehmann M, Nikolic DS, Piguet V. How HIV-1 takes advantage of the cytoskeleton during replication and cell-to-cell transmission. *Viruses*. 2011;3:1757-1776. doi:10.3390/v3091757.

349. Brancolini C, Benedetti M, Schneider C. Microfilament reorganization during apoptosis: the role of Gas2, a possible substrate for ICE-like proteases. *EMBO J*. 1995;14(21):5179-5190.

350. Spano a., Sciola L, Monaco G, Barni S. Relationship between actin microfilaments and plasma membrane changes during apoptosis of neoplastic cell lines in different culture conditions. *Eur J Histochem*. 2000;44(3):255-267.

351. Matarrese P, Malorni W. Human immunodeficiency virus (HIV)-1 proteins and cytoskeleton: partners in viral life and host cell death. *Cell Death Differ*. 2005;12 Suppl 1:932-941. doi:10.1038/sj.cdd.4401893.

352. Schonhofen P, de Medeiros LM, Chatain CP, Bristot IJ, Klamt F. Cofilin/Actin rod formation by dysregulation of cofilin-1 activity as a central initial step in neurodegeneration. *Mini Rev Med Chem*. 2014;14(5):393-400. doi:10.2174/1389557514666140506161458.

353. Goellner B, Aberle H. The synaptic cytoskeleton in development and disease. *Dev Neurobiol*. 2012;72(1):111-125. doi:10.1002/dneu.20892.

354. Ethell IM, Pasquale EB. Molecular mechanisms of dendritic spine development

and remodeling. *Prog Neurobiol*. 2005;75:161-205. doi:10.1016/j.pneurobio.2005.02.003.

355. Messaoudi E, Kanhema T, Soulé J, et al. Sustained Arc/Arg3.1 synthesis controls long-term potentiation consolidation through regulation of local actin polymerization in the dentate gyrus in vivo. *J Neurosci*. 2007;27(39):10445-10455. doi:10.1523/JNEUROSCI.2883-07.2007.

356. Fukazawa Y, Saitoh Y, Ozawa F, Ohta Y, Mizuno K, Inokuchi K. Hippocampal LTP is accompanied by enhanced F-actin content within the dendritic spine that is essential for late LTP maintenance in vivo. *Neuron*. 2003;38:447-460. doi:10.1016/S0896-6273(03)00206-X.

357. Qualmann B, Boeckers TM, Jeromin M, Gundelfinger ED, Kessels MM. Linkage of the actin cytoskeleton to the postsynaptic density via direct interactions of Abp1 with the ProSAP/Shank family. *J Neurosci*. 2004;24(10):2481-2495. doi:10.1523/JNEUROSCI.5479-03.2004.

358. Garvalov BK, Flynn KC, Neukirchen D, et al. Cdc42 regulates cofilin during the establishment of neuronal polarity. *J Neurosci*. 2007;27(48):13117-13129. doi:10.1523/JNEUROSCI.3322-07.2007.

359. Wegner AM, Nebhan C a., Hu L, et al. N-WASP and the Arp2/3 complex are critical regulators of actin in the development of dendritic spines and synapses. *J Biol Chem*. 2008;283(23):15912-15920. doi:10.1074/jbc.M801555200.

360. Du Y, Weed S a, Xiong WC, Marshall TD, Parsons JT. Identification of a novel cortactin SH3 domain-binding protein and its localization to growth cones of cultured neurons. *Mol Cell Biol*. 1998;18(10):5838-5851.

361. Teng B, Lukasz A, Schiffer M. The ADF/cofilin-pathway and actin dynamics in podocyte injury. *Int J Cell Biol*. 2012;2012. doi:10.1155/2012/320531.

362. HIV compromises integrity of the podocyte actin cytoskeleton through.pdf.crdownload.

363. Manuscript A, Zebrafish R, Development E. The Non-core Subunit eIF3h of Translation Initiation Factor eIF3 Regulates Zebrafish Embryonic Development. 2011;239(6):1632-1644. doi:10.1002/dvdy.22289.The.

364. Sertie AL, de Alencastro G, De Paula VJ, Passos-Bueno MR. Collybistin and gephyrin are novel components of the eukaryotic translation initiation factor 3 complex. *BMC Res Notes*. 2010;3:242. doi:10.1186/1756-0500-3-242.

365. Manadas B, Santos AR, Szabadfi K, et al. BDNF-induced changes in the expression of the translation machinery in hippocampal neurons: Protein levels and dendritic mRNA. *J Proteome Res*. 2009;8(10):4536-4552. doi:10.1021/pr900366x.

366. Schratt GM, Nigh E a, Chen WG, Hu L, Greenberg ME. BDNF regulates the translation of a select group of mRNAs by a mammalian target of rapamycin-phosphatidylinositol 3-kinase-dependent pathway during neuronal development. *J Neurosci*. 2004;24(33):7366-7377. doi:10.1523/JNEUROSCI.1739-04.2004.

367. Bliss T V, Cooke SF. Long-term potentiation and long-term depression: a clinical perspective. *Clinics*. 2011;1:3-17. doi:10.1590/S1807-59322011001300002.

368. Ying S-W, Futter M, Rosenblum K, et al. Brain-derived neurotrophic factor induces long-term potentiation in intact adult hippocampus: requirement for ERK activation coupled to CREB and upregulation of Arc synthesis. *J Neurosci*. 2002;22(5):1532-1540. doi:22/5/1532 [pii].

369. Wu J, Rowan MJ, Anwyl R. Long-term potentiation is mediated by multiple kinase cascades involving CaMKII or either PKA or p42/44 MAPK in the adult rat dentate gyrus in vitro. *J Neurophysiol*. 2006;95:3519-3527. doi:10.1152/jn.01235.2005.

370. Howe AK. Regulation of actin-based cell migration by cAMP/PKA. *Biochim Biophys Acta - Mol Cell Res*. 2004;1692:159-174. doi:10.1016/j.bbamcr.2004.03.005.

371. Warren K, Wei T, Li D, et al. Eukaryotic elongation factor 1 complex subunits are critical HIV-1 reverse transcription cofactors. *Proc Natl Acad Sci*. 2012;109(24):9587-9592. doi:10.1073/pnas.1204673109.

372. Inamura N, Nawa H, Takei N. Enhancement of translation elongation in neurons by brain-derived neurotrophic factor: Implications for mammalian target of rapamycin signaling. *J Neurochem*. 2005;95(5):1438-1445. doi:10.1111/j.1471-4159.2005.03466.x.

373. MacEwan DJ. TNF ligands and receptors--a matter of life and death. *Br J Pharmacol*. 2002;135(4):855-875. doi:10.1038/sj.bjp.0704549.

374. Twu YC, Gold MR, Teh HS. TNFR1 delivers pro-survival signals that are required for limiting TNFR2-dependent activation-induced cell death (AICD) in CD8 + T cells. *Eur J Immunol*. 2011;41(2):335-344. doi:10.1002/eji.201040639.

375. Rauert H, Stühmer T, Bargou R, Wajant H, Siegmund D. TNFR1 and TNFR2 regulate the extrinsic apoptotic pathway in myeloma cells by multiple mechanisms. *Cell Death Dis*. 2011;2:e194. doi:10.1038/cddis.2011.78.

376. Gary DS, Mattson MP. PTEN regulates Akt kinase activity in hippocampal neurons and increases their sensitivity to glutamate and apoptosis. *Neuromolecular Med*. 2002;2(2):261-269. doi:10.1385/NMM:2:3:261.

377. Zhao T, Adams MH, Zou S-P, El-Hage N, Hauser KF, Knapp PE. Silencing the PTEN gene is protective against neuronal death induced by human immunodeficiency virus type 1 Tat. *J Neurovirol*. 2007;13(2):97-106. doi:10.1080/13550280701236841.

378. Kim N, Kukkonen S, Gupta S, Aldovini A. Association of Tat with promoters of PTEN and PP2A subunits is key to transcriptional activation of apoptotic pathways in HIV-infected CD4+ T cells. *PLoS Pathog*. 2010;6(9):e1001103. doi:10.1371/journal.ppat.1001103.

379. Shanley TP, Vasi N, Denenberg a, Wong HR. The serine/threonine phosphatase, PP2A: endogenous regulator of inflammatory cell signaling. *J Immunol*. 2001;166(2):966-972. doi:10.1097/00003246-199912001-00013.

380. Wallace AM, Hardigan A, Geraghty P, et al. Protein phosphatase 2A regulates innate immune and proteolytic responses to cigarette smoke exposure in the lung. *Toxicol Sci*. 2012;126(2):589-599. doi:10.1093/toxsci/kfr351.

381. Schabbauer G, Matt U, Günzl P, et al. Myeloid PTEN promotes inflammation but impairs bactericidal activities during murine pneumococcal pneumonia. *J Immunol*. 2010;185(1):468-476. doi:10.4049/jimmunol.0902221.

382. Wang X, Blanchard J, Kohlbrenner E, et al. The carboxy-terminal fragment of inhibitor-2 of protein phosphatase-2A induces Alzheimer disease pathology and cognitive impairment. *FASEB J*. 2010;24(1):4420-4432. doi:10.1096/fj.10-158477.

383. Shanley TP, Vasi N, Denenberg a, Wong HR. The serine/threonine phosphatase, PP2A: endogenous regulator of inflammatory cell signaling. *J Immunol*. 2001;166:966-972. doi:10.1097/00003246-199912001-00013.

384. Alison M. Wallace*, Andrew Hardigan†, Patrick Geraghty†, Shaneeza Salim*, Adam Gaffney*, Jincy Thankachen*, Leo Arellanos* JMDa and RF, Foronjy†. PROTEIN PHOSPHATASE 2A (PP2A) REGULATES INNATE IMMUNE AND PROTEOLYTIC RESPONSES TO CIGARETTE SMOKE EXPOSURE IN THE LUNG Alison. 2012;(212):1-32.

385. Buss H, Dörrie A, Schmitz ML, et al. Phosphorylation of serine 468 by GSK-3beta negatively regulates basal p65 NF-kappaB activity. *J Biol Chem*. 2004;279(48):49571-49574. doi:10.1074/jbc.C400442200.

386. Schwabe RF, Brenner D a. Role of glycogen synthase kinase-3 in TNF-alpha-induced NF-kappaB activation and apoptosis in hepatocytes. *Am J Physiol Gastrointest Liver Physiol*. 2002;283:G204-G211. doi:10.1152/ajpgi.00016.2002.

387. Mayo MW, Madrid L V, Westerheide SD, et al. PTEN blocks tumor necrosis factor-induced NF-kB-dependent transcription by inhibiting the transactivation potential of the p65 subunit. *J Biol Chem*. 2002;277(13):11116-11125. doi:10.1074/jbc.M108670200.

388. Barisic S, Strozyk E, Peters N, Walczak H, Kulms D. Identification of PP2A as a crucial regulator of the NF-kappaB feedback loop: its inhibition by UVB turns NF-kappaB into a pro-apoptotic factor. *Cell Death Differ*. 2008;15:1681-1690. doi:10.1038/cdd.2008.98.

389. Willie Wilson III ASB. Maintenance of Constitutive IκB Kinase Activity by Glycogen Synthase Kinase-3 α/β in Pancreatic Cancer. *Cancer Res*. 2008;68(19):8156-8163. doi:10.1016/j.biotechadv.2011.08.021.Secreted.

390. Dogra C, Changotra H, Wedhas N, Qin X, Wergedal JE, Kumar A. TNF-related weak inducer of apoptosis (TWEAK) is a potent skeletal muscle-wasting cytokine. *FASEB J*. 2007;21(8):1857-1869. doi:10.1096/fj.06-7537com.

391. Zhang D, Kanthasamy A, Yang Y, Anantharam V, Kanthasamy A. Protein kinase C delta negatively regulates tyrosine hydroxylase activity and dopamine synthesis by enhancing protein phosphatase-2A activity in dopaminergic neurons. *J Neurosci*. 2007;27(20):5349-5362. doi:10.1523/JNEUROSCI.4107-06.2007.

392. Ahn J-H, McAvoy T, Rakhilin S V, Nishi A, Greengard P, Nairn AC. Protein kinase A activates protein phosphatase 2A by phosphorylation of the B56delta subunit. *Proc Natl Acad Sci U S A*. 2007;104(8):2979-2984. doi:10.1073/pnas.0611532104.

393. Cysique L a, Brew BJ, Halman M, et al. Undetectable cerebrospinal fluid HIV RNA and beta-2 microglobulin do not indicate inactive AIDS dementia complex in highly active antiretroviral therapy-treated patients. *J Acquir Immune Defic Syndr*. 2005;39(4):426-429. doi:10.1097/01.qai.0000165799.59322.f5.

394. Maggirwar SB, Tong N, Ramirez S, Gelbard H a., Dewhurst S. HIV-1 Tat-mediated activation of glycogen synthase kinase-3B contributes to Tat-mediated neurotoxicity. *J Neurochem*. 1999;73(2):578-586. doi:10.1046/j.1471-4159.1999.0730578.x.

395. Focosi D, Azzarà A, Kast RE, Carulli G, Petrini M. Lithium and hematology: established and proposed uses. *J Leukoc Biol*. 2009;85(1):20-28. doi:10.1189/jlb.0608388.

396. Lenox RH, Wang L. Molecular basis of lithium action: integration of lithium-responsive signaling and gene expression networks. *Mol Psychiatry*. 2003;8(2):135-144. doi:10.1038/sj.mp.4001306.

397. Chuang D-M, Wang Z, Chiu C-T. GSK-3 as a Target for Lithium-Induced Neuroprotection Against Excitotoxicity in Neuronal Cultures and Animal Models of Ischemic Stroke. *Front Mol Neurosci*. 2011;4(August):15. doi:10.3389/fnmol.2011.00015.

398. Beurel E, Michalek SM, Jope RS. Innate and adaptive immune responses regulated by glycogen synthae kinase-3 (GSK3). *Tremds Immunol*. 2010;31(1):1-16. doi:10.1016/j.it.2009.09.007.Innate.

399. Beaulieu JM. A role for Akt and glycogen synthase kinase-3 as integrators of dopamine and serotonin neurotransmission in mental health. *J Psychiatry Neurosci*. 2012;37(1):7-16. doi:10.1503/jpn.110011.

400. Smillie KJ, Cousin MA. The Role of GSK3 in Presynaptic Function. *Int J Alzheimers Dis*. 2011;2011:263673. doi:10.4061/2011/263673.

401. Mendes CT, Mury FB, de Sá Moreira E, et al. Lithium reduces Gsk3b mRNA levels: implications for Alzheimer Disease. *Eur Arch Psychiatry Clin Neurosci*. 2009;259(1):16-22. doi:10.1007/s00406-008-0828-5.

402. Schifitto G, Zhong J, Gill D, et al. Lithium therapy for human immunodeficiency virus type 1-associated neurocognitive impairment. *J Neurovirol*. 2009;15(2):176-186. doi:10.1080/13550280902758973.

403. Li X, Jope RS. Is glycogen synthase kinase-3 a central modulator in mood regulation? *Neuropsychopharmacology*. 2010;35(11):2143-2154. doi:10.1038/npp.2010.105.

404. Liang MH, Chuang DM. Differential roles of glycogen synthase kinase-3 isoforms in the regulation of transcriptional activation. *J Biol Chem*. 2006;281(41):30479-30484. doi:10.1074/jbc.M607468200.

405. Jaeger LB, Nath a. Modeling HIV-associated neurocognitive disorders in mice: new approaches in the changing face of HIV neuropathogenesis. *Dis Model Mech*. 2012;5(3):313-322. doi:10.1242/dmm.008763.

406. Bagashev A, Sawaya BE. Roles and functions of HIV-1 Tat protein in the CNS: an overview. *Virol J*. 2013;10:358. doi:10.1186/1743-422X-10-358.

407. Cruceanu C, Alda M, Turecki G. Lithium: a key to the genetics of bipolar disorder. *Genome Med*. 2009;1(8):79. doi:10.1186/gm79.

408. Baum a E, Akula N, Cabanero M, et al. A genome-wide association study implicates diacylglycerol kinase eta (DGKH) and several other genes in the etiology of bipolar disorder. *Mol Psychiatry*. 2008;13(2):197-207. doi:10.1038/sj.mp.4002012.

409. Wiśniewski JR, Zougman A, Nagaraj N, Mann M. Universal sample preparation method for proteome analysis. *Nat Methods*. 2009;6(5):359-362. doi:10.1038/nmeth.1322.

410. Pirmoradian M, Budamgunta H, Chingin K, Zhang B, Zubarev RA. Rapid and deep human proteome analysis by single- dimension shotgun proteomics Rapid and deep single-dimension shotgun proteomics. 2013:1-32.

411. Alonso M, Medina JH, Pozzo-miller L. ERK1 / 2 Activation Is Necessary for BDNF to Increase Dendritic Spine Density in Hippocampal CA1 Pyramidal Neurons. 2004:172-178. doi:10.1101/lm.67804.tant.

412. Audoly G, Popoff MR, Gluschankof P. Involvement of a small GTP binding protein in HIV-1 release. *Retrovirology*. 2005;2:48. doi:10.1186/1742-4690-2-48.

413. Sirois M, Robitaille L, Allary R, et al. TRAF6 and IRF7 control HIV replication in macrophages. *PLoS One*. 2011;6(11). doi:10.1371/journal.pone.0028125.

414. Depaepe V, Cuvelier L, Thöny B, Résibois A. Pterin-4α-carbinolamine dehydratase in rat brain. I. Patterns of co-localization with tyrosine hydroxylase. *Mol Brain Res*. 2000;75(1):76-88. doi:10.1016/S0169-328X(99)00297-1.

415. Eskinazi R, Thöny B, Svoboda M, et al. Overexpression of pterin-4a-carbinolamine dehydratase/dimerization cofactor of hepatocyte nuclear factor 1 in human colon cancer. *Am J Pathol*. 1999;155(4):1105-1113.

416. Andersen JL, Le Rouzic E, Planelles V. HIV-1 Vpr: Mechanisms of G2 arrest and apoptosis. *Exp Mol Pathol*. 2008;85(1):2-10. doi:10.1016/j.yexmp.2008.03.015.

417. Liu H, Nakazawa T, Tezuka T, Yamamoto T. Physical and Functional Interaction of Fyn Tyrosine Kinase with a Brain-enriched Rho GTPase-activating Protein TCGAP *. *J Biol Chem*. 2006;281(33):23611-23619. doi:10.1074/jbc.M511205200.

418. Mcmanus EJ, Sakamoto K, Armit LJ, et al. Role that phosphorylation of GSK3 plays in insulin and Wnt signalling defined by knockin analysis. *EMBO J*. 2005;24:1571-1583.

419. Tyler W a, Jain MR, Cifelli SE, et al. Proteomic identification of novel targets regulated by the mammalian target of rapamycin pathway during oligodendrocyte differentiation. *Glia*. 2011;59(11):1754-1769.

doi:10.1002/glia.21221.

420. Beltran L, Chaussade C, Vanhaesebroeck B, Cutillas PR. Calpain interacts with class IA phosphoinositide 3-kinases regulating their stability and signaling activity. *Proc Natl Acad Sci*. 2011;108(39):16217-16222. doi:10.1073/pnas.1107692108.

421. Amini M, Ma C-L, Farazifard R, et al. Conditional Disruption of Calpain in the CNS Alters Dendrite Morphology, Impairs LTP, and Promotes Neuronal Survival following Injury. *J Neurosci*. 2013;33(13):5773-5784. doi:10.1523/JNEUROSCI.4247-12.2013.

422. Liu J, Liu MC, Wang KKW. Calpain in the CNS: from synaptic function to neurotoxicity. *Sci Signal*. 2008;1(14):re1. doi:10.1126/stke.114re1.

423. Chakrabarti A, Chen AW, Varner JD. A review of the Mammalian Unfoded Protein Response. *Biotechnol Bioeng*. 2012;108(12):2777-2793. doi:10.1002/bit.23282.A.

424. Mekahli D, Bultynck G, Parys JB, de Smedt H, Missiaen L. Endoplasmic-reticulum calcium depletion and disease. *Cold Spring Harb Perspect Biol*. 2011;3(6):1-30. doi:10.1101/cshperspect.a004317.

425. Germain D, Russell a, Thompson a, Hendley J. Ubiquitination of free cyclin D1 is independent of phosphorylation on threonine 286. *J Biol Chem*. 2000;275(16):12074-12079. http://www.ncbi.nlm.nih.gov/pubmed/10766840.

426. Forgacs G. Role of the cytoskeleton in signaling networks. *J Cell Sci*. 2004;117(13):2769-2775. doi:10.1242/jcs.01122.

427. Stupack DG, Cheresh D a. Get a ligand, get a life: integrins, signaling and cell survival. *J Cell Sci*. 2002;115(Pt 19):3729-3738. doi:10.1242/jcs.00071.

428. Calderwood D a., Shattil SJ, Ginsberg MH. Integrins and actin filaments: reciprocal regulation of cell adhesion and signaling. *J Biol Chem*. 2000;275(30):22607-22610. doi:10.1074/jbc.R900037199.

429. Mosser S, Alattia J-R, Dimitrov M, et al. The adipocyte differentiation protein APMAP is an endogenous suppressor of A production in the brain. *Hum Mol Genet*. 2014;24(2):371-382. doi:10.1093/hmg/ddu449.

430. Matsuki T, Pramatarova A, Howell BW. Reduction of Crk and CrkL expression blocks reelin-induced dendritogenesis. *J Cell Sci*. 2008;121(Pt 11):1869-1875. doi:10.1242/jcs.027334.

431. Il Hwan Kim, Bence Racz, Hong Wang, Lauren Burianek RW, Ryohei Yasuda WCW and SHS. Disruption of Arp2/3 Results in Asymmetric Structural Plasticity of Dendritic Spines and Progressive Synaptic and Behavioral Abnormalities. *J Neurosci*. 2013;33(14):6081-6092. doi:10.1523/JNEUROSCI.0035-13.2013.Disruption.

432. Reddy-Alla S, Schmitt B, Birkenfeld J, et al. PH-Domain-driven targeting of collybistin but not Cdc42 activation is required for synaptic gephyrin clustering. *Eur J Neurosci*. 2010;31:1173-1184. doi:10.1111/j.1460-9568.2010.07149.x.

433. Braga VM, Machesky LM, Hall a, Hotchin N a. The small GTPases Rho and Rac are required for the establishment of cadherin-dependent cell-cell contacts. *J Cell Biol*. 1997;137(6):1421-1431. http://www.pubmedcentral.nih.gov/articlerender.fcgi?artid=2132529&tool=pmcentrez&rendertype=abstract.

434. Aznar S, Lacal JC. Rho signals to cell growth and apoptosis. *Cancer Lett*. 2001;165(1):1-10. doi:10.1016/S0304-3835(01)00412-8.

435. Seasholtz TM, Majumdar M, Brown JH. Rho as a mediator of G protein-coupled receptor signaling. *Mol Pharmacol*. 1999;55(6):949-956.

436. Whitehead IP, Zohn IE, Der CJ. Rho GTPase-dependent transformation by G protein-coupled receptors. *Oncogene*. 2001;20(13):1547-1555. doi:10.1038/sj.onc.1204188.

437. Woo J a, Zhao X, Khan H, et al. Slingshot-Cofilin activation mediates mitochondrial and synaptic dysfunction via Aβ ligation to β1-integrin conformers. *Cell Death Differ*. 2015;22(6):921-934. doi:10.1038/cdd.2015.5.

438. Valdiglesias V, Fernández-Tajes J, Pásaro E, Méndez J, Laffon B. Identification of differentially expressed genes in SHSY5Y cells exposed to okadaic acid by suppression subtractive hybridization. *BMC Genomics*. 2012;13(1):46. doi:10.1186/1471-2164-13-46.

439. Kinoshita a, Kinoshita M, Akiyama H, et al. Identification of septins in neurofibrillary tangles in Alzheimer's disease. *Am J Pathol*. 1998;153(5):1551-1560. doi:10.1016/S0002-9440(10)65743-4.

440. Ochs SM, Dorostkar MM, Aramuni G, et al. Loss of neuronal GSK3β reduces dendritic spine stability and attenuates excitatory synaptic transmission via β-catenin. *Mol Psychiatry*. 2014;(August 2013):1-8. doi:10.1038/mp.2014.55.

441. Takahashi M, Yasutake K, Tomizawa K. Lithium inhibits neurite growth and tau protein kinase I/glycogen synthase kinase-3beta-dependent phosphorylation of juvenile tau in cultured hippocampal neurons. *J Neurochem*. 1999;73(5):2073-2083.

442. S. M. Shaha, C. H. Patela, A. S. Fenga and RK. Lithium Alters the Morphology of Neurites Regenerating from Cultured Adult Spiral Ganglion Neurons. *Hear Res*. 2013;304:137-144. doi:10.1016/j.biotechadv.2011.08.021.Secreted.

443. Gómez-sintes R, Lucas JJ. NFAT / Fas signaling mediates the neuronal apoptosis and motor side effects of GSK-3 inhibition in a mouse model of lithium therapy. *J Clin Invest*. 2010;120(7):2432-2445. doi:10.1172/JCI37873.2432.

444. Gaskill PJ, Calderon TM, Luers AJ, Eugenin E a, Javitch J a, Berman JW. Human immunodeficiency virus (HIV) infection of human macrophages is increased by dopamine: a bridge between HIV-associated neurologic disorders and drug abuse. *Am J Pathol*. 2009;175(3):1148-1159. doi:10.2353/ajpath.2009.081067.

445. Silvers J, Aksenova M, Aksenov M, Mactutus C, Booze R. Neurotoxicity of HIV-1 Tat protein: Involvement of D1 dopamine receptor. *Neurotoxicology*. 2007;28(6):1184-1190. doi:10.1016/j.neuro.2007.07.005.

446. Church LD, Hessler G, Goodall JE, et al. TNFR1-induced sphingomyelinase activation modulates TCR signaling by impairing store-operated Ca2+ influx. *J Leukoc Biol*. 2005;78(1):266-278. doi:10.1189/jlb.1003456.

447. Homaidan FR, El-Sabban ME, Chakroun I, El-Sibai M, Dbaibo GS. IL-1 stimulates ceramide accumulation without inducing apoptosis in intestinal epithelial cells. *Mediators Inflamm*. 2002;11(1):39-45. doi:10.1080/09629350210313.

448. An H, Zhao W, Hou J, et al. SHP-2 Phosphatase Negatively Regulates the TRIF Adaptor Protein-Dependent Type I Interferon and Proinflammatory Cytokine Production. *Immunity*. 2006;25(6):919-928. doi:10.1016/j.immuni.2006.10.014.

449. Hartman ZR, Schaller MD, Agazie YM. The tyrosine phosphatase SHP2 regulates focal adhesion kinase to promote EGF-induced lamellipodia persistence and cell migration. *Mol Cancer Res*. 2013;11(6):651-664. doi:10.1158/1541-7786.MCR-12-0578.

450. Lee SH, Peng IF, Ng YG, et al. Synapses are regulated by the cytoplasmic tyrosine kinase Fer in a pathway mediated by p120catenin, Fer, SHP-2, and ??-catenin. *J Cell Biol*. 2008;183(5):893-908. doi:10.1083/jcb.200807188.

451. Kusakari S, Saitow F, Ago Y, et al. Shp2 in Forebrain Neurons Regulates Synaptic Plasticity, Locomotion, and Memory Formation in Mice. *Mol Cell Biol*. 2015;35(9):1557-1572. doi:10.1128/MCB.01339-14.

452. Yao X-Q, Zhang X-X, Yin Y-Y, et al. Glycogen synthase kinase-3β regulates Tyr307 phosphorylation of protein phosphatase-2A via protein tyrosine phosphatase 1B but not Src. *Biochem J*. 2011;437(2):335-344. doi:10.1042/BJ20110347.

453. Sohyun A, Ginty DD, Linden DJ. A late phase of cerebellar long-term depression requires activation of CaMKIV and CREB. *Neuron*. 1999;23(3):559-568. doi:10.1016/S0896-6273(00)80808-9.

454. Du K, Montminy M. Communication CREB Is a Regulatory Target for the Protein Kinase Akt / PKB *. *J Biol Chem*. 1998;273(9):32377-32379. doi:10.1074/jbc.273.49.32377.

455. Pugazhenthi S, Wang M, Pham S, Sze C-I, Eckman CB. Downregulation of CREB expression in Alzheimer's brain and in Aβ-treated rat hippocampal neurons. *Mol Neurodegener*. 2011;6(1):60. doi:10.1186/1750-1326-6-60.

456. Ye X, Deng Y, Lai ZC. Akt is negatively regulated by Hippo signaling for growth inhibition in Drosophila. *Dev Biol*. 2012;369(1):115-123. doi:10.1016/j.ydbio.2012.06.014.

457. Larsson M, Shankar EM, Che KF, et al. Molecular signatures of T-cell inhibition in HIV-1 infection. *Retrovirology*. 2013;10:31. doi:10.1186/1742-4690-10-31.

458. Zhao B, Li L, Lei Q, Guan KL. The Hippo-YAP pathway in organ size control and tumorigenesis: An updated version. *Genes Dev*. 2010;24(9):862-874. doi:10.1101/gad.1909210.

459. Manuscript A. Negative regulation of Yap during neuronal differentiation. *Changes*. 2012;29(6):997-1003. doi:10.1016/j.biotechadv.2011.08.021.Secreted.

460. Liu Z, Lv Y, Zhao N, Guan G, Wang J. Protein kinase R-like ER kinase and its role in endoplasmic reticulum stress-decided cell fate. *Cell Death Dis*. 2015;6(7):e1822. doi:10.1038/cddis.2015.183.

461. Datta B, Datta R, Mukherjee S, Zhang Z. Increased phosphorylation of eukaryotic initiation factor 2alpha at the G2/M boundary in human osteosarcoma cells correlates with deglycosylation of p67 and a decreased rate of protein synthesis. *Exp Cell Res*. 1999;250(1):223-230. doi:10.1006/excr.1999.4508.

462. Sudhakar a, Ramachandran a, Ghosh S, Hasnain SE, Kaufman RJ, Ramaiah K V. Phosphorylation of serine 51 in initiation factor 2 alpha (eIF2 alpha) promotes complex formation between eIF2 alpha(P) and eIF2B and causes inhibition in the guanine nucleotide exchange activity of eIF2B. *Biochemistry*. 2000;39(42):12929-12938.

463. Stephen Bertsch, Charles H. Lang TCV. Inhibition of GSK-3β Activity with Lithium In Vitro Attenuates Sepsis-Induced Changes in Muscle Protein Turnover. *shock*. 2011;35(3):266-274. doi:10.1016/j.biotechadv.2011.08.021.Secreted.

464. Bosetti F, Seemann R, Rapoport SI. Chronic lithium chloride administration to rats decreases brain protein level of epsilon subunit of eukaryotic initiation factor-2B. *Neurosci Lett*. 2002;327(1):71-73. doi:10.1016/S0304-3940(02)00354-3.

465. Liu ZH, Huang T, Smith CB. Lithium reverses increased rates of cerebral protein synthesis in a mouse model of fragile X syndrome. *Neurobiol Dis*. 2012;45(3):1145-1152. doi:10.1016/j.nbd.2011.12.037.

466. Brown LA, Scarola J, Smith AJ, Sanberg PR, Tan J, Giunta B. The role of tau protein in HIV-associated neurocognitive disorders. *Mol Neurodegener*. 2014;9(1):40. doi:10.1186/1750-1326-9-40.

467. Rankin C a, Sun Q, Gamblin TC. Tau phosphorylation by GSK-3beta promotes tangle-like filament morphology. *Mol Neurodegener*. 2007;2:12. doi:10.1186/1750-1326-2-12.

468. Caccamo A, Oddo S, Tran LX, LaFerla FM. Lithium reduces tau phosphorylation but not A beta or working memory deficits in a transgenic model with both plaques and tangles. *Am J Pathol*. 2007;170(5):1669-1675. doi:10.2353/ajpath.2007.061178.

469. Zhu L-Q, Wang S-H, Liu D, et al. Activation of glycogen synthase kinase-3 inhibits long-term potentiation with synapse-associated impairments. *J Neurosci*. 2007;27(45):12211-12220. doi:10.1523/JNEUROSCI.3321-07.2007.

470. Martin M, Geudens I, Bruyr J, et al. PP2A regulatory subunit Bα controls endothelial contractility and vessel lumen integrity via regulation of HDAC7. *EMBO J*. 2013;32(18):2491-2503. doi:10.1038/emboj.2013.187.

471. Chacon MR, Navarro a. I, Cuesto G, et al. Focal adhesion kinase regulates actin nucleation and neuronal filopodia formation during axonal growth. *J Cell Sci*. 2012;125(17):e1-e1. doi:10.1242/jcs.120741.

472. Yu-Chih Lin AJK. Mechanisms of Synapse and Dendrite Maintenance and Their

Disruption in Psychiatric and Neurodegenerative Disorders. *Annu Rev Neurosci*. 2010;33:349-378. doi:10.1146/annurev-neuro-060909-153204.Mechanisms.

473. Gomez TM, Roche FK, Letourneau PC. Chick sensory neuronal growth cones distinguish fibronectin from laminin by making substratum contacts that resemble focal contacts. *J Neurobiol*. 1996;29(1):18-34. doi:10.1002/(SICI)1097-4695(199601)29:1<18::AID-NEU2>3.0.CO;2-A.

474. Myers JP, Gomez TM. Focal Adhesion Kinase Promotes Integrin Adhesion Dynamics Necessary for Chemotropic Turning of Nerve Growth Cones. *J Neurosci*. 2011;31(38):13585-13595. doi:10.1523/JNEUROSCI.2381-11.2011.

475. Renaudin a, Lehmann M, Girault J, McKerracher L. Organization of point contacts in neuronal growth cones. *J Neurosci Res*. 1999;55(4):458-471.

476. Yamaguchi Y, Katoh H, Yasui H, Mori K, Negishi M. RhoA Inhibits the Nerve Growth Factor-induced Rac1 Activation through Rho-associated Kinase-dependent Pathway. *J Biol Chem*. 2001;276(22):18977-18983. doi:10.1074/jbc.M100254200.

477. Sharma N, Deppmann CD, Harrington AW, et al. Long distance control of synapse assembly by target-derived NGF. *Neuron*. 2010;67(3):422-434. doi:10.1016/j.neuron.2010.07.018.Long.

478. Drubin D, Feinstein SC, Shooter EM, Kirschner M. Nerve growth factor induced neurite outgrowth in PC12 cells involves the coordinate induction of microtubule assembly and assembly-promoting factors. *J Cell Biol*. 1985;101(15):1790-1807. doi:10.1083/jcb.101.5.1799.

479. Prencipe G, Minnone G, Strippoli R, et al. Nerve growth factor downregulates inflammatory response in human monocytes through TrkA. *J Immunol*. 2014;192(7):3345-3354. doi:10.4049/jimmunol.1300825.

480. Equils O, Faure E, Thomas L, Bulut Y, Trushin S, Arditi M. Bacterial lipopolysaccharide activates HIV long terminal repeat through Toll-like receptor 4. *J Immunol*. 2001;166(4):2342-2347. doi:10.4049/jimmunol.166.4.2342.

481. De Jong M a WP, De Witte L, Oudhoff MJ, Gringhuis SI, Gallay P, Geijtenbeek TBH. TNFα and TLR agonists increase susceptibility to HIV-1 transmission by human Langerhans cells ex vivo. *J Clin Invest*. 2008;118(10):3440-3452. doi:10.1172/JCI34721.

482. Kessing LV, Søndergård L, Forman JL, Andersen PK. Lithium treatment and risk of dementia. *Arch Gen Psychiatry*. 2008;65(11):1331-1335. doi:10.1001/archpsyc.65.11.1331.

Appendix

Appendix 1

SILAC incorporation test peptides

Sequence	Intensity	Intensity L	Intensity H
AAAAAAALQAK	31983000	0	31983000
AAAAVGAGHGAGGPGAASSSGGAR	2358900	0	2358900
AAADLMAYCEAHAK	11847000	0	11847000
AAAEAANCIMEVSCGQAESSEKPNAEDMTSK	4461600	0	4461600
AAAEVNQDYGLDPK	3921900	0	3921900
AAAGEFADDPCSSVK	55136000	0	55136000
AAAGGGGGGAAAAGR	59439000	0	59439000
AAAMDVDTPSGTNSGAGK	8302200	0	8302200
AAAMDVDTPSGTNSGAGKK	1636200	0	1636200
AAANFSDR	26771000	0	26771000
AAASTDYYK	6348200	0	6348200
AAATAEEPDPK	4593100	0	4593100
AAATGPSFWLGNETLK	44271000	0	44271000
AAAVSALAK	13317000	0	13317000
AACDLVR	41071000	0	41071000
AADIDQEVK	0	0	0
AADIGVAMGQTGTDVCK	0	0	0
AADTQVSETLKR	0	0	0
AAEADGPLKR	26292000	0	26292000

AAECNIVVTQPR	69769000	0	69769000
AAEDDEDDDVDTK	5326600	0	5326600
AAEDLFVNIR	6192200	0	6192200
AAESLADPTEYENLFPGLK	2887000	0	2887000
AAFDDAIAELDTLSEESYK	7232100	0	7232100
AAFGLELEEMK	65375000	0	65375000
AAFNSGK	806630	0	806630
AAFQLGSPWR	0	0	0
AAGGDHGSPDSYR	3967900	0	3967900
AAGPSLSHTSGGTQSK	9892900	0	9892900
AAGTLYTYPENWR	10265000	0	10265000
AAGVNVEPFWPGLFAK	6859400	0	6859400
AAILPTSIFLTNK	17033000	0	17033000
AALAGGTTMIIDHVVPEPESSLTEAYEK	41880000	0	41880000
AALAPLPPLPAQFK	3027300	0	3027300
AALEALGSCLNNK	2536400	0	2536400
AALEALLPYTER	4227800	0	4227800
AALETDENLLLCAPTGAGK	2232500	0	2232500
AALEYLEDIDLK	30975000	0	30975000
AALLELWELR	3748800	0	3748800
AALNALQPPEFR	3468800	0	3468800
AALQELLSK	91358000	0	91358000
AALSALESFLK	85076000	0	85076000
AAMEALVVEVTK	5544100	0	5544100
AANDAGYFNDEMAPIEVK	31139000	0	31139000

AANGVVLATEK	20098000	0	20098000
AANILVGENLVCK	3222600	0	3222600
AANSLEAFIFETQDK	34043000	0	34043000
AAQDFFSTCR	0	0	0
AAQEEYVK	146680000	0	146680000
AAQELQEGQR	48475000	2050100	46425000
AAQGEPQVQFK	59656000	0	59656000
AASDIAMTELPPTHPIR	1505000	0	1505000
AASITSEVFNK	0	0	0
AASLIQGYWR	867720	0	867720
AATAAADFTAK	39164000	0	39164000
AATASAGAGGIDGKPR	0	0	0
AATQFWR	49972000	0	49972000
AAVAWEAGKPLSIEEIEVAPPK	13171000	0	13171000
AAVENLPTFLVELSR	4455700	0	4455700
AAVPSGASTGIYEALELR	149490000	0	149490000
AAYFGIYDTAK	70866000	0	70866000
AAYFGVYDTAK	99519000	0	99519000
AAYPDLENPPLLVTPSQQAK	0	0	0
ACADATLSQITNNIDPVGR	30423000	0	30423000
ACAEIAAQR	9596100	0	9596100
ACANPAAGSVILLENLR	108510000	0	108510000
ACGDSTLTQITAGLDPVGR	13026000	0	13026000
ACGLNFADLMAR	113140000	2304200	110840000
ACGLVASNLNLKPGECLR	20475000	0	20475000

ACGNFGIPCELR	62772000	0	62772000
ACIDSNEDGDLSK	4751100	0	4751100
ACIGDTLCQK	20590000	0	20590000
ACLDYPVTSVLPPASLCK	11821000	0	11821000
ACNPQPNGENAISAR	6699800	0	6699800
ACYALENFVENLGPK	7169900	0	7169900
ADAEEEAATR	5347100	0	5347100
ADALQAGASQFETSAAK	35540000	0	35540000
ADCASGIFLAAEK	0	0	0
ADDYEQVK	5922600	0	5922600
ADEASELACPTPK	14676000	0	14676000
ADEGISFR	214610000	1659100	212950000
ADFPAGIPECGTDALR	20258000	0	20258000
ADFQGISPER	63516000	0	63516000
ADGELNVDSLITR	14251000	0	14251000
ADGGTQVIDTK	69659000	0	69659000
ADGLLGMFLK	10521000	0	10521000
ADGYVLEGK	15798000	0	15798000
ADIFMFDEPSSYLDVK	5806300	0	5806300
ADKEAAFDDAVEER	0	0	0
ADLDKLNIDSIIQR	11841000	0	11841000
ADLFPILMR	2245800	0	2245800
ADLIAYLK	298630000	0	298630000
ADLINNLGTIAK	41046000	0	41046000
ADLLLSTQPGREEGSPLELER	22350000	0	22350000

ADLYLEGK	13226000	0	13226000
ADMETLQR	21957000	1303200	20654000
ADMGGAATICSAIVSAAK	31321000	0	31321000
ADQIETQQLMR	7594400	0	7594400
ADSWVEKEEPAPSN	6940900	0	6940900
ADTLTLEER	67712000	0	67712000
ADTLTLK	65029000	0	65029000
ADTLTPEECQQFK	39379000	0	39379000
ADTQTYQPYNK	18948000	0	18948000
ADVIQATGDAICIFR	13099000	0	13099000
AEAGGGWEGSASYK	2876000	0	2876000
AEAGPEGVAPAPEGEK	10823000	0	10823000
AEDGATPSPSNETPK	8127200	0	8127200
AEDKEWMPVTK	149520000	0	149520000
AEDNADTLALVFEAPNQEK	12126000	0	12126000
AEEDEILNR	42976000	0	42976000
AEEILEK	80385000	0	80385000
AEEVATFFAK	3794900	0	3794900
AEEYEFLTPVEEAPK	527740000	0	527740000
AEFVEVTK	420680000	420680000	0
AEGPGLSR	28167000	0	28167000
AEGPQEWVFQECK	0	0	0
AEGSDVANAVLDGADCIMLSGETAK	1949900	0	1949900
AEGYEVAHGGR	13349000	382030	12966000
AEHDSILAEK	3692300	0	3692300

AEKDEPGAWEETFK	11961000	0	11961000
AELDDTPMR	5815600	0	5815600
AELGEYIR	0	0	0
AELLDNEKPAAVVAPITTGYTVK	21063000	0	21063000
AELNEFLTR	0	0	0
AELQLDPAMAGLGGGAGSR	19324000	19324000	0
AELVQLVSPFLGK	828360	0	828360
AEMDAAIASCK	14184000	0	14184000
AEMVVPDFSELFK	2164600	0	2164600
AENFFILR	110610000	2663400	107950000
AENQVLAMR	51903000	0	51903000
AENYDIPSADR	25284000	0	25284000
AEPEDHYFLLTEPPLNTPENR	37550000	0	37550000
AEQWNVNYVETSAK	0	0	0
AESEEMETSQAGSK	28282000	0	28282000
AESMLQQADK	8361100	0	8361100
AESTPEIAEQR	16779000	0	16779000
AEVAAEFLNDR	9699000	0	9699000
AEVLSEEPILK	5335400	0	5335400
AEVSIQNNK	5786400	0	5786400
AEVSPMYGVQK	5573000	0	5573000
AEYLASIFGTEK	871450	0	871450
AFALEVIK	28900000	0	28900000
AFAVGVQQVLLK	52810000	0	52810000
AFCEPGNVENNGVLSFIK	0	0	0

AFCQEMLQEEPR	816340	0	816340
AFDLIVDRPVTLVR	10249000	0	10249000
AFDLVPPEAVPEQK	1873000	0	1873000
AFDSGIIPMEFVNK	95893000	0	95893000
AFDTAGNGYCR	14337000	0	14337000
AFEPATGR	24896000	0	24896000
AFFAGSQR	92043000	0	92043000
AFFESHPAPSAER	3691200	0	3691200
AFFSEVER	13950000	0	13950000
AFGGQSLK	18078000	0	18078000
AFGPGLQGGSAGSPAR	45265000	0	45265000
AFHNEAQVNPER	30923000	0	30923000
AFLADPSAFVAAAPVAAATTAAPAAAAAPAK	123090000	0	123090000
AFLASGPYLTHQQK	77405000	0	77405000
AFLASPEYVNLPINGNGK	124630000	3865600	120760000
AFLEENNLDYIIR	76855000	0	76855000
AFLLFPTIER	4988100	0	4988100
AFLTLAEDILR	40600000	0	40600000
AFNDPFIQK	0	0	0
AFPAWADTSVLSR	6871600	0	6871600
AFPMPGFDEH	0	0	0
AFPNPYADYNK	11015000	0	11015000
AFSGYLGTDQSK	24768000	0	24768000
AFSPTTVNTGR	105380000	4041600	101340000
AFTHTAQYDEAISDYFR	9149600	0	9149600

AFTYINLDK	27381000	0	27381000
AFVDFLSDEIK	0	0	0
AFVDFLSDEIKEER	17612000	0	17612000
AFVEAQNK	0	0	0
AFYGDTLVTGFAR	1417200	0	1417200
AFYNNVLGEYEEYITK	4984500	0	4984500
AFYYPEEAGLAFGGPGSSR	145810000	0	145810000
AGAGSAAVSGAGTPVAGPTGR	0	0	0
AGAGSATLSMAYAGAR	18115000	0	18115000
AGALQCSPSDAYTK	20045000	0	20045000
AGAVAEEVLAAIR	28904000	0	28904000
AGAYDFPSPEWDTVTPEAK	977240	0	977240
AGDEFVEK	56211000	0	56211000
AGDEIDEPSER	1563200	0	1563200
AGDISCNADINPLK	6058000	0	6058000
AGDMENAENILTVMR	25906000	0	25906000
AGDQIICMDDVYGGTNR	0	0	0
AGDTVIPLYIPQCGECK	16706000	0	16706000
AGELTEDEVER	168020000	6571300	161440000
AGFAGDDAPR	2536500000	38362000	2498100000
AGFFGTVVEYGAER	11356000	0	11356000
AGGAAVVITEPEHTK	3647600	0	3647600
AGGEAGVTLGQPHLSR	0	0	0
AGGFLMK	22101000	0	22101000
AGGSASAMLQPLLDNQVGFK	22128000	0	22128000

AGIISTVEVLK	13245000	0	13245000
AGIPVYAWK	1287200	0	1287200
AGLGSGLSLSGLVHPELSR	8363400	0	8363400
AGLQFPVGR	855710	0	855710
AGLQVYNK	21627000	0	21627000
AGMSAEQAQGLLEK	24015000	0	24015000
AGNEKEEGETADTVGCCSLR	16544000	0	16544000
AGNELLESSAGDDASSLR	2403400	0	2403400
AGNFYVPAEPK	91318000	0	91318000
AGPESDAQYQFTGIK	7288000	0	7288000
AGPIWDLR	15347000	0	15347000
AGQLSQGAAEEDHGCR	32300000	0	32300000
AGQPLQLLDASWYLPK	0	0	0
AGQTTYSGVIDCFR	0	0	0
AGQVFLEELGNHK	8413200	0	8413200
AGSDGESIGNCPFSQR	22278000	0	22278000
AGVLAHLEEER	31320000	0	31320000
AGYAGEDCPK	5615600	0	5615600
AGYGTCNCFPEEEK	4389200	0	4389200
AGYIIPLQGPGLTTTESR	0	0	0
AGYPQYVSEILEK	22638000	0	22638000
AHIAQLCEK	27292000	0	27292000
AHQVVEDGYEFFAK	36235000	0	36235000
AHSSMVGVNLPQK	85578000	0	85578000
AIADTGANVVVTGGK	17187000	0	17187000

AIAGVINQPYYNYEAGPDAVLGR	7626200	0	7626200
AIDLFTDAIK	21010000	0	21010000
AIEAVAISPWK	4492200	0	4492200
AIEEQMVAAK	6442700	0	6442700
AIELLQEFSDQHPENAAEIK	7559400	0	7559400
AIENELLAR	7504600	0	7504600
AIEPNDYTGK	13943000	0	13943000
AIEPPPLDAVIEAEHTLR	8876200	0	8876200
AIFENTLSTYPK	4708800	0	4708800
AIFTGYYGK	10757000	0	10757000
AIGAVPLIQGEYMIPCEK	44614000	0	44614000
AIGNIELGIR	8192100	0	8192100
AIGNTELENK	22028000	0	22028000
AIGSASEGAQSSLQEVYHK	74511000	0	74511000
AIITALGVER	0	0	0
AIITDSVK	10977000	0	10977000
AILILDNDGDR	4035300	0	4035300
AILPCIK	29557000	0	29557000
AILPCQDTPSVK	6039800	0	6039800
AIMYEETTYSK	11849000	0	11849000
AINNYNPK	5224000	0	5224000
AINQGGLTSVAVR	9450500	0	9450500
AINVQEEK	13768000	0	13768000
AIPQLQGYLR	36576000	0	36576000
AIQDPAFSDGIR	13163000	0	13163000

AISTTCIPNYPDR	13862000	0	13862000
AITGASLADIMAK	18450000	0	18450000
AITIANQTNCPLYITK	0	0	0
AITIASQTNCPLYVTK	16700000	0	16700000
AITSAYYR	0	0	0
AIVAGDQNVEYK	84070000	0	84070000
AIVAIENPADVSVISSR	534400000	0	534400000
AIVDSPCIYEAEQK	2939900	0	2939900
AIVQLVNER	43473000	0	43473000
AIVQQWLEYR	0	0	0
AIWGYCDQLK	0	0	0
AIYDTPCIQAESEK	4759900	0	4759900
AIYNNMK	70866000	0	70866000
ALAAAGYDVEK	789680000	9221500	780460000
ALADDDFLTVTGK	0	0	0
ALADVATVLGR	26182000	0	26182000
ALAEIAK	15485000	0	15485000
ALAESWNAAFLESSAK	16723000	0	16723000
ALAGCDFLTISPK	41598000	0	41598000
ALANSLACQGK	203560000	0	203560000
ALAPEYAK	44791000	0	44791000
ALAYFEQLK	4051600	0	4051600
ALCADLSPR	4634200	0	4634200
ALCDLGPWVK	8184300	0	8184300
ALCDVGTAISCSR	6147300	0	6147300

ALCEAAGCGSALLWPR	3449200	0	3449200
ALDDMISTLK	21404000	0	21404000
ALDFIASK	0	0	0
ALDIAENEMPGLMR	145770000	0	145770000
ALDIPLVK	21282000	0	21282000
ALDLLYGMVSK	41564000	0	41564000
ALDQFVNFSEQK	1222500	0	1222500
ALDTMNFDVIK	26710000	0	26710000
ALEAFETFK	27927000	0	27927000
ALEDVDYVQTFK	1388400	0	1388400
ALEEAGFK	11940000	0	11940000
ALEHFTDLYDIK	24124000	0	24124000
ALELCEILAK	11754000	0	11754000
ALELDSNLYR	54906000	0	54906000
ALELDSNNEK	8989400	0	8989400
ALELNMLSLK	112210000	0	112210000
ALELTGLK	18894000	0	18894000
ALEPTGQSGEAVK	1357500	0	1357500
ALEQFATVVEAK	25915000	0	25915000
ALESDMAPVLIMATNR	2099800	0	2099800
ALESGDVNTVWK	0	0	0
ALESPERPFLAILGGAK	217420000	0	217420000
ALESSIAPIVIFASNR	20424000	0	20424000
ALFAVPK	4382400	0	4382400
ALFNGAQK	7096800	0	7096800

ALGAQIEK	9162400	0	9162400
ALGGLLK	46756000	0	46756000
ALGTEVIQLFPEK	151190000	0	151190000
ALIAAQYSGAQVR	0	0	0
ALIEHEMK	0	0	0
ALIEVLQPLIAEHQAR	11631000	0	11631000
ALIQCAK	7452800	0	7452800
ALLANALTSALR	48385000	0	48385000
ALLEVVQSGGK	2844400	0	2844400
ALLFIPR	146360000	0	146360000
ALLFVPR	121000000	0	121000000
ALLGSVK	4568600	0	4568600
ALLIFLEK	4989000	0	4989000
ALLLLCGEDD	0	0	0
ALLNVVDNAR	0	0	0
ALLQEMPLTALLR	3544400	0	3544400
ALLQQQPEDDSK	16726000	0	16726000
ALLQQQPEDDSKR	9936200	0	9936200
ALLQSSASR	38556000	0	38556000
ALLTPVAIAAGR	66725000	0	66725000
ALLVTASQCQQPAENK	18805000	0	18805000
ALMDEVVK	0	0	0
ALMQVVDFLSR	4557600	0	4557600
ALNEACESVIQTACK	0	0	0
ALNMAIPGGPK	23354000	1305200	22049000

ALNSAANNVYQYGR	2196900	0	2196900
ALPAVQQNNLDEDLIR	1519200	0	1519200
ALPFWNEEIVPQIK	15217000	0	15217000
ALPGQLKPFETLLSQNQGGK	269310000	0	269310000
ALPIPAWESQPR	21666000	0	21666000
ALQAAIQQLAEAQPEATAK	4627200	0	4627200
ALQASALK	124850000	0	124850000
ALQATVGNSYK	216490000	0	216490000
ALQEGEGDLSISADR	9234400	0	9234400
ALQSVGQIVGEVLK	10532000	0	10532000
ALSEALTELGYK	0	0	0
ALSPLEEWLR	24476000	0	24476000
ALSQLAEVEEK	19069000	0	19069000
ALSVETEK	20004000	0	20004000
ALTGGIAHLFK	6814200	0	6814200
ALTLIAGSPLK	78925000	0	78925000
ALTLPGSSENEYIMK	8457900	0	8457900
ALTTMGFR	0	0	0
ALTVPELTQQMFDAK	3947400	0	3947400
ALTVPELTQQVFDAK	60581000	0	60581000
ALTYDEK	6911300	0	6911300
ALVAYYQK	25649000	0	25649000
ALVDILSEVSK	29983000	0	29983000
ALVILAK	0	0	0
ALVPFEDLFGQAPGGER	0	0	0

ALVSAQWVAEALR	6153000	0	6153000
ALYLIATNGTPELQNPEK	0	0	0
ALYTYESK	7833900	0	7833900
AMADALLER	43123000	0	43123000
AMDLVQEEFLQR	60239000	0	60239000
AMDQVNALCEQLVK	2730900	0	2730900
AMEAVAAQGK	36848000	0	36848000
AMGAAQVVVTDLSATR	19235000	0	19235000
AMGIMNSFVNDIFER	401570000	2791900	398780000
AMGPLVLTEVLFNEK	3075100	0	3075100
AMLESIGVPLEK	122650000	0	122650000
AMQDAEVSK	47343000	0	47343000
AMTEDGFLAVCSEAK	0	0	0
AMTLMEYLIK	5900900	0	5900900
AMVDPAQTVEQR	0	0	0
ANCIDSTASAEAVFASEVK	9169000	0	9169000
ANDDLADAGLEK	11350000	0	11350000
ANDDVAQEIAER	5437500	0	5437500
ANEAYPCPCDIGHR	0	0	0
ANINIEK	57770000	0	57770000
ANIQAVSLK	10218000	0	10218000
ANIVHLMLSSPEQIQK	24154000	0	24154000
ANNMQEVSR	0	0	0
ANTFVAELK	0	0	0
ANYWWLR	4315200	0	4315200

APDFVFYAPR	15818000	0	15818000
APEAWDYGQGFVNEEMIR	5536100	0	5536100
APFDLFENK	349770000	0	349770000
APFDLFENR	225800000	0	225800000
APGAEEYAQQDVLK	6466700	0	6466700
APGAGLGQDR	40266000	0	40266000
APGEQTVPALNLQNAFR	39422000	0	39422000
APGFGDNR	69858000	0	69858000
APGLGAFR	41606000	0	41606000
APIIAVTR	0	0	0
APIVTVGVNNDPADVR	550510	0	550510
APPSVFAEVPQAQPVLVFK	12977000	0	12977000
APQETYADIGGLDNQIQEIK	5900800	0	5900800
APSDLYQIILK	27562000	0	27562000
APSVPAAEPEYPK	10239000	0	10239000
APTNIVYK	33150000	0	33150000
APVAGTCYQAEWDDYVPK	34687000	0	34687000
APVDITGQFEK	39276000	0	39276000
APVLLSSLDR	5798400	0	5798400
APVLSDSSCK	1315800000	1315800000	0
APVPTGEVYFADSFDR	7765800	0	7765800
APVSYPNTLPESFTK	0	0	0
APWELLELR	65106000	0	65106000
AQDGSHPLSLQDLIEK	18533000	0	18533000
AQDPDQLR	0	0	0

AQDQGEKENPMR	19146000	0	19146000
AQFAQPEILIGTIPGAGGTQR	14209000	0	14209000
AQFEGIVTDLIR	76068000	0	76068000
AQGPQQQPGSEGPSYAK	6691100	0	6691100
AQLGPDESK	25651000	0	25651000
AQQEFATGVMSNK	2192500	0	2192500
AQQEQELAADAFK	169240000	0	169240000
AQQLEQIR	20442000	0	20442000
AQTEGINISEEALNHLGEIGTK	0	0	0
AQVADVVVSR	0	0	0
AQYYLPDGSTIEIGPSR	16833000	0	16833000
ARFEELNADLFR	22228000	0	22228000
ASADLMSYCEEHAR	24151000	0	24151000
ASAELALGENSEVLK	23797000	0	23797000
ASAETVDPASLWEY	0	0	0
ASAFALQEQPVVNAVIDDTTK	9832600	0	9832600
ASALEQFVNSVR	2647200	0	2647200
ASANMDLMR	40697000	23764000	16933000
ASAQGDPDVPECLK	6829500	0	6829500
ASCLYGQLPK	0	0	0
ASENAIVWK	0	0	0
ASGPPVSELITK	51046000	0	51046000
ASGTTTTAVK	2833800	0	2833800
ASGTVYSGEEK	0	0	0
ASIPFSVVGSNQLIEAK	10787000	0	10787000

ASLNGADIYSGCCTLK	3740900	0	3740900
ASSAQSGGSSGGPAVPTVQR	5311300	0	5311300
ASSGLLYPLER	89554000	0	89554000
ASSLISLLK	15809000	0	15809000
ASSTSPVEISEWLDQK	2926800	0	2926800
ASVGFGGSCFQK	0	0	0
ASVTVGGEQISAIGR	3967600	0	3967600
ASWSSLSMDEK	0	0	0
ATAAELLR	21256000	0	21256000
ATAEQISSQTGNK	10082000	0	10082000
ATAFNEQVDK	12503000	0	12503000
ATAGDTHLGGEDFDNR	48378000	0	48378000
ATAVMPDGQFK	873620000	0	873620000
ATAVVDGAFK	319320000	0	319320000
ATCAPQHGAPGPGPADASK	20353000	1140200	19212000
ATCIGNNSAAAVSMLK	0	0	0
ATDAQLCLESSPK	3638200	0	3638200
ATDFVVPGPGK	35441000	0	35441000
ATEGMVVADK	66939000	0	66939000
ATENDIANFFSPLNPIR	2906500	0	2906500
ATESGAQSAPLPMEGVDISPK	14478000	0	14478000
ATGPPVSELITK	0	0	0
ATIELCSTHANDASALR	0	0	0
ATIGADFLTK	16782000	0	16782000
ATLQEILPEVLK	5998800	0	5998800

ATLSSIR	38977000	0	38977000
ATLYVTAIEDR	62214000	0	62214000
ATNDEIFSILK	43463000	0	43463000
ATPLAVNSAASLWGPYK	1832800	0	1832800
ATQALVLAPTR	23283000	0	23283000
ATQMPEGGQGAPPMYQLYK	7262300	0	7262300
ATSFLLALEPELEAR	8985700	0	8985700
ATSTATSGFAGAIGQK	1496600	0	1496600
ATVLTTER	46019000	0	46019000
ATVQQLEGR	6384500	0	6384500
ATYDGNHDTFR	1922600	0	1922600
AVAISLPK	8591200	0	8591200
AVANYDSVEEGEK	10388000	0	10388000
AVASQLDCNFLK	8311800	0	8311800
AVAVVVDPIQSVK	0	0	0
AVCMLSNTTAIAEAWAR	86954000	0	86954000
AVDCLLDSK	31965000	1032900	30932000
AVDIPHMDIEALK	301770000	0	301770000
AVDLLYAMCDR	2243500	0	2243500
AVDQSIEK	133110000	0	133110000
AVDSQILPK	62351000	0	62351000
AVEAVVNDTSGENK	0	0	0
AVECPPPR	1501900	0	1501900
AVELAANTK	28108000	0	28108000
AVENSSTAIGIR	125680000	0	125680000

AVFPSIVGR	1536300000	62170000	1474100000
AVFWDIK	15010000	0	15010000
AVGPEITK	9969900	0	9969900
AVGPSGGGGETPR	0	0	0
AVGQGCVEIGSQR	8613600	0	8613600
AVGWNELEGR	22620000	0	22620000
AVLASTPR	6689400	0	6689400
AVLCPPPVK	0	0	0
AVLENNLGAAVLR	3739900	0	3739900
AVLGTSNFK	64127000	0	64127000
AVLIAGQPGTGK	20276000	0	20276000
AVLLAGPPGTGK	5003400	0	5003400
AVLLGPPGAGK	0	0	0
AVLNPLCQVDYR	29783000	0	29783000
AVLQEFGR	0	0	0
AVMISAIEK	33983000	0	33983000
AVNYFSK	42598000	0	42598000
AVPETRPNHTIYINNLNEK	22092000	0	22092000
AVPLALALISVSNPR	3721400	0	3721400
AVQGMLDFDYVCSR	17846000	0	17846000
AVQPTSGEPR	864480	0	864480
AVSDWIDEQEK	5424900	0	5424900
AVSDWLIASVEGR	9411700	0	9411700
AVTELNEPLSNEDR	0	0	0
AVTEQGAELSNEER	11680000	0	11680000

AVTEQGHELSNEER	5915200	0	5915200
AVTHTSPEDVSFAESR	16750000	0	16750000
AVTQALNR	0	0	0
AVTVMMDPNSTQR	2455400	0	2455400
AVVISGAGK	44390000	0	44390000
AVVIVDDR	0	0	0
AVVLMGK	27022000	0	27022000
AVVVTDGER	19758000	0	19758000
AVYEAVLR	27704000	0	27704000
AVYMMPTEGDDSSK	10508000	0	10508000
AVYTQDCPLAAAK	90221000	0	90221000
AWDIAIATMK	77770000	0	77770000
AWGAVVPLVGK	27788000	0	27788000
AWGPGLEGGVVGK	0	0	0
AWSATFDELIGR	10827000	0	10827000
AYAALAALEK	8739500	0	8739500
AYAALTDEESR	5426400	0	5426400
AYADFYR	58016000	0	58016000
AYAQGISR	97459000	1407600	96051000
AYAYLFK	16075000	0	16075000
AYDGTTYLPGIVGLNNIK	13669000	0	13669000
AYEFAER	70055000	0	70055000
AYGENIGYSEK	4296500	0	4296500
AYGGSMCAK	23133000	0	23133000
AYGPGIEPTGNMVK	14059000	0	14059000

AYGQALAK	38658000	0	38658000
AYHSFLVEPISCHAWNK	4349700	0	4349700
AYIDSFR	27303000	0	27303000
AYILNLVK	39107000	0	39107000
AYSEAHEISK	220790000	0	220790000
AYVAVDGIPQGVLER	3382600	0	3382600
AYVPALQMAFK	38212000	0	38212000
CDKEFMWALK	16749000	0	16749000
CTGGEVGATSALAPK	11808000	0	11808000
DAASGEVVGK	18070000	0	18070000
DAATIMQPYFTSNGLVTK	23083000	0	23083000
DACDGHEIGR	946850	0	946850
DADVQNFVSFISK	10957000	0	10957000
DAEGILEDLQSYR	33785000	0	33785000
DAEQESQMR	0	0	0
DAFLGSFLYEYSR	93582000	93582000	0
DAFVAIVQSVK	17556000	0	17556000
DAGMQLQGYR	246040000	5089600	240950000
DAGQISGLNVLR	0	0	0
DAGTIAGLNVLR	703030000	0	703030000
DAIAALGLLQK	8325300	0	8325300
DAIAQAVR	9279000	0	9279000
DAIPENLPPLTADFAEDK	54850000	54850000	0
DAIPENLPPLTADFAEDKDVCK	145210000	145210000	0
DAITQALFLR	8948100	0	8948100

DALSDLALHFLNK	50720000	0	50720000
DAMQYASESK	98028000	0	98028000
DANCSVMR	12261000	0	12261000
DANGNSFATR	43810000	0	43810000
DANNGNLQLR	20603000	0	20603000
DAPQDFHPDR	27951000	0	27951000
DAQQSSSPAADNLR	1736900	0	1736900
DASQCYVK	2983800	0	2983800
DATNVGDEGGFAPNILENK	386430000	0	386430000
DATSRPTDNILIPQLIR	15037000	0	15037000
DAVITVPVFFNQAER	4794900	0	4794900
DAVLLLFANK	23987000	0	23987000
DAVLLVFANK	8083200	0	8083200
DAVTYTEHAK	228390000	0	228390000
DAVVYPILVEFTR	3434400	0	3434400
DCFTCSNCK	19345000	0	19345000
DCGATWVVLGHSER	103550000	0	103550000
DCLLELIEQK	9214700	0	9214700
DCPDSAEEYER	1152100	0	1152100
DCPLNAEAASSK	27537000	0	27537000
DCVGPEVEK	0	0	0
DDDIAALVVDNGSGMCK	420550000	3373000	417170000
DDETMYVESK	16953000	0	16953000
DDEYDYLFK	8961900	0	8961900
DDFSSGTSSR	4689900	0	4689900

DDGEEEFAGAK	6228300	0	6228300
DDGSWEVIEGYR	0	0	0
DDIIENAPTTHTEEYSGEEK	16700000	0	16700000
DDIPVFLR	18510000	0	18510000
DDLLGFALR	18120000	0	18120000
DDMIFEDCGDVPSEPK	0	0	0
DDNMFQIGK	6328400	0	6328400
DDPHACYSTVFDK	50185000	50185000	0
DDPLTNLNTAFDVAEK	11776000	0	11776000
DDPLVTPVPAAENPFR	131550000	5060700	126490000
DDPSTIEK	23601000	0	23601000
DDPVTNLNNAFEVAEK	5980500	0	5980500
DDSPDLPK	88769000	88769000	0
DEAAYGELR	31338000	0	31338000
DEAQNEGPATESEAPLKEDGLLPK	12689000	0	12689000
DECPEVR	27045000	0	27045000
DEFEGLFK	9752800	0	9752800
DEFLIQASPR	4923300	0	4923300
DEIIWLLR	1752900	0	1752900
DEILPTTPISEQK	0	0	0
DELHIVEAEAMNYEGSPIK	7434200	0	7434200
DENSVELTMAEGPYK	3310600	0	3310600
DEPDTNLVALMK	51787000	0	51787000
DEPSVAAMVYPFTGDHK	11494000	0	11494000
DETLETEK	1404700	0	1404700

DETNYGIPQR	242010000	15797000	226210000
DEVLYVFPSDFCR	127110000	4921700	122190000
DFEEYPEHR	13594000	0	13594000
DFFQSYGNVVELR	2286700	0	2286700
DFIDSLGLLHEQNMAK	16653000	0	16653000
DFIIFEAAPQETR	30482000	0	30482000
DFINFISDK	31251000	0	31251000
DFLAGGIAAAISK	113580000	0	113580000
DFLAGGVAAAISK	121600000	0	121600000
DFLIPIGK	11979000	0	11979000
DFLLKPELLR	2264000	0	2264000
DFLLQQTMLR	118750000	2559200	116190000
DFLVQIK	22495000	0	22495000
DFLYSYFK	22354000	0	22354000
DFMIQGGDFTR	1114500000	10816000	1103700000
DFPAMVQELHQGGR	8139400	0	8139400
DFPLNDLLSATELDK	20834000	0	20834000
DFQSGQHVIVR	3751500	0	3751500
DFSPSGIFGAFQR	31289000	0	31289000
DFSVFFQK	2344300	0	2344300
DFTATDLSEFAAK	43628000	0	43628000
DFTPVCTTELGR	0	0	0
DFTVSAMHGDMDQK	24802000	0	24802000
DFVQVMR	7697600	0	7697600
DGATILTHAYSR	4491600	0	4491600

DGDILGK	16411000	0	16411000
DGDSVMVLPTIPEEEAK	265520000	0	265520000
DGEAVWFGCDVGK	36291000	0	36291000
DGEDLMDESVLK	0	0	0
DGENYVVLLDSTLPR	6063800	0	6063800
DGETLEELMK	32771000	0	32771000
DGETPDPEDPSR	3823600	0	3823600
DGGAWGTEQR	0	0	0
DGGFCEVCK	19861000	0	19861000
DGIDDESYGQIFKPIISK	10424000	0	10424000
DGIEPMWEDEK	0	0	0
DGIVLGADTR	36272000	0	36272000
DGLEMEK	16064000	0	16064000
DGLILTSR	0	0	0
DGMEYPFIGEGEPHVDGEPGDLR	10827000	0	10827000
DGPGETDAFGNSEGK	3723700	0	3723700
DGPNALTPPPTTPEWIK	13843000	0	13843000
DGQAMLWDLNEGK	163790000	0	163790000
DGQILPVPNVVVR	81719000	0	81719000
DGSAFEDGLR	6601900	234280	6367600
DGTACAEVSR	6009200	0	6009200
DGTQCLSGSSDGTIR	4463300	0	4463300
DGTVTAGNASGVADGAGAVIIASEDAVK	4931700	0	4931700
DGVYVLDLAAK	80191000	0	80191000
DHDTFLAVR	22165000	0	22165000

DHINLPGFSGQNPLR	19651000	0	19651000
DIAAYIK	7356800	0	7356800
DICNDVLSLLEK	62859000	0	62859000
DIDDDLEGEVTEECGK	2856900	0	2856900
DIDEVSSLLR	17913000	0	17913000
DIDIHEVR	114210000	0	114210000
DIELVMSQANVSR	4813200	0	4813200
DIEREDIEFICK	0	0	0
DIFQEIFDK	3543000	0	3543000
DIFQEIYDK	43053000	0	43053000
DIGEGNLSTAAAAALAAAAVK	2508900	0	2508900
DIIACGFDINK	58686000	0	58686000
DIICQIAYAR	52885000	0	52885000
DIISIAEDEDLR	50370000	0	50370000
DILADLIPK	42841000	0	42841000
DILETHLR	0	0	0
DILIDPIR	7213400	0	7213400
DILIQYDR	0	0	0
DILLRPELEELR	26660000	0	26660000
DILPCLDGYLK	6590200	0	6590200
DILQNVFK	34049000	0	34049000
DINAVAASLR	12379000	0	12379000
DINAYNCEEPTEK	314690000	1027900	313660000
DINELNLPK	0	0	0
DINQEVYNFLATAGAK	1428800	0	1428800

DIPNENEAQFQIR	0	0	0
DIPNENELQFQIK	6213400	0	6213400
DIQEDSGMEPR	20306000	0	20306000
DIQENDEEAVQVK	25686000	0	25686000
DIQTNVYIK	8295500	0	8295500
DIREEAEK	0	0	0
DISEASVFDAYVLPK	7890500	0	7890500
DISLSDYK	74554000	0	74554000
DISTTLNADEAVAR	0	0	0
DIVQFVPFR	41390000	2862100	38528000
DIVVQETMEDIDK	27285000	0	27285000
DKDPPIPVAK	7369100	0	7369100
DKLNNLVLFDK	11500000	0	11500000
DKLSGEYEK	4665300	0	4665300
DKYPNLQVIGGNVVTAAQAK	7614600	0	7614600
DLAACIK	26161000	0	26161000
DLADELALVDVIEDK	18755000	0	18755000
DLAEITTLDR	6093700	0	6093700
DLAPIGIR	0	0	0
DLASVQALLR	9741800	0	9741800
DLEALMFDR	15062000	0	15062000
DLEGENIEIVFAKPPDQK	15304000	0	15304000
DLEGSDIDTR	32445000	0	32445000
DLFDPIIEDR	37688000	0	37688000
DLFEDELVPLFEK	16815000	0	16815000

DLFLASCSQDCLIR	9763300	0	9763300
DLFLQGAYDTVR	6177000	0	6177000
DLFQVAFNR	38837000	0	38837000
DLGEEHFK	68011000	68011000	0
DLGFFGIYK	88980000	0	88980000
DLGFNGAPYR	2217500	0	2217500
DLGLAQDSATSTK	6764200	0	6764200
DLGLSESGEDVNAAILDESGK	6614600	0	6614600
DLGLSESGEDVNAAILDESGKK	259060000	0	259060000
DLGREAWDIESTPIMMK	140500000	0	140500000
DLGTESQIFISR	0	0	0
DLIGIDNLVVPGR	2706400	0	2706400
DLIGVQNLLK	3298000	0	3298000
DLILADYGK	4128400	0	4128400
DLILPTIQK	0	0	0
DLILQCLDDKDESIR	6378600	0	6378600
DLIPYLEK	9779600	0	9779600
DLIQMLVQR	0	0	0
DLISHDEMFSDIYK	54626000	0	54626000
DLIVTPATILK	88598000	0	88598000
DLKPQNILVTSSGQIK	6012900	0	6012900
DLLGLCEQK	2725200	0	2725200
DLLLTCAQDR	7168800	0	7168800
DLLLTSSYLSDSGSTGEHTK	48088000	0	48088000
DLLQSSYNK	9225100	0	9225100

DLNCVPEIADTLGAVAK	8997100	0	8997100
DLNGIDLTPVQDTPVASR	0	0	0
DLNSDMDSILASLK	4040600	0	4040600
DLNSQADSLMTSSAFDTSQVK	3059700	0	3059700
DLNSYLEDK	3401600	0	3401600
DLPDVQELITQVR	6843400	0	6843400
DLPLLLFR	28423000	731550	27692000
DLPVSEQQER	0	0	0
DLQMVNISLR	40939000	14170000	26768000
DLSLDDFK	111320000	0	111320000
DLSLLQIQMR	15442000	0	15442000
DLSSQLLK	0	0	0
DLSSVQTLLTK	22651000	0	22651000
DLSTIEPLK	0	0	0
DLSTIEPLKK	11756000	0	11756000
DLSTVEALQNLK	94333000	0	94333000
DLTDYLMK	11944000000	86976000	1.1857E+10
DLTGQVPTPVVK	11481000	0	11481000
DLTGVQNLR	0	0	0
DLTLDQAYSYAVENAK	221720000	0	221720000
DLTNVQNLQK	17263000	0	17263000
DLTPEHLPLLR	3674400	0	3674400
DLTSWVTEMK	7265900	0	7265900
DLTTAGAVTQCYR	59059000	15234000	43825000
DLTTGYDDSQPDKK	0	0	0

DLTYNITPTQVFK	3007000	0	3007000
DLVGELGTALR	7290500	0	7290500
DLYANNVLSGGTTMYPGIADR	3164500	0	3164500
DLYANTVLSGGTTMYPGIADR	1099400000	0	1099400000
DLYEDELVPLFEK	17060000	0	17060000
DLYSALIK	36035000	0	36035000
DMFQETMEAMR	7428800	0	7428800
DMLLANK	0	0	0
DMNQVLDAYENK	13523000	0	13523000
DMSGTMGFNEFK	3263100	0	3263100
DMSIIQWK	0	0	0
DMVGIAQTGSGK	23391000	0	23391000
DMYSFLQDMGLK	859690	859690	0
DNFTAIPEGTNGVEER	66486000	396170	66090000
DNFTLIPEGTNGTEER	0	0	0
DNGNGTYSCSYVPR	9781700	0	9781700
DNHLLGTFDLTGIPPAPR	78310000	0	78310000
DNINIEEAAR	4179800	0	4179800
DNIQGITK	131020000	0	131020000
DNIQGITKPAIR	341600000	0	341600000
DNLAEDIMR	33211000	0	33211000
DNLEFFLAGIGR	29091000	0	29091000
DNLQLPLQFLSR	2474700	0	2474700
DNLTLWTSDMQGDGEEQNK	12236000	0	12236000
DNMALQR	9351600	0	9351600

DNNLLGK	39656000	0	39656000
DNNQFASASLDR	2963600	0	2963600
DNPGVVTCLDEAR	0	0	0
DNPNLLFNMCGFECR	1210100	0	1210100
DNSGMIDKNELK	4987300	0	4987300
DNTNEIYSGK	50088000	0	50088000
DNVDDPTGNFR	61131000	0	61131000
DNYTCPTEEEYK	5670900	0	5670900
DPAEGDGAQPEETPR	14929000	0	14929000
DPAQPMSPGEATQSGAR	11936000	0	11936000
DPCAGPVCDCK	6009400	0	6009400
DPEEIEKEEQAAAEK	80826000	0	80826000
DPEFVFYDQLK	11977000	0	11977000
DPENFPFVVLGNK	47025000	7572900	39452000
DPETLVGYSMVGCQR	0	0	0
DPFYMGLYQK	4031900	0	4031900
DPGVITYDLPTPPGEK	7022500	0	7022500
DPLLLAIIPK	5562600	0	5562600
DPLNPIK	56479000	0	56479000
DPMIDNNR	34585000	0	34585000
DPNNLFMVR	81233000	0	81233000
DPNTYFIVGTAMVYPEEAEPK	2443900	0	2443900
DPPDPYVSLLLLPDK	0	0	0
DPQHDLDR	4781900	0	4781900
DPSTESGEEENEEQDELNEQILR	15084000	0	15084000

DPVQEAWAEDVDLR	26191000	0	26191000
DQDLEPGAPSMGAK	8911400	0	8911400
DQDNMQAELNR	7843000	0	7843000
DQELSPR	5702000	0	5702000
DQFTTTEVNMAR	0	0	0
DQILTDSR	7475300	0	7475300
DQIPSPGLMVFPK	0	0	0
DQIYDIFQK	139050000	0	139050000
DQLIYNLLK	336160000	0	336160000
DQLLPNLR	0	0	0
DQLQTFSEEHPVLLTEAPLNPR	10771000	0	10771000
DQNIFVQK	55380000	0	55380000
DQQEAALVDMVNDGVEDLR	25538000	0	25538000
DQTVIQNTDGNNNEAWAK	0	0	0
DQVANSAFVER	754980000	15846000	739130000
DQVTAQEIFQDNHEDGPTAK	7482400	0	7482400
DRDVTFSPATIENELIK	13928000	0	13928000
DRPFFAGLVK	290590000	0	290590000
DRPFFPGLVK	579160000	0	579160000
DRPMEESLLLFEAMR	658180	0	658180
DRPQEADGIDSVIVVDNVPQVGPDR	13123000	0	13123000
DSAQCAAIAER	15050000	0	15050000
DSAQNSVIIVDK	28368000	0	28368000
DSAVNAICYGAK	12352000	0	12352000
DSLIIIDELGR	8715500	0	8715500

DSLVYQYLQK	13850000	0	13850000
DSPDLLLLLR	3547400	0	3547400
DSPLETK	25495000	0	25495000
DSPSVWAAVPGK	24451000	0	24451000
DSQDAGGFGPEDR	0	0	0
DSQICELK	0	0	0
DSSQILSASFDQTIR	14093000	0	14093000
DSSQSPSQVDQFCK	0	0	0
DSTLIMQLLR	1035600000	26394000	1009200000
DSWVDIFR	25704000	25704000	0
DSYLILETLPTEYDSR	0	0	0
DSYVGDEAQSK	3997300000	39752000	3957500000
DSYVGDEAQSKR	44182000	0	44182000
DTDIVDEAIYYFK	7067000	0	7067000
DTDSINLYK	0	0	0
DTEMLATGAQDGK	29964000	0	29964000
DTFLGPVLK	0	0	0
DTGNIGQER	2763900	0	2763900
DTLDYSSNTMESALQYEK	2133300	0	2133300
DTLYEAVR	48396000	0	48396000
DTNFGTNCICR	913400	0	913400
DTNGSQFFITTVK	487070000	0	487070000
DTPGFIVNR	0	0	0
DTPQEMEQTR	3098600	0	3098600
DTQTSITDSCAVYR	13766000	0	13766000

DTSASAVAVGLK	47584000	0	47584000
DTYMLSSTVSSK	0	0	0
DVACGANHTLVLDSQK	113480000	0	113480000
DVAIKEPLVDVVDPK	0	0	0
DVATVCR	6683400	0	6683400
DVAWAPSIGLPTSTIASCSQDGR	63605000	0	63605000
DVCLYPR	50431000	0	50431000
DVDFMYVELIQR	2742000	0	2742000
DVFSPIGER	0	0	0
DVIAQSQSGTGK	75772000	0	75772000
DVIATDKEDVAFK	286600000	0	286600000
DVIEEYFK	66214000	0	66214000
DVIIADCGK	0	0	0
DVLEVGELAK	0	0	0
DVLLDVAYAYGK	7185400	0	7185400
DVLSVAFSSDNR	196100000	0	196100000
DVMDSTTTQK	28220000	0	28220000
DVMPEVNK	82176000	2391500	79785000
DVNAAIATIK	551890000	0	551890000
DVNQQEFVR	195970000	6738400	189230000
DVPNPNQDDDDDEGFSFNPLK	7300900	0	7300900
DVQDSLTVSNEAQTAK	29906000	0	29906000
DVQEIFR	0	0	0
DVQELLTQYTK	0	0	0
DVQIGDIVTVGECRPLSK	175560000	0	175560000

DVSELTGFPEMLGGR	20108000	0	20108000
DVSGPMPDSYSPR	8378800	0	8378800
DVTEAEQAEEQAR	2390500	0	2390500
DVTFSPATIENELIK	17734000	0	17734000
DVTNNVHYENYR	18563000	0	18563000
DVTYEEAK	0	0	0
DVVHTSEEAR	21486000	374450	21111000
DVVICPDASLEDAKK	28036000	0	28036000
DVVMEPTMK	3459700	0	3459700
DVVQAYPEVR	76359000	0	76359000
DVWGIEGPIDAAFTR	26846000	26846000	0
DVYIVQDLMETDLYK	0	0	0
DVYTGDALR	87773000	0	87773000
DWNTLIVGK	23364000	0	23364000
DWNVDLIPK	145770000	0	145770000
DWTDTNYYSEK	1059000	0	1059000
DYEILFK	17795000	0	17795000
DYETATLSDIK	0	0	0
DYFEEYGK	49757000	0	49757000
DYFEQYGK	167040000	0	167040000
DYFGAHTYELLAK	12001000	0	12001000
DYFNVPYPLPK	17997000	0	17997000
DYGNSPLHR	54073000	0	54073000
DYGVLLEGSGLALR	75365000	0	75365000
DYGVYLEDSGHTLR	1027000	0	1027000

DYIPVDQEELR	0	0	0
DYIVVGSDSGR	0	0	0
DYLEAAIR	0	0	0
DYLHLPPEIVPATLR	9127000	0	9127000
DYNVTANSK	68027000	0	68027000
DYPFHEEF	0	0	0
DYPLASK	5115800	0	5115800
DYSGQGVVK	12372000	0	12372000
DYSVTANSK	153520000	0	153520000
DYTSGAMLTGELK	0	0	0
DYTSGAMLTGELKK	2738400	0	2738400
DYVAPTANLDQK	84333000	0	84333000
DYVDLFR	45183000	0	45183000
DYVQEVTK	13623000	0	13623000
DYYINIR	0	0	0
EAAENSLVAYK	312520000	0	312520000
EAAEVLQNNR	45229000	890590	44338000
EAALSTALSEK	32449000	0	32449000
EAATQAQQTLGSTIDK	26819000	0	26819000
EAAWAISNLTISGR	15239000	0	15239000
EACFAVEGPK	42085000	42085000	0
EADASPASAGICR	6178600	0	6178600
EADDIVNWLK	11481000	0	11481000
EAEILEVLR	8865000	0	8865000
EAELLEPLMPAIR	23725000	0	23725000

EAEPDLLAVLR	3913900	0	3913900
EAESLIAK	19502000	0	19502000
EAESSPFVER	77308000	0	77308000
EAFEISK	51073000	7073200	44000000
EAFLQEVWK	39531000	0	39531000
EAFSDGITSVK	11681000	1856400	9824600
EAFSLFDKDGDGTITTK	3054900	0	3054900
EAGAGGLAIAVEGPSK	10805000	0	10805000
EAGEGGEAEAPAAEGGK	63304000	0	63304000
EAGLAPVPMIIFAK	5714700	0	5714700
EAGVEMGDEDDLSTPNEK	6827300	0	6827300
EAHEPLAVADAK	4767300	0	4767300
EAIEGTYIDKK	14090000	0	14090000
EAIESAIGGNAYQHSK	45870000	0	45870000
EAINLLEPMTNDPVNYVR	13676000	0	13676000
EAINVEQAFQTIAR	34298000	0	34298000
EAIQLIAR	9848100	0	9848100
EALDVLGAVLK	11056000	0	11056000
EALELTDTGLLSGSEER	3986900	0	3986900
EALENANTNTEVLK	0	0	0
EALENCITLQDFNR	3665100	0	3665100
EALLELLR	12891000	0	12891000
EALLGDTGTGDFLK	19486000	0	19486000
EALLSSAVDHGSDEVK	17246000	0	17246000
EALQDDLQR	2631600	0	2631600

EALQLMATYLPK	90565000	0	90565000
EAMEADLK	4873200	0	4873200
EAMEDGEIDGNK	14433000	0	14433000
EAMMGLAQLYK	2223000	0	2223000
EANNFLWPFK	59318000	0	59318000
EANQQQQFNR	5496200	0	5496200
EANSIIITPGYGLCAAK	40994000	0	40994000
EAPAEGEAAEPGSPTAAEGEAASAASSTSSPK	33098000	0	33098000
EAQELSQNSAIK	43714000	0	43714000
EAQNLSAMEIR	15899000	0	15899000
EASDPQPEEADGGLK	13869000	0	13869000
EASFDGISK	19374000	0	19374000
EATAGNPGGQTVR	2538200	0	2538200
EATDAIGHLDR	100180000	0	100180000
EATDEELEK	2311600	0	2311600
EAVEAIQNSTSIK	14144000	0	14144000
EAVLNAYR	10193000	0	10193000
EAVTEILGIEPDR	25032000	0	25032000
EAVTEILGIEPDREK	59475000	0	59475000
EAYFWLR	1989800	0	1989800
EAYMGNVLQGGEGQAPTR	26180000	0	26180000
EAYPDHTQFEK	2360200	0	2360200
EAYPEEAYIADLDAK	1510000	0	1510000
ECCDKPLLEK	14647000	14647000	0
ECCHGDLLECADDR	113130000	113130000	0

ECLPLIIFLR	102000000	2353100	99648000
ECPSVLEYK	119220000	0	119220000
ECVPNSNER	9299000	9299000	0
ECVQQLAENTR	8309700	0	8309700
EDCSPDEFIDVIVGNR	911550	0	911550
EDDLNSFNATDLK	13831000	0	13831000
EDEEESLNEVGYDDIGGCR	3664900	0	3664900
EDFDSLLQSAK	353110000	1158900	351950000
EDGLAQQQTQLNLR	3758300	0	3758300
EDGSEVGVGGAQVTGSNTR	7746700	0	7746700
EDGSGDRGDGPFR	10804000	0	10804000
EDGTFYEFGEDIPEAPER	3530000	0	3530000
EDIEFICK	0	0	0
EDIQSVMTEIR	58206000	0	58206000
EDITQSAQHALR	20319000	0	20319000
EDIYAVEIVGGATR	49903000	0	49903000
EDLECLIQEQMK	11018000	0	11018000
EDLNCQEEEDPMNK	4430400	0	4430400
EDLQLDKPASGVK	13237000	0	13237000
EDLTEIR	88468000	2618200	85849000
EDLVYQAK	24370000	0	24370000
EDLYLKPIQR	8417600	0	8417600
EDMAALEK	446150000	0	446150000
EDPLIIPVPASENPFR	7493200	0	7493200
EDPLLTPVPASENPFR	52823000	0	52823000

EDPTVSALLTSEK	6683600	0	6683600
EDQSILCTGESGAGK	37437000	0	37437000
EDQTEYLEER	162630000	6104100	156530000
EDTEEYNLR	33444000	0	33444000
EDTESLEIFQNEVAR	14725000	0	14725000
EDVLTLLLPVMGDSK	8201600	0	8201600
EEAADLSSLK	10594000	0	10594000
EEACDCLFEVVNK	2730000	0	2730000
EEAENTLQSFR	158390000	4042700	154350000
EEASDYLELDTIK	46360000	1340700	45019000
EEASGSSVTAEEAK	22025000	0	22025000
EEDPATGTGDPPR	1515100	0	1515100
EEEDVSGEPEASPSADTTILFVK	3928500	0	3928500
EEEIAALVIDNGSGMCK	75469000	0	75469000
EEEVTGPVIAPLFPQK	9719100	0	9719100
EEIAQLAR	25967000	0	25967000
EEIQSSISGVTAAYNR	0	0	0
EELEALFLPYDLK	2628000	0	2628000
EELEEVIK	4707600	0	4707600
EELEEVIKDI	37687000	0	37687000
EELFVTSK	5356200	0	5356200
EELGLIEQAYDNPHEALSR	48955000	0	48955000
EELQANGSAPAADKEEPAAAGSGAASPSAAEK	22309000	0	22309000
EELVAEQALK	9717400	0	9717400
EELVEESQTK	7223100	0	7223100

EEMIHNLQ	0	0	0
EENAEQQALAAK	18688000	0	18688000
EEPGSDSGTTAVVALIR	47673000	0	47673000
EEQMDGTVTLK	6983000	0	6983000
EESDDEAAVEEEEEEK	23897000	0	23897000
EESGVSVSNSQPTNESHSIK	7117600	0	7117600
EEVVTVETWQEGSLK	0	0	0
EFADSLGIPFLETSAK	42220000	0	42220000
EFAGEDTSDLFLEER	33447000	0	33447000
EFCENLSADCR	91726000	0	91726000
EFCQQEVEPMCK	7271200	0	7271200
EFEDAFPADFIAEGIDQTR	6823000	0	6823000
EFEEDLTGIDDR	51863000	0	51863000
EFEENGLEK	10364000	0	10364000
EFGATECINPQDFSK	17303000	0	17303000
EFGEPWDLNSGDGAFYGPK	2894400	0	2894400
EFGFSGLNVK	32117000	0	32117000
EFGTNIK	141850000	0	141850000
EFHLNESGDPSSK	92138000	0	92138000
EFIQEPAK	40471000	0	40471000
EFLPEGQDIGAFVAEQK	13116000	0	13116000
EFLVAGGEDFK	4842600	0	4842600
EFMWALK	3189600	0	3189600
EFVICDK	5850100	0	5850100
EGALCEENMR	394030000	0	394030000

EGATVYATGTHAQVEDGR	7092700	0	7092700
EGDCGFGDGGPSGASGR	0	0	0
EGEAVVLPEVEPGLTAR	2033700	0	2033700
EGEEATAEAEEK	3517800	0	3517800
EGFLLALTQGR	9613000	0	9613000
EGFYDLSSEDPFGCK	11820000	0	11820000
EGGDFVCCALSPR	13583000	0	13583000
EGGGNNLYGEEMVQALK	18509000	0	18509000
EGGLGPLNIPLLADVTR	1986200	0	1986200
EGGTVVYGGK	10078000	0	10078000
EGIAQTVFLGLNR	4969700	0	4969700
EGIPALDNFLDK	54395000	0	54395000
EGIPPDQQR	1430300000	33640000	1396700000
EGITTYFSGNCTMEDAK	0	0	0
EGIVTATEQEVK	6638200	0	6638200
EGLELPEDEEEK	0	0	0
EGLELPEDEEEKK	9953300	0	9953300
EGLLAIFK	35794000	0	35794000
EGLLFEGR	3748800	0	3748800
EGLLGLQNLLK	2896000	0	2896000
EGLLLWCQR	77737000	1768900	75968000
EGMEAAVEK	0	0	0
EGMNIVEAMER	379910000	10130000	369780000
EGPAVVGQFIQDVK	22542000	0	22542000
EGPLCDELIR	12818000	0	12818000

EGPYDVVVLPGGNLGAQNLSESAAVK	19384000	0	19384000
EGPYSISVLYGDEEVPR	6607100	0	6607100
EGQEIASVSDDHTCR	10620000	0	10620000
EGQNYQQNCIK	25791000	0	25791000
EGQTICVR	4160500	0	4160500
EGSLVINSK	59587000	0	59587000
EGSPVLLNCLMYK	31988000	0	31988000
EGSQGELTPANSQSR	6158500	0	6158500
EGTGTEMPMIGDR	0	0	0
EGTLSDSTGSEK	2737100	0	2737100
EGVECEVINMR	1669000	0	1669000
EGVHGGLINK	57320000	0	57320000
EGVVECSFVK	188610000	0	188610000
EHALLAYTLGVK	113110000	0	113110000
EHINSVSAMK	1986400	0	1986400
EHVIEALR	71128000	0	71128000
EHYVDLK	169790000	0	169790000
EIAEAYLGK	11688000	0	11688000
EIAQDFK	1406000000	3516500	1402500000
EIAQEFKTDLR	41831000	0	41831000
EIATVVK	126030000	0	126030000
EICCYSISCK	15891000	0	15891000
EIEDPEDR	78162000	0	78162000
EIEQEAAVELSQLR	15183000	0	15183000
EIEVGGGR	266330000	9038400	257290000

EIFNFVLK	102510000	0	102510000
EIGSTMSGR	25883000	0	25883000
EIIDLVLDR	3995300000	117580000	3877700000
EIIEAMLK	83925000	0	83925000
EIIQDVTLHDLDVANAR	23514000	0	23514000
EILAELTGR	11791000	0	11791000
EILETLIK	0	0	0
EILGTAQSVGCNVDGR	150150000	966780	149180000
EILIPVFK	56335000	0	56335000
EILSEENEMQPNGK	0	0	0
EILTLLQGVHQGAGFQDIPK	42425000	0	42425000
EIQTAVR	50194000	1140200	49054000
EIQTTTGNQQVLVR	3629300	0	3629300
EIRPALELLEPIEQK	80344000	0	80344000
EISYENTQISR	16641000	0	16641000
EITALAPSTMK	5178000000	0	5178000000
EIVESCDLK	33350000	0	33350000
EIVLADVIDNDSWR	35491000	0	35491000
EIVNNVR	17092000	0	17092000
EIVPVLVSTR	2167800	0	2167800
EIVQDGDHMIIR	44009000	0	44009000
EKLQEEMLQR	7115700	0	7115700
EKPYFPIPEEYTFIQNVPLEDR	11629000	0	11629000
EKVESELR	32002000	0	32002000
EKYIDQEELNK	3472100	0	3472100

ELAEDGYSGVEVR	147390000	0	147390000
ELAESDFASTFR	0	0	0
ELAFQISK	0	0	0
ELAILLGMLDPAEK	3469000	0	3469000
ELAILLGMLDPAEKDEK	28414000	0	28414000
ELALQPK	45291000	0	45291000
ELAMPGEDLK	22193000	5907500	16286000
ELANSPDCPQMCAYK	28248000	0	28248000
ELAPAVSVLQLFCSSPK	1006600	0	1006600
ELAPLFEELR	9691600	0	9691600
ELAPLQELIEK	21871000	0	21871000
ELAPYDENWFYTR	19115000	0	19115000
ELAQQIQK	162740000	602650	162140000
ELATVLSDQPGLLGPK	36073000	0	36073000
ELAVQIQK	27745000	0	27745000
ELDALDANDELTPLGR	51237000	0	51237000
ELDQWIEQLNECK	69563000	0	69563000
ELDSLQTEAESLDNTVK	0	0	0
ELEAENYHDIK	7666300	0	7666300
ELEEESIR	15883000	0	15883000
ELEEETGYK	9477000	0	9477000
ELEEIVQPIISK	68301000	0	68301000
ELEQVCNPIISGLYQGAGGPGPGGFGAQGPK	4326900	0	4326900
ELEVLLMCNK	23868000	0	23868000
ELFSNLQEFAGPSGK	10314000	0	10314000

ELFSPLHALNFGIGGDTTR	18181000	0	18181000
ELGENLDQILR	19973000	0	19973000
ELGIWEPLAVK	27018000	0	27018000
ELGSECGIEFDEEK	0	0	0
ELGSSTNALR	9251500	0	9251500
ELHINLIPNK	5910200	0	5910200
ELIDYLR	2685500	0	2685500
ELIFEETAR	13618000	0	13618000
ELISNASDALDK	143250000	0	143250000
ELISNSSDALDK	397980000	0	397980000
ELITILEK	0	0	0
ELLAVPDNYK	9854200	0	9854200
ELLEIVK	8315900	0	8315900
ELLEQISAFDNVPR	10415000	0	10415000
ELLESNFTLVGDDGTNK	13296000	0	13296000
ELLGQGLLLR	5768200	0	5768200
ELLLQPVTISR	150860000	0	150860000
ELLNPVVEFVSHPSTTCR	54440000	0	54440000
ELLSNVDEGIYQLEK	3689900	0	3689900
ELLTLDEKDPR	8771400	0	8771400
ELLVPLTSSMYVPGK	43744000	0	43744000
ELLYFLDSCEPEFK	3687900	0	3687900
ELMAWNQAENR	3850100	0	3850100
ELNGTAPEEK	2822700	0	2822700
ELNITAAK	168080000	0	168080000

ELNYFAK	103160000	0	103160000
ELPAAVAPAGPASLAR	0	0	0
ELPEQLQEHAIEDK	6412500	0	6412500
ELQCLTPR	28578000	0	28578000
ELQDSTQMNEK	7791600	0	7791600
ELQEQLK	0	0	0
ELQEQMSR	53451000	8164300	45287000
ELQSMADQEK	5812900	0	5812900
ELQSVEQEVR	32306000	0	32306000
ELSDFISYLQR	17027000	0	17027000
ELSDSVTLSSSDR	7836800	0	7836800
ELSEALTR	69300000	0	69300000
ELSEYVR	31674000	0	31674000
ELSGTIK	93742000	0	93742000
ELSNFYFSIIK	2864000	0	2864000
ELSQIEACQGPMQMR	0	0	0
ELSTTLNADEAVTR	14355000	0	14355000
ELTAPDENIPAK	0	0	0
ELTAVVQK	249610000	0	249610000
ELTDEEAER	18944000	0	18944000
ELTEEKESAFEFLSSA	9685100	0	9685100
ELTGEDVLVR	0	0	0
ELTIGSK	9006700	0	9006700
ELTVSNNDINEAGVR	8466100	0	8466100
ELVALMSAIR	0	0	0

ELVEGEMK	17443000	0	17443000
ELVLDNSR	0	0	0
ELVSCSNCTDYQAR	66359000	642880	65717000
ELVSDANQHVK	10428000	0	10428000
ELWDSIMTR	34715000	0	34715000
ELYPVEFR	3009700	0	3009700
EMDVVSQHK	0	0	0
EMEENFAVEAANYQDTIGR	1138300	0	1138300
EMFGSGTACVVCPVSDILYK	16923000	0	16923000
EMLGGEIIPR	17770000	0	17770000
EMLQQSK	15234000	0	15234000
EMQNLSFQDCYSSK	1544300	0	1544300
EMQPTHPIR	37096000	0	37096000
EMQQLSGGQK	0	0	0
EMTADVIELK	4186700	0	4186700
EMVECFNK	63791000	0	63791000
EMVELPLR	21389000	0	21389000
EMVQNLMVLR	30668000	0	30668000
ENCMYQACPTQDCNKK	4284900	0	4284900
ENELTYYCCK	0	0	0
ENFSCLTR	162460000	12452000	150010000
ENGGYTGCPFPAK	780650	0	780650
ENGLPLEYQEK	7647200	0	7647200
ENILEEFSK	71437000	0	71437000
ENITEDEAK	21061000	0	21061000

ENIVEAIIHSPELIR	7295700	0	7295700
ENLATVEGNFASIDER	2937800	0	2937800
ENLFMDLLR	15370000	3118000	12252000
ENLISALEEAK	17739000	0	17739000
ENLLDFIK	197560000	1719800	195840000
ENLSYDLVPLK	7217500	0	7217500
ENMTLQPK	8009600	0	8009600
ENQTAVDVFR	8653100	0	8653100
ENSETVVTGSLDDLVK	13608000	0	13608000
ENTELVQK	3577200	0	3577200
ENVNATENCISAVGK	2084500	0	2084500
ENVSNCIQLK	55822000	0	55822000
EPELGLEELLR	6379200	0	6379200
EPESILQVLSQMEK	10138000	0	10138000
EPEVLSTMAIIVNK	26056000	0	26056000
EPFLQQLK	0	0	0
EPLYVGVDDDK	21387000	0	21387000
EPNPPIDEVISTPGVVAR	0	0	0
EPNSENVDISSGGGVTGWK	2901900	0	2901900
EPPYGADVLR	41903000	0	41903000
EPVAVLK	12558000	0	12558000
EPVETAVDNNSK	14230000	0	14230000
EPVQLETLSIR	2205700	0	2205700
EPWLLPSQHNDIIR	26768000	0	26768000
EQADFAVEALAK	17475000	0	17475000

EQAYQER	5228700	0	5228700
EQEAGLLQFLR	35158000	0	35158000
EQESCNMANIR	0	0	0
EQFLDGDGWTSR	144940000	1496100	143450000
EQGFLSFWR	4989900	0	4989900
EQGPYETYEGSPVSK	11465000	0	11465000
EQGVLSFWR	295750000	1882100	293870000
EQGVTFPSGDIQEQLIR	65918000	0	65918000
EQICEVEEGDKPDVDK	6451000	0	6451000
EQILEEFSK	23585000	0	23585000
EQIYDVYR	31901000	0	31901000
EQLAIAEFAR	10787000	0	10787000
EQLDAFIDQLYK	4502200	0	4502200
EQLDNQLDAYMSK	0	0	0
EQLGEEIDSK	26701000	0	26701000
EQLMSQEER	4686300	0	4686300
EQLWLANEGLITR	12660000	0	12660000
EQPEKEPELQQYVPQLQNNTILR	7594700	0	7594700
EQPVFAMTGLR	30371000	0	30371000
EQQEAIEHIDEVQNEIDR	0	0	0
EQQIVIQSSGGLSK	4789200	0	4789200
EQSGPSPLEETR	13853000	0	13853000
EQSILELGSLLAK	7084400	0	7084400
EQTADGVAVIPVLQR	47002000	0	47002000
EQVANSAFVER	37877000	0	37877000

EQWDTIEELIR	2937500	0	2937500
EQYGSVDQYAR	0	0	0
ESALILLQTVPK	8052100	0	8052100
ESCLEAYTGIVQGLK	101740000	0	101740000
ESDYFTPQGEFR	0	0	0
ESFAEMNR	168410000	3719100	164690000
ESIEEPSAK	40130000	0	40130000
ESISDVGFGMLK	13478000	0	13478000
ESLDDLTNLVVK	0	0	0
ESLPELSTAQQNK	11459000	0	11459000
ESLVALLSR	0	0	0
ESNCYDPER	122220000	0	122220000
ESPFSTSASPLLSGSQHFDVPPR	16436000	0	16436000
ESPNITDR	4323400	0	4323400
ESQDTSFTTLVER	4560800	0	4560800
ESSLTEPVIVGLLK	15148000	0	15148000
ESSSEQYVPDVFYK	4172500	0	4172500
ESSVPMCQGELR	0	0	0
ESTAEKDEL	244740000	0	244740000
ESTLHLVLR	44155000	0	44155000
ESTSCPVVQK	13331000	0	13331000
ESVVDYCNR	28404000	0	28404000
ESYDYLK	7611900	0	7611900
ESYSVYVYK	109160000	0	109160000
ETAENYLGHTAK	4041600	0	4041600

ETAFILTGYCTDK	0	0	0
ETANAIVSQQTPQR	4908400	0	4908400
ETDLLILFK	3434100	0	3434100
ETDLQELFR	9996200	0	9996200
ETEEILADVLK	19364000	0	19364000
ETEGDVTSVK	8819700	0	8819700
ETENDDLTNVIQK	48396000	0	48396000
ETENDDVTNVIQK	6694600	0	6694600
ETGCMVYEK	0	0	0
ETLAQLQQEFQR	12327000	0	12327000
ETLIQFLR	4591200	0	4591200
ETLLAMFK	41388000	0	41388000
ETLLNGVGYLHEGLSPMER	11293000	0	11293000
ETLPAEQDLTTK	28789000	0	28789000
ETLVYLTHLDYVDTER	10178000	0	10178000
ETMVTSTTEPSR	129290000	2701000	126590000
ETQALILAPTR	9842800	0	9842800
ETSGNLEQLLLAVVK	4097300	0	4097300
ETSMVHELNR	9653900	4060700	5593200
ETTGTGPNVYHENDTIAK	24097000	0	24097000
ETTNIFSNCGCVR	0	0	0
ETVDSFLDLAR	17514000	0	17514000
ETVEEQASTTER	2864200	0	2864200
ETVSEESNVLCLSK	2614500	0	2614500
ETYGDMADCCEK	156900000	156900000	0

EVAALCR	6314200	0	6314200
EVAEAATGEDASSPPPK	8220300	0	8220300
EVATAIR	48440000	750470	47690000
EVCFACVDGK	0	0	0
EVDEQMLNVQNK	539740000	0	539740000
EVDIYTVK	0	0	0
EVEMGPFK	0	0	0
EVEPALELLEPIDQK	15204000	0	15204000
EVEQFTQVAK	0	0	0
EVEQLIK	88138000	0	88138000
EVFEMATR	21240000	0	21240000
EVFLVMPTGGGK	60129000	0	60129000
EVGSIIGK	37652000	0	37652000
EVIAVSCGPAQCQETIR	0	0	0
EVIDLLK	22407000	0	22407000
EVLCPESQSPNGVR	2136900	0	2136900
EVLDSFLDLAR	17980000	0	17980000
EVLEGLEYLHK	5394000	0	5394000
EVLEYNAIGGK	0	0	0
EVLLEAQDMAVR	0	0	0
EVLLPEVGAK	0	0	0
EVLNEEDEVQPNGK	8348800	0	8348800
EVLQNLGPK	18558000	0	18558000
EVNEVIQNPATITR	0	0	0
EVNLAVQNAK	54096000	0	54096000

EVPCYVFDEELR	2372100	0	2372100
EVPGPDCR	29136000	0	29136000
EVQVEHIK	2456500	0	2456500
EVQYLLNK	16151000	0	16151000
EVQYTLEMIK	0	0	0
EVSEEQPVVTLEK	6926300	0	6926300
EVSQPDWTPPPEVTLVLTK	18188000	0	18188000
EVSSATNALR	74406000	0	74406000
EVSSSFDHVIK	0	0	0
EVSTYIK	941000000	0	941000000
EVTPEGLQMVK	22270000	0	22270000
EVVCTNCPTGTTGK	5274300	0	5274300
EVVEAHVDQK	10292000	0	10292000
EVVEEAENGR	736760000	20592000	716170000
EVVEQGLLK	14890000	0	14890000
EVWNTYELDLVNYQNK	26225000	0	26225000
EWLNSCDLK	2840000	0	2840000
EWLTELFQQSK	8180600	0	8180600
EYAEDDNIYQQK	4241100	0	4241100
EYCIQAFESFVR	14825000	0	14825000
EYEATLEECCAK	234630000	234630000	0
EYFGGFGEVESIELPMDNK	6156600	0	6156600
EYGCGPSGQVVSR	4145400	0	4145400
EYINCNR	4999100	0	4999100
EYLLGSTAEEK	0	0	0

EYLPIGGLAEFCK	161010000	1436900	159570000
EYLSEEVQAVHK	22322000	0	22322000
EYNEFAEVFLK	32710000	0	32710000
EYQDLLNVK	4026200	0	4026200
EYQTQLIQR	51918000	0	51918000
EYSLQVLK	5862300	0	5862300
EYTAAVEAK	3653700	0	3653700
EYTDVYPEIIER	30702000	0	30702000
EYTLDVYR	2510000	0	2510000
EYVTCHTCR	1241900	0	1241900
FAAATGATPIAGR	389240000	9604600	379640000
FAANPNQNK	5965200	0	5965200
FAAQATQQR	0	0	0
FAAYFQQGDMESNGK	27628000	0	27628000
FADFMVK	3252000	0	3252000
FADIGNTVK	6069200	0	6069200
FAEALGSTEAK	32393000	1925900	30467000
FAETQPK	0	0	0
FAEVYFAQSQQK	3200700	0	3200700
FAFQAEVNR	0	0	0
FAIQDISVEETSAK	44940000	0	44940000
FAMEPEEFDSDTLR	238650000	0	238650000
FAMEQSFSADTGGGGR	0	0	0
FASGGCDNLIK	51695000	0	51695000
FATEYCNTIEGTAK	0	0	0

FAVALLDDSVR	14263000	0	14263000
FAVFGLGNK	11901000	0	11901000
FAVGSGSR	26926000	0	26926000
FCANTCVECR	13250000	0	13250000
FCDNSSAIQGK	2709200	0	2709200
FCECDNFNCDR	79221000	2811200	76410000
FCENTQAGEGR	1156400	0	1156400
FCIWTESAFR	44059000	0	44059000
FCNPGFPIGCYITDK	16887000	0	16887000
FCNVDDDELR	39530000	0	39530000
FCPEADSK	12204000	0	12204000
FCPFAER	52317000	0	52317000
FCQLLWR	6245500	0	6245500
FCTGLTQIETLFK	35726000	0	35726000
FDAGELITQR	0	0	0
FDDAVVQSDMK	21867000	0	21867000
FDDESAEEIR	7608000	0	7608000
FDDPLLGPR	4685500	0	4685500
FDEISFVNFAR	79109000	3583600	75525000
FDGCYCDSLENLADGYK	2551100	0	2551100
FDGILTEGEGPR	18671000	0	18671000
FDLLGDFGR	5169200	0	5169200
FDLMYAK	88640000	0	88640000
FDLNSPWEAFPVYR	0	0	0
FDNLYGCR	70179000	0	70179000

FDNPAAVSPTPTR	12286000	0	12286000
FDQPLEASTWLK	33481000	25185000	8296100
FDSNCITPGTEFMDNLAK	3093600	0	3093600
FDSSLDR	67372000	2112500	65260000
FDTEEEFK	9463300	0	9463300
FDTGNLCMVTGGANLGR	16611000	0	16611000
FDTQYPYGEK	3651600	0	3651600
FDVPGDENAEMDAR	0	0	0
FDVSGYPTLK	82372000	0	82372000
FDYSGVGSSDGNSEESTLGK	0	0	0
FEDENFILK	2107400000	0	2107400000
FEDYLNAESR	0	0	0
FEEAVEK	37911000	0	37911000
FEEFLQR	18004000	0	18004000
FEELGVK	30994000	0	30994000
FEELNADLFR	154380000	2100400	152280000
FEELTNLIR	44753000	0	44753000
FEETGQELAELLEEEK	4769800	0	4769800
FEETTADGR	13330000	0	13330000
FEHCNFNDVTTR	4618400	0	4618400
FEIWDTAGQER	67913000	0	67913000
FELDTSER	20675000	0	20675000
FENYGDK	35364000	0	35364000
FESILPR	0	0	0
FEVGDIMLIR	18288000	0	18288000

FEVNNTILHPEIVECR	0	0	0
FEVQGLQPNGEEMTLK	60155000	0	60155000
FEWELPLDEAQR	10753000	0	10753000
FFDANYDGK	9584400	0	9584400
FFDDPMLLELAK	4765500	0	4765500
FFDGELTK	0	0	0
FFEHFIEGGR	21857000	0	21857000
FFEILSPVYR	0	0	0
FFEVFDNSMK	2955000	0	2955000
FFGGYVPEMVLTPDDQR	26823000	0	26823000
FFGNLMDASK	0	0	0
FFLSSGLIDK	12585000	0	12585000
FFNVLTTNTDGK	59874000	0	59874000
FFPASFPNR	0	0	0
FFPLESWQIGK	48541000	0	48541000
FFQEENTEK	16561000	0	16561000
FFQPTEMASQDFFQR	4665000	0	4665000
FFVAPFPEVFGK	9106600	9106600	0
FFVGGNWK	0	0	0
FFVSSSQGR	74848000	0	74848000
FFYSDQNVDSR	0	0	0
FGALTAEK	70766000	0	70766000
FGAMLDMLTDR	9134400	0	9134400
FGAPPHAGGGIGLER	9609100	0	9609100
FGAVWTGDNTAEWDHLK	34749000	0	34749000

FGELVMTK	0	0	0
FGEVTSASNCTDFQSR	2482800	0	2482800
FGEVVDCTLK	26358000	0	26358000
FGFEIIETK	21124000	0	21124000
FGFPAFSGISR	19491000	0	19491000
FGFPEGSVELYAEK	11311000	0	11311000
FGFYEVFK	111070000	0	111070000
FGGALDAAAK	103810000	0	103810000
FGGGNPELLTQMVSK	108900000	0	108900000
FGGLAAGEDNGQR	22998000	1353900	21644000
FGGSGSQVDSAR	23760000	0	23760000
FGIDDQDYQNSVTR	4922700	0	4922700
FGIQAQMVTTDFQK	35316000	0	35316000
FGNEITQLAR	0	0	0
FGPYYTEPVIAGLDPK	17876000	0	17876000
FGQVYTEAK	10276000	0	10276000
FGSEFSPELQASFQK	87520000	87520000	0
FGSLLPIHPVTSG	0	0	0
FGTINIVHPK	0	0	0
FGVIFAGAQK	117200000	0	117200000
FGVLSDNFK	6937000	0	6937000
FGVVLDEIKPSSAPELQAVR	5326700	0	5326700
FGWDCHGLPVEYEIDK	23117000	0	23117000
FGYVDFESAEDLEK	18121000	0	18121000
FHEICSNLVK	23769000	0	23769000

FHMVDGNVSGEFTDLVPEK	10235000	0	10235000
FHVEEEGK	5149000	0	5149000
FIASTGMDR	58932000	0	58932000
FIAYQFTDTPLQIK	7136100	0	7136100
FIDDVVSAVLR	2797700	0	2797700
FIEEHATK	39387000	0	39387000
FIEIAAR	25912000	0	25912000
FIGELFK	43075000	0	43075000
FIHDQTSPNPK	1440000	0	1440000
FIIPNVVK	999060000	0	999060000
FIIPQIVK	2071000000	15505000	2055400000
FIMESGAK	281100000	0	281100000
FINDQYEK	29023000	0	29023000
FIPCSPFSDYVYK	216360000	0	216360000
FIPEGSQR	34442000	0	34442000
FIPGSALNGMVEMMDR	6415200	0	6415200
FIQLLSDQSDQSVLIQK	36448000	0	36448000
FIQTFGK	23418000	0	23418000
FISLASLEYSDYSK	21412000	0	21412000
FITDNTVEER	14008000	0	14008000
FKDIFQEIYDK	17184000	0	17184000
FLAEEGFYK	20415000	0	20415000
FLDGNELTLADCNLLPK	5084300	2607700	2476500
FLEEYLSSTPQR	19815000	0	19815000
FLELLPK	22452000	0	22452000

FLEMCNDLLAR	165510000	0	165510000
FLEMHQL	0	0	0
FLESPDFQPNIAK	3820200	0	3820200
FLESQEFQPSIAK	9047800	0	9047800
FLFDSVSSQNVGLR	0	0	0
FLFSLFGQK	4965300	0	4965300
FLFVDADQIVR	42454000	0	42454000
FLGDIEVWDQAEK	45269000	0	45269000
FLICTDVAAR	0	0	0
FLILPDMLK	47396000	0	47396000
FLINLEGGDIR	36972000	0	36972000
FLIPNASQAESK	503920000	0	503920000
FLIQNVLR	64842000	0	64842000
FLITGADQNR	17766000	0	17766000
FLIVAHDDGR	12737000	0	12737000
FLLADNLYCK	34002000	0	34002000
FLLDHQGELFPSPDPSGL	0	0	0
FLLSESGSGK	0	0	0
FLNAENAQK	46426000	0	46426000
FLNEMIAPVMR	159390000	2142100	157240000
FLNVPMFR	47490000	0	47490000
FLPGYVGGIQEGAVTPAGVVNK	13088000	0	13088000
FLPLFDR	52530000	0	52530000
FLQDTIEEMALK	40591000	0	40591000
FLQEVDFFQR	7397500	0	7397500

FLQFVTGTSK	0	0	0
FLQMCNDDPDVLPDLK	10249000	0	10249000
FLSAIVSSVDK	7058800	0	7058800
FLSLYGDQIDMHR	88961000	0	88961000
FLSNGYIPIPGQQDK	8947900	0	8947900
FLTAVNLEHPEMLEK	13064000	0	13064000
FLTVMMK	6213700	0	6213700
FLVGFTNK	29872000	0	29872000
FLVYVANFDEK	43314000	0	43314000
FLYSELMK	79562000	0	79562000
FMADIDLDPGCTLNK	27295000	0	27295000
FMEQVIFK	70797000	0	70797000
FMGTELNGK	54555000	0	54555000
FMQASEDLLK	566180000	0	566180000
FMQDPMEIFVDDETK	30519000	0	30519000
FMQDPMEVFVDDETK	19616000	0	19616000
FNADEFEDMVAEK	28601000	0	28601000
FNAHGDANTIVCNSK	36772000	0	36772000
FNEEHIPDSPFVVPVASPSGDAR	9572300	0	9572300
FNESGDPSCVIMQNWAR	7813600	0	7813600
FNLTYVSHDGDDK	21955000	0	21955000
FNQVLDQFGEK	65022000	0	65022000
FNTANDDNVTQVR	10946000	0	10946000
FNTGPVGK	23190000	0	23190000
FNVDEYSDLVTLTK	9702100	0	9702100

FNVEDGEIVQQVR	3967100	0	3967100
FNVLQYVVPEVK	9515200	0	9515200
FNVWDTAGQEK	43273000	0	43273000
FNYGFEYLGVQDK	11865000	0	11865000
FPAEQYYR	28094000	0	28094000
FPDENFK	324570000	0	324570000
FPEEEAPSTVLSQNLFTPK	9656600	0	9656600
FPGQLNADLR	53528000	0	53528000
FPLFGGWK	13194000	0	13194000
FPSGNYPPCIGDNR	4469000	0	4469000
FPSLLTHNENMVAK	214210000	0	214210000
FPTLTNINENNPTLLNPIK	6100200	0	6100200
FQASQGENLEGK	8335600	0	8335600
FQDGDLTLYQSNTILR	112180000	0	112180000
FQDGVLEPDFPR	15117000	15117000	0
FQDLGAAYEVLSDSEK	19811000	0	19811000
FQGEWNLQPLPK	10815000	0	10815000
FQGQTCEMCQTCLGVCAEHK	14235000	0	14235000
FQIATVTEK	0	0	0
FQLLEGPPESMGR	7751300	0	7751300
FQMPDQGMTSADDFFQGTK	87360000	0	87360000
FQSGDFHVINGVLR	0	0	0
FQSISTEFLALMK	4454100	0	4454100
FQSIVIGCALEDQK	3470300	0	3470300
FQTEIQTVNK	71723000	0	71723000

FQVDPSGEIVELAK	3233900	0	3233900
FRIDELEPR	16984000	0	16984000
FRPDMEEEEAK	50765000	0	50765000
FSASGELGNGNIK	0	0	0
FSDQFPLPLK	54086000	0	54086000
FSDSYASVIK	4744200	0	4744200
FSELTAEK	39726000	0	39726000
FSFTLPYPVK	27434000	0	27434000
FSGDLDDQTCR	21296000	0	21296000
FSGGYPALMDCMNK	28218000	0	28218000
FSGWYDADLSPAGHEEAK	22672000	0	22672000
FSHEEIAMATVTALR	78341000	0	78341000
FSHQGVQLIDFSPCER	6604100	0	6604100
FSIEDLK	6012900	0	6012900
FSIIAEPLVR	248840000	17100000	231740000
FSIQTMCPIEGEGNIAR	108720000	0	108720000
FSMVVQDGIVK	11267000	0	11267000
FSPNSSNPIIVSCGWDK	90234000	0	90234000
FSPTDFLAK	30748000	0	30748000
FSSSSGYGGGSSR	11758000	11758000	0
FSTIASSYEECR	4613200	0	4613200
FSTVAGESGSADTVR	11204000	0	11204000
FSVCVLGDQQHCDEAK	28221000	0	28221000
FSWFAGEK	2911300	0	2911300
FTADEAR	15759000	0	15759000

FTAGDFSTTVIQNVNK	1182600	0	1182600
FTASAGIQVVGDDLTVTNPK	0	0	0
FTAVEDQYYCVDCYK	8478700	0	8478700
FTCSESQVNSR	5685300	0	5685300
FTEYETQVK	28945000	0	28945000
FTITPSTTQVVGILK	8926300	0	8926300
FTNMLGQPGSTALDLFK	3431700	0	3431700
FTPGTFTNQIQAAFR	73432000	0	73432000
FTPLPEGK	58126000	0	58126000
FVADGIFK	8371200	0	8371200
FVASCGFTPDVK	1706800	0	1706800
FVCAPPSR	6465600	0	6465600
FVDGLMIHSGD	0	0	0
FVEGLPINDFSR	135210000	0	135210000
FVETPGQK	198070000	0	198070000
FVFDRPLPVSR	33029000	0	33029000
FVFSLVDAMNGK	104980000	0	104980000
FVGQDVEGER	0	0	0
FVIATSTK	35192000	0	35192000
FVIGGPQGDAGLTGR	19045000	0	19045000
FVIQGAGAK	48599000	0	48599000
FVLSGANIMCPGLTSPGAK	44931000	0	44931000
FVLSQAKDEL	0	0	0
FVLSSGK	0	0	0
FVPYYDLFMPSLK	11415000	0	11415000

FVSISDLLVPK	143010000	0	143010000
FVTETLEDGSR	2754300	0	2754300
FVTVQTISGTGALR	0	0	0
FVVQNVSAQK	11006000	0	11006000
FWEQSVR	24929000	0	24929000
FWESPETVSQLDSVR	9966500	0	9966500
FWPAIDDGLR	31682000	3292100	28390000
FWQTYSSAEEVLQK	1775800	0	1775800
FWSLEDGLNR	0	0	0
FYALSASFEPFSNK	70885000	0	70885000
FYDDAIVSQK	25999000	0	25999000
FYEAFSK	1133200000	5408100	1127800000
FYEQFSK	1693800000	0	1693800000
FYFNGEYAGFDETQPTAESGGK	11364000	0	11364000
FYGDEEKDK	21444000	0	21444000
FYNLVLLPR	4881800	0	4881800
FYPLEIDYGQDEEAVK	9817400	0	9817400
FYQASTSELYGK	0	0	0
FYSLPQSPQQFK	0	0	0
FYSLWDTGYAK	5312700	0	5312700
FYTEDSPGLK	58556000	0	58556000
FYTQQWEDYR	5222800	0	5222800
FYVEDLK	7440200	0	7440200
FYVHNDIFR	0	0	0
GAAGALLVYDITR	16617000	0	16617000

GACLLPK	218780000	218780000	0
GACSVGTNVR	0	0	0
GADCCVLVFDVTAPNTFK	2227900	0	2227900
GADFCQFR	39719000	39719000	0
GADFLVTEVENGGSLGSK	15080000	0	15080000
GADIMYTGTVDCWR	21237000	0	21237000
GAEDDLNTVAAGTMTGMLYK	11883000	0	11883000
GAEEMETVIPVDVMR	51627000	0	51627000
GAEILEVLHSLPAVR	4349200	0	4349200
GAEYVSAR	30903000	0	30903000
GAFASLSELHCDK	37969000	37969000	0
GAFGKPQGTVAR	17494000	0	17494000
GAGQQQSQEMMEVDR	2271400	0	2271400
GAGSEETAAAAAPSR	1285600	0	1285600
GAGTDDHTLIR	28809000	0	28809000
GAGTDDSTLVR	6515500	0	6515500
GAIILAK	51018000	0	51018000
GALPLDTVTFYK	58160000	0	58160000
GALQNIIPASTGAAK	1679700000	0	1679700000
GANDFMCDEMER	3034700	0	3034700
GATQQILDEAER	0	0	0
GAVGALLVYDIAK	33827000	0	33827000
GAVLVCDMSSNFLSK	30634000	0	30634000
GAVLVCDMSSNFLSKPVDVSK	85347000	0	85347000
GAVSAEQVIAGFNR	10236000	0	10236000

GAVWGATLNK	14780000	0	14780000
GAVYSFDPVGSYQR	27295000	0	27295000
GAWSNVLR	32058000	0	32058000
GCALQCAILSPAFK	50546000	0	50546000
GCDVVVIPAGVPR	92946000	0	92946000
GCEVIQEIK	11933000	0	11933000
GCEVVVSGK	225880000	0	225880000
GCILTLVER	22748000	0	22748000
GCITIIGGGDTATCCAK	37889000	0	37889000
GCPEDAAVCAVDK	13947000	0	13947000
GCTATLGNFAK	5155100	0	5155100
GCVITISGR	3123100	0	3123100
GDAMIMEETGK	88817000	0	88817000
GDDQLELIKDDEK	49201000	0	49201000
GDECGLALGR	2971400	0	2971400
GDEELDSLIK	12820000	0	12820000
GDFCIQVGR	404790000	8438200	396350000
GDFDENLNYPEQK	0	0	0
GDFILVGDLMR	3014800	0	3014800
GDKVDILYNNIK	11797000	0	11797000
GDLGIEIPAEK	26952000	0	26952000
GDLLFLTNR	48322000	0	48322000
GDPQVYEELFSYSCPK	4196000	0	4196000
GDQENVHPDVMLVQPR	0	0	0
GDQPAASGDSDDDEPPPLPR	5022300	0	5022300

GDTVATLSER	18926000	0	18926000
GDVENIEVVQK	85299000	0	85299000
GDVSNLDPNFSFEGTK	65835000	0	65835000
GDVVNQDDLYQALASGK	5665000	0	5665000
GDYPLEAVR	28971000	0	28971000
GEAAAERPGEAAVASSPSK	27998000	0	27998000
GEDEEENNLEVR	13369000	0	13369000
GEDFPANNIVK	29965000	0	29965000
GEDFYCVTCHETK	15478000	0	15478000
GEEVDVAR	10816000	0	10816000
GEEVGELSR	10176000	0	10176000
GEFTIETEGK	15083000	0	15083000
GEGQLGPAER	796890000	30286000	766610000
GEHGFIGCR	38049000	0	38049000
GEHPGLSIGDVAK	93421000	0	93421000
GEIFLDEK	0	0	0
GELLEAIK	8583700	0	8583700
GELSGDFEK	7936200	0	7936200
GEMMDLQHGSLFLQTPK	232530000	0	232530000
GEMMDLQHGSLFLR	181980000	0	181980000
GENLVSMTVEGPPPK	6271800	0	6271800
GENSWFSTQVDTVATK	93072000	0	93072000
GEPAAAAAPEAGASPVEK	16226000	0	16226000
GEQGQYLQQDANECWIQMMR	5653300	0	5653300
GESDPAYQQYQDAANNLR	0	0	0

GESLPCVK	4745900	0	4745900
GESPVDYDGGR	69944000	0	69944000
GETDLIQK	18466000	0	18466000
GETLGLIGFGR	7686100	0	7686100
GETVNDCHAEIISR	48799000	0	48799000
GETVPLDVLQIK	20304000	0	20304000
GEVDEEDAALYR	3682400	0	3682400
GEVFNELVGK	25988000	0	25988000
GFAFVQYVNER	104410000	0	104410000
GFAFVTFDDHDSVDK	199140000	0	199140000
GFAFVTFDDHDTVDK	113540000	0	113540000
GFAFVYFENVDDAK	3246800	0	3246800
GFALVGVGSEASSK	5108000	0	5108000
GFAVSER	100660000	4013400	96649000
GFCFITFK	65748000	0	65748000
GFCFLEYEDHK	61178000	0	61178000
GFDILGIKPVQR	18739000	0	18739000
GFDQDMANK	26981000	0	26981000
GFDVFNALDLMENK	1877700	0	1877700
GFELTFK	1067300	0	1067300
GFGFGLVK	38426000	0	38426000
GFGFVDFNSEEDAK	214610000	0	214610000
GFGFVLFK	7623800	0	7623800
GFGFVSFER	12224000	0	12224000
GFGFVTFDDHDPVDK	183170000	0	183170000

GFIGPGIDVPAPDMSTGER	49793000	0	49793000
GFLNSSELSGLPAGPDR	10249000	0	10249000
GFPTDATLDDIK	0	0	0
GFQEDSEIR	2793100	0	2793100
GFQEVVTPNIFNSR	7945400	0	7945400
GFSIPECQK	27356000	0	27356000
GFTIPEAFR	25593000	0	25593000
GFVEIQTPK	7495200	0	7495200
GFVPSPTSQPGGHESLVDR	0	0	0
GFVQVDDGR	22808000	0	22808000
GGADLFVENMPGFPDNIR	10444000	0	10444000
GGADVNIR	22139000	0	22139000
GGDCLTSQTR	6298900	0	6298900
GGEIQPVSVK	106160000	0	106160000
GGELVYTDSEAR	2683100	0	2683100
GGGPAGAGGEAPAALR	14646000	0	14646000
GGIMLPEK	45973000	0	45973000
GGIVGMTLPIAR	70526000	0	70526000
GGKPEPPAMPQPVPTA	29817000	0	29817000
GGLGYVEETSEFEAR	0	0	0
GGLQEVAEQLELER	0	0	0
GGPEVQQVPAGER	27563000	0	27563000
GGPNYQEGLR	39694000	0	39694000
GGSWIQEINVAEK	47359000	0	47359000
GGVVGIK	0	0	0

GGWGISPR	18314000	0	18314000
GGYFDEFGIIR	8834900	0	8834900
GHLENNPALEK	394780000	0	394780000
GHYTEGAELVDSVLDVVR	0	0	0
GIAAQPLYAGYCNHENM	0	0	0
GIAPGDER	60432000	1445100	58987000
GIATNDVGIQK	3447700	0	3447700
GICECGVCK	3442700	0	3442700
GIDPFSLDSLAK	36596000	0	36596000
GIEMSEVR	0	0	0
GIFGFTDSDCIGK	170040000	0	170040000
GIFGSSAVPQPK	0	0	0
GIIGYDV	0	0	0
GILAADESTGSIAK	16088000	0	16088000
GILEQGWQADSTTR	569580	0	569580
GINAGQLPAPK	55674000	0	55674000
GIQEEMEALVK	10827000	0	10827000
GISCMNTTLSESPFK	38169000	0	38169000
GISDPLTVFEQTEAAAR	0	0	0
GISEETTTGVHNLYK	46567000	0	46567000
GISLNPEQWSQLK	25678000	0	25678000
GISQEQMQEFR	18648000	0	18648000
GITFDSGGISIK	0	0	0
GITPLLER	12763000	0	12763000
GIVDQSQQAYQEAFEISK	971480000	6373000	965110000

GIVFEDVK	2034300	0	2034300
GIVLLEELLPK	16591000	0	16591000
GIVNEQFLLQR	31589000	0	31589000
GIYAVGDVCGK	0	0	0
GIYFADMVSK	74329000	0	74329000
GLALGIAK	0	0	0
GLALWEAYR	4801800	0	4801800
GLAPDLPEDLYHLIK	43162000	0	43162000
GLCAIAQAESLR	62907000	0	62907000
GLDNTEFQGK	2210500	0	2210500
GLEALLADPQQK	0	0	0
GLEVTAYSPLGSSDR	9858000	0	9858000
GLFDEYGSK	0	0	0
GLFIIDDK	68952000	0	68952000
GLFIIDGK	28870000	0	28870000
GLFTGLTPR	0	0	0
GLGAGAGAGEESPATSLPR	14433000	0	14433000
GLGDCLVK	397250000	0	397250000
GLGILSLK	0	0	0
GLLLYGPPGTGK	0	0	0
GLLPQLLGVAPEK	56817000	0	56817000
GLLQTEPQNNQAK	61868000	0	61868000
GLNVDQLNMLGEK	8140700	0	8140700
GLQEGYENSR	0	0	0
GLQQQNSDWYLK	0	0	0

GLQTSQDAR	1613500	0	1613500
GLSEDVSISK	7041500	0	7041500
GLSFSEATASNLVK	0	0	0
GLSSLLCNFTK	53122000	0	53122000
GLSSLLYGSIPK	6557000	0	6557000
GLTPSQIGVILR	106780000	0	106780000
GLTSVINQK	794440000	0	794440000
GLVEPVDVVDNADGTQTVNYVPSR	0	0	0
GLVGEIIK	64361000	0	64361000
GLVGEIIKR	0	0	0
GLVLGPIHK	15558000	0	15558000
GLYCYELDEK	11588000	11588000	0
GLYDGPVCEVSVTPK	28247000	0	28247000
GMGLSLMR	0	0	0
GMSAEYSFPIWK	4732900	0	4732900
GMTSLQCDCTEK	6076600	0	6076600
GMTTVDDFFQGTK	147100000	0	147100000
GMYDGPVFDLTTTPK	164340000	0	164340000
GNAGGIQPDLLISLTAPK	37678000	0	37678000
GNDIIAAAK	14633000	0	14633000
GNDISSGTVLSDYVGSGPPK	114280000	0	114280000
GNDTPLALESTNTEK	6836000	0	6836000
GNEFFCEVDEDYIQDK	5969100	0	5969100
GNEIVLSAGSTPR	19359000	0	19359000
GNENANGAPAITLLIR	18763000	0	18763000

GNILIPGINEAVAAVTEEEHK	4071500	0	4071500
GNLANVIR	141560000	0	141560000
GNPTVEVDLFTSK	65406000	0	65406000
GNVGFVFTK	0	0	0
GPAAAQGSAAAPAEPK	28762000	0	28762000
GPCIIYNEDNGIIK	0	0	0
GPCVSENEIGTGGTCQWK	2803500	0	2803500
GPDGLTAFEATDNQAIK	8277200	0	8277200
GPDWILGEIK	53112000	0	53112000
GPFADENFK	24372000	0	24372000
GPGDGAEEDEAASGGPGGR	11840000	0	11840000
GPGLYYVDSEGNR	42160000	0	42160000
GPLGPNWK	8995600	0	8995600
GPLMMYISK	28965000	0	28965000
GPNSEDLNR	917150	0	917150
GPNVVGPYGLLQPFADAMK	6869500	0	6869500
GPPCGPVNCNEK	4416000	0	4416000
GPQLVCTGSDDGTVK	6374500	0	6374500
GPSGCVESLEVTCR	4840300	0	4840300
GPSGGGEEPALSQYQR	8000100	0	8000100
GPSSVEDIK	86262000	0	86262000
GPVEGYEENEEFLR	0	0	0
GPVFAGDVSSSVR	6085400	0	6085400
GPWTCVGDMNR	6593400	0	6593400
GQAFVIFK	42173000	0	42173000

GQAVDYEGSR	56925000	0	56925000
GQCDLELINVCNENSLFK	2235100	0	2235100
GQESAGIVTSDGSSVPTFK	0	0	0
GQEVETSVTYYR	11429000	0	11429000
GQFSTDELVAEVEK	164740000	0	164740000
GQFSTDELVAEVEKR	32562000	0	32562000
GQGSMDEGTADER	7465300	0	7465300
GQGSVSASVTEGQQNEQ	0	0	0
GQISETLK	6895200	0	6895200
GQLCELSCSTDYR	33682000	0	33682000
GQLESIVENIR	40461000	0	40461000
GQQQVFK	7576800	0	7576800
GQTPGGAQFVGLELYK	15717000	0	15717000
GQVLNIQMR	19242000	0	19242000
GSAITGPVAK	52564000	0	52564000
GSAPPGPVPEGSIR	85392000	0	85392000
GSDFDCELR	100820000	0	100820000
GSELQLPFQACLK	0	0	0
GSELQNYFTK	0	0	0
GSFSEQGINEFLR	220980000	0	220980000
GSIDEVDKR	12222000	0	12222000
GSIVWQEVFDDK	4976000	0	4976000
GSLESPATDVFGSTEEGEKR	0	0	0
GSLLFTAGPLEEER	15848000	0	15848000
GSLVAPDR	10746000	0	10746000

GSNSLPLLR	19060000	0	19060000
GSNTCELIFEDCK	2146200	0	2146200
GSNTIASAAADK	62793000	0	62793000
GSPLVVISQGK	45544000	0	45544000
GSSASLVLK	162140000	0	162140000
GSSDVDQLGK	13516000	0	13516000
GSTAPVGGGAFPTIVER	139560000	0	139560000
GSVSCPTCQAVGR	1555200	0	1555200
GTAFGGWK	0	0	0
GTAVAICR	0	0	0
GTAVVNGEFK	115240000	0	115240000
GTAYVVYEDIFDAK	24207000	0	24207000
GTDIMYTGTLDCWR	32597000	0	32597000
GTEASSGTEAATGLEGEEK	4934500	0	4934500
GTEDITSPHGIPLDLLDR	34660000	0	34660000
GTFDNAETK	25761000	0	25761000
GTGGVDTAATGGVFDISNLDR	37784000	0	37784000
GTGGVDTAAVGGVFDVSNADR	330400000	0	330400000
GTGIVSAPVPK	161330000	0	161330000
GTGLQPGEEELPDIAPPLVTPDEPK	20555000	0	20555000
GTIQVITQGTSLK	14104000	0	14104000
GTLDPVEK	51016000	0	51016000
GTMVTIEGPR	13673000	0	13673000
GTPLISPLIK	90586000	0	90586000
GTQVYSPEK	13161000	0	13161000

GTRDDEYDYLFK	30251000	0	30251000
GTTAVLTEK	50663000	0	50663000
GTVEPQLEAR	69943000	1750400	68192000
GTVQGQLQGPISK	10220000	0	10220000
GTYQGLTATVLK	0	0	0
GVAPLWMR	70405000	0	70405000
GVDDLDFFIGDEAIEKPTYATK	13829000	0	13829000
GVDIVMDPLGGSDTAK	165630000	0	165630000
GVDLHEQSQQNK	20091000	0	20091000
GVDLQENNPASR	191780000	0	191780000
GVDLTEPTQPTR	26123000	0	26123000
GVDLVLNSLAEEK	70053000	0	70053000
GVEAVGSYAENQR	17176000	0	17176000
GVEEEEEDGEMR	0	0	0
GVEEEEEDGEMRE	15925000	0	15925000
GVESVFDIMEMEDEER	1868300	0	1868300
GVETIANDVVSLATK	8017000	0	8017000
GVEWAAFGR	0	0	0
GVIDLIFEK	46947000	0	46947000
GVIQAIQK	116120000	0	116120000
GVLFGVPGAFTPGCSK	67544000	0	67544000
GVNEDTYSGILDCAR	9721700	0	9721700
GVNLPGAAVDLPAVSEK	3337200	0	3337200
GVNTDSGSVCR	95638000	691690	94946000
GVPESLASGEGAGAGLPALDLAK	11565000	0	11565000

GVQVETISPGDGR	0	0	0
GVSAIVYMVDAADQEK	4901800	0	4901800
GVTCLSFSK	7655000	0	7655000
GVTFNVTTVDTK	0	0	0
GVTQYYAYVTER	3522500	0	3522500
GVTSILPVLR	11856000	0	11856000
GVVDSDDLPLNVSR	205470000	0	205470000
GVVDSEDLPLNISR	2578800000	98630000	2480200000
GVVEVTHDLQK	44678000	0	44678000
GVVPLAGTDGETTTQGLDGLSER	2710700	0	2710700
GVVPLAGTNGETTTQGLDGLSER	29873000	0	29873000
GWDENVYYTVPLVR	13767000	0	13767000
GWEEGVAQMSVGQR	9810600	0	9810600
GWPLELLCEK	199990000	0	199990000
GWPLYLSTK	19179000	0	19179000
GYAFNHSADFETVR	10135000	0	10135000
GYAVLGGER	94714000	0	94714000
GYDVIAQAQSGTGK	48381000	0	48381000
GYGFVHFETQEAAER	0	0	0
GYGLFAGPCK	0	0	0
GYIWNYGAIPQTWEDPGHNDK	3472600	0	3472600
GYLGPEQLPDCLK	508450000	0	508450000
GYPTLLLFR	5305500	0	5305500
GYSFTTTAER	103880000000	0	1.0388E+10
GYSYDLEVEQAYDLAR	3929400	0	3929400

HALIIYDDLSK	1772000	0	1772000
HASNMLGELR	6876900	0	6876900
HAYTLNNNSTTK	2154600	2154600	0
HCECSTDEVNSEDMDAYCR	24737000	0	24737000
HCLLTCEECK	0	0	0
HCNMVLENVK	57986000	0	57986000
HEEFEEGCK	23513000	0	23513000
HEELMLGDPCLK	0	0	0
HEGLGAFYK	28971000	0	28971000
HELIEFR	22565000	0	22565000
HEQEYMEVR	9855300	0	9855300
HEQNIDCGGGYVK	277920000	0	277920000
HESQMDSVVK	7171100	0	7171100
HETLTSLNLEK	0	0	0
HFCPNVPIILVGNK	1683200	0	1683200
HFILDECDK	20105000	0	20105000
HFIMQVVCEATQCPDTR	30659000	0	30659000
HFVALSTNTTK	99138000	0	99138000
HFVLDECDK	5543300	0	5543300
HGDLPDIQIK	0	0	0
HGESAWNLENR	50617000	0	50617000
HGLYLPTR	32197000	0	32197000
HGVESTLER	10207000	0	10207000
HGVIVAADSR	6258900	0	6258900
HIDLVEGDEGR	3770000	0	3770000

HIYYITGETK	385520000	99268000	286250000
HLIPAANTGESK	441760000	0	441760000
HLLPVETQR	46133000	0	46133000
HLMDPQVLEFLGSR	31005000	0	31005000
HLQLAIR	238730000	0	238730000
HLSVNDLPVGR	0	0	0
HLTDAYFK	80574000	0	80574000
HLTGEFEK	444590000	0	444590000
HLTYENVER	3727200	0	3727200
HLVDEPQNLIK	67839000	67839000	0
HLYTLDGGDIINALCFSPNR	715680	0	715680
HMLPSGFR	18977000	0	18977000
HNDLDDVGK	0	0	0
HNDMPIYEAADK	5215100	0	5215100
HNLQDFINIK	2084200	0	2084200
HNQLPLVIEFTEQTAPK	68926000	0	68926000
HPDASVNFSEFSK	2501300	0	2501300
HPDSSVNFAEFSK	6809400	0	6809400
HPHDIIDDINSGAVECPAS	0	0	0
HPYFYAPELLYYANK	15568000	15568000	0
HQAQIDQYLGLVR	23054000	0	23054000
HQEGEIFDTEK	7855500	0	7855500
HQGVMVGMGQK	1995000000	20551000	1974500000
HQNVQLPR	194970000	0	194970000
HQPTAIIAK	39922000	0	39922000

HSGNITFDEIVNIAR	29462000	0	29462000
HSQFIGYPITLY	0	0	0
HSSLAGCQIINYR	35532000	0	35532000
HSSLITPLQAVAQR	2137400	0	2137400
HSTENDSPTNVQQ	0	0	0
HTGPGILSMANAGPNTNGSQFFICTAK	3176200	0	3176200
HTLADNFNPVSEER	4204400	0	4204400
HTLNQIDSVK	25877000	25877000	0
HVFGESDELIGQK	121900000	0	121900000
HVGMAVAGLLADAR	33100000	0	33100000
HVMDGSLPTSLK	2771200	0	2771200
HVQLLGR	20782000	0	20782000
HVTFNQVK	95993000	0	95993000
HVTNPAFTK	20864000	0	20864000
HWGGNVLGPK	0	0	0
HYFQNTQGLIFVVDSNDR	4315100	0	4315100
HYGGLTGLNK	89662000	0	89662000
HYGPGWVSMANAGK	24670000	0	24670000
HYLFDVQR	20015000	0	20015000
IAAAILNTPDLR	38886000	0	38886000
IAAANGIGR	0	0	0
IAAEIAQAEEQAR	5544400	0	5544400
IAAYLFK	13181000	0	13181000
IAAYLQSDQFCK	8891300	0	8891300
IACTTLCPVDGR	4135400	0	4135400

IADDKYNDTFWK	11931000	0	11931000
IADISQVYTQNAEMR	2385300	0	2385300
IAEFTTNLTEEEEK	0	0	0
IAEGAQQGDPLSR	4503200	0	4503200
IAEVDCTAER	11999000	0	11999000
IAFAITAIK	14365000	0	14365000
IAFGGETDEATR	27698000	0	27698000
IAGQVAAANK	15036000	0	15036000
IAIPGLAGAGNSVLLVSNLNPER	0	0	0
IAIVNHDK	9279900	0	9279900
IAIYELLFK	14042000	0	14042000
IALLPLLQAETDR	4751300	0	4751300
IALTDNALIAR	150740000	0	150740000
IALYETPTGWK	6232400	0	6232400
IALYGLGSIPDER	4701400	0	4701400
IANPDQLLTQDVEK	4973700	0	4973700
IAPPEAPVTGYMFGK	3281400	0	3281400
IAPYSVEIK	42372000	0	42372000
IAQGVSGSIQDK	7308100	0	7308100
IASPEGQDYLK	15571000	0	15571000
IATEAIENFR	19944000	0	19944000
IATGQIAGVDK	0	0	0
IATGSFLK	130250000	1623100	128630000
IAVAAQNCYK	329940000	0	329940000
IAVEPVNPSELPK	2746500	0	2746500

IAVVGEGR	12006000	0	12006000
ICDDELILIK	5619400	0	5619400
ICDVYNAVMDVVK	18881000	0	18881000
ICGDIHGQYTDLLR	0	0	0
ICGDIHGQYYDLLR	9763800	0	9763800
ICLDILK	18932000	0	18932000
IDATSASVLASR	30891000	0	30891000
IDDMTAAPMDVR	29852000	0	29852000
IDELEPR	155960000	0	155960000
IDFYFDENPYFENK	7714900	0	7714900
IDGGITGNMR	19228000	0	19228000
IDGLLIDQIQR	2687900	0	2687900
IDIIPNPQER	58146000	0	58146000
IDINMSGFNETDDLKR	0	0	0
IDISNVK	114940000	0	114940000
IDISPVLLQK	21756000	0	21756000
IDKTDYMVGSYGPR	32032000	0	32032000
IDNLDVNR	34777000	0	34777000
IDNSQVESGSLEDDWDFLPPK	9176600	0	9176600
IDNSQVESGSLEDDWDFLPPKK	29010000	0	29010000
IDPLAPLDK	14984000	0	14984000
IDTIEIITDR	95635000	1337000	94298000
IDVFSPVEFNK	4577000	0	4577000
IDYGEYMDK	40143000	0	40143000
IEAINQAIANEYEVR	0	0	0

IEALQNHENESVYK	13728000	0	13728000
IECDDKGDGSCDVR	44191000	0	44191000
IEDFLER	0	0	0
IEDGNDFGVAIQEK	20852000	0	20852000
IEDGNNFGVAVQEK	8017100	0	8017100
IEDLSQQAQLAAAEK	28675000	0	28675000
IEDYFPEFAR	22957000	0	22957000
IEEELGSK	0	0	0
IEELDQENEAALENGIK	0	0	0
IEESDQGPYAIILAPTR	0	0	0
IEEVPELPLVVEDK	61564000	0	61564000
IEFISTMEGYK	34731000	0	34731000
IEGDETSTEAATR	24981000	0	24981000
IEGDMIVCAAYAHELPK	150410000	0	150410000
IEGLLAAFPK	2900700	0	2900700
IEGTPLETIQK	20738000	0	20738000
IEIEQNYAK	5301300	0	5301300
IEISELNR	17695000	17695000	0
IENLCAMGFDR	0	0	0
IENSLTYSK	2336100	0	2336100
IENVVLDANCSR	5517000	0	5517000
IENVVLVVPVK	0	0	0
IEPSPYK	7136600	0	7136600
IEPSVNFLK	26549000	0	26549000
IEQLQNHENEDIYK	38867000	0	38867000

IETIEVMEDR	71661000	0	71661000
IETQDIQALR	0	0	0
IEVEKPFAIAK	0	0	0
IEVIEIMTDR	88862000	0	88862000
IEVLQQHENEDIYK	11718000	0	11718000
IEWLESHQDADIEDFK	123660000	0	123660000
IEYDCELVPR	5879900	0	5879900
IEYNDQNDGSCDVK	17665000	0	17665000
IEYQFFEDR	926830	0	926830
IEYVTVTPEGFR	1968000	0	1968000
IFANTESYLK	15760000	0	15760000
IFAPNHVVAK	14090000	0	14090000
IFAQDGEGQR	34622000	1099100	33523000
IFCCHGGLSPDLQSMEQIR	183520000	0	183520000
IFFAGDTIPK	8619900	0	8619900
IFFDDYVACCVK	1696900	0	1696900
IFGGLDMLAEK	125550000	0	125550000
IFGPIWNR	18144000	0	18144000
IFGVTTLDIVR	427970000	9315400	418650000
IFIGTFK	0	0	0
IFNETPINPR	0	0	0
IFNLYPR	10524000	0	10524000
IFSIVEQR	5217200	0	5217200
IFSQETLTK	15113000	0	15113000
IFTSIGEDYDER	0	0	0

IFVFEPPPGVK	50850000	0	50850000
IFVGGIKEDTEEYNLR	0	0	0
IFVGGLSPDTPEEK	15392000	0	15392000
IFYPETTDIYDR	2871100	0	2871100
IGADFLAR	0	0	0
IGAEVYHNLK	67657000	0	67657000
IGAFGYMECSAK	15746000	0	15746000
IGALEGYR	290030000	0	290030000
IGASFLQR	40982000	2595600	38386000
IGASTLLSDIER	0	0	0
IGAVNCGDDR	8653600	0	8653600
IGDEDVGR	447110000	12578000	434530000
IGDELDSNMELQR	7618700	0	7618700
IGDLQAFQGHGAGNLAGLK	106060000	0	106060000
IGDTPMVR	75856000	0	75856000
IGDVVGSSGANQQTSGK	2335700	0	2335700
IGEHTPSALAIMENANVLAR	0	0	0
IGFFQGDIR	2242300	0	2242300
IGGIGTVPVGR	880980000	24288000	856690000
IGGVQQDTILAEGLHFR	32024000	0	32024000
IGHPAPNFK	10465000	0	10465000
IGIFGQDEDVTSK	0	0	0
IGIIDGEYVVNPTR	0	0	0
IGIIGGTGLDDPEILEGR	0	0	0
IGLETSLR	11256000	0	11256000

IGLFYMDNDLITR	4662300	0	4662300
IGLGTLQPWLHAAAR	0	0	0
IGLINDMVR	26343000	0	26343000
IGNCPFSQR	10798000	0	10798000
IGPITPLEFYR	102640000	0	102640000
IGPLGLSPK	92047000	0	92047000
IGPYQPNVPVGIDYVIPK	14085000	0	14085000
IGSLIDVNQSK	109660000	0	109660000
IGTDIQDNK	9060900	0	9060900
IGTVTSGCPSPSLK	6224200	0	6224200
IGVLDEGK	319830000	0	319830000
IGVNQPK	6209400	0	6209400
IGVVGGSDFEK	0	0	0
IHCLENVDK	18553000	0	18553000
IHFPLATYAPVISAEK	170130000	0	170130000
IHPVSTMVK	251060000	0	251060000
IHQETFGK	4729300	0	4729300
IHQIEYAMEAVK	3902000	0	3902000
IHVSDQELQSANASVDDSR	11987000	0	11987000
IIAEGANGPTTPEADK	25537000	0	25537000
IIAEGANGPTTPEADKIFLER	3440000	0	3440000
IIAPPER	8041000000	241640000	7799400000
IIAQCLNK	19843000	0	19843000
IICAQQCSGR	10433000	616050	9817400
IIDDSEITKEDDALWPPPDR	42053000	0	42053000

IIDGLLVMR	21274000	0	21274000
IIDISDVFR	14819000	0	14819000
IIDSLFNTVTDK	25014000	0	25014000
IIDVVYNASNNELVR	85657000	0	85657000
IIEDCSNSEETVK	3227500	0	3227500
IIENELEGFGIR	4957400	0	4957400
IIEVGDTPK	151370000	4283800	147080000
IIEVSGQK	29841000	0	29841000
IIFDDFR	49567000	0	49567000
IIGLDQVAGMSETALPGAFK	1207400	0	1207400
IIHEDGYSEDECK	15835000	0	15835000
IIIPEIQK	17609000	0	17609000
IILDLISESPIK	35823000	0	35823000
IILLAEGR	30142000	0	30142000
IINDLLQSLR	10764000	0	10764000
IINDNATYCR	23774000	0	23774000
IINEPTAAAIAYGLDK	171330000	0	171330000
IINEPTAAAIAYGLDKK	44615000	0	44615000
IINNTENLVR	116650000	2624200	114030000
IINPMGLLVEELK	1332400	0	1332400
IIPGFMCQGGDFTR	2558400000	69832000	2488600000
IIPLVVK	0	0	0
IIPTLEEYQHYK	0	0	0
IIQFNPGPEK	20790000	0	20790000
IIQLIEGK	20142000	0	20142000

IIQLLDDYPK	1039200000	1906700	1037300000
IISDNLTYCK	22476000	0	22476000
IISNASCTTNCLAPLAK	1099400000	1224500	1098200000
IISSIEQK	0	0	0
IITEGASILR	0	0	0
IITHPNFNGNTLDNDIMLIK	184200000	184200000	0
IITIPPFLAYGEDGDGK	1866600	0	1866600
IITSELYR	0	0	0
IIVDELK	0	0	0
IIVDELKQEVISTSSK	222900000	0	222900000
IIVLGLLPR	16015000	0	16015000
ILADAAAEGVPVR	26153000	0	26153000
ILADNPR	23899000	2939000	20960000
ILAQVVGDVDTSLPR	0	0	0
ILATPPQEDAPSVDIANIR	82145000	0	82145000
ILCQEEQDAYR	2820800	0	2820800
ILDAVVAQEPLHR	3641400	0	3641400
ILDDWGETCK	17199000	0	17199000
ILDGMFAICGVSDSK	20778000	0	20778000
ILDIDNVDLAMGK	20193000	0	20193000
ILDILGETCK	0	0	0
ILDWHVANTDK	13412000	0	13412000
ILDYSCSQDR	7883200	3364100	4519100
ILEAHQNVAQMSLIEAK	16725000	0	16725000
ILEAWEMNEK	0	0	0

ILEDDLK	6441900	0	6441900
ILEFFGLK	159650000	0	159650000
ILELDQFK	0	0	0
ILEPPEGQDEGVWK	0	0	0
ILFEDFR	10102000	0	10102000
ILFFNTPK	65105000	0	65105000
ILFIFIDSDHTDNQR	2419900	0	2419900
ILFNNAVK	30821000	0	30821000
ILGIPVIVTEQYPK	249670000	0	249670000
ILGLLDAYLK	30873000	0	30873000
ILGPGLNK	492960000	1072800	491880000
ILGTAGTEEGQK	40855000	0	40855000
ILIEDWK	6507300	0	6507300
ILILGLDGAGK	48140000	0	48140000
ILILQGLK	15537000	0	15537000
ILITTVPPNLR	9850500	0	9850500
ILLEAAR	12957000	0	12957000
ILLLGLDNAGK	30244000	0	30244000
ILLNYLPLER	1723100	0	1723100
ILMLGLDAAGK	51696000	0	51696000
ILMVGLDAAGK	215210000	0	215210000
ILNPEEIEK	27332000	0	27332000
ILPDILK	28758000	0	28758000
ILPEQGLMLTGSADK	8448600	0	8448600
ILPTLEAVAALGNK	135470000	0	135470000

ILQDIASGSHPFSQVLK	3892800	0	3892800
ILQEDPTNTAAR	2528700	0	2528700
ILQEYITQEGHK	0	0	0
ILQVSFK	0	0	0
ILSFIQDQEEDYLK	3028900	0	3028900
ILSGVVTK	17411000	0	17411000
ILTDYGFEGHPFR	35985000	0	35985000
ILTFDQLALDSPK	97068000	0	97068000
ILTGLNYEAPK	19255000	0	19255000
ILTTSEDSNAQEIK	6803400	0	6803400
ILVATNLFGR	35303000	0	35303000
ILYLTPEQEK	24109000	0	24109000
ILYMTDEVNDPSLTIK	49914000	0	49914000
IMADNPSWDGEK	7290400	0	7290400
IMASSPDMDLATVSALR	10114000	0	10114000
IMCCVAQQASEK	14763000	0	14763000
IMDCVGCFK	24295000	0	24295000
IMEFTTTLLNTSPEGWK	4872500	0	4872500
IMEIVDAITTTAQSHQR	18136000	0	18136000
IMGPNYTPGK	45387000	0	45387000
IMLEDGNLHVTQGAGR	0	0	0
IMLGDEAALLEQK	37974000	0	37974000
IMLPGVLR	56063000	0	56063000
IMLPWDPTGK	28589000	0	28589000
IMMLSVLK	11954000	0	11954000

IMQVVDEK	0	0	0
IMVDMLDSDGSGK	0	0	0
INDALSCEYECR	0	0	0
INDFVLSPGPQPYK	9441300	7113300	2327900
INELMPK	16174000	0	16174000
INEWLTLVEK	92985000	0	92985000
INFYCPGSALGR	3625500	0	3625500
INGSALSPHPGLR	476260000	0	476260000
INISEGNCPER	104200000	0	104200000
INMNGINNSSGMVDAR	0	0	0
INMNGVNSSNGVVDPR	6294300	0	6294300
INNFSADIK	13286000	0	13286000
INQILMEK	9663700	0	9663700
INQLYEQAK	63517000	0	63517000
INSAPQQIEVFPPFR	10204000	0	10204000
INSITVDNCK	50910000	0	50910000
INTQEYLDVLGR	10074000	0	10074000
INVLAAQYQSLLNSYGEPVDDK	2464100	0	2464100
INVSGLTTK	12236000	0	12236000
INYTEGR	163810000	0	163810000
IPALDLLIK	31319000	0	31319000
IPDEIIDMVK	21656000	0	21656000
IPDPEAVKPDDWDEDAPAK	5385200	0	5385200
IPDWFLNR	99971000	0	99971000
IPDYLWMGLDGMK	4472100	0	4472100

IPEGLFDPSNVK	1699400	0	1699400
IPEISIQDMTAQVTSPSGK	2094800	0	2094800
IPETLEEDQQFMLK	7637200	0	7637200
IPGGIIEDSCVLR	8142200	0	8142200
IPGLLGVFQK	21406000	0	21406000
IPGSPPESMGR	84410000	0	84410000
IPLLSDLTHQISK	15205000	0	15205000
IPLNNGAGCR	0	0	0
IPLNTEQK	25028000	0	25028000
IPNPDFFEDLEPFR	23146000	0	23146000
IPSEQEQLR	11024000	0	11024000
IPVDTYNNILTVLK	7019000	0	7019000
IPVENILGEVGDGFK	5259900	0	5259900
IQASTMAFK	11021000	0	11021000
IQDFNDTFYR	4481900	0	4481900
IQDKEGIPPDQQR	232390000	0	232390000
IQEAGTEVVK	691450000	0	691450000
IQEEGTEVELTGK	14718000	14718000	0
IQEGVFDINNEANGIK	0	0	0
IQEPNTFPAILR	35552000	0	35552000
IQEVADELQK	60735000	0	60735000
IQFVGACNPPTDPGR	0	0	0
IQGLTVEQAEAVVR	0	0	0
IQLIFER	3092100	0	3092100
IQLINNMLDK	72551000	0	72551000

IQLLVFK	9377600	0	9377600
IQLQDAGR	12284000	0	12284000
IQNTLHCCGVTDYR	16906000	0	16906000
IQQEIAVQNPLVSER	0	0	0
IQQGALELLR	2657200	0	2657200
IQQLAISGLK	10226000	0	10226000
IQSGQCLR	26142000	0	26142000
IQSLLDIQEK	0	0	0
IQSTVTQPGGK	14456000	0	14456000
IQTLTSSVR	20880000	0	20880000
IQTQPGYANTLR	25206000	0	25206000
IQVLQQQADDAEER	6585500	0	6585500
IRDEMVATEQER	16621000	0	16621000
ISAPQER	16019000	0	16019000
ISATSIFFESMPYK	38904000	0	38904000
ISAVSVAER	138700000	3447500	135250000
ISDDLMQK	12506000	0	12506000
ISDEDWDIIHR	0	0	0
ISDIQSQLEK	32578000	0	32578000
ISEACSLAQQSGDHR	3530800	0	3530800
ISEQFTAMFR	462860000	10770000	452090000
ISESPSEIMESLTK	3346100	0	3346100
ISGAIGPCVSLNSK	0	0	0
ISGETIFVTAPHEATAGIIGVNR	23468000	0	23468000
ISGLIYEETR	701940000	4408700	697530000

ISLGLPVGAVINCADNTGAK	177470000	0	177470000
ISLQAIQQLVR	11260000	0	11260000
ISNYGWDQSDK	33835000	0	33835000
ISSDLDGHPVPK	58957000	0	58957000
ISSIQSIVPALEIANAHR	141500000	0	141500000
ISSMVVMENVGQQK	978490	0	978490
ISSTLYQAAAPVLTPAK	1136800	0	1136800
ISVAAASK	27024000	0	27024000
ISVGSDSDLVIWDPDAVK	14172000	0	14172000
ISVNDFIIK	33874000	0	33874000
ITADLLSNGIDVYPQK	1421400	0	1421400
ITAEEMYDIFGK	36547000	0	36547000
ITAFVVER	0	0	0
ITCLCQVPQNAANR	9972000	0	9972000
ITDGTMLQAIER	4591500	0	4591500
ITDVALDFWR	10351000	0	10351000
ITEFCHR	37445000	0	37445000
ITENIGCVMTGMTADSR	6117700	0	6117700
ITFDDYIACCVK	55632000	0	55632000
ITFDVAPSR	7943700	0	7943700
ITIADCGQLE	0	0	0
ITITNDK	371390000	3436500	367950000
ITITNDQNR	0	0	0
ITLPVDFVTADK	57794000	0	57794000
ITLPVDFVTADKFDENAK	382210000	0	382210000

ITNNINVLIK	0	0	0
ITNQVHGLK	10617000	0	10617000
ITNQVIYLNPPIEECR	1186100	0	1186100
ITPSYVAFTPEGER	0	0	0
ITQDIFQQLLK	4363600	0	4363600
ITSAPDMEDILTESEIK	0	0	0
ITSDEPLTK	27190000	0	27190000
ITSEALLVTQQLVK	35067000	0	35067000
ITSEMGSASQANIR	10102000	0	10102000
ITSPLMEPSSIEK	0	0	0
ITVPGNFQGHSGAQCITCSYK	18825000	0	18825000
ITVTSEVPFSK	54965000	0	54965000
ITWSNPPAQGAR	9105700	0	9105700
IVADKDYSVTANSK	685340000	0	685340000
IVAERPGTNSTGPAPMAPPR	3950200	0	3950200
IVALSSSLSNAK	16466000	0	16466000
IVASTLSNPELFEEWTGNVK	14888000	0	14888000
IVAVTGAEAQK	69036000	0	69036000
IVCTPGQGLGDLR	8199700	0	8199700
IVDDWANDGWGLK	124840000	0	124840000
IVEDEPNKICEADR	23288000	0	23288000
IVEMSTSK	251950000	0	251950000
IVEPPENIQEK	12632000	0	12632000
IVEWNGK	87128000	0	87128000
IVFNLCPLQTEDDK	16470000	0	16470000

IVFQEFR	11923000	3165000	8757600
IVGPSGAAVPCK	40619000	0	40619000
IVIGLFGK	22047000	0	22047000
IVILEYQPSK	85362000	0	85362000
IVIVPSLNPDGR	0	0	0
IVLANDPDADR	39684000	0	39684000
IVLDNSVFSEHR	0	0	0
IVLEDGTLHVTEGSGR	9015300	0	9015300
IVLTNPVCTEVGEK	0	0	0
IVLVDDSIVR	0	0	0
IVNSAQTGSFK	61694000	0	61694000
IVNSSMELAQTAK	0	0	0
IVPGQFLAVDPK	54090000	0	54090000
IVPNVLLEQGK	45776000	0	45776000
IVQAEGEAEAAK	3835400	0	3835400
IVQMTEAEVR	31663000	0	31663000
IVVEMIK	0	0	0
IVVFQYSDGK	29714000	0	29714000
IVVLFYK	0	0	0
IVVNLTGR	96537000	0	96537000
IVVSNTPR	25081000	0	25081000
IVVVTAGVR	746730000	13444000	733290000
IVYLYTK	8884700	0	8884700
IWDLEGK	0	0	0
IWDTASGQCLK	27948000	0	27948000

IWGDCTVR	34425000	0	34425000
IYADTFGDINYQEFAK	25105000	0	25105000
IYAMHWGTDSR	11594000	0	11594000
IYANFFPYGDASK	23229000	0	23229000
IYDLNKPEAEPK	2865000	0	2865000
IYELAAGGTAVGTGLNTR	11491000	0	11491000
IYFMAGSSR	0	0	0
IYGISFPDPK	18896000	0	18896000
IYGLGSLALYEK	32607000	0	32607000
IYIGDQVQK	5006200	0	5006200
IYLDMLNVYK	16481000	0	16481000
IYLYLTK	0	0	0
IYNDDKNTYIR	9656600	0	9656600
IYQIYEGTSQIQR	0	0	0
IYQTEELR	0	0	0
IYSYVVSR	6253700	0	6253700
IYVISLAEPR	52003000	0	52003000
KACADATLSQITNNIDPVGR	0	0	0
KAEEIANEMIEAAK	0	0	0
KALAAAGYDVEK	8894500	0	8894500
KDCEVVMMIGLPGAGK	657010	0	657010
KDDEVQVVR	9798600	0	9798600
KDDPVTNLNNAFEVAEK	20857000	0	20857000
KDLYANTVLSGGTTMYPGIADR	667900000	0	667900000
KEAAENSLVAYK	4800500	0	4800500

KEGGLGPLNIPLLADVTR	1688600	0	1688600
KESYSVYVYK	65569000	0	65569000
KEVVEEAENGR	71172000	0	71172000
KGDIFLVR	0	0	0
KGIVDQSQQAYQEAFEISK	0	0	0
KIPNPDFFEDLEPFR	23206000	0	23206000
KITIADCGQLE	161910000	0	161910000
KLELSDNR	61936000	0	61936000
KPEDVLDDDDAGSAPLK	12160000	0	12160000
KPEDWDEEMDGEWEPPVIQNPEYK	23623000	0	23623000
KPITDDDVDR	9906400	0	9906400
KQSLGELIGTLNAAK	26739000	0	26739000
KQTIDNSQGAYQEAFDISK	0	0	0
KSDVEAIFSK	9436700	0	9436700
KVDWLTEK	0	0	0
KVEDMMK	85073000	0	85073000
KVESLQEEIAFLK	118240000	0	118240000
KVMDLCFSK	1360600000	0	1360600000
KVMHLQDVEVK	31252000	2330000	28922000
KVPQVSTPTLVEVSR	127250000	127250000	0
KVTGTLDANR	7097400	0	7097400
KYDAFLASESLIK	145150000	0	145150000
KYEDICPSTHNMDVPNIK	10568000	0	10568000
LAAIAESGVER	22396000	0	22396000
LAAIVAK	133870000	0	133870000

LAALNPESNTAGLDIFAK	25426000	0	25426000
LAASGEGGLQELSGHFENQK	15451000	0	15451000
LAATNALLNSLEFTK	127510000	0	127510000
LAAVDATVNQVLASR	94415000	0	94415000
LAAVVSACK	54977000	0	54977000
LACDVDQVTR	206350000	18869000	187480000
LACTSCTFVTSVGDAMAK	0	0	0
LADFGLAR	28921000	0	28921000
LAEAEETAR	4020000	0	4020000
LAECCIAANK	3268100	0	3268100
LAELCGVLK	0	0	0
LAEQAER	1256700	0	1256700
LAETVFNFQEK	5172800	0	5172800
LAETYLHR	5339700	0	5339700
LAEVGQYEQVK	23825000	0	23825000
LAFLNVQAAEEALPR	32581000	7071000	25510000
LAGEELAGEEAPQEK	3726500	0	3726500
LAGESESNLR	47977000	0	47977000
LAGFLDLTEQEFR	18054000	0	18054000
LAGTQPLEVLEAVQR	10275000	0	10275000
LALFNPDVCWDR	112670000	4057500	108610000
LALGDDSPALK	47835000	0	47835000
LALGIPLPELR	1890600	0	1890600
LALLAHPR	83760000	0	83760000
LAMQEFMILPVGAANFR	3445800	0	3445800

LANDAAQVK	26094000	0	26094000
LANILFTQELAR	16673000	0	16673000
LAPEYEK	12593000	0	12593000
LAPGTIVEVWK	0	0	0
LAPITSDPTEATAVGAVEASFK	9503100	0	9503100
LAQAAQSSVATITR	0	0	0
LAQFEPSQR	16216000	0	16216000
LAQLAGDHECGSSSQR	0	0	0
LAQLDDVK	75115000	0	75115000
LAQLEEAK	197250000	0	197250000
LAQMFSDMVLK	33637000	0	33637000
LAQQISDEASR	6283000	0	6283000
LAQVSPELLLASVR	13272000	0	13272000
LASALDLPLLR	0	0	0
LASDLLEWIR	23970000	0	23970000
LASEEPPDDEEALATIR	6207200	0	6207200
LASGEDDPFDSDFSCPVK	1213900	0	1213900
LASQANIAQVLAELK	14264000	0	14264000
LASTLVHLGEYQAAVDGAR	0	0	0
LASVLGSEPSLDSEVTSK	0	0	0
LATALQK	17830000	0	17830000
LATQLTGPVMPVR	20365000	0	20365000
LAVDEEENADNNTK	22154000	0	22154000
LAVEALSSLDGDLAGR	23986000	0	23986000
LAVNMVPFPR	540920000	0	540920000

LAVNNIAGIEEVNMIK	5787500	0	5787500
LAVSAQSEPAR	0	0	0
LAVVDPLFGMQPIR	63341000	0	63341000
LAYINPDLALEEK	10144000	0	10144000
LCAAAASILGK	7185200	0	7185200
LCDEQLSSQSHYDFGLR	0	0	0
LCFSTAQHAS	0	0	0
LCGDTSLNNMQR	48495000	0	48495000
LCGQDLNK	22699000	0	22699000
LCIEVTPQSK	0	0	0
LCLISTFLEDGIR	11747000	0	11747000
LCMSLMQNK	10356000	0	10356000
LCQIFSDLNATYR	1580800	0	1580800
LCSLFYTNEEVAK	0	0	0
LCSLLDSEDYNTCEGAFGALQK	16525000	0	16525000
LCTSATESEVAR	15624000	0	15624000
LCVLHEK	27033000	27033000	0
LCVQNSPQEAR	0	0	0
LCYDAFTENMAGENQLLER	2439800	0	2439800
LCYVALDFEQEMATAASSSSLEK	6283200	0	6283200
LCYYIGATDDAATK	0	0	0
LDDFVETGDIR	1775900	0	1775900
LDECEEAFQGTK	9043700	0	9043700
LDEFGEQLSK	11354000	0	11354000
LDELEELLTNNR	51696000	0	51696000

LDEQYQK	0	0	0
LDFGNSQGK	17441000	0	17441000
LDFVCSFLQK	22127000	0	22127000
LDGEASINNR	115100000	2728800	112370000
LDGFPLLR	11077000	0	11077000
LDGFSVLMR	22273000	0	22273000
LDGNLLTQPGQAR	0	0	0
LDHVVTIIK	14012000	0	14012000
LDILDMFTEIK	930790	0	930790
LDLQQGQNLLQGLSK	0	0	0
LDNLMLELDGTENK	5248600	0	5248600
LDNLVAILDINR	3191800	0	3191800
LDPHLVLDQLR	41437000	0	41437000
LDPSIFESLQK	4390000	0	4390000
LDQPMTEIVSR	13161000	0	13161000
LDQVSSEIK	0	0	0
LDSSAVLDTGK	77795000	0	77795000
LDTAMWLSR	5451500	0	5451500
LDTMNTTCVDR	69971000	0	69971000
LDVGNAEVK	41956000	0	41956000
LDVPQNLMFGK	27150000	0	27150000
LDVQFSGLTK	4942100	0	4942100
LDYGQHVVAGTPGR	41039000	0	41039000
LDYILGLK	140890000	0	140890000
LDYLSSLK	33982000	0	33982000

LEAADEGSGDVK	3166700	0	3166700
LEAEIATYRR	12782000	0	12782000
LEAGDYADLVK	3982500	0	3982500
LEAIEDDSVKETDSSSASAATPSK	0	0	0
LEALEEK	21000000	0	21000000
LEALSVK	16140000	0	16140000
LEATGELVDK	18430000	0	18430000
LECSEELGDLVK	0	0	0
LECVEPNCR	15868000	0	15868000
LEDCTPQR	62894000	0	62894000
LEDLVCDVVDR	51954000	0	51954000
LEDSEVR	17101000	0	17101000
LEEDAEMK	0	0	0
LEELTMDGAK	0	0	0
LEELYTK	78973000	0	78973000
LEEPESTK	7290000	0	7290000
LEETLPVIR	0	0	0
LEGGSGGDSEVQR	14120000	0	14120000
LEGNSPQGSNQGVK	3154700	0	3154700
LEGQGDVPTPK	12540000	0	12540000
LEGQMGEDGNSIK	9408000	0	9408000
LEGTNVQEAQK	6543600	0	6543600
LELEAAQK	14251000	0	14251000
LELFLPEEYPMAAPK	1779900	0	1779900
LELNYCVPMGVQTGDR	3612000	0	3612000

LEMDYYQLR	41703000	0	41703000
LEMYVLNPVK	0	0	0
LENDQIESLR	0	0	0
LENEHLNNCGEFR	7125500	0	7125500
LENGEIETIAR	0	0	0
LENPDEACAVSQK	1757900	0	1757900
LENYPIPEPGPNEVLLR	10702000	0	10702000
LEQGQAIDDLMPAQK	40561000	0	40561000
LEQLASR	95430000	0	95430000
LEQSEAQLGR	13112000	0	13112000
LESCGVTSDNCR	9120100	0	9120100
LESEEEGVPSTAIR	7111800	0	7111800
LETHMTPEMFR	23270000	0	23270000
LETLGIGQR	8807000	0	8807000
LEVEANNAFDQYR	3072800	0	3072800
LEVNIDR	131500000	0	131500000
LEVQATDREENK	1781900	0	1781900
LEYCEALAMLR	102520000	0	102520000
LFCVGFTK	23816000	0	23816000
LFDDCTQQFK	0	0	0
LFDFVNAK	32563000	0	32563000
LFDHPESPTPNPTEPLFLAQAEVYK	6426600	0	6426600
LFDSICNNK	42723000	0	42723000
LFEFAGYDVLR	45081000	8044700	37036000
LFEGNALLR	120230000	0	120230000

LFELLEK	22916000	0	22916000
LFEVGGSPANTR	0	0	0
LFFPVIYDVK	6015400	0	6015400
LFFVGSR	4777000	0	4777000
LFFWMQEPK	20471000	0	20471000
LFGAAEVQR	15660000	0	15660000
LFGNMEGDCPSDWK	0	0	0
LFGQESGPSAEK	30879000	0	30879000
LFGYEMAEFK	8032100	0	8032100
LFGYEPTIYYPK	105320000	0	105320000
LFIYNPTTGEFLGR	15443000	0	15443000
LFLAGYDPTPTMR	41950000	5429500	36521000
LFLNETQTQEITEDIPVK	12440000	0	12440000
LFLVQLQEK	52509000	0	52509000
LFNTAVCESK	12951000	0	12951000
LFPDTPLALDANK	5004700	0	5004700
LFPGFEIETVK	71071000	0	71071000
LFPNMLPSTFETQSLK	6581800	0	6581800
LFQECCPHSTDR	154020000	1022700	153000000
LFQEDDEIPLYLK	67034000	0	67034000
LFQPNLNMDR	17719000	0	17719000
LFQSNDQTLR	2390000	0	2390000
LFQSVAQCCMGQK	0	0	0
LFSDEAANIYER	5103300	0	5103300
LFSQETVMK	48605000	0	48605000

LFSSVTFETVEESK	0	0	0
LFTAESLIGLK	0	0	0
LFTEVEGTCTGK	20731000	0	20731000
LFTFHADICTLPDTEK	38003000	38003000	0
LFTLTALR	14370000	0	14370000
LFTTMELMR	25898000	0	25898000
LFVGNLPADITEDEFK	19599000	0	19599000
LFVGNLPPDITEEEMR	36789000	0	36789000
LFVGSIPK	16986000	0	16986000
LFVVPADEAQAR	8046400	0	8046400
LGAQALLGAAK	5287500	0	5287500
LGAVDESLSEETQK	41226000	0	41226000
LGAVFNQVAFPLQYTPR	3922800	0	3922800
LGDLLISQFSGPSAEQMCK	0	0	0
LGDLYEEEMR	36953000	0	36953000
LGDPEELMFQYFK	6314200	0	6314200
LGEDLNK	23055000	0	23055000
LGEHNIDVLEGNEQFINAAK	1650900000	1650900000	0
LGEHNIEVLEGNEQFINAAK	116600000	116600000	0
LGELPSWILMR	4967200	0	4967200
LGEMWNNLNDSEK	8581400	0	8581400
LGEMWNNTAADDK	1595700	0	1595700
LGEMWNNTAADDKQPYEK	233060000	0	233060000
LGEMWSEQSAK	57713000	0	57713000
LGEQVFGTTGK	0	0	0

LGEYGFQNALIVR	36518000	36518000	0
LGFEEFK	12509000	0	12509000
LGGIGQFLAK	111180000	0	111180000
LGGSLADSYLDEGFLLDK	10065000	0	10065000
LGGSPFGPAGTGK	66656000	0	66656000
LGGSPTSLGTWGSWIGPDHDK	16850000	0	16850000
LGGSQEDQIK	25053000	0	25053000
LGGTCVNVGCVPK	18480000	0	18480000
LGIGQSQEMNTLFR	28224000	0	28224000
LGIHEDSQNR	1538200000	34964000	1503200000
LGIHEDSTNR	1741400000	93951000	1647400000
LGLDYEER	15003000	0	15003000
LGLENAEALIR	34546000	0	34546000
LGLPPLTPEQQEALQK	17414000	0	17414000
LGLQNDLFSLAR	7119900	0	7119900
LGLSIPDLTPK	895970	0	895970
LGMLSPEGTCK	103230000	0	103230000
LGNNCVFAPADVTSEK	0	0	0
LGNPIVPLNIR	18383000	0	18383000
LGNTISSLFGGGTTPDAK	36479000	0	36479000
LGNYAGAVQDCER	8875100	0	8875100
LGPALATGNVVVMK	19322000	0	19322000
LGPEGELLIR	0	0	0
LGPLLDILADSR	9806600	0	9806600
LGPNDQYK	152550000	0	152550000

LGQASLGVIK	12507000	0	12507000
LGQEATVGK	15148000	0	15148000
LGQIYQSWLDK	38478000	0	38478000
LGSAVVTR	4578600	0	4578600
LGVELGLK	419750000	0	419750000
LGVENCYFPMFVSQSALEK	26573000	0	26573000
LGVIEDHSNR	756160000	9295400	746870000
LGVTANDVK	142310000	0	142310000
LGYILTCPSNLGTGLR	23123000	0	23123000
LGYTPVCR	50215000	0	50215000
LHEEGIIYR	6746400	0	6746400
LIAEEGVDSLNVK	0	0	0
LIAEQPPHLTPGIR	3725800	0	3725800
LIAINANDPEASK	8828900	0	8828900
LIANMPESGPSYEFHLTR	34687000	0	34687000
LIANNTTVER	0	0	0
LIAPVAEEEATVPNNK	3739100	0	3739100
LICCDILDVLDK	133570000	1167100	132400000
LIDDMVAQAMK	221500000	0	221500000
LIDDMVAQVLK	38730000	0	38730000
LIDFLESGK	0	0	0
LIDVLENR	0	0	0
LIEGLSHEVIVSAACGR	8701100	0	8701100
LIEVANLACSISNNEEGVK	3206300	0	3206300
LIFYDLR	12572000	0	12572000

LIINELSNVMEANAAR	12865000	0	12865000
LIINSLYK	57154000	0	57154000
LIIWDSYTTNK	195310000	0	195310000
LILDLSMK	17051000	0	17051000
LILIESR	149140000	0	149140000
LIMAMQTLIPIDEAK	6089400	0	6089400
LIPTLVSIMQAPADK	25666000	0	25666000
LIPVLVNGMK	0	0	0
LIQEQHPEEELIK	11854000	0	11854000
LIQESPTLSK	2420200	0	2420200
LIQQQLEK	11956000	0	11956000
LIQYCQSK	65159000	0	65159000
LISTLIYK	12977000	0	12977000
LISWYDNEFGYSNR	502160000	13140000	489020000
LITEDVQGK	110190000	6385600	103800000
LITPAEK	14592000	0	14592000
LITPAVVSER	204550000	0	204550000
LITTQQWLIK	64578000	0	64578000
LIVDEAINEDNSVVSLSQPK	68262000	0	68262000
LIVDHNIADYMTAK	11226000	0	11226000
LKDDEVAQLK	70194000	0	70194000
LKPDPNTLCDEFK	0	0	0
LLADQAEAR	79381000	0	79381000
LLAEMSSFCGDMEK	56594000	0	56594000
LLALNSLYSPK	31078000	0	31078000

LLAPDCEIIQEVGK	16686000	0	16686000
LLAQDQGQGAPLLEPAP	0	0	0
LLATGSQDR	10581000	0	10581000
LLCGLLAER	860320000	3229800	857090000
LLCTVAR	14333000	0	14333000
LLDEVFFSEK	147210000	0	147210000
LLDSITVPVAR	0	0	0
LLDSSTVTHLFK	23009000	0	23009000
LLDSWFTSTQEK	5931700	0	5931700
LLDVDNR	153680000	0	153680000
LLDVTGGLGTDELR	11183000	0	11183000
LLDYVPIGPR	5066000	0	5066000
LLEAAITPETK	7378800	0	7378800
LLEEALLR	24250000	0	24250000
LLEELEEGQK	9778600	0	9778600
LLEGEESR	146830000	0	146830000
LLELFPVNR	10093000	0	10093000
LLEPVLLLGK	31861000	0	31861000
LLEQGLR	168150000	0	168150000
LLESGDLSMSSIK	0	0	0
LLETECPQYIR	0	0	0
LLEVVQPCLQAAK	0	0	0
LLEVYDQLFK	31739000	0	31739000
LLEYDTVTR	48448000	0	48448000
LLFEGAGSNPGDK	8081500	0	8081500

LLFPAVDDNLLK	50825000	0	50825000
LLGAALPLLTK	3918000	0	3918000
LLGELLQDNAK	18611000	7146400	11464000
LLGMGDIEGLIDK	2684600	0	2684600
LLGPNASPDGLIPWTR	7893300	0	7893300
LLGQFSEK	41107000	0	41107000
LLGWIQNK	38542000	0	38542000
LLHVAVSDVNDDVR	0	0	0
LLIAAQK	10104000	0	10104000
LLIDEAILK	53450000	0	53450000
LLIEMEQR	284050000	0	284050000
LLILADMADVYK	15868000	0	15868000
LLILALER	3473500	0	3473500
LLIVSTTPYSEK	1874600	0	1874600
LLLDTFEYQGLVK	11026000	0	11026000
LLLIDWPELK	539010	0	539010
LLLIGDSGVGK	146800000	0	146800000
LLLLAGVDR	0	0	0
LLLLGAGESGK	51303000	0	51303000
LLLLGTGESGK	0	0	0
LLLNLAENPAMTR	8224500	0	8224500
LLLNNDNLLR	9779000	0	9779000
LLLNNGAK	107780000	1882300	105890000
LLLPGELAK	127750000	0	127750000
LLLPWLEAR	134600000	0	134600000

LLLQVQHASK	52651000	0	52651000
LLLSIPHSDLLDYPK	3913400	0	3913400
LLLSSETPIEGK	14507000	0	14507000
LLLWDTKTMK	0	0	0
LLMLGLDNAGK	0	0	0
LLMMAGIDDCYTSAR	23925000	0	23925000
LLNCSDFAFTDMTK	5788700	0	5788700
LLNDSGLTGSK	3942100	0	3942100
LLNFPTIVER	41759000	0	41759000
LLPDDPYEK	18911000	0	18911000
LLPEQLIK	3893800	0	3893800
LLPQLTYLDGYDR	1032100000	36314000	995810000
LLPQLTYLDGYDRDDK	46497000	0	46497000
LLQAPDTDLR	12243000	0	12243000
LLQDFFNGK	252530000	0	252530000
LLQDFFNGR	81814000	0	81814000
LLQQEEEIK	33952000	0	33952000
LLQSIGQAPESISEK	1942700	0	1942700
LLQTGQER	6481000	0	6481000
LLSEGADVNAK	7515400	0	7515400
LLSGGSVLDIIK	57105000	0	57105000
LLSLSSLYSPK	6420800	6420800	0
LLSNDEVTIK	64142000	0	64142000
LLSPTER	12391000	0	12391000
LLSQEPSNGISSDPTVFLDR	0	0	0

LLTAEADK	12282000	0	12282000
LLTDDGNK	43670000	0	43670000
LLTEEGQK	7612200	0	7612200
LLTFYNLADCIAEK	1274100	0	1274100
LLVGLVQSR	0	0	0
LLVPILLPEK	79308000	0	79308000
LLVSASQDGK	461340000	0	461340000
LLVTDMSDAEQYR	0	0	0
LLWIDTK	53763000	0	53763000
LLYEALVDCK	173330000	0	173330000
LLYFMMFLKR	20661000	0	20661000
LLYNNVSNFGR	7513500	0	7513500
LLYVTPEK	33364000	0	33364000
LMCPQEIVDYIADK	7626200	0	7626200
LMDEAVLALR	5003500	0	5003500
LMDEVAGIVAAR	86648000	0	86648000
LMDLLADSR	0	0	0
LMEDLDR	31226000	0	31226000
LMELFPANK	24677000	0	24677000
LMIEMDGTENK	7150300	0	7150300
LMLAQDEER	39153000	5813800	33339000
LMLISMANDLK	123120000	0	123120000
LMMDPLSGQNR	11689000	0	11689000
LMMDPLTGLNR	63682000	0	63682000
LMMLQSCSGPTCR	0	0	0

LMNDMTAVALNYGIYK	21811000	0	21811000
LMQGDEICLR	6522300	0	6522300
LMSSGNEESLR	7885800	0	7885800
LMSSNSTDLPLNIECFMNDKDVSGK	0	0	0
LMTDTINEPILLCR	24951000	0	24951000
LMTTGNNTVR	23122000	0	23122000
LMVEPLQAILIR	1277000	0	1277000
LMVMEIR	0	0	0
LMVSMLDR	21763000	0	21763000
LNAIYQNNLTK	0	0	0
LNDGNEYLFQAK	878270	0	878270
LNDYIFSFDK	5551100	0	5551100
LNEAQPSTIATSMR	1893100	0	1893100
LNECVDHTPK	62235000	0	62235000
LNEILQAR	5104300	0	5104300
LNEQASEEILK	0	0	0
LNESTFDTQITK	66132000	0	66132000
LNFELTDALK	10516000	0	10516000
LNGDFAQLNLK	5631500	0	5631500
LNILDTLSK	104530000	0	104530000
LNIPATNVFANR	0	0	0
LNIQPSEADYAVDIR	0	0	0
LNLGTVGFYR	0	0	0
LNLYELK	9275200	0	9275200
LNMTPEEAER	48451000	0	48451000

LNNLVLFDK	236880000	0	236880000
LNPEDIK	18582000	0	18582000
LNQVCFDDDGTSSPQDR	15089000	0	15089000
LNQVIFPVSYNDK	0	0	0
LNQYFQK	194290000	0	194290000
LNSGVDYR	15955000	0	15955000
LNSLMSLVNK	50483000	0	50483000
LNTLLQR	109870000	0	109870000
LNVCVSK	14326000	0	14326000
LNVEGEHCDVCK	0	0	0
LNVTEQEK	321760000	0	321760000
LNVWDLSK	10141000	0	10141000
LNWTGTSK	15927000	0	15927000
LPAAGVGDMVMATVK	155760000	0	155760000
LPAIALDLLR	1713900	0	1713900
LPCIFICENNR	5440800	0	5440800
LPEADDIQYPSMLLLTADHDDR	7804700	0	7804700
LPEGDLGK	74149000	0	74149000
LPENYTDETWQK	7753100	0	7753100
LPESNQTLLR	4234000	0	4234000
LPETNLFETEETR	1636500	0	1636500
LPFAAAQIGNSFR	0	0	0
LPFPIIDDR	862260000	25962000	836300000
LPGAICSLTCGGADIGTAMAK	8790100	0	8790100
LPGLLGNFPGPFEEEMK	6904400	0	6904400

LPLISGFYK	17447000	0	17447000
LPLPEPWR	26070000	0	26070000
LPLQDVYK	331910000	0	331910000
LPLQLDDAVRPEAEGEEEGR	18862000	0	18862000
LPNFGFVVFDDSEPVQK	5058100	0	5058100
LPPNTNDEVDEDPTGNK	8771900	0	8771900
LPPTPLLLFPEEEATNGR	2938400	0	2938400
LPQLPITNFSR	5433000	0	5433000
LPQPPEGQCYSN	0	0	0
LPQPPEGQTYNN	0	0	0
LPTDLTACDNR	49777000	1262000	48515000
LPVLAGCLK	0	0	0
LPVPESITGFAR	86378000	0	86378000
LQAASPELTQAAIMEK	3671900	0	3671900
LQAENDASKEEVK	10383000	0	10383000
LQAFSAAIESCNK	1777300	0	1777300
LQDAEIAR	127380000	0	127380000
LQDAINILK	14908000	0	14908000
LQDAYYIFQEMADK	8495200	0	8495200
LQDEEASMGASYSK	2373600	0	2373600
LQDEFENR	3647800	0	3647800
LQDEIQNMK	138520000	0	138520000
LQDEIQNMKEEMAR	16603000	0	16603000
LQDLVNR	4154200	0	4154200
LQEEINEVK	8366500	0	8366500

LQEEMLQR	175640000	0	175640000
LQEEYWDLQDMLTNR	4213000	0	4213000
LQELSAEER	0	0	0
LQETEMMDPELDYTLMR	3432600	0	3432600
LQETLSAADR	14527000	0	14527000
LQETTLVANQLR	4570500	0	4570500
LQEVPHEGPMCDLLWSDPDDR	3315500	0	3315500
LQGETLDQQLGR	1996000	0	1996000
LQGINCGPDFTPSFANLGR	4521000	0	4521000
LQGQLEQGDDTAAER	8508600	0	8508600
LQIEDFEAR	0	0	0
LQIVEMPLAHK	57217000	0	57217000
LQIWDTAGQESFR	47193000	0	47193000
LQKEEEIEFLYNENTVR	0	0	0
LQLDSPEDAEFIVAK	46145000	0	46145000
LQLEIDQK	10519000	0	10519000
LQLLEDDKENR	59493000	0	59493000
LQLWDIAGQER	10896000	0	10896000
LQLWDTAGQER	9477000	0	9477000
LQMEAPHIIVGTPGR	16271000	0	16271000
LQMEQQQQLQQR	118750000	0	118750000
LQPFATEADVEEALR	6091700	0	6091700
LQQLPADFGR	36537000	0	36537000
LQQVLQMESHIQSTSDR	112070000	1550800	110520000
LQSIGTENTEENR	17944000	0	17944000

LQSIGTENTEENRR	58172000	0	58172000
LQSSQEPEAPPPR	1933200	0	1933200
LQTASDESYKDPTNIQSK	10833000	0	10833000
LQTQGLGTALK	69079000	0	69079000
LQTQVFK	119120000	0	119120000
LQVMANSR	6861800	0	6861800
LQVSQQEDITK	54512000	0	54512000
LQVTNVLSQPLTQATVK	7440400	0	7440400
LQVVDQPLPVR	0	0	0
LSAAVTEAFVR	0	0	0
LSAETLQQVNR	6562300	0	6562300
LSAIPVSAFCNSETK	11869000	0	11869000
LSALGNVTTCNDYVALVHPDLDR	7615900	0	7615900
LSANQQNILK	105810000	0	105810000
LSASDMLQVR	218910000	0	218910000
LSCFAQTVSPAEK	100210000	0	100210000
LSDIPEGK	0	0	0
LSDLLAPISEQIK	17707000	0	17707000
LSDMPLK	22379000	0	22379000
LSEELSGGR	22152000	0	22152000
LSEETTTSSSR	1364000	0	1364000
LSEFGLIQEK	6219800	0	6219800
LSESGAIMTDLEENPK	0	0	0
LSFAVPFR	14869000	0	14869000
LSGQDVER	6059200	0	6059200

LSGSNPYTTVTPQIINSK	4156300	0	4156300
LSGTGSAGATIR	32717000	1670600	31046000
LSILYPATTGR	213030000	0	213030000
LSIVPVR	35202000	0	35202000
LSKEDIER	9447300	0	9447300
LSLDGQNIYNACCTLR	118540000	0	118540000
LSLLCIDFNK	0	0	0
LSLLLNDISR	0	0	0
LSLNIDPDAK	29054000	0	29054000
LSMSQLNEK	447010000	0	447010000
LSNIFVIGK	0	0	0
LSNTSPEFQEMSLLER	8125200	0	8125200
LSNVNLQEK	16377000	0	16377000
LSPEELLLR	10042000	0	10042000
LSPQAVNSIAK	123500000	0	123500000
LSPTDNLPR	36731000	0	36731000
LSQLEGVNVER	14129000	0	14129000
LSQMAVQGLQQFK	9046200	0	9046200
LSQNNFALGYK	61789000	4730600	57059000
LSQVPDNPPDYQK	12653000	0	12653000
LSSAMSAAK	47062000	0	47062000
LSSDVCPTSDK	11763000	0	11763000
LSSPATLNSR	3495900000	3495900000	0
LSSTWEGIQAGK	55974000	0	55974000
LSSVVTQHDSK	9156600	0	9156600

LSTLCPSAVLQR	16252000	0	16252000
LSTLVETTLK	6492800	0	6492800
LSVADSQAEAK	25504000	0	25504000
LSVDYGKK	0	0	0
LSVEESEAAGDGVDTK	14286000	0	14286000
LSVEGFAVDK	0	0	0
LSVENVPCIVTLCK	0	0	0
LSVLGAITSVQQR	2349800	0	2349800
LSVNSVTAGDYSR	21840000	0	21840000
LSYNTASNK	17012000	0	17012000
LTDADAMK	57473000	0	57473000
LTDCVVMR	19978000	0	19978000
LTDIQYGR	27609000	2185200	25424000
LTDQLPLIIVCDR	130890000	24398000	106500000
LTEGCSFR	6029700	0	6029700
LTEMETLQSQLMAEK	37495000	0	37495000
LTFDSSFSPNTGK	0	0	0
LTFDTTFSPNTGK	0	0	0
LTFSCLGGSDNFK	2963300	0	2963300
LTGADGTPPGFLLK	0	0	0
LTGMAFR	844580000	29289000	815290000
LTGSLSGWSSPK	9576000	0	9576000
LTGSVLEDAWK	0	0	0
LTGVFAPR	245120000	0	245120000
LTIAEER	11618000	0	11618000

LTLDTIFVPNTGK	10852000	0	10852000
LTLHGLQQYYVK	8027400	0	8027400
LTLSALLDGK	12115000	0	12115000
LTLSALVDGK	4609500	0	4609500
LTLSQFQK	0	0	0
LTNFPEMMNR	0	0	0
LTNVAATSGDGYR	11684000	0	11684000
LTPEFSQR	87688000	0	87688000
LTPITYPQGLAMAK	99841000	0	99841000
LTPQMFQQLMK	51143000	0	51143000
LTPTEVK	9514400	0	9514400
LTQDQDVDVK	14291000	0	14291000
LTQEQVSDSQVLIR	3437500	0	3437500
LTQVSPR	2419600	0	2419600
LTSDSTVYDYAGK	3189800	0	3189800
LTSEPQPQR	66247000	0	66247000
LTTLPSDFCGLTHLVK	347710000	347710000	0
LTVAENEAETK	46878000	16569000	30309000
LTVEDPVTVEYITR	57497000	0	57497000
LTVNDFVR	2403500	0	2403500
LTVNPGTK	65033000	0	65033000
LVAGEMGQNEPDQGGQR	16587000	0	16587000
LVAIVDVIDQNR	4150800	0	4150800
LVALAVIDEK	12637000	0	12637000
LVALLNTLDR	42067000	0	42067000

LVARPEPATGYTLEFR	76028000	0	76028000
LVASAEQLLK	9178300	0	9178300
LVCSGLLQASK	436890000	411250000	25644000
LVDAGEECDCGTPK	1607100	0	1607100
LVDEYSLNAGK	0	0	0
LVDVICEK	22354000	0	22354000
LVEAISR	30964000	0	30964000
LVEALAAATEK	0	0	0
LVEALCAEHQINLIK	0	0	0
LVEDEER	21584000	780440	20803000
LVEDMENK	26457000	0	26457000
LVEQYTK	38354000	0	38354000
LVFDEYLK	57209000	0	57209000
LVFLGLDNAGK	286960000	0	286960000
LVFPQDLLEK	91464000	0	91464000
LVFSNVNLK	3721100	0	3721100
LVGMPAK	17949000	0	17949000
LVGPEEALSPGEAR	8768000	0	8768000
LVGQGASAVLLDLPNSGGEAQAK	73556000	0	73556000
LVGSVNLFSDENVPR	13365000	0	13365000
LVIEEAER	121970000	0	121970000
LVIITAGAR	154040000	0	154040000
LVILANNCPALR	34743000	0	34743000
LVILEGELER	0	0	0
LVINGNPITIFQER	1216100000	128410000	1087700000

LVIPSELGYGER	16328000	0	16328000
LVIVGDGACGK	160740000	7526300	153220000
LVKPGNQNTQVTEAWNK	16869000	0	16869000
LVLEAEER	47989000	0	47989000
LVLLGESAVGK	101540000	0	101540000
LVLMSATGDNER	12684000	0	12684000
LVLVGDGGTGK	282140000	0	282140000
LVMELSGEMVR	0	0	0
LVNANGEAVYCK	14833000	0	14833000
LVNELTEFAK	138380000	138380000	0
LVNLADCLCNEDLESR	5497400	0	5497400
LVPADNEK	6772600	0	6772600
LVPDLLAIVQR	1697200	0	1697200
LVPEAVGDQK	30299000	0	30299000
LVPLLDTGDIIIDGGNSEYR	1248600	0	1248600
LVPLNQESVEER	29105000	0	29105000
LVPQLVR	3067600	0	3067600
LVPSQEETK	16954000	0	16954000
LVPTGLDFGQEGFTR	1887400	0	1887400
LVQAFQFTDK	34015000	0	34015000
LVQAFQYTDK	33514000	0	33514000
LVQGSILK	80155000	0	80155000
LVQLGQAEK	6585300	0	6585300
LVQSPNSYFMDVK	85456000	19077000	66379000
LVQTAAQQVAEDK	18804000	0	18804000

LVSDGNINSDR	11734000	0	11734000
LVSEYMSK	117920000	0	117920000
LVSIDSK	41041000	0	41041000
LVSIGAEEIVDGNAK	21653000	0	21653000
LVSIGAEEIVDGNVK	0	0	0
LVSLGTCFGK	5987900	0	5987900
LVSLIGSK	99144000	0	99144000
LVSLYFDTK	24785000	0	24785000
LVSPGSANETSSILVESVTR	3010900	0	3010900
LVTDEDVFPTK	0	0	0
LVTMQIWDTAGQER	47917000	0	47917000
LVVECVMNNVTCTR	29260000	0	29260000
LVVLGSGGVGK	18589000	0	18589000
LVVLGSSQESNSK	0	0	0
LVVPATQCGSLIGK	0	0	0
LVWIETPTNPTQK	0	0	0
LVYLVENPGGYVAYSK	0	0	0
LWAPDSPNR	11004000	0	11004000
LWDFQGFECIR	2926600	0	2926600
LWDIGGQPR	0	0	0
LWDLTTGTTTR	54512000	0	54512000
LWDLVAGK	0	0	0
LWEEQLAAAK	28003000	0	28003000
LWGDIYFNPK	3745200	0	3745200
LWGLTEMFPER	2314800	0	2314800

LWNLLMPTK	0	0	0
LWNTLGVCK	0	0	0
LWVPDEEVSPETMVK	5714400	0	5714400
LYAMQTGMK	19574000	0	19574000
LYCPVEFSK	0	0	0
LYDAYELK	19145000	0	19145000
LYDLVAGSNCLK	5652900	0	5652900
LYDMADVWVK	6502600	0	6502600
LYDVVAVFPK	0	0	0
LYELIITR	0	0	0
LYENFISEFEHR	44975000	0	44975000
LYEQLSGK	102620000	0	102620000
LYEWTTEK	19101000	0	19101000
LYGDDALDNALQTFIK	1799900	0	1799900
LYGEFADPFK	3130100	0	3130100
LYGPSSVSFADDFVR	1437900	0	1437900
LYGSAGPPPTGEEDTAEKDEL	12957000	0	12957000
LYIDSYEK	9258900	0	9258900
LYLVSDVLYNSSAK	5007400	0	5007400
LYNNHEIR	35302000	0	35302000
LYPEGLAQLAR	32950000	0	32950000
LYQPEYQEVSTEEQR	16554000	0	16554000
LYQVEYAFK	18450000	0	18450000
LYSEDELPAEFK	2680000	0	2680000
LYSESLAR	258950000	0	258950000

LYTLQDK	119710000	0	119710000
LYTLVLTDPDAPSR	17639000	0	17639000
LYVYNTDTDNCR	7359900	0	7359900
MADLHAVPR	118750000	0	118750000
MADMQNLVER	0	0	0
MAEDEAETIGNLIEECGGLEK	3403000	0	3403000
MAGAIPLVTAGSQK	0	0	0
MAGATPVFIPLR	16437000	0	16437000
MAGTAFDFENMK	0	0	0
MAILQIMK	30748000	0	30748000
MAIMVQSPMFDGK	28277000	0	28277000
MAIQTQQSK	20278000	0	20278000
MALLMAEMSR	40313000	0	40313000
MASTFIGNSTAIQELFK	3112900	0	3112900
MATEVAADALGEEWK	23554000	0	23554000
MATFEIDEK	0	0	0
MAVLALLAK	12273000	0	12273000
MAVQDAVDALMQK	0	0	0
MCQGGDFTR	6065700	0	6065700
MDASTGDAIK	41920000	0	41920000
MDATANDVPSDR	93987000	0	93987000
MDCQECPEGYR	25708000	0	25708000
MDDREDLVYQAK	216740000	0	216740000
MDELQLFR	145610000	4054600	141560000
MDENQFVAVTSTNAAK	14535000	0	14535000

MDGTYACSYTPVK	15223000	0	15223000
MDKNELVQK	37824000	0	37824000
MDLVTYFGK	7052300	0	7052300
MDMEEIIQR	2863600	0	2863600
MDPNTIIEALR	7164600	0	7164600
MDQAIIFCR	15486000	0	15486000
MDQYFNQMEK	11051000	0	11051000
MDSTANEVEAVK	131650000	0	131650000
MDSTEPPYSQK	22362000	0	22362000
MEADPDGQQPEK	2505600	0	2505600
MEAEDYVMAVVDK	8048500	0	8048500
MEANIDR	8595500	0	8595500
MEEADALIESLCR	48569000	0	48569000
MEEANIQPNR	65120000	0	65120000
MEEETEVR	14831000	0	14831000
MEEVVIAGMSGK	15617000	0	15617000
MEGGTENDLR	5308700	0	5308700
MEGVEEK	1388300	0	1388300
MELITILEK	12258000	0	12258000
MELVQVLK	4660700	0	4660700
MESVLGAGGK	10916000	7250800	3665600
MESYHKPDQQK	16039000	0	16039000
METLGENEYFR	5389800	0	5389800
MFDVGGQR	22516000	0	22516000
MFEFYER	8523300	0	8523300

MFGMVLEK	109060000	0	109060000
MFIGGLSWDTTK	27733000	0	27733000
MFLSFPTTK	12727000	12727000	0
MFLYADNEDR	826350	0	826350
MFQDIGVSK	0	0	0
MFVLDEADEMLSR	166700000	0	166700000
MFVTPGAGR	29771000	0	29771000
MGESDDSILR	12765000	0	12765000
MGGDIANR	19210000	0	19210000
MGGEEAEIR	98586000	0	98586000
MGITEYNNQCR	65513000	0	65513000
MGPGAASGGER	405580	0	405580
MGPGAASGGERPNLK	7699200	0	7699200
MGPGATAGGAEK	18309000	0	18309000
MGPNIYELR	32174000	0	32174000
MGVVECAK	0	0	0
MIAAVDTDSPR	103700000	0	103700000
MIAILTENYGGK	97031000	0	97031000
MIDLIIPR	5277400	0	5277400
MIDLSGNPVLR	29210000	0	29210000
MIFDVESMK	102990000	0	102990000
MIFVGIK	6096700	0	6096700
MIIEEAK	10595000	0	10595000
MILELFSK	52946000	0	52946000
MINTDLSR	56407000	0	56407000

MIPCDFLIPVQTQHPIR	96956000	0	96956000
MISDAIPELK	136240000	0	136240000
MISGMYLGEIVR	15622000	0	15622000
MISLTDTQK	6511400	0	6511400
MIVDPVEPHGEMK	8495600	0	8495600
MLAEDELR	90673000	0	90673000
MLALALLDR	6321400	0	6321400
MLAQQAVK	14484000	0	14484000
MLDAEDIVGTARPDEK	0	0	0
MLDAEDIVNTARPDEK	20801000	0	20801000
MLENTDNSSPSTEHSQGLEK	0	0	0
MLEQLDMR	1750900	0	1750900
MLFDYLADK	75500000	0	75500000
MLLADQGQSWK	0	0	0
MLLCEAVAAVMAK	17429000	0	17429000
MLLNDFLNDQNR	9531600	0	9531600
MLLQSSEGR	13389000	0	13389000
MLLSLPEK	23008000	0	23008000
MLLVDELR	149500000	889910	148610000
MLLYTEVTR	31384000	0	31384000
MLPLIWSK	2279600	0	2279600
MLQIQPEK	7467400	0	7467400
MLQPCGPPADKPEEN	3035000	0	3035000
MLQPSSSPLWGK	0	0	0
MLSCAGADR	65334000	0	65334000

MLTAQDMSYDEAR	6002900	0	6002900
MLTGPVYSQSTALTHK	25769000	0	25769000
MLVIEQCK	52197000	0	52197000
MLVLDEADEMLNK	118440000	0	118440000
MLVNENFEEYLR	98589000	0	98589000
MLVQCMQDQEHPSIR	4402500	0	4402500
MLVVGGIDR	3211100	0	3211100
MMADEALGSGLVSR	0	0	0
MMCGAPSATQPATAETQHIADQVR	39269000	0	39269000
MMMQSGR	14129000	0	14129000
MMVAGFK	24983000	0	24983000
MNEFLENFEK	35762000	0	35762000
MNGMLLNDR	20297000	0	20297000
MNGMSVLMK	2215700	0	2215700
MNLGVGAYR	115550000	0	115550000
MNLSAIQDR	128480000	28973000	99507000
MNPEYDYLFK	10517000	0	10517000
MNYSDAIVWLK	16062000	0	16062000
MPCTEDYLSLILNR	24269000	24269000	0
MPPYDEQTQAFIDAAQEAR	120960000	0	120960000
MPSLPSYK	12133000	0	12133000
MPTTQETDGFQVK	0	0	0
MQASIEK	70051000	0	70051000
MQGQSPPAPTR	2110500	0	2110500
MQLSGEGAK	14744000	0	14744000

MQVDPQK	50087000	0	50087000
MQVDQEEPHVEEQQQQTPAENK	36283000	0	36283000
MREDYDSVEQDGDEPGPQR	1666800	0	1666800
MSAEDIEK	31531000	0	31531000
MSASDPNSSIFLTDTAK	20251000	0	20251000
MSATFIGNSTAIQELFK	3112900	0	3112900
MSPDEGQEELEEVQAELK	3089300	0	3089300
MSSFGDFVALSDVCDVPTAK	7063600	0	7063600
MSTMTPK	7801900	0	7801900
MSTSPEAFLALR	2126200	0	2126200
MSVIWDK	63771000	0	63771000
MTALAQDFAVGLGPR	1132500	0	1132500
MTDSFTEQADQVTAEVGK	0	0	0
MTFTSNK	12163000	0	12163000
MTLSNPSELDELMSEEAYEK	6048300	0	6048300
MTQNPNYYNLQGISHR	0	0	0
MTTETASEDDNFGTAQSNK	0	0	0
MTVDESGQLISCSMDDTVR	2901000	0	2901000
MVCSSTCYR	4074000	0	4074000
MVDVGGQR	23700000	0	23700000
MVEGYQGLR	5260500	0	5260500
MVGSQDILCSENK	0	0	0
MVGVPAALDMMLTGR	2439300	0	2439300
MVLVGDVK	15660000	0	15660000
MVMAEGTAVLR	0	0	0

MVNHFIAEFK	25604000	0	25604000
MVQQCCTYVEEITDLPIK	0	0	0
MVRPNQDGTLIASCSNDQTVR	7243800	0	7243800
MVSDEYEQLSSEALEAAR	3346400	0	3346400
MVVESAYEVIK	436950000	0	436950000
MVVLSLPR	7098900	0	7098900
MVVPAALK	0	0	0
MVYDMEK	8628400	0	8628400
MWFQWSEQR	35899000	0	35899000
MYVGECQGPGVR	3379800	0	3379800
NAAPCAVSYLLFDQNDK	5473100	0	5473100
NACIECSVNQNSIR	38589000	0	38589000
NADMSEDMQQDAVDCATQAMEK	36381000	0	36381000
NADMSEEMQQDSVECATQALEK	161020000	0	161020000
NAENAIEALK	48628000	0	48628000
NAENAIEALKEYEPEMGK	12251000	0	12251000
NAFMMLIHADQDR	7185600	0	7185600
NAGFTPQER	187360000	0	187360000
NAGNCLSPAVIVGLLK	22303000	0	22303000
NAGNEQDLGIQYK	4170600	0	4170600
NAIQEIQR	0	0	0
NALDLLLPK	44146000	0	44146000
NALDPMSVLLAR	6014200	0	6014200
NALESYAFNMK	36851000	0	36851000
NALLQLTDSQIADVAR	2556700	0	2556700

NALSSLWGK	32054000	0	32054000
NAPNDASYDAVR	17881000	0	17881000
NAQAIEDMVGYAQETQHEK	11809000	0	11809000
NASNDIVR	73908000	0	73908000
NATNVEQAFMTMAAEIK	3820900	0	3820900
NATNVEQSFMTMAAEIK	0	0	0
NAYVWSQK	10258000	0	10258000
NCAAYLK	62602000	0	62602000
NCAVEFNFGQR	5845700	0	5845700
NCETDTLINYMAK	2143300	0	2143300
NCFASVFEK	10465000	0	10465000
NCGQMSEIEAK	4976900	0	4976900
NCIDITGVR	35526000	0	35526000
NCISTVVHQGLIR	6651400	0	6651400
NCIVLIDSTPYR	10596000	0	10596000
NCLTNFHGMDLTR	76703000	0	76703000
NCNDFQYESK	41661000	0	41661000
NCPHIVVGTPGR	41358000	0	41358000
NCTIVSPDAGGAK	6461200	0	6461200
NDCEENGLAK	2743100	0	2743100
NDEELNK	1119000	0	1119000
NDEELNKLLGK	0	0	0
NDFTEEEEAQVR	0	0	0
NDGAAILAAVSSIAQK	25777000	0	25777000
NDGVLLLQALTR	20772000	0	20772000

NDLAVVDVR	29018000	0	29018000
NDLDDPER	0	0	0
NDLSPASSGNAVYDFFIGR	3725700	0	3725700
NDNDTFTVK	29396000	0	29396000
NDQCYDDIR	29062000	0	29062000
NDQCYEDIR	16292000	0	16292000
NDQDTWDYTNPNLSGQGDPGSNPNKR	0	0	0
NEAIQAAHDAVAQEGQCR	5934100	0	5934100
NEALAALLR	45539000	0	45539000
NECFLSHK	43885000	43885000	0
NEDITEPQSILAAAEK	0	0	0
NEDLNAEDVYSR	4529300	0	4529300
NEEDAAELVALAQAVNAR	164420000	0	164420000
NEEEGNSEEIK	10170000	0	10170000
NEFIPTNFEILPLEK	0	0	0
NEGNIFPNPEATFVK	96875000	0	96875000
NELEIPGQYDGR	8479000	0	8479000
NELSGALTGLTR	111790000	0	111790000
NENQLIIFADDTYPR	0	0	0
NEPQNATGAPGR	12327000	0	12327000
NETGGGEGIEVLK	0	0	0
NETLGGTCLNVGCIPSK	29473000	0	29473000
NFALLGVGTSK	20194000	0	20194000
NFATSLYSMIK	5955300	0	5955300
NFDEILR	24892000	0	24892000

NFDFEDVFVK	27695000	0	27695000
NFEDVAFDEK	0	0	0
NFGAENPDPFVPVLNTAVK	1814200	0	1814200
NFGASLLLPGLK	14428000	0	14428000
NFGDQPDIR	35386000	0	35386000
NFGEDMDDER	8044300	0	8044300
NFGIWLR	17986000	0	17986000
NFGLYNER	0	0	0
NFGSYVTHETK	46039000	0	46039000
NFIEFVFPYR	76003000	5501100	70502000
NFILDQCNVYNSGQR	0	0	0
NFILDQTNVSAAAQR	0	0	0
NFLSTPQFLYR	5245700	0	5245700
NFNETFLK	4918800	0	4918800
NFPQTALVSFATTGEK	0	0	0
NFVDSPIIVDITK	47112000	0	47112000
NGAPIIMSFPHFYQADER	2165400	0	2165400
NGDYLCVK	8381300	0	8381300
NGETELCMEGR	9398600	0	9398600
NGGQILIADLR	17256000	0	17256000
NGLSLAALK	18032000	0	18032000
NGQDLGVAFK	52208000	0	52208000
NGQVIGIGAGQQSR	25284000	0	25284000
NGYELSPTAAANFTR	6332200	0	6332200
NHDEESLECLCR	33682000	0	33682000

NHQSAAEYNIFEGMELR	19986000	0	19986000
NICFTVWDVGGQDK	22034000	0	22034000
NICFTVWDVGGQDR	39740000	0	39740000
NIDEHANEDVER	109650000	0	109650000
NIEDVIAQGIGK	140830000	0	140830000
NIEEHASADVEK	4020800	0	4020800
NIEIDSPYEISR	2565500	0	2565500
NIEMTQEDVR	2700400	0	2700400
NIFLLFK	6549200	0	6549200
NIFPSNLVSAAFR	4581600	0	4581600
NIGWGTDQGIGGFGEEPGIK	66142000	7918400	58223000
NIIGYFEQK	6545600	0	6545600
NIIHGSDSVESAEK	121120000	0	121120000
NIIHGSDSVK	213230000	0	213230000
NILGGTVFR	62762000	0	62762000
NILIDFTK	20694000	0	20694000
NILTEIYR	60038000	0	60038000
NINDAWVCTNDMFR	15721000	0	15721000
NINLIVQK	0	0	0
NIPGITLLNVSK	135650000	0	135650000
NIQESNFDR	4471400	0	4471400
NISFTVWDVGGQDK	133960000	693010	133260000
NISPIEVEYSQAEMK	39724000	0	39724000
NIVEAAAVR	266740000	2460400	264280000
NIVLSGGSTMFR	41313000	0	41313000

NIYSEELR	8414500	0	8414500
NIYVLQELDNPGAK	117420000	0	117420000
NKFDVDAADEK	0	0	0
NLAMGVNLTSMSK	5451900	0	5451900
NLANTVTEEILEK	61428000	0	61428000
NLATTVTEEILEK	138810000	0	138810000
NLDCPELISEFMK	3412700	0	3412700
NLDDGIDDER	19661000	0	19661000
NLDEQLSAPK	6580300	0	6580300
NLDGISHAPNAVK	9939000	0	9939000
NLDIERPTYTNLNR	52563000	0	52563000
NLDKEYLPIGGLAEFCK	78639000	0	78639000
NLDLAVLELMQSSVDNTK	0	0	0
NLDPDVFNQIVK	16907000	0	16907000
NLEAMNPPLFLR	2987300	0	2987300
NLEAVETLGSTSTICSDK	0	0	0
NLEGYVGFANLPNQVYR	4437900	0	4437900
NLFEDQNTLTSICEK	98873000	0	98873000
NLGESEIR	12138000	0	12138000
NLGLYVK	17902000	0	17902000
NLIDAGVDALR	72892000	0	72892000
NLIDEDGNNQWPEGLK	27690000	0	27690000
NLIEWLNK	15000000	0	15000000
NLLDVIDQAR	2215700	0	2215700
NLLQNIH	0	0	0

NLLQVDLTK	5872200	0	5872200
NLLSVAYK	220780000	0	220780000
NLLTPLMEK	62585000	0	62585000
NLLTVTSSDEMMK	0	0	0
NLLVAFR	0	0	0
NLMFLVLR	3493600	0	3493600
NLNEDDTFLVFSK	5891100	0	5891100
NLPIYSENIIEMYR	9220000	0	9220000
NLPPEEQMISALPDIK	19548000	0	19548000
NLQEAEEWYK	10469000	0	10469000
NLQEVLGEEK	0	0	0
NLQLFMENK	15300000	0	15300000
NLQNLLILTAIK	14304000	0	14304000
NLQYYDISAK	41589000	0	41589000
NLSGQPNFPCR	93315000	0	93315000
NLSSNEAISLEEIR	9161600	0	9161600
NLTEDNSQNQDLIAK	10543000	0	10543000
NLTWIDSPAPER	9570900	0	9570900
NLVDSYVAIINK	1707600	0	1707600
NLVTEDVMR	23991000	0	23991000
NLVVIPK	82703000	0	82703000
NLYIISVK	41585000	0	41585000
NLYVTFPIPDLQK	19098000	0	19098000
NMAALDAADR	28037000	0	28037000
NMACVQR	12135000	0	12135000

NMALSIAER	20155000	0	20155000
NMDPLNDNIATLLHQSSDK	12488000	0	12488000
NMGLYGER	32388000	0	32388000
NMGYVQQR	8310800	0	8310800
NMMAACDPR	153140000	1767700	151370000
NMSGSLYEMVSR	45470000	0	45470000
NMVPQQALVIR	4279900	0	4279900
NNALNQVVLWDK	47678000	0	47678000
NNASTDYDLSDK	237990000	0	237990000
NNAYLAQSPQLYK	0	0	0
NNDFYVTGESYAGK	7007000	0	7007000
NNDLCYWVPELVR	5791300	0	5791300
NNFAVGYR	67288000	0	67288000
NNFEGEVTK	242410000	0	242410000
NNFSDGFR	14007000	0	14007000
NNIIQTWR	10421000	0	10421000
NNIPYFETSAK	40500000	0	40500000
NNLCPSGSNIISNLFK	28114000	0	28114000
NNNQQLAQLQK	24431000	0	24431000
NNNSNQNFFK	12183000	0	12183000
NNNTDLMILK	0	0	0
NNPEPWNK	79395000	0	79395000
NNQFQALLQYADPVSAQHAK	137340000	0	137340000
NNSELLNNLGNFINR	47031000	0	47031000
NNSGLSFEELYR	3409300	0	3409300

NNSPMAANQTPTLR	2787200	0	2787200
NNTQVLINCR	73251000	1639500	71612000
NNVNVASLTQSEIR	0	0	0
NNWEVSALSR	0	0	0
NNYENYIDIVK	17545000	0	17545000
NPASPYNLAYK	25373000	3722700	21650000
NPAVQAGSIVVLQGGEETQR	6380700	0	6380700
NPDDITNEEYGEFYK	51116000	0	51116000
NPDDITQEEYGEFYK	360230000	0	360230000
NPDGTMNLMNWECAIPGK	8520200	0	8520200
NPELPNAAQAQK	7306900	0	7306900
NPELQNLLLDDFFK	6362600	0	6362600
NPEPELLVR	0	0	0
NPQNSSQSADGLR	1023000	0	1023000
NPSNCYGEESNAVCEK	5477600	5477600	0
NPTIVNFPITNVDLR	46375000	0	46375000
NPVMELNEK	29894000	0	29894000
NPYYGGESASITPLEDLYK	125160000	0	125160000
NPYYGGESSSITPLEELYK	77305000	0	77305000
NQDLAPNSAEQASILSLVTK	47464000	0	47464000
NQGGGLSSSGAGEGQGPK	7511800	0	7511800
NQGIEEALK	30133000	0	30133000
NQKDDVAQTDLLQIDPNFGSK	0	0	0
NQNIQKPEYSE	4510700	0	4510700
NQSETLNWLSNAIK	16966000	0	16966000

NQSFCPTVNLDK	0	0	0
NQTAEKEEFEHQQK	59734000	0	59734000
NQVAMNPTNTVFDAK	0	0	0
NQVFEPSCLDAFPNLK	22095000	0	22095000
NQYDNDVTVWSPQGR	3894800	0	3894800
NREPVQLETLSIR	21350000	808520	20541000
NSAFESLYQDK	2790300	0	2790300
NSAQGNVYVK	8542500	0	8542500
NSILFLNSLDAK	8636600	0	8636600
NSIVNSQPPEK	14344000	0	14344000
NSLDCEIVSAK	36411000	0	36411000
NSLESYAFNMK	267370000	0	267370000
NSNILEDLETLR	0	0	0
NSNPALNDNLEK	11460000	0	11460000
NSQFAGGPLGNPNTTAK	20062000	0	20062000
NSSTYWEGK	5245500	0	5245500
NSSYFVEWIPNNVK	775650000	2511500	773140000
NSTFSEIFK	78970000	0	78970000
NSTTDQVYQAIAAK	0	0	0
NSVFQQGMK	37186000	0	37186000
NSVTPDMMEEMYK	0	0	0
NSVVEASEAAYK	23317000	0	23317000
NSYLEVLLK	73482000	0	73482000
NSYVAGQYDDAASYQR	2379600	0	2379600
NTCTSVYTK	25885000	0	25885000

NTDQASMPDNTAAQK	18033000	0	18033000
NTGIICTIGPASR	0	0	0
NTISLLVAGLK	18849000	0	18849000
NTLANSCGTGIR	1623800	0	1623800
NTLCAPEVISLINTR	9652400	0	9652400
NTLIQFEDFGNHNAFR	6414800	0	6414800
NTNDANSCQIIIPQNQVNR	88772000	0	88772000
NTNPNFVR	73000000	0	73000000
NTPLCDSFVFR	5650400	0	5650400
NTPSFLIACNK	0	0	0
NTTGALTTR	5022300	0	5022300
NTVANSPQTLLAGMNK	1525200	0	1525200
NTVCSLSSGK	15124000	0	15124000
NTVVATGGYGR	30011000	0	30011000
NTVVLFVPQQEAWVVER	6391300	0	6391300
NTWDCGLQILK	15485000	0	15485000
NVAQYNANHPDFPMQIEQLER	29545000	0	29545000
NVDILKDPETVK	1523500	0	1523500
NVDLLSDMVQEHDEPILK	23409000	0	23409000
NVEAMNFADIER	0	0	0
NVEDFTGPR	70633000	0	70633000
NVEGQDMLYQSLK	13914000	0	13914000
NVEMFMNIEK	0	0	0
NVFDEAILAALEPPEPK	4895700	0	4895700
NVFLLGFIPAK	1649400	0	1649400

NVFNALIR	29566000	0	29566000
NVGQFSGFPFEK	22093000	0	22093000
NVIDGDLCEQFNSMEPNK	0	0	0
NVIIWGNHSSTQYPDVNHAK	5087900	0	5087900
NVIQSVLQAIR	2156800	0	2156800
NVIVNGLVLASDGQK	64313000	0	64313000
NVLCSACSGQGGK	19511000	0	19511000
NVLDSEDEIEELSK	20641000	0	20641000
NVLIVEDIIDTGK	5444100	0	5444100
NVMTIITGYPTPGSK	233970000	0	233970000
NVNSNLITWNR	6716600	0	6716600
NVQGIIEILK	3233000	0	3233000
NVQLTENEIR	93480000	0	93480000
NVTELNEPLSNEER	175890000	2127500	173770000
NVVAECLGK	0	0	0
NVVTIFSAPNYCYR	20523000	0	20523000
NVVVVDGVR	26165000	0	26165000
NWADVQSQLR	0	0	0
NWFGLPGR	19584000	19584000	0
NWQYQETIK	39119000	0	39119000
NYAQVFNK	43075000	0	43075000
NYDVMKDFEEMR	16852000	0	16852000
NYDYYASR	8141800	0	8141800
NYELLCGDNTR	2795300	2795300	0
NYFLEEDNYK	0	0	0

NYILDQTNVYGSAQR	3326400	0	3326400
NYIMDFQVGK	186320000	0	186320000
NYLEPGKECVQPATK	26695000	0	26695000
NYLLQCTR	27460000	0	27460000
NYLSIFR	15350000	0	15350000
NYLSLAPLFFK	2612000	0	2612000
NYMMPAK	10295000	0	10295000
NYNECIR	22415000	0	22415000
NYPDPVSIIQK	5191800	0	5191800
NYTDEAIETDDLTIK	29233000	0	29233000
NYVLQTLGTETYR	63109000	0	63109000
NYYEQWGK	75542000	0	75542000
PAAPPAPGPGQLTLR	8444800	0	8444800
PAAVVLQTK	34072000	0	34072000
PADEIAVDR	256410000	0	256410000
PADTEPPPLLVYK	1972600	0	1972600
PADVYLIDEPSAYLDSEQR	3970900	0	3970900
PAEIDSLWEISK	1930500	0	1930500
PAGQNLQGIEDK	2733900	0	2733900
PALELLEPIEQK	36014000	0	36014000
PASGCEAETQTEELK	4934100	0	4934100
PASPATETVPAFSER	2457300	0	2457300
PDISPYFGLFYEK	1293000	0	1293000
PEPATGYTLEFR	0	0	0
PGDGEFVEVISLPK	22976000	0	22976000

PLSSGGEEEEKPR	8449100	0	8449100
PMEIFVDDETK	11702000	0	11702000
PMFIVNTNVPR	4199200	1978800	2220400
PPSAASAAPSSSK	247390000	0	247390000
PPYTVVYFPVR	77904000	0	77904000
PSQVVAETR	23951000	0	23951000
PVAVGPYGQSQPSCFDR	0	0	0
PVDFTGYWK	19198000	0	19198000
PVIDNPNYK	105690000	0	105690000
PVNLGLWDTAGQEDYDR	4018700	0	4018700
QEYDESGPSIVHR	175740000	6090200	169650000
QIDNPDYK	12724000	0	12724000
QMFLTQTDTGDDR	0	0	0
QSLGELIGTLNAAK	5851100	0	5851100
QVHPDTGISSK	11858000	0	11858000
QVTIFINSGGK	32214000	32214000	0
QVVESAYEVIK	2989200	0	2989200
RAPFDLFENK	42689000	0	42689000
RAPFDLFENR	73188000	0	73188000
RFDDAVVQSDMK	61628000	0	61628000
RFPGYDSESK	5995600	0	5995600
RGTGGVDTAAVGGVFDVSNADR	11007000	0	11007000
RLTDADAMK	0	0	0
RPCFSALTPDETYVPK	14356000	14356000	0
RPTPQDSPIFLPVDDTSFR	42122000	0	42122000

RQVDQLTNDK	6564200	0	6564200
RYDDPEVQK	29489000	0	29489000
SAADLISQAR	54151000	0	54151000
SAADSISESVPVGPK	27043000	0	27043000
SADESGQALLAAGHYASDEVR	11203000	0	11203000
SADGSAPAGEGEGVTLQR	84883000	2759600	82123000
SADTLWDIQK	27606000	0	27606000
SADTLWGIQK	22893000	0	22893000
SAEAYENFLR	17476000	0	17476000
SAGACTAAAFLK	0	0	0
SAHLQWMVVR	0	0	0
SALALAIK	0	0	0
SALLDFYMK	33849000	0	33849000
SALQSINEWAAQTTDGK	34410000	0	34410000
SALYYVDLIGGK	36831000	0	36831000
SANSELGGIWSVGQR	5147300	0	5147300
SANVNEFPVLK	0	0	0
SASAPAAEGEGTPTQPASEKEPEMPGPR	0	0	0
SASVVSVISR	1562600	0	1562600
SATLLQLITK	15727000	0	15727000
SATQFTGR	29983000	0	29983000
SATYVNTEGR	11129000	0	11129000
SAVDAGFLQK	0	0	0
SAVEDEGLK	43095000	0	43095000
SAVENCQDSWR	99572000	0	99572000

SAVVAAGGGSSGQVTSNGSIGR	5607400	0	5607400
SAYDSTMETMNYAQIR	0	0	0
SCAAAGTECLISGWGNTK	50230000	50230000	0
SCDGNQELLNFLR	18038000	5011100	13026000
SCNCLLLK	465070000	0	465070000
SCQFVAVR	0	0	0
SCSGVEFSTSGSSNTDTGK	34029000	0	34029000
SCSPELQQK	11801000	0	11801000
SCSSSCAVHDLIFWR	26848000	0	26848000
SCTTESCDFVR	14310000	0	14310000
SCYDLSCHAR	79969000	0	79969000
SDAAVDTSSEITTK	7710700	0	7710700
SDALETLGFLNHYQMK	39529000	0	39529000
SDASPSSIR	24135000	0	24135000
SDATADDLIDVVEGNR	8450400	0	8450400
SDGGYTYDTSDLAAIK	11657000	2975000	8682500
SDGIYIINLK	254260000	0	254260000
SDHPGISITDLSK	0	0	0
SDIGEVILVGGMTR	6373300	0	6373300
SDLLLEGFNNYR	0	0	0
SDPGLLTNTMDVFVK	18386000	0	18386000
SDPLLIGIPTSENPFK	23832000	0	23832000
SDPVVSYR	34466000	0	34466000
SDQDYILK	57334000	0	57334000
SDTIANIQLNK	6694400	6694400	0

SDTPLIYK	65617000	0	65617000
SDVEAIFSK	70929000	0	70929000
SDVLELTDDNFESR	21320000	0	21320000
SDVLQPGAEVTTDDR	2064500	0	2064500
SDVLVEYQGEGR	13424000	0	13424000
SDYDMVDYLNELR	179220000	0	179220000
SDYLNTFEFMDK	38464000	0	38464000
SEALPTDLPAPSAPDLTEPK	2062400	0	2062400
SEAVVEYVFSGSR	0	0	0
SEDFSLPAYMDR	109290000	0	109290000
SEDGEIVSTPR	7341700	0	7341700
SEDLLDYGPFR	22947000	0	22947000
SEEEFIHINNK	32950000	0	32950000
SEENEEPMETDQNAKEEEK	4019200	0	4019200
SEEPEVPDQEGLQR	0	0	0
SEEQLKEEGIEYK	125310000	0	125310000
SEETNQQEVANSLAK	5348200	0	5348200
SEGALELADVSNELPGLK	0	0	0
SEGDSVGESVHGK	22907000	0	22907000
SEGDSVGESVHGKPSVVYR	31611000	0	31611000
SEGFDTYR	101920000	0	101920000
SEGGFIWACK	5220400	0	5220400
SEGTYCCGPVPVR	3561400	0	3561400
SEGVVAVLLTK	100110000	13524000	86590000
SEHPGLSIGDTAK	337470000	0	337470000

SEIDLFNIR	42568000	0	42568000
SEIEYYAMLAK	34528000	0	34528000
SEISLLPSDIDR	2971400	0	2971400
SELDMLDIR	10742000	0	10742000
SELDQLRQEAEQLK	20263000	0	20263000
SEMEVQDAELK	53486000	0	53486000
SEMTPEELQK	65106000	0	65106000
SENENQEQIEESK	4233100	0	4233100
SENFEELLK	93172000	0	93172000
SENGLEFTSSGSANTETTK	2931800	0	2931800
SEPIPESNDGPVK	25899000	0	25899000
SEQDQAENEGEDSAVLMER	0	0	0
SESPKEPEQLR	0	0	0
SESVTTQAELEEK	3370700	0	3370700
SETELKDTYAR	3808300	0	3808300
SETITEEELVGLMNK	38042000	0	38042000
SEVATLTAAGK	70869000	0	70869000
SEVSSDEDIQFR	9796800	0	9796800
SFAFVGPSR	0	0	0
SFAVGMFK	4580800	0	4580800
SFDLLILK	6359000	0	6359000
SFDLLVK	121980000	0	121980000
SFDVNKPGCEVDDLK	17820000	0	17820000
SFEEAFQK	8157500	0	8157500
SFENISK	30088000	0	30088000

SFGGGTGSGFTSLLMER	44457000	0	44457000
SFITTDVNPYYDSFVR	16286000	0	16286000
SFLDDPIWR	0	0	0
SFLEDIR	0	0	0
SFLEDIRK	0	0	0
SFLLDLLNATGK	0	0	0
SFQDYLGK	22837000	0	22837000
SFYPEEVSSMVLTK	57118000	0	57118000
SFYQGEK	10412000	0	10412000
SGALDVLQMK	566640000	0	566640000
SGALDVLQMKEEDVLK	11632000	0	11632000
SGANVLICGPNGCGK	636580	0	636580
SGAYLIPLLER	8558400	0	8558400
SGCIVNNLAEFTVDPK	16695000	0	16695000
SGDETPGSEVPGDK	15893000	0	15893000
SGDSEVYQLGDVSQK	93839000	0	93839000
SGEENPASKPTPVQDVQGDGR	52652000	0	52652000
SGELLAK	9244900	0	9244900
SGENAASLANELAK	0	0	0
SGFQINLNPLK	4878900	0	4878900
SGGGGGGGLGSGGSIR	4488900	4488900	0
SGGVGGSNTNWK	2346500	0	2346500
SGLGELILPENEPGSSIMPGK	42640000	0	42640000
SGNELPLAVASTADLIR	11841000	0	11841000
SGNYPSSLSNETDR	20268000	0	20268000

SGPGAYESGIMVSK	2076900	0	2076900
SGSAAQAEGLCK	0	0	0
SGSGTMNLGGSLTR	28527000	0	28527000
SGSMATAEASGSDGK	32100000	0	32100000
SGSMSAYEMR	16013000	0	16013000
SGTVDPQELQK	100870000	0	100870000
SGVGNIFIK	0	0	0
SGVGTALLLK	0	0	0
SGVNSELVK	51231000	0	51231000
SGVSLAALK	70327000	0	70327000
SHCIAEVEK	126130000	126130000	0
SHMMDVQGSTQDSAIK	3242400	0	3242400
SHQTGIQASEDVK	0	0	0
SIAFPSIGSGR	16179000	0	16179000
SIAPSIFGGTDMK	0	0	0
SIASEPTEK	15786000	0	15786000
SICTTVLELLDK	10842000	0	10842000
SIDMSWDSVTMK	25206000	0	25206000
SIDSNPYDTDK	12450000	0	12450000
SIDTGMGLER	1820900	0	1820900
SIEDFAHSSFQMALSK	7013200	0	7013200
SIEEQLGTEIKPIPSNIDK	11682000	0	11682000
SIEVIENR	17616000	0	17616000
SIFDFSALK	34793000	0	34793000
SIFLFLDR	4569400	0	4569400

SIFSLDTPEQYQEAFQK	7766800	0	7766800
SIGTANRPMGAGEALR	113630000	0	113630000
SIIECVDDFR	0	0	0
SIIQEVAR	10479000	0	10479000
SIISMFDR	4565200	0	4565200
SILYDER	86257000	0	86257000
SIMSYNGGAVMAMK	3010800	0	3010800
SINNPDMR	59435000	0	59435000
SINPDEAVAYGAAVQAAILSGDK	10085000	0	10085000
SINSILDYISTSK	14553000	0	14553000
SIPMTVDFIR	48684000	0	48684000
SIPVLAK	10413000	0	10413000
SIQFVDWCPTGFK	118260000	0	118260000
SISFIPPDGEFELMR	8881300	0	8881300
SITCWTLSR	0	0	0
SIVEHVASK	51733000	0	51733000
SIYGEKFEDENFILK	240040000	0	240040000
SIYSLILGQDNAADQSR	0	0	0
SKFDEMAK	29693000	0	29693000
SKFDNLYGCR	0	0	0
SLAASSSFYGQR	1101000	0	1101000
SLADELALVDVLEDK	122510000	0	122510000
SLAEGYFDAAGR	0	0	0
SLAGSSGPGASSGTSGDHGELVVR	30893000	0	30893000
SLANVILGGYGTTSTAGGK	16800000	0	16800000

SLAPSLLDR	46623000	0	46623000
SLCNLEESITSAGR	0	0	0
SLDDSQCGITYK	0	0	0
SLDECCHSESSTACLNAK	3821900	3821900	0
SLDFYTR	39557000	0	39557000
SLDLDISK	27518000	0	27518000
SLDLFNCEITNLEDYR	1480900	0	1480900
SLDLFNCEVTNLNDYR	273000000	9924200	263080000
SLDLIESLLR	576360	0	576360
SLDLVTMK	0	0	0
SLDTSEEGGR	0	0	0
SLEDQVEMLR	10106000	0	10106000
SLEEGEGPIAVIMTPTR	5622100	0	5622100
SLEEIYLFSLPIK	3983000	0	3983000
SLESINSR	117660000	0	117660000
SLETCMYDHK	8750500	0	8750500
SLETENAGLR	0	0	0
SLFNNAER	10810000	0	10810000
SLFSNVVTK	0	0	0
SLFSSIGEVESAK	4023600	0	4023600
SLFTDVVAEK	36724000	36724000	0
SLGNVIHPDVVVNGGQDQSK	16422000	0	16422000
SLGPPQGEEDSVPR	188070000	0	188070000
SLGTDLMNEMR	1760100	0	1760100
SLHDALCVIR	33803000	0	33803000

SLHTLFGDELCK	446270000	446270000	0
SLIEEGGDWDR	0	0	0
SLIGCFNLDPNR	1997700	0	1997700
SLILTALQR	35628000	0	35628000
SLLDFLPR	16009000	0	16009000
SLLDGNIDSSQYEDSLR	0	0	0
SLLEGEGSSGGGGR	18852000	16446000	2406100
SLLINAVEASCIR	22986000	0	22986000
SLLIPYLDNLVK	4255600	0	4255600
SLLQGTILQYVK	6372700	0	6372700
SLLSILQR	8155200	0	8155200
SLLVQTK	102870000	0	102870000
SLLVTELGSSR	19083000	0	19083000
SLMEQDVK	10645000	0	10645000
SLPVEEQPK	13035000	0	13035000
SLQMYLER	0	0	0
SLQSVAEER	79397000	0	79397000
SLQSYYFYDELR	3694800	0	3694800
SLSFVPGNDFEMSK	15879000	0	15879000
SLTAEIDR	25340000	0	25340000
SLTNDWEDHLAVK	227230000	0	227230000
SLTYLSILR	14807000	923020	13884000
SLVASLAEPDFVVTDFAK	17444000	0	17444000
SLVDLTAVDVPTR	94911000	0	94911000
SLVEIADTVPK	64510000	0	64510000

SLVQEMVGSFGK	9236200	0	9236200
SLYQSAGVAPESFEYIEAHGTGTK	30099000	0	30099000
SLYYYIQQDTK	3370500	0	3370500
SMEEDPQTSR	40064000	0	40064000
SMENYYQESGR	23078000	0	23078000
SMFAGVPTMR	5010600	0	5010600
SMQGFPFYDK	39219000	0	39219000
SMSTEGLMK	217350000	88855000	128490000
SMVAVMDSDTTGK	32617000	0	32617000
SMVNLMDR	3949800	0	3949800
SNDEEAFTFAR	0	0	0
SNEILTAIIQGMR	39254000	0	39254000
SNELWTEIK	0	0	0
SNFGYNIPLK	59554000	0	59554000
SNGLICGGNGVCK	27507000	0	27507000
SNILTLMYQCMQDK	0	0	0
SNIWLAAVTK	11045000	0	11045000
SNLNSLDEQEGVK	25197000	0	25197000
SNLQVSNEPGNR	9280800	0	9280800
SNNSMAQAMK	9314400	0	9314400
SNPEDQILYQTER	1911500	0	1911500
SNQQNLGTIK	4918900	0	4918900
SNTPILVDGK	191010000	0	191010000
SNVSDAVAQSTR	592780000	16717000	576060000
SNVVDDMVQSNPVLYTPGEEPDHCVVIK	22889000	0	22889000

SPAAECLSEK	0	0	0
SPAESCDLLGDIQTCIR	15069000	0	15069000
SPAGSIVHELNPNFQPPK	0	0	0
SPASDTYIVFGEAK	27952000	0	27952000
SPDTNYLFMGDYVDR	82684000	1347300	81336000
SPEACCELTLQPLR	0	0	0
SPEDLER	268630000	5052300	263580000
SPELVQAMFPK	1763400	0	1763400
SPEVLSGGEDGAVR	2016400	0	2016400
SPFLQVFNNSPDESSYYR	6764400	0	6764400
SPFSVAVSPSLDLSK	0	0	0
SPFTVGVAAPLDLSK	24984000	0	24984000
SPIEFLENAYEK	10579000	0	10579000
SPLIIFSDCDMNNAVK	29744000	0	29744000
SPLSWIEEK	20797000	0	20797000
SPLVMDVLNIQGVQR	72773000	0	72773000
SPNDFALWK	3852800	0	3852800
SPPGQVTEAVK	170260000	0	170260000
SPPTVLVICGPGNNGGDGLVCAR	16279000	0	16279000
SPVYLTVLK	1613500	0	1613500
SPYTVTVGQACNPSACR	29284000	0	29284000
SQADQFCQR	6048100	0	6048100
SQAIDLLYWR	54281000	0	54281000
SQDIYLR	254830000	4399400	250430000
SQETECTYFSTPLLLGK	205650000	0	205650000

SQFEELCAELLQK	38875000	0	38875000
SQGGEPTYNVAVGR	59206000	0	59206000
SQICDNAALYAQK	72849000	0	72849000
SQIFSTASDNQPTVTIK	0	0	0
SQIHDIVLVGGSTR	130150000	0	130150000
SQLSCVVVDDIER	27396000	0	27396000
SQMDGLIPGVEPR	0	0	0
SQNFDILQSAISK	33513000	0	33513000
SQSPTCQMCGEK	4862800	0	4862800
SQVEPADYK	29027000	0	29027000
SQYEQLAEQNR	15278000	15278000	0
SQYPEIIFLGTGSAIPMK	1697200	0	1697200
SSAEVIAQAR	13660000	0	13660000
SSALQWLTPEQTSGK	4018300	0	4018300
SSAQDPQAVLGALGR	22577000	0	22577000
SSAYESLMEIVK	196210000	0	196210000
SSDSADPFYWMR	9886000	0	9886000
SSEAVIWEVLR	26426000	0	26426000
SSEHINEGETAMLVCK	20468000	0	20468000
SSFLPSYIIDVR	2402800	0	2402800
SSFTVDCSK	117340000	0	117340000
SSFYVNGLTLGGQK	126280000	0	126280000
SSGEIVYCGQVFEK	0	0	0
SSGGFVWACK	1821400	0	1821400
SSGSALTVWGTGNPR	0	0	0

SSGSSYPSLLQCLK	496300000	496300000	0
SSIDSEPALVLGPLK	8295800	0	8295800
SSIGTGYDLSASTFSPDGR	16370000	0	16370000
SSLAEFISER	4461700	0	4461700
SSLNPILFR	45298000	0	45298000
SSLQSQCLNEVLK	0	0	0
SSLSSAQADFNQLAELDR	23469000	0	23469000
SSMNPEYDYLFK	2496900	0	2496900
SSPSGPSNPSNPSVEEK	23916000	0	23916000
SSSGLLEWESK	0	0	0
SSSSSSASAAAAAAAASSSASCSR	9883700	0	9883700
SSVNCPFSSQDMK	5307100	0	5307100
SSYPGQITGNMICVGFLEGGK	34914000	34914000	0
STAGDTHLGGEDFDNR	912900000	27369000	885540000
STCIYGGAPK	28940000	0	28940000
STELLIR	1596300000	21217000	1575000000
STESLQANVQR	19982000	0	19982000
STFVLDEFKR	12530000	0	12530000
STGEAFVQFASQEIAEK	25111000	0	25111000
STGGAPTFNVTVTK	244240000	0	244240000
STGSFVGELMYK	30566000	0	30566000
STGTFVVSQPLNYR	11460000	0	11460000
STIIGESISR	21838000	0	21838000
STLEPVEK	17292000	0	17292000
STLINSLFLTDLYPER	877140	0	877140

STLINTLFK	40091000	0	40091000
STLMDTLFNTK	10878000	0	10878000
STNCFGDNDPIDVCEIGSK	0	0	0
STNGDTFLGGEDFDQALLR	24571000	0	24571000
STPAITLESPDIK	0	0	0
STPEYFAER	30181000	0	30181000
STPVTVVLPDTK	5511600	0	5511600
STPYECGFDPMSPAR	10901000	0	10901000
STQFEYAWCLVR	6850600	0	6850600
STSLETQDDDNIR	13020000	0	13020000
STTELPLTVSYDK	1887900	0	1887900
STTQVADSGYQR	7233800	0	7233800
STTTGHLIYK	384790000	0	384790000
STVAQLVK	84055000	0	84055000
STVNCSTTPVAER	23133000	0	23133000
STVVQLLER	18248000	0	18248000
STYIESSTK	3044800	0	3044800
SVAGGFVYTYK	8101800	0	8101800
SVDETLR	147810000	1939600	145870000
SVDIPENR	7485700	0	7485700
SVEEISTLVQK	0	0	0
SVEETLR	137630000	2299600	135330000
SVESVPK	33272000	0	33272000
SVILEAFSSPSEEVK	26779000	0	26779000
SVLDAAQIVGLNCLR	41468000	0	41468000

SVLGEADQK	71930000	0	71930000
SVLIGEFLEK	9315800	0	9315800
SVLQAVQK	134240000	0	134240000
SVMDATQIAGLNCLR	0	0	0
SVMEELKR	14336000	0	14336000
SVNELIYK	30146000	0	30146000
SVPLAATSMLITQGLISK	2027700	0	2027700
SVQTTLQTDEVK	57744000	0	57744000
SVSAFAPICNPVLCPWGK	14993000	0	14993000
SVSFSDVFFK	17835000	0	17835000
SVSGTDVQEECR	19614000	0	19614000
SVTEQGAELSNEER	213790000	6371600	207420000
SVVALHNLINNK	9990400	0	9990400
SVVSQSVCDYFFEAQEK	6459500	0	6459500
SVVTSIFGVK	6943100	0	6943100
SVVYQETNGETR	1684600	0	1684600
SVYQDNESETGK	5851800	0	5851800
SWCPDCVQAEPVVR	0	0	0
SWLLPVIR	2433200	0	2433200
SWLPQNCTLVDMK	103770000	0	103770000
SWNDCLNK	27487000	0	27487000
SWQDELAQQAEEGSAR	1604800	0	1604800
SWVNQMESQTGEASK	1547600	0	1547600
SYAEELAK	51847000	0	51847000
SYCAEIAHNVSSK	142780000	0	142780000

SYCNDQSTGDIK	33689000	0	33689000
SYCSNLVR	0	0	0
SYDYQSVCEPGAAPK	42096000	0	42096000
SYEECIIESR	5136700	0	5136700
SYELPDGQVITIGNER	8771300000	290650000	8480600000
SYEPLEDPGVK	45630000	0	45630000
SYGATATSPGER	6142600	0	6142600
SYLMTNYESAPPSPQYK	918940	0	918940
SYSEDDIHR	6670400	0	6670400
SYSPYDMLESIR	66282000	1993700	64288000
SYSSGGEDGYVR	12692000	0	12692000
SYVDLLK	14387000	0	14387000
SYVTTSTR	7806200	0	7806200
TAAYVNAIEK	35985000	0	35985000
TAEENLDR	1300900	0	1300900
TAEEVAALIR	0	0	0
TAEVLANK	15808000	0	15808000
TAFDDAIAELDTLNEDSYK	715830	0	715830
TAFDEAIAELDTLNEDSYK	13361000	0	13361000
TAFDEAIAELDTLNEESYK	13996000	0	13996000
TAIEEVQAER	11080000	0	11080000
TALAATNPAVR	22723000	0	22723000
TALALAIAQELGSK	3184100	0	3184100
TALAMGADR	2664100	0	2664100
TALNLFFK	32430000	0	32430000

TAMNVNEIFMAIAK	7401100	0	7401100
TAPGPATTQAGDAAR	2493000	0	2493000
TAPYVVTGSVDQTVK	0	0	0
TAQCFLR	17111000	0	17111000
TASSVIELTCTK	0	0	0
TASTNNIAQAR	3662100	0	3662100
TATPQQAQEVHEK	857320000	4588000	852730000
TATQLAVNK	91994000	0	91994000
TATTQETDGFQVK	35068000	0	35068000
TATVYPEPQNK	0	0	0
TAVAPIER	351180000	7035100	344150000
TAVCDIPPR	771120000	0	771120000
TAVETAVLLLR	23061000	0	23061000
TAVVVGTITDDVR	0	0	0
TAWGQQPDLAANEAQLLR	15744000	0	15744000
TAWLDGK	249730000	0	249730000
TCAAQLVSYPGK	0	0	0
TCDGVQCAFEELVEK	4619600	0	4619600
TCEESSFCK	102100000	0	102100000
TCGFDFTGAVEDISK	163250000	0	163250000
TCLICADTFR	2888600	0	2888600
TCNCETEDYGEK	84483000	0	84483000
TCNTMNQFVNK	13435000	0	13435000
TCTTVAFTQVNSEDK	67383000	0	67383000
TCTTVAFTQVNSEDKGALAK	21208000	0	21208000

TCVADESHAGCEK	173200000	173200000	0
TDAPQPDVK	2594300	0	2594300
TDDEVVQR	13654000	0	13654000
TDDYLDQPCLETVNR	18973000	0	18973000
TDDYLDQPCYETINR	0	0	0
TDEATFSK	6854900	0	6854900
TDEGIAYR	135190000	0	135190000
TDFEEFFLR	11901000	0	11901000
TDGCHAYLSK	61866000	0	61866000
TDGFGIDTCR	9260500	0	9260500
TDITYPAGFMDVISIDK	27200000	0	27200000
TDLLLEPYNK	0	0	0
TDLVPAFQNLMK	30785000	0	30785000
TDMDNQIVVSDYAQMDR	0	0	0
TDPALNPADTLAPADYTGANAALK	39721000	39721000	0
TDSDIIAK	0	0	0
TDTESELDLISR	0	0	0
TDTLEDLFPTTK	105030000	0	105030000
TDTVLILCR	32490000	0	32490000
TDYMVGSYGPR	143960000	0	143960000
TDYNASVSVPDSSGPER	50151000	0	50151000
TECGCQFTSK	1608500	0	1608500
TEEEEIDR	10076000	1429600	8646500
TEELKPQVEEK	4898700	0	4898700
TEFLGFFYK	9016800	0	9016800

TEIIILATR	8188300	0	8188300
TELAEPIAIRPTSETVMYPAYAK	0	0	0
TEQAISFAK	0	0	0
TEQGPQIDQK	0	0	0
TEQGPQVDETQFK	14632000	0	14632000
TESSGGWQNR	7008400	0	7008400
TETVEEPMEEEEAAK	49883000	0	49883000
TETVEEPMEEEEAAKEEK	75454000	0	75454000
TEWLDGK	14398000	0	14398000
TEYTVAVQTASK	15864000	0	15864000
TFAPEEISAMVLTK	31049000	0	31049000
TFCQLILDPIFK	74735000	0	74735000
TFDHYCEYR	2792300	0	2792300
TFDSIVMDPK	0	0	0
TFDTNGDGTIDFR	0	0	0
TFEGIDPK	25852000	0	25852000
TFEGVDPQTTSMR	101300000	0	101300000
TFESLVDFSK	32379000	0	32379000
TFEVTPIR	0	0	0
TFFSFPAVVAPFK	25284000	0	25284000
TFIAIKPDGVQR	359010000	0	359010000
TFLVGER	92130000	2399500	89731000
TFLVWVNEEDHLR	13125000	0	13125000
TFNMDEYVGLPR	67973000	0	67973000
TFPTVNPSTGEVICQVAEGDKEDVDK	0	0	0

TFQGPNCPATCGR	3849600	0	3849600
TFSEACLMVR	0	0	0
TFSEILNR	11748000	0	11748000
TFSYAGFEMQPK	11643000	0	11643000
TFTDCFNCLPIAAIVDEK	40460000	0	40460000
TFTTQETITNAETAK	172940000	0	172940000
TFVNITPAEVGVLVGK	0	0	0
TGAAPIIDVVR	0	0	0
TGCNVLLIQK	48010000	0	48010000
TGDLGDINAEQLPGR	0	0	0
TGEAIVDAALSALR	17477000	0	17477000
TGENVEDAFLEAAK	7294200	0	7294200
TGFFEFQAAK	18836000	0	18836000
TGGQVPDTNYIFMGDFVDR	3465900	0	3465900
TGIEQGSDAGYLCESQK	11764000	0	11764000
TGIYEEK	89559000	0	89559000
TGLYNYYDDEK	10551000	0	10551000
TGLYNYYDDEKEK	152270000	0	152270000
TGNIPALVR	63590000	0	63590000
TGPNLHGLFGR	29266000	0	29266000
TGQAAELGGLLK	0	0	0
TGQAPGYSYTAANK	203290000	0	203290000
TGQATVASGIPAGWMGLDCGPESSK	61821000	0	61821000
TGQATVASGIPAGWMGLDCGPESSKK	33130000	0	33130000
TGQEVVFVAEPDNK	24029000	0	24029000

TGQYSGIYDCAK	30319000	0	30319000
TGTSCALDCGAGIGR	2160100	0	2160100
TGTVSLEVR	18196000	0	18196000
TGVAVNKPAEFTVDAK	62792000	0	62792000
TGVVTDGVK	10806000	0	10806000
TGWISTSSIWK	3240100	0	3240100
TGYTLDVTTGQR	86444000	0	86444000
TGYTPDEK	1829200	0	1829200
THINAVVAK	73374000	0	73374000
THLPGFVEQAEALK	21230000	0	21230000
THNSSLEYNIFEGMECR	10161000	0	10161000
THVADFAPEVAWVTR	6110000	0	6110000
TIADHCPDSACK	6414900	0	6414900
TIAECLADELINAAK	19083000	0	19083000
TIAEIFGNPNYLR	13759000	0	13759000
TIAPALVSK	893420000	0	893420000
TIAQDYGVLK	64778000	0	64778000
TIAQGNLSNTDVQAAK	2100200	0	2100200
TIAVDFASEDIYDK	56669000	0	56669000
TICSSVDK	7558200	0	7558200
TIDDLEEK	28926000	0	28926000
TIDPELLGK	17146000	0	17146000
TIEAEAAHGTVTR	4207100	0	4207100
TIEEYAVCPDLK	2130900	0	2130900
TIEKFEK	10266000	0	10266000

TIELDGK	27592000	0	27592000
TIFAYFTGSK	5517800	0	5517800
TIFQGIAAK	22742000	0	22742000
TIGGGDDSFNTFFSETGAGK	44482000	0	44482000
TIIPLISQCTPK	288570000	0	288570000
TIIQNPTDQQK	14901000	0	14901000
TIISYIDEQFER	12790000	0	12790000
TILATGELGTLTNVYK	8764500	0	8764500
TILPAAAQDVYYR	0	0	0
TINLYPLTNYTFGTK	13597000	0	13597000
TIPGTALVEMGDEYAVER	0	0	0
TIPIDGDFFSYTR	5197900	0	5197900
TIQEMQQK	37159000	0	37159000
TIQVDNTDAEGR	55782000	0	55782000
TIQVSDFVR	4710700	0	4710700
TISETIER	22719000	1260000	21459000
TITLEVEPSDTIENVK	3908300000	0	3908300000
TITVALADGGRPDNTGR	35426000	0	35426000
TIVTDVFQGSMR	24314000	0	24314000
TKVEAFQTTISK	7998800	0	7998800
TLADAEGDVFR	0	0	0
TLADIIMEK	2335000	0	2335000
TLAMDTILANAR	45278000	0	45278000
TLAQLNPESSLFIIASK	36693000	0	36693000
TLASAGGPDNLVLLNPEK	2773900	0	2773900

TLATWATK	11869000	0	11869000
TLDELGIHLTK	6335500	0	6335500
TLDNLGYR	7237000	0	7237000
TLDPDPAIR	22219000	0	22219000
TLEDPDLNVR	4588000	0	4588000
TLEEDEEELFK	10613000	0	10613000
TLETANCMSSQTK	21567000	0	21567000
TLFATEDALEVR	0	0	0
TLFLAVQVQNEEGK	0	0	0
TLFNELR	6723700	0	6723700
TLFPLIEAK	30681000	0	30681000
TLGECGFTSQTAR	35539000	0	35539000
TLGILGLGR	79924000	0	79924000
TLGLYGK	446880000	0	446880000
TLGVDLVALATR	4947300	0	4947300
TLHPDLGTDK	8015400	0	8015400
TLIDDDNPPVSFVK	24607000	0	24607000
TLIEFLLR	2501100	0	2501100
TLIQNCGASTIR	22484000	4022300	18462000
TLLDSLR	0	0	0
TLLEFLK	13619000	0	13619000
TLLENTAITIGR	0	0	0
TLLETLQK	0	0	0
TLLVNNNR	20694000	0	20694000
TLLYNPFPPTNESDVIR	8065700	0	8065700

TLMNTIMQLR	6428000	0	6428000
TLNAGAYSK	16547000	0	16547000
TLQEVLTMEYR	10403000	0	10403000
TLQLDNNFEVK	0	0	0
TLQSLLTPQPPLLK	12982000	0	12982000
TLQTISLLGYMK	7342200	0	7342200
TLSDYNIQK	13498000	0	13498000
TLSGLEVSMVTAVPGR	0	0	0
TLSPTGNISSAPK	5216900	0	5216900
TLTDELAALQITGVK	12938000	0	12938000
TLTLVDTGIGMTK	57511000	0	57511000
TLTTMAPYLSTEDVPLAR	11070000	0	11070000
TLVECWK	11386000	0	11386000
TLVEDLFADK	12735000	0	12735000
TLVLLDNLNVR	16927000	0	16927000
TLVLLMGK	69690000	0	69690000
TLVSVTK	142200000	0	142200000
TLYNNQPIDFLK	64298000	0	64298000
TMGFCYQILTEPNADPR	1837100	0	1837100
TMLESAGGLIQTAR	0	0	0
TMQNTNDVETAR	24338000	0	24338000
TMQNTSDLDTAR	2314100	0	2314100
TMQTLLSLVR	3213800	0	3213800
TMSIVSYNHLGNNDGENLSAPLQFR	4231000	0	4231000
TMTITETADK	41659000	0	41659000

TMVQELLDFK	3793300	0	3793300
TNADTDGMVK	25305000	0	25305000
TNAENEFVTIK	4862000	4862000	0
TNDEVIHGIFK	0	0	0
TNEAQAIETAR	251120000	2441800	248680000
TNHIYVSSDDIK	3881800	0	3881800
TNIVTASVDAINFHDK	77465000	0	77465000
TNLDESDVQPVK	2270100	0	2270100
TNNPLPLEQR	20167000	0	20167000
TNSTFNQVVLK	148560000	0	148560000
TNTLAVTGGEDDK	2453800	0	2453800
TNYNDRYDEIR	20987000	0	20987000
TPADCPVIAIDSFR	28282000	0	28282000
TPAFAESVTEGDVR	0	0	0
TPAQYDASELK	58577000	0	58577000
TPCEEILVK	95395000	0	95395000
TPCNAGTFSQPEK	30938000	0	30938000
TPEEYPESAK	9540100	0	9540100
TPEGLTLLFK	341030000	0	341030000
TPELNLDQFHDK	2121600	0	2121600
TPEQCPSVVSLLSESYNPHVR	19895000	0	19895000
TPLLLMLGQEDR	62725000	0	62725000
TPPLLENSLPQCYQR	0	0	0
TPSALAILENANVLAR	1217500	0	1217500
TPTEALASFDYIVR	10961000	0	10961000

TPTLLNEGAVR	0	0	0
TPVEEVPAAIAPFQGR	95737000	0	95737000
TPVIVTLK	5600700	0	5600700
TPVPSDIDISR	32875000	0	32875000
TPVSITEHPK	9642600	0	9642600
TPVTDPATGAVK	13268000	0	13268000
TPVTQVNEVTGTLR	0	0	0
TPYTDVNIVTIR	0	0	0
TQEEIVAK	129130000	0	129130000
TQGFLALFSGDTGEIK	3327000	0	3327000
TQIDHYVGIAR	126520000	0	126520000
TQIIQDFLR	8223800	0	8223800
TQIPTQR	97129000	0	97129000
TQLEELEDELQATEDAK	3345700	0	3345700
TQLVSNLK	217580000	0	217580000
TQLYEYLQNR	4582100	0	4582100
TQMTSAVR	70414000	2152700	68262000
TQNVLGEK	143160000	0	143160000
TQPVQGEPSAPK	2012300	0	2012300
TQPYDVYDQVEFDVPVGSR	0	0	0
TQQYDDLIDEFMK	25351000	0	25351000
TQSSLVPALTDFVR	21668000	0	21668000
TQVTVQYMQDR	19062000	0	19062000
TQYACPPFDLTECSFK	4019300	0	4019300
TSAPITCELLNK	0	0	0

TSDANINWNNLK	9791900	9791900	0
TSDFNTFLAQEGCTK	1740400	0	1740400
TSDLIVLGLPWK	0	0	0
TSDQTWVK	12611000	0	12611000
TSEFTAAFVGR	8097300	0	8097300
TSESLCQNNMVILK	5210000	0	5210000
TSFVNFTDICK	63291000	0	63291000
TSGNVEDDLIIFPDDCEFK	9646000	0	9646000
TSIAIDTIINQK	0	0	0
TSIDAYDNFDNISLAQR	57139000	0	57139000
TSLDWWITDK	187410000	0	187410000
TSLMNQYVNK	68150000	0	68150000
TSNSYLR	15148000	0	15148000
TSQTVATFLDELAQK	4158600	0	4158600
TSSAETPTIPLGSAVEAIK	3210500	0	3210500
TSSAFVGK	6185400	0	6185400
TSSDPTCVEK	42159000	0	42159000
TSSQPGFLER	39108000	0	39108000
TSTSQAVFR	40042000	0	40042000
TSVETALR	25160000	0	25160000
TSYGWIEIVGCADR	35565000	0	35565000
TTAAMWALQTVEK	0	0	0
TTANAIYCPPK	4447400	0	4447400
TTAQVLIR	2119000	0	2119000
TTDGYLLR	37410000	0	37410000

TTECSNTFK	9564900	0	9564900
TTEINFK	13929000	0	13929000
TTETQVFVATPQK	1361200	0	1361200
TTETQVLVASAQK	38553000	0	38553000
TTGEVVSGVVSK	13228000	0	13228000
TTGFGMIYDSLDYAK	127680000	0	127680000
TTGIVMDSGDGVTHTVPIYEGYALPHAILR	88773000	0	88773000
TTIAQQVK	17824000	0	17824000
TTIFTDAK	10018000	0	10018000
TTLVIMER	52845000	0	52845000
TTNFAGILSQGLR	66120000	0	66120000
TTPECGPTGYVEK	0	0	0
TTPLNQESDR	28432000	0	28432000
TTPSVVAFTADGER	2507000	0	2507000
TTPSYVAFTDTER	4498000	0	4498000
TTPTFFPK	10163000	0	10163000
TTQFSCTLGEK	10419000	0	10419000
TTQVPQFILDDFIQNDR	9235100	0	9235100
TTTGSYIANR	43672000	0	43672000
TTVVYPATEK	4337500	0	4337500
TTYQALPCLPSMYGYPNR	9240400	0	9240400
TVAGGAWTYNTTSAVTVK	0	0	0
TVALWDLR	40263000	0	40263000
TVAQSQQLETNSQR	2994300	0	2994300
TVCGVVSR	13946000	0	13946000

TVDFTQDSNYLLTGGQDK	36887000	0	36887000
TVDNFVALATGEK	1824000000	13330000	1810700000
TVEAEAAHGTVTR	17833000	0	17833000
TVEALYK	0	0	0
TVEDVFLR	21168000	0	21168000
TVELLSGVVDQTK	21383000	0	21383000
TVENFVALATGEK	34048000	0	34048000
TVENVTVFGTASASK	0	0	0
TVESEAASYLDQISR	0	0	0
TVESITDIR	124060000	0	124060000
TVFAEHISDECK	169250000	0	169250000
TVGAALDILCPSGPIK	26382000	0	26382000
TVGALQVLGTEAQSSLLK	84789000	0	84789000
TVGATALPR	26555000	0	26555000
TVGQCLETTAQR	22129000	0	22129000
TVGQLYK	15925000	0	15925000
TVIDYNGER	69209000	0	69209000
TVIGCSGFHGDCLTLTK	0	0	0
TVLDPVTGDLSDTR	26730000	4740200	21990000
TVLDQQQTPSR	74997000	0	74997000
TVLGTPEVLLGALPGAGGTQR	9148700	0	9148700
TVLIMELINNVAK	1254400	0	1254400
TVLLLADQMISR	7526100	0	7526100
TVLMLADQMISR	5136000	0	5136000
TVMENFVAFVDK	656740000	656740000	0

TVNTFSQSVSSLFGEDNVR	4256900	0	4256900
TVNVVQFEPSK	0	0	0
TVPWEQPATK	5196300	0	5196300
TVQIEASTVEIEER	2696900	0	2696900
TVQLTSSELESTLETLK	21541000	0	21541000
TVQSNSPISALAPTGK	36044000	0	36044000
TVQVSATEDGNVTK	22065000	0	22065000
TVSQIISLQTLK	46471000	0	46471000
TVTAEVQPQCGR	5413800	0	5413800
TVTAMDVVYALK	38353000	0	38353000
TVTATFGYPFR	40887000	0	40887000
TVTEIDEK	20984000	0	20984000
TVTNAVVTVPAYFNDSQR	8476100	0	8476100
TVVAPSAVAGK	15229000	0	15229000
TVVSGSCAAHSLLITTEGK	0	0	0
TWIEVSGSSAK	17795000	0	17795000
TWNDPSVQQDIK	5749000	0	5749000
TWTVVDAK	43935000	0	43935000
TYADYESVNECMEGVCK	0	0	0
TYCCDLK	33885000	0	33885000
TYDATTHFETTCDDIK	28323000	0	28323000
TYDLLFK	36737000	0	36737000
TYDSYLGDDYVR	1561300	1561300	0
TYGGCEGPDAMYVK	0	0	0
TYIPPKGETK	2562400	0	2562400

TYIQCIAAISR	21487000	0	21487000
TYLPSQVSR	29127000	0	29127000
TYLQALPYFDR	51876000	0	51876000
TYSWDNAQVLLVGNK	0	0	0
TYSYLTPDLWK	3562700	0	3562700
TYTDELTPIESAVSVFK	0	0	0
VAAAESMPLLLECAR	0	0	0
VAAALPGMESTQDR	19678000	0	19678000
VAADMFSDGNFNWGR	9674900	0	9674900
VAAGLQIK	46849000	0	46849000
VAAIEALNDGELQK	9591200	0	9591200
VAALIQK	9893600	0	9893600
VAALQNLVK	137280000	0	137280000
VAALTGLPFVTAPNK	16968000	0	16968000
VAAPDVVVPTLDTVR	86351000	0	86351000
VAASCGAIQYIPTELDQVR	46303000	0	46303000
VAASNIVQMK	176900000	0	176900000
VAASPEDIK	5893900	0	5893900
VACITEQVLTLVNK	6389700	0	6389700
VADGGGAGGTFQPYLDTLR	24305000	0	24305000
VADIGLAAWGR	45530000	0	45530000
VADISGDTQK	115120000	1180300	113940000
VAECSTGTLDYILQR	1088200	0	1088200
VAEDEAEAAAAAK	60635000	0	60635000
VAEITELILK	17624000	0	17624000

VAEQTPLTALYVANLIK	5432100	0	5432100
VAEQVLNAVNK	29429000	0	29429000
VAFITGGGTGLGK	12712000	0	12712000
VAFTGSTEIGR	10385000	0	10385000
VAGDCLDEK	45549000	0	45549000
VAGSPGWVR	0	0	0
VAGTQACATETIDTSR	6348800	0	6348800
VAGYAALLEQYQK	10028000	0	10028000
VAHALAEGLGVIACIGEK	2509200	0	2509200
VAIEPGAPR	27786000	0	27786000
VAIFIEK	0	0	0
VALDMTTLTIMR	12107000	0	12107000
VALIGSPVDLTYTYDHLGDSPK	7605700	0	7605700
VAMGAFDK	20376000	0	20376000
VANPSGNLTETYVQDR	0	0	0
VANVELYYR	35061000	0	35061000
VAPADGFSDLAMQVMTSPSK	5700700	0	5700700
VAPDEHPILLTEAPLNPK	10104000	0	10104000
VAPEEHPILLTEAPLNPK	612900000	612900000	0
VAPEEHPVLLTEAPLNPK	1422000000	0	1422000000
VAPPGLTQIPQIQK	12577000	0	12577000
VAQGVSGAVQDK	83945000	0	83945000
VAQLEQVYIR	60974000	0	60974000
VAQPTITDNK	3587600	0	3587600
VAQVAEITYGQK	0	0	0

VASGCLDINSSVK	9564800	0	9564800
VASQGEVVR	3811500	0	3811500
VASVEMVK	61287000	0	61287000
VATMLATGGNR	21614000	0	21614000
VATPVDWK	95334000	0	95334000
VATSSLDQTVK	7689100	0	7689100
VATVSLPR	4869700000	4869700000	0
VATWFNQPAR	0	0	0
VAVAIPNRPPDAVLTDTTSLNQAALYR	6322700	0	6322700
VAVEYLDPSPEVQK	0	0	0
VAVLSQNR	8975000	0	8975000
VAVTPPGLAR	1488500	0	1488500
VAVYVPGSK	17696000	0	17696000
VCALLSCTSHK	2899800	0	2899800
VCDIAAELAR	38012000	0	38012000
VCEEIAIIPSK	0	0	0
VCEEIAIIPSKK	0	0	0
VCENIPIVLCGNK	254180000	0	254180000
VCGSDGVTYGNECQLK	1677600	0	1677600
VCLLGCGISTGYGAAVNTAK	89195000	0	89195000
VCMDFNIIR	31016000	0	31016000
VCMVYDLYK	4049300	0	4049300
VCNYGLTFTQK	3002300	0	3002300
VCNYVNWIQQTIAAN	0	0	0
VCQCDSNGDCTDVDR	6232100	0	6232100

VCQGIGMVNR	11517000	0	11517000
VCTLAIIDPGDSDIIR	85693000	0	85693000
VDALLSAQPK	30504000	0	30504000
VDATADYICK	53480000	0	53480000
VDATAETDLAK	163170000	0	163170000
VDATEESDLAQQYGVR	0	0	0
VDCDQHSDIAQR	10598000	0	10598000
VDCQAYAQTCQK	2288700	0	2288700
VDCTAHSDVCSAQGVR	21273000	0	21273000
VDCTQHYELCSGNQVR	22777000	0	22777000
VDDESMQR	3062900	0	3062900
VDDFLANEAK	9946000	0	9946000
VDDQIAIVFK	0	0	0
VDDSSGSIGR	106530000	5266000	101260000
VDEFVTHNLSFDEINK	26389000	0	26389000
VDFPQDQLTALTGR	349840000	0	349840000
VDFTEEEINNMK	16073000	0	16073000
VDGALCTEK	10300000	10300000	0
VDGMDILCVR	19443000	0	19443000
VDIIENQVMDFR	52185000	3564700	48620000
VDLGVLGK	0	0	0
VDNDENEHQLSLR	23070000	0	23070000
VDNIQAGELTEGIWR	7285500	0	7285500
VDQETLTEMVKPSIDYVR	13229000	0	13229000
VDQIQEIVTGNPTVIK	3427300	0	3427300

VDQSTTSMAK	1600500	0	1600500
VDSDKEDDITELK	12151000	0	12151000
VDSLLENLEK	66627000	0	66627000
VDTILEFSQNMNTK	5099600	0	5099600
VDVGKDQEFTVK	0	0	0
VDVTEQPGLSGR	72199000	0	72199000
VEAFQTTISK	12411000	0	12411000
VEDLTFTSPFCLQVK	16296000	0	16296000
VEDPTFLNQLQSGVNR	0	0	0
VEDVVVSDECR	38795000	0	38795000
VEEIAASK	30236000	0	30236000
VEEQEPELTSTPNFVVEVIK	29213000	0	29213000
VEESSWLIEDGK	10525000	0	10525000
VEEVEDVSPGPWGLVK	25634000	25634000	0
VEEVELPVEK	7030900	0	7030900
VEEVGPYTYR	57031000	0	57031000
VEFILEQMR	21178000	0	21178000
VEFNVNYTQDLDK	1158300	0	1158300
VEGELEEMER	48382000	0	48382000
VEGFPTIYFAPSGDK	67198000	0	67198000
VEIATLTR	53225000	865490	52360000
VEILANDQGNR	85840000	12170000	73670000
VEITYTPSDGTQK	120610000	0	120610000
VELDNMPLR	10148000	0	10148000
VELSEQQLQLWPSDVDK	9926600	0	9926600

VELVPPTPAEIPR	64314000	0	64314000
VENFIQK	70935000	0	70935000
VENQENVSNLVIEDTELK	91610000	0	91610000
VEPGLGADNSVVR	39751000	0	39751000
VEQDLAMGTDAEGEK	13994000	0	13994000
VEQIEAGTPGR	103240000	0	103240000
VESLQEEIAFLK	36159000	0	36159000
VESVEPSENEASK	10114000	0	10114000
VETGVLKPGMVVTFAPVNVTTEVK	41724000	0	41724000
VETPLEEAIK	12031000	0	12031000
VETYNDESR	9088200	0	9088200
VEVCCFDK	25012000	0	25012000
VEVGKDQEFTVDTR	6807300	0	6807300
VEVTEFEDIK	49661000	0	49661000
VEYPIMYSTDPENGHIFNCIQR	17959000	0	17959000
VEYTLGEESEAPGQR	0	0	0
VFDAIMNFK	249920000	0	249920000
VFDFTFSPEEMK	17410000	0	17410000
VFDGIPPPYDK	0	0	0
VFDPQNDKPSK	25104000	0	25104000
VFDPVPVGVTK	16161000	0	16161000
VFEDESGK	10294000	0	10294000
VFEEDALSWEDK	6846600	0	6846600
VFEGNRPTNSIVFTK	41295000	0	41295000
VFEISPFEPWITR	11186000	0	11186000

VFFDLMR	34090000	0	34090000
VFIGNLNTLVVK	219350000	0	219350000
VFITDDFHDMMPK	114810000	0	114810000
VFIWTCDDASSNTWSPK	28309000	0	28309000
VFLATNSDYK	18003000	0	18003000
VFLDFFTYAPPK	9616700	0	9616700
VFLDVLMK	8416300	0	8416300
VFLENVIR	2003000000	56058000	1947000000
VFLLGEEVAQYDGAYK	12029000	0	12029000
VFMQEFK	21683000	0	21683000
VFNCISYSPLCK	9806000	0	9806000
VFNDTCR	6078100	0	6078100
VFNLYPR	0	0	0
VFQFLNAK	0	0	0
VFQSSTSQEQVYNDCAK	1618900	0	1618900
VFSGLVSTGLK	0	0	0
VFSIGPVFR	27739000	0	27739000
VFSLSSEFK	9451000	0	9451000
VFTAGSEER	6147000	0	6147000
VFVDLLPATQCTK	0	0	0
VFVMPNGMLK	0	0	0
VFVPLPGSTVMLCDYK	9640400	0	9640400
VFYYLVQDLK	96489000	0	96489000
VGAEELTADQNLK	26934000	0	26934000
VGDAIPAVEVFEGEPGNK	6412800	0	6412800

VGDPQELNGITR	12155000	0	12155000
VGEEFEEQTVDGRPCK	28214000	0	28214000
VGEFSGANK	88438000	0	88438000
VGEGFEEETVDGR	8079900	0	8079900
VGEGPGVCWLAPEQTAGK	565500	0	565500
VGEIEFEGLMR	22032000	0	22032000
VGEIVVFR	37442000	0	37442000
VGENADSQIK	0	0	0
VGFLPSAGK	17298000	0	17298000
VGGDVPETNYLFMGDFVDR	4610700	0	4610700
VGGTSDVEVNEK	2202400	0	2202400
VGGVQSLGGTGALR	43962000	0	43962000
VGINYQPPTVVPGGDLAK	398710000	0	398710000
VGIPVTDENGNR	25919000	0	25919000
VGLVASQK	31178000	0	31178000
VGMVETNSQDRPVDDVK	46876000	0	46876000
VGNLTVVGK	39937000	0	39937000
VGPGAGESPGTPPFR	0	0	0
VGQALELPLR	20450000	0	20450000
VGQAMASTEEK	59930000	0	59930000
VGQAVDVVGQAGKPK	18967000	0	18967000
VGQDPVLR	113400000	0	113400000
VGQEIEVRPGIVSK	20618000	0	20618000
VGQLSEGAIAAIMQK	56984000	0	56984000
VGSTSENITQK	7277200	0	7277200

VGSVEEFQGQER	9521300	0	9521300
VGTVIGSNK	96191000	0	96191000
VGVNGFGR	978150000	23371000	954780000
VGWEQLLTTIAR	1428000	0	1428000
VGYTPDWIFLLR	5107200	0	5107200
VHAAVQPGSLDSESGIFACAFDQSESR	3005600	0	3005600
VHAPEVDWIK	0	0	0
VHLVGIDIFTGK	3012100	0	3012100
VHPVSTMIK	176870000	0	176870000
VHVDCMTSQK	2553300	0	2553300
VIAALLQTMEDQGNQR	96434000	0	96434000
VIADNVK	81450000	0	81450000
VIAINVDDPDAANYNDINDVKR	7203900	0	7203900
VIATDINESK	8325900	0	8325900
VIATFTCSGEK	10733000	0	10733000
VIAYNSEGK	8791900	0	8791900
VIDQQNGLYR	15044000	0	15044000
VIECSYTSADGQR	32517000	0	32517000
VIEDIYEK	0	0	0
VIEDNEYTAR	1981500	0	1981500
VIEEQLEPAVEK	18065000	0	18065000
VIFGLFGK	238500000	1831500	236670000
VIFLENYR	13517000	0	13517000
VIGIECSSISDYAVK	0	0	0
VIGNQSLVNELAFTAR	12965000	0	12965000

VIGSGCNLDSAR	3695700000	126600000	3569100000
VIISAPSADAPMFVMGVNHEK	2399400000	8282500	2391100000
VIISCDLISPSVPPK	812010000	812010000	0
VIITGDAFVPGER	3625300	0	3625300
VILDLTPNYR	57838000	0	57838000
VILGSEAAQQHPEEVR	17469000	0	17469000
VIMGEEVEPVGLMTGSGVVGVK	9315000	0	9315000
VIMVGSGGVGK	13403000	0	13403000
VINEPTAAALAYGLDK	71714000	0	71714000
VIPAADLSQQISTAGTEASGTGNMK	0	0	0
VIPELNGK	1365900000	3445700	1362500000
VIPGAAEK	38040000	0	38040000
VIPSFMCQAGDFTNHNGTGGK	0	0	0
VIQALAMK	7568000	0	7568000
VIQCFAETGQVQK	102000000	0	102000000
VIQDCEDENIQR	18139000	0	18139000
VIQEGLEGLVLK	2351400	0	2351400
VIQEIVDK	31175000	0	31175000
VIQVAAGSSNLK	52289000	0	52289000
VISELNGK	85267000	0	85267000
VISLEDFMEK	46446000	0	46446000
VISTLEEPTPQCPTSQGR	9650000	0	9650000
VISYEEGK	15203000	0	15203000
VIVDFSSPNIAK	0	0	0
VIVVGNPANTNCLTASK	0	0	0

VKNPEDLSAETMAK	3129800	0	3129800
VLAGETLSVNDPPDVLDR	9252400	0	9252400
VLANNSLSFEK	6534900	0	6534900
VLANPGNSQVAR	101540000	0	101540000
VLANQYK	6355200	0	6355200
VLATAFDTTLGGR	21290000	0	21290000
VLAVNQENEHLMEDYEK	7435600	0	7435600
VLAVNQENEQLMEDYEK	30838000	0	30838000
VLDMPTQELGLPAYR	5494700	0	5494700
VLDNAIETEK	73013000	0	73013000
VLDPASSDFTR	0	0	0
VLDPFTIKPLDR	43191000	0	43191000
VLEACSIACNK	12063000	0	12063000
VLECLASGIVMPDGSGIYDPCEK	27980000	0	27980000
VLEDNKLPGAICSLTCGGADIGTAMAK	7160000	0	7160000
VLEEYGAGVCSTR	7830200	0	7830200
VLEFNCR	6489800	0	6489800
VLEGMEVVR	516530000	0	516530000
VLEGNEQFINAAK	4707900	4707900	0
VLELVSITANK	55657000	0	55657000
VLENAEGAR	25615000	0	25615000
VLENIELNK	7308800	0	7308800
VLEQLIVAHFPMQSR	18435000	0	18435000
VLEQLTGQTPVFSK	62177000	0	62177000
VLESLDR	8653600	0	8653600

VLESVAR	36067000	0	36067000
VLFDNTGR	34067000	0	34067000
VLFLLGADGGCITR	0	0	0
VLFPGNSTQYNILEGLEK	4192400	0	4192400
VLFSSNGGVVK	11124000	0	11124000
VLGATLLPDLIQK	42102000	0	42102000
VLGGSFADQK	0	0	0
VLGLVLLR	17420000	0	17420000
VLGMDPLPSK	0	0	0
VLGMTLIQK	0	0	0
VLGQLTETGVVSPEQFMK	18156000	0	18156000
VLGSDTNCSAPR	240650000	12979000	227670000
VLGTAFDPFLGGK	179510000	0	179510000
VLGTEELYGYLK	18645000	0	18645000
VLIDPVSVQDK	25528000	0	25528000
VLIFSQMTK	29575000	0	29575000
VLIFSQMTR	5087200	0	5087200
VLIGGDETPEGQR	2371200	0	2371200
VLIGVGK	20668000	0	20668000
VLITTDLLAR	11756000	0	11756000
VLLDNVENK	0	0	0
VLLDQLR	13083000	0	13083000
VLLSALER	0	0	0
VLLVPGPEKEN	0	0	0
VLNLGQALER	5013900	0	5013900

VLNNMEIGTSLFDEEGAK	80756000	0	80756000
VLNSYWVGEDSTYK	9042600	0	9042600
VLNTNIDGR	357970000	0	357970000
VLPGSSVLFLCDMQEK	1885500	0	1885500
VLPMNTGVEAGETACK	7684100	0	7684100
VLPQEAEEENR	12817000	0	12817000
VLPSITTEILK	21528000	0	21528000
VLPSIVNEVLK	35124000	0	35124000
VLQALEGLK	7274600	0	7274600
VLQATVVAVGSGSK	7359900	0	7359900
VLQDMGLPTGAEGR	13107000	0	13107000
VLQGDLVMNVYR	31702000	0	31702000
VLQNMEQCQK	4743700	0	4743700
VLQQTMTK	1667100	0	1667100
VLQSALAAIR	29498000	0	29498000
VLQSDEYEEVEDK	9224400	0	9224400
VLSECSPLMNDIFNK	96073000	0	96073000
VLSGQDTEDR	5000800	0	5000800
VLSQQAASVVK	11502000	0	11502000
VLSSIEQK	322240000	0	322240000
VLSTPDLEVR	13253000	0	13253000
VLTEIIASR	15435000	0	15435000
VLTGVAGEDAECHAAK	113620000	0	113620000
VLTIDPTEFK	22088000	0	22088000
VLTNITVSCQEK	1019000	0	1019000

VLTSDIEK	39423000	0	39423000
VLTTAGSYVR	19011000	8437700	10573000
VLTVINQTQK	60583000	0	60583000
VLVDSLVEDDR	3318500	0	3318500
VLVEGPLNNLR	9090500	0	9090500
VLVEPDAGAGVAVMK	0	0	0
VLVEWLR	9504400	0	9504400
VLVIGAGGLGCELLK	2142500	0	2142500
VLVLSQDYGK	18200000	0	18200000
VLVPATDR	67954000	0	67954000
VLVSPTNPPGATSSCQK	14394000	0	14394000
VLVWDLR	25406000	0	25406000
VLYAYGYYTGEPSK	12930000	0	12930000
VLYPNDNFFEGK	43594000	0	43594000
VLYSNMLGEENTYLWR	5680300	0	5680300
VLYVQDSLEGEAR	0	0	0
VMATTGGTNLR	16336000	0	16336000
VMEIVDADEK	106000000	0	106000000
VMEMYQPSAVVLQCGADSLSGDR	24032000	0	24032000
VMEYINR	63094000	0	63094000
VMFEVWR	35965000	0	35965000
VMLGETNPADSK	56688000	0	56688000
VMLGETNPADSKPGTIR	643710000	0	643710000
VMQQQQQTTQQQLPQK	2566300	0	2566300
VMQVLNADAIVVK	105040000	0	105040000

VMVELLGSYTEDNASQAR	7434900	0	7434900
VMVLDFVTPTPLGTR	6364100	0	6364100
VMVQPINLIFR	53352000	1100300	52251000
VNAELQAR	0	0	0
VNASASSLK	8299900	0	8299900
VNEAAPEKPQDDSGTAGGISSTSASVNR	0	0	0
VNEALLQR	17492000	0	17492000
VNEIVETNRPDSK	1971800	0	1971800
VNEVNQFAAK	37475000	0	37475000
VNFAMNVGK	44866000	0	44866000
VNFDDYTVNLGGLK	12532000	0	12532000
VNFTVDQIR	0	0	0
VNGDASPAAAESGAK	17664000	0	17664000
VNIFGVESGK	0	0	0
VNIIGEVVDQGSTNLK	30281000	0	30281000
VNIIPLIAK	63869000	0	63869000
VNIVPVIAK	3573100	0	3573100
VNLAELFK	101770000	0	101770000
VNLFTDFDK	56334000	0	56334000
VNLGVGAYR	10070000	0	10070000
VNLLQIVR	12639000	0	12639000
VNLLSVLEAAK	16648000	0	16648000
VNNSTMLGASGDYADFQYLK	64903000	0	64903000
VNPIQGLASK	162520000	0	162520000
VNQAIWLLCTGAR	14195000	0	14195000

VNQIGSVTESLQACK	85137000	0	85137000
VNTLIRPDGEK	18588000	0	18588000
VNVPVIGGHAGK	136740000	0	136740000
VPADTEVVCAPPTAYIDFAR	300830000	6179700	294650000
VPAGLEK	25075000	0	25075000
VPAGNWVLIEGVDQPIVK	3152700	0	3152700
VPAINVNDSVTK	317880000	0	317880000
VPDVLVADPPIAR	5869600	0	5869600
VPEANSSWMDTVIR	20566000	0	20566000
VPEILQLSDALR	5676000	0	5676000
VPELNVQNGVLK	0	0	0
VPEPGVPTETIK	19573000	0	19573000
VPEWVDTVK	2311800	0	2311800
VPFLPGDSDLDQLTR	6966200	0	6966200
VPFLVLECPNLK	126250000	0	126250000
VPGLPTPIENMILR	7788000	0	7788000
VPLAIVNK	15377000	0	15377000
VPLQGFAALEGMNGIQK	7476900	0	7476900
VPLVAPEDLR	12455000	0	12455000
VPMASCDFSIR	0	0	0
VPPAINQFTQALDR	163550000	0	163550000
VPQVSTPTLVEVSR	24003000	24003000	0
VPSENVLGEVGSGFK	39656000	0	39656000
VPSLVGSFIR	6362100	0	6362100
VPSTETEALASNLMGMFEK	15156000	0	15156000

VPTANVSVVDLTCR	596670000	0	596670000
VPTWGPLR	0	0	0
VPVNLLR	23591000	0	23591000
VQAHAAAALINFTEDCPK	64245000	0	64245000
VQAQGPGLK	5066700	0	5066700
VQAQVIQETIVPK	1230400	0	1230400
VQEGETIEDGAR	4777400	0	4777400
VQEMVESNEAK	10773000	0	10773000
VQENCIDLVGR	0	0	0
VQEQLGNDVVEK	11336000	0	11336000
VQESADELQK	119080000	2285200	116790000
VQIAANEETQER	28175000	0	28175000
VQIPIMLVGNK	31271000	0	31271000
VQIQESVR	15325000	0	15325000
VQQTVQDLFGR	25349000	0	25349000
VQSDGQIVLVDDWIK	3310100	0	3310100
VQTAALR	15800000	0	15800000
VQTGEEGMPLSTIR	2568200	0	2568200
VQVALEELQDLK	14839000	0	14839000
VQVMVPEAETR	3553700	0	3553700
VQVQDNEGCPVEALVK	0	0	0
VQVYQEPNR	5332600	0	5332600
VQYPQSQACK	7545600	0	7545600
VSASPLLYTLIEK	23600000	0	23600000
VSEEIEDIIK	14797000	0	14797000

VSEYVPEIVNFVQK	13838000	0	13838000
VSFELFADK	527320000	0	527320000
VSGGLEVLAEK	244530000	0	244530000
VSGVDGYETEGIR	2157300	0	2157300
VSQAAADLK	5487500	0	5487500
VSQAAAELLAFCETHAK	46733000	0	46733000
VSQGQLVVMQPEK	73658000	0	73658000
VSQGSKDPAEGDGAQPEETPR	17246000	0	17246000
VSQMAQYFEPLTLAAVGAASK	1563100	0	1563100
VSQPIEGHAASFAQFK	14988000	0	14988000
VSSDNVADLHEK	52752000	3431700	49320000
VSSFEEK	65337000	363020	64974000
VSTEVDAR	65966000	0	65966000
VSYGIGDEEHDQEGR	43178000	0	43178000
VSYYENVIK	41015000	0	41015000
VTAQGPGLEPSGNIANK	68648000	0	68648000
VTAVPTLLK	12715000	0	12715000
VTCIDPNPNFEK	29172000	0	29172000
VTDDLVCLVYK	15566000	0	15566000
VTDFGDKVEDPTFLNQLQSGVNR	20618000	0	20618000
VTDLVQFLLFK	927410	0	927410
VTEGGEPYR	3997200	0	3997200
VTEGLTDVILYHQPDDK	16250000	0	16250000
VTEGLVDVILYHQPDDK	52960000	0	52960000
VTEGSFVYK	117800000	0	117800000

VTELALTASDR	47932000	0	47932000
VTGQFPWSSLR	20044000	0	20044000
VTGTLDANR	375860000	3169600	372690000
VTIAQGGVLPNIQAVLLPK	1108400	0	1108400
VTLGTQPTVLR	16655000	0	16655000
VTLLDLMIAK	6029800	0	6029800
VTLMQLPTR	12727000	0	12727000
VTLNPPGTFLEGVAK	1879400	0	1879400
VTLPGQEEPWDIR	0	0	0
VTLTSEEEAR	585000000	6797400	578200000
VTMNFEPNK	6207800	0	6207800
VTMQNLNDR	3581800	3581800	0
VTNGAFTGEISPGMIK	54036000	0	54036000
VTNLLMLK	14885000	0	14885000
VTNLSEDTR	35782000	0	35782000
VTPPAVTGSPEFER	18374000	0	18374000
VTQDELK	40231000	0	40231000
VTQSNFAVGYK	86022000	0	86022000
VTQVDGNSPVR	7380500	0	7380500
VTSAVEALLSADSASR	11427000	0	11427000
VTSEGAGLQLQK	11920000	0	11920000
VTTGTSNTTAIK	8433700	0	8433700
VTWDSSFCAVNPR	0	0	0
VTYMEEER	2825500	0	2825500
VVAEPVELAQEFR	10683000	0	10683000

VVAIGECGLDFDR	6768600	0	6768600
VVAPTISSPVCQEQLVEAGR	0	0	0
VVDLLNQAALITNDSK	7534000	0	7534000
VVDLMAHMASK	37282000	0	37282000
VVDLMAHMASKE	0	0	0
VVDYTTAK	6452500	0	6452500
VVEDGILK	33806000	0	33806000
VVEGSFVYK	34737000	4537600	30199000
VVEGTPLIDGR	14589000	0	14589000
VVEQLEK	11969000	0	11969000
VVESGGPEILK	5265800	0	5265800
VVFEQTK	515270000	0	515270000
VVFQEFR	0	0	0
VVFVFGPDK	96302000	710660	95591000
VVGAMQLYSVDR	0	0	0
VVGAQSLK	49971000	0	49971000
VVHIMDFQR	12996000	0	12996000
VVHVNGYGK	1690900	0	1690900
VVIEDEQLVLGASQEPVGR	2643600	0	2643600
VVIFQQEQENK	0	0	0
VVIIGAGK	26897000	0	26897000
VVINGQEVK	21514000	0	21514000
VVLAYEPVWAIGTGK	173230000	0	173230000
VVLIGDSGVGK	15381000	0	15381000
VVLIGGKPDR	8842900	0	8842900

VVLLGEFLHPCEDDIVCK	15664000	0	15664000
VVLLTGETSTDLK	7242500	0	7242500
VVLPIEAPIR	73277000	1666200	71611000
VVLVLAGR	3834900	0	3834900
VVMDGVISDHECQELQR	2841400	0	2841400
VVNDEEVVR	5358600	0	5358600
VVNEINIEDLCLTK	46666000	0	46666000
VVNIVPVIAK	27480000	0	27480000
VVSLSEYR	0	0	0
VVSPWNSEDAK	18062000	0	18062000
VVSSIEQK	801880000	3677800	798200000
VVSTQAPDR	1602900	0	1602900
VVSVHPGDVLITSCTYNTEDR	18233000	0	18233000
VVTDTDETELAR	7483200	0	7483200
VVTGVANALAHR	32775000	32775000	0
VVTQNICQYR	71519000	0	71519000
VVTVGQFK	31602000	0	31602000
VVTYGMANLLTGPK	64069000	0	64069000
VVVLGLLPR	34601000	0	34601000
VVVLNCEPSK	16865000	0	16865000
VVVQVLAEEPEAVLK	8211800	0	8211800
VVVVTGANTGIGK	19979000	0	19979000
VVYIFGPPVK	0	0	0
VVYTGTYDTEGVTPTK	0	0	0
VWDISGLR	17394000	0	17394000

VWNLANCK	68614000	0	68614000
VWQLQDLSFQTAAR	10772000	0	10772000
VYATILNAGTNTDGFK	12498000	0	12498000
VYAVATSTNTPCAR	6480400	0	6480400
VYEGERPLTK	13135000	0	13135000
VYIYSSGSVEAQK	10799000	0	10799000
VYLQNEYK	0	0	0
VYMGEMGR	16080000	0	16080000
VYNVTQHAVGIVVNK	5131100	0	5131100
VYPSSLSK	37824000	0	37824000
VYQVTEQQISEK	0	0	0
VYSYALALK	0	0	0
VYTPVGK	22682000	0	22682000
VYVGNLGTGAGK	14277000	0	14277000
VYVVEGSK	19439000	0	19439000
VYYVSEK	8263500	0	8263500
WADNFMAEGCGGSK	0	0	0
WAPNENK	24509000	0	24509000
WCEYGLTFTEK	18873000	0	18873000
WDPTANEDPEWILVEK	5947500	0	5947500
WDTGENPIYK	1649700	0	1649700
WDVLIQQATQCLNR	33936000	22246000	11691000
WDYLTQVEK	39905000	0	39905000
WELNSGDGAFYGPK	30752000	0	30752000
WFEENASQSTVK	61736000	0	61736000

WFLTCINQPQFR	38642000	0	38642000
WFVLDAETR	24453000	0	24453000
WGEEEAELNK	8955000	0	8955000
WGLGGTCVNVGCIPK	20497000	0	20497000
WGSNELPAEEGK	34362000	0	34362000
WGTLTDCVVMR	22849000	0	22849000
WIDETPPVDQPSR	15684000	0	15684000
WIDFDNDYK	24312000	0	24312000
WIDLTMEDIR	32765000	0	32765000
WISDWNLTTEK	7118900	0	7118900
WISIMTER	27318000	0	27318000
WLAIDANAR	0	0	0
WLAPDGLIFPDR	111470000	0	111470000
WLDESDAEMELR	16849000	0	16849000
WLLLCNPGLADTIVEK	1885700	0	1885700
WLLLTGISAQQNR	6840100	0	6840100
WLNENAVEK	176890000	0	176890000
WMVSSWLPSEVHPDINR	6855600	0	6855600
WNFDDLLEK	0	0	0
WNSPAEEGSSDCEVFSK	1819000	0	1819000
WPFSLSEQQLDAR	8388100	0	8388100
WSLQSEAHR	18388000	0	18388000
WSPLENK	0	0	0
WSSLACNIALDAVK	18596000	0	18596000
WSTISENLFATTGYPGK	8849600	0	8849600

WSTLVEDYGMELR	28444000	0	28444000
WTDENIDTVALK	46146000	0	46146000
WTELAGCTADFR	5069600	0	5069600
WTEYGLTFTEK	3756300	0	3756300
WTGMIIGPPR	34891000	0	34891000
WTMSSWTMKMMR	1512500	1512500	0
WTNQLNSLNQAVVSK	0	0	0
WTSQDSLLGMEFSGR	19386000	0	19386000
WTTEQQQR	26464000	0	26464000
WVTTASLLDYDTVAGADK	27742000	0	27742000
WYVVQTNYDR	1986400	0	1986400
YAACNAVGQMATDFAPGFQK	12256000	0	12256000
YADLTEDQLPSCESLK	10901000	0	10901000
YAEAVTR	251570000	0	251570000
YAILNEPFK	3897200	0	3897200
YALPLVGHR	6560800	0	6560800
YALTGDEVK	304170000	0	304170000
YALTTTLSAR	0	0	0
YAMEQSIK	14071000	0	14071000
YANEVNSDAGAFK	17931000	0	17931000
YASACQMK	1903600	0	1903600
YASICQQNGIVPIVEPEILPDGDHDLK	36030000	0	36030000
YATLATVSR	3443100	1367500	2075600
YAVLYQPLFDK	20553000	0	20553000
YAVPSAGLR	62757000	0	62757000

YCALLLPLLK	4402800	0	4402800
YCAQDAFFQVK	3185400	0	3185400
YCFGVEDTLK	0	0	0
YCGLCDSIITIYR	0	0	0
YCTDTGVLFR	10677000	0	10677000
YDAFLASESLIK	50485000	0	50485000
YDDAIQLYDR	1023100	0	1023100
YDDMAAAMK	127630000	0	127630000
YDDMAACMK	78805000	0	78805000
YDDPEVQK	16286000	0	16286000
YDEEFQR	19203000	0	19203000
YDEMVESMK	332520000	0	332520000
YDGLVGMFDPK	32734000	0	32734000
YDGQVAVFGSDLQEK	12734000	0	12734000
YDLSPITVK	0	0	0
YDLTVPFAR	111770000	0	111770000
YDPTIEDSYR	0	0	0
YDQNYDIR	5131400	0	5131400
YDYEEVEAEGANK	36076000	0	36076000
YDYNSGEELESYK	9897200	0	9897200
YEAAGTLVTLSSAPTAIK	60425000	0	60425000
YEAAYGK	7063800	0	7063800
YEDAYQYQNIFGPLVK	2927800	0	2927800
YEDICPSTHNMDVPNIK	14311000	0	14311000
YEDLAPCITLK	11765000	0	11765000

YEFLWGPR	2163500	0	2163500
YEGGYPALTEVMNK	4799800	0	4799800
YEILTPNSIPK	8652800	0	8652800
YEIMDGAPVR	2397500	0	2397500
YEITEQR	21919000	0	21919000
YENNVMNIR	24989000	0	24989000
YEPIVTK	86068000	0	86068000
YEQGTGCWQGPNR	64454000	1986600	62468000
YESLTDPSK	374300000	0	374300000
YEWDVAEAR	0	0	0
YFAYDCEASFPGISTGPMK	5895300	0	5895300
YFDEISQDTGK	11889000	0	11889000
YFDPANGK	204540000	0	204540000
YFDSCNGDLDPEIVK	9037400	0	9037400
YFDTVPVAAAMCVLK	10365000	0	10365000
YFEGVSPK	55628000	0	55628000
YFEVEEADGNK	2206400	0	2206400
YFFDFLDEQAEK	2909400	0	2909400
YFFFDDGNGLK	51014000	0	51014000
YFGDIISVGQR	0	0	0
YFGGTEDR	17463000	0	17463000
YFLFYDGETVSGK	1108200	0	1108200
YFPFMDLK	11353000	0	11353000
YFPTQALNFAFK	48074000	0	48074000
YFQFQEEGK	6268500	0	6268500

YFTLGLPTGSTPLGCYK	18683000	0	18683000
YFTWDPSR	111240000	0	111240000
YFVISNTTGYNDR	2333500	0	2333500
YGALALQEIFDGIQPK	5192200	0	5192200
YGDAFIR	12418000	0	12418000
YGDSGEQIAGFVK	0	0	0
YGEPGEVFINK	33241000	0	33241000
YGEYFPGTGDLR	58809000	0	58809000
YGGPPPDSVYSGVQPGIGTEVFVGK	8450000	0	8450000
YGGQPVPNFPSK	5294800	0	5294800
YGIENVK	14412000	0	14412000
YGIEPTMVVQGVK	0	0	0
YGIVDYMIEQSGPPSK	90441000	0	90441000
YGLECLFR	5889000	0	5889000
YGMGTSVER	38175000	0	38175000
YGPADVEDTTGSGATDSK	2879300	0	2879300
YGPFVADFADK	70265000	0	70265000
YGPMEEPLVIEK	0	0	0
YGQFSGLNPGGR	19276000	0	19276000
YGSPGNVSK	34310000	0	34310000
YGSQVEDQR	4473900	0	4473900
YGTCPHGGYGLGLER	42667000	0	42667000
YGVSGYPTLK	55705000	0	55705000
YHNVGLSK	12124000	0	12124000
YHTSQSGDEMTSLSEYVSR	249460000	3814800	245650000

YIAENGTDPINNQPLSEEQLIDIK	17760000	0	17760000
YIAIVSTTVETK	0	0	0
YICDNQDTISSK	444840000	444840000	0
YIDQEELNK	835800000	4810400	830980000
YIETSELCGGAR	14601000	0	14601000
YIIIGDMGVGK	27163000	0	27163000
YIIIGDTGVGK	24858000	0	24858000
YILAATLDNTLK	6506900	0	6506900
YIMVPSGNMGVFDPTEIHNR	15532000	0	15532000
YIQAEPPTNK	18343000	0	18343000
YIQELWR	2876500	0	2876500
YISLIYTNYEAGK	46440000	0	46440000
YISLIYTNYEAGKDDYVK	13631000	0	13631000
YISPDQLADLYK	513920000	0	513920000
YITDWQNVFR	0	0	0
YITGDQLGALYQDFVR	1783200	0	1783200
YITGTDILDMK	23064000	0	23064000
YITQNGDYQLR	2351600	0	2351600
YIYIMGIQER	18584000	0	18584000
YKPESEELTAER	158420000	0	158420000
YLAADKDGNVTCER	62896000	0	62896000
YLAEFATGNDR	832040000	20466000	811580000
YLAEFATGNDRK	108760000	0	108760000
YLAEVAAGDDK	164080000	0	164080000
YLAEVAAGDDKK	254090000	0	254090000

YLAEVACGDDR	163520000	4253200	159270000
YLAEVACGDDRK	44125000	0	44125000
YLAEVASGEK	73870000	0	73870000
YLAEVATGEK	321680000	0	321680000
YLAIAPPIIK	39389000	0	39389000
YLCDEQK	17177000	0	17177000
YLDLILNDFVR	8225500	0	8225500
YLDSIPPGQYMDSSLVK	10496000	0	10496000
YLEAGAAGLR	28549000	0	28549000
YLEANMTQSALPK	7041000	0	7041000
YLEAVEK	31879000	0	31879000
YLEMIYSMCK	19452000	0	19452000
YLEPLYNDYR	15380000	0	15380000
YLFLGDYVDR	25946000	0	25946000
YLGLLENLR	9557800	0	9557800
YLIANATNPESK	86709000	0	86709000
YLIATSEQPIAALHR	34769000	0	34769000
YLIPNATQPESK	82193000	0	82193000
YLLADCNEAFIK	20932000	0	20932000
YLLAMER	3154000	0	3154000
YLLDSCAPLLR	0	0	0
YLLGDMEGR	0	0	0
YLLLMDLQDR	1721600	0	1721600
YLMEEDEDAYKK	28042000	0	28042000
YLNIFGESQPNPK	0	0	0

YLQQIFESQR	10926000	0	10926000
YLQSLLAEVER	7392500	0	7392500
YLSEVASGDNK	63057000	0	63057000
YLSNAYAR	11530000	0	11530000
YLTGTYVQEESPEGGR	4921800	0	4921800
YLTLDGFDAMFR	8953000	0	8953000
YLTMDDLTTALEGNR	37091000	0	37091000
YLTTAVITNK	25344000	0	25344000
YLYEIAR	57818000	57818000	0
YMACCLLYR	64515000	0	64515000
YMDAWNTVSR	2157700	0	2157700
YMEENDQLKK	27235000	0	27235000
YMLPLDNLK	18057000	0	18057000
YMMIVDPAISSSGPAGSYRPYDEGLR	3582100	0	3582100
YMSPEQISSQDYGK	0	0	0
YMTDGMLLR	0	0	0
YNACILEYK	2981200	0	2981200
YNAQCQETIR	7905600	0	7905600
YNDTFWK	16939000	0	16939000
YNGVFQECCQAEDK	192620000	192620000	0
YNILGTNTIMDK	171090000	0	171090000
YNPNVLPVQCTGK	10868000	0	10868000
YNPTWHCIVGR	11302000	0	11302000
YNQPFFVTSLPDDK	4460100	0	4460100
YPEAPPFVR	0	0	0

YPEETLSLMTK	14056000	0	14056000
YPENFFLLR	53089000	0	53089000
YPIEHGIITNWDDMEK	1145800000	1647100	1144200000
YPQLLPGIR	22897000	0	22897000
YPSATNNTPAK	3378800	0	3378800
YPSPFFVFGEK	15548000	0	15548000
YPVNSVNILK	0	0	0
YQAVTATLEEK	64369000	0	64369000
YQEALAK	31951000	0	31951000
YQEALHLGSQLLR	35457000	0	35457000
YQEELNFDNPLGMR	2602700	0	2602700
YQETFNVIER	0	0	0
YQEVTNNLEFAK	2419900	0	2419900
YQILPLHSQIPR	17017000	0	17017000
YQLDKDGVVLFK	92681000	0	92681000
YQLNLPPYPDTECVYR	0	0	0
YQQGDFGYCPR	46491000	0	46491000
YQQLFEDIR	0	0	0
YQSHDYAFSSVEK	5030000	0	5030000
YQYVDCGR	44602000	0	44602000
YRPGTVALR	232180000	0	232180000
YRVPDVLVADPPIAR	0	0	0
YSDIEPSTEGEVIFR	13140000	0	13140000
YSDSLVQK	13305000	0	13305000
YSEEGVYNVQYSFIK	3289000	0	3289000

YSELTTVQQQLIR	25125000	0	25125000
YSEVFEAINITNNEK	11428000	0	11428000
YSFLQFDPAPR	46563000	0	46563000
YSGDQILIR	7982800	0	7982800
YSIDQEFLK	1691800	0	1691800
YSLEPVAVELK	108060000	0	108060000
YSNDPVVASLAQDIFK	7006300	0	7006300
YSNSALGHVNCTIK	74053000	0	74053000
YSNSEVVTGSGR	11542000	0	11542000
YSQVLANGLDNK	61341000	0	61341000
YSQYQQAIYK	24320000	0	24320000
YSSTEEVLVAAK	6572500	0	6572500
YSTDVSVDEVK	19862000	0	19862000
YSTSGSSGLTTGK	8191700	0	8191700
YSVQTADHR	321780000	5065600	316710000
YSYQYTVANK	31384000	0	31384000
YSYVCPDLVK	0	0	0
YTAESSDTLCPR	10981000	0	10981000
YTCGEAPDYDR	18904000	0	18904000
YTCSFCGK	18246000	0	18246000
YTEGVQSLNWTK	0	0	0
YTFEEIQQETDIPER	1164800	0	1164800
YTGEDFDEDLR	9616100	0	9616100
YTGTLDCAK	12864000	0	12864000
YTMGDAPDYDR	1118600	0	1118600

YTPEEIAMATVTALR	1983000	0	1983000
YTQGGLENLELSR	0	0	0
YTQSNSVCYAK	28907000	0	28907000
YTSQIVGR	28727000	0	28727000
YTTPEDATPEPGEDPR	13941000	0	13941000
YTTTQQVVK	1312800	0	1312800
YTVQDESHSEWVSCVR	9249300	0	9249300
YVAAAFPSACGK	0	0	0
YVAEIEK	63688000	0	63688000
YVALTSLLK	30023000	0	30023000
YVALVQEK	12154000	0	12154000
YVANLFPYK	6251700	0	6251700
YVASYLLAALGGNSSPSAK	3588300	0	3588300
YVECSALTQK	0	0	0
YVENFGLIDGR	0	0	0
YVIYIER	14645000	0	14645000
YVLCTAPR	7260900	0	7260900
YVLEPEISFTSDNSFAK	6762400	0	6762400
YVLGDTAMQK	0	0	0
YVLINWVGEDVPDAR	5631800	0	5631800
YVMTTTTLER	5248300	0	5248300
YVPYVGDSK	52850000	0	52850000
YVQLPADEVDTQLLQDAAR	33097000	0	33097000
YVQQLQR	6759000	0	6759000
YVVEMAEGSNGNK	777120	0	777120

YVVVTGITPTPLGEGK	22298000	0	22298000
YWLCAATGPSIK	177680000	0	177680000
YWTLTATGGVQSTASSK	0	0	0
YWYLGPLK	8640000	0	8640000
YYAVNFPMR	56276000	0	56276000
YYDDTYPSVK	53441000	0	53441000
YYDQICSIEPK	18388000	0	18388000
YYEAADTVTQFDNVR	973740	0	973740
YYGLQILENVIK	1621200	0	1621200
YYMNQVEETR	28287000	0	28287000
YYNAESYEVER	1506400	0	1506400
YYNDYGDIIK	0	0	0
YYPTEDVPR	41146000	0	41146000
YYTEFPTVLDITAEDPSK	10138000	0	10138000
YYTPTISR	117820000	0	117820000
YYTSASGDEMVSLK	431650000	1249500	430400000
YYVLNALK	2847200	0	2847200
YYVTIIDAPGHR	461920000	0	461920000

Appendix 2

Dysregulated SILAC proteins

Uniprot accession #	Symbol	Entrez gene name	Fold change	Depleted_ p_value	Phospho_ p_value
A0AVT1	UBA6	ubiquitin-like modifier activating enzyme 6	1.105	0.006	
A6ZKI3	FAM127A	family with sequence similarity 127, member A	1.273		0.021
B1AKJ5	NRD1	nardilysin (N-arginine dibasic convertase)	1.074		0.002
B1AKZ3	PEA15	phosphoprotein enriched in astrocytes 15	1.075		0.004
B1AVU8			-1.195		0.017
B3KQV7	SLC29A1	solute carrier family 29 (equilibrative nucleoside transporter), member 1	1.230	0.02	
B3KS98	EIF3H	eukaryotic translation initiation factor 3, subunit H	-1.203	0.035	
B4DNJ6	STRAP	serine/threonine kinase receptor associated protein	1.049		0.003
B4DR61	SEC61A1	Sec61 alpha 1 subunit (S. cerevisiae)	1.123	0.008	
B4E1G6	GALK1	galactokinase 1	-1.100	0	
B7Z254	PDIA6	protein disulfide isomerase family A, member 6	1.245	0.003	0.001
B7Z7Q0	PITPNB	phosphatidylinositol transfer protein, beta	1.391		0.02
B9A064	IGLL1/IGLL5	immunoglobulin lambda-like polypeptide 1	-5.039		0.001
C9IZQ1	SSR1	signal sequence receptor, alpha	1.131	0.021	
C9JEA7	PLCD4	phospholipase C, delta 4	1.131		0.002
C9JEH3	AAMP	angio-associated, migratory cell protein	-1.078		0.026
C9JWM7	ARPC4	actin related protein 2/3 complex, subunit 4, 20kDa	1.098		0.014
D3DQV9	EIF4G2	eukaryotic translation initiation factor 4 gamma, 2	1.121	0.029	
E7EPA7	TKT	transketolase	1.258	0.023	0.046
E7EX17	EIF4B	eukaryotic translation initiation factor 4B	-1.112		0.021
E9PCK7	RRP12	ribosomal RNA processing 12 homolog	1.032		0.02
E9PFM1	EIF4G1	eukaryotic translation initiation factor 4 gamma, 1	1.048		0.038
E9PHK9			-1.245	0.03	
E9PK25	CFL1	cofilin 1 (non-muscle)	1.018	0.017	
E9PNQ8	THY1	Thy-1 cell surface antigen	-1.282	0.019	

F5H3A1	ATP1A1	ATPase, Na+/K+ transporting, alpha 1 polypeptide	1.061	0.018	
F5H3J8			6.521		0.028
F5HFY4	NAP1L4	nucleosome assembly protein 1-like 4	-1.062		0.027
F8W7C6	RPL10	ribosomal protein L10	-1.078	0.004	
F8W8S0			1.089		0.037
G3V2N0	GNG2	guanine nucleotide binding protein (G protein), gamma 2	-1.205	0	
G3V4T6	GSTZ1	glutathione S-transferase zeta 1	-1.194	0.004	
G3V5Z7	PSMA6	proteasome (prosome, macropain) subunit, alpha type, 6	1.048		0.048
H0YBA3	NRG1	neuregulin 1	1.012	0.002	
H0YHU6			-23.605	0.036	
H3BPE7	FUS	FUS RNA binding protein	-1.093	0.004	
H7BYM6			-1.091		0.038
H7C2I1	PRMT1	protein arginine methyltransferase 1	1.048	0.008	
I3NI00			-1.108	0.021	
J3KN16	KIAA0368	KIAA0368	1.109	0.028	
J3KN36	NOMO1 (includes others)	NODAL modulator 1	1.075	0.021	
J3KPP7			1.117		0.018
J3KPV7	MPST	mercaptopyruvate sulfurtransferase	1.035	0.009	
J3KTA4	DDX5	DEAD (Asp-Glu-Ala-Asp) box helicase 5	1.063	0.016	
J3QLS3	MRPS7	mitochondrial ribosomal protein S7	-1.050	0.02	
J3QT22	PPME1	protein phosphatase methylesterase 1	-1.058	0.027	
O00116	AGPS	alkylglycerone phosphate synthase	1.073	0.013	
O00571	DDX3X	DEAD (Asp-Glu-Ala-Asp) box helicase 3, X-linked	1.084	0.029	0.011
O00629	KPNA4	karyopherin alpha 4 (importin alpha 3)	-1.016		0.039
O14579	COPE	coatomer protein complex, subunit epsilon	1.087		0.004
O14979	HNRNPDL	heterogeneous nuclear ribonucleoprotein D-like	-1.047		0.015
O14980	XPO1	exportin 1	-1.008	0.032	
O15116	LSM1	LSM1 homolog, mRNA degradation associated	1.264		0.017
O15143	ARPC1B	actin related protein 2/3 complex, subunit 1B, 41kDa	1.137	0.016	
O15144	ARPC2	actin related protein 2/3 complex, subunit 2, 34kDa	1.056	0.047	
O15397	IPO8	importin 8	-1.067		0.012
O15511	ARPC5	actin related protein 2/3 complex, subunit 5, 16kDa	1.089	0.032	

O43175	PHGDH	phosphoglycerate dehydrogenase	-1.076	0.015	
O43447	PPIH	peptidylprolyl isomerase H (cyclophilin H)	-1.128	0	
O43633	CHMP2A	charged multivesicular body protein 2A	1.087		0.047
O43707	ACTN4	actinin, alpha 4	1.119		0
O43760	SYNGR2	synaptogyrin 2	1.193	0	
O60763-2	USO1	USO1 vesicle transport factor	1.097		0.039
O75083	WDR1	WD repeat domain 1	1.209	0.015	
O75367	H2AFY	H2A histone family, member Y	1.004	0.026	
O75369-8	FLNB	filamin B, beta	1.254		0.038
O75475	PSIP1	PC4 and SFRS1 interacting protein 1	-1.179		0.049
O75569	PRKRA	protein kinase, interferon-inducible double stranded RNA dependent activator	-1.173		0.035
O75688	PPM1B	protein phosphatase, Mg2+/Mn2+ dependent, 1B	-1.159		0.044
O75718	CRTAP	cartilage associated protein	1.119		0.031
O75874	IDH1	isocitrate dehydrogenase 1 (NADP+), soluble	1.101	0.009	
O75915	ARL6IP5	ADP-ribosylation factor-like 6 interacting protein 5	1.172	0.045	
O75976	CPD	carboxypeptidase D	1.050	0.02	
O94888	UBXN7	UBX domain protein 7	-3.555	0.004	
O94925-3	GLS	glutaminase	-1.181	0.029	
O95372	LYPLA2	lysophospholipase II	1.147	0.016	
O95399-2	UTS2	urotensin 2	1.134		0.015
O95433	AHSA1	AHA1, activator of heat shock 90kDa protein ATPase homolog 1 (yeast)	1.025		0.042
O95864	FADS2	fatty acid desaturase 2	1.248	0.006	
O96019	ACTL6A	actin-like 6A	-1.193	0.017	
P00338-3	LDHA	lactate dehydrogenase A	1.105		0.001
P00374			-1.289	0.038	
P01040	CSTA	cystatin A (stefin A)	-4.740	0.037	
P01876	IGHA1	immunoglobulin heavy constant alpha 1	-9.966	0.032	0.022
P02786	TFRC	transferrin receptor	1.240	0.041	0.027
P05109	S100A8	S100 calcium binding protein A8	-5.529	0.021	
P05141	SLC25A5	solute carrier family 25 (mitochondrial carrier; adenine nucleotide translocator), member 5	1.091	0.026	
P05198	EIF2S1	eukaryotic translation initiation factor 2, subunit 1 alpha, 35kDa	1.036		0.047
P05386	RPLP1	ribosomal protein, large, P1	-1.078	0.011	
P05388	RPLP0	ribosomal protein, large, P0	-1.053	0.013	
P05455	SSB	Sjogren syndrome antigen B (autoantigen La)	1.045		0.018
P06493	CDK1	cyclin-dependent kinase 1	-1.229	0.019	0.008

P06730-2	EIF4E	eukaryotic translation initiation factor 4E	1.070	0.013	0.041
P06753-2	TPM3	tropomyosin 3	1.041		0.028
P07339	CTSD	cathepsin D	-1.247		0.017
P07814	EPRS	glutamyl-prolyl-tRNA synthetase	-1.024	0.042	
P07900-2	HSP90AA1	heat shock protein 90kDa alpha (cytosolic), class A member 1	-1.035		0.002
P07954	FH	fumarate hydratase	-1.048	0.014	
P08107			-1.162		0.011
P08133	ANXA6	annexin A6	-1.119		0.024
P08183	ABCB1	ATP-binding cassette, sub-family B (MDR/TAP), member 1	1.271	0.035	
P08195-4	SLC3A2	solute carrier family 3 (amino acid transporter heavy chain), member 2	1.202	0.046	
P08243	ASNS	asparagine synthetase (glutamine-hydrolyzing)	1.272	0.036	
P08559-4	PDHA1	pyruvate dehydrogenase (lipoamide) alpha 1	1.037	0.049	
P08754	GNAI3	guanine nucleotide binding protein (G protein), alpha inhibiting activity polypeptide 3	1.113	0.034	
P08865	RPSA	ribosomal protein SA	-1.032	0.016	
P09172	DBH	dopamine beta-hydroxylase (dopamine beta-monooxygenase)	1.672		0.028
P09211	GSTP1	glutathione S-transferase pi 1	-1.197	0.01	
P09429	HMGB1	high mobility group box 1	-1.048		0.016
P09936	UCHL1	ubiquitin carboxyl-terminal esterase L1 (ubiquitin thiolesterase)	1.127	0.003	
P0C0S5	H2AFZ	H2A histone family, member Z	-1.091	0	
P10412	HIST1H1E	histone cluster 1, H1e	-1.251	0.006	
P10645	CHGA	chromogranin A	2.095		0.009
P11142	HSPA8	heat shock 70kDa protein 8	-1.016		0.019
P11166	SLC2A1	solute carrier family 2 (facilitated glucose transporter), member 1	-1.340	0.02	
P11233	RALA	v-ral simian leukemia viral oncogene homolog A (ras related)	-1.064	0.028	
P11413-2	G6PD	glucose-6-phosphate dehydrogenase	1.137	0.034	
P11498	PC	pyruvate carboxylase	-1.026	0.011	
P11586	MTHFD1	methylenetetrahydrofolate dehydrogenase (NADP+ dependent) 1, methenyltetrahydrofolate cyclohydrolase, formyltetrahydrofolate synthetase	-1.033	0.021	
P12004	PCNA	proliferating cell nuclear antigen	-1.056	0.04	
P12956	XRCC6	X-ray repair complementing defective repair in Chinese hamster cells 6	1.054		0.039

P13073	COX4I1	cytochrome c oxidase subunit IV isoform 1	1.217	0.01	
P13591	NCAM1	neural cell adhesion molecule 1	-1.243	0.037	
P13639	EEF2	eukaryotic translation elongation factor 2	-1.117	0.012	0.017
P13667	PDIA4	protein disulfide isomerase family A, member 4	1.122		0.017
P13674-2	P4HA1	prolyl 4-hydroxylase, alpha polypeptide I	1.116		0.011
P14324	FDPS	farnesyl diphosphate synthase	1.168	0.019	
P14618	PKM	pyruvate kinase, muscle	1.035	0	
P14625	HSP90B1	heat shock protein 90kDa beta (Grp94), member 1	1.109		0.032
P14868	DARS	aspartyl-tRNA synthetase	1.040	0.019	
P15121	AKR1B1	aldo-keto reductase family 1, member B1 (aldose reductase)	-1.183	0.023	
P15311	EZR	ezrin	1.096		0.005
P15880	RPS2	ribosomal protein S2	-1.011	0.032	
P15924	DSP	desmoplakin	-5.506		0
P16401	HIST1H1B	histone cluster 1, H1b	-1.256	0.014	0.007
P16403	HIST1H1C	histone cluster 1, H1c	-1.227	0.003	
P17987	TCP1	t-complex 1	1.037	0.015	
P18077	RPL35A	ribosomal protein L35a	1.064	0.006	0
P18085	ARF4	ADP-ribosylation factor 4	1.064	0.021	
P18669	PGAM1	phosphoglycerate mutase 1 (brain)	-1.111		0.007
P18754-2	RCC1	regulator of chromosome condensation 1	1.151		0.026
P20700	LMNB1	lamin B1	-1.106		0.019
P21266	GSTM3	glutathione S-transferase mu 3 (brain)	1.059	0.038	
P22102	GART	phosphoribosylglycinamide formyltransferase, phosphoribosylglycinamide synthetase, phosphoribosylaminoimidazole synthetase	1.064	0.009	
P22234	PAICS	phosphoribosylaminoimidazole carboxylase, phosphoribosylaminoimidazole succinocarboxamide synthetase	1.039	0.02	
P22626	HNRNPA2B1	heterogeneous nuclear ribonucleoprotein A2/B1	-1.052	0.008	0
P22695	UQCRC2	ubiquinol-cytochrome c reductase core protein II	1.101	0.024	
P23284	PPIB	peptidylprolyl isomerase B (cyclophilin B)	1.132		0.046
P23396	RPS3	ribosomal protein S3	1.062		0.004
P24386	CHM	choroideremia (Rab escort protein 1)	1.282		0.03
P24534	EEF1B2	eukaryotic translation elongation factor 1 beta 2	-1.091		0.018

P25205	MCM3	minichromosome maintenance complex component 3	-1.291	0.017	0.006
P25789	PSMA4	proteasome (prosome, macropain) subunit, alpha type, 4	-1.093	0.007	
P26583	HMGB2	high mobility group box 2	-1.091		0.008
P26641	EEF1G	eukaryotic translation elongation factor 1 gamma	-1.023		0.008
P27348	YWHAQ	tyrosine 3-monooxygenase/tryptophan 5-monooxygenase activation protein, theta	-1.075	0.006	
P27797	CALR	calreticulin	1.087		0.035
P28070	PSMB4	proteasome (prosome, macropain) subunit, beta type, 4	1.047		0.041
P28074	PSMB5	proteasome (prosome, macropain) subunit, beta type, 5	1.037		0.028
P30044	PRDX5	peroxiredoxin 5	1.094	0.041	
P31944	CASP14	caspase 14, apoptosis-related cysteine peptidase	-2.454		0.028
P32119	PRDX2	peroxiredoxin 2	-1.112	0.009	
P33316	DUT	deoxyuridine triphosphatase	-1.168		0.043
P33947	KDELR2	KDEL (Lys-Asp-Glu-Leu) endoplasmic reticulum protein retention receptor 2	1.177	0.005	
P33991	MCM4	minichromosome maintenance complex component 4	-1.124	0.048	
P33992	MCM5	minichromosome maintenance complex component 5	-1.171		0.031
P33993	MCM7	minichromosome maintenance complex component 7	-1.213		0.018
P34932	HSPA4	heat shock 70kDa protein 4	-1.008		0.026
P35030	PRSS3	protease, serine, 3	-11.081	0.009	0.043
P35611-3	ADD1	adducin 1 (alpha)	-1.152		0.049
P35908	KRT2	keratin 2, type II	-6.462		0.031
P35998	PSMC2	proteasome (prosome, macropain) 26S subunit, ATPase, 2	-1.068	0.002	0.019
P36543	ATP6V1E1	ATPase, H+ transporting, lysosomal 31kDa, V1 subunit E1	1.084	0.016	
P38606	ATP6V1A	ATPase, H+ transporting, lysosomal 70kDa, V1 subunit A	1.060	0.04	
P38646	HSPA9	heat shock 70kDa protein 9 (mortalin)	-1.048		0.045
P39019	RPS19	ribosomal protein S19	1.082	0.003	
P40227	CCT6A	chaperonin containing TCP1, subunit 6A (zeta 1)	1.038	0.004	
P40616	ARL1	ADP-ribosylation factor-like 1	1.142	0.029	
P40926	MDH2	malate dehydrogenase 2, NAD (mitochondrial)	-1.121	0.033	
P41091	EIF2S3	eukaryotic translation initiation factor 2, subunit 3 gamma, 52kDa	1.091		0.044
P43304	GPD2	glycerol-3-phosphate	-1.219	0.033	

		dehydrogenase 2 (mitochondrial)			
P43487	RANBP1	RAN binding protein 1	-1.032		0.001
P43490	NAMPT	nicotinamide phosphoribosyltransferase	1.148	0.009	
P46108	CRK	v-crk avian sarcoma virus CT10 oncogene homolog	1.016		0.001
P46778	RPL21	ribosomal protein L21	-1.014	0.047	
P46782	RPS5	ribosomal protein S5	1.213		0.049
P46783	RPS10	ribosomal protein S10	-1.067	0.043	
P47914	RPL29	ribosomal protein L29	-1.275	0.025	
P48643	CCT5	chaperonin containing TCP1, subunit 5 (epsilon)	-1.092		0.04
P48735	IDH2	isocitrate dehydrogenase 2 (NADP+), mitochondrial	-1.103	0	
P49006	MARCKSL1	MARCKS-like 1	-1.162	0.046	
P49321	NASP	nuclear autoantigenic sperm protein (histone-binding)	-1.087		0.012
P49327	FASN	fatty acid synthase	1.142		0.028
P49354	FNTA	farnesyltransferase, CAAX box, alpha	1.145		0
P49366	DHPS	deoxyhypusine synthase	-1.059		0.021
P49589-3	CARS	cysteinyl-tRNA synthetase	1.127	0.002	
P49643	PRIM2	primase, DNA, polypeptide 2 (58kDa)	-1.247		0.01
P49720	PSMB3	proteasome (prosome, macropain) subunit, beta type, 3	1.045		0.018
P49959	MRE11A	MRE11 homolog A, double strand break repair nuclease	-1.073	0.037	
P50148	GNAQ	guanine nucleotide binding protein (G protein), q polypeptide	-1.089	0.024	
P50213	IDH3A	isocitrate dehydrogenase 3 (NAD+) alpha	1.112	0.003	
P50897	PPT1	palmitoyl-protein thioesterase 1	1.062	0	
P51114	FXR1	fragile X mental retardation, autosomal homolog 1	-1.027		0.007
P51659	HSD17B4	hydroxysteroid (17-beta) dehydrogenase 4	1.087	0.007	
P51809	VAMP7	vesicle-associated membrane protein 7	-1.091	0.021	
P51991	HNRNPA3	heterogeneous nuclear ribonucleoprotein A3	-1.027		0.036
P52298	NCBP2	nuclear cap binding protein subunit 2, 20kDa	1.110		0.015
P52565	ARHGDIA	Rho GDP dissociation inhibitor (GDI) alpha	-1.046		0.036
P52732	KIF11	kinesin family member 11	-1.188	0.042	
P53396	ACLY	ATP citrate lyase	1.158		0.033
P53634	CTSC	cathepsin C	1.091		0.038
P53999	SUB1	SUB1 homolog (S. cerevisiae)	1.165		0.03
P54136	RARS	arginyl-tRNA synthetase	1.047	0.01	
P54727	RAD23B	RAD23 homolog B, nucleotide	1.178		0.001

		excision repair protein			
P54920	NAPA	N-ethylmaleimide-sensitive factor attachment protein, alpha	1.087	0.035	
P55060	CSE1L	CSE1 chromosome segregation 1-like (yeast)	-1.084	0.001	0.008
P55072	VCP	valosin containing protein	1.037		0.015
P60468	SEC61B	Sec61 beta subunit	1.073	0.041	
P60953	CDC42	cell division cycle 42	-1.027	0.024	
P61081	UBE2M	ubiquitin-conjugating enzyme E2M	1.118	0.049	
P61158	ACTR3	ARP3 actin-related protein 3 homolog (yeast)	1.042		0.007
P61163	ACTR1A	ARP1 actin-related protein 1 homolog A, centractin alpha (yeast)	1.087	0.021	
P61289-2	PSME3	proteasome (prosome, macropain) activator subunit 3 (PA28 gamma; Ki)	1.117	0.049	
P61513	RPL37A	ribosomal protein L37a	1.075	0.037	
P62191	PSMC1	proteasome (prosome, macropain) 26S subunit, ATPase, 1	-1.092		0.016
P62263	RPS14	ribosomal protein S14	-1.092	0.001	
P62277	RPS13	ribosomal protein S13	-1.036	0.041	
P62333	PSMC6	proteasome (prosome, macropain) 26S subunit, ATPase, 6	1.097	0.037	
P62424	RPL7A	ribosomal protein L7a	-1.001	0	
P62753	RPS6	ribosomal protein S6	-1.047	0.021	
P62805			-1.056	0.001	
P62820	RAB1A	RAB1A, member RAS oncogene family	1.108	0.041	
P62913	RPL11	ribosomal protein L11	-1.078	0.005	0.009
P62917	RPL8	ribosomal protein L8	1.017	0.016	
P62937	PPIA	peptidylprolyl isomerase A (cyclophilin A)	-1.053		0.009
P62979	RPS27A	ribosomal protein S27a	-1.076	0.006	
P63173	RPL38	ribosomal protein L38	-1.010		0
P67775	PPP2CA	protein phosphatase 2, catalytic subunit, alpha isozyme	-1.129		0.004
P68104	EEF1A1	eukaryotic translation elongation factor 1 alpha 1	1.017	0.042	
P78347	GTF2I	general transcription factor IIi	-1.116		0.038
P78371	CCT2	chaperonin containing TCP1, subunit 2 (beta)	1.018	0.019	
P81605	DCD	dermcidin	-10.770	0.002	
P82663	MRPS25	mitochondrial ribosomal protein S25	1.139	0.031	
P82921	MRPS21	mitochondrial ribosomal protein S21	1.167	0.048	
P83916	CBX1	chromobox homolog 1	-1.082		0.013
P84090	ERH	enhancer of rudimentary homolog (Drosophila)	-1.064	0.033	
Q00534	CDK6	cyclin-dependent kinase 6	1.253	0.006	0.019

Q00577	PURA	purine-rich element binding protein A	1.095		0.048
Q00610	CLTC	clathrin, heavy chain (Hc)	1.050	0.03	
Q01105-2	SET	SET nuclear proto-oncogene	-1.012		0.022
Q01581	HMGCS1	3-hydroxy-3-methylglutaryl-CoA synthase 1 (soluble)	1.155	0.038	
Q01844-5	EWSR1	EWS RNA-binding protein 1	-1.085	0.008	
Q02543	RPL18A	ribosomal protein L18a	1.065	0.002	
Q02790	FKBP4	FK506 binding protein 4, 59kDa	-1.067		0.006
Q04323	UBXN1	UBX domain protein 1	1.121		0.023
Q04837	SSBP1	single-stranded DNA binding protein 1, mitochondrial	1.110		0.042
Q05639	EEF1A2	eukaryotic translation elongation factor 1 alpha 2	-1.163	0.04	
Q06323	PSME1	proteasome (prosome, macropain) activator subunit 1 (PA28 alpha)	1.235		0.006
Q08499-6	PDE4D	phosphodiesterase 4D, cAMP-specific	-15.232	0.016	
Q12904-2	AIMP1	aminoacyl tRNA synthetase complex-interacting multifunctional protein 1	1.048	0.002	
Q12905	ILF2	interleukin enhancer binding factor 2	-1.070	0.041	0.026
Q12912	LRMP	lymphoid-restricted membrane protein	-418.476	0.003	0
Q13151	HNRNPA0	heterogeneous nuclear ribonucleoprotein A0	-1.040	0.033	0.025
Q13257	MAD2L1	MAD2 mitotic arrest deficient-like 1 (yeast)	-1.138	0.003	0.042
Q13263	TRIM28	tripartite motif containing 28	-1.078	0.013	
Q13630	TSTA3	tissue specific transplantation antigen P35B	1.196	0.017	
Q13813	SPTAN1	spectrin, alpha, non-erythrocytic 1	-1.123	0.003	
Q13838	DDX39B	DEAD (Asp-Glu-Ala-Asp) box polypeptide 39B	-1.011		0.01
Q14103	HNRNPD	heterogeneous nuclear ribonucleoprotein D (AU-rich element RNA binding protein 1, 37kDa)	-1.179	0.01	0.017
Q14108	SCARB2	scavenger receptor class B, member 2	1.169	0.027	
Q14152	EIF3A	eukaryotic translation initiation factor 3, subunit A	1.102	0.038	
Q14194-2	CRMP1	collapsin response mediator protein 1	-1.754	0.026	
Q14195-2	DPYSL3	dihydropyrimidinase-like 3	1.094	0.015	
Q14204	DYNC1H1	dynein, cytoplasmic 1, heavy chain 1	1.090	0.006	
Q14566	MCM6	minichromosome maintenance complex component 6	-1.164	0.047	0.019
Q14683	SMC1A	structural maintenance of	-1.132	0.015	

		chromosomes 1A			
Q15008	PSMD6	proteasome (prosome, macropain) 26S subunit, non-ATPase, 6	1.118	0.038	
Q15056	EIF4H	eukaryotic translation initiation factor 4H	1.126		0.039
Q15149	PLEC	plectin	1.048		0.007
Q15181	PPA1	pyrophosphatase (inorganic) 1	1.101	0.025	
Q15291	RBBP5	retinoblastoma binding protein 5	1.079		0.031
Q15293	RCN1	reticulocalbin 1, EF-hand calcium binding domain	1.073		0.011
Q15365	PCBP1	poly(rC) binding protein 1	1.016	0.016	
Q15393	SF3B3	splicing factor 3b, subunit 3, 130kDa	-1.109		0.044
Q15691	MAPRE1	microtubule-associated protein, RP/EB family, member 1	-1.031		0
Q15738	NSDHL	NAD(P) dependent steroid dehydrogenase-like	1.142	0.003	
Q15785	TOMM34	translocase of outer mitochondrial membrane 34	-1.300	0.014	
Q15904	ATP6AP1	ATPase, H+ transporting, lysosomal accessory protein 1	1.236	0.044	
Q16539	MAPK14	mitogen-activated protein kinase 14	1.052		0
Q16555	DPYSL2	dihydropyrimidinase-like 2	-1.149	0.011	0.003
Q16629	SRSF7	serine/arginine-rich splicing factor 7	1.135	0.026	
Q16630-2	CPSF6	cleavage and polyadenylation specific factor 6, 68kDa	-1.069		0
Q16658	FSCN1	fascin actin-bundling protein 1	-1.041	0.024	
Q16836-2	HADH	hydroxyacyl-CoA dehydrogenase	-1.140	0.02	
Q16850	CYP51A1	cytochrome P450, family 51, subfamily A, polypeptide 1	1.125	0.036	
Q16878	CDO1	cysteine dioxygenase type 1	1.446	0.005	
Q1KMD3	HNRNPUL2	heterogeneous nuclear ribonucleoprotein U-like 2	-1.090		0.006
Q4KWH8	PLCH1	phospholipase C, eta 1	1.185		0.013
Q53EL6	PDCD4	programmed cell death 4 (neoplastic transformation inhibitor)	1.055		0.019
Q5SSJ5	HP1BP3	heterochromatin protein 1, binding protein 3	-1.207	0.01	
Q5T4U5	ACADM	acyl-CoA dehydrogenase, C-4 to C-12 straight chain	1.208	0.031	
Q68D91	MBLAC2	metallo-beta-lactamase domain containing 2	-1.067	0.041	
Q69YN4	KIAA1429	KIAA1429	-1.454	0	
Q6GMV2	SMYD5	SMYD family member 5	-1.374	0.013	
Q6IBS0	TWF2	twinfilin actin binding protein 2	1.100		0.044
Q6JUT2	TICAM2	toll-like receptor adaptor molecule 2	1.202	0.022	
Q7Z2Z2	EFTUD1	elongation factor Tu GTP binding	1.119		0.042

		domain containing 1			
Q8IUE6	HIST2H2AB	histone cluster 2, H2ab	-1.149		0.01
Q8IZ81	ELMOD2	ELMO/CED-12 domain containing 2	1.090	0.01	
Q8N0U8	VKORC1L1	vitamin K epoxide reductase complex, subunit 1-like 1	1.050	0.043	
Q8N183	NDUFAF2	NADH dehydrogenase (ubiquinone) complex I, assembly factor 2	-1.071	0.011	
Q8N5I4	DHRSX	dehydrogenase/reductase (SDR family) X-linked	-1.034	0.032	
Q8NC51	SERBP1	SERPINE1 mRNA binding protein 1	-1.081		0.011
Q8NE71	ABCF1	ATP-binding cassette, sub-family F (GCN20), member 1	1.084		0.021
Q8NFH5	NUP35	nucleoporin 35kDa	-1.061	0	
Q8NFQ8	TOR1AIP2	torsin A interacting protein 2	1.179		0.048
Q8TBQ9	TMEM167A	transmembrane protein 167A	1.043	0.028	
Q8TF72	SHROOM3	shroom family member 3	-103.752	0.002	0.014
Q8WVY7	UBLCP1	ubiquitin-like domain containing CTD phosphatase 1	1.058		0.036
Q8WWC4	C2orf47	chromosome 2 open reading frame 47	-1.087	0.044	
Q8WWM9	CYGB	cytoglobin	1.273		0.011
Q8WWY3	PRPF31	pre-mRNA processing factor 31	1.079		0.009
Q8WXE1	ATRIP	ATR interacting protein	-1.033		0.045
Q8WY54	PPM1E	protein phosphatase, Mg2+/Mn2+ dependent, 1E	1.076		0.045
Q92522	H1FX	H1 histone family, member X	-1.081	0	
Q92598	HSPH1	heat shock 105kDa/110kDa protein 1	1.254	0.002	
Q92616	GCN1	GCN1 eIF2 alpha kinase activator homolog	-1.055	0.003	
Q969X5	ERGIC1	endoplasmic reticulum-golgi intermediate compartment 1	1.050	0.032	
Q96DA0	ZG16B	zymogen granule protein 16B	-11.811		0.023
Q96DR8	MUCL1	mucin-like 1	-6.653		0.001
Q96E39	RBMXL1	RNA binding motif protein, X-linked-like 1	1.201		0
Q96FX7	TRMT61A	tRNA methyltransferase 61A	-1.007	0.045	
Q96HE7	ERO1A	endoplasmic reticulum oxidoreductase alpha	1.070		0.018
Q96ND0	FAM210A	family with sequence similarity 210, member A	1.089		0.035
Q96P70	IPO9	importin 9	1.039		0.026
Q96PE2	ARHGEF17	Rho guanine nucleotide exchange factor (GEF) 17	-8.556	0.035	
Q96QK1	VPS35	VPS35 retromer complex component	1.022	0.021	
Q96RP9-2	GFM1	G elongation factor, mitochondrial 1	-1.097	0.002	
Q96S97	MYADM	myeloid-associated differentiation	-1.075	0.029	

		marker			
Q96SI1	KCTD15	potassium channel tetramerization domain containing 15	-1.331		0.026
Q96SI9	STRBP	spermatid perinuclear RNA binding protein	-1.067		0.011
Q96SL4	GPX7	glutathione peroxidase 7	-1.030	0.023	
Q99470	SDF2	stromal cell-derived factor 2	1.138		0.005
Q99627	COPS8	COP9 signalosome subunit 8	-1.219	0.023	0.024
Q99714	HSD17B10	hydroxysteroid (17-beta) dehydrogenase 10	-1.027	0	
Q99729-2	HNRNPAB	heterogeneous nuclear ribonucleoprotein A/B	-1.040		0.029
Q99832	CCT7	chaperonin containing TCP1, subunit 7 (eta)	1.035	0.042	
Q99986	VRK1	vaccinia related kinase 1	-1.131	0.004	
Q9BPX5	ARPC5L	actin related protein 2/3 complex, subunit 5-like	1.175		0.035
Q9BQA1	WDR77	WD repeat domain 77	-1.117		0.046
Q9BRJ2	MRPL45	mitochondrial ribosomal protein L45	-1.002	0.017	
Q9BRX8	FAM213A	family with sequence similarity 213, member A	1.064		0.011
Q9BUJ2	HNRNPUL1	heterogeneous nuclear ribonucleoprotein U-like 1	-1.044		0.047
Q9BUL8	PDCD10	programmed cell death 10	-1.065	0.023	
Q9BV86	NTMT1	N-terminal Xaa-Pro-Lys N-methyltransferase 1	1.153		0.003
Q9BVA1	TUBB2B	tubulin, beta 2B class IIb	-1.078		0.028
Q9BVG4	PBDC1	polysaccharide biosynthesis domain containing 1	1.074		0.043
Q9BWD1	ACAT2	acetyl-CoA acetyltransferase 2	1.048	0.002	
Q9BY50	SEC11C	SEC11 homolog C, signal peptidase complex subunit	1.200	0.023	
Q9BYD1	MRPL13	mitochondrial ribosomal protein L13	1.077	0.007	
Q9BYD6	MRPL1	mitochondrial ribosomal protein L1	-1.039		0.007
Q9BZC1	CELF4	CUGBP, Elav-like family member 4	1.123		0.016
Q9H3U1	UNC45A	unc-45 myosin chaperone A	1.050	0.012	
Q9H444	CHMP4B	charged multivesicular body protein 4B	-1.073		0.017
Q9HAV7	GRPEL1	GrpE-like 1, mitochondrial (E. coli)	-1.138	0.028	
Q9HBD4	SMARCA4	SWI/SNF related, matrix associated, actin dependent regulator of chromatin, subfamily a, member 4	-1.201	0.037	
Q9HCC0	MCCC2	methylcrotonoyl-CoA carboxylase 2 (beta)	1.180	0.031	
Q9NP55	BPIFA1	BPI fold containing family A, member 1	-26.410	0.009	0.011
Q9NPD8	UBE2T	ubiquitin-conjugating enzyme E2T	-1.234		0.003
Q9NPL8	TIMMDC1	translocase of inner mitochondrial	1.218		0.019

		membrane domain containing 1			
Q9NQ48	LZTFL1	leucine zipper transcription factor-like 1	1.169		0.022
Q9NQ50	MRPL40	mitochondrial ribosomal protein L40	-1.035		0.009
Q9NR28	DIABLO	diablo, IAP-binding mitochondrial protein	1.081		0.034
Q9NSD9	FARSB	phenylalanyl-tRNA synthetase, beta subunit	-1.127	0.048	
Q9NTJ3	SMC4	structural maintenance of chromosomes 4	-1.202	0.013	
Q9NTX5	ECHDC1	ethylmalonyl-CoA decarboxylase 1	-1.211	0.019	
Q9NVP1	DDX18	DEAD (Asp-Glu-Ala-Asp) box polypeptide 18	-1.056		0.027
Q9NZL4	HSPBP1	HSPA (heat shock 70kDa) binding protein, cytoplasmic cochaperone 1	1.166		0.018
Q9P0J7	KCMF1	potassium channel modulatory factor 1	1.138	0.02	
Q9P258	RCC2	regulator of chromosome condensation 2	-1.048		0.04
Q9P2R7	SUCLA2	succinate-CoA ligase, ADP-forming, beta subunit	-1.089	0.007	
Q9P2X0-2	DPM3	dolichyl-phosphate mannosyltransferase polypeptide 3	1.228	0.032	
Q9UBE0	SAE1	SUMO1 activating enzyme subunit 1	-1.106	0.049	0.002
Q9UBK7-3	RABL2A	RAB, member of RAS oncogene family-like 2A	1.230		0.019
Q9UBP6	METTL1	methyltransferase like 1	-1.097	0	
Q9UBT2	UBA2	ubiquitin-like modifier activating enzyme 2	-1.053		0.035
Q9UEU0	VTI1B	vesicle transport through interaction with t-SNAREs 1B	-1.222	0.002	
Q9UHD8-5	SEPT9	septin 9	1.155	0.047	0.041
Q9UHN1	POLG2	polymerase (DNA directed), gamma 2, accessory subunit	1.095	0.024	
Q9UL46	PSME2	proteasome (prosome, macropain) activator subunit 2 (PA28 beta)	1.400	0	0.004
Q9UQ80	PA2G4	proliferation-associated 2G4, 38kDa	-1.034		0.031
Q9Y266	NUDC	nudC nuclear distribution protein	1.144	0.013	
Q9Y285	FARSA	phenylalanyl-tRNA synthetase, alpha subunit	-1.081	0.049	
Q9Y291	MRPS33	mitochondrial ribosomal protein S33	1.186	0	
Q9Y295	DRG1	developmentally regulated GTP binding protein 1	-1.176		0.036
Q9Y3A5	SBDS	Shwachman-Bodian-Diamond syndrome	-1.115	0.003	
Q9Y3B4	SF3B6	splicing factor 3b, subunit 6, 14kDa	1.085	0.031	

Q9Y3D9	MRPS23	mitochondrial ribosomal protein S23	1.075	0.006	
Q9Y3E7	CHMP3	charged multivesicular body protein 3	-1.021		0.043
Q9Y3L5	RAP2C	RAP2C, member of RAS oncogene family	-1.052	0.013	
Q9Y4L1	HYOU1	hypoxia up-regulated 1	1.103	0.043	
Q9Y520-7	PRRC2C	proline-rich coiled-coil 2C	-31.889	0.019	
Q9Y5K8	ATP6V1D	ATPase, H+ transporting, lysosomal 34kDa, V1 subunit D	1.061	0	
Q9Y5L0	TNPO3	transportin 3	1.059	0.049	
Q9Y5M8	SRPRB	signal recognition particle receptor, B subunit	1.058	0.043	
Q9Y5S9	RBM8A	RNA binding motif protein 8A	1.053		0.001
Q9Y6E2	BZW2	basic leucine zipper and W2 domains 2	1.206		

Appendix 3

Dysregulated gene expression genes

Gene Symbol	Gene Name	fold change	p-value
7-Sep	septin 7	-1.4984401	0.00608128
A1CF	APOBEC1 complementation factor	1.40399642	0.00257006
AADAT	aminoadipate aminotransferase	-1.6651491	0.00993689
AATF	apoptosis antagonizing transcription factor	-1.5335361	0.00467496
ABAT	4-aminobutyrate aminotransferase	1.32180711	0.00720804
ABCA5	ATP-binding cassette, sub-family A (ABC1), member 5	1.50720344	0.00209641
ABHD11	abhydrolase domain containing 11	1.45037732	0.00616103
ABLIM2	actin binding LIM protein family, member 2	1.70232289	0.00815331
ACADVL	acyl-CoA dehydrogenase, very long chain	1.44375247	0.00437243
ACAT1	acetyl-CoA acetyltransferase 1	-1.4087298	0.00808636
ACD	adrenocortical dysplasia homolog (mouse)	1.38843469	0.00633468
ACHE	acetylcholinesterase	1.4125532	0.00280107
ACOT2	acyl-CoA thioesterase 2	1.40818223	0.00349595
ACR	acrosin	1.36912597	0.00351268
ACSL5	acyl-CoA synthetase long-chain family member 5	-1.5060511	0.0016866
ACTL6B	actin-like 6B	1.43279035	0.00764492
ACTL9	actin-like 9	1.488417	0.00605686
ACTRT3	actin-related protein T3	1.38756845	0.00298979
ADAM20	ADAM metallopeptidase domain 20	1.61847785	0.00247439
ADAM28	ADAM metallopeptidase domain 28	1.36116056	0.00752962
ADAM29	ADAM metallopeptidase domain 29	1.36611509	0.0039063
ADM	adrenomedullin	1.53747418	0.00199026
ADSS	adenylosuccinate synthase	-1.6332631	0.00682018
AFAP1	actin filament associated protein 1	1.34664961	0.004574
AGAP3	ArfGAP with GTPase domain, ankyrin repeat and PH domain 3	1.36901629	0.00130042
AGGF1	angiogenic factor with G patch and FHA domains 1	-1.3011144	0.00594638
AGRN	agrin	1.41911852	0.00288114
AGT	angiotensinogen (serpin peptidase inhibitor, clade A, member 8)	-1.383402	0.00889442
AGTR2	angiotensin II receptor, type 2	1.47805562	0.00497075
AHR	aryl hydrocarbon receptor	1.52516676	0.00739662
AKAP5	A kinase (PRKA) anchor protein 5	-1.4289685	0.00372443
ALG5	ALG5, dolichyl-phosphate beta-glucosyltransferase	-1.4734871	0.00490963
ALKBH1	alkB, alkylation repair homolog 1 (E. coli)	-1.3183499	0.00425537
ANKRD20A11P	ankyrin repeat domain 20 family, member A11, pseudogene	-1.3887586	0.00261117
ANKRD20A8P	ankyrin repeat domain 20 family, member A8, pseudogene	-2.0980388	0.0034523
ANKRD24	ankyrin repeat domain 24	1.39065038	0.00593802
ANKRD36	ankyrin repeat domain 36	-1.3519997	0.00703186
ANKRD36B	ankyrin repeat domain 36B	-1.4952863	0.00903325

ANXA3	annexin A3	-1.3593938	0.00329835
ANXA7	annexin A7	1.3879872	0.00861895
AP1S2	adaptor-related protein complex 1, sigma 2 subunit	-1.4852222	0.00754761
APH1B	anterior pharynx defective 1 homolog B (C. elegans)	1.34792774	0.00330927
API5	apoptosis inhibitor 5	-1.9076431	0.00256648
APIP	APAF1 interacting protein	1.4747703	0.00823354
APOBEC3B	apolipoprotein B mRNA editing enzyme, catalytic polypeptide-like 3B	1.36878993	0.00308093
APOBEC3F	apolipoprotein B mRNA editing enzyme, catalytic polypeptide-like 3F	1.35529586	0.0072492
APOC1	apolipoprotein C-I	1.2949613	0.00709404
APOL4	apolipoprotein L, 4	-1.3302259	0.00396969
AQP2	aquaporin 2 (collecting duct)	1.51969647	0.00732511
AQP4	aquaporin 4	1.33282589	0.00865278
AQP6	aquaporin 6, kidney specific	1.48499542	0.00296404
ARHGAP36	Rho GTPase activating protein 36	-1.4976739	0.0012076
ARRDC3	arrestin domain containing 3	1.43125423	0.00358846
ARSG	arylsulfatase G	-1.3183171	0.00820076
ARSI	arylsulfatase family, member I	1.40122219	0.0063748
ARV1	ARV1 homolog (S. cerevisiae)	-1.5342957	0.00334069
ASAP1	ArfGAP with SH3 domain, ankyrin repeat and PH domain 1	-1.3351206	0.00503114
ASCL1	achaete-scute complex homolog 1 (Drosophila)	-1.9005652	0.00480802
ASIC2	acid-sensing (proton-gated) ion channel 2	1.46177904	0.00817559
ASIP	agouti signaling protein	1.45381678	0.00768403
ASMT	acetylserotonin O-methyltransferase	1.46262452	0.00265487
ASMT	acetylserotonin O-methyltransferase	1.39635483	0.00377306
ATG10	autophagy related 10	-1.3860079	0.00463556
ATP1B3	ATPase, Na+/K+ transporting, beta 3 polypeptide	-1.6961035	0.0055613
ATP6V0C	ATPase, H+ transporting, lysosomal 16kDa, V0 subunit c	1.58077695	0.00172218
ATP8A2	ATPase, aminophospholipid transporter, class I, type 8A, member 2	1.33934957	0.00987716
AVIL	advillin	-1.4720667	0.00534935
B3GALT4	UDP-Gal:betaGlcNAc beta 1,3-galactosyltransferase, polypeptide 4	1.43925088	0.00960861
B3GALT4	UDP-Gal:betaGlcNAc beta 1,3-galactosyltransferase, polypeptide 4	1.43925088	0.00960861
B3GALT6	UDP-Gal:betaGal beta 1,3-galactosyltransferase polypeptide 6	1.39830758	0.00516814
B3GNT9	UDP-GlcNAc:betaGal beta-1,3-N-acetylglucosaminyltransferase 9	1.86549119	0.00071363
BAAT	bile acid CoA: amino acid N-acyltransferase (glycine N-choloyltransferase)	1.34871741	0.00526872
BAG5	BCL2-associated athanogene 5	-1.7306534	0.00087346
BAIAP2-AS1	BAIAP2 antisense RNA 1 (head to head)	1.49395372	0.00845472

BCL2L2	BCL2-like 2	1.31212254	0.00668409
BCL7C	B-cell CLL/lymphoma 7C	1.60381277	0.0028725
BMP10	bone morphogenetic protein 10	-1.4691914	0.00131576
BMP8B	bone morphogenetic protein 8b	-1.6078147	0.00444957
BMS1P4	BMS1 pseudogene 4	-1.5559773	0.00578774
BRCA2	breast cancer 2, early onset	-1.4770358	0.00074779
BSPRY	B-box and SPRY domain containing	1.24937758	0.0097779
BST2	bone marrow stromal cell antigen 2	1.61629272	0.0001938
BTF3L4	basic transcription factor 3-like 4	-1.5678655	0.00641156
BTF3P11	basic transcription factor 3 pseudogene 11	-1.3259101	0.0041633
C10orf107	chromosome 10 open reading frame 107	-1.5162638	0.00857738
C10orf55	chromosome 10 open reading frame 55	1.30532068	0.00753963
C12orf40	chromosome 12 open reading frame 40	1.4014459	0.00466736
C12orf76	chromosome 12 open reading frame 76	-1.6305819	0.00823317
C14orf169	chromosome 14 open reading frame 169	-1.4850804	0.00746659
C14orf180	chromosome 14 open reading frame 180	1.63106991	0.00203119
C14orf37	chromosome 14 open reading frame 37	-1.6401752	0.00081278
C15orf27	chromosome 15 open reading frame 27	1.35307939	0.00884666
C19orf66	chromosome 19 open reading frame 66	1.35430929	0.00603134
C1orf63	chromosome 1 open reading frame 63	-1.3277417	0.00539741
C1orf64	chromosome 1 open reading frame 64	1.27409371	0.00745309
C1RL-AS1	C1RL antisense RNA 1	1.38351101	0.00743235
C21orf119	chromosome 21 open reading frame 119	1.49057083	0.00311083
C2orf27A	chromosome 2 open reading frame 27A	1.34125981	0.00269092
C2orf54	chromosome 2 open reading frame 54	1.44893254	0.00275162
C3	complement component 3	1.38248576	0.0083961
C3orf67	chromosome 3 open reading frame 67	-1.3201351	0.0070835
C4orf21	chromosome 4 open reading frame 21	-1.4462947	0.0032078
C5AR1	complement component 5a receptor 1	1.71196499	0.00480311
C5orf34	chromosome 5 open reading frame 34	-1.40708	0.00347049
C5orf54	chromosome 5 open reading frame 54	-1.6470839	0.00228177
C5orf63	chromosome 5 open reading frame 63	-1.5581383	0.00234503
C7orf13	chromosome 7 open reading frame 13	1.49351643	0.00908752
C7orf61	chromosome 7 open reading frame 61	1.45028055	0.00276623
C7orf69	chromosome 7 open reading frame 69	-1.8157076	0.00483134
C9orf57	chromosome 9 open reading frame 57	1.41127778	0.00619903
C9orf64	chromosome 9 open reading frame 64	-1.3627049	0.0075531
C9orf66	chromosome 9 open reading frame 66	1.9172585	0.00680794
C9orf72	chromosome 9 open reading frame 72	-1.3983	0.00534874
CA5A	carbonic anhydrase VA, mitochondrial	1.3107483	0.0090998
CA5B	carbonic anhydrase VB, mitochondrial	-1.2934834	0.0060258
CABP1	calcium binding protein 1	-1.3602423	0.00348499
CACNA1C	calcium channel, voltage-dependent, L type, alpha 1C subunit	1.63876109	0.00396931
CALD1	caldesmon 1	-1.5088737	0.00738752
CALY	calcyon neuron-specific vesicular protein	1.60071309	0.00399234
CASP7	caspase 7, apoptosis-related cysteine peptidase	1.42146028	0.00775724
CBLN2	cerebellin 2 precursor	-2.0585125	0.00321421
CC2D2B	coiled-coil and C2 domain containing 2B	1.98785278	0.00795639

CCDC105	coiled-coil domain containing 105	1.36741386	0.00912022
CCDC111	coiled-coil domain containing 111	-1.3868754	0.0078463
CCDC125	coiled-coil domain containing 125	-1.6005917	0.00210689
CCDC130	coiled-coil domain containing 130	1.33314167	0.00478115
CCDC15	coiled-coil domain containing 15	-1.4132657	0.00353545
CCDC157	coiled-coil domain containing 157	1.32041743	0.0092776
CCDC23	coiled-coil domain containing 23	-1.5998012	0.00171056
CCDC59	coiled-coil domain containing 59	-1.9050684	0.00568834
CCDC85B	coiled-coil domain containing 85B	1.73615813	0.00326807
CCDC97	coiled-coil domain containing 97	-1.2775654	0.00677263
CCL2	chemokine (C-C motif) ligand 2	6.458198	0.00896644
CCL27	chemokine (C-C motif) ligand 27	1.42775251	0.0027912
CCNB1	cyclin B1	-1.3905987	0.00654906
CCT6A	chaperonin containing TCP1, subunit 6A (zeta 1)	-1.6108124	0.00918703
CCT8	chaperonin containing TCP1, subunit 8 (theta)	-1.3019616	0.00652346
CD40	CD40 molecule, TNF receptor superfamily member 5	1.42851339	0.00083145
CD83	CD83 molecule	1.40233474	0.00101099
CD99	CD99 molecule	-1.3174832	0.00734419
CDC123	cell division cycle 123	-1.366842	0.0092751
CDC42EP2	CDC42 effector protein (Rho GTPase binding) 2	1.32872277	0.00711512
CDH9	cadherin 9, type 2 (T1-cadherin)	1.48060011	0.00937582
CDK5R2	cyclin-dependent kinase 5, regulatory subunit 2 (p39)	1.49163182	0.00410361
CDKL4	cyclin-dependent kinase-like 4	-1.5971317	0.00648699
CDKN2B	cyclin-dependent kinase inhibitor 2B (p15, inhibits CDK4)	1.45764553	0.00312511
CELP	carboxyl ester lipase pseudogene	1.55045311	0.00460831
CEMP1	cementum protein 1	1.6356154	0.00349869
CEP290	centrosomal protein 290kDa	-1.4888556	0.00102782
CHMP2A	charged multivesicular body protein 2A	1.32885604	0.00636408
CHORDC1	cysteine and histidine-rich domain (CHORD) containing 1	-1.5063194	0.00078603
CHP2	calcineurin-like EF-hand protein 2	1.59184573	0.00524852
CHRM1	cholinergic receptor, muscarinic 1	1.3192699	0.00884907
CHRNA4	cholinergic receptor, nicotinic, alpha 4 (neuronal)	1.30875715	0.00731808
CHRNA5	cholinergic receptor, nicotinic, alpha 5 (neuronal)	-1.5958122	0.0040677
CHRNB1	cholinergic receptor, nicotinic, beta 1 (muscle)	1.54829912	0.00575994
CHRNE	cholinergic receptor, nicotinic, epsilon (muscle)	1.35489472	0.00913969
CHST12	carbohydrate (chondroitin 4) sulfotransferase 12	1.4633345	0.00881797
CIRBP-AS1	CIRBP antisense RNA 1	1.37470967	0.00528761
CLEC11A	C-type lectin domain family 11, member A	1.54520065	0.00649744

CLEC3B	C-type lectin domain family 3, member B	1.2624645	0.00869212
CLGN	calmegin	-1.3504835	0.00558512
CLHC1	clathrin heavy chain linker domain containing 1	-1.4331775	0.00720207
CLNS1A	chloride channel, nucleotide-sensitive, 1A	-1.5241125	0.0055801
CLP1	cleavage and polyadenylation factor I subunit 1	1.53066795	0.00960602
CMTM3	CKLF-like MARVEL transmembrane domain containing 3	1.44262758	0.00558042
CNTNAP3	contactin associated protein-like 3	-2.2148939	0.00336497
CNTNAP3	contactin associated protein-like 3	-2.2148939	0.00336497
CNTNAP4	contactin associated protein-like 4	1.46528097	0.00118182
COL11A2	collagen, type XI, alpha 2	1.41880415	0.00221912
COL11A2	collagen, type XI, alpha 2	1.41880415	0.00221912
COL8A1	collagen, type VIII, alpha 1	1.7937738	0.0008596
COLEC10	collectin sub-family member 10 (C-type lectin)	1.49982659	0.00205082
CORO1A	coronin, actin binding protein, 1A	1.74995054	0.00308974
CPXM2	carboxypeptidase X (M14 family), member 2	-1.4630577	0.00175754
CRABP2	cellular retinoic acid binding protein 2	2.04259509	0.00040643
CSF1	colony stimulating factor 1 (macrophage)	1.33213696	0.00635303
CSNK1G3	casein kinase 1, gamma 3	-1.4132806	0.00542341
CSPG4	chondroitin sulfate proteoglycan 4	1.50334185	0.00878242
CSPG4P1Y	chondroitin sulfate proteoglycan 4 pseudogene 1, Y-linked	1.40630483	0.0067943
CSPG4P1Y	chondroitin sulfate proteoglycan 4 pseudogene 1, Y-linked	1.40630483	0.0067943
CSRP2	cysteine and glycine-rich protein 2	1.45401889	0.00191152
CST7	cystatin F (leukocystatin)	1.40451305	0.00737404
CSTB	cystatin B (stefin B)	1.39686613	0.00556535
CT47A1	cancer/testis antigen family 47, member A1	-2.1145286	0.0007563
CT47A1	cancer/testis antigen family 47, member A1	-2.1145286	0.0007563
CT47A1	cancer/testis antigen family 47, member A1	-1.7790009	0.00163196
CT47A10	cancer/testis antigen family 47, member A10	-2.1145286	0.0007563
CTAGE4	CTAGE family, member 4	-1.7717865	0.00300301
CTAGE4	CTAGE family, member 4	-2.2499671	0.00445651
CTAGE6P	CTAGE family, member 6, pseudogene	-1.8224788	0.00642042
CTAGE6P	CTAGE family, member 6, pseudogene	-1.7496182	0.00959033
CTBP2	C-terminal binding protein 2	1.32923091	0.00927575
CTRL	chymotrypsin-like	1.41886492	0.00385596
CTSB	cathepsin B	1.41956895	0.00793897
CTSL3P	cathepsin L family member 3, pseudogene	-1.4041411	0.00592271
CWF19L2	CWF19-like 2, cell cycle control (S. pombe)	1.30034654	0.00750656
CXADR	coxsackie virus and adenovirus receptor	-1.6140047	0.00282615
CXCL16	chemokine (C-X-C motif) ligand 16	1.69772233	0.00689009
CXCR6	chemokine (C-X-C motif) receptor 6	1.35796347	0.00192341
CXXC11	CXXC finger protein 11	1.3771677	0.00694307
CYLC2	cylicin, basic protein of sperm head cytoskeleton 2	1.55461898	0.00564163

CYP2C18	cytochrome P450, family 2, subfamily C, polypeptide 18	1.360413	0.00342202
CYP4F30P	cytochrome P450, family 4, subfamily F, polypeptide 30, pseudogene	-1.5124396	0.00994937
CYP4F30P	cytochrome P450, family 4, subfamily F, polypeptide 30, pseudogene	-1.5118029	0.00995343
DAB2IP	DAB2 interacting protein	1.39833554	0.00408515
DAPL1	death associated protein-like 1	-1.5213054	0.00203877
DARC	Duffy blood group, chemokine receptor	-1.6685878	0.00203222
DARS	aspartyl-tRNA synthetase	-1.3490682	0.00996349
DBF4B	DBF4 homolog B (S. cerevisiae)	-1.2904874	0.00873128
DCAF13	DDB1 and CUL4 associated factor 13	-1.4742775	0.0047464
DCLRE1A	DNA cross-link repair 1A	-1.379613	0.00908365
DCP1B	DCP1 decapping enzyme homolog B (S. cerevisiae)	-2.0860606	0.00248041
DCTN4	dynactin 4 (p62)	-1.4243972	0.00883326
DDR1	discoidin domain receptor tyrosine kinase 1	1.42115861	0.00143806
DDR1	discoidin domain receptor tyrosine kinase 1	1.37493496	0.00524051
DDR1	discoidin domain receptor tyrosine kinase 1	1.35094709	0.00676501
DDX58	DEAD (Asp-Glu-Ala-Asp) box polypeptide 58	1.38267202	0.00320914
DEFB127	defensin, beta 127	1.43552994	0.00189834
DEFB132	defensin, beta 132	1.60853438	0.00673306
DEK	DEK oncogene	-1.3201203	0.00515759
DEPDC7	DEP domain containing 7	1.43919931	0.00707205
DEXI	Dexi homolog (mouse)	1.41242428	0.00382427
DEXI	Dexi homolog (mouse)	1.41242428	0.00382427
DHFR	dihydrofolate reductase	-1.7358712	0.00719605
DHRS3	dehydrogenase/reductase (SDR family) member 3	1.46097631	0.0062481
DHRS7C	dehydrogenase/reductase (SDR family) member 7C	1.41439583	0.00160991
DHX9	DEAH (Asp-Glu-Ala-His) box polypeptide 9	-1.5584467	0.00377462
DLEU7	deleted in lymphocytic leukemia, 7	-1.7198129	0.00826711
DLK1	delta-like 1 homolog (Drosophila)	1.46805722	0.0081591
DLL3	delta-like 3 (Drosophila)	1.58841027	0.00403631
DNAJA4	DnaJ (Hsp40) homolog, subfamily A, member 4	1.29654171	0.00631861
DNAJB1	DnaJ (Hsp40) homolog, subfamily B, member 1	1.707447	0.00478467
DNAJC12	DnaJ (Hsp40) homolog, subfamily C, member 12	-1.5329817	0.00752884
DNAJC15	DnaJ (Hsp40) homolog, subfamily C, member 15	-1.5891888	0.00368321
DNAJC19	DnaJ (Hsp40) homolog, subfamily C, member 19	-1.6480697	0.00688969
DNAJC2	DnaJ (Hsp40) homolog, subfamily C, member 2	-1.3726308	0.00871237
DNAJC4	DnaJ (Hsp40) homolog, subfamily C, member 4	1.4289938	0.00441396
DNAL1	dynein, axonemal, light chain 1	1.44219731	0.00198364

DPY19L3	dpy-19-like 3 (C. elegans)	-1.416202	0.00740495
DRD4	dopamine receptor D4	1.36312751	0.00339405
DUOXA1	dual oxidase maturation factor 1	1.45333388	0.00734303
DUSP15	dual specificity phosphatase 15	1.40349034	0.00129605
DYNC1LI1	dynein, cytoplasmic 1, light intermediate chain 1	-1.4536471	0.00892579
E2F5	E2F transcription factor 5, p130-binding	-1.7964338	0.0076987
E4F1	E4F transcription factor 1	1.57362678	0.00997376
EDEM1	ER degradation enhancer, mannosidase alpha-like 1	1.46055622	0.00532533
EFEMP2	EGF containing fibulin-like extracellular matrix protein 2	1.42547617	0.0033326
EFHA1	EF-hand domain family, member A1	-1.3260019	0.00468515
EFHD2	EF-hand domain family, member D2	1.33964624	0.00286356
EFNA1	ephrin-A1	1.57769161	0.00023888
EIF3E	eukaryotic translation initiation factor 3, subunit E	-1.4484499	0.0087005
EIF4B	eukaryotic translation initiation factor 4B	-1.9230901	0.00219707
EIF4B	eukaryotic translation initiation factor 4B	-1.4264988	0.00681525
ELMO3	engulfment and cell motility 3	1.52645526	0.00534868
ELOVL2-AS1	ELOVL2 antisense RNA 1	1.63848915	0.00433533
EME1	essential meiotic endonuclease 1 homolog 1 (S. pombe)	-1.3270693	0.00337762
EMILIN1	elastin microfibril interfacer 1	1.54017784	0.00050776
EML3	echinoderm microtubule associated protein like 3	1.31209933	0.00600673
ENGASE	endo-beta-N-acetylglucosaminidase	1.41250267	0.00238552
EPHA1	EPH receptor A1	1.4674116	0.00413348
EPHA2	EPH receptor A2	1.46136946	0.00190208
EPHA7	EPH receptor A7	1.36845249	0.00510077
EPHX1	epoxide hydrolase 1, microsomal (xenobiotic)	1.41816857	0.00203623
EPS8L2	EPS8-like 2	1.50639134	0.00247935
EQTN	equatorin, sperm acrosome associated	1.37320394	0.00371442
ERAS	ES cell expressed Ras	1.41960967	0.00636028
ERCC6L	excision repair cross-complementing rodent repair deficiency, complementation group 6-like	1.39565452	0.00140245
ERCC6L2	excision repair cross-complementing rodent repair deficiency, complementation group 6-like 2	-1.3681732	0.00692221
ERVFC1-1	endogenous retrovirus group FC1, member 1	-1.4655461	0.00121988
ESR2	estrogen receptor 2 (ER beta)	-1.5617064	0.00126234
EXOC3L2	exocyst complex component 3-like 2	1.45093729	0.00240619
FADD	Fas (TNFRSF6)-associated via death domain	1.35225764	0.00431984
FAF2	Fas associated factor family member 2	-1.5132243	0.00345403
FAM115C	family with sequence similarity 115, member C	-1.4252672	0.00716198
FAM129A	family with sequence similarity 129,	1.36310846	0.00157227

	member A		
FAM136A	family with sequence similarity 136, member A	-1.7674728	0.00445093
FAM185A	family with sequence similarity 185, member A	-1.5247677	0.00414397
FAM209B	family with sequence similarity 209, member B	-1.4630168	0.00933243
FAM221A	family with sequence similarity 221, member A	-1.6049817	0.00532264
FAM3A	family with sequence similarity 3, member A	1.4714046	0.00583562
FAM46A	family with sequence similarity 46, member A	1.79445762	0.00433952
FAM65A	family with sequence similarity 65, member A	1.44720088	0.0033097
FAM86B1	family with sequence similarity 86, member B1	-1.3604455	0.00905306
FAM86DP	family with sequence similarity 86, member D, pseudogene	1.28026391	0.0092316
FAM90A10P	putative protein FAM90A10	-1.8280389	0.00498387
FAM92B	family with sequence similarity 92, member B	1.30662303	0.0090668
FAM98C	family with sequence similarity 98, member C	1.50010248	0.00840963
FBL	fibrillarin	1.49126141	0.00646627
FBXL6	F-box and leucine-rich repeat protein 6	1.37595072	0.00221666
FBXL8	F-box and leucine-rich repeat protein 8	1.46982553	0.0087072
FBXO25	F-box protein 25	-1.9463862	0.00171204
FBXO5	F-box protein 5	-1.7847546	0.00900986
FBXO9	F-box protein 9	-1.2782382	0.00541704
FBXW5	F-box and WD repeat domain containing 5	1.32319329	0.00656749
FCGR2A	Fc fragment of IgG, low affinity IIa, receptor (CD32)	-1.6495348	0.00832779
FER1L5	fer-1-like 5 (C. elegans)	1.48256544	0.00257805
FHIT	fragile histidine triad	1.53404805	0.00402755
FIBIN	fin bud initiation factor homolog (zebrafish)	1.35599533	0.00501094
FKTN	fukutin	-1.3956176	0.00412904
FLJ00290	FLJ00290 protein	1.52515281	0.00453387
FLJ16124	FLJ16124 protein	-1.7418576	7.16E-05
FLJ40852	uncharacterized LOC285962	-1.8054055	0.00215123
FLJ46010	FLJ46010 protein	1.4487022	0.00225245
FN1	fibronectin 1	-1.3736624	0.00293406
FNDC5	fibronectin type III domain containing 5	1.59671738	0.00101517
FOXE1	forkhead box E1 (thyroid transcription factor 2)	1.55931804	0.00688943
FOXG1	forkhead box G1	1.53894988	0.007729
FOXN1	forkhead box N1	1.6681649	0.00392401
FOXN3-AS2	FOXN3 antisense RNA 2	1.37860911	0.00822837
FOXP4	forkhead box P4	1.3407025	0.00454256
FRAT2	frequently rearranged in advanced T-cell	-1.2957657	0.00836044

	lymphomas 2		
FUT11	fucosyltransferase 11 (alpha (1,3) fucosyltransferase)	1.34367056	0.00589971
FZD2	frizzled family receptor 2	1.38438984	0.00744227
GABPA	GA binding protein transcription factor, alpha subunit 60kDa	-1.3623306	0.00615479
GABRA2	gamma-aminobutyric acid (GABA) A receptor, alpha 2	1.32804344	0.00492319
GABRA5	gamma-aminobutyric acid (GABA) A receptor, alpha 5	1.36064086	0.00669276
GAFA3	FGF-2 activity-associated protein 3	-1.7600028	0.00726059
GAGE12B	G antigen 12B	-1.572379	0.00615968
GAGE12G	G antigen 12G	-1.9396781	0.00544343
GAREML	GRB2 associated, regulator of MAPK1-like	1.36089057	0.00390282
GAS6	growth arrest-specific 6	1.48624367	0.00806804
GATSL3	GATS protein-like 3	1.4847895	0.00064202
GBAP1	glucosidase, beta, acid pseudogene 1	-1.9873666	0.00203203
GCFC2	GC-rich sequence DNA-binding factor 2	-1.5057776	0.00947834
GCSH	glycine cleavage system protein H (aminomethyl carrier)	-1.5826448	0.00636755
GDF15	growth differentiation factor 15	2.31406546	0.00015991
GDF2	growth differentiation factor 2	-1.4440709	0.00194197
GET4	golgi to ER traffic protein 4 homolog (S. cerevisiae)	1.41244627	0.00444028
GFOD1	glucose-fructose oxidoreductase domain containing 1	1.61610342	0.00556383
GFRA1	GDNF family receptor alpha 1	1.37344454	0.00876855
GINM1	glycoprotein integral membrane 1	-1.6341205	0.00392617
GJB4	gap junction protein, beta 4, 30.3kDa	1.37927908	0.00534821
GLI1	GLI family zinc finger 1	1.57201614	0.00131998
GLUL	glutamate-ammonia ligase	1.48196185	0.00415082
GM2A	GM2 ganglioside activator	-1.3751475	0.00279776
GNG11	guanine nucleotide binding protein (G protein), gamma 11	-2.3585267	0.00342451
GNPDA2	glucosamine-6-phosphate deaminase 2	-1.4574169	0.00333011
GOLGA6A	golgin A6 family, member A	-1.7096381	0.00188026
GOLGA6A	golgin A6 family, member A	-1.6265027	0.00287806
GOLGA6B	golgin A6 family, member B	-1.7126347	0.00073422
GOLGA6B	golgin A6 family, member B	-1.6230647	0.00218616
GOLGA7B	golgin A7 family, member B	1.4952246	0.00059627
GOLGA8CP	golgin A8 family, member C, pseudogene	-1.678006	0.00293306
GOLGA8DP	golgin A8 family, member D, pseudogene	-1.779009	0.00161121
GOLGA8DP	golgin A8 family, member D, pseudogene	-1.6518255	0.00293684
GOLGA8EP	golgin A8 family, member E, pseudogene	-1.7444265	0.00137293
GOLGA8F	golgin A8 family, member F	-1.9352733	0.00053522
GOLGA8F	golgin A8 family, member F	-1.6924449	0.00271074
GOLGA8G	golgin A8 family, member G	-1.7804466	0.00188902
GOLGA8G	golgin A8 family, member G	-1.7804466	0.00188902
GOLGA8I	golgin A8 family, member I	-1.3641628	0.00270222
GOLGA8I	golgin A8 family, member I	-1.4977994	0.00627908

GP9	glycoprotein IX (platelet)	1.66180114	0.00032157
GPAM	glycerol-3-phosphate acyltransferase, mitochondrial	-4.759574	0.00717223
GPC2	glypican 2	1.64693456	0.0075887
GPR125	G protein-coupled receptor 125	-1.5266338	0.00771512
GPR87	G protein-coupled receptor 87	-1.5929989	0.00194725
GRAMD2	GRAM domain containing 2	1.29447278	0.00692641
GREM1	gremlin 1, DAN family BMP antagonist	1.32903588	0.00762051
GRWD1	glutamate-rich WD repeat containing 1	1.30629598	0.00523252
GSPT1	G1 to S phase transition 1	-1.5684938	0.00313961
GSTM1	glutathione S-transferase mu 1	1.31207878	0.00659851
GTF3A	general transcription factor IIIA	-1.3804047	0.00958578
GTPBP10	GTP-binding protein 10 (putative)	-1.6148176	0.00049488
GUCA1C	guanylate cyclase activator 1C	-1.582679	0.00980018
GUCY1B3	guanylate cyclase 1, soluble, beta 3	1.38543556	0.0043242
GULP1	GULP, engulfment adaptor PTB domain containing 1	-1.4634208	0.00918897
GZMH	granzyme H (cathepsin G-like 2, protein h-CCPX)	1.37546617	0.00794708
H3F3C	H3 histone, family 3C	-1.6823724	0.00382094
HAS1	hyaluronan synthase 1	1.41519769	0.00992248
HAUS6	HAUS augmin-like complex, subunit 6	-1.8477691	0.00795401
HBE1	hemoglobin, epsilon 1	-1.5284297	0.00056329
HBZ	hemoglobin, zeta	1.92565434	0.00057246
HCFC1R1	host cell factor C1 regulator 1 (XPO1 dependent)	1.49173279	0.00183157
HCG27	HLA complex group 27 (non-protein coding)	1.56250825	0.00335795
HCLS1	hematopoietic cell-specific Lyn substrate 1	1.38988023	0.00532845
HCRTR2	hypocretin (orexin) receptor 2	1.51845962	0.00916578
HES1	hairy and enhancer of split 1, (Drosophila)	1.47571979	0.00855364
HES6	hairy and enhancer of split 6 (Drosophila)	1.38612243	0.00932072
HHEX	hematopoietically expressed homeobox	1.75030403	0.00282441
HIF3A	hypoxia inducible factor 3, alpha subunit	1.30562014	0.00457406
HIST1H1B	histone cluster 1, H1b	-1.535788	0.0060165
HIST1H2AK	histone cluster 1, H2ak	-1.6132711	0.00056287
HIST1H2BE	histone cluster 1, H2be	-1.5123396	0.00374242
HIST1H2BF	histone cluster 1, H2bf	-2.2472862	0.00235658
HIST1H2BM	histone cluster 1, H2bm	-1.3689334	0.00743264
HIST1H3G	histone cluster 1, H3g	-2.263027	0.00303331
HIST1H4D	histone cluster 1, H4d	-1.4654363	0.00905834
HIST1H4E	histone cluster 1, H4e	-1.3594196	0.002829
HIST1H4I	histone cluster 1, H4i	-1.7975941	0.00467047
HIST1H4L	histone cluster 1, H4l	-1.3410717	0.00684357
HIST2H2AB	histone cluster 2, H2ab	-1.3630564	0.00510716
HLA-A	major histocompatibility complex, class I, A	1.56363877	0.00063651
HLA-A	major histocompatibility complex, class I, A	1.53365882	0.0008735
HLA-C	major histocompatibility complex, class I, C	1.34192597	0.00244172
HLA-C	major histocompatibility complex, class I, C	1.42304192	0.00299471
HLA-DMA	major histocompatibility complex, class II, DM alpha	-1.3896835	0.00940659

HLA-H	major histocompatibility complex, class I, H (pseudogene)	1.51814758	0.00522171
HNRNPA1	heterogeneous nuclear ribonucleoprotein A1	-1.4376811	0.00520577
HNRNPCL1	heterogeneous nuclear ribonucleoprotein C-like 1	-1.4814942	0.00614308
HNRNPF	heterogeneous nuclear ribonucleoprotein F	1.33321998	0.00345261
HNRNPH2	heterogeneous nuclear ribonucleoprotein H2 (H')	-1.4524954	0.00222474
HNRPDL	heterogeneous nuclear ribonucleoprotein D-like	-1.3431189	0.00680819
HOXB8	homeobox B8	1.28594309	0.00633524
HOXC10	homeobox C10	1.5462776	0.00150971
HOXD12	homeobox D12	1.60087824	0.00096138
HOXD9	homeobox D9	1.43285396	0.00150592
HS3ST2	heparan sulfate (glucosamine) 3-O-sulfotransferase 2	-1.9846779	0.00561259
HS6ST2	heparan sulfate 6-O-sulfotransferase 2	-1.4053567	0.00387087
HSD17B6	hydroxysteroid (17-beta) dehydrogenase 6	-1.3156976	0.00347008
HSPA1A	heat shock 70kDa protein 1A	1.72426529	0.00363717
HSPA1B	heat shock 70kDa protein 1B	1.88830445	0.0065915
HSPB2	heat shock 27kDa protein 2	1.8551688	0.00149319
ICAM1	intercellular adhesion molecule 1	2.39147761	0.00019756
IDI2	isopentenyl-diphosphate delta isomerase 2	-1.3436748	0.00442506
IFIH1	interferon induced with helicase C domain 1	1.45435091	0.00432776
IFIT1B	interferon-induced protein with tetratricopeptide repeats 1B	-1.9139157	0.00244303
IFITM1	interferon induced transmembrane protein 1	1.51286565	0.00204425
IFNA14	interferon, alpha 14	1.70719931	0.00025261
IFNA16	interferon, alpha 16	1.45914449	0.00734769
IGF2BP3	insulin-like growth factor 2 mRNA binding protein 3	-1.9498267	0.00358878
IGFBP6	insulin-like growth factor binding protein 6	1.40837088	0.00536374
IGK@	immunoglobulin kappa locus	1.37239261	0.0050714
IL12A	interleukin 12A (natural killer cell stimulatory factor 1, cytotoxic lymphocyte maturation factor 1, p35)	1.46324993	0.00313229
IL16	interleukin 16	-1.4779732	0.0019272
IL17D	interleukin 17D	1.36329967	0.00605238
IL17REL	interleukin 17 receptor E-like	1.48870221	0.00781906
IL27RA	interleukin 27 receptor, alpha	1.40220621	0.00120901
IMP3	IMP3, U3 small nucleolar ribonucleoprotein, homolog (yeast)	1.60611058	0.0027704
IMPAD1	inositol monophosphatase domain containing 1	-1.7274307	0.00063132
INO80C	INO80 complex subunit C	1.55243986	0.00516809
INSRR	insulin receptor-related receptor	1.4060464	0.00537082
INTU	inturned planar cell polarity effector homolog (Drosophila)	1.27585607	0.00717194

IPO11	importin 11	-1.3423521	0.00716138
IRAK1	interleukin-1 receptor-associated kinase 1	1.49286546	0.00742093
IRF1	interferon regulatory factor 1	1.91788448	0.00090356
IRF7	interferon regulatory factor 7	1.49339277	0.00457725
IRX2	iroquois homeobox 2	1.47034547	0.00821892
ISCA1	iron-sulfur cluster assembly 1 homolog (S. cerevisiae)	-1.6565667	0.00229221
ITPA	inosine triphosphatase (nucleoside triphosphate pyrophosphatase)	1.254876	0.00843721
JAKMIP2	janus kinase and microtubule interacting protein 2	-1.6737238	0.0017846
JKAMP	JNK1/MAPK8-associated membrane protein	-1.2723758	0.00641461
JUNB	jun B proto-oncogene	1.38850101	0.00711351
KBTBD3	kelch repeat and BTB (POZ) domain containing 3	1.64771659	0.0005275
KCNJ3	potassium inwardly-rectifying channel, subfamily J, member 3	1.58606947	0.00108532
KCNJ5	potassium inwardly-rectifying channel, subfamily J, member 5	1.4005271	0.0086741
KCNK10	potassium channel, subfamily K, member 10	-1.257699	0.00985841
KCNQ1DN	KCNQ1 downstream neighbor (non-protein coding)	1.58414366	0.00957277
KDM4D	lysine (K)-specific demethylase 4D	-1.5036161	0.00248182
KDM6B	lysine (K)-specific demethylase 6B	1.29050416	0.00811393
KERA	keratocan	1.53515126	0.00729617
KIAA0947	KIAA0947	-1.3011333	0.00751556
KIAA1143	KIAA1143	-1.4715957	0.00731705
KIAA1586	KIAA1586	-1.7882312	0.00150098
KIAA1671	KIAA1671	1.68718788	0.00233698
KIAA1804	mixed lineage kinase 4	-1.5361622	0.00740112
KIF11	kinesin family member 11	-2.0951566	0.00175736
KIF17	kinesin family member 17	1.55583395	0.00753366
KIF18A	kinesin family member 18A	-1.4441497	0.00991971
KIF1A	kinesin family member 1A	1.35109502	0.00194876
KIF25-AS1	KIF25 antisense RNA 1	1.40402907	0.00969577
KIF4A	kinesin family member 4A	-1.489318	0.00260038
KIF4B	kinesin family member 4B	-1.3546668	0.00723938
KLF17	Kruppel-like factor 17	1.77478947	0.00102835
KLF6	Kruppel-like factor 6	1.60932411	0.00079512
KLHDC10	kelch domain containing 10	-1.6346608	0.00030588
KLK2	kallikrein-related peptidase 2	-1.3431813	0.00562813
KNTC1	kinetochore associated 1	-1.510823	0.0044797
KPNA3	karyopherin alpha 3 (importin alpha 4)	-1.7303641	0.00525414
KRCC1	lysine-rich coiled-coil 1	-1.870309	0.00391615
KRT6C	keratin 6C	-1.4216889	0.00912623
KRT72	keratin 72	-1.3264305	0.00581181
KRT79	keratin 79	1.37945574	0.00616254
KRTAP1-1	keratin associated protein 1-1	-1.325578	0.00531899
KRTAP4-2	keratin associated protein 4-2	-1.4842331	0.00402215
KRTAP4-7	keratin associated protein 4-7	-1.4406273	0.00697999

KRTAP4-9	keratin associated protein 4-9	-1.3548083	0.00729224
KRTAP9-2	keratin associated protein 9-2	-2.8523007	0.00327308
KRTAP9-4	keratin associated protein 9-4	-1.4936662	0.00434703
L3MBTL2	l(3)mbt-like 2 (Drosophila)	1.68197215	0.00311585
LATS2	LATS, large tumour suppressor, homolog 2 (Drosophila)	1.37800108	0.0038231
LBX1	ladybird homeobox 1	1.56433088	0.00035289
LCE1F	late cornified envelope 1F	1.3278228	0.00817019
LCE3C	late cornified envelope 3C	1.55088577	0.00462421
LCE4A	late cornified envelope 4A	1.37132554	0.00587565
LENG1	leukocyte receptor cluster (LRC) member 1	1.70075471	0.00047482
LGALS1	lectin, galactoside-binding, soluble, 1	1.52084084	0.00454816
LGALS2	lectin, galactoside-binding, soluble, 2	1.2866337	0.00681117
LGALS3	lectin, galactoside-binding, soluble, 3	1.49789804	0.00362271
LGALS8	lectin, galactoside-binding, soluble, 8	1.47635865	0.00390088
LGALS9	lectin, galactoside-binding, soluble, 9	1.31894271	0.0055027
LIF	leukemia inhibitory factor	1.63742325	0.00224831
LILRA6	leukocyte immunoglobulin-like receptor, subfamily A (with TM domain), member 6	1.60948964	0.00800949
LIMD1-AS1	LIMD1 antisense RNA 1	-2.9987612	0.0014607
LIN7A	lin-7 homolog A (C. elegans)	1.40496514	0.00702178
LINC00083	long intergenic non-protein coding RNA 83	1.4480573	0.00184392
LINC00161	long intergenic non-protein coding RNA 161	1.51438514	0.00352098
LINC00324	long intergenic non-protein coding RNA 324	-1.4150558	0.00270479
LINC00326	long intergenic non-protein coding RNA 326	1.80331777	0.00430523
LINC00328	long intergenic non-protein coding RNA 328	-1.561099	0.00621697
LINC00334	long intergenic non-protein coding RNA 334	1.41292223	0.00495078
LINC00470	long intergenic non-protein coding RNA 470	1.48930379	0.00886861
LINC00652	long intergenic non-protein coding RNA 652	-1.6462011	0.00223502
LLPH	LLP homolog, long-term synaptic facilitation (Aplysia)	-1.7370629	0.00400387
LOC100128356	protein transactivated by hepatitis B virus E antigen	1.55525094	0.00167317
LOC100128644	LMNE6487	1.52616314	0.00947376
LOC100130876	uncharacterized LOC100130876	-1.7583144	0.0061228
LOC100132319	uncharacterized LOC100132319	-1.5413939	0.00342226
LOC149373	uncharacterized LOC149373	-1.6067554	0.00155708
LOC157740	uncharacterized protein C8orf9	1.49149715	0.00165635
LOC1720	dihydrofolate reductase pseudogene	-2.6252688	0.00226471
LOC286359	uncharacterized LOC286359	1.46330034	0.00568533
LOC349196	uncharacterized LOC349196	-2.6553267	0.00378863
LOC349196	uncharacterized LOC349196	-2.6553267	0.00378863
LOC349196	uncharacterized LOC349196	-2.6188928	0.00431395
LOC349196	uncharacterized LOC349196	-2.6188928	0.00431395
LOC349196	uncharacterized LOC349196	-1.8389346	0.00692405
LOC349196	uncharacterized LOC349196	-1.6917143	0.00696358
LOC440461	Rho GTPase activating protein 27	1.5425584	0.00640761

	pseudogene		
LOC440518	golgin A2 pseudogene	1.54903821	0.00157767
LOC441233	uncharacterized LOC441233	-1.453047	0.00165581
LOC441601	septin 7 pseudogene	-1.574438	0.00125853
LOC728093	putative POM121-like protein 1-like	-2.8302117	0.00207992
LOC728093	putative POM121-like protein 1-like	-2.3596391	0.00222753
LOC728093	putative POM121-like protein 1-like	-2.4893059	0.00347276
LOC728093	putative POM121-like protein 1-like	-2.5346682	0.00405898
LOC728093	putative POM121-like protein 1-like	-2.5899449	0.00624563
LOC729866	hCG1994895	-1.2495077	0.00962286
LRRC37A2	leucine rich repeat containing 37, member A2	-1.7499196	0.00615896
LRRC37A2	leucine rich repeat containing 37, member A2	-1.7258521	0.00878025
LRRC37A4P	leucine rich repeat containing 37, member A4, pseudogene	-2.0324506	0.00379769
LRRC37A4P	leucine rich repeat containing 37, member A4, pseudogene	-1.6011804	0.00829862
LRRFIP1	leucine rich repeat (in FLII) interacting protein 1	-1.6428484	0.00089113
LRRFIP1	leucine rich repeat (in FLII) interacting protein 1	-1.4372556	0.00499763
LRRN4	leucine rich repeat neuronal 4	1.40567939	0.00337612
LSM5	LSM5 homolog, U6 small nuclear RNA associated (S. cerevisiae)	-2.0118102	4.83E-05
LYVE1	lymphatic vessel endothelial hyaluronan receptor 1	-1.4640346	0.00758696
LYZL2	lysozyme-like 2	-1.4001227	0.00697368
MAG	myelin associated glycoprotein	1.39009697	0.0064814
MAGEC3	melanoma antigen family C, 3	1.37428423	0.00978512
MAGED2	melanoma antigen family D, 2	1.36221039	0.00496031
MAL	mal, T-cell differentiation protein	1.79307625	0.00637814
MAML3	mastermind-like 3 (Drosophila)	-1.6547906	0.007928
MANSC1	MANSC domain containing 1	-1.4001226	0.00717139
MAP3K8	mitogen-activated protein kinase kinase kinase 8	1.40791861	0.00295065
MAP9	microtubule-associated protein 9	-1.4694117	0.00139462
MATK	megakaryocyte-associated tyrosine kinase	1.32979381	0.00237734
MBL1P	mannose-binding lectin (protein A) 1, pseudogene	1.46393234	0.0016882
MBOAT2	membrane bound O-acyltransferase domain containing 2	-1.5002044	0.00823811
MC3R	melanocortin 3 receptor	-1.3504471	0.0021511
MCM4	minichromosome maintenance complex component 4	-1.583085	0.00940137
MECOM	MDS1 and EVI1 complex locus	1.68820312	0.00162863
MED11	mediator complex subunit 11	1.38848832	0.00785458
METTL17	methyltransferase like 17	-1.3259692	0.00831058
MFSD10	major facilitator superfamily domain containing 10	1.36115892	0.00656932

MFSD12	major facilitator superfamily domain containing 12	1.46004333	0.00578763
MGC2752	CENPB DNA-binding domains containing 1 pseudogene	1.57841007	0.00301383
MIOX	myo-inositol oxygenase	1.58155366	0.00019451
MIR101-2	microRNA 101-2	-1.450115	0.00468929
MIR124-2	microRNA 124-2	1.57538479	0.00685616
MIR127	microRNA 127	-1.717711	0.00038283
MIR132	microRNA 132	1.44681707	0.00845629
MIR194-1	microRNA 194-1	1.38033729	0.00324537
MIR199A1	microRNA 199a-1	1.4838612	0.00094699
MIR200A	microRNA 200a	1.65129884	0.00046954
MIR217	microRNA 217	1.72579811	0.00297348
MIR24-2	microRNA 24-2	1.64948761	0.00157753
MIR331	microRNA 331	1.62489997	0.0097712
MIR9-1	microRNA 9-1	1.33770284	0.00631658
MIRLET7A2	microRNA let-7a-2	-1.91675	0.00103118
MIS18BP1	MIS18 binding protein 1	-1.63245	0.00331005
MKNK1	MAP kinase interacting serine/threonine kinase 1	1.52856379	0.00994782
MLF1IP	MLF1 interacting protein	-2.0947479	0.0027028
MLYCD	malonyl-CoA decarboxylase	1.44228622	0.00178723
MMADHC	methylmalonic aciduria (cobalamin deficiency) cblD type, with homocystinuria	-1.6050085	0.00464214
MMP15	matrix metallopeptidase 15 (membrane-inserted)	1.50356421	0.00739363
MORN2	MORN repeat containing 2	-1.7053174	0.00682951
MPLKIP	M-phase specific PLK1 interacting protein	-1.6346498	0.00697653
MPLKIP	M-phase specific PLK1 interacting protein	-1.6251707	0.00979526
MRE11A	MRE11 meiotic recombination 11 homolog A (S. cerevisiae)	-1.434089	0.00350256
MRPL36	mitochondrial ribosomal protein L36	-1.3477643	0.00638591
MRPL42	mitochondrial ribosomal protein L42	-1.8062143	0.00344433
MRPL43	mitochondrial ribosomal protein L43	1.43490952	0.00745007
MRPS16	mitochondrial ribosomal protein S16	-1.3824089	0.00153061
MS4A10	membrane-spanning 4-domains, subfamily A, member 10	-1.448379	0.00206776
MS4A5	membrane-spanning 4-domains, subfamily A, member 5	-1.5262421	0.00431019
MSANTD3	Myb/SANT-like DNA-binding domain containing 3	1.3132095	0.00750806
MT1IP	metallothionein 1I, pseudogene	1.56545655	0.00916121
MT1P2	metallothionein 1H-like	-1.7032556	0.0086519
MTERF	mitochondrial transcription termination factor	-1.7032065	4.08E-05
MTF1	metal-regulatory transcription factor 1	-1.3340475	0.00906641
MTHFD1L	methylenetetrahydrofolate dehydrogenase (NADP+ dependent) 1-like	-1.9765297	0.00742429
MTHFD1L	methylenetetrahydrofolate dehydrogenase (NADP+ dependent) 1-like	-1.9765297	0.00742429

MTHFD1L	methylenetetrahydrofolate dehydrogenase (NADP+ dependent) 1-like	-1.7744804	0.00810297
MTSS1L	metastasis suppressor 1-like	1.40796112	0.00387123
MYC	v-myc myelocytomatosis viral oncogene homolog (avian)	-1.5293125	0.00144542
MYL3	myosin, light chain 3, alkali; ventricular, skeletal, slow	1.4229427	0.00379969
MYO1F	myosin IF	1.34349144	0.00491486
MZF1	myeloid zinc finger 1	1.4015913	0.00342834
NAA30	N(alpha)-acetyltransferase 30, NatC catalytic subunit	1.38611291	0.00874639
NAALAD2	N-acetylated alpha-linked acidic dipeptidase 2	-1.4439501	0.00149197
NAB2	NGFI-A binding protein 2 (EGR1 binding protein 2)	1.36139019	0.00665619
NANOGP1	Nanog homeobox pseudogene 1	-1.427557	0.00317513
NARFL	nuclear prelamin A recognition factor-like	1.62211979	0.00227088
NARG2	NMDA receptor regulated 2	-1.6981767	0.00397781
NBPF15	neuroblastoma breakpoint family, member 15	-1.4531656	0.00495607
NBPF3	neuroblastoma breakpoint family, member 3	-1.7415064	0.00556132
NCOR1P1	nuclear receptor corepressor 1 pseudogene 1	-1.263402	0.00978249
NDOR1	NADPH dependent diflavin oxidoreductase 1	1.48046061	0.00587505
NDUFA7	NADH dehydrogenase (ubiquinone) 1 alpha subcomplex, 7, 14.5kDa	1.3531688	0.00839612
NEBL	nebulette	-1.4208168	0.00665693
NEDD9	neural precursor cell expressed, developmentally down-regulated 9	1.33779803	0.00601474
NET1	neuroepithelial cell transforming 1	-1.4640557	0.00937576
NEUROD2	neuronal differentiation 2	1.96644622	0.00291419
NF1	neurofibromin 1	-1.5079174	0.00483154
NF1	neurofibromin 1	-1.5079174	0.00483154
NFIA	nuclear factor I/A	-1.4665809	0.00881149
NFKB2	nuclear factor of kappa light polypeptide gene enhancer in B-cells 2 (p49/p100)	1.84070992	0.00321834
NFKBIA	nuclear factor of kappa light polypeptide gene enhancer in B-cells inhibitor, alpha	1.7531713	0.00257873
NFKBIE	nuclear factor of kappa light polypeptide gene enhancer in B-cells inhibitor, epsilon	1.41831309	0.00527512
NGEF	neuronal guanine nucleotide exchange factor	1.49417589	0.00869222
NMU	neuromedin U	1.56099287	0.00060394
NOBOX	NOBOX oogenesis homeobox	1.64413558	7.37E-05
NOL7	nucleolar protein 7, 27kDa	-1.4421621	0.00649029
NOS3	nitric oxide synthase 3 (endothelial cell)	1.34222472	0.00757502
NPPA	natriuretic peptide A	1.26857443	0.00664999
NPTX2	neuronal pentraxin II	1.35667558	0.00224272
NR4A1	nuclear receptor subfamily 4, group A,	1.35130357	0.00808884

	member 1		
NR5A1	nuclear receptor subfamily 5, group A, member 1	1.59169884	0.0059521
NRM	nurim (nuclear envelope membrane protein)	1.7354009	0.00214796
NSMAF	neutral sphingomyelinase (N-SMase) activation associated factor	-1.6719728	0.00417878
NSRP1	nuclear speckle splicing regulatory protein 1	-1.6125228	0.00470031
NT5C3	5'-nucleotidase, cytosolic III	1.45312089	0.00909778
NUF2	NUF2, NDC80 kinetochore complex component, homolog (S. cerevisiae)	-1.673213	0.00130638
NUP107	nucleoporin 107kDa	-1.4960766	0.00774131
NUP37	nucleoporin 37kDa	-1.3838821	0.00765852
NXF4	nuclear RNA export factor 4 pseudogene	1.32129466	0.00660328
OCIAD1	OCIA domain containing 1	-1.4659436	0.00935387
OGDHL	oxoglutarate dehydrogenase-like	1.3766824	0.0065033
OGFOD2	2-oxoglutarate and iron-dependent oxygenase domain containing 2	1.29189231	0.00548823
OIT3	oncoprotein induced transcript 3	1.39035564	0.00594665
OK/SW-CL.36	OK/SW-CL.36	1.80690112	0.00251412
OR10A4	olfactory receptor, family 10, subfamily A, member 4	1.36045724	0.00307227
OR10A7	olfactory receptor, family 10, subfamily A, member 7	1.38487134	0.00734019
OR10G3	olfactory receptor, family 10, subfamily G, member 3	-1.3730261	0.00477705
OR10H5	olfactory receptor, family 10, subfamily H, member 5	-1.5041112	0.00204324
OR2B11	olfactory receptor, family 2, subfamily B, member 11	-1.5288092	0.00639621
OR2T11	olfactory receptor, family 2, subfamily T, member 11	1.32432744	0.00655848
OR2T29	olfactory receptor, family 2, subfamily T, member 29	1.38156558	0.00698807
OR2T5	olfactory receptor, family 2, subfamily T, member 5	1.34198452	0.00768327
OR3A1	olfactory receptor, family 3, subfamily A, member 1	1.56202554	0.00120887
OR4K17	olfactory receptor, family 4, subfamily K, member 17	1.51869215	0.00483456
OR4K5	olfactory receptor, family 4, subfamily K, member 5	1.47721168	0.00654816
OR4S1	olfactory receptor, family 4, subfamily S, member 1	1.63160583	0.00780147
OR52E2	olfactory receptor, family 52, subfamily E, member 2	1.51517958	0.00122487
OR52N4	olfactory receptor, family 52, subfamily N, member 4	1.42003733	0.00403946
OR5M9	olfactory receptor, family 5, subfamily M, member 9	1.41642243	0.00206395
OR6C1	olfactory receptor, family 6, subfamily C,	1.29796113	0.00646662

	member 1		
OR8G5	olfactory receptor, family 8, subfamily G, member 5	1.63997691	0.00786227
OTX2	orthodenticle homeobox 2	1.31161593	0.00463197
OVOS	ovostatin	-1.4968429	0.00937502
OXR1	oxidation resistance 1	-1.3910238	0.00188538
PAGE5	P antigen family, member 5 (prostate associated)	-1.7145755	0.00875443
PAPL	iron/zinc purple acid phosphatase-like protein	1.2908762	0.00852893
PAQR5	progestin and adipoQ receptor family member V	1.53823354	0.00349553
PAQR9	progestin and adipoQ receptor family member IX	1.35331256	0.00937692
PARP12	poly (ADP-ribose) polymerase family, member 12	-1.5751495	0.00238174
PARP14	poly (ADP-ribose) polymerase family, member 14	-1.534117	0.00756498
PAX1	paired box 1	1.37632675	0.00511245
PAX7	paired box 7	1.33140805	0.00499699
PBK	PDZ binding kinase	-1.8980533	0.00518191
PCBP1	poly(rC) binding protein 1	1.40954459	0.00707651
PCDH8	protocadherin 8	1.33689978	0.00325469
PCDHA8	protocadherin alpha 8	1.36943955	0.00565029
PDLIM7	PDZ and LIM domain 7 (enigma)	1.41179562	0.00319649
PDS5B	PDS5, regulator of cohesion maintenance, homolog B (S. cerevisiae)	-1.3458781	0.00714099
PDXDC2P	pyridoxal-dependent decarboxylase domain containing 2, pseudogene	-1.4340272	0.00551439
PFKL	phosphofructokinase, liver	1.31330404	0.00928331
PGAM1	phosphoglycerate mutase 1 (brain)	-1.5187871	0.00680149
PHF1	PHD finger protein 1	1.45882846	0.0034018
PHF6	PHD finger protein 6	-1.3391933	0.00358065
PHLDA3	pleckstrin homology-like domain, family A, member 3	1.58904443	0.00833364
PHOX2B	paired-like homeobox 2b	-1.9186995	0.00037861
PIEZO1	piezo-type mechanosensitive ion channel component 1	1.61231735	0.00350699
PIGA	phosphatidylinositol glycan anchor biosynthesis, class A	-1.6351627	0.00341186
PIGW	phosphatidylinositol glycan anchor biosynthesis, class W	-1.9345698	0.00201181
PIM3	pim-3 oncogene	1.33392885	0.00474499
PINX1	PIN2/TERF1 interacting, telomerase inhibitor 1	-1.3345843	0.0086471
PIWIL3	piwi-like RNA-mediated gene silencing 3	-1.3698656	0.00487864
PLAG1	pleiomorphic adenoma gene 1	-1.5802292	0.00075659
PLEC	plectin	1.42493828	0.00434097
PLEK2	pleckstrin 2	1.33459652	0.00893016
PLIN3	perilipin 3	1.35921699	0.0068674

PMM1	phosphomannomutase 1	1.36014741	0.00562909
PMS2P5	postmeiotic segregation increased 2 pseudogene 5	-1.4492919	0.00737318
PNLIPRP1	pancreatic lipase-related protein 1	-1.4463829	0.00888997
POLR3K	polymerase (RNA) III (DNA directed) polypeptide K, 12.3 kDa	-1.4319111	0.00422938
POTEE	POTE ankyrin domain family, member E	-1.9021442	0.00458446
POU1F1	POU class 1 homeobox 1	1.48075686	0.00342383
PP7080	uncharacterized LOC25845	1.42000423	0.0023527
PPAPDC1B	phosphatidic acid phosphatase type 2 domain containing 1B	1.33097883	0.00854024
PPBPP2	pro-platelet basic protein pseudogene 2	1.59275099	0.00190216
PPDPF	pancreatic progenitor cell differentiation and proliferation factor homolog (zebrafish)	1.58908589	0.00405252
PPIP5K2	diphosphoinositol pentakisphosphate kinase 2	-1.4963792	0.0049785
PPP1R14C	protein phosphatase 1, regulatory (inhibitor) subunit 14C	1.50470617	0.00945794
PPP1R2P9	protein phosphatase 1, regulatory (inhibitor) subunit 2 pseudogene 9	-1.3179065	0.00764159
PRAME	preferentially expressed antigen in melanoma	1.30881928	0.00979463
PRAMEF24P	PRAME family member 24, pseudogene	1.41045915	0.0073604
PRAMEF3	PRAME family member 3	-1.3712788	0.00362342
PRAP1	proline-rich acidic protein 1	1.40158517	0.00210265
PRELP	proline/arginine-rich end leucine-rich repeat protein	-1.2831075	0.00767429
PRH1	proline-rich protein HaeIII subfamily 1	1.35080916	0.00597129
PRICKLE3	prickle homolog 3 (Drosophila)	1.39723334	0.0063454
PRIM2	primase, DNA, polypeptide 2 (58kDa)	-1.3915371	0.005428
PRKAG1	protein kinase, AMP-activated, gamma 1 non-catalytic subunit	-1.2934552	0.00942534
PRKD3	protein kinase D3	-1.4473024	0.00397071
PRM2	protamine 2	1.38121441	0.00428374
PROCA1	protein interacting with cyclin A1	1.54721086	0.00517252
PROM1	prominin 1	-1.5004625	0.00523099
PRORSD1P	prolyl-tRNA synthetase associated domain containing 1, pseudogene	1.29014823	0.00711071
PRR25	proline rich 25	1.46600522	0.00785079
PRTN3	proteinase 3	1.38999153	0.00733455
PS1TP4	HBV preS1-transactivated protein 4	-1.4758125	0.00355916
PSMB6	proteasome (prosome, macropain) subunit, beta type, 6	1.30293645	0.00606505
PTGES	prostaglandin E synthase	1.69442917	0.0026536
PTGES2	prostaglandin E synthase 2	1.2818581	0.00560912
PTPLAD2	protein tyrosine phosphatase-like A domain containing 2	1.3687682	0.00160185
PTPN12	protein tyrosine phosphatase, non-receptor type 12	-1.5686677	0.00901474
PURG	purine-rich element binding protein G	1.30422311	0.00951276

PUS7	pseudouridylate synthase 7 homolog (S. cerevisiae)	-1.6901236	0.00557966
PYDC1	PYD (pyrin domain) containing 1	1.43569886	0.0018279
PYY2	peptide YY, 2 (pseudogene)	1.63744248	0.00317913
RAB14	RAB14, member RAS oncogene family	-1.2915067	0.00888837
RAB19	RAB19, member RAS oncogene family	1.64965203	0.00609239
RAB27A	RAB27A, member RAS oncogene family	1.43318218	0.00360747
RAB42	RAB42, member RAS oncogene family	1.31382673	0.00958148
RAB4A	RAB4A, member RAS oncogene family	-1.3561917	0.00819289
RABL3	RAB, member of RAS oncogene family-like 3	-1.3432457	0.00864677
RAD51	RAD51 homolog (S. cerevisiae)	-1.5156276	0.00651326
RAG2	recombination activating gene 2	-1.354598	0.00289187
RANBP6	RAN binding protein 6	-1.7880422	0.00510804
RAP1A	RAP1A, member of RAS oncogene family	-1.337501	0.00744466
RAP1GAP2	RAP1 GTPase activating protein 2	1.31380105	0.00310572
RARG	retinoic acid receptor, gamma	1.35476562	0.00324248
RBBP6	retinoblastoma binding protein 6	-1.4090555	0.00583859
RBM11	RNA binding motif protein 11	1.52910124	0.00359926
RBM38	RNA binding motif protein 38	1.34503441	0.00363068
RBMS1	RNA binding motif, single stranded interacting protein 1	-1.7175682	0.00951117
RBMY1A1	RNA binding motif protein, Y-linked, family 1, member A1	1.8539554	0.00801024
RBPJ	recombination signal binding protein for immunoglobulin kappa J region	1.41361912	0.00809874
RCN1	reticulocalbin 1, EF-hand calcium binding domain	-1.515104	0.00678496
RD3	retinal degeneration 3	1.30390824	0.0080413
REG1P	regenerating islet-derived 1 pseudogene	1.33162613	0.00792155
REM2	RAS (RAD and GEM)-like GTP binding 2	1.34968204	0.00462349
REN	renin	1.44590412	0.00475158
RET	ret proto-oncogene	1.26585469	0.00713909
RETNLB	resistin like beta	1.29320572	0.00889996
RFC1	replication factor C (activator 1) 1, 145kDa	-7.2552632	0.00527569
RFK	riboflavin kinase	-1.4953205	0.00359816
RFPL3	ret finger protein-like 3	-1.3269688	0.00726742
RFPL4A	ret finger protein-like 4A	-1.476346	0.00791465
RFT1	RFT1 homolog (S. cerevisiae)	1.3952342	0.00287894
RFX1	regulatory factor X, 1 (influences HLA class II expression)	1.58346735	0.00867333
RGCC	regulator of cell cycle	1.47637621	0.00722517
RGPD4	RANBP2-like and GRIP domain containing 4	-1.3038347	0.00378976
RGS14	regulator of G-protein signaling 14	1.35304669	0.00486376
RGS20	regulator of G-protein signaling 20	1.33421915	0.00783578
RGS8	regulator of G-protein signaling 8	-2.0691151	0.00084814
RHBDF2	rhomboid 5 homolog 2 (Drosophila)	1.28935138	0.0056114
RHPN2	rhophilin, Rho GTPase binding protein 2	1.36015241	0.00509987
RIMKLB	ribosomal modification protein rimK-like family member B	-1.4352475	0.00396861
RLTPR	RGD motif, leucine rich repeats,	1.43561157	0.008175

	tropomodulin domain and proline-rich containing		
RNASEH2B	ribonuclease H2, subunit B	-1.4996089	0.00482342
RNF113A	ring finger protein 113A	1.62304463	0.00465788
RNF128	ring finger protein 128, E3 ubiquitin protein ligase	1.32013923	0.00786633
RNF130	ring finger protein 130	-1.3814472	0.00192864
RNF207	ring finger protein 207	2.44355276	0.00106254
RNF39	ring finger protein 39	1.76726332	0.00116754
RNF39	ring finger protein 39	1.3303209	0.0099667
RNF7	ring finger protein 7	1.36223459	0.00819957
RNU105C	RNA, U105C small nucleolar	1.35588643	0.00429825
RNU4-1	RNA, U4 small nuclear 1	1.46850289	0.0012848
RNY4P8	RNA, Ro-associated Y4 pseudogene 8	2.17829883	0.00260147
RP1	retinitis pigmentosa 1 (autosomal dominant)	-1.3788828	0.00821927
RPF2	ribosome production factor 2 homolog (S. cerevisiae)	-1.6113262	0.00715953
RPL13P5	ribosomal protein L13 pseudogene 5	1.59037257	0.00764284
RPL15	ribosomal protein L15	-1.3448405	0.00888981
RPL17	ribosomal protein L17	-1.7196792	0.00735713
RPL21	ribosomal protein L21	-1.5732435	0.00310483
RPL21	ribosomal protein L21	-1.3868593	0.00731918
RPL23AP7	ribosomal protein L23a pseudogene 7	-1.3259939	0.0045243
RPL23AP82	ribosomal protein L23a pseudogene 82	-1.3902583	0.00892742
RPL41	ribosomal protein L41	-1.5784134	0.00762604
RPL7	ribosomal protein L7	-2.1837556	0.005671
RPS12	ribosomal protein S12	1.3201093	0.00680787
RPS18P9	ribosomal protein S18 pseudogene 9	-1.2980697	0.00840981
RPS4Y2	ribosomal protein S4, Y-linked 2	1.42324841	0.00484915
RPS8	ribosomal protein S8	1.41301781	0.00501818
RRAS	related RAS viral (r-ras) oncogene homolog	1.51736198	0.00041811
RSPO2	R-spondin 2	1.42088121	0.00353461
S100A10	S100 calcium binding protein A10	1.36525336	0.00711731
SAA2	serum amyloid A2	-1.3730322	0.00337943
SACS	spastic ataxia of Charlevoix-Saguenay (sacsin)	-1.4809056	0.00269208
SART1	squamous cell carcinoma antigen recognized by T cells	1.37693948	0.00913641
SASS6	spindle assembly 6 homolog (C. elegans)	-2.0661429	0.0019406
SCAND2P	SCAN domain containing 2 pseudogene	1.34497816	0.00408092
SCARNA11	small Cajal body-specific RNA 11	1.31937452	0.00923161
SCARNA4	small Cajal body-specific RNA 4	-1.3060213	0.00902797
SCARNA9L	small Cajal body-specific RNA 9-like	-1.8012527	0.002488
SCRG1	stimulator of chondrogenesis 1	1.31446062	0.0074904
SEC14L2	SEC14-like 2 (S. cerevisiae)	1.35376988	0.00393954
SEC61G	Sec61 gamma subunit	-1.620669	0.00367282
SELT	selenoprotein T	-1.5993055	0.006961
SEMA3E	sema domain, immunoglobulin domain (Ig), short basic domain, secreted, (semaphorin)	1.49366159	0.00925837

	3E		
SEMG2	semenogelin II	1.26795925	0.0091194
SERF2	small EDRK-rich factor 2	1.63545225	0.00244993
SERPINA5	serpin peptidase inhibitor, clade A (alpha-1 antiproteinase, antitrypsin), member 5	1.5675072	0.00092058
SERPINA7	serpin peptidase inhibitor, clade A (alpha-1 antiproteinase, antitrypsin), member 7	1.46611768	0.00587476
SERPINB11	serpin peptidase inhibitor, clade-B (ovalbumin), member 11 (gene/pseudogene)	-1.3802507	0.00305391
SETD9	SET domain containing 9	-1.2850054	0.00818042
SFMBT2	Scm-like with four mbt domains 2	1.34111786	0.00410599
SFRP1	secreted frizzled-related protein 1	1.47104681	0.00056471
SH2D6	SH2 domain containing 6	1.3404933	0.00378496
SH3KBP1	SH3-domain kinase binding protein 1	-1.504401	0.00590555
SHC3	SHC (Src homology 2 domain containing) transforming protein 3	-1.3120228	0.00873297
SHH	sonic hedgehog	1.45585993	0.00656163
SIKE1	suppressor of IKBKE 1	-1.3388263	0.00802696
SIRPG	signal-regulatory protein gamma	-1.5527818	0.00240301
SIX5	SIX homeobox 5	1.3669927	0.00629323
SKA2	spindle and kinetochore associated complex subunit 2	-1.4885727	0.00322029
SKP2	S-phase kinase-associated protein 2, E3 ubiquitin protein ligase	-1.2682071	0.00977842
SLC16A3	solute carrier family 16, member 3 (monocarboxylic acid transporter 4)	-1.4473994	0.00072852
SLC17A9	solute carrier family 17, member 9	1.41618011	0.00778823
SLC24A5	solute carrier family 24, member 5	1.63362584	0.00555133
SLC25A32	solute carrier family 25 (mitochondrial folate carrier) , member 32	-1.2585664	0.00992027
SLC25A35	solute carrier family 25, member 35	1.29761502	0.00853233
SLC2A3	solute carrier family 2 (facilitated glucose transporter), member 3	-1.9464176	9.12E-05
SLC2A6	solute carrier family 2 (facilitated glucose transporter), member 6	1.42111487	0.0038238
SLC30A2	solute carrier family 30 (zinc transporter), member 2	1.47578691	0.00795333
SLC30A7	solute carrier family 30 (zinc transporter), member 7	-1.2903243	0.00902701
SLC34A3	solute carrier family 34 (sodium phosphate), member 3	1.30802151	0.0078593
SLC35B2	solute carrier family 35, member B2	1.48209054	0.00200942
SLC38A9	solute carrier family 38, member 9	-1.5667527	0.00247208
SLC43A2	solute carrier family 43, member 2	1.4601023	0.00096276
SLC45A2	solute carrier family 45, member 2	1.45526895	0.00620841
SLC7A4	solute carrier family 7 (orphan transporter), member 4	1.32406	0.00411189
SLCO6A1	solute carrier organic anion transporter family, member 6A1	1.4338976	0.00891736
SLED1	proteoglycan 3 pseudogene	-1.4765682	0.0061134

SLITRK4	SLIT and NTRK-like family, member 4	1.46804986	0.00967883
SLPI	secretory leukocyte peptidase inhibitor	1.38786264	0.00775953
SMIM11	small integral membrane protein 11	1.76415226	0.0037342
SMIM8	small integral membrane protein 8	1.33019823	0.00658544
SMR3B	submaxillary gland androgen regulated protein 3B	1.62169363	0.0084304
SNORA24	small nucleolar RNA, H/ACA box 24	1.29909036	0.00927678
SNORA40	small nucleolar RNA, H/ACA box 40	-1.5253876	0.00903804
SNORA73A	small nucleolar RNA, H/ACA box 73A	-1.9718843	0.005879
SNORA80B	small nucleolar RNA, H/ACA box 80B	1.427043	0.0070032
SNORD114-26	small nucleolar RNA, C/D box 114-26	1.93853041	0.00066389
SNORD114-6	small nucleolar RNA, C/D box 114-6	1.45298892	0.00789582
SNORD116-21	small nucleolar RNA, C/D box 116-21	-1.8655778	0.00494818
SNORD116-22	small nucleolar RNA, C/D box 116-22	-1.784712	0.00287197
SNORD28	small nucleolar RNA, C/D box 28	-2.5267856	0.00537802
SNORD32A	small nucleolar RNA, C/D box 32A	1.47125976	0.00613069
SNORD47	small nucleolar RNA, C/D box 47	-2.765056	0.00415733
SNORD53	small nucleolar RNA, C/D box 53	1.4480991	0.00110322
SNORD54	small nucleolar RNA, C/D box 54	-1.4986839	0.00867576
SNORD83A	small nucleolar RNA, C/D box 83A	1.41092744	0.00995603
SNORD83B	small nucleolar RNA, C/D box 83B	1.42814595	0.00395453
SNRNP25	small nuclear ribonucleoprotein 25kDa (U11/U12)	-1.4662124	0.00753144
SNRNP35	small nuclear ribonucleoprotein 35kDa (U11/U12)	-1.3707088	0.00700775
SNRPB2	small nuclear ribonucleoprotein polypeptide B	-1.4427687	0.00836926
SNRPE	small nuclear ribonucleoprotein polypeptide E	-1.8486403	0.00662544
SNX14	sorting nexin 14	-1.7011032	0.00815084
SNX29P2	sorting nexin 29 pseudogene 2	-1.4904836	0.00624199
SNX29P2	sorting nexin 29 pseudogene 2	-1.4901777	0.00686328
SOS1	son of sevenless homolog 1 (Drosophila)	-1.3383185	0.00597408
SOX8	SRY (sex determining region Y)-box 8	1.5408732	0.00909677
SPA17	sperm autoantigenic protein 17	-1.9149208	0.00469728
SPAG7	sperm associated antigen 7	1.41376129	0.0007959
SPATA31C1	SPATA31 subfamily C, member 1	-1.4574866	0.00447166
SPATA31C1	SPATA31 subfamily C, member 1	-1.433493	0.00838289
SPC25	SPC25, NDC80 kinetochore complex component, homolog (S. cerevisiae)	-1.8092176	0.00540351
SPDL1	spindle apparatus coiled-coil protein 1	-1.7985188	0.00522621
SPDYE4	speedy homolog E4 (Xenopus laevis)	-1.5408145	0.00103508
SPG21	spastic paraplegia 21 (autosomal recessive, Mast syndrome)	-1.3780475	0.00632969
SPINK9	serine peptidase inhibitor, Kazal type 9	1.47378834	0.00551911
SPINT3	serine peptidase inhibitor, Kunitz type, 3	1.62702221	0.00666778
SQSTM1	sequestosome 1	1.48262713	0.00595664
SRSF10	serine/arginine-rich splicing factor 10	-1.2960057	0.00856662
SSC5D	scavenger receptor cysteine-rich domain containing (5 domains)	1.75015926	0.00285319

SSX4	synovial sarcoma, X breakpoint 4	-2.0625988	0.00783906
ST6GALNAC4	ST6 (alpha-N-acetyl-neuraminyl-2,3-beta-galactosyl-1,3)-N-acetylgalactosaminide alpha-2,6-sialyltransferase 4	1.5746846	0.00314745
ST6GALNAC5	ST6 (alpha-N-acetyl-neuraminyl-2,3-beta-galactosyl-1,3)-N-acetylgalactosaminide alpha-2,6-sialyltransferase 5	1.43032786	0.00815716
STARD10	StAR-related lipid transfer (START) domain containing 10	1.49107363	0.0008294
STK3	serine/threonine kinase 3	-1.3846451	0.0018806
STK33	serine/threonine kinase 33	1.33745193	0.00255048
STMN4	stathmin-like 4	1.29553666	0.00601313
STPG1	sperm-tail PG-rich repeat containing 1	-1.3828801	0.00176296
SUCNR1	succinate receptor 1	1.42610767	0.00813748
SULT1A1	sulfotransferase family, cytosolic, 1A, phenol-preferring, member 1	1.92884127	0.00086885
SUMO1	SMT3 suppressor of mif two 3 homolog 1 (S. cerevisiae)	-2.1213541	0.00208169
SUMO1P3	SUMO1 pseudogene 3	-1.7127261	0.00242378
SUPT7L	suppressor of Ty 7 (S. cerevisiae)-like	-1.4939791	0.00612014
SYNPO	synaptopodin	1.31865022	0.00949869
SYNPO2L	synaptopodin 2-like	1.30501233	0.00372278
SYT5	synaptotagmin V	1.26285709	0.00929044
TAB2	TGF-beta activated kinase 1/MAP3K7 binding protein 2	-1.6617923	0.00011505
TAS2R38	taste receptor, type 2, member 38	-1.3884273	0.00839776
TAS2R45	taste receptor, type 2, member 45	1.61375704	0.00242476
TBC1D21	TBC1 domain family, member 21	1.61730397	0.00050047
TBC1D2B	TBC1 domain family, member 2B	-1.3459318	0.00565615
TBCA	tubulin folding cofactor A	-1.5293579	0.00731506
TBCE	tubulin folding cofactor E	-1.395743	0.0067436
TBX10	T-box 10	1.45086373	0.00772717
TBX2	T-box 2	1.44814986	0.00832134
TBXA2R	thromboxane A2 receptor	1.36438974	0.00528757
TCF7L1	transcription factor 7-like 1 (T-cell specific, HMG-box)	1.30948469	0.00331539
TCTE1	t-complex-associated-testis-expressed 1	1.30828204	0.00585674
TCTE3	t-complex-associated-testis-expressed 3	-1.4036072	0.00385406
TEAD2	TEA domain family member 2	1.37822941	0.00437832
TECTA	tectorin alpha	-1.3435151	0.00492826
TENM3	teneurin transmembrane protein 3	-1.2692944	0.0098579
TERF1	telomeric repeat binding factor (NIMA-interacting) 1	-1.5291117	0.00165372
TET1	tet methylcytosine dioxygenase 1	-1.3351282	0.00833343
TET2	tet methylcytosine dioxygenase 2	-1.486639	0.00318103
TEX30	testis expressed 30	-1.555587	0.0075745
TEX35	testis expressed 35	-1.3467975	0.00319399
TFAP2B	transcription factor AP-2 beta (activating enhancer binding protein 2 beta)	-1.4505479	0.00891461
TFDP2	transcription factor Dp-2 (E2F dimerization	-1.4233727	0.00580582

	partner 2)		
TFE3	transcription factor binding to IGHM enhancer 3	1.29237942	0.0073865
TFPI2	tissue factor pathway inhibitor 2	1.34645625	0.00550187
THAP5	THAP domain containing 5	-1.877235	0.003309
THBS1	thrombospondin 1	-1.5170703	0.00442329
THSD7B	thrombospondin, type I, domain containing 7B	1.30895332	0.00559285
TIMD4	T-cell immunoglobulin and mucin domain containing 4	1.46649258	0.00972391
TLR2	toll-like receptor 2	1.64211905	0.00606061
TMA7	translation machinery associated 7 homolog (S. cerevisiae)	-1.3928834	0.007475
TMC4	transmembrane channel-like 4	1.63392816	0.00217606
TMEM11	transmembrane protein 11	1.4180403	0.00420597
TMEM115	transmembrane protein 115	1.62280795	0.00549541
TMEM171	transmembrane protein 171	1.36285049	0.00855559
TMEM176B	transmembrane protein 176B	1.3930882	0.0014476
TMEM177	transmembrane protein 177	1.98955487	0.00614044
TMEM194A	transmembrane protein 194A	-1.3879439	0.00993134
TMEM204	transmembrane protein 204	1.43163773	0.00888
TMEM209	transmembrane protein 209	-1.4436199	0.00867761
TMEM225	transmembrane protein 225	1.5085165	0.00149641
TMEM243	transmembrane protein 243, mitochondrial	-1.5778268	0.00316234
TMEM254	transmembrane protein 254	-1.8876126	0.00158038
TMEM256	transmembrane protein 256	1.37153361	0.00668196
TMEM5	transmembrane protein 5	-1.2904889	0.00559558
TMOD4	tropomodulin 4 (muscle)	-1.2916232	0.00785128
TMPRSS5	transmembrane protease, serine 5	1.40191466	0.00944558
TMSB15A	thymosin beta 15a	1.49996513	0.00225184
TMSB4X	thymosin beta 4, X-linked	-1.5713019	0.00747261
TMX1	thioredoxin-related transmembrane protein 1	-1.4590948	0.00325232
TNF	tumour necrosis factor	1.82325585	0.00072702
TNF	tumour necrosis factor	1.82325585	0.00072702
TNF	tumour necrosis factor	1.82325585	0.00072702
TNFAIP8L3	tumour necrosis factor, alpha-induced protein 8-like 3	1.35518061	0.00803936
TNFRSF12A	tumour necrosis factor receptor superfamily, member 12A	1.54373297	0.00218968
TNFSF9	tumour necrosis factor (ligand) superfamily, member 9	1.68404209	0.00138506
TOMM20L	translocase of outer mitochondrial membrane 20 homolog (yeast)-like	1.38014745	0.00287146
TOMM22	translocase of outer mitochondrial membrane 22 homolog (yeast)	-1.6306566	0.00988361
TOP1	topoisomerase (DNA) I	-1.6673634	0.00672314
TP53I3	tumour protein p53 inducible protein 3	1.66905815	0.00402356
TP53TG3	TP53 target 3	-1.9318329	8.78E-05
TP53TG3	TP53 target 3	-1.6287949	0.0009121

TP53TG3	TP53 target 3	-1.6287949	0.0009121
TPP1	tripeptidyl peptidase I	1.45244389	0.00641158
TPST1	tyrosylprotein sulfotransferase 1	1.44451452	0.00733
TRA2A	transformer 2 alpha homolog (Drosophila)	-1.5328577	0.00804863
TRAF1	TNF receptor-associated factor 1	1.55324292	0.00061575
TRAF3IP1	TNF receptor-associated factor 3 interacting protein 1	-1.2780399	0.00699101
TREML3P	triggering receptor expressed on myeloid cells-like 3, pseudogene	1.66003587	0.00287719
TRERF1	transcriptional regulating factor 1	-1.3912537	0.00763847
TRIAP1	TP53 regulated inhibitor of apoptosis 1	1.59804827	0.00329516
TRIM16	tripartite motif containing 16	1.41190575	0.00179349
TRIM64	tripartite motif containing 64	-1.3495948	0.00449859
TRIM73	tripartite motif containing 73	1.48081582	0.00483609
TRIM73	tripartite motif containing 73	1.39492202	0.00710298
TRIM9	tripartite motif containing 9	-1.4913546	0.00641607
TRIML1	tripartite motif family-like 1	-1.3552718	0.00509419
TSC22D1	TSC22 domain family, member 1	1.37398511	0.00562496
TSC22D2	TSC22 domain family, member 2	1.38974221	0.00798312
TTC23L	tetratricopeptide repeat domain 23-like	1.37299446	0.00425825
TTC8	tetratricopeptide repeat domain 8	-1.4693999	0.00260307
TTR	transthyretin	1.44484577	0.00976102
TTTY9A	testis-specific transcript, Y-linked 9A (non-protein coding)	1.49342992	0.0078765
TTTY9A	testis-specific transcript, Y-linked 9A (non-protein coding)	1.49342992	0.0078765
TUBA3E	tubulin, alpha 3e	-1.3872365	0.00291494
TUBB7P	tubulin, beta 7, pseudogene	1.35601924	0.00364905
TUBGCP5	tubulin, gamma complex associated protein 5	1.27890851	0.00727431
TXNL4B	thioredoxin-like 4B	-1.6051395	0.00779487
TXNRD2	thioredoxin reductase 2	1.34274581	0.00953194
U2AF1L4	U2 small nuclear RNA auxiliary factor 1-like 4	1.34505745	0.00819291
UAP1L1	UDP-N-acteylglucosamine pyrophosphorylase 1-like 1	1.34907951	0.00799782
UBE2D2	ubiquitin-conjugating enzyme E2D 2	-1.3275287	0.00910058
UBE2E2	ubiquitin-conjugating enzyme E2E 2	-1.3276831	0.00839816
UBE2G1	ubiquitin-conjugating enzyme E2G 1	-1.4353923	0.00913833
UBE2V2	ubiquitin-conjugating enzyme E2 variant 2	-1.3019873	0.00461406
UCA1	urothelial cancer associated 1 (non-protein coding)	-1.4823698	0.00224772
UGP2	UDP-glucose pyrophosphorylase 2	-1.4987398	0.00559773
UPF2	UPF2 regulator of nonsense transcripts homolog (yeast)	-1.2824097	0.00870346
UQCR11	ubiquinol-cytochrome c reductase, complex III subunit XI	-1.3592465	0.00862442
UQCRB	ubiquinol-cytochrome c reductase binding protein	1.34193808	0.00568602
UQCRQ	ubiquinol-cytochrome c reductase, complex	-1.3673093	0.00930787

	III subunit VII, 9.5kDa		
USP14	ubiquitin specific peptidase 14 (tRNA-guanine transglycosylase)	-1.579024	0.00494022
USP17L2	ubiquitin specific peptidase 17-like family member 2	-2.2207348	0.00740727
USP17L2	ubiquitin specific peptidase 17-like family member 2	-2.2207348	0.00740727
USP45	ubiquitin specific peptidase 45	-1.3385195	0.00808387
UTP20	UTP20, small subunit (SSU) processome component, homolog (yeast)	-1.3717251	0.00789091
UXT	ubiquitously-expressed, prefoldin-like chaperone	1.33168676	0.00594137
VASN	vasorin	1.39630102	0.00794552
VASP	vasodilator-stimulated phosphoprotein	1.50416798	0.00804549
VEGFA	vascular endothelial growth factor A	1.24902079	0.00913782
VPS18	vacuolar protein sorting 18 homolog (S. cerevisiae)	1.38912296	0.005355
VSX2	visual system homeobox 2	1.59156912	0.00909056
VWA5B1	von Willebrand factor A domain containing 5B1	1.38829849	0.0048921
WASF3	WAS protein family, member 3	-1.5654037	0.00093818
WASH1	WAS protein family homolog 1	1.34409994	0.00950598
WBSCR27	Williams Beuren syndrome chromosome region 27	1.41031331	0.0094696
WDR35	WD repeat domain 35	-1.4454092	0.00661542
WDR63	WD repeat domain 63	1.68327869	0.00211679
WDSUB1	WD repeat, sterile alpha motif and U-box domain containing 1	-1.3518602	0.00295526
WNT6	wingless-type MMTV integration site family, member 6	1.40519357	0.00865265
WSB1	WD repeat and SOCS box containing 1	1.4090423	0.00720225
XAF1	XIAP associated factor 1	1.33882372	0.00468846
XAGE2	X antigen family, member 2	-1.6098678	0.0023911
XAGE2	X antigen family, member 2	-1.6098678	0.0023911
XAGE5	X antigen family, member 5	-1.5601156	0.00286432
XCL1	chemokine (C motif) ligand 1	-1.284046	0.00996633
XPNPEP1	X-prolyl aminopeptidase (aminopeptidase P) 1, soluble	1.30114391	0.00849348
XRCC2	X-ray repair complementing defective repair in Chinese hamster cells 2	-1.8648728	0.00176591
YAE1D1	Yae1 domain containing 1	-2.1929167	0.00526492
YEATS4	YEATS domain containing 4	-1.8012026	0.00739336
YY2	YY2 transcription factor	1.42602643	0.00714733
ZBED3	zinc finger, BED-type containing 3	1.57525522	0.00033457
ZBTB32	zinc finger and BTB domain containing 32	1.56160979	0.00897679
ZBTB33	zinc finger and BTB domain containing 33	-1.8679142	6.00E-05
ZBTB4	zinc finger and BTB domain containing 4	1.40499132	0.00214602
ZFAND2B	zinc finger, AN1-type domain 2B	1.46027419	0.00245805
ZFAND5	zinc finger, AN1-type domain 5	1.33062735	0.00497071
ZFP30	ZFP30 zinc finger protein	-1.4637022	0.00561004

ZFP36	ZFP36 ring finger protein	1.75330753	0.00087569
ZFP37	ZFP37 zinc finger protein	-1.5327128	0.0059632
ZNF100	zinc finger protein 100	-1.3551788	0.00959488
ZNF219	zinc finger protein 219	1.44279837	0.00411836
ZNF253	zinc finger protein 253	-1.8274146	0.00239955
ZNF257	zinc finger protein 257	-1.8850459	8.25E-05
ZNF29P	zinc finger protein 29, pseudogene	1.31390376	0.00674269
ZNF320	zinc finger protein 320	-1.6288505	0.00370094
ZNF385C	zinc finger protein 385C	1.39273293	0.00596903
ZNF428	zinc finger protein 428	1.50080629	0.00917844
ZNF474	zinc finger protein 474	1.76398737	0.00196361
ZNF493	zinc finger protein 493	-1.3924263	0.00974746
ZNF516	zinc finger protein 516	1.33961751	0.00487458
ZNF558	zinc finger protein 558	-1.4043754	0.00708913
ZNF585B	zinc finger protein 585B	-1.4414827	0.00149728
ZNF587	zinc finger protein 587	1.3198051	0.00575996
ZNF599	zinc finger protein 599	1.26968155	0.00941448
ZNF610	zinc finger protein 610	-1.5649062	0.00327722
ZNF618	zinc finger protein 618	1.41839742	0.0089143
ZNF624	zinc finger protein 624	1.37589647	0.0092119
ZNF69	zinc finger protein 69	-1.4420076	0.00441717
ZNF695	zinc finger protein 695	-1.3716037	0.00348576
ZNF724P	zinc finger protein 724, pseudogene	-2.1577577	9.39E-05
ZNF777	zinc finger protein 777	1.66307478	0.00805479
ZNF780B	zinc finger protein 780B	-1.6066267	0.00909869
ZNF808	zinc finger protein 808	-1.308982	0.006736
ZNF93	zinc finger protein 93	-1.3084894	0.00987301
ZNF98	zinc finger protein 98	-1.6267553	0.00384123
ZSCAN2	zinc finger and SCAN domain containing 2	1.26545921	0.00750236

Appendix 4

Dysregulated-LF_TatvsBme proteins

Uniprot accession #	Symbol	Entrez gene name	Log2 Ratio	p-value
B0UX83			0.082	
B1AKZ5	PEA15	phosphoprotein enriched in astrocytes 15	-0.428	0.045443598
B1ANR0	PABPC4	poly(A) binding protein, cytoplasmic 4 (inducible form)	-0.514	0.001105763
B4DGU4	CTNNB1	catenin (cadherin-associated protein), beta 1, 88kDa	-0.554	0.01856624
B4DJP7	SNRPD3	small nuclear ribonucleoprotein D3 polypeptide 18kDa	0.593	0.025934802
B4DT77	ANXA7	annexin A7	0.230	0.019274764
B4DVY1	EIF3D	eukaryotic translation initiation factor 3, subunit D	0.363	0.019730813
B7Z254	PDIA6	protein disulfide isomerase family A, member 6	0.569	3.85E-05
B7Z972	PCMT1	protein-L-isoaspartate (D-aspartate) O-methyltransferase	0.245	0.005413453
B7Z9I1	ACADM	acyl-CoA dehydrogenase, C-4 to C-12 straight chain	-0.230	0.040270643
C9J2Y9	POLR2B	polymerase (RNA) II (DNA directed) polypeptide B, 140kDa	0.059	0.037345812
C9JAZ1	MTX2	metaxin 2	0.970	0.012058425
C9JQV0	C7orf50	chromosome 7 open reading frame 50	0.354	0.019054514
E5RIW3	TBCA	tubulin folding cofactor A	-0.289	0.000376615
E7EQ72	TMED2	transmembrane emp24 domain trafficking protein 2	-0.689	0.001651738
E7ESY4	MTA1	metastasis associated 1	0.072	0.003827555
E9PC52	RBBP7	retinoblastoma binding protein 7	-0.287	0.022834008
E9PID8	CSTF2	cleavage stimulation factor, 3' pre-RNA, subunit 2, 64kDa	-0.472	0.000723888
F5H2Q7			-0.325	0.023732276
F5H669	CPSF7	cleavage and polyadenylation specific factor 7, 59kDa	-0.616	0.018739581
F5H8E5			-0.405	0.008226516
F8VQE1	LIMA1	LIM domain and actin binding 1	-0.497	0.001412543
F8W7S5	RRBP1	ribosome binding protein 1	-0.330	0.014946706
F8WBH3			-0.467	0.035213753
G5EA52			-0.183	0.001501007
G8JLB2	XPNPEP1	X-prolyl aminopeptidase (aminopeptidase P) 1, soluble	0.224	0.01806039
H0YNG3	SEC11A	SEC11 homolog A, signal peptidase complex subunit	0.475	0.005757513
H7BXW3			0.150	0.005826958
J3KNF8	CYB5B	cytochrome b5 type B (outer mitochondrial membrane)	-0.382	0.018389348

J3KNU8	ALDH6A1	aldehyde dehydrogenase 6 family, member A1	0.308	0.016323129
J3KSI4	MPDU1	mannose-P-dolichol utilization defect 1	0.158	0.038081134
J3KTL7	CDK11B	cyclin-dependent kinase 11B	0.441	0.012701995
J3QLE5	SNRPN	small nuclear ribonucleoprotein polypeptide N	0.181	0.043153114
J3QQT2	RPL17	ribosomal protein L17	0.256	0.001907946
M0QX07	BABAM1	BRISC and BRCA1 A complex member 1	-1.173	0.012172722
M0R366	FSD1	fibronectin type III and SPRY domain containing 1	-0.847	0.00106746
O00159-2	MYO1C	myosin IC	0.649	0.029072883
O00170	AIP	aryl hydrocarbon receptor interacting protein	-0.324	0.032252991
O00231	PSMD11	proteasome (prosome, macropain) 26S subunit, non-ATPase, 11	0.210	0.009084319
O00267-2	SUPT5H	suppressor of Ty 5 homolog (S. cerevisiae)	-0.389	0.028515076
O00303	EIF3F	eukaryotic translation initiation factor 3, subunit F	0.368	0.006535552
O00425	IGF2BP3	insulin-like growth factor 2 mRNA binding protein 3	0.082	1.45E-05
O00429	DNM1L	dynamin 1-like	0.395	0.024417694
O00505	KPNA3	karyopherin alpha 3 (importin alpha 4)	0.200	0.006959562
O00746	NME4	NME/NM23 nucleoside diphosphate kinase 4	-0.487	0.011667398
O14617	AP3D1	adaptor-related protein complex 3, delta 1 subunit	-0.642	0.027695712
O14737	PDCD5	programmed cell death 5	-0.412	0.032949515
O14745	SLC9A3R1	solute carrier family 9, subfamily A (NHE3, cation proton antiporter 3), member 3 regulator 1	-0.556	0.000603427
O15020-2	SPTBN2	spectrin, beta, non-erythrocytic 2	-0.602	0.002623003
O15145	ARPC3	actin related protein 2/3 complex, subunit 3, 21kDa	-0.410	0.011093358
O15305	PMM2	phosphomannomutase 2	-0.290	0.014129737
O15372	EIF3H	eukaryotic translation initiation factor 3, subunit H	-0.424	0.032432987
O15498	YKT6	YKT6 v-SNARE homolog (S. cerevisiae)	0.096	0.034785993
O43175	PHGDH	phosphoglycerate dehydrogenase	0.147	0.047639549
O43583	DENR	density-regulated protein	-0.771	0.029782219
O43670-2	ZNF207	zinc finger protein 207	-0.627	3.91E-05
O43681	ASNA1	arsA arsenite transporter, ATP-binding, homolog 1 (bacterial)	0.359	6.02E-05
O43719	HTATSF1	HIV-1 Tat specific factor 1	-0.557	0.00389311

O43765	SGTA	small glutamine-rich tetratricopeptide repeat (TPR)-containing, alpha	-0.502	0.001057483
O43776	NARS	asparaginyl-tRNA synthetase	0.269	0.034875669
O43795-2	MYO1B	myosin IB	0.142	0.003765677
O43813	LANCL1	LanC lantibiotic synthetase component C-like 1 (bacterial)	-0.256	0.011796272
O60264	SMARCA5	SWI/SNF related, matrix associated, actin dependent regulator of chromatin, subfamily a, member 5	-0.391	0.000584404
O60493	SNX3	sorting nexin 3	-0.436	0.048396362
O60762	DPM1	dolichyl-phosphate mannosyltransferase polypeptide 1, catalytic subunit	0.408	0.033786561
O75340	PDCD6	programmed cell death 6	0.828	4.79E-05
O75380	NDUFS6	NADH dehydrogenase (ubiquinone) Fe-S protein 6, 13kDa (NADH-coenzyme Q reductase)	-0.329	0.042182932
O75475	PSIP1	PC4 and SFRS1 interacting protein 1	-0.376	0.002330608
O75531	BANF1	barrier to autointegration factor 1	0.531	0.001832361
O75534-2	CSDE1	cold shock domain containing E1, RNA-binding	-0.396	0.021190425
O75947	ATP5H	ATP synthase, H+ transporting, mitochondrial Fo complex, subunit d	-0.367	0.00755882
O76003	GLRX3	glutaredoxin 3	0.453	0.00138796
O76031	CLPX	caseinolytic mitochondrial matrix peptidase chaperone subunit	0.158	0.043543373
O94826	TOMM70A	translocase of outer mitochondrial membrane 70 homolog A (S. cerevisiae)	-0.219	0.037064899
O95202	LETM1	leucine zipper-EF-hand containing transmembrane protein 1	0.222	0.001029447
O95336	PGLS	6-phosphogluconolactonase	0.316	1.34E-06
O95777	LSM8	LSM8 homolog, U6 small nuclear RNA associated	-0.471	0.048219459
O96019	ACTL6A	actin-like 6A	-0.308	0.016686857
P00403	MT-CO2	cytochrome c oxidase subunit II	0.654	0.001062871
P00491	PNP	purine nucleoside phosphorylase	-0.796	0.005539035
P00568	AK1	adenylate kinase 1	-0.744	0.009042188
P02786	TFRC	transferrin receptor	0.166	0.012157298
P04632	CAPNS1	calpain, small subunit 1	-0.392	0.009963709
P04843	RPN1	ribophorin I	0.129	0.01575029
P05386	RPLP1	ribosomal protein, large, P1	0.840	0.046852382
P05556	ITGB1	integrin, beta 1 (fibronectin receptor, beta polypeptide,	-0.272	0.045382388

		antigen CD29 includes MDF2, MSK12)		
P06493	CDK1	cyclin-dependent kinase 1	-0.319	0.02122772
P06576	ATP5B	ATP synthase, H+ transporting, mitochondrial F1 complex, beta polypeptide	0.117	0.013590792
P06730	EIF4E	eukaryotic translation initiation factor 4E	-0.287	0.008713543
P07814	EPRS	glutamyl-prolyl-tRNA synthetase	-0.266	0.029286659
P07900	HSP90AA1	heat shock protein 90kDa alpha (cytosolic), class A member 1	0.235	0.044852392
P08107			0.269	0.002719511
P08238	HSP90AB1	heat shock protein 90kDa alpha (cytosolic), class B member 1	0.160	0.01038445
P08240-2	SRPR	signal recognition particle receptor (docking protein)	0.278	0.039556951
P08670	VIM	vimentin	0.103	0.004665877
P08754	GNAI3	guanine nucleotide binding protein (G protein), alpha inhibiting activity polypeptide 3	0.297	0.01107521
P08758	ANXA5	annexin A5	0.293	0.02942688
P09104	ENO2	enolase 2 (gamma, neuronal)	-0.330	0.005592507
P09211	GSTP1	glutathione S-transferase pi 1	0.340	0.003381664
P09382	LGALS1	lectin, galactoside-binding, soluble, 1	-0.433	0.004883304
P09429	HMGB1	high mobility group box 1	-0.299	0.025815199
P09543-2	CNP	2',3'-cyclic nucleotide 3' phosphodiesterase	0.245	0.002577887
P09661	SNRPA1	small nuclear ribonucleoprotein polypeptide A'	0.123	0.010740883
P0CW22	RPS17	ribosomal protein S17	0.151	0.02656002
P10155-3	TROVE2	TROVE domain family, member 2	-0.506	0.000505333
P11021	HSPA5	heat shock 70kDa protein 5 (glucose-regulated protein, 78kDa)	0.071	0.043558806
P11172	UMPS	uridine monophosphate synthetase	0.374	0.007431418
P11279	LAMP1	lysosomal-associated membrane protein 1	-0.467	0.004927886
P12081-4	HARS	histidyl-tRNA synthetase	0.201	0.013696079
P12235	SLC25A4	solute carrier family 25 (mitochondrial carrier; adenine nucleotide translocator), member 4	0.771	0.000115263
P12277	CKB	creatine kinase, brain	0.544	0.00286631
P13010	XRCC5	X-ray repair complementing defective repair in Chinese hamster cells 5 (double-strand-break rejoining)	0.248	0.001809585
P13693	TPT1	tumour protein, translationally-controlled 1	-0.499	0.017251213

P14174	MIF	macrophage migration inhibitory factor (glycosylation-inhibiting factor)	0.443	0.003671885
P14324-2	FDPS	farnesyl diphosphate synthase	0.535	0.039145724
P14406	COX7A2	cytochrome c oxidase subunit VIIa polypeptide 2 (liver)	0.563	0.033127375
P14618	PKM	pyruvate kinase, muscle	0.804	0.039669197
P16152	CBR1	carbonyl reductase 1	0.457	0.038822816
P16401	HIST1H1B	histone cluster 1, H1b	-0.242	0.003551272
P16402	HIST1H1D	histone cluster 1, H1d	-0.139	0.001206152
P16403	HIST1H1C	histone cluster 1, H1c	-0.449	0.040337038
P16435	POR	P450 (cytochrome) oxidoreductase	0.469	0.000543216
P17174	GOT1	glutamic-oxaloacetic transaminase 1, soluble	0.102	0.032003235
P18085	ARF4	ADP-ribosylation factor 4	0.188	0.005527608
P18615	NELFE	negative elongation factor complex member E	-0.340	0.017185736
P20700	LMNB1	lamin B1	-0.309	0.031811377
P21283	ATP6V1C1	ATPase, H+ transporting, lysosomal 42kDa, V1 subunit C1	0.309	0.049697488
P23381	WARS	tryptophanyl-tRNA synthetase	0.242	0.034644942
P23588	EIF4B	eukaryotic translation initiation factor 4B	-0.422	0.006041669
P24534	EEF1B2	eukaryotic translation elongation factor 1 beta 2	-0.394	0.038391208
P24539	ATP5F1	ATP synthase, H+ transporting, mitochondrial Fo complex, subunit B1	-0.986	0.002829824
P24752	ACAT1	acetyl-CoA acetyltransferase 1	0.237	0.025930951
P24928	POLR2A	polymerase (RNA) II (DNA directed) polypeptide A, 220kDa	0.563	0.023544105
P25398	RPS12	ribosomal protein S12	-0.293	0.001422152
P25685	DNAJB1	DnaJ (Hsp40) homolog, subfamily B, member 1	0.455	0.000284744
P25787	PSMA2	proteasome (prosome, macropain) subunit, alpha type, 2	0.515	0.010493039
P26368-2	U2AF2	U2 small nuclear RNA auxiliary factor 2	0.315	0.015725768
P27348	YWHAQ	tyrosine 3-monooxygenase/tryptophan 5-monooxygenase activation protein, theta	-0.388	0.001196978
P27695	APEX1	APEX nuclease (multifunctional DNA repair enzyme) 1	-0.314	0.043311557
P27824	CANX	calnexin	0.253	0.003954031
P28072	PSMB6	proteasome (prosome, macropain) subunit, beta type, 6	-0.488	0.001224471
P28838-2	LAP3	leucine aminopeptidase 3	0.095	0.001129042
P29373	CRABP2	cellular retinoic acid binding protein 2	0.539	0.008597304

P29401	TKT	transketolase	0.142	0.000387931
P30041	PRDX6	peroxiredoxin 6	0.089	0.000261694
P30044-2	PRDX5	peroxiredoxin 5	0.334	0.003820306
P30520	ADSS	adenylosuccinate synthase	0.107	0.041450692
P31150	GDI1	GDP dissociation inhibitor 1	0.109	0.007036114
P31323	PRKAR2B	protein kinase, cAMP-dependent, regulatory, type II, beta	0.983	0.005932705
P31939	ATIC	5-aminoimidazole-4-carboxamide ribonucleotide formyltransferase/IMP cyclohydrolase	0.050	0.003169244
P31942-2	HNRNPH3	heterogeneous nuclear ribonucleoprotein H3 (2H9)	0.195	0.008746671
P31946-2	YWHAB	tyrosine 3-monooxygenase/tryptophan 5-monooxygenase activation protein, beta	-0.517	0.015157519
P32969	RPL9	ribosomal protein L9	0.529	0.000139254
P34897-3	SHMT2	serine hydroxymethyltransferase 2 (mitochondrial)	0.123	0.006594307
P35232	PHB	prohibitin	0.272	0.004338721
P35244	RPA3	replication protein A3, 14kDa	0.556	0.000359465
P35269	GTF2F1	general transcription factor IIF, polypeptide 1, 74kDa	-0.231	0.036534819
P35520	CBS/CBSL	cystathionine-beta-synthase	-0.194	0.030952861
P35637-2	FUS	FUS RNA binding protein	-0.547	0.004726813
P36404	ARL2	ADP-ribosylation factor-like 2	0.086	0.0329326
P36405	ARL3	ADP-ribosylation factor-like 3	0.880	1.52E-06
P39656	DDOST	dolichyl-diphosphooligosaccharide--protein glycosyltransferase subunit (non-catalytic)	0.211	0.023055399
P39748	FEN1	flap structure-specific endonuclease 1	-0.245	0.005524999
P42167	TMPO	thymopoietin	0.699	0.000369519
P43487	RANBP1	RAN binding protein 1	-0.332	0.03233675
P43490	NAMPT	nicotinamide phosphoribosyltransferase	0.154	0.023995371
P45974-2	USP5	ubiquitin specific peptidase 5 (isopeptidase T)	0.298	0.000881193
P46087	NOP2	NOP2 nucleolar protein	0.376	0.005212805
P46778	RPL21	ribosomal protein L21	0.379	0.006529396
P46781	RPS9	ribosomal protein S9	0.111	0.001643832
P47813	EIF1AX	eukaryotic translation initiation factor 1A, X-linked	-0.411	0.011437671
P48147	PREP	prolyl endopeptidase	0.301	0.001508054
P48637	GSS	glutathione synthetase	-0.364	0.024064817
P48643	CCT5	chaperonin containing TCP1, subunit 5 (epsilon)	0.193	0.036522519
P49006	MARCKSL1	MARCKS-like 1	-0.204	0.018781147
P49189	ALDH9A1	aldehyde dehydrogenase 9	-0.240	0.046929468

		family, member A1		
P49321	NASP	nuclear autoantigenic sperm protein (histone-binding)	-0.236	0.008490313
P49327	FASN	fatty acid synthase	0.169	0.003200218
P49419-2	ALDH7A1	aldehyde dehydrogenase 7 family, member A1	0.209	0.000599184
P49720	PSMB3	proteasome (prosome, macropain) subunit, beta type, 3	0.246	0.000396092
P49770	EIF2B2	eukaryotic translation initiation factor 2B, subunit 2 beta, 39kDa	0.368	0.048224022
P49773	HINT1	histidine triad nucleotide binding protein 1	-0.314	0.017456701
P50395	GDI2	GDP dissociation inhibitor 2	0.159	0.00898103
P50416-2	CPT1A	carnitine palmitoyltransferase 1A (liver)	-0.404	0.00255797
P50454	SERPINH1	serpin peptidase inhibitor, clade H (heat shock protein 47), member 1, (collagen binding protein 1)	0.212	0.001632399
P51571	SSR4	signal sequence receptor, delta	0.424	0.005549936
P51572	BCAP31	B-cell receptor-associated protein 31	-1.069	0.010820127
P51858	HDGF	hepatoma-derived growth factor	-0.470	0.004108056
P52948-6	NUP98	nucleoporin 98kDa	-0.354	0.003666415
P53396	ACLY	ATP citrate lyase	0.152	0.00549645
P53990-2	IST1	increased sodium tolerance 1 homolog (yeast)	-0.873	0.004194261
P54136	RARS	arginyl-tRNA synthetase	0.106	0.033211941
P54725-2	RAD23A	RAD23 homolog A, nucleotide excision repair protein	-0.407	0.010940519
P54727	RAD23B	RAD23 homolog B, nucleotide excision repair protein	-0.289	0.010281498
P55010	EIF5	eukaryotic translation initiation factor 5	0.314	0.000261544
P55072	VCP	valosin containing protein	0.116	0.007046351
P56134-3	ATP5J2	ATP synthase, H+ transporting, mitochondrial Fo complex, subunit F2	0.566	0.013201036
P56192	MARS	methionyl-tRNA synthetase	0.298	0.005426432
P57088	TMEM33	transmembrane protein 33	0.166	0.030099849
P59998	ARPC4	actin related protein 2/3 complex, subunit 4, 20kDa	0.390	0.000254598
P60174-1	TPI1	triosephosphate isomerase 1	0.257	0.000220944
P60900	PSMA6	proteasome (prosome, macropain) subunit, alpha type, 6	0.265	0.035478676
P60953	CDC42	cell division cycle 42	0.805	0.031915193
P60981	DSTN	destrin (actin depolymerizing factor)	0.129	0.031555097
P61457	PCBD1	pterin-4 alpha-carbinolamine dehydratase/dimerization cofactor of hepatocyte nuclear	0.612	0.002354626

		factor 1 alpha		
P61586	RHOA	ras homolog family member A	1.049	0.022155991
P61964	WDR5	WD repeat domain 5	-0.650	0.032739535
P61970	NUTF2	nuclear transport factor 2	-0.252	0.039000347
P61978-2	HNRNPK	heterogeneous nuclear ribonucleoprotein K	0.715	0.00051122
P62158			-0.506	0.023916164
P62258	YWHAE	tyrosine 3-monooxygenase/tryptophan 5-monooxygenase activation protein, epsilon	-0.355	0.018444203
P62277	RPS13	ribosomal protein S13	0.629	0.003166966
P62304	SNRPE	small nuclear ribonucleoprotein polypeptide E	0.986	0.041112866
P62333	PSMC6	proteasome (prosome, macropain) 26S subunit, ATPase, 6	0.132	0.021977644
P62805			0.442	0.000401869
P62851	RPS25	ribosomal protein S25	0.091	0.036012958
P62854	RPS26	ribosomal protein S26	0.425	0.02948157
P62906	RPL10A	ribosomal protein L10a	0.328	0.003436465
P62937	PPIA	peptidylprolyl isomerase A (cyclophilin A)	1.367	0.009318894
P62993	GRB2	growth factor receptor-bound protein 2	-0.217	0.041832128
P63151	PPP2R2A	protein phosphatase 2, regulatory subunit B, alpha	-0.452	0.036236488
P63173	RPL38	ribosomal protein L38	0.635	0.006371542
P67809	YBX1	Y box binding protein 1	-0.618	0.004101063
P67936	TPM4	tropomyosin 4	-0.654	0.014615316
P68036	UBE2L3	ubiquitin-conjugating enzyme E2L 3	-0.770	0.004876744
P68104	EEF1A1	eukaryotic translation elongation factor 1 alpha 1	0.520	0.035438597
P78344	EIF4G2	eukaryotic translation initiation factor 4 gamma, 2	0.363	0.010928649
P78347-2	GTF2I	general transcription factor IIi	-0.338	0.015313238
P78417	GSTO1	glutathione S-transferase omega 1	0.147	0.002584711
P80723	BASP1	brain abundant, membrane attached signal protein 1	-0.169	0.001525792
P84090	ERH	enhancer of rudimentary homolog (Drosophila)	-0.623	0.000601542
Q00534	CDK6	cyclin-dependent kinase 6	0.190	0.005641734
Q01105-2	SET	SET nuclear proto-oncogene	-0.221	0.020957902
Q01581	HMGCS1	3-hydroxy-3-methylglutaryl-CoA synthase 1 (soluble)	0.556	0.022832346
Q02880-2	TOP2B	topoisomerase (DNA) II beta 180kDa	0.175	0.041260933
Q04837	SSBP1	single-stranded DNA binding protein 1, mitochondrial	-0.237	0.027445965

Q04917	YWHAH	tyrosine 3-monooxygenase/tryptophan 5-monooxygenase activation protein, eta	-0.471	0.001324838
Q06124-2	PTPN11	protein tyrosine phosphatase, non-receptor type 11	-0.548	0.049978081
Q06210-2	GFPT1	glutamine--fructose-6-phosphate transaminase 1	-0.502	0.049062088
Q06830	PRDX1	peroxiredoxin 1	-0.291	0.04197834
Q07021	C1QBP	complement component 1, q subcomponent binding protein	1.157	0.003213479
Q07866-3	KLC1	kinesin light chain 1	-0.347	0.035934002
Q07955	SRSF1	serine/arginine-rich splicing factor 1	-0.431	8.94E-05
Q08211	DHX9	DEAH (Asp-Glu-Ala-His) box helicase 9	0.070	0.005106558
Q09028-3	RBBP4	retinoblastoma binding protein 4	-0.280	0.030264444
Q12765	SCRN1	secernin 1	-0.236	0.044460004
Q12792	TWF1	twinfilin actin binding protein 1	-0.497	0.037497558
Q12905	ILF2	interleukin enhancer binding factor 2	0.288	0.020516523
Q13126	MTAP	methylthioadenosine phosphorylase	-0.474	0.016168697
Q13185	CBX3	chromobox homolog 3	-0.548	0.012643541
Q13242	SRSF9	serine/arginine-rich splicing factor 9	-0.297	0.002083675
Q13247-3	SRSF6	serine/arginine-rich splicing factor 6	-0.340	0.015129061
Q13283	G3BP1	GTPase activating protein (SH3 domain) binding protein 1	0.451	0.000636466
Q13347	EIF3I	eukaryotic translation initiation factor 3, subunit I	-0.357	0.003122779
Q13409-3	DYNC1I2	dynein, cytoplasmic 1, intermediate chain 2	-0.713	8.36E-05
Q13442	PDAP1	PDGFA associated protein 1	-0.283	0.015009881
Q13573	SNW1	SNW domain containing 1	-0.419	0.027973685
Q13620-3	CUL4B	cullin 4B	-0.348	0.044921914
Q13630	TSTA3	tissue specific transplantation antigen P35B	-0.391	0.039148057
Q14247	CTTN	cortactin	-0.503	0.021203064
Q14699	RFTN1	raftlin, lipid raft linker 1	-0.419	0.015627758
Q14789	GOLGB1	golgin B1	0.345	0.046124634
Q15005	SPCS2	signal peptidase complex subunit 2	-0.309	0.016031277
Q15102	PAFAH1B3	platelet-activating factor acetylhydrolase 1b, catalytic subunit 3 (29kDa)	0.120	0.04812527
Q15435	PPP1R7	protein phosphatase 1, regulatory subunit 7	0.283	0.004758079
Q15437	SEC23B	Sec23 homolog B (S. cerevisiae)	-0.565	5.44E-05
Q15631	TSN	translin	0.146	0.041458753

Q15785	TOMM34	translocase of outer mitochondrial membrane 34	-0.707	0.01154691
Q16527	CSRP2	cysteine and glycine-rich protein 2	-0.492	0.010790443
Q16531	DDB1	damage-specific DNA binding protein 1, 127kDa	0.182	0.01691446
Q16629-3	SRSF7	serine/arginine-rich splicing factor 7	-0.542	0.000607116
Q16643	DBN1	drebrin 1	-0.426	0.009415594
Q16777	HIST2H2AC	histone cluster 2, H2ac	2.064	0.049313512
Q16836	HADH	hydroxyacyl-CoA dehydrogenase	-0.707	0.047898125
Q16850	CYP51A1	cytochrome P450, family 51, subfamily A, polypeptide 1	0.218	0.027623103
Q29RF7	PDS5A	PDS5 cohesin associated factor A	-0.352	0.03846805
Q2TAY7	SMU1	smu-1 suppressor of mec-8 and unc-52 homolog (C. elegans)	-0.396	0.027164747
Q3ZCM7	TUBB8	tubulin, beta 8 class VIII	1.174	0.035422051
Q4G0J3	LARP7	La ribonucleoprotein domain family, member 7	-0.318	0.029982683
Q58FF8	HSP90AB2P	heat shock protein 90kDa alpha (cytosolic), class B member 2, pseudogene	4.015	0.011673008
Q5JP53	TUBB	tubulin, beta class I	1.153	0.004274
Q5JRA6-2	MIA3	melanoma inhibitory activity family, member 3	-0.774	0.034839608
Q5VW32	BROX	BRO1 domain and CAAX motif containing	0.159	0.01279061
Q5VYK3	KIAA0368	KIAA0368	-0.733	0.0005437
Q6NUK1-2	SLC25A24	solute carrier family 25 (mitochondrial carrier; phosphate carrier), member 24	0.546	6.60E-05
Q6UXN9	WDR82	WD repeat domain 82	-0.772	0.017572548
Q7L2H7	EIF3M	eukaryotic translation initiation factor 3, subunit M	0.426	0.013155595
Q7RTV0	PHF5A	PHD finger protein 5A	-0.629	0.000657565
Q7Z2T5	TRMT1L	tRNA methyltransferase 1 homolog (S. cerevisiae)-like	-0.509	0.014048953
Q86U42-2	PABPN1	poly(A) binding protein, nuclear 1	0.407	0.01029432
Q86U44	METTL3	methyltransferase like 3	-0.442	0.025804632
Q8IV08	PLD3	phospholipase D family, member 3	0.098	0.009767724
Q8IY81	FTSJ3	FtsJ homolog 3 (E. coli)	0.362	0.00079843
Q8N1F7	NUP93	nucleoporin 93kDa	-0.292	0.001125018
Q8NBS9-2	TXNDC5	thioredoxin domain containing 5 (endoplasmic reticulum)	-0.312	0.018531569
Q8NE71-2	ABCF1	ATP-binding cassette, sub-family F (GCN20), member 1	-0.329	0.004131324
Q8NFH4	NUP37	nucleoporin 37kDa	-0.509	0.035242145
Q8NI36	WDR36	WD repeat domain 36	-0.277	7.63E-06
Q8TEA8	DTD1	D-tyrosyl-tRNA deacylase 1	-0.605	0.045645079
Q8TEM1	NUP210	nucleoporin 210kDa	0.797	0.020627459

Q8TEX9	IPO4	importin 4	0.550	0.013265677
Q8WVC2	RPS21	ribosomal protein S21	-0.906	1.16E-06
Q8WW12	PCNP	PEST proteolytic signal containing nuclear protein	-0.528	0.032298365
Q8WZA9	IRGQ	immunity-related GTPase family, Q	-0.365	0.001219965
Q92499	DDX1	DEAD (Asp-Glu-Ala-Asp) box helicase 1	0.191	0.006214171
Q92598-2	HSPH1	heat shock 105kDa/110kDa protein 1	0.134	0.003464985
Q92878	RAD50	RAD50 homolog, double strand break repair protein	-0.593	0.00937218
Q92879-2	CELF1	CUGBP, Elav-like family member 1	-0.565	0.003576203
Q92896	GLG1	golgi glycoprotein 1	-0.541	0.018680487
Q92973-2	TNPO1	transportin 1	0.255	0.045079054
Q96AG4	LRRC59	leucine rich repeat containing 59	0.380	0.020465995
Q96B54	ZNF428	zinc finger protein 428	-0.455	0.018265545
Q96C01	FAM136A	family with sequence similarity 136, member A	-0.376	0.004017361
Q96CN7	ISOC1	isochorismatase domain containing 1	0.561	0.000454077
Q96CT7	CCDC124	coiled-coil domain containing 124	-0.400	0.011840373
Q96DH6-2	MSI2	musashi RNA-binding protein 2	0.589	0.0054224
Q96FC7	PHYHIPL	phytanoyl-CoA 2-hydroxylase interacting protein-like	-0.288	0.001842916
Q96HS1	PGAM5	phosphoglycerate mutase family member 5	-0.254	0.029029066
Q96I25	RBM17	RNA binding motif protein 17	-0.730	0.047584769
Q96KR1	ZFR	zinc finger RNA binding protein	-0.191	0.01527677
Q96PZ0	PUS7	pseudouridylate synthase 7 (putative)	-0.296	0.008884381
Q96TA2-3	YME1L1	YME1-like 1 ATPase	-0.316	0.045235908
Q99543-2	DNAJC2	DnaJ (Hsp40) homolog, subfamily C, member 2	-0.717	0.018107404
Q99733	NAP1L4	nucleosome assembly protein 1-like 4	-0.275	0.003225905
Q99880	HIST1H2BL	histone cluster 1, H2bl	-0.305	0.028954221
Q9BQ52-4	ELAC2	elaC ribonuclease Z 2	0.250	0.04884852
Q9BQA1	WDR77	WD repeat domain 77	0.526	0.040263099
Q9BRX8-2	FAM213A	family with sequence similarity 213, member A	1.238	0.003133277
Q9BTT0	ANP32E	acidic (leucine-rich) nuclear phosphoprotein 32 family, member E	0.346	0.027030894
Q9BVG4	PBDC1	polysaccharide biosynthesis domain containing 1	-0.489	0.009572317
Q9H307	PNN	pinin, desmosome associated protein	-0.626	0.015287906
Q9H9B4	SFXN1	sideroflexin 1	0.202	0.000283261
Q9HAV4	XPO5	exportin 5	0.140	0.006611309

Q9NQ48-2	LZTFL1	leucine zipper transcription factor-like 1	0.417	0.025634072
Q9NR45	NANS	N-acetylneuraminic acid synthase	0.588	0.000642731
Q9NWU5	MRPL22	mitochondrial ribosomal protein L22	-0.512	0.025994698
Q9NZZ3	CHMP5	charged multivesicular body protein 5	0.331	0.036155523
Q9P258	RCC2	regulator of chromosome condensation 2	-0.279	0.021193485
Q9P2J5	LARS	leucyl-tRNA synthetase	0.155	0.016734573
Q9UBM7	DHCR7	7-dehydrocholesterol reductase	0.142	0.017369289
Q9UHB9	SRP68	signal recognition particle 68kDa	0.282	0.013372805
Q9UHD8-5	SEPT9	septin 9	0.192	1.49E-05
Q9UJA5	TRMT6	tRNA methyltransferase 6	-0.328	0.015156387
Q9UJS0	SLC25A13	solute carrier family 25 (aspartate/glutamate carrier), member 13	0.277	0.004092393
Q9UNS2	COPS3	COP9 signalosome subunit 3	0.276	0.01101695
Q9UQ80	PA2G4	proliferation-associated 2G4, 38kDa	-0.339	0.024150782
Q9Y230	RUVBL2	RuvB-like AAA ATPase 2	-0.202	0.018236837
Q9Y265	RUVBL1	RuvB-like AAA ATPase 1	0.361	0.001286532
Q9Y2A7	NCKAP1	NCK-associated protein 1	0.994	0.008558676
Q9Y2W1	THRAP3	thyroid hormone receptor associated protein 3	-0.224	0.00018084
Q9Y394-2	DHRS7	dehydrogenase/reductase (SDR family) member 7	0.435	0.001591339
Q9Y3B3-2	TMED7	transmembrane emp24 protein transport domain containing 7	0.419	0.010425221
Q9Y3B7-2	MRPL11	mitochondrial ribosomal protein L11	0.071	0.00760537
Q9Y4C2	TCAF1	TRPM8 channel-associated factor 1	0.370	0.003850379
Q9Y5B8-2	NME7	NME/NM23 family member 7	0.445	0.044338155
Q9Y5K5-2	UCHL5	ubiquitin carboxyl-terminal hydrolase L5	0.224	0.020980893
Q9Y678	COPG1	coatomer protein complex, subunit gamma 1	0.688	0.02646428
Q9Y6G9	DYNC1LI1	dynein, cytoplasmic 1, light intermediate chain 1	-0.390	0.010044682
R4GNH3	PSMC3	proteasome (prosome, macropain) 26S subunit, ATPase, 3	-0.329	4.08E-05
S4R3H4	ACIN1	apoptotic chromatin condensation inducer 1	-0.372	0.039298841

Appendix 5

Dysregulated LF_TatLivsBme proteins

Uniprot accession #	Symbol	Log2 ratio	p-value
Q5JRA6-2	MIA3	-0.6913835	0
O95782-2	AP2A1	-0.3804217	4.54E-212
P08574	CY1	0.10743022	2.02E-13
Q12972-2	PP1R8	-0.4955246	1.09E-08
Q5VTU3	Q5VTU3	-0.8494605	2.85E-07
O95202	LETM1	0.34496839	8.11E-07
P06576	ATPB	0.27184662	1.66E-06
P04406	G3P	0.394625	1.88E-06
R4GNH3	R4GNH3	-0.4366067	3.87E-06
P08670	VIME	0.19422923	4.17E-06
P00403	COX2	0.81210021	4.26E-06
Q7RTV0	PHF5A	-1.071474	4.30E-06
P18085	ARF4	0.40627647	4.38E-06
Q2NL82	TSR1	0.29527683	6.99E-06
Q9NS69	TOM22	-0.9187857	7.87E-06
Q99832	TCPH	0.13640894	8.60E-06
O43681	ASNA	0.29959877	1.21E-05
Q07955	SRSF1	-0.3124895	1.88E-05
P80723	BASP1	-0.8429613	2.08E-05
Q13126	MTAP	-0.5017758	2.20E-05
P40227	TCPZ	0.11978615	2.23E-05
Q8WX93-4	PALLD	-0.4270714	2.24E-05
Q16629-3	SRSF7	-0.5301607	2.38E-05
Q8WZA9	IRGQ	-0.6128187	2.39E-05
P68402	PA1B2	-0.8240464	2.65E-05
Q9UHD8-5	9-Sep	0.20512801	2.78E-05
O00231	PSD11	0.36036241	2.99E-05
O00159-2	MYO1C	0.60850023	3.02E-05
P14406	CX7A2	1.17743944	3.04E-05
P09543-2	CN37	0.49754354	3.68E-05
E9PH29	E9PH29	0.3535852	3.76E-05
Q96CN7	ISOC1	0.73326151	3.78E-05
P67809	YBOX1	-1.1842305	4.03E-05
Q99460	PSMD1	0.45609209	4.30E-05
P60981	DEST	0.23838071	4.73E-05
P62847-2	RS24	0.71227512	5.21E-05
Q9NQT5	EXOS3	-0.199944	5.43E-05
P51149	RAB7A	0.31675595	5.79E-05
Q9UHB9	SRP68	0.40451927	7.09E-05
P33993	MCM7	0.35686876	7.36E-05
P32969	RL9	0.49312255	9.39E-05
O95816	BAG2	0.4141795	0.00010021
Q9ULC4	MCTS1	0.6502271	0.00010042
P62805	H4	0.58873181	0.00010299
Q15435	PP1R7	0.5653714	0.00012916

P49419-2	AL7A1	-0.3558217	0.00013573
P62854	RS26	0.85358842	0.00013625
O15020-2	SPTN2	-0.6219199	0.00013697
P49327	FAS	0.18085568	0.00013993
P35637-2	FUS	-0.7959033	0.0001459
E7ETZ4	E7ETZ4	0.42629914	0.00014615
P13639	EF2	0.26289713	0.00016338
Q15005	SPCS2	0.29766686	0.00017046
Q15437	SC23B	-0.5238638	0.0001718
Q15631	TSN	0.29110765	0.00017778
Q09028-3	RBBP4	-0.6549413	0.00020218
Q12765	SCRN1	-0.4158813	0.00021311
P10645	CMGA	-0.5043355	0.00021611
Q92598-2	HS105	0.14392028	0.00024121
Q9HDC9	APMAP	0.13566251	0.00024593
P13010	XRCC5	0.28389073	0.00026392
Q5T6V5	CI064	0.34167259	0.00027018
Q969Z0	TBRG4	-0.551933	0.00027558
P50454	SERPH	0.21550018	0.00027761
P16403	H12	-1.0704551	0.00029289
M0R366	M0R366	-1.0472801	0.00031372
Q96DI7	SNR40	-0.2612973	0.00032262
P49189	AL9A1	-0.5386639	0.00033088
P25705	ATPA	0.10089093	0.00033684
P61313	RL15	-0.8859813	0.00036589
Q9BRP8-2	WIBG	-0.557871	0.00036781
P35269	T2FA	-0.750707	0.00039315
B7Z1R5	B7Z1R5	0.41918661	0.00039984
P25205	MCM3	0.2057147	0.00042497
O75475	PSIP1	-0.3911358	0.00042856
Q9Y678	COPG1	1.35046477	0.00043262
P27348	1433T	-0.2690067	0.00044048
D6RGI3	D6RGI3	-0.6501962	0.00045681
Q16850	CP51A	0.44211141	0.00046437
Q96DH6-2	MSI2H	0.56611172	0.00047658
O60264	SMCA5	-0.3794155	0.00048387
P49591	SYSC	0.74228698	0.00051216
O75439	MPPB	-0.3940763	0.00052998
Q08211	DHX9	0.12503582	0.00053439
O43776	SYNC	0.6129039	0.00054543
Q9Y6G9	DC1L1	-0.5967029	0.00057668
P00491	PNPH	-0.4468672	0.00058958
P25685	DNJB1	0.40883102	0.00059779
E9PC52	E9PC52	-0.6175613	0.00059799
Q9BZZ5-2	API5	0.18755361	0.00065178
Q14137	BOP1	-0.6678439	0.00070141
P07741	APT	-0.8223015	0.00071759
Q04637-5	IF4G1	0.33946656	0.00072613
P84090	ERH	-0.4974438	0.00073588
P53396	ACLY	0.12581246	0.00074102

B7Z972	B7Z972	0.48607445	0.00074664
Q15813	TBCE	0.28057711	0.00075679
O15173	PGRC2	0.17460716	0.00077015
D6RIY6	D6RIY6	-0.2203475	0.00077136
Q16527	CSRP2	-0.633395	0.00080209
Q14699	RFTN1	-0.729051	0.00081062
Q9UNS2	CSN3	0.36843005	0.00081642
H3BRV0	H3BRV0	-0.3526311	0.00082685
Q9NYF8-2	BCLF1	-0.6260714	0.00083073
P25787	PSA2	0.88791971	0.00087008
O43657	TSN6	-0.7004303	0.00088783
Q14011	CIRBP	-0.5904156	0.00094096
P13591-1	NCAM1	-0.4624239	0.00097145
P54725-2	RD23A	-0.3513324	0.00098206
Q9UJS0	CMC2	0.43969872	0.00099077
P56192	SYMC	0.43151661	0.00105197
O15143	ARC1B	-0.3703162	0.00105317
P30566	PUR8	0.43717649	0.00106918
P43490	NAMPT	0.19149716	0.0010968
Q9H2J4	PDCL3	-0.440774	0.00113636
P29966	MARCS	-0.3840245	0.00114418
Q9BVG4	PBDC1	-0.7763724	0.0011836
P49589-2	SYCC	0.82772412	0.00119031
P36543	VATE1	0.42888244	0.00121953
Q14444-2	CAPR1	-0.3828671	0.0012707
P09211	GSTP1	0.37461177	0.00131937
Q9BR76	COR1B	-0.465043	0.00134989
P48735	IDHP	0.23950955	0.00142385
Q9UKD2	MRT4	-0.381532	0.00143845
P62851	RS25	0.30495983	0.00146125
P47897	SYQ	0.12043223	0.00146328
P16435	NCPR	0.46421825	0.00146421
P50395	GDIB	0.23390987	0.0014973
B4E363	B4E363	-0.4007379	0.00152665
P27695	APEX1	-0.4140086	0.00159289
P27824	CALX	0.3880622	0.00162241
O43719	HTSF1	-0.548108	0.00163042
Q9UJZ1	STML2	-0.2170229	0.00165471
P40222	TXLNA	-0.4781395	0.00172115
P35520	CBS	-0.3297285	0.0017519
F8VQX6	F8VQX6	0.74411293	0.00177144
P05556	ITB1	-0.3721782	0.00177538
J3QT28	J3QT28	-0.3692807	0.00179301
O14980	XPO1	0.22796556	0.00183118
P08754	GNAI3	0.39814519	0.00184264
P51571	SSRD	0.23822864	0.00187765
Q15126	PMVK	-0.4000686	0.0019073
Q8WWM7	ATX2L	-0.4059125	0.00192826
P09172	DOPO	-0.4091666	0.00194118
P19367	HXK1	0.09818375	0.00194851

O43765	SGTA	-0.402194	0.00195333
P61163	ACTZ	-0.3811932	0.00198359
P12236	ADT3	0.41996109	0.00200616
Q8TEX9	IPO4	0.63212103	0.0020598
H0Y9Y3	H0Y9Y3	-0.2679842	0.00209834
Q14157	UBP2L	-0.602968	0.00211704
O14737	PDCD5	-0.5365084	0.00213991
P42167	LAP2B	0.62035446	0.00214649
P11940	PABP1	0.27347677	0.00218204
Q92879-2	CELF1	-0.4805355	0.00220402
P60174-1	TPIS	0.22767786	0.002205
Q92896	GSLG1	-0.7413966	0.00220662
Q13409-3	DC1I2	-0.4794948	0.00220917
O00170	AIP	-0.4327176	0.0022471
Q9Y2W1	TR150	-0.1297525	0.00228458
P05141	ADT2	0.63203981	0.00232517
P15374	UCHL3	-0.3124247	0.00234625
P35221	CTNA1	0.15767077	0.00235113
P21266	GSTM3	-0.4476481	0.00237385
O75531	BAF	0.40968063	0.00237661
P62241	RS8	0.27092144	0.00242905
Q9BUQ8	DDX23	0.14943694	0.00253154
Q8WXF1-2	PSPC1	0.68135665	0.00255108
P22626	ROA2	-0.2729841	0.00268263
Q9Y2A7	NCKP1	1.93878879	0.00271167
O14813	PHX2A	-0.6629725	0.00271825
O75691	UTP20	-0.8269714	0.00277623
P56537	IF6	-0.6390248	0.00278537
P61978-2	HNRPK	-0.6605611	0.00286167
Q9NPJ3-2	ACO13	0.4282369	0.00290099
O95433	AHSA1	0.16265704	0.0029059
O43670-2	ZN207	-0.5631164	0.00299797
P11216	PYGB	-0.2476821	0.00311436
Q9H223	EHD4	-0.6131218	0.00312966
Q07021	C1QBP	1.26926778	0.00313453
P62873	GBB1	0.07908513	0.00315873
Q13347	EIF3I	-0.3753692	0.00317877
Q9H0D6	XRN2	0.73306622	0.00336384
Q8IY81	SPB1	0.17355028	0.00336601
Q12788	TBL3	-0.425691	0.0033717
O00505	IMA4	0.23250164	0.0034379
Q00796	DHSO	0.16439367	0.0034572
E9PB90	E9PB90	-0.5987672	0.00347569
P00558	PGK1	0.23134701	0.00355768
P61247	RS3A	0.19417847	0.0035776
P07355	ANXA2	0.15504899	0.00363759
P30044-2	PRDX5	0.4382393	0.00368916
P53990-2	IST1	-0.7871176	0.00371996
Q9UKN8	TF3C4	-0.4590048	0.00374872
O43795-2	MYO1B	0.09947394	0.00376079

Q9UGI8-2	TES	-0.4302656	0.00381761
Q9Y265	RUVB1	0.32102313	0.00384167
H7C2G3	H7C2G3	-1.4669421	0.00391854
Q96FW1	OTUB1	-0.4695218	0.00394749
P51858	HDGF	-0.3768478	0.00395912
Q14232	EI2BA	0.21313358	0.00396993
P08238	HS90B	0.18087664	0.00397999
Q9BS26	ERP44	0.16943397	0.0040288
O43290	SNUT1	-0.4725547	0.00404638
Q8WXI9	P66B	-0.4430816	0.00406468
P09661	RU2A	0.24548928	0.00412568
Q8NFH4	NUP37	-0.820406	0.00414214
Q5T3Q7	Q5T3Q7	-0.5545054	0.00416612
P63104	1433Z	0.26411472	0.00427475
O43324-2	MCA3	0.16495326	0.00442892
Q96B54	ZN428	-1.1368546	0.00448403
Q99714	HCD2	0.1771657	0.00453754
Q9BVJ6-3	UT14A	-0.4580056	0.00455009
O95747	OXSR1	0.16401103	0.00461377
P12277	KCRB	0.4962872	0.00462627
Q9Y696	CLIC4	0.35594049	0.00463604
O75822	EIF3J	0.39575154	0.00467686
E5RHG8	E5RHG8	-0.2827243	0.00471655
Q53EL6-2	PDCD4	-0.5651363	0.0047467
Q29RF7	PDS5A	-0.5509964	0.00475802
P0CW22	RS17L	0.21929951	0.00476877
P54136	SYRC	0.12583971	0.004805
Q7Z2W4	ZCCHV	-0.5470989	0.00483703
Q969X5-2	ERGI1	-0.4495811	0.00486926
P18615	NELFE	-0.6070631	0.00487531
P20042	IF2B	0.24356705	0.0050198
Q14669-4	TRIPC	-0.290539	0.00528327
O00429	DNM1L	0.53488622	0.00533045
P02545	LMNA	0.20251626	0.00543886
O96019	ACL6A	-0.3322127	0.00544566
B7Z7F3	B7Z7F3	-0.7223731	0.00558113
A6NNI4	A6NNI4	-0.4085948	0.00558911
P38117	ETFB	-0.3231112	0.00562632
Q9NP72	RAB18	0.74084635	0.00569053
Q9Y4C2	F115A	0.29572689	0.00573443
Q9UBQ7	GRHPR	-0.459955	0.00593059
P10515	ODP2	0.24678235	0.00594362
P50991	TCPD	0.09244949	0.0060505
O15305	PMM2	-0.279776	0.00610123
F8VR84	F8VR84	0.11784407	0.00617176
Q8NE71-2	ABCF1	-0.3052054	0.00626591
Q15365	PCBP1	0.68246099	0.00636012
O43813	LANC1	-0.2332036	0.00636935
F8W7S5	F8W7S5	-0.3456749	0.00647795
B4DVE7	B4DVE7	0.07870376	0.00659698

P68036	UB2L3	-0.9579576	0.00664704
Q9HD42	CHM1A	0.20170304	0.0066865
P37235	HPCL1	-0.4770035	0.00669488
P12081-4	SYHC	0.29243974	0.00680897
P61981	1433G	-0.451085	0.00689884
Q13573	SNW1	-0.3028767	0.00703074
P11233	RALA	0.34242002	0.00711418
Q5T760	Q5T760	0.54801135	0.00751645
Q09161	NCBP1	0.32402347	0.00752466
P33991	MCM4	0.17501827	0.00763259
P61158	ARP3	-0.1676225	0.00767887
P32322	P5CR1	-0.3619812	0.0077413
P06132	DCUP	0.64250357	0.0077813
Q9UJW0	DCTN4	-0.3836373	0.00778488
P49790	NU153	-0.3002443	0.0078699
Q13724-2	MOGS	-0.6258741	0.0078796
Q96TA2-3	YMEL1	-0.2713002	0.00800716
F5H669	F5H669	-0.6889427	0.00802406
Q99627-2	CSN8	0.54311538	0.00811039
Q9H4A4	AMPB	0.28656988	0.00812161
Q99733	NP1L4	-0.3033602	0.00814527
P14618	KPYM	0.85579993	0.00819258
J3KSI4	J3KSI4	0.86514115	0.00822442
Q9BRX8-2	F213A	0.49370444	0.00824029
O43809	CPSF5	0.12044263	0.00828998
I3L1P8	I3L1P8	-0.3461458	0.00833072
Q8NBS9-2	TXND5	-0.3083553	0.00833188
P35232	PHB	0.2961273	0.00837994
Q15019	2-Sep	0.12700618	0.00844986
P62277	RS13	0.50690244	0.00845313
E5RGR0	E5RGR0	-0.3983663	0.00845585
O75874	IDHC	0.09126657	0.00850118
P61081	UBC12	0.21750876	0.00855251
Q9UIA9	XPO7	-0.4437967	0.00861995
Q13362-4	2A5G	-0.4489363	0.0088225
F5H2Q7	F5H2Q7	-0.5764061	0.00887743
P24666	PPAC	-0.4159461	0.0089195
P62906	RL10A	0.52360575	0.00904041
Q9NYH9	UTP6	-0.3383785	0.00904961
P57740	NU107	-0.4823143	0.00905945
Q9P258	RCC2	-0.3254391	0.00909171
P28072	PSB6	-0.5312568	0.00912911
Q9Y333	LSM2	1.42370605	0.00919397
P78347-2	GTF2I	-0.3622572	0.009364
O00483	NDUA4	-1.0439633	0.00938736
Q92878	RAD50	-0.2357025	0.00941604
Q14108	SCRB2	0.32033788	0.00943686
P12235	ADT1	0.39586674	0.00949142
Q13151	ROA0	0.60628708	0.00961192
P25788-2	PSA3	-0.3071643	0.00983277

P54577	SYYC	0.45138201	0.00989364
P40926	MDHM	0.21476603	0.00994247
E5RJI7	E5RJI7	-0.597278	0.01001409
E7EU96	E7EU96	0.38112146	0.01010198
Q04837	SSBP	-0.2819044	0.01012469
O00410	IPO5	-0.1015946	0.01023345
P24539	AT5F1	-0.9352183	0.01024696
P34897-3	GLYM	0.06382125	0.01026703
P04181	OAT	-0.3388927	0.01036417
Q8TEM1	PO210	0.54121991	0.01040082
Q8N8S7-2	ENAH	-0.6264979	0.01042338
Q99453	PHX2B	-0.1727332	0.01043904
Q86V81	THOC4	0.42407696	0.01055297
P51148	RAB5C	-0.3186011	0.01055781
Q9Y3B3-2	TMED7	0.35647331	0.01077864
P67936	TPM4	-0.4529101	0.01108349
P29373	RABP2	0.47852169	0.01117547
P53004	BIEA	0.20142911	0.01120686
Q14257	RCN2	0.6228945	0.01130158
O75348	VATG1	-0.3611296	0.01149301
Q92522	H1X	-0.6206284	0.01220216
Q9ULV4	COR1C	-0.2694564	0.01238347
P35658-2	NU214	-0.417129	0.01240852
Q14254	FLOT2	0.46130544	0.01242215
Q9Y262	EIF3L	0.13848467	0.01257534
O60271-4	JIP4	-0.5336622	0.0126379
Q9NTI5-2	PDS5B	-0.3011565	0.01276182
P21283	VATC1	0.28852194	0.01285924
P60953	CDC42	0.74285151	0.01305653
P22059	OSBP1	-0.3744546	0.01320858
Q13247-3	SRSF6	-0.3050024	0.01322571
Q16555	DPYL2	0.32150776	0.01333187
P00505	AATM	0.19262043	0.01344204
P35244	RFA3	0.31507644	0.01369819
O75340	PDCD6	0.38111105	0.01373106
P26583	HMGB2	-0.3327729	0.01385569
O00232	PSD12	0.2103367	0.01392224
Q1KMD3	HNRL2	0.2150828	0.01405858
Q9UKM9-2	RALY	0.24226031	0.01414952
O75223	GGCT	-0.3521439	0.01446901
O43847	NRDC	-0.1416122	0.01451422
P22695	QCR2	-0.3081495	0.01468315
Q9H0A0	NAT10	0.82910196	0.01486666
P02786	TFR1	0.23754606	0.01490123
P08621	RU17	-0.2453147	0.01496919
Q8IZL8	PELP1	-0.3634902	0.01501083
P55010	IF5	0.27337664	0.01502639
G8JLB2	G8JLB2	0.17879285	0.01533227
O60762	DPM1	0.56962807	0.01533798
Q16401-2	PSMD5	0.49305294	0.01534479

P07858	CATB	-0.2130324	0.01561901
P62140	PP1B	0.32255179	0.01578671
P62829	RL23	0.41025496	0.01581577
Q9H3P7	GCP60	-0.389451	0.01609769
F5H8E5	F5H8E5	-0.3043434	0.01610484
H7BXW3	H7BXW3	0.17810516	0.01621557
E7EVA0	E7EVA0	-0.2885021	0.01634682
Q7KZF4	SND1	-0.1971671	0.01646028
Q96H79	ZCCHL	-0.5092706	0.01682556
H3BV80	H3BV80	0.15234408	0.01690784
P47813	IF1AX	-0.2582713	0.0170173
P10599	THIO	0.25052679	0.01702853
E3W994	E3W994	-0.6317961	0.01706636
F8VPD4	F8VPD4	0.12723512	0.01713474
O15240	VGF	0.42540049	0.01724866
Q16543	CDC37	-0.2184469	0.0173562
P49736	MCM2	0.50708332	0.0175659
P61586	RHOA	0.7291954	0.01774152
O00461	GOLI4	-0.5442628	0.01775416
P48147	PPCE	0.21758558	0.01799724
B4DEK4	B4DEK4	-0.3754769	0.01803957
Q16643	DREB	-0.3170894	0.01806144
B7Z254	B7Z254	0.20615248	0.0181571
B4DUS9	B4DUS9	0.18896909	0.0185763
Q13442	HAP28	-0.2282016	0.01888934
J3QRD1	J3QRD1	-0.3801315	0.01890638
O00299	CLIC1	0.22426383	0.0189139
P36578	RL4	0.22025837	0.01893942
M0QX07	M0QX07	-1.5950906	0.0194857
O00746	NDKM	-0.324535	0.01955966
P40938-2	RFC3	-0.4032543	0.01961431
P61964	WDR5	-0.638016	0.01975557
P47985	UCRI	2.60047344	0.01992551
Q7L014	DDX46	-0.1865038	0.01995713
B4DP61	B4DP61	-0.231257	0.01997915
O00303	EIF3F	0.21213578	0.02013508
Q01581	HMCS1	0.58108685	0.02024099
Q96B26	EXOS8	0.34624596	0.02102707
P61970	NTF2	0.16422304	0.02115015
Q96AG4	LRC59	0.37932661	0.02116035
Q13148	TADBP	-0.5056326	0.0212743
Q9Y2Q3	GSTK1	-0.6583139	0.02129402
Q9HB71	CYBP	-0.2815207	0.02162537
Q13526	PIN1	0.51007236	0.02169703
Q4VC31	CCD58	-0.114858	0.02192572
Q9Y6C9	MTCH2	-0.1879274	0.02199233
H0Y362	H0Y362	-0.7620361	0.0220115
Q13162	PRDX4	-0.1973549	0.02208853
P31939	PUR9	0.08847242	0.02215771
Q9NV06	DCA13	0.15307215	0.02217835

Q14498-3	RBM39	0.45535835	0.02236653
P62266	RS23	-0.4109626	0.02244679
O00148	DX39A	0.38479895	0.02266198
P18859	ATP5J	-1.0988631	0.02275873
Q8TEA8	DTD1	-0.3598152	0.02280051
P24928	RPB1	0.56164381	0.02283175
Q9HD20	AT131	-0.5606333	0.02293079
P20618	PSB1	0.1517247	0.02297074
B7Z9I1	B7Z9I1	-0.2774859	0.02325851
Q99459	CDC5L	0.29794268	0.02326376
Q9P2J5	SYLC	0.13197715	0.02346955
P04843	RPN1	0.11049842	0.02363949
O00267-2	SPT5H	-0.3332797	0.02366301
Q9UNZ2	NSF1C	-0.671253	0.02369701
E2QRM6	E2QRM6	-0.6299637	0.02410387
P09429	HMGB1	-0.3808071	0.02432337
P15880	RS2	0.18402184	0.02453162
Q9H2M9	RBGPR	-0.7110106	0.02453565
O95487-2	SC24B	-1.2776102	0.02469893
B7Z3Y2	B7Z3Y2	-0.1389802	0.0247272
P62826	RAN	-0.2296955	0.02495393
O15355	PPM1G	0.12472678	0.02505325
Q8IV08	PLD3	0.19304616	0.02508805
P54289-5	CA2D1	-0.4235853	0.02530562
Q01082	SPTB2	-0.2641796	0.02539493
O00154-4	BACH	0.38720599	0.02545483
Q5JP53	Q5JP53	0.83222482	0.02567824
Q9NZB2	F120A	-0.6030013	0.02603678
Q86U42-2	PABP2	0.41383839	0.02604857
P62280	RS11	0.22916979	0.02624602
P52948-6	NUP98	-0.3547756	0.02634268
Q9Y315	DEOC	-0.1619873	0.02643924
P61011	SRP54	0.30486451	0.02649424
O00425	IF2B3	-0.1100721	0.02666259
Q6NUK1-2	SCMC1	0.16252869	0.02685506
Q13045-2	FLII	-0.3962422	0.02728717
P11047	LAMC1	-0.6461229	0.02735778
Q9BVP2-2	GNL3	0.28730727	0.02753233
Q99622	C10	-0.462872	0.02763465
B7Z7Q6	B7Z7Q6	1.23090513	0.02769174
Q9NX46	ARHL2	-0.3560116	0.02780972
P28070	PSB4	0.27908864	0.02784361
Q9Y394-2	DHRS7	0.19102527	0.02785022
Q9H910	HN1L	-0.3882719	0.02807951
P19338	NUCL	0.1223577	0.0281829
Q9Y570	PPME1	0.73716308	0.02828869
Q15056	IF4H	0.34381821	0.02830909
P53597	SUCA	-0.5895135	0.02836441
E7EQ72	E7EQ72	-0.340146	0.02850739
O95881	TXD12	-0.43143	0.02851135

P23193	TCEA1	-0.3144191	0.02854349
Q9H9H4	VP37B	0.43845239	0.02859007
A6NHR9	SMHD1	-0.6833407	0.0286715
P63151	2ABA	-0.5007296	0.0291499
Q01081	U2AF1	-0.2775706	0.03000987
Q9UM54-6	MYO6	-0.3231186	0.03039797
P54886-2	P5CS	0.31098732	0.0305444
P63244	GBLP	0.25801247	0.03087214
Q9P0J0	NDUAD	0.30410154	0.03089417
Q9Y5M8	SRPRB	-0.3251541	0.03101928
P05388	RLA0	0.06867191	0.03120403
P84095	RHOG	-0.5556166	0.03123039
Q9BT78	CSN4	0.49677642	0.03134711
Q9HC38-2	GLOD4	0.24668376	0.03148872
P59998	ARPC4	0.19196373	0.03161036
Q16181	7-Sep	-0.2492034	0.03185862
Q7L2H7	EIF3M	0.42027179	0.03194377
Q15717	ELAV1	0.12760223	0.03201372
C9JG97	C9JG97	-0.5084527	0.03220341
Q9NQ48-2	LZTL1	-0.264396	0.03232106
Q96CW1-2	AP2M1	0.06532179	0.03320072
P63092	GNAS2	-0.3550469	0.03325483
Q96PK6	RBM14	-0.2897838	0.03347358
Q53GQ0	DHB12	1.12531917	0.03353059
Q49AR2	CE022	-0.3750434	0.03360422
Q13363-2	CTBP1	-0.3557922	0.0336296
P49006	MRP	-0.5129918	0.03405043
O43395	PRPF3	0.30222216	0.03450002
P23368	MAOM	0.23961596	0.03467032
Q99543-2	DNJC2	-0.823313	0.03499295
F8VQE1	F8VQE1	-0.1669062	0.03517794
Q9P289-2	MST4	0.08208894	0.03597858
O60443	DFNA5	-0.4177737	0.03616795
A6NKG5	RTL1	-0.3425707	0.03617421
Q15424	SAFB1	-0.3006997	0.03633811
P78417	GSTO1	-0.2072622	0.03641052
Q96EK6	GNA1	0.61253634	0.03654984
Q9NYY8-2	FAKD2	-0.9443297	0.03658897
Q99426	TBCB	-0.2930028	0.03659576
B1ALU1	B1ALU1	-0.3315986	0.03670205
B4DJP7	B4DJP7	0.62809837	0.03678863
B7Z452	B7Z452	0.24349333	0.03705886
O75396	SC22B	-0.2515568	0.03729855
P23921	RIR1	-0.2817969	0.03740107
B9A018	B9A018	0.33971415	0.03751816
Q9Y4L1	HYOU1	0.04644909	0.03791438
Q14697	GANAB	-0.2625225	0.03822151
Q9NZZ3	CHMP5	0.22072787	0.03862693
P23381	SYWC	0.18235385	0.03881231
Q8IYB3-2	SRRM1	-0.6195964	0.03907963

P35579	MYH9	0.07577479	0.03909937
P50502	F10A1	-0.3946793	0.03942084
Q9H4M9	EHD1	0.16213619	0.03975718
P48681	NEST	-0.134334	0.03996942
P18583-2	SON	0.2439199	0.03997056
O60841	IF2P	-0.3909038	0.04066065
Q13155	AIMP2	-0.2628297	0.04098395
P55263	ADK	0.07447996	0.04253146
P49792	RBP2	-0.3511754	0.04270022
P09525	ANXA4	-0.1629169	0.04286451
Q9H8Y8-2	GORS2	0.46304416	0.04389657
Q12906	ILF3	-0.1767016	0.04432012
Q8NCW5-2	NNRE	0.30792536	0.04462927
Q14195-2	DPYL3	0.05430598	0.04492902
Q9UIG0-2	BAZ1B	0.31603205	0.04509509
O14929	HAT1	-0.3393296	0.04532541
P06730	IF4E	-0.6308994	0.04570401
E9PF19	E9PF19	-0.2223048	0.04576374
H3BPJ9	H3BPJ9	-0.5487046	0.04657484
Q9NRR5	UBQL4	-0.3687411	0.04674124
Q15477	SKIV2	-0.2740043	0.04698422
P07737	PROF1	0.29339578	0.04701896
P46821	MAP1B	-0.2355988	0.04704407
Q9H0S4-2	DDX47	-0.4317449	0.04760638
Q14258	TRI25	0.25492191	0.04762559
P22314	UBA1	0.07135596	0.04780925
Q8N1F7	NUP93	-0.1394137	0.04790679
E9PN17	E9PN17	-0.754698	0.04790809
Q9Y6H1	CHCH2	-0.5063266	0.04810517
O95347	SMC2	-0.3909784	0.04810562
Q8WWM9	CYGB	-0.5002084	0.04844401
Q86TX2	ACOT1	-0.1777046	0.04865176
P61006	RAB8A	0.57423884	0.04894231
P39019	RS19	0.13328324	0.04930969
P13667	PDIA4	-0.1062504	0.04944285
Q13620-3	CUL4B	-0.2918901	0.04954965